

## **INFORMATION TO USERS**

This manuscript has been reproduced from the microfilm master. UMI films the text directly from the original or copy submitted. Thus, some thesis and dissertation copies are in typewriter face, while others may be from any type of computer printer.

**The quality of this reproduction is dependent upon the quality of the copy submitted.** Broken or indistinct print, colored or poor quality illustrations and photographs, print bleedthrough, substandard margins, and improper alignment can adversely affect reproduction.

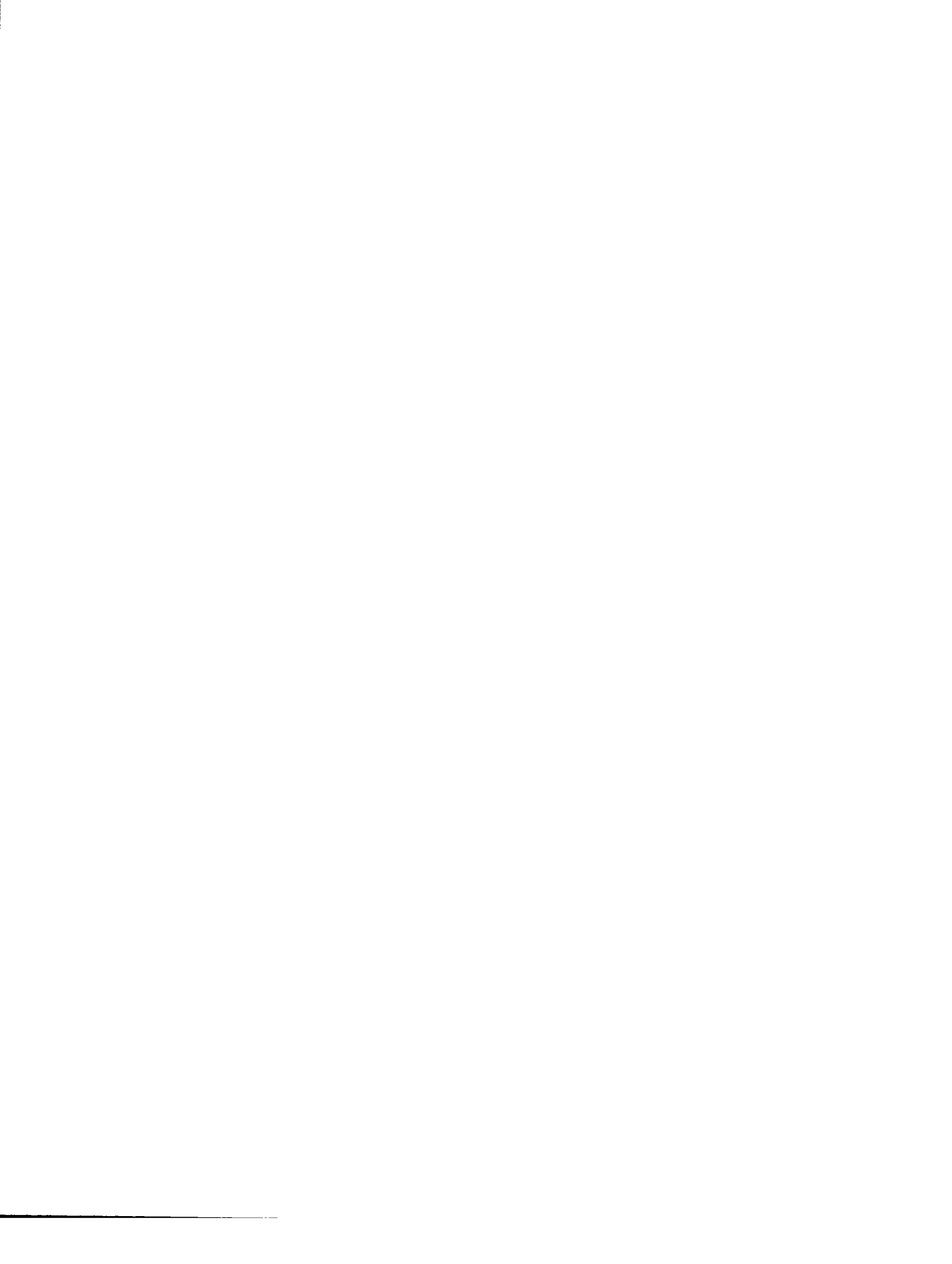
In the unlikely event that the author did not send UMI a complete manuscript and there are missing pages, these will be noted. Also, if unauthorized copyright material had to be removed, a note will indicate the deletion.

Oversize materials (e.g., maps, drawings, charts) are reproduced by sectioning the original, beginning at the upper left-hand corner and continuing from left to right in equal sections with small overlaps. Each original is also photographed in one exposure and is included in reduced form at the back of the book.

Photographs included in the original manuscript have been reproduced xerographically in this copy. Higher quality 6" x 9" black and white photographic prints are available for any photographs or illustrations appearing in this copy for an additional charge. Contact UMI directly to order.

**UMI**

A Bell & Howell Information Company  
300 North Zeeb Road, Ann Arbor MI 48106-1346 USA  
313/761-4700 800/521-0600



## **NOTE TO USERS**

**The original manuscript received by UMI contains pages with  
indistinct and slanted print. Pages were microfilmed as  
received.**

**This reproduction is the best copy available**

**UMI**



THE UNIVERSITY OF OKLAHOMA

GRADUATE COLLEGE

TEMPORAL AND SPATIAL SOURCE ROCK VARIATIONS AND THE  
CONSEQUENCE ON CRUDE OIL COMPOSITION IN THE TERTIARY  
PETROLEUM SYSTEM OF THE UNTA BASIN, UTAH, U.S.A.

A Dissertation

SUBMITTED TO THE GRADUATE FACULTY

in partial fulfillment of the requirements for the

degree of

Doctor of Philosophy

By

ERIC MUELLER  
Norman, Oklahoma  
1998

**UMI Number: 9911867**

---

**UMI Microform 9911867**  
**Copyright 1999, by UMI Company. All rights reserved.**

**This microform edition is protected against unauthorized  
copying under Title 17, United States Code.**

---

**UMI**  
**300 North Zeeb Road**  
**Ann Arbor, MI 48103**

**© Copyright Eric Mueller  
All rights reserved**

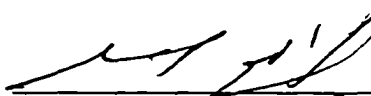
TEMPORAL AND SPATIAL SOURCE ROCK VARIATIONS AND THE  
CONSEQUENCE ON CRUDE OIL COMPOSITION IN THE TERTIARY  
PETROLEUM SYSTEM OF THE UNTA BASIN, UTAH, U.S.A.

A Dissertation APPROVED FOR THE  
SCHOOL OF GEOLOGY AND GEOPHYSICS

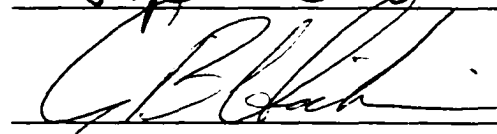
BY



James M. Ferguson



Steven W. Eller



## **Acknowledgements**

I am most grateful to my advisor R. Paul Philp for his support and trust, which allowed me to pursue those aspects of the study which were personally the most interesting and also made it possible to complete the study in a timely manner. Needless to say, the discussions and advices through the thesis work were most helpful. Also, I am most indebted to Tim Ruble (CISRO) for his advices, discussions and support during the field work and for pointing out a number of interesting aspects of the geology of the Uinta Basin. A particular salute to his patience having me around for an extended period of time during work in the core libraries at the U.S. Geological Survey (USGS) in Denver. Mike Engel, J. Forgotson, L. Williams and G. Hieshima are acknowledged for their reviews and the effort they put into serving on the Ph.D. committee. In particular, the detailed and critical review of Dr. Glenn Hieshima was much appreciated.

A number of individuals have provided logistic support and samples to this study. John Allen assisted in the analytical part of the thesis. I am indebted to Mike Lewan and Ted Daws (USGS, Denver) for running the Rock-Eval analysis on the samples. Paul Lillis (USGS, Denver) permitted taking aliquots of crude oil samples stored at the USGS. Additional samples were donated by Samir Gazi (Conoco Inc.), who also supplied a large number of well logs to this study. John Osmond (Consultant, Denver) and Tom Ault (CNG, Houston) provided samples from the West Willow Creek field, John also shared his knowledge about this unusual field. Larry Tedesco (Chevron Inc., Houston) was very helpful in tracking down the necessary data for the oils samples, most of which have been taken by Chevron Inc. Additional information came from the PI database, made available by D. Northcuff (PI Dwight's Inc., Oklahoma City). Craig Morgan (Utah Geological Survey) also helped with retrieving information available at the UGS. Mary McPherson (Chevron Inc.) provided information and maps for the Greater Red Wash area. Dr. Mike Richman

from the Department of Meteorology at the University of Oklahoma gave guidance through the world of multivariate statistics.

The study was supported through grants of the Japanese National Oil Company and Chevron Inc. The fieldwork was made possible through grants of the Geological Society of America, American Association of Petroleum Geologists and the School of Geology and Geophysics, University of Oklahoma.

This thesis is dedicated to my wife Madeleine, who was supportive and understanding all the way through, and who had to tolerate this endeavor for much too long.

## Table of Contents

<b>List of Figures</b> .....	.ix
<b>List of Tables</b> .....	.xv
<b>List of Appendices</b> .....	.xvii
<b>Abstract</b> .....	.xviii
<b>1. Introduction</b> .....	.1
<b>2. Purpose</b> .....	.3
<b>3. The Tertiary Uinta Basin</b> .....	.5
<b>3.1. Physical-tectonic Setting</b> .....	.5
<b>3.2. Lacustrine Facies</b> .....	.7
<b>3.3. Tertiary Stratigraphy and Evolution of the Uinta Basin</b> .....	.12
<b>3.4. Lacustrine Environments of Lake Uinta</b> .....	.16
<b>3.5. The Green River Petroleum System</b> .....	.19
<b>4. Samples</b> .....	.24
<b>4.1. Source Rock Samples</b> .....	.24
<b>4.2. Oil Samples</b> .....	.24
<b>5. Experimental</b> .....	.30
<b>5.1. Rock-Eval Analysis</b> .....	.30
<b>5.2. Source rock extraction</b> .....	.30
<b>5.3. Asphalt Precipitation and Fractionation of Source Rock Extracts and Oils</b> .....	.31
<b>5.4. Gas Chromatography (GC) and Gas Chromatography-Mass spectrometry (GC-MS)</b> .....	.32
<b>5.5. Statistical Methods</b> .....	.34

<b>6. Data Analysis and Interpretation .....</b>	39
<b>6.1. Source Rock Analysis .....</b>	39
<b>6.1.1. General Observations .....</b>	40
<b>6.1.1.1 Bulk Data .....</b>	40
<b>6.1.1.2 High Temperature Gas-Chromatography (GC) Analysis.....</b>	44
<b>6.1.2. Gas Chromatography-Mass Spectrometry (GC-MS) Analysis .....</b>	48
<b>6.1.2.1 Biomarker Distribution in the Source Rock Extracts .....</b>	49
<b>6.1.2.2 Principal Component Analysis (PCA) of Source Rock Extract GC-MS data .....</b>	65
<b>6.1.2.2.1 Principal Component Loadings - Source Rock Extract Analysis .....</b>	66
<b>6.1.2.2.3 Source Rock Extract Principal Component Scores .....</b>	75
<b>6.1.2.2.3 Correlation of PCA Sample Scores and other Geochemical Parameters .....</b>	81
<b>6.2 Stratigraphic and Facies Related Aspects of Source Rock Geochemistry.....</b>	35
<b>6.2.1 Altamont-Bluebell Area - Map-group 1 .....</b>	87
<b>6.2.2 Greater Red Wash Area - Map-group 2 .....</b>	100
<b>6.2.3 South Central Area - Map-group 3.....</b>	109
<b>6.3 Crude Oil Analysis.....</b>	117
<b>6.3.1 General Observations .....</b>	117
<b>6.3.2 Crude Oil Biomarker Composition - GC-MS Analysis.....</b>	122
<b>6.3.2.1 Principal Component Analysis of Crude Oil GC-MS Data.....</b>	123
<b>6.3.2.1.1 Principal Component Loadings - Crude Oil Analysis .....</b>	125
<b>6.3.2.1.2 Principal Component Scores of the Crude Oil Analysis - Correlation to Source Rocks .....</b>	127
<b>6.3.2.1.3 Other Geochemical Data of the Crude Oils .....</b>	138

<b>7. Synthesis of the Source Rock and Crude Oil Geochemistry and Implications for the Petroleum System of the Uinta Basin .....</b>	<b>144</b>
<b>7.1 Green River Formation Source Rocks in the Uinta Basin .....</b>	<b>144</b>
<b>7.2 Uinta Basin Crude Oils and their Correlation to Source Rocks.....</b>	<b>146</b>
<b>7.3 Secondary Migration .....</b>	<b>150</b>
<b>8. Conclusions .....</b>	<b>155</b>
<b>9. References.....</b>	<b>156</b>

## List of Figures

Figure 1: Location of the Uinta Basin and extent of the Green River Formation in Laramide basins of Wyoming, Utah and Colorado (adapted from Tuttle, 1991). The figure also indicates the structural elements surrounding the Uinta Basin.....	6
Figure 2: Schematic cross-section through the Uinta Basin (adapted from Fouch, 1975) showing the asymmetric structure, formations and lithofacies of the Tertiary sediments. Prominent subsurface markers used for correlation in the basin are also indicated.....	6
Figure 3: Location and extent of Lake Gosiute and Lake Uinta during the Middle Eocene (modified from Remy, 1992). Note that in this interpretation no hydrological connection exists between Lake Uinta and Lake Gosiute.....	9
Figure 4: Lacustrine facies model showing Ryder's <i>et al.</i> (1976) tripartitioned facies belts in Lake Uinta.....	9
Figure 5: Generalized lithofacies maps for (a) the Eocene-Paleocene boundary, (b) units deposited midway between carbonate marker and Paleocene-Eocene boundary, (c) strata equivalent to the carbonate marker and (d) the middle marker time (modified from Fouch, 1975). .....	11
Figure 6: Generalized and simplified development of the Lake Uinta depositional system in the Uinta Basin. Note that the figure includes faciesbelts, the facies succession and stratigraphic terminology. Lake level fluctuations and climate changes are schematic and indicate only major changes in lake extent and ambient conditions in the area of the Green River Formation depositional system.....	13
Figure 7: Overpressure region in the Uinta Basin assumed to coincide with an active hydrocarbon kitchen. (a) Section shown also in Figure 2 with superimposed area of fluid pressure gradients $>0.5\text{ psi}/\text{ft}$ (after Chidsey, 1993). (b) Generalized pore pressure vs. depth for the Altamont Bluebell area (Montgomery and Morgan, 1998). (c) Regional map showing the distribution of fluid pressure gradients $>0.6 \text{ psi}/\text{ft}$ (Chidsey, 1993). .....	20
Figure 8: Location of source rock samples obtained from cored wells drilled in the Uinta Basin. Map-groups refer to samples grouped together depending on well location.....	26
Figure 9: Location of the Uinta Basin oil and gas fields from which samples have been investigated for this study. The map has been adapted from the Utah Geological Survey Map 68 (1982) and most fields have been extended since publication. Stippled pattern are oil fields, hatched pattern are gas fields.....	27
Figure 10: Location of oil samples obtained from various fields (see Figure 9) of the Uinta Basin. Map-groups refer to samples grouped together based on well location.....	28
Figure 11: Histograms of TOC (a) and HI-Indices (b) of Green River Formation source rock samples analyzed in this study. Bimodal distribution in (a) is caused by high TOC in oil-shales. Extremely high TOC value represents coal sample UB42E, maximum value in (b) is from mahogany zone outcrop sample UB39E. Note class change at TOC $>16\%$ in (a).....	41

Figure 12: Oxygen- vs. Hydrogen-Index (a) and $T_{max}$ vs. Hydrogen-Index (b) derived from Rock-Eval analyses of source rock core samples. Displayed samples were used for detailed geochemical study. Standard kerogen type pathways adopted from Tissot <i>et al.</i> (1987). The difference between regular type and oil-shale type samples is explained the text.....	43
Figure 13: Representative high-temperature gas chromatograms of source rock extract saturated hydrocarbon fractions (oil-shale type (a and b) and regular type (c and d)). Samples in (b) and (d) show possible evaporative loss of lower molecular weight fractions. *= Internal standard $C_{24}D_{50}$ .....	46
Figure 14: Representative reconstructed ion current chromatograms of source rock extract branched and cyclic fraction obtained with MID GC-MS. Regular type source rock in (a), oil-shale type source rock in (b). *=internal standard $C_{24}D_{50}$ (approx. 287 ppm); Pr=pristane, Ph=phytane.....	50
Figure 15: Representative mass-chromatograms m/z 191 of source rock extracts branched and cyclic fractions. Peak labels refer to compounds listed in Appendix 1.2. Chromatogram (a) and (b) show regular type source rock, (c) is oil-shale type; peak labeled ? in (a) is possibly $C_{24}$ -tetracyclic terpane.....	51
Figure 16: Methyl hopanes(shaded peaks) in two representative source rock extract branched and cyclic fractions. Chromatogram (a) shows regular source rock type, chromatogram (b) shows oil-shale type sample; peak identification in Appendix 1.2.....	54
Figure 17: Representative mass-chromatograms m/z 217 of source rock extract branched and cyclic fraction ((a and b) regular type, (c) oil-shale type). Peak labels refer to compounds listed in Appendix 1.2. $4\alpha(Me)$ -steranes refer to $4\alpha(Me)$ -24-ethyl- $14\beta(H), 17\beta(H), 20S+R$ -cholestanes.....	57
Figure 18: Ternary diagram of desmethyl sterane distribution (using $14a(H), 17a(H), 20R$ isomers) in Uinta Basin source rock extracts. Graph differentiates between map-groups and oil-shale vs. regular type extracts. Samples and % sterane values listed in Appendix 5.....	58
Figure 19: Methyl sterane identification in representative source rock extracts. Chromatograms (a) and (b) show metastable ion transitions, (c) compares characteristic ions obtained from MID GC-MS analysis. Note the distinct pattern of $3\beta(Me)$ - and $4a(Me)\beta\beta$ -isomers in m/z 232. Labels refer to compounds listed in Appendix 1.2.....	60
Figure 20: Representative chromatograms of monoaromatic steroids in the saturate fractions of Uinta Basin source rock extracts. Sample in (a) is a regular source rock type, sample (b) shows the m/z 253 chromatogram of an oil-shale type sample. Peak identification is tentative because of coelution of a number of compounds; peak labels refer to compounds listed in Appendix 1.2.....	62
Figure 21: Representative examples for sesquiterpane and diterpane distributions in Uinta Basin source rock extract branched and cyclic fractions, determined with MID GC-MS. Chromatogram (a and b) are from regular type source rocks, (c) is an oil-shale type source rock. Peak labels refer to compounds listed in Appendix 1.2.....	64

Figure 22a: Loadings on principal components PC1 (a), PC2 (b) and PC3 (c), source rock extract GC-MS analysis; m=96, variance-covariance matrix based PCA. Bar labels and numbers on x-axis are the variables and refer to peak numbers listed in Appendix 1.2.....	69
Figure 22b: Loadings on principal components PC1 (a), PC2 (b) and PC3 (c), source rock extract GC-MS analysis; m=20, variance-covariance matrix based PCA. Bar labels and numbers on x-axis are the variables and refer to peaks listed in the accompanying table. This PCA method has been used to characterize source rock biomarker composition.....	70
Figure 22c: Loadings on principal components PC1 (a), PC2 (b) and PC3 (c), source rock extract GC-MS analysis; m=20, correlation matrix based PCA. Bar labels and numbers on x-axis are the variables and refer to peak numbers listed in Appendix 1.2.....	71
Figure 23: Comparison of PC2 and absolute gammacerane concentration vs. depth relative to a datum in map-groups 1-3 of the Uinta Basin. Note logarithmic scale for gammacerane concentration in the Altamont-Bluebell field (left panel) and the varying depth scales.....	74
Figure 24a: Principal component cross plot PC1 vs. PC2. Both components include variances associated with the source of organic material and environmental conditions (see text). Labels are sample numbers.....	76
Figure 24b and c: Principal component cross plots PC1 vs. PC3 (b) and PC2 vs. PC3 (c). Variances associated with PC3 are due to maturity differences.....	77
Figure 25: PCA interpretation illustrated with sample UB25E as an example. Refer to Figures 24a-c for location of the sample within PC ordination. (a) is the HTGC trace, (b) to (e) show the RIC, m/z 191, 217, 123 and 253 MID chromatograms. Peak labels refer to compounds listed in Appendix 1.2. *=Internal standard C <sub>24</sub> D <sub>50</sub> .....	78
Figure 26: Schematic overview over the approximate relative stratigraphic positions of the cores summarized into map-groups 1 to 3.....	86
Figure 27: HTGC analysis of source rock extract saturate fractions from cores of the Altamont-Bluebell area (map-group 1). Sample depths are referenced to the middle marker datum (see text); stratigraphy adopted from well Mapco George E Fisher (SW NE, Sec7-T1S-R3W) published by Fouch (1981). Sample information includes sample number, depth of sample in well and Rock-Eval bulk data. *= Internal standard C <sub>24</sub> D <sub>50</sub> ; black rectangles=cores, hatched rectangles=core chips.....	94
Figure 28a: Maturity related biomarker indices and principal component 3 vs. depth in the Altamont-Bluebell area (map-group 1). Sample depth datum is the middle marker (see text); stratigraphy adopted from well Mapco George E Fisher (SW NE, Sec7-T1S-R3W) published by Fouch (1981); abbreviations and ratios are explained in Appendix 1.1.; black rectangles=cores, hatched rectangles=core chips.....	95
Figure 28b: Biomarkers and principal components 1 and 2 vs. depth in the Altamont-Bluebell area (map-group 1). Sample depth datum is the middle marker (see text); stratigraphy adopted from well Mapco George E Fisher (SW NE, Sec7-T1S-R3W) published by Fouch (1981); abbreviations and ratios are explained in Appendix 1.1.; black rectangles=cores, hatched rectangles=core chips.....	96

Figure 28c: Biomarker ratios as proxies for clastic and higher plant organic matter input vs. depth in the Altamont-Bluebell area (map-group 1). Sample depth datum is the middle marker (see text); stratigraphy adopted from well Mapco George E Fisher (SW NE, Sec 7-T1S-R3W) published by Fouch (1981); abbreviations and ratios are explained in Appendix 1.1 black rectangles=cores, hatched rectangles=core chips.....	97
Figure 29: Rock-Eval vs. depth profile from well Blanchard 1-33-3 from the Altamont Bluebell area. Core comprises mostly the green shale facies and Parachute Creek Member below the mahogany zone. Legend in Appendix 3.....	98
Figure 29a: Biomarkers and principal components 1 and 2 vs. depth in the Altamont-Bluebell area (map-group 1). Sample depth datum is the middle marker (see text).....	103
Figure 30: HTGC analysis of source rock extract saturated fractions from cores of the Greater Red Wash area. Sample depths relative to top of Douglas Creek Member (K-marker) datum (see text). Sample information includes sample number, depth of sample in well and Rock-Eval bulk data. *=Internal standard C <sub>24</sub> D <sub>50</sub> ; abbreviations and ratios are explained in Appendix 1.1; black rectangles=cores, hatched rectangles=core chips.....	104
Figure 31a: Maturity related biomarker indices and principal component 3 vs. depth in the Greater Red Wash area (map-group 2). Sample depth datum is the top of the Douglas Creek Member (see text); black rectangles=cores, hatched rectangles=core chips.....	105
Figure 31b: Selected biomarkers and principal components 1 and 2 vs. depth in the Greater Red Wash area (map-group 2). Sample depth datum is the top of the Douglas Creek Member (see text). Sample information includes sample number, depth of sample in well and Rock-Eval bulk data; abbreviations and ratios are explained in Appendix 1.1 black rectangles=cores, hatched rectangles=core chips.....	106
Figure 31c: Biomarker ratios as proxies for clastic and higher plant organic matter input vs. depth in the Greater Red Wash area (map-group 2). Sample depth datum is the top of the Douglas Creek Member (see text); abbreviations and ratios are explained in Appendix 1.1.; black rectangles=cores, hatched rectangles=core chips.....	107
Figure 32: Rock-Eval vs. depth profile for well 23-24 Federal from the Greater Red Wash area. Rocks are from the upper Douglas Creek Member. Legend in Appendix 3.....	108
Figure 33: HTGC analysis of source rocks from cores of the South-central area (map-group 3). Sample depths relative to the 3pt. marker datum Colburn <i>et al.</i> (1985). Sample information includes sample number, depth of sample in well and Rock-Eval data. *=Internal standard C <sub>24</sub> D <sub>50</sub> ; black rectangles=cores.....	112
Figure 34a: Maturity related biomarker indices and principal component 3 vs. depth in the south-central area (map-group 2) of the Uinta Basin. Sample depth datum is the 3pt. marker of Colburn <i>et al.</i> (1985); black rectangles=cores.....	113
Figure 34b: Selected biomarkers and principal components 1 and 2 vs. depth in the south-central area (map-group 3) of the Uinta Basin. Sample depth datum is the 3pt. marker of Colburn <i>et al.</i> (1985); black rectangles=cores.....	114

Figure 34c: Biomarker ratios as proxies for clastic and higher plant organic matter input vs. depth in the south-central area of the Uinta Basin (map-group 3). Sample depth datum is the 3pt. marker of Colburn <i>et al.</i> (1985; see text); ratios are explained in Appendix 1.1.; black rectangles=cores.....	115
Figure 35: Ternary diagrams of crude oil saturated, aromatic and polar fractions in the three different oil types (a) (note axis scales); <i>n</i> -alkanes, aromatics+polars and cyclic & branched fractions of samples separated into map-groups (labels indicate sample numbers) (b). Based on classification suggested by Tissot and Welte (1984) oils are paraffinic and naphthenic crudes.....	119
Figure 36: HTGC of representative samples of oils produced in the Uinta Basin. Chromatogram in (a) is an immature type oil, (b) and (c) are regular type oils and (d) is a waxy (yellow) crude oil sample * =Internal standard C <sub>24</sub> D <sub>50</sub> .....	120
Figure 37: Loadings on principal components PC1 (a), PC2 (b), crude oil GC-MS analysis; m=20, variance-covariance matrix based PCA. Bar labels and numbers on x-axis are the variables and refer to peaks listed in the accompanying table. Only PC1 and PC2 are retained according to the broken-stick model. ....	126
Figure 38: Principal component cross plot PC1 vs. PC2, crude oil GC-MS analysis. PC interpretations are annotated. Samples are separated into map-groups (see text); sample labels for map-groups 5, 7 and 10 were omitted. Areas comprising samples from Wonsits Valley (5), Coyote Basin (6), Walker Hollow (7), Brennan Bottom/Horseshoe Bend (8), and immature type samples are outlined with patterns (numbers in parenthesis are map-group numbers).....	128
Figure 39.1: GC-MS m/z 191 chromatograms of representative crude oil samples from different fields of the Uinta Basin. Immature oil type in (a), samples from the Pariette Bench (map-group 4) in (b), Wonsits Valley (map-group 5) in (c), Coyote Basin (map-group 6) in (d), and Walker Hollow (map-group 7) in (e). Peak labels identified in Appendix 1.2.....	129
Figure 39.2: GC-MS m/z 217 chromatograms of representative crude oil samples from different fields of the Uinta Basin. Immature oil type in (a), samples from the Pariette Bench (map-group 4) in (b), Wonsits Valley (map-group 5) in (c), Coyote Basin (map-group 6) in (d), Walker Hollow and (map-group 7) in (e). Peak labels identified in Appendix 1.2.....	130
Figure 39.3: GC-MS m/z 123 chromatograms of representative crude oil samples from different fields of the Uinta Basin. Immature oil type in (a), samples from the Pariette Bench (map-group 4) in (b), Wonsits Valley (map-group 5) in (c), Coyote Basin (map-group 6) in (d), and Walker Hollow (map-group 7) in (e). Peak labels identified in Appendix 1.2.....	131
Figure 39.4: GC-MS m/z 253 chromatograms of representative crude oil samples from different fields of the Uinta Basin. Immature oil type in (a), samples from the Pariette Bench (map-group 4) in (b), Walker Hollow (map-group 5) in (c), Coyote Basin (map-group 6) in (d), and Wonsits Valley (map-group 7) in (e). Peak labels identified in Appendix 1.2.....	132

Figure 40: Comparison of biomarker ratios of representative samples from map-groups 4-7 (GC-MS chromatograms for the samples are shown in Fig.39.1-4). Sample UB1o is an immature sample from the Cedar Rim area (map-group 1). Numbers in parenthesis in legend are the map-group numbers. Indices are explained in Appendix 1.1; numerical values in Appendix 8.1.....	141
Figure 41: Ternary diagram of sterane distributions in crude oil samples from the Uinta Basin. Samples are separated into map-groups (see text); numbers in legend are the map-groups.....	142
Figure 42: Comparison of the loadings on principal components PC1 and PC2, source rock extract (a) and crude oil (b) GC-MS analysis; m=20, variance-covariance matrix based PCA. Bar labels and numbers on x-axis are the variables and refer to peak numbers listed in Appendix 1.2.....	147
Figure 43: Overlay of PC1 and PC2 cross plots obtained from the PCA of source rock extract and crude oil GC-MS data. This overlay provides a means to quickly compare geochemical compositions for correlation purposes. ....	149
Figure 44a: Examples for PCA based source rock and crude oil correlation. Source rock UB18E (a) was obtained from lower black shale facies/green shale facies sediments in the Altamont-Bluebell area (source rock map-group 1). Crude oil sample UB71o is a representative sample oil for map-group 5 (Wonsits Valley). Peak labels identified in Appendix 1.2.....	151
Figure 44b: Examples for PCA based source rock and crude oil correlation. Source rock UB12E (a) was obtained from basal Green River Formation sediments (lower black shale facies) in the south-central area (source rock map-group 3). Crude oil sample UB67o is a representative sample oil for map-group 7 (Coyote Basin). Peak labels identified in Appendix 1.2.....	152
Figure 45: Conceptual interpretation of migration patterns in the Tertiary petroleum system of the Uinta Basin, based on geochemical analysis of source rocks and oils, and geographic distribution of crude oils. Size of arrows symbolizes quantity of migrating hydrocarbons.....	154

## List of tables

Table 1: Overview of fields in the Uinta Basin from which oil samples were analyzed (for locations see Figure 9 and 10). sdst. = sandstone; ppt. = pour point; Map-group 4A-E are summarized as south-central fields; cum. prod. = cumulative production as of 1998; Utah Division of Energy and Mineral Resources, Oil, Gas and Mining Production Handbook. *1: Montgomery and Morgan, 1998; *2: Clem, 1985; *3: Hill and Bereskin, 1993; *4: Pitman <i>et al.</i> , 1982; *5: Osmond, written communication; *6: CNG Producing Company, written communication; *7: Colburn <i>et al.</i> , 1985; *8: Borer and McPherson, 1996; *9: Castle, 1990; *10: Kelly and Castle, 1990; *11: Osmond, 1992; *12: Morgan <i>et al.</i> , 1998 .....	29
Table 2: List of compounds in branched and cyclic fractions obtained from source rock extracts and crude oils which were used for the principal component analysis with 20 variables (m=20). .....	36
Table 3: Selected averages and ranges for geochemical parameters of source rock extract saturated fractions investigated in this study. Source rocks are separated into groups as described in the text. Abbreviations in Appendix 1.1; n = number of samples.....	44
Table 4: Brief summary of biomarker interpretations described in Chapter 6.1; after Peters and Moldowan (1993), Fu Jiamo <i>et al.</i> (1990) and references listed in the text. ....	48
Table 5: Principal component analysis results (using 96 variables in (a) and 20 variables in (b)), based on the variance-covariance matrix of GC-MS peak-heights obtained from the analysis of the branched and cyclic fractions of source rock extracts. Results of the PCA using a correlation matrix with 20 variables (m=20) are shown in (c).....	65
Table 6: Normalized peak-heights of 20 GC-MS peaks used in the PCA (m=20), source rock extracts; peak (variable) numbers are listed in Appendix 1.2. var = variance; std.dev. = standard deviation. ....	68
Table 7: Correlation coefficient matrix (Pearson's correlation coefficient r) relating source rock principal components and other parameters obtained from GC and Rock-Eval analysis; $r >  0.45 $ highlighted. ....	82
Table 8: Averages and ranges of selected geochemical parameters for waxy, immature, and regular oil types produced in the Uinta Basin (n=number of samples, avg.= average). ....	118
Table 9: Principal component analysis results using 20 variables, based on the variance-covariance matrix of GC-MS peak-heights obtained from the analysis of the saturate fractions of 47 crude oil samples. ....	123
Table 10: Normalized peak-heights of 20 GC-MS peaks used in the PCA (m=20), crude oils; peak (variable) numbers are listed in Appendix 1.2; var = variance, std.dev. = standard deviation. ....	124

Table 11: Comparison of averages and ranges of biomarker ratios and parameters between different map-groups (a) and immature vs. regular type oils (b). Abbreviations and ratio formulas are listed in Appendix 1.1 .....	135
Table 12: Correlation coefficient matrix (Pearson's correlation coefficient r) relating crude oil principal components to other parameters obtained by GC analysis; $r >  0.45 $ are highlighted.....	139

## List of Appendices

Appendix 1.1: Abbreviations and formulas used in the text and appendices.....	A1.1
Appendix 1.2: List of peaks identified in the GC-MS analysis and peak numbers.....	A1.2
Appendix 2: Core description.....	A2
Appendix 3: Core well data and source rock samples.....	A3
Appendix 4.1: Source rock extracts - GC-MS peak heights [response in $\mu$ V] .....	A4.1
Appendix 4.2: PCA results, source rock extract analysis .....	A4.2
Appendix 5: Source rock Extracts - Rock-Eval, GC and GC-MS parameters .....	A5
Appendix 6: Source rock Extracts - High temperature gas chromatograms of outcrop samples and samples from wells outside area with datum control. ....	A6
Appendix 7: Crude oils - Well locations and sample data.....	A7
Appendix 8.1: Crude oils - GC-MS peak heights [response in $\mu$ V].....	A8.1
Appendix 8.2: PCA results, crude oil analysis .....	A8.2
Appendix 9: Crude oils - Fractionation, GC and GC-MS parameters. ....	A9
Appendix 10: Crude oils - High temperature gas chromatograms of Uinta Basin crude oils. ..	A10

## **Abstract**

In this study a number of source rock samples obtained from cores of wells drilled in different parts of the Green River Formation of the Uinta Basin were analyzed in order to characterize the geochemical variations associated with lacustrine organic-rich rocks. The analysis of crude oil samples from various fields in the basin was intended to document whether the variation in source rock geochemistry has a consequence on the composition of the oils produced in the basin and if these variations permit inferences about hydrocarbon generation and migration patterns.

Organic matter composition and biomarker analysis of the source rocks can be related to lake evolution in the Tertiary lacustrine depositional system of the Uinta Basin, Utah. Biomarker data, integrated into a stratigraphic framework, and used as molecular fossils, provided additional information for the identification of changes in the depositional environment through time. A gradual transformation from a freshwater lacustrine system in the lower Green River Formation through a shallow water stage with fluctuating lake water chemistry is manifested in the chemical composition of the organic matter. Lean oil shale deposition also took place in a shallow, anoxic water regime and produced lithologically similar, but geochemically different source rock types than those of the mahogany zone.

Crude oils produced in the basin inherited the stratigraphic signature of source rocks and biomarker distributions which permits detailed correlation to specific source rock sections. Apart from the waxy oils produced in the deepest reservoirs of the basin, 6 additional oil groups have been differentiated. Geographical distribution of oil types and their correlation to the source rocks permit inferences about direction and timing of hydrocarbon migration and trapping. The hydrocarbon kitchen is located in the north central part of the basin, where oils were generated from successively younger source rocks with increasing subsidence and migrated in south easterly

direction into the peripheral fields of the basin. Oils from the stratigraphically oldest source rocks are produced farthest away from the kitchen. Smaller pools in the central part of the basin received charges from distinct local sources, some with contribution from hydrocarbon migrating along the main pathway. Molecular thermal maturity parameters indicate that the peak hydrocarbon generation currently is occurring in the Colton Tongue and stratigraphically equivalent marginal and open lacustrine facies in the north-central part of the basin. Basal Green River Formation source rocks in this area are in the late generation stage. In addition, it is suspected that nearshore open lacustrine source rocks in the south-central part of the basin are in the late early generation to beginning peak generation stage. Source rock samples from the Grater Red Wash area are immature and probably have not contributed significantly to hydrocarbon generation. However, immature oils, possibly generated by other mechanisms than thermal maturation, are related to the oil-shales occurring in this area.

The overall results of the study demonstrate how organic geochemical data, when integrated into a stratigraphic framework, can assist the investigation of different aspects of lacustrine petroleum systems, ranging from hydrocarbon generation and migration patterns to the characterization of lake evolution through time. Relatively simple multivariate statistical evaluation of the source rock extract and crude oil analyses greatly facilitated the interpretation and correlation of the samples.

## 1. Introduction

The alluvial-fluvial-lacustrine depositional system of the Tertiary Green River Formation of Wyoming, Colorado and Utah has been the subject of numerous geological, structural and geochemical investigations since Bradley's pioneering work published by the U.S. Geological Survey (USGS) in 1929 and 1931. The formation is considered a classic example for lacustrine depositional environments and a number of studies describe the stratigraphy, sedimentology and geochemistry in the Uinta Basin (for review see Fouch *et al.*, 1994). Green River oil-shales have been examined extensively and provided the base material for the definition of the classic kerogen type I (Tissot and Welte, 1984). Some of the well established biomarkers such as gammacerane (Hills *et al.*, 1966) and  $\beta$ -carotane (Murphy *et al.*, 1967) were first described from extracts of Green River Formation source rocks. Green River oil-shales have also been a popular material for studies of kerogen composition and structure (Burnham *et al.*, 1982), pyrolysis and maturation research (Sweeney *et al.*, 1987). Most published investigations, however, deal with isolated aspects of the Green River Formation. Observations and subsequent interpretations made in one basin containing the Green River Formation depositional system often are extrapolated to all other basins, disregarding the fact that the formation was deposited in two different lake systems (Lake Gosiute and Lake Uinta), which probably were neither connected for most of their existence, nor entirely contemporaneous.

A number of descriptions and analyses of the Green River Formation in the Uinta Basin have focused on outcrops located in the southwest and southern areas (e.g. Picard *et al.*, 1973), and at Raven Ridge to the northeast (e.g. Koesomatinada, 1970). A relatively smaller number of studies, particularly those involving geochemical investigations, have tried to trace and analyze the sediments in the deep subsurface (e.g. Anders *et al.*, 1992). Source rock analyses often have been confined to the analysis of "oil-shales", most of which came from unspecified locations and

stratigraphic positions. The investigation of core samples by Tissot's *et al.* (1978) and Ruble's (1996) work on outcrop source rocks provide detailed geochemical analyses combined with stratigraphic interpretation. Reed and Henderson (1972) demonstrated the stratigraphic control of crude oil composition based on gas chromatographic analyses. Few other detailed accounts of source rock geochemistry and the relationship to the various crude oils produced in the basin have been published, despite the application of the Uinta Basin as a model for a prolific lacustrine petroleum system (e.g. Powell, 1986). Green River source rocks are considered classic type I kerogen representatives, but it has been established that the Tertiary lacustrine environment underwent significant physical changes during the evolution of the Uinta Basin. These changes affected the biological system, part of which was preserved in the organic-rich sediments.

The present study is an attempt to extend Ruble's (1996) outcrop based documentation of the temporal variations of source rock composition in the Green River Formation into the subsurface of the north-central and eastern part of the Uinta Basin. Core samples from wells drilled in different parts of the basin also provide a lateral component in the investigation of organic facies variations. In contrast to the source rocks, lacustrine crude oils from the Uinta Basin have received considerable less attention. The effect of the environmental variations on the organic matter of the source rocks on the composition of crude oils produced in the basin is virtually unknown. The stratigraphic intervals which have generated the crude oils in the basin have not been documented in detail. In particular, the sources of the crude oils produced in the peripheral fields southeast and south of the Altamont-Bluebell trend have not been unambiguously established.

The investigation presented in the following study may be important for resource estimation in some of the marginal fields of the Uinta Basin, but will not necessarily provide a significant alternative exploration technique for this particular basin. However, if the Uinta Basin is considered an analog for other less well explored petroliferous lacustrine basins, the results will

demonstrate that it is important to consider the potential variability of source rock composition. This variability may have consequences on hydrocarbon geochemistry and needs to be evaluated if geochemistry is to be used for generation, correlation and migration studies. Results based on the relatively simple and structurally undisturbed evolution of the Uinta Basin offer a model for interpreting lacustrine basins that are structurally and stratigraphically more complicated, are transitional with other depositional environments or may have a stratigraphic record of more than one lacustrine phase. The investigation also shows that molecular organic geochemistry has the potential to provide important evidence and parameters for paleoenvironmental characterization, stratigraphy/facies analysis and evaluation of subsurface flow phenomena.

## **2. Purpose of the Study**

Despite the large number of investigations on the Green River Formation source rocks, no comprehensive description, employing modern analytical equipment, is available for different organic facies and genetically related crude oils. This study is intended to provide additional documentation of source rock organic matter variations within the Green River Formation of the Uinta Basin and how these variations relate to changes in lacustrine environmental conditions. It is also intended to demonstrate how integration of geochemical data into a stratigraphic framework can supplement paleoenvironmental analysis.

The detailed analysis of source rock samples within a stratigraphic and sedimentary facies framework and the correlation to a number of crude oil samples from various fields in the basin is supposed to document that geochemical variations in the source rocks may be inherited by the hydrocarbons generated from them. Geochemical characterization of the compositional variations in crude oils is useful for differentiation of oil groups and the assessment of their relationship to specific source intervals within the petroleum system. The geochemical data provide a basis for the

interpretation of hydrocarbon generation, kitchen location and identification of migration patterns in the basin. Interpretations are assisted by relatively simple multivariate statistical processing of the geochemical data. The study will show how statistical evaluation can differentiate genetic groups which are otherwise difficult to distinguish based on traditional qualitative analysis. These techniques provide a simple procedure to visualize and compare source rock and crude oil geochemical data for correlation purposes.

### **3. The Tertiary Uinta Basin**

#### ***3.1 Physical-tectonic Setting***

The Uinta Basin is a structural and topographic trough located in northeast Utah (Figure 1) with a structural axis presently located only a few miles south of the Uinta Mountains range. The steeply south dipping Tertiary strata in the basin at the northern margin and gently north and northeast dipping sections at the southern margin (Figure 2) give the basin the typical asymmetric geometry of Laramide basins in the Rocky Mountain region. The Uinta Basin presently comprises an area of approximately 24,000 km<sup>2</sup> today (Osmond, 1964) and is filled with a section of fluvial-lacustrine sediments estimated to reach a total thickness between 3,600 m (11,811 ft; Franczyk and Pitman, 1989) and 5,500 m (18,045 ft; Picard, 1985). Uppermost Cretaceous to lowermost Tertiary (pre-Lake Uinta) sediments are encountered at depths of about 6,100 m (20,000 ft) in the north-central part of the basin (Fouch *et al.*, 1994). Tertiary lacustrine/fluvial deposits south of the present limit of the Green River Formation were eroded during syn- and post-Laramide uplifts.

Several Laramide and pre-Laramide structural features surrounding the basin (Figure 1) influenced depositional patterns and facies development. The presence of these structural features explains in part the complicated temporal and spatial facies associations, because they provided variable quantities of clastic material either contemporaneously or at different times. The most pronounced structural element is the Uinta Mountain range to the north, a basement cored, fault bounded uplift, which was formed by two distinct uplift pulses during the Laramide orogeny (Bradley, 1995). The Uinta Basin boundary thrust fault separates the Uinta Basin section from the northern Mesozoic and Paleozoic rocks, and southerly directed thrusting along this fault line caused the pronounced asymmetry of the Uinta Basin sedimentary fill. The Wasatch Plateau/Sevier orogenic belt marks the western boundary of the basin. Its tectonic activity is distinguished by thin skinned thrusting, predating Laramide deformation (Dickinson *et al.*, 1988). Sevier and Laramide

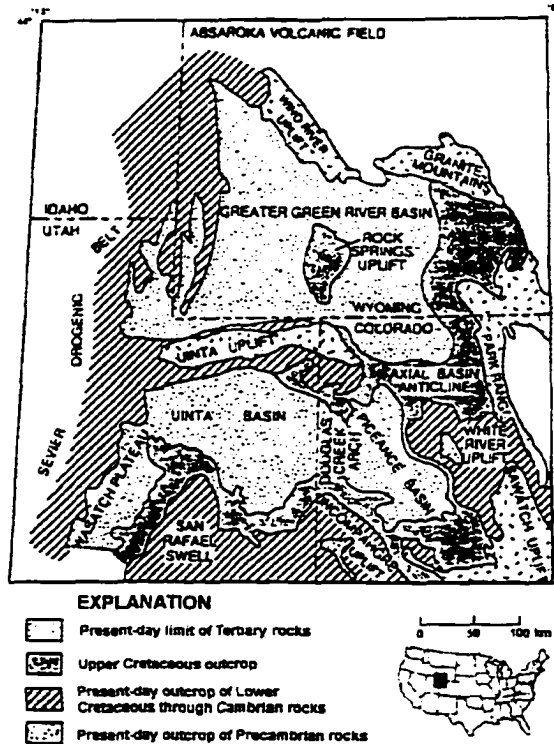


**Figure 1:** Location of the Uinta Basin and extent of the Green River Formation in Laramide basins of Wyoming, Utah and Colorado (adapted from Tuttle, 1991). The figure also indicates the structural elements surrounding the Uinta Basin.

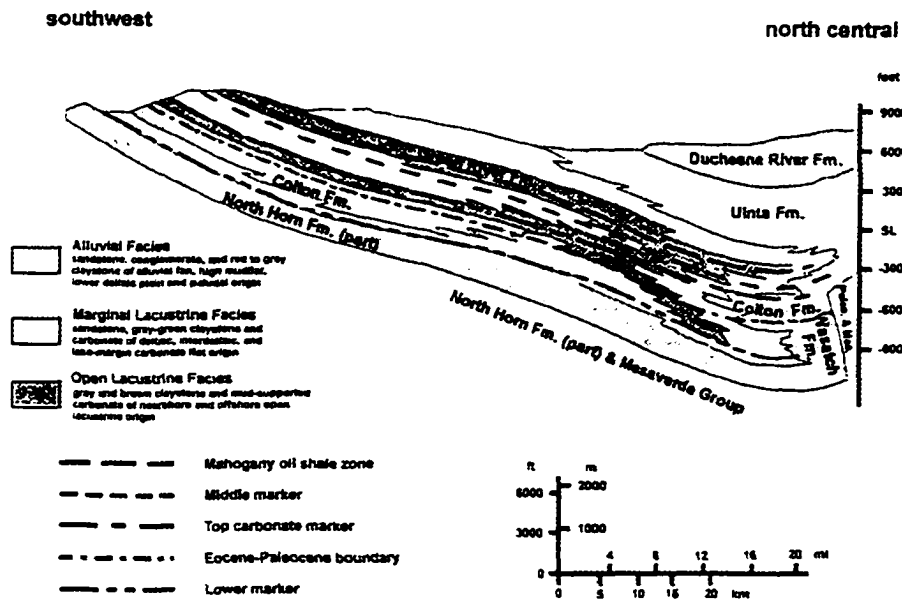


**Figure 2:** Schematic cross-section through the Uinta Basin (adapted from Fouch, 1975) showing the asymmetric structure, formations and lithofacies of the Tertiary sediments. Prominent subsurface markers used for correlation in the basin are also indicated.

orogenic activity is partly contemporaneous in the area (Johnson, 1992). The Uinta Basin was formed after the late Maastrichtian and during the transition of the interior Rocky Mountain region from a Sevier foreland basin into an area characterized by segmentation through numerous continental Laramide basins and uplifts (Johnson, 1988). Epirogenic movements and sediment supply on the southern margin were controlled by the San Juan and Uncompahgre uplifts. The Douglas Creek Arch, which connects the Uinta Mountains with the Uncompahgre Uplift, forms the eastern boundary of the Uinta Basin and was an effective barrier separating the Uinta Basin from the Piceance Creek Basin to the east during the Paleocene and Early to Middle Eocene (Moncure and Surdam, 1980). According to Johnson and Finn (1976), the Douglas Creek Arch, unlike the other Laramide structures surrounding the Uinta Basin, has never been a major topographic feature.

The Uinta Basin is only one of several basins containing sediments of the Green River Formation depositional system. The regional distribution of the formation in Wyoming, Colorado and Utah records the deposition in Lake Gosiute located north of the Uinta Mountains, and Lake Uinta south of the mountains which covered the Uinta and the Piceance Creek Basins (Figure 1). The illustration in Figure 3 is an interpretation of the extent of the lakes at maximum highstands during the Middle Eocene. The Uinta Basin is the only basin in which the Green River Formation is petroliferous and contains both source rocks and reservoirs, thereby forming an individual petroleum system (Fouch *et al.*, 1994).

### **3.2 Lacustrine facies**

The confusing array of local stratigraphic terms used in the Uinta Basin prompted Ryder *et al.* (1976) to propose a facies model for the subdivision of the Green River and Colton/Wasatch Formations. Using this facies model, the sedimentary succession can be interpreted based on three

associated facies belts illustrated schematically in Figure 4:

1. open lacustrine facies.
2. marginal lacustrine facies.
3. alluvial facies.

The distal open lacustrine facies is characterized by predominately dark (gray-brown to black) mud-supported carbonates and calcareous claystones/shales, local sand-/siltstones and carbonate packstones. This facies is associated with the bulk of organic-rich source rocks including the oil-shales. Ryder *et al.* (1976) and Wiggins and Harris (1994) differentiated a nearshore and an offshore open lacustrine facies. The latter is distinguished by the distinct lamination bedding and lack of (macro-) fossils. The former is characterized by the absence of lamination and the presence of locally abundant ostracodes, bivalve and gastropod shells.

The marginal lacustrine facies contains fluvial, carbonate flat, deltaic, and interdeltaic sediments, characterized by light gray to brown colors, an important property in distinguishing facies in outcrop and cores. Lithofacies include mud- and grain-supported carbonates, stromatolite boundstones, calcareous claystone/shales and locally channelform sandstones. Paludal coals may form viable source rocks within these facies (Fouch and Hanley, 1977; Franczyk and Pitman, 1989; Ruble, 1996) but in general marginal lacustrine sediments are the reservoirs in the basin (Fouch *et al.*, 1994). In addition to the marginal lacustrine sub-environments mentioned above, shoreline facies (Borer and McPherson, 1996) and offshore sandbars (Castle, 1990) have been identified.

The alluvial facies is divided into lower deltaic plain, high mudflat and alluvial fan environments. Channelform sandstones deposited from braided and meandering streams distinguish the upper deltaic plain and are characteristically associated with non-calcareous red claystone and siltstone units, which show abundant desiccation cracks or other exposure features. These

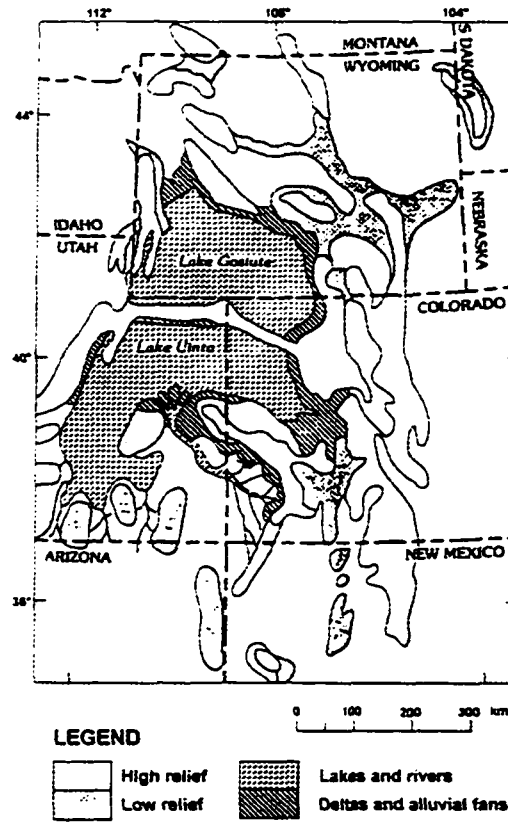


**Figure 3:** Location and extent of Lake Gosiute and Lake Uinta during the Middle Eocene (modified from Remy, 1992). Note that in this interpretation no hydrological connection exists between Lake Uinta and Lake Gosiute.

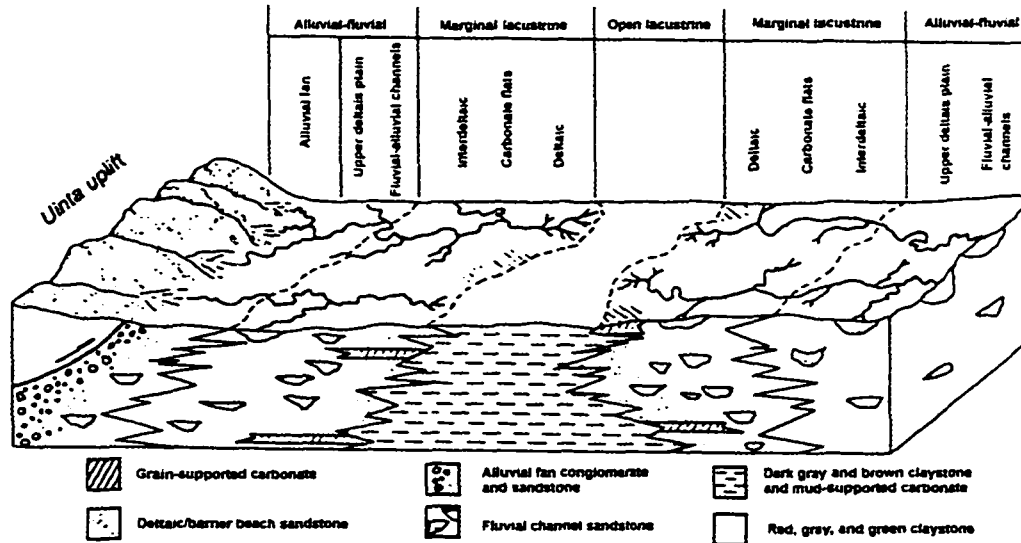


**Figure 4:** Lacustrine facies model showing Ryder's *et al.* (1976) tripartitioned facies belts in Lake Uinta.

sediments originated in floodplain and/or periodically flooded high mudflat environments. Coarse grained clastics and conglomerates characterize the alluvial fans.

In map-view the facies belts more or less show a characteristic concentric arrangement in the basin. However, along the relatively steep northern margin, the thrusting associated with the Uinta Mountain uplift and the proximity of the uplift to the basin center render the facies belts relatively narrow (Figure 5). This is contrasted by the laterally extensive facies belts on the southern margin. The maps reproduced in Figure 5 indicate the lateral facies variations and superposition of facies during the Paleocene-Eocene to middle marker times. Particularly remarkable is the extent of the open lacustrine facies during the first major lake expansion associated with deposition of the black shale facies (Fig.5c) and subsequent development of a broad marginal lacustrine facies belt in the southern and southeastern part of the basin (Fouch, 1975; Fig.5d). Not shown here is the second major expansion of open lacustrine facies during the deposition of the mahogany zone (see Ryder *et al.*, 1976).

The lacustrine sediments in the Uinta Basin are petrographically complex sections containing mixed siliciclastic-carbonate lithology (Ryder *et al.*, 1976) and rapid alternations of siliciclastics and carbonates. These types of lithologies were deposited simultaneously in different locations within the basin. The frequently employed term marlstone appears to have been used for sediments in the basin which are otherwise difficult to classify (Picard, 1953). Wiggins and Harris (1994) relate clastic vs. carbonate dominated deposition in the lower Green River Formation to changes in climate. They developed a wet climate model (high fluvial discharge) for predominately clastic deposition and a dry-climate model (low fluvial discharge) for dominantly carbonate sedimentation.

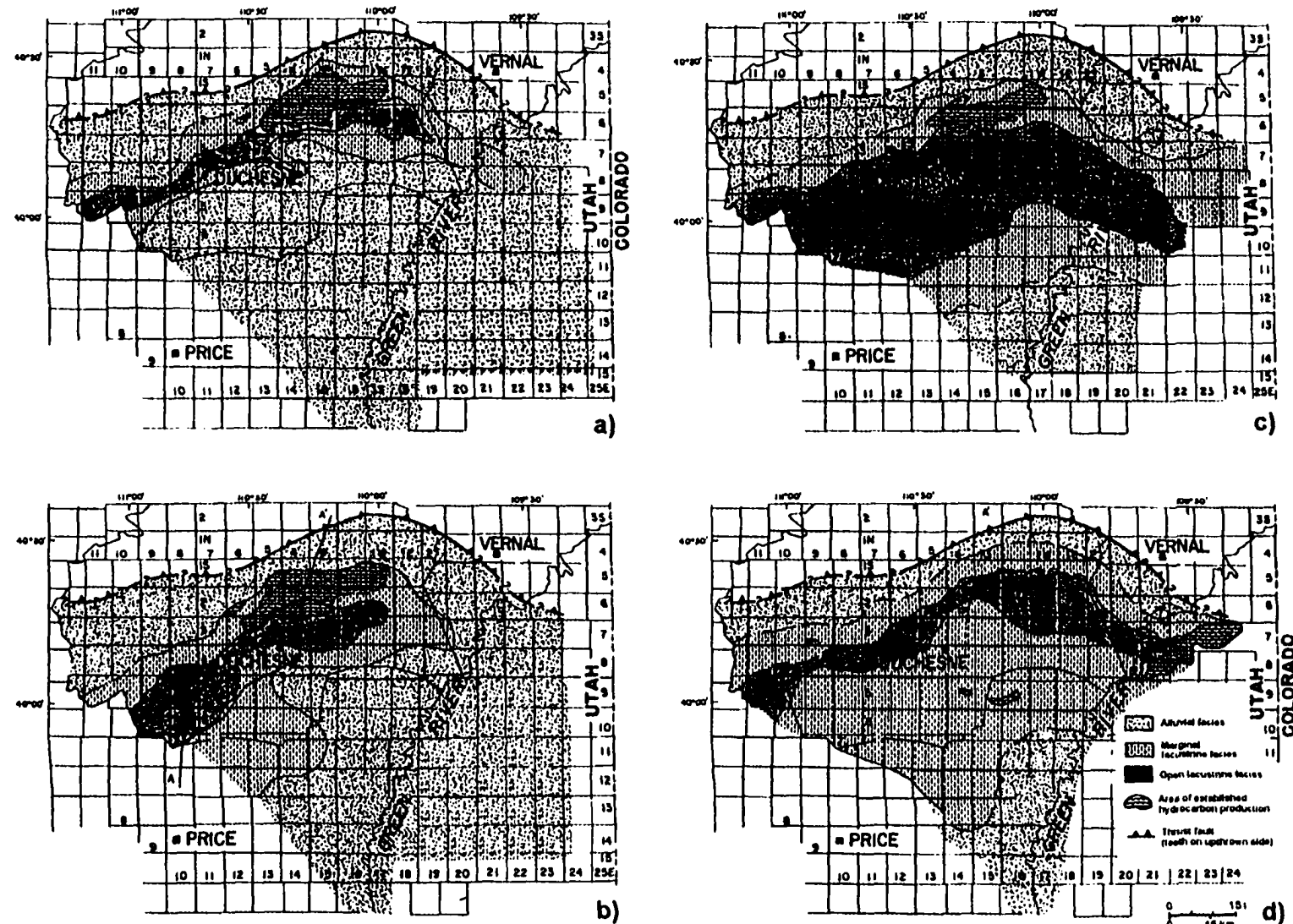


**Figure 5:** Generalized lithofacies maps for (a) the Eocene-Paleocene boundary, (b) units deposited midway between carbonate marker and Paleocene-Eocene boundary, (c) strata equivalent to the carbonate marker and (d) the middle marker time (modified from Fouch, 1975).

### **3.3 Tertiary Stratigraphy and Evolution of the Uinta Basin**

A comprehensive summary of the geological evolution of the Uinta Basin during the Paleogene is shown in Figure 6 and will be briefly explained in the following sections. The stratigraphic terms were adopted from Ryder *et al.* (1976) and are incorporated in Figure 6 to provide a simplified but consistent overview of the nomenclature, association and temporal relation of facies, differences between the southern and northern/northeastern part of the basin, geological time, major expansion and contraction of the lake system, and climate. A generalized cross section from the southwestern to the northern margin, illustrating the structural asymmetry of the basin. Succession of the formations, and lithofacies association is shown in Figure 2. A detailed review of the stratigraphic and stratigraphic nomenclature can be found in Ruble (1996) and Ruble and Philp (1998).

The “basement” of the Tertiary alluvial to lacustrine section deposited in and around Lake Uinta consists of the North Horn Formation which recorded the last step of the transition between marine - marginal marine - continental deposition during the Cretaceous - Paleocene after the complete retreat of the Cretaceous Interior Seaway from the area (Franczyk *et al.*, 1992). The Flagstaff Limestone records the earliest lacustrine sediments in the basin deposited in Lake Flagstaff, which in part can be considered the Paleocene precursor of Lake Uinta (Johnson, 1985). Stanley and Collison (1979) documented the extent of Lake Flagstaff which occupied much of central Utah and expanded into the central Uinta Basin during the Paleocene. In the western and central Uinta Basin the Flagstaff and Green River Formation form a continuous lacustrine section, prompting Fouch (1976) to include the Flagstaff Limestone as a member of the Green River Formation. The eastern part of the Uinta Basin was dominated by fluvial and alluvial processes during the Paleocene-Early Eocene.

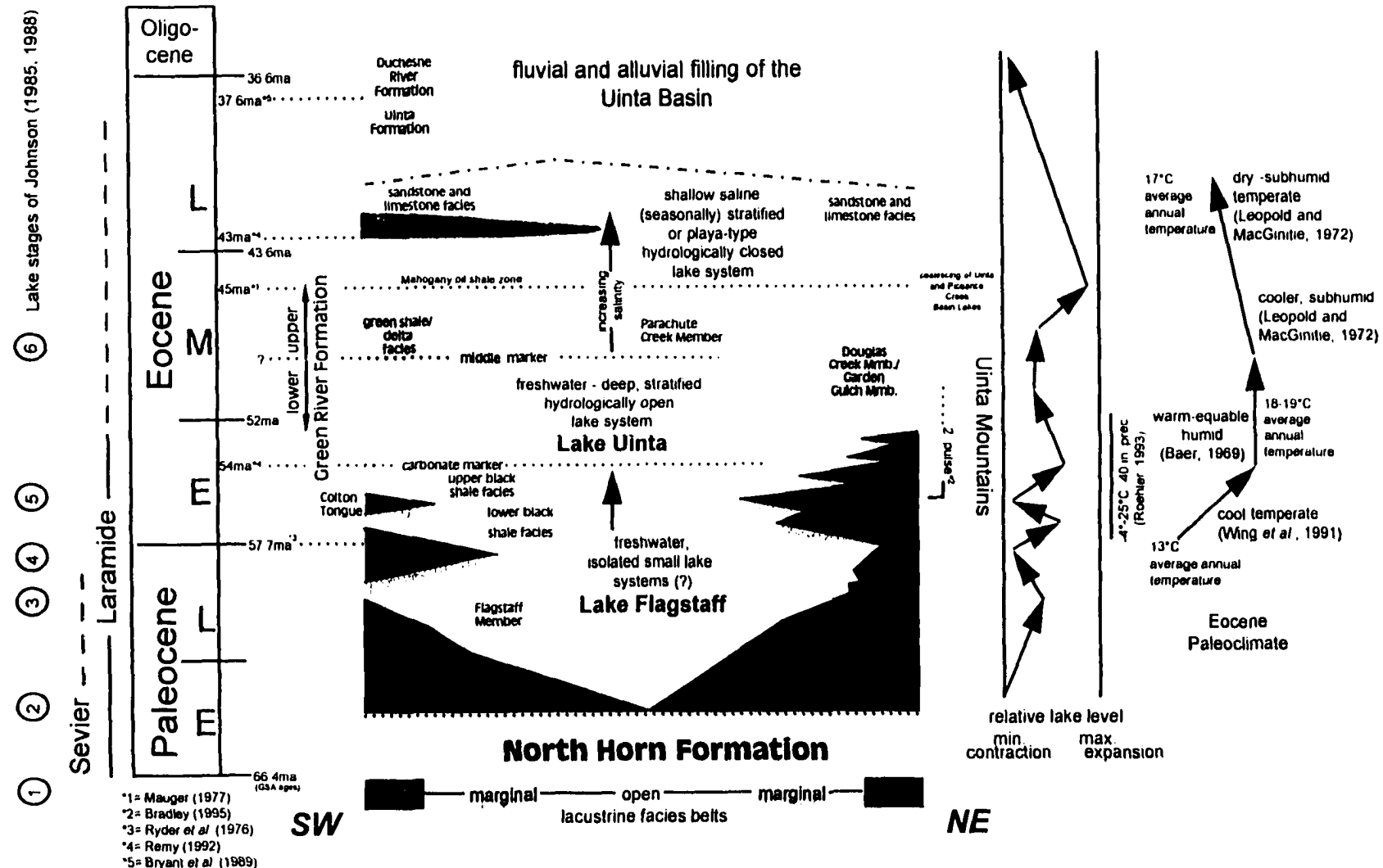


**Figure 6:** Generalized and simplified development of the Lake Uinta depositional system in the Uinta Basin. Note that the figure includes faciesbelts, the facies succession and stratigraphic terminology. Lake level fluctuations and climate changes are schematic and indicate only major changes in lake extent and ambient conditions in the area of the Green River Formation depositional system.

A thick clastic wedge separates the Flagstaff Member from the overlying section of the Green River Formation in the southern part of the basin. According to Ryder *et al.* (1976) the Paleocene-Eocene boundary falls within the upper 1/3 of this unit. This alluvial/fluvial wedge is apparently only partly contemporaneous with a similar clastic wedge on the northern margin of the basin, which records a period of major uplift in the Uinta Mountains. Both of these wedges are termed Colton Formation, which Fouch (1976) defines as alluvial-fluvial sediments separated by the Flagstaff Member from the underlying North Horn Formation. In the northernmost part of the basin close to the Uinta Mountains a continuous alluvial-fluvial section developed which is termed the Wasatch Formation.

A major expansion of Lake Uinta is recorded by the deposition of the marginal and predominately open lacustrine black shale facies (Picard, 1955) during the Early Eocene. On the southern margin this section is separated by the alluvial-fluvial Tongue of the Wasatch, which splits the black shale facies section into an upper and lower unit (Abott, 1957). The black shale facies is similarly separated into a lower and upper unit by a thick Colton sequence in the northern part of the basin (see also cross-section in Figure 2). The top of the black shale facies unit is formed by the carbonate marker (Ruble, 1996), a continuous carbonate horizon signaling a first major expansion of Lake Uinta based on facies maps published by Fouch (1975; Figure 5c). The overlying and partly contemporaneous extensive marginal lacustrine sediments in the southwestern part of the basin have been termed green shale facies (Picard, 1957) or delta facies (Bradley, 1931). They comprise deposits of a large deltaic system dominating sedimentation in the area (compare areas of deltas and alluvial fans at the southern margin of Lake Uinta in Figure 3). Remy (1992) interprets the increasing amount of oil-shales and carbonaceous mudstones in the upper parts of this unit as indicators for a gradual expansion of the lake. Johnson (1989) named the oil-shale zones below the mahogany zone R4-6 and correlated them in the basin. Towards the basin

center the green shale facies merges with open lacustrine sediments of the upper black shale facies and Parachute Creek member (Ruble, 1996). Marginal lacustrine strata in the east and northeast parts of the basin include the Douglas Creek and Garden Gulch members of Bradley (1931) which were later summarized into Douglas Creek Member by Picard (1957). These units occupied large parts of the basin after the first major expansion of the lake and formed a broad facies belt on the southern margin (Figure 5d). A prominent subsurface marker called middle marker within or at the base of these units separates calcareous claystones from the underlying mud-supported carbonates (Fouch, 1975). In this study, the middle marker is also used to informally subdivide the Green River Formation into an upper and lower unit (Figure 6).

Another major expansive stage of the Lake Uinta began during the early Middle Eocene after deposition of the green shale and stratigraphically equivalent strata. This expansion culminated in the transgression of the lake over the Douglas Creek Arch and the connection of the Piceance Creek and Uinta Basins. Johnson (1985) argued for possible intermittent hydrological connection between the Uinta Basin and Piceance Creek Basins beginning in the late Paleocene, but significant differences in oil-shale composition and evaporite mineral occurrence point to a physical separation of the basins up to this point. The mahogany oil-shales mark the maximum highstand of the lake (Franczyk and Pitman, 1989; Fig.3) and provide an important stratigraphic marker in the basins (Fouch and Cashion, 1979). Tuff horizons in the Parachute Creek Member below the mahogany zone record the volcanic activity in the Absaroka volcanic complex in Wyoming (Surdam and Stanley, 1980). Radiometric dating of tuff horizons intercalated into the mahogany zone suggest an approximate age of 45 ma (Mauger, 1977). The top of the Parachute Creek Member indicates the end of the major phase of open lacustrine deposition during the Late Eocene in the Uinta Basin.

The saline facies, included within the Green River Formation according to Dyni *et al.* (1985), records a regressive phase of Lake Uinta and the retreat of the lake into the north-central areas. This unit represents the final lacustrine stage involving oil-shale deposition in Lake Uinta. Saline minerals (Dyni *et al.*, 1985) are evidence for hypersaline conditions of the lake water at this stage. Marginal lacustrine equivalents and overlying units are included into the sandstone and limestone facies of the Green River Formation (Dane, 1954). Alluvial and fluvial sediments of the Uinta and Duchesne River Formations represent the filling of the Uinta Basin after cessation of lacustrine deposition approximately in the latest Eocene to Early Oligocene.

### **3.4 Lacustrine Environments of Lake Uinta**

Paleontological evidence (LaRoque, 1960) indicates that Lake Uinta and its precursor Lake Flagstaff developed as a hydrologically open (water inflow  $\geq$  evaporation) system (Johnson, 1985) during the late Paleocene to Early Eocene, possibly with alkaline water (Franczyk *et al.*, 1992) from which gypsum precipitated (Ryder *et al.*, 1976). During the Middle Eocene the water apparently became more saline, although, unlike in other Green River Formation basins, no record of evaporite mineral deposition has been reported (Tuttle, 1991). Immediately before the deposition of the mahogany oil-shales a change of lake water chemistry and an increase in salinity is evidenced by the deposition of saline minerals such as nahcolite (Johnson, 1985). The modifications in lake water chemistry signal the change in hydrological conditions during the late Early to Middle Eocene from an open to a closed lake system in which evaporation exceeded water supply. It is unclear, however, exactly when these conditions changed, how fast they changed and whether there was a fluctuation between fresh-brackish-saline stages of the lake.

The deposition of oil-shale in the Green River Formation has been alternatively explained based on the playa lake and meromictic deep lake models. The stratified lake model invokes a deep

perennial lake containing a stratified water column and a lower anaerobic hypolimnion (monimolimnion). Bradley (1931) originally interpreted the Green River Formation as a deposit of a deep stratified lake. In contrast, the playa lake model involves a shallow, ephemeral, hypersaline lake, surrounded by an extensive playa mudflat complex. The playa lake model of Eugster and Surdam (1973) was developed from investigations of the Wilkins Peak Member of the Green River Formation in the Green River Basin of Wyoming. Later, the model was applied to the interpretation of the Tipton Member (Surdam and Wolfbauer, 1975) and the Laney Member (Wolfbauer and Surdam, 1975; Surdam and Stanley, 1979) within this basin. It has also been used to explain Green River Formation depositional environments in the Piceance Creek Basin (Lundell and Surdam, 1975) and Fossil Lake Basin (Buchheim, 1994), and subsequently has become a general depositional model for the Green River Formation. Other authors (Desborough, 1978; Boyer, 1982; Johnson, 1981) rejected the model and reinterpreted the formation as a deep, stratified lake deposit. Picard (1985) summarized arguments and interpretations for the formation of oil-shales in the various basins of the Green River Formation. The questionable connection and correlation of Lake Uinta and Lake Gosiute, different hydrological conditions through time, and varying basin subsidence histories (*e.g.* Johnson and Finn, 1976) cast considerable doubt upon the scientific basis on the application of a model developed in one basin to explain depositional environments in other basins.

The above discussion evolved mostly around the origin and genesis of dolomite in the oil-shales, their sedimentary structures (*e.g.* lamination *vs.* mudcracks as evidence for subaerial exposure), facies association and the presence of evaporite minerals. The models were therefore developed strictly for sections of the basins which contain oil-shales (*i.e.* laminated organic-rich rocks yielding hydrocarbons (3 gal/t rock (Brobst and Tucker, 1973) to 15 gal/t (Ryder *et al.*, 1976)) upon pyrolysis (500°C) and/or evaporites, thus not necessarily include the early lacustrine

stage (late Paleocene to early Middle Eocene) in the Uinta Basin. The playa lake vs. deep meromictic lake model discussion is therefore restricted to the upper part of the Green River Formation in the Uinta Basin. It is noteworthy, though, that the term oil-shale has a rather universal meaning in the Green River Basins and it appears that any rock containing sufficient organic matter to give it a dark color is called oil-shale.

In contrast to the Greater Green River and Piceance Creek Basin fewer interpretations of the Green River depositional environments and the limnological characteristics through time are available for the Uinta Basin (*e.g.* Katz, 1995). Lake Uinta is interpreted as a relatively deep, permanently stratified or meromictic, perennial lake from Paleocene (Lake Flagstaff) to early middle Eocene (Ryder *et al.*, 1976, Stanley and Collinson, 1979; Powell, 1986). Johnson (1985) believes that similar limnological conditions existed during the Middle Eocene until the end of lacustrine deposition. However, according to Ryder *et al.* (1976), Lake Uinta became hypersaline after deposition of the richest oil-shales (*i.e.* the mahogany zone) and the playa lake model may explain the sedimentology of the upper part of the Green River Formation above the middle marker. Johnson (1985) places the beginning of saline Lake Uinta (his stage 6; Figure 6) in the early Middle Eocene, an interpretation supported by Tuttle (1991), who described the lake conditions as saline enough to kill off freshwater fauna but not to deposit evaporite minerals. No doubt exists about the final hypersaline stage of Lake Uinta in which bedded halite and associated evaporite minerals were directly precipitated from lake brines (Dyni *et al.*, 1985).

It is well established that lakes, unlike marine systems, are strongly influenced by climatic factors and respond rapidly to environmental changes (*e.g.* Glenn and Kelts, 1991). Therefore, paleoclimatic information has been included on Figure 6, to show the relationship between stratigraphy/facies and climate in the region. Most data have been derived from research done in the Greater Green River Basin (Leopold and McGinitie, 1972; Roehler, 1993), Bighorn Basin

(Wing *et al.*, 1991), and interpretations based on paleoecological work on sediments of the Uinta Basin by MacGinitie (1969) and Baer (1969). The Eocene was the warmest interval of the Cenozoic and generally represents a period of extreme planetary warmth (Barron and Moore, 1994). A rather radical change in climate occurred at the Paleocene-Eocene boundary in the low latitude setting of the area. Average annual temperatures of 18°-19°C and a warm-humid, equable climate allowed a diverse assemblage of fauna and flora to flourish during the deposition of the Lower Green River Formation in Lake Uinta. Average annual temperatures fell during the middle Eocene and according to MacGinitie (1969), in the Middle Eocene the climate had marked seasonal changes with frost-free winters until dry-subhumid and temperate conditions prevailed at the end of the Middle Eocene.

### ***3.5 The Green River Petroleum System***

The Uinta Basin accommodates a significant petroleum system in the Green River Formation in contrast to related basins of the Green River Formation depositional system in Wyoming and Colorado and contains one of the world's largest nonmarine petroleum accumulations (Kelly and Caste, 1990). A second petroleum system, which comprises thermogenic non-associated gases (Group A gases of Rice *et al.*, 1992) generated from the Cretaceous Mancos Formation and produced from tight Wasatch/Colton reservoirs will not be considered here. Cumulative crude oil production in the Uinta Basin (Duchesne and Uintah counties) was 467 Mbbl in 1998 (Utah Division of Mineral and Energy Resources; Oil, Gas and Mining Production Book, 1998).

The general scheme of the Green River petroleum system in which hydrocarbons are being generated from open lacustrine facies in the deep north-central part of the basin was summarized by Fouch *et al.* (1994; see Figure 7). The hydrocarbons partly fill fractured and matrix-porosity

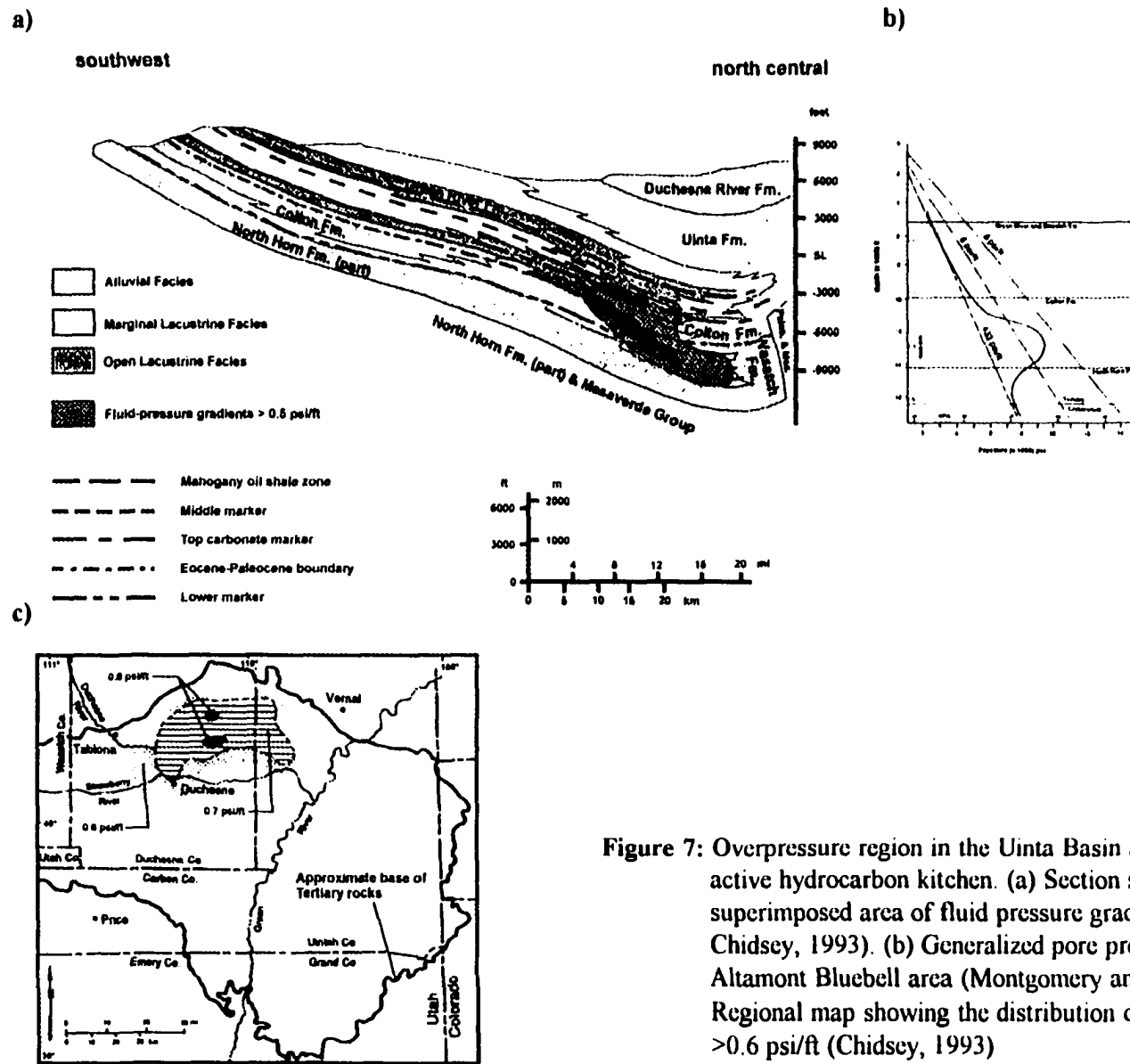


**Figure 7:** Overpressure region in the Uinta Basin assumed to coincide with an active hydrocarbon kitchen. (a) Section shown also in Figure 2 with superimposed area of fluid pressure gradients  $> 0.5 \text{ psi/ft}$  (after Chidsey, 1993). (b) Generalized pore pressure vs. depth for the Altamont Bluebell area (Montgomery and Morgan, 1998). (c) Regional map showing the distribution of fluid pressure gradients  $> 0.6 \text{ psi/ft}$  (Chidsey, 1993)

reservoirs adjacent to the source rocks or migrate laterally through fractures and porous strata into mostly channelform, lenticular sandstone reservoirs. These reservoirs are mostly marginal lacustrine sediments located in the peripheral eastern and southern parts of the basin. The importance of fracturing is minor in these areas and no major faulting (except the Duchesne fault zone; Hintze, 1981) has been reported from the areas south of the Uinta Mountain thrust fault zone. Stratigraphic pinchouts against impermeable alluvial facies form the hydrocarbon traps. Economically most important are the deep fractured reservoirs and reservoirs in open lacustrine facies (e.g. turbidites) of the Altamont-Bluebell area (Fouch *et al.*, 1994). In addition, offshore sandbars (Castle, 1990) and shoreline deposits in the Greater Red Wash area (Borer and McPherson, 1996) have been described. Fouch *et al.* (1992) distinguished two groups of reservoirs containing oil and associated gas (Group B gases of Rice *et al.*, 1992). Group I reservoirs are overpressured, low permeability, fractured deep reservoirs below 10,000 ft (3,048 m) in the lower Green River Formation of the Altamont-Bluebell field. Fractures and overpressure control the production in these reservoirs (Montgomery and Morgan, 1998). Group II reservoirs, characterized by high matrix porosities and normal pressures, are encountered in the eastern and southern peripheral fields (e.g. Greater Red Wash area, Pariette Bench) and in shallow Altamont-Bluebell reservoirs at depths < 9,500 ft (2,896 m).

Petroleum source rocks are assumed to occur mostly in open lacustrine facies (Fouch, 1975), are TOC- and hydrogen-rich, and contain predominately type I kerogen. The organic matter consists mainly of lipid-rich algal and bacterial organic matter in various proportions (Tissot *et al.*, 1978). Maximum TOC values of 33% and oil-shale hydrogen indices exceeding 1,000 mg HC/g TOC have been reported (Katz, 1995). Additional proposed source rock facies comprise hydrogen-rich paludal and algal coals particularly in the lower Green River Formation (Fouch and Hanley, 1977; Ruble, 1996). The composition of the organic matter appears to generally change to more

hydrogen-rich and less reworked material in the upper Green River Formation (Tissot *et al.*, 1978; Katz, 1995).

Despite a number of investigations the depth, extent, and timing of oil-generation in the basin is rather speculative. Anders and Gerrild (1984) suggested a depth of 8,500-12,500 ft (2,590-3,810 m) as the depth of the principal zone of hydrocarbon generation. Powell (1986) estimates a depth of 3,900-4,500 m (12,795-14,764 ft) for the onset of extensive hydrocarbon generation, with the peak and base of generation occurring at 5,500 m and 5,800 m (18,045-19,029 ft), respectively. Thermal modeling by Fouch *et al.* (1994) suggests that gas is currently generated at depths >3,050 m (10,000 ft) and that generation began in the lower Green River Formation some 40 ma ago. According to their model the productive zone coincides with the zone of overpressuring (Figure 7) which is believed to be caused by active hydrocarbon generation (Spencer, 1987; Bredehoeft *et al.*, 1994). However, hydrocarbon generation is still considered an unproven explanation for overpressure (Osborne and Swabrick, 1997). Tissot *et al.* (1978) suggested a deeper oil-generation window (13,000-18,500 ft (3,962-5,693 m)) due to the high generation threshold ( $R_o \approx 0.7\%$ ) of lipid-rich organic matter with low heteroatom content. Ruble (1996) in his recent kinetic model, indicates that only the black shale facies and Flagstaff Member could have attained a maturity level for significant hydrocarbon generation, rendering these units the most likely hydrocarbon source. Shallow immature oils in Ruble's (1996) model are being expelled as a bitumen from upper Green River Formation oil-shales.

After generation and expulsion it is assumed that hydrocarbons migrated south- and eastward into the reservoirs of the marginal fields in the basin (Anders *et al.*, 1992). Based on investigations in the Red Wash area (Kelly and Castle, 1990; Rice *et al.*, 1992), Pariette Bench (Pitman *et al.*, 1982) and other peripheral fields (Anders *et al.*, 1992) it is speculated that hydrocarbon generating source rocks are present in stratigraphically equivalent (Middle Eocene)

open lacustrine units in the deeper north-central part of the basin. These interpretations demonstrated that the oils in the reservoirs are relatively mature compared to the maturity of organic-rich sediments associated with the reservoir rocks (see also Anders *et al.*, 1992). The migration models proposed comprise expulsion and migration of the generally very waxy hydrocarbons through fracture networks in the deep central core of the basin. Hydrodynamic and buoyancy driven flow caused oil migration to the east and south through permeable carrier beds into the peripheral reservoirs of the basin (e.g. Bredehoeft *et al.*, 1994).

Ruble (1996) distinguished three crude oil types occurring in the Altamont-Bluebell area:

1. black, viscous and immature aromatic types of oils produced from shallow reservoirs;
2. black, solid (at standard temperatures and pressures (STP)) paraffinic crudes from reservoirs >8,500 ft (2,951 m);
3. yellow-brown solid (at STP) paraffinic crude oils from the deepest reservoirs (>10,000 ft).

Based on hydrous pyrolysis experiments, Ruble (1996) interpreted the mahogany type oil-shales as the source for type 1 oils and the black shale facies as the source for oil types 2 and 3. Montgomery and Morgan (1998) similarly reported the occurrence of yellow waxes in the Flagstaff and Colton members and black waxes in the overlying lower Green River Formation. The API gravity for the oils is reportedly between 25-54°, with most oils falling into the 31-34° range. Boiling points vary between about 60-140°F (compare Table 1).

Ruble (1996) noted a stratigraphic control on oil composition which was reported earlier by Reed and Henderson (1972). In the latter study high geochemical variability and strong stratigraphic signatures in the composition of oils from several fields in the basin were reported based on gas chromatographic analysis of whole oils, indicating that distinct sources for individual fields may be present. Bass (1964) also detected significant differences in bulk oil composition based on gravity and boiling points.

## **4. Samples**

### **4.1 Source rock samples**

Source rock samples of wells drilled in different parts of the basin (Figure 8) were obtained from cores stored in the core libraries of the US Geological Survey (USGS) in Lakewood, Colorado, and the Utah Geological Survey (UGS) in Salt Lake City, Utah. Core analysis and sampling, field investigation and outcrop sampling were completed during two field seasons. Cores were separated into map-groups based on well locations (Figure 8). The core samples analyzed were identified as follows: UB for Uinta Basin, sample number and capital E for extract (e.g. UB1E).

Selection of source rock samples taken from the cores after core analysis was based on color, lithology and facies association. Detailed core descriptions are given in Appendix 3. Outcrop samples collected from known stratigraphic positions were included as reference samples. Prior to sample processing and chemical analysis fresh center portions of the core samples were cut or broken off, and sample surfaces cleaned. The core fragments were subsequently crushed and powdered in a shatterbox (SPEX Industries, 2 min. at ca. 900 rpm) to a grainsize of 200 mesh. The shatterbox metal grinding container was cleaned with soap and water, and rinsed with distilled water and acetone after each sample to avoid cross-contamination.

### **4.2 Oil samples**

The Geochemistry Department of the USGS made available a collection of oil samples and donated aliquots to this study. The sample set covers most of the larger fields and a number of smaller, peripheral fields from the south-central and southeastern part of the basin. A schematic overview of the oil field locations is given in Figure 9. The location of oil producing wells from which samples were obtained are shown in Figure 10. For further reference, oil samples were

separated into 9 map-groups depending on field location (see also Table 1). Map-groups 5 to 7 are sometimes referred to as Greater Red Wash area. Well and sample data were taken from the USGS and/or the Petroleum Institute database. All relevant well information is listed in Appendix 2, field and reservoir data are summarized in Table 1. Samples were identified as follows: UB for Uinta Basin, sample number and small letter o for oil sample (*e.g.* UB1o).

---

**Captions (next 4 pages):**

**Figure 8:** Location of source rock samples obtained from cored wells drilled in the Uinta Basin. Map-groups refer to samples grouped together depending on well location.

**Figure 9:** Location of the Uinta Basin oil and gas fields from which samples have been investigated for this study. The map has been adapted from the Utah Geological Survey Map 68 (1982) and most fields have been extended since publication. Stippled pattern are oil fields, hatched pattern are gas fields

**Figure 10:** Location of oil samples obtained from various fields (see Figure 9) of the Uinta Basin. Map-groups refer to samples grouped together based on well location.

**Table 1:** Overview of fields in the Uinta Basin from which oil samples were analyzed (for locations see Figure 9 and 10).

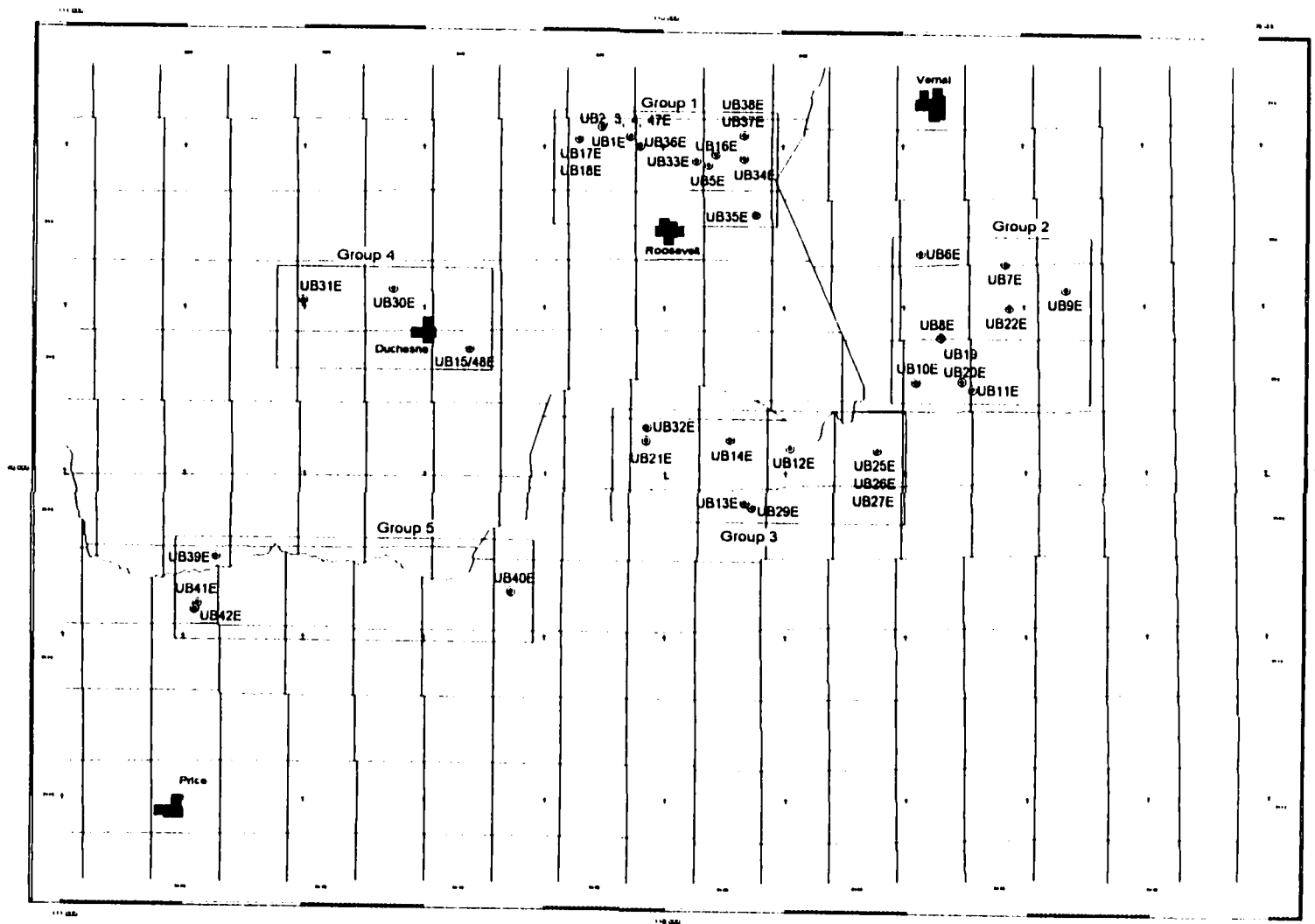
sdst. = sandstone;

ppt. = pour point;

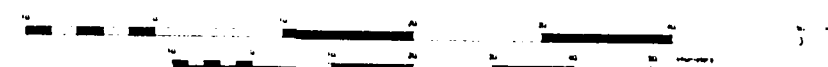
Map-group 4A-E are summarized as south-central fields;

cum. prod. = cumulative production as of 1998; Utah Division of Energy and Mineral Resources, Oil, Gas and Mining Production Handbook.

\*1: Montgomery and Morgan, 1998; \*2: Clem, 1985; \*3: Hill and Bereskin, 1993; \*4: Pitman *et al.*, 1982; \*5: Osmond, written communication; \*6: CNG Producing Company, written communication; \*7: Colburn *et al.*, 1985; \*8: Borer and McPherson, 1996; \*9: Castle, 1990; \*10: Kelly and Castle, 1990; \*11: Osmond, 1992; \*12: Morgan *et al.*, 1998



**Figure 8**



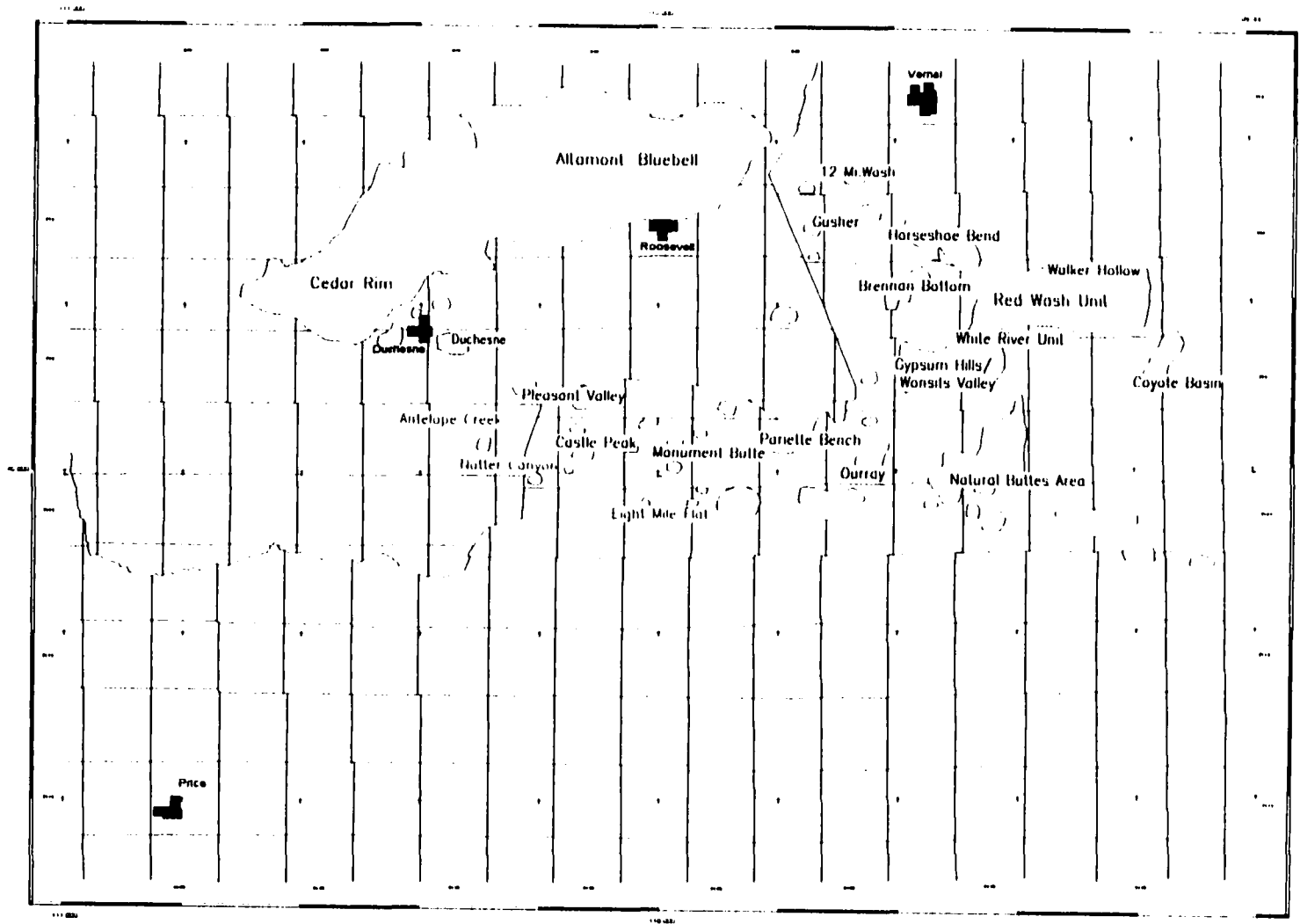
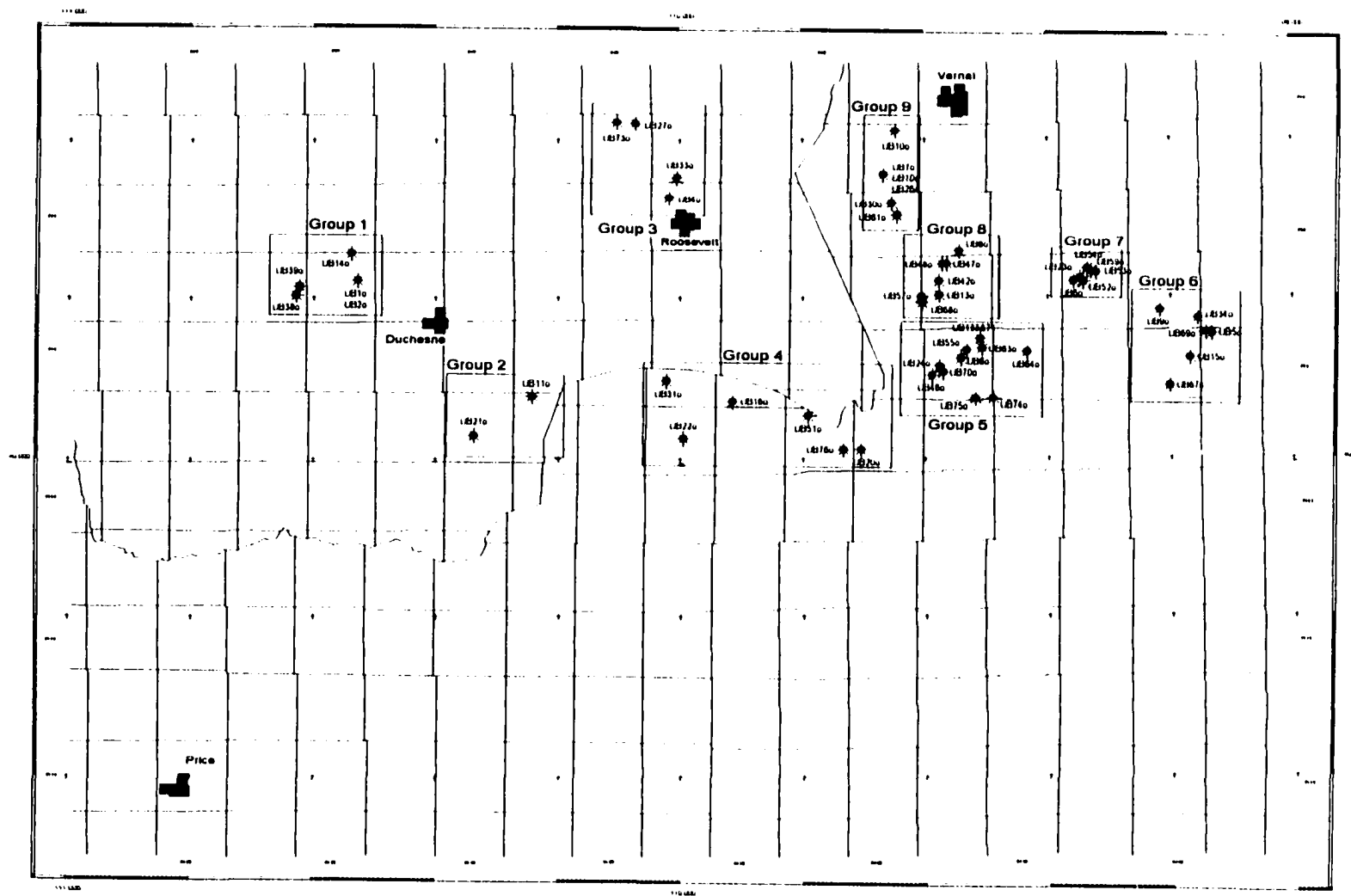


Figure 9



**Figure 10**

Map-group	Field	Depth of production ft	Stratigraphy of producing horizon	Cum. prod. Mbbl	Gravity (API°)/ppt.	Reservoir character	Sample number
1	Cedar Rim	3700-12595 <sup>*2</sup>	Green River Fm., Wasatch <sup>*2</sup>	8832	22-54°/90-125°F <sup>*2</sup>	fractured sdst. and siltstones <sup>*2</sup>	1, 2, 14, 38, 39
2	Antelope Creek	6027-6296 <sup>*3</sup>	Colton, upper Green River Fm. <sup>*3</sup>	2245	40°/90-100°F <sup>*3</sup>	fracture enhanced pointbars and channels <sup>*3</sup>	11, 21
3	Altamont Bluebell	10500-13000 <sup>*1</sup>	Flagstaff Mmb., lower Green River Fm., Colton <sup>*1</sup>		39°/110-125°F <sup>*1</sup>	overpressure, fractured fluvial deltaic, delta front and beach sdst. <sup>*1</sup>	4, 27, 33, 73
4 A	Eight Mile Wash	5205-5215 <sup>*2</sup>	Lower Green River Fm., green shale facies, black shale facies <sup>*7</sup>	61.1	33-37°/95°F <sup>*2</sup>	delta channel sdst., point bars <sup>*7</sup>	16
4 B	Monument Butte	3568-5747 <sup>*2</sup>	Lower Green River Fm., green shale facies, black shale facies <sup>*7</sup>	8767	31-34°/85-90°F <sup>*2</sup>	fluvial-deltaic distributary mouth bars and channels <sup>*12</sup> , pointbars <sup>*7</sup> , offshore bars <sup>*3</sup>	31
4 C	Pariette Bench	4000-4900 <sup>*2</sup>	Douglas Creek <sup>*4</sup>	966	22-40°/90°F <sup>*2</sup>	interbedded fluvial-alluvial channel sdst. <sup>*4</sup>	51
4 D	Pleasant Valley	4000-6000 <sup>*7</sup>	Lower Green River Fm., green shale facies, black shale facies <sup>*7</sup>	60.3	17-44°/82-140°F <sup>*2</sup>	delta channel sdst., pointbars <sup>*7</sup>	20, 22
4 E	West Willow Creek	4600-4800 <sup>*3</sup>	lower Green River Fm. <sup>*3</sup>	759	32°/n.a. <sup>*6</sup>	stromatoporid reef <sup>*3</sup>	76
5 A	Gypsum Hills/Wonsits Valley	5385-5495/5118-5740 <sup>*2</sup>	Douglas Creek <sup>*9</sup> , lower Green River Fm. <sup>*3</sup>		27-31/n.a. <sup>*2</sup>	nearshore barrier beach, bars, fluvial deltaic channels <sup>*9</sup>	46, 70/6, 24, 55, 63, 71
5 B	White River	4349-5823 <sup>*2</sup>	Douglas Creek <sup>*9</sup> , lower Green River Fm. <sup>*3</sup>	1472	28-29°/n.a. <sup>*3</sup>	fluvial deltaic channels <sup>*9</sup> , ostracodal limestone <sup>*3</sup>	64
5 C	Natural Buttes	3015-9272 <sup>*2</sup>	Douglas Creek <sup>*4</sup> , lower Green River Fm. <sup>*11</sup>	3107	29-48°/60-90°F <sup>*2</sup>	marginal lacustrine channels and point bars <sup>*3</sup>	74, 75
6	Coyote Basin	4204-4618 <sup>*2</sup>	lower Douglas Creek <sup>*9</sup>	1379	31-36°/95°F <sup>*2</sup>	fluvial-deltaic channels <sup>*3</sup>	5, 9, 15, 34, 67, 69
7	Walker Hollow	4341-5742 <sup>*2</sup>	Douglas Creek <sup>*9</sup>	14428	26-33°/n.a. <sup>*2</sup>	storm/waved dominated. shoreface, gravity flows <sup>*8</sup>	23, 52, 53, 54, 59, 60
8 A	Brennan Bottom	2290-7275 <sup>*2</sup>	Uinta Fm. <sup>*2</sup> , Lower Green River Fm. <sup>*3</sup> , Wasatch <sup>*2</sup>	1141	25-34°/95-105°F <sup>*2</sup>	sandy ostracodal limestone <sup>*3</sup>	13, 42, 57, 68
8 B	Horseshoe Bend	2578-7516 <sup>*2</sup>	Uinta Fm., Green River Fm., Wasatch <sup>*2</sup>	1411	27°/80°F <sup>*2</sup>	marginal lacustrine, channel sdst. <sup>*2</sup>	8, 47, 48
9 A	12 Mile Wash	6956-6960 <sup>*2</sup>	Green River Fm. <sup>*2</sup>	5.1	27°/n.a. <sup>*2</sup>	n.a.	7, 10, 26
9 B	Gusher	7750-12638 <sup>*2</sup>	Green River Fm., Wasatch <sup>*2</sup>	232	26-38°/85-95°F	fractured oil-shale and sdst. lenses <sup>*2</sup>	30, 61

Table 1

## **5. Experimental**

### **5.1 Rock-Eval Analysis**

Rock-Eval analyses were performed at the Geochemistry Division of the USGS in Lakewood, Colorado using a Delsi Instruments Inc. Rock Eval II<sup>®</sup> pyrolysis system with TOC module. Prior to analysis, samples were decarbonized with hydrochloric acid. Initially, samples were pyrolyzed isothermally at 250°C for 3 minutes to determine S1 (thermally distillable C<sub>1</sub>–C<sub>3</sub>, hydrocarbons). Temperature programmed pyrolysis from 250° to 600°C at 25°C/min yielded S2 (thermal decomposition of kerogen) and via a splitter S3 (carbon dioxide, CO<sub>2</sub>). The carrier gas was He (2 ml/min) which transported the pyrolysis products through a splitter set at 500°C to either a flame ionization detector (FID; determination of S1 and S2) or thermal conductivity detector (TCD; determination of S3). The samples were subsequently transferred into the oxidation module to be heated to 600°C in air for 13 minutes. The carbon monoxide (CO) produced was passed to a second furnace where it was converted via a copper oxide catalyst to CO<sub>2</sub> and detected by a TCD to compute S4. The TOC content was determined by addition of the S1, S2 and S4 peaks. Calibration of the Rock Eval system was performed using the IFP#55000 standard.

### **5.2 Source Rock Extraction**

Samples selection for further processing was based on TOC, location and hydrocarbon content determined by Rock-Eval analysis. Powdered samples (20-100 mg depending on TOC, see Appendix 5) were extracted using a Soxhlet apparatus in which ca. 350 ml of a mixture of HPLC grade methanol (MeOH) and dichloromethane (DCM) solvents (1:1 vol.) was circulated for 24 hours. Pre-extracted (12 hours) cotton cellulose thimbles containing the samples were closed at the top with cleaned glass wool. Solvent and extracts were collected in 500 ml round bottom flasks, which also contained boileezer chips and activated Cu for sulfur removal. Ruble (1996) reported

high sulfur content in some source rock samples (e.g. 3.87% S for the black shale facies sample), but actual sulfur reaction on the Cu was not observed. After the extraction procedure excess solvent was removed in a rotoevaporator and the extracts placed in tarred 4 ml sample vials to quantify extractable organic matter (Appendix 5).

### **5.3 Asphaltene Precipitation and Fractionation of Source Rock Extracts and Oils**

Source rock extracts and oils were treated in the same manner for deasphalting and fractionation and are described together. Pentane (100 ml) and sample (130-500 mg) were placed into glass centrifuge tubes and stored in a freezer for 24 hours. The tubes were centrifuged subsequently at 3000 rpm for 10 minutes and the pentane soluble maltene fraction decanted into 250 ml round bottom flasks. The precipitated asphaltene fraction was rinsed with pentane, centrifuged again and dissolved in DCM for transfer into pre-weighted 4 ml vials after decanting the pentane and any remaining maltene fraction. Pentane was removed by rotoevaporation and the maltene fractions were placed in 4 ml vials for weighting. Fractionation of the maltenes was performed using high pressure liquid chromatography (HPLC) for which sample aliquots were dissolved in hexane at a ratio of 20 ml/50 mg sample. Samples were warmed before injection into the HPLC system (ELDEX 9600 equipped with a Whatman Partisil 5 Pac column, 25 cm). Saturated, aromatic and polar fractions were eluted according to a modified gradient program adapted from McDonald and Mahlon (1992) using hexane, DCM and ethylacetate as eluents. Hexane elution was extended to 20 minutes to insure complete fractionation of high molecular weight saturated compounds. This program modification was developed after test runs using an *n*-alkane standard which included *n*-C<sub>50</sub> (Mueller and Philp, 1998). Elution was also monitored using a Kratos Inc. UV Spectroflow 783 set at  $\lambda=254$  nm. Saturated, aromatic and polar fractions were collected in 100 ml round bottom flasks, excess solvent evaporated and the fractions weighted.

Several saturated fractions of oils and source rock extracts were selected for branched and cyclic compound isolation (method after West *et al.*, 1990) to improve resolution and enhance relative concentration in the gas chromatography-mass spectrometry (GC-MS) analysis. Saturated fraction aliquots (3-10 mg, depending on availability) were dissolved in pentane and eluted through powdered, activated (350°C, 24 hrs) silicalite (UOP Molecular Sieves, S-115). The silicalite was placed into 3 ml Pasteur pipettes, which were sealed at the tip with cleaned glass wool, and rinsed with 3 bed volumes prior to sample elution. Samples were placed on the silicalite and forced through the column at very low pressures. The branched and cyclic fraction eluate was collected, tarred and the silicalite stored for later isolation of *n*-alkanes. The quality of the isolation procedure was monitored by GC-analysis of selected branched and cyclic fractions.

#### **5.4 Gas Chromatography (GC) and Gas Chromatography-Mass Spectrometry (GC-MS)**

Saturated fractions of oils and extracts were prepared for GC analysis by dissolving aliquots in *p*-xylene to 2-3 mg/ml solutions. Aliquots of branched and cyclic fractions were processed with concentrations of 3-4 mg/ml DCM. In addition, an internal standard C<sub>24</sub>D<sub>50</sub> was added to the samples. The amount of β-carotane normalized to µg/g TOC was calculated using this standard (calculation procedure in Ruble, 1996). Samples were warmed up prior to on-column injection of 1.0 µl sample volume. Analysis was performed using an HP GC5890 GC equipped with a J&W DB-1HT fused silica column (30 m x 0.32 mm i.d., 0.1 µm film). The temperature program was initially set to 40°C for 1.5 min., ramping 40°-360°C at 4°C/min and a final hold at 360°C for 37.5 min, resulting in a total run time of 120 min. Carrier gas was He set at 2 ml/min; detection system was a flame ionization detector (FID) set at 370°C.

Gas chromatographic setting for GC-MS analysis was as follows: a Varian 3400GC equipped with a J&W DB-5 (60 m x 0.32 mm i.d., 0.25 µm film) was programmed to 40°C hold

for 1.5 min, 40°-310°C at 4°C/min, and 310°C hold for 31 min. The column was operated in slit/splitless mode using He as carrier gas at 2 ml/min flow rate. Eluents were transported through a transfer line set at 310°C to a Finnigan Mat TSQ70 mass spectrometer operated in electron impact (EI) mode at 70 eV. The mass spectrometer was operated in the multiple ion detection mode (MID) to analyze the following ions:

<b>Ion m/z</b>	<b>Compound class</b>	<b>GCMS\MS ion transitions m/z</b>
95, 98	Dinosteranes	
114	Internal standard C <sub>24</sub> D <sub>50</sub>	
123	Sesquiterpanes	123 → 194, 208, 222
	Diterpanes	123 → 248, 262, 276
177	Demethylated hopanes	
183	Isoprenoids	
191	Tricyclic terpanes	191 → 416, 430
	Pentacyclic terpanes	191 → 370, 384, 398, 412
205	Methylated hopanes	
217	Desmethyl steranes and diasteranes	217 → 372, 386, 400
218	ββ-steranes	
231	Methyl steranes, diasteranes	231 → 386, 400, 414
232	ββ methyl steranes	
253	Monoaromatic steranes	
400	C <sub>29</sub> desmethyl steranes	
414	C <sub>30</sub> desmethyl steranes	
426	Extended (C <sub>31</sub> ) hopanes	

Biomarker identification was based on GC-MS\MS experiments performed on selected samples and the results were used to identify compounds in all other samples. The collision gas was argon at 0.5 mtorr and a collision energy of -10eV was used. In addition, published chromatograms and analyses of standard samples were used to assist in compound identification.

## **5.5 Statistical methods**

Traditionally, organic geochemical data in the form of chromatograms are interpreted by visual comparison, computation of ratios of biomarkers or quantitative analysis. Only relatively few publications describe the application of multivariate statistical methods for the analysis of organic geochemical data in petroleum exploration (e.g. Telnaes and Dahl, 1986; Engel *et al.*, 1988). In some studies principal component analysis (PCA) was employed, which is basically the most primitive form of factor analysis performed on dispersion matrices (Davis, 1986). Chatfield and Collins (1980) state that PCA “*consists of finding an orthogonal transformation of the original variables to a new set of uncorrelated variables, called principal components, which are derived in decreasing order of importance. The analyst hopes that the first principal components will account for most variation in the original data, so that the effective dimensionality of the data can be reduced*” . As such, PCA is not strictly a statistical method but merely a data ordination, which does not make assumptions about the data and has no underlying model (Rock, 1988). Under favorable circumstances, PCA allows reduction of the variance associated with a multidimensional data set into just a few components representing a large portion of the variance.

Statistical analysis in this study was performed using the GC-MS response peak heights of 96 compounds measured in ions m/z 123, 191, 217 and 253 of source rock extract and crude oil saturated fractions (Appendix 4.1 and 8.1). The process was subsequently repeated using 20 of the dominant peaks measured in m/z 123, 191 and 217. Peak heights were used instead of peak areas because of multiple coelutions associated with significant peaks (e.g. 17 $\alpha$ (H),21 $\beta$ (H)-norhopane and 18 $\alpha$ (H)-norhopane (C<sub>29</sub>-Ts)).

Eigenanalysis provides information about the structure of a matrix, and in case of the PCA, about the location and magnitude of maximum variances. Principal components are the eigenvalues of a dispersion matrix and can be visualized as mutually orthogonal axis defining an

envelope which encloses all sample points in the n-dimensional data space, and in which the principal components describe the maximum spread (maximum variance) in the data set (Davis, 1986). The direction of the axis is given by the associated eigenvectors. Matrix inversion allows the calculation of associated eigenvectors who's elements provide the loadings of each respective variable. The loadings describe the relative influence of the variables on a given principal component. Reference of original observations to the new coordinate system defined by the principal components and their eigenvectors, *i.e.* calculation of principal component scores, is performed by simple matrix multiplication of the eigenvector matrix and the original data matrix. Working backwards from a principal component score cross plot to the principal component loadings allows interpretation of which variables influences the composition of a sample and how variables interrelate.

The first PCA applied in this study using 96 variables (peaks) is not statistically sound, since a dispersion (variance-covariance) matrix technically cannot be estimated from a number of samples smaller than the number of variables. Statistical valid estimation of the dispersion matrix demands that the number of samples is clearly higher than the number of variables, although the first principal components are affected very little by whether or not the matrix is of full rank (Legendre and Legendre, 1983). Grossman *et al.* (1991) also demonstrated that the performance of tests of significance of eigenvalues depends on the ratio of number of samples and variables. The PCA for source rock extracts and crude oils was therefore repeated using a selected number of peaks (Table 2) which showed comparable absolute magnitudes of variance. The results of using 96 and 20 variables were almost identical, both in terms of variable interrelationship and sample scores. Including a high number of variables suggested more details about the relationship between biomarkers and biomarker groups, therefore the results of this analysis are reported, too. However, many of the small coefficients are not significant according to the cut-off values suggested below.

peak no.	compound	ion m/z	peak no.	compound	ion m/z
3	C <sub>21</sub> tricyclic terpane	191	33	17α(H),21 β(H),22R-30-homohopane	191
5	C <sub>23</sub> tricyclic terpane	191	34	gammacerane	191
16	18α(H)-22,29,30-normehopane (Ts)	191	45	8β(H)-drimane	123
19	17α(H)-22,29,30-trisnorhopane (Tm)	191	49	8β(H)-homodrimane	123
25	17α(H),21 β(H)-30-norhopane	191	54	4β(H)-19-norisoprimarane	123
26	C <sub>30</sub> diahopane	191	58	isopimarane	123
28	17β(H),21α(H)-30-normoretane	191	59	16β(H)-phylocladane	123
30	17α(H),21 β(H)-hopane	191	71	14α(H),17α(H),20R-cholestane	217
31	17β(H),21α(H)-moretane	191	77	24-methyl-14α(H),17α(H),20R-cholestane	217
32	17α(H),21 β(H),22S-30-homohopane	191	81	24-ethyl-14α(H),17α(H),20R-cholestane	217

**Table 2:** List of compounds in branched and cyclic fractions obtained from source rock extracts and crude oils which were used for the principal component analysis with 20 variables ( $m=20$ ).

Most published PCA of organic geochemical data used in petroleum exploration studies are based on data sets in which the number of variables clearly exceed the number of samples. Mello *et al.* (1988) performed PCA on 94 samples using 962 variables, and Telnaes and Cooper (1991) explicitly state that the requirement of number of samples larger than the number of variables is a misconception.

Both variance-covariance and correlation matrices were tested as input matrices for the PCA. In the PCA of variance-covariance matrices the variables with the highest absolute variance will contribute most to the first principal components (Rock, 1988). Standardization (*i.e.* performing an eigenanalysis of a correlation matrix) normalizes variances to zero mean and unit variance, thereby compensating for the differences in absolute variance magnitudes. Generally, the use of variance-covariance (centered) matrices are recommended in geochemical applications if all variables are measured in the same units or if the absolute magnitudes of variances are of interest (LeMaitre, 1982, and references therein; Rock, 1988). Anderson (1963) stressed the incongruity of standardizing all variances and then trying to maximize the variance of certain linear combinations

by computing principal components. It is possible that with the data set in this study important information associated with minor peaks may be lost without standardization. *e.g.* the steranes were present only in minor concentrations in most samples. Normalization and computation of principal components for a reduced number of variables with comparable variances (within two orders of magnitude) partly compensated for this problem. However, it is also apparent that the variation of the normalized magnitudes of peaks within the sample set contains valuable information as well. Attempts using the correlation matrices in the PCA applied in this study resulted in loss of variance associated with the first principal components, and because of the difficult interpretation and unclear sample separation, data interpretation was based on the analysis of variance-covariance matrices. It is legitimate to select which method to use based on performance and PC interpretability (*e.g.* Gower, 1966), although James and McCulloch (1990) cautioned about circular reasoning when multivariate statistics is judged based on interpretability.

Tests for evaluation of the significance of eigenvalues obtained from PCA have been developed. Several of these tests have been evaluated by Jackson (1993) who found the broken-stick model to be one of the most reliable tests in the evaluation of simulated data matrices. This model considers the variance as a resource shared between principal components. The distribution of variance by chance can be regarded as a stick of unit length randomly broken into a number of pieces equivalent to the number of principal components. The method was developed by Frontier (1976) (*cf.* Legendre and Legendre, 1983) who also published a table listing the % variance associated with successive eigenvalues according to the broken-stick model. Comparison of observed eigenvalues with broken-stick eigenvalues shows which principal component comprises more variance than can be expected by chance alone (*i.e.* observed eigenvalue > broken-stick eigenvalue).

In contrast the issue of the significance of the eigenvector loadings in PCA and what levels should be used to discard insignificant loadings has not been discussed widely in the literature. Flury and Riedwyl (1988) suggested formulas for the calculation of standard errors of loadings, but their validity depends on large samples sizes and assumption of multivariate normality. A recent discussion can be found in Richman and Gong (1999) who experimentally tested magnitudes of eigenvector coefficients (loadings) which can be considered important in meteorological applications based on samples size and components retained. Since no formal test is available which does not assume normally distributed data and independence of variables, arbitrary cut-off values have been employed in some studies (Richman and Gong (1999) and references therein). Richman (personal comm.) recommended calculation of cut-off values using 0.2 times the maximum loading in a given PC as a rule of thumb when employing eigenanalysis of variance-covariance matrices. Choosing these cut-off values prevents overinterpretation of the numerical values and also compensates for the error in GC-MS reproducability.

Principal component analysis in this study is considered a tool for initial (exploratory) data evaluation and sample interpretation, which needs to be corroborated by comparison with conventional geochemical parameters. The method greatly aids in systematic evaluation of biomarker relationships and correlation of samples but does not replace the need to investigate the data individually and verify interpretations made on PCA results. The statistics software PC-Ord Version 2.0, written for ecological studies, was used for the PCA. The software allows flexible calculations based on different dispersion matrices and reports the broken-stick eigenvalues as a measure of how many components to retain in the analysis.

## **6. Data Analysis and Interpretation**

Source rock extract and crude oil analyses were performed using standard biomarker techniques and bulk geochemical parameters in case of the source rocks. The interpretations and correlations described in the following sections are based on the data obtained from these methods. Many of the biomarkers detected and used for interpretations are synthesized by a number of different organisms and occur in different depositional environments, thus have only a limited specificity for the interpretation of source rocks organic matter and depositional environment. Although interpretations made in this study are substantiated employing several geochemical parameters simultaneously, additional data obtained from other geochemical methods such as carbon isotopic measurements (bulk analysis, hydrocarbon fractions, and compound specific analysis), porphyrin analysis, elemental analysis (sulfur, nitrogen) *etc.* would be desirable.

### **6.1. Source Rock Analysis**

Before describing source rock geochemistry in detail it is worthwhile to examine the data set as a whole using bulk, Rock-Eval and gas chromatographic analyses. These analyses allow an initial grouping of the large number of samples investigated. In subsequent chapters the geochemical character of the source rocks will be interpreted based on multivariate statistics of GC-MS data as described in Chapter 5.5. The interpretation will then be verified by correlation to other data obtained from GC and Rock-Eval analysis and supplemented by observations from core descriptions (Appendix 3). All relevant source rock geochemical data and sample descriptions are summarized in Appendix 5; abbreviations used are listed in Appendix 1.1.

### 6.1.1. General Observations

#### 6.1.1.1. Bulk Data

Histograms of TOC-values of source rocks (41 samples) which have been processed for detailed geochemical analysis show an expected lognormal distribution (Fig. 11a), with the most frequent values varying between 2-4% TOC (median=2.4%). Maximum TOC values (>30%) occur in coaly samples (UB26E, UB42E and UB45E). High values were also measured in outcrop samples from the mahogany zone. Sample UB29E from the south-central area (map-group 3) shows extremely high TOC-values, but is classified as a massive shaley mudstone with occasional large pelecypod shells, similar to the nearshore open lacustrine facies of Wiggins and Harris (1994). However, most other samples do not show exceptionally high TOC values, although some would qualify as oil-shales based on lithology, lamination and color. The distribution of HI values is less consistent (Fig. 11b) which may be explained by source, maturity range or organic matter oxidation levels. A maximum value of 1,020 mg HC/g TOC was measured in an outcrop sample from the mahogany zone (UB39E).

Rock-Eval data for samples used for extraction are illustrated in conventional Hydrogen-Index (HI) vs. Oxygen-Index (OI) and  $T_{max}$  cross plots (Fig. 12). Although oil-shale type samples (see Chapter 6.1.2.) plot along the expected pathway of type I kerogens in Figure 12a, a number of samples classify as type II and possible mixtures of types I+II or II+III. An alternative explanation for the apparent mixing are oxidation processes prior or soon after burial through bacterial reworking or weathering. Horsfield *et al.* (1994) favor bacterial reworking in their investigation of Green River Formation samples from the Greater Green River Basin in Wyoming. Extensive reworking has also been interpreted for upper Green River Formation oil-shales in the Uinta and Piceance Creek Basins by Dean and Anders (1991). Despite the analytical problems associated with the OI (Peters, 1986), this parameter is nevertheless an indication of extensive organic matter

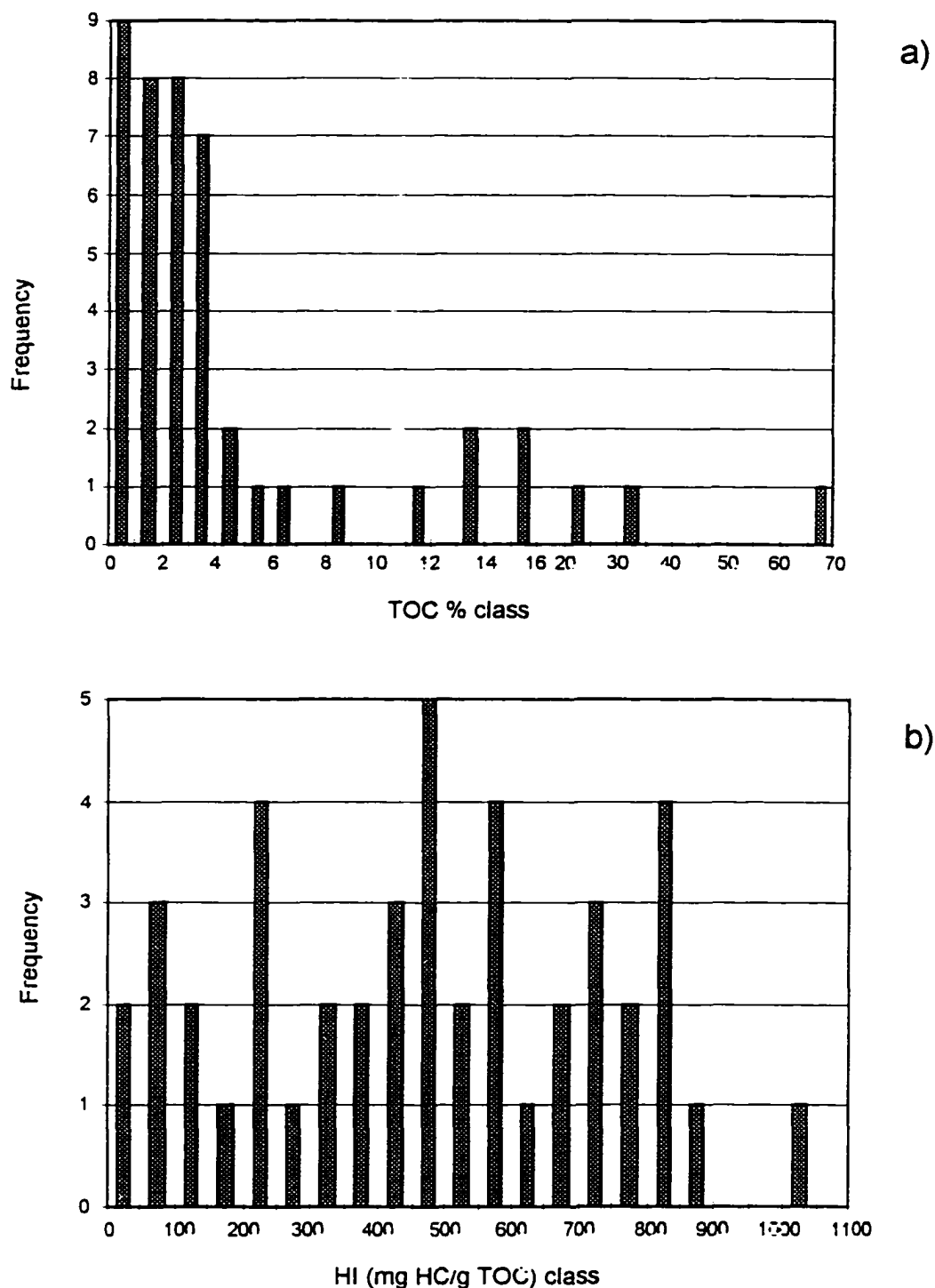


**Figure 11:** Histograms of TOC (a) and HI-Indices (b) of Green River Formation source rock samples analyzed in this study. Bimodal distribution in (a) is caused by high TOC in oil-shales. Extremely high TOC value in (a) represents coal sample UB42E, and the maximum value in (b) was obtained from the mahogany zone outcrop sample UB39E. Note class change at TOC >16% in (a).

reworking in the analyzed core samples, since weathering can be excluded, and petrographic analyses in other studies do not indicate sufficiently high vitrinite contents to decrease HI markedly (e.g. Ruble, 1996; Dean and Anders, 1991). Comparison of the HI vs. OI distribution of the investigated samples with analyses published elsewhere (e.g. Tissot *et al.*, 1978; Dean and Anders, 1991), in which samples generally plot close to the type I pathway, makes the bias of published Green River Formation source rock investigations towards the analysis of oil shales (at least for the Uinta Basin) apparent.

Rock-Eval  $T_{max}$ -values have been used extensively for source rock maturity studies, although the quality of the measurement depends strongly on the kerogen type and is often inconclusive for type I kerogens (Tissot *et al.*, 1987). Figure 12b shows the sample distribution in a  $T_{max}$  vs. HI cross plot. The HI-values decrease with increasing maturity, whilst  $T_{max}$  increases. The beginning of the oil window (hydrocarbon generation zone) has been proposed to correlate with a  $T_{max}$ -value of 440°C for kerogen type I (Espitalié, 1986). Most of the samples in this study fall below or within this oil-window. A few samples (Appendix 5) show erroneous  $T_{max}$  values, possibly caused by extensive weathering (outcrop sample UB44E) and extremely low TOC (UB30E) and are not displayed in the graph. Sample UB31E also appears to have a anomalously high  $T_{max}$ -value, considering its location (Cedar Rim field) and shallow depth (8507 ft). All other samples plot below the suggested upper oil window level of 460°C (Anders *et al.*, 1992). In pyrolysis experiments, Huizinger *et al.* (1988) reported invariable trends for  $T_{max}$  in Green River oil-shales, while Ruble (1996) demonstrated that  $T_{max}$  may be useful for certain source facies in the Uinta Basin. In naturally matured samples, Anders and Gerrild (1984) and Anders *et al.* (1992) reported considerable scatter or invariant  $T_{max}$  vs. depth profiles for samples from various fields in the basin.

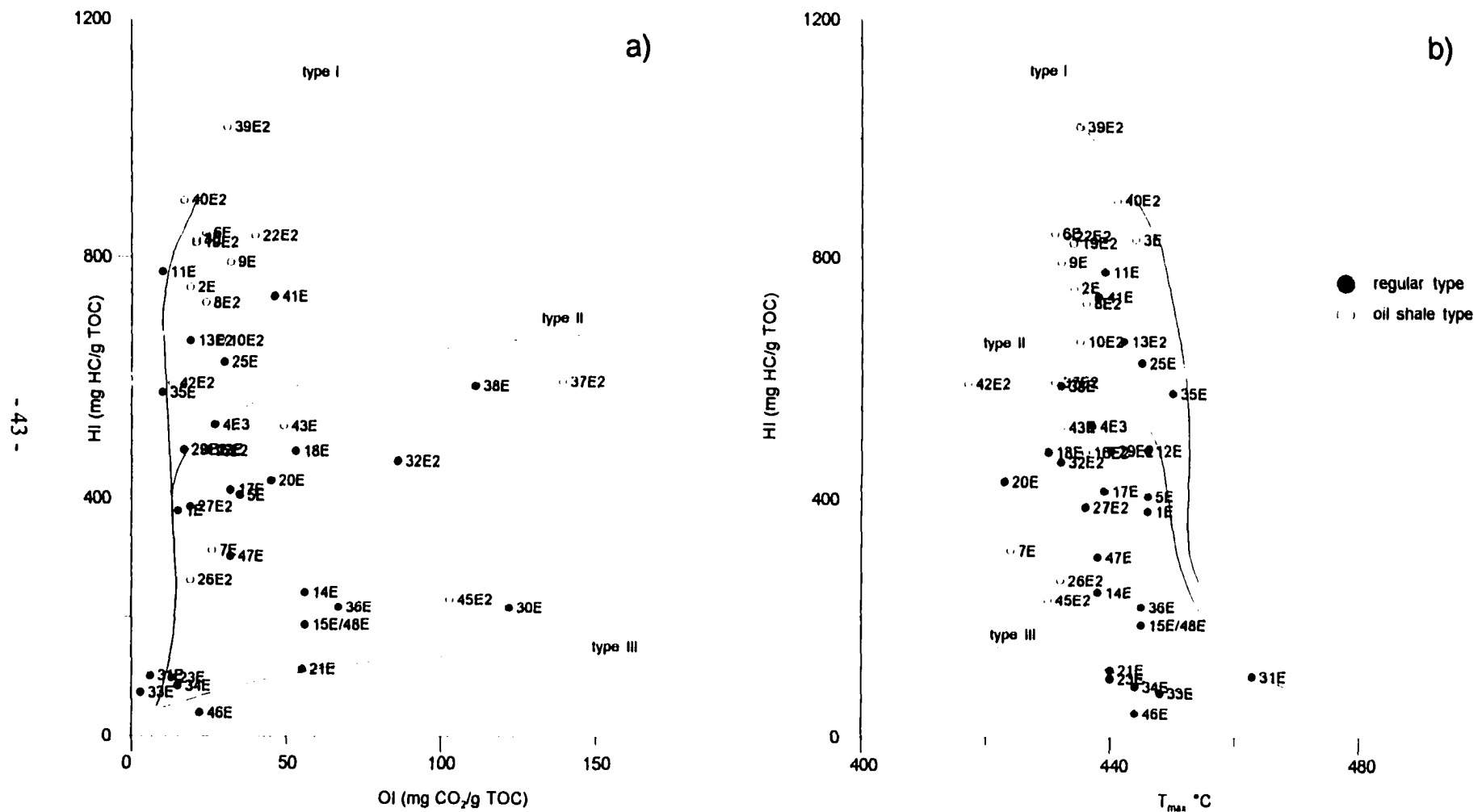


**Figure 12:** Oxygen- vs. Hydrogen-Index (a) and  $T_{max}$  vs. Hydrogen-Index (b) derived from Rock-Eval analyses of source rock core samples. Displayed samples were used for detailed geochemical study. Standard kerogen type pathways adopted from Tissot *et al.* (1987). The difference between regular type and oil shale type samples is explained the text.

### 6.1.1.2. High Temperature Gas-Chromatography (GC) Analysis

Gas chromatographic analysis of the saturated fractions permits separation of two types of source rocks based on *n*-alkane abundance and distribution relative to isoprenoids and naphthenic compounds. A third group comprises samples identified as coals in outcrop and core. Examples for comparison of the former two groups are given in Figure 13 and average bulk and GC derived geochemical parameters are summarized in Table 3. Individual samples of these sample groups are differentiated in Appendix 5.

Source rock type		ASPH %	SAT %	EOM ppm	Pr/Ph	CPI	$\beta$ -carotane ( $\mu\text{g/g TOC}$ )	TOC %	HI (mg HC/g TOC)	T <sub>max</sub> °C
Oil-shale type n=29	avg.	23.5	38.9	1065	1.39	1.23	971	4.02	721	434
	range	14.6-34.8	1.2-60	267-2486	0.19-1.31	0.75-2.64	59-5038	1.2-13.6	314-1020	424-444
	std.dev.	5.4	15.0	669	0.57	0.52	1446	3.51	188	4.6
Regular type n=12	avg.	17.2	58.5	490	1.78	1.04	82	3.3	359	441
	range	2.6-22.0	32.8-67.2	12-2684	0.77-3.48	0.95-1.17	0-581	0.31-15.7	39-775	423-450
	std.dev.	13.8	11.4	625	1.05	0.37	133	11.1	270	314
Coals n=3	avg.	59.7	25.9	6410	4.11	1.68	0	40.4	261	426
	range	43.5-75	31.8-39.5	2245-13494	3.36-5.37	1.24-2.11	0	21.3-67.7	230-589	417-432
	std.dev.	15.7	3.8	6158	1.10	0.62	0	24.3	198	8.1

Table 3: Selected averages and ranges for geochemical parameters of source rock extract saturated fractions investigated in this study. Source rocks are separated into groups as described in the text. Abbreviations in Appendix 1.1; n = number of samples.

Samples of the first group are here referred to as oil-shale type samples and include samples known to originate from the mahogany zone (outcrop samples UB39E, UB40E). The oil-shale type group is distinguished by GC traces characteristically dominated by isoprenoids (pristane and phytane), pentacyclic terpanes, gammacerane and  $\beta$ -carotane and show only minor *n*-alkane abundances (Fig. 13a and b). Similar geochemical characteristics of organic-rich lacustrine sediments have been reported from Brazil (e.g. Mello and Maxwell, 1990) and China (e.g. Carroll *et al.*, 1992).  $\beta$ -Carotane has been interpreted as a general biomarker for algal, archaeabacterial or

photosynthetic bacterial derived compounds deposited in hypersaline and anoxic environments (Jiang and Fowler, 1986; Fu Jiamo *et al.*, 1990). High concentrations of  $\beta$ -carotane generally indicate a biosphere of low diversity but high productivity (Killops and Killops, 1993, and references therein). Whilst the typical mahogany zone oil-shale shows a dominance of  $\beta$ -carotane and Pr/Ph values < 1.0 (see sample chromatograms in Appendix 6), this is not necessarily true for other samples of this type (Table 3). Ruble (1996) detected similar geochemical variations in outcrop samples stratigraphically ranging from the upper black shale facies to the saline facies (see Fig. 6 for stratigraphy). Bulk and biomarker parameters are also highly variable, TOC-values e.g. vary from 1.2% to 13.6% in the oil-shale type samples, EOM is also generally high in these samples (Table 3). The geochemical signature of the oil-shale type samples is in part related to their low thermal maturity. The relative concentration of *n*-alkanes in source rock extracts increases with maturity, as a result of their generation from the kerogen matrix during maturation (Tissot and Welte, 1984). Thermal generation and destruction of compounds may have obliterated an initial oil-shale type signature in samples from the stratigraphically deeper sections of the basin. However, hydrous pyrolysis of mahogany zone samples by Ruble (1996) demonstrated that distinct geochemical features such as high relative pristane, phytane and  $\beta$ -carotane concentrations were still visible at elevated pyrolysis temperatures (330°C/72 hrs; Lewan's (1993) beginning primary oil generation stage). Since  $T_{max}$  and molecular thermal maturity indicators suggest that most of the samples investigated in this study are immature to early mature, it is assumed that the proposed distinction of extracts is valid for the majority of the samples investigated and reflects major differences in source and depositional environment of the source rocks (see also Tissot *et al.*, 1978). However, the differentiation to samples of regular type samples described below may be transitional.

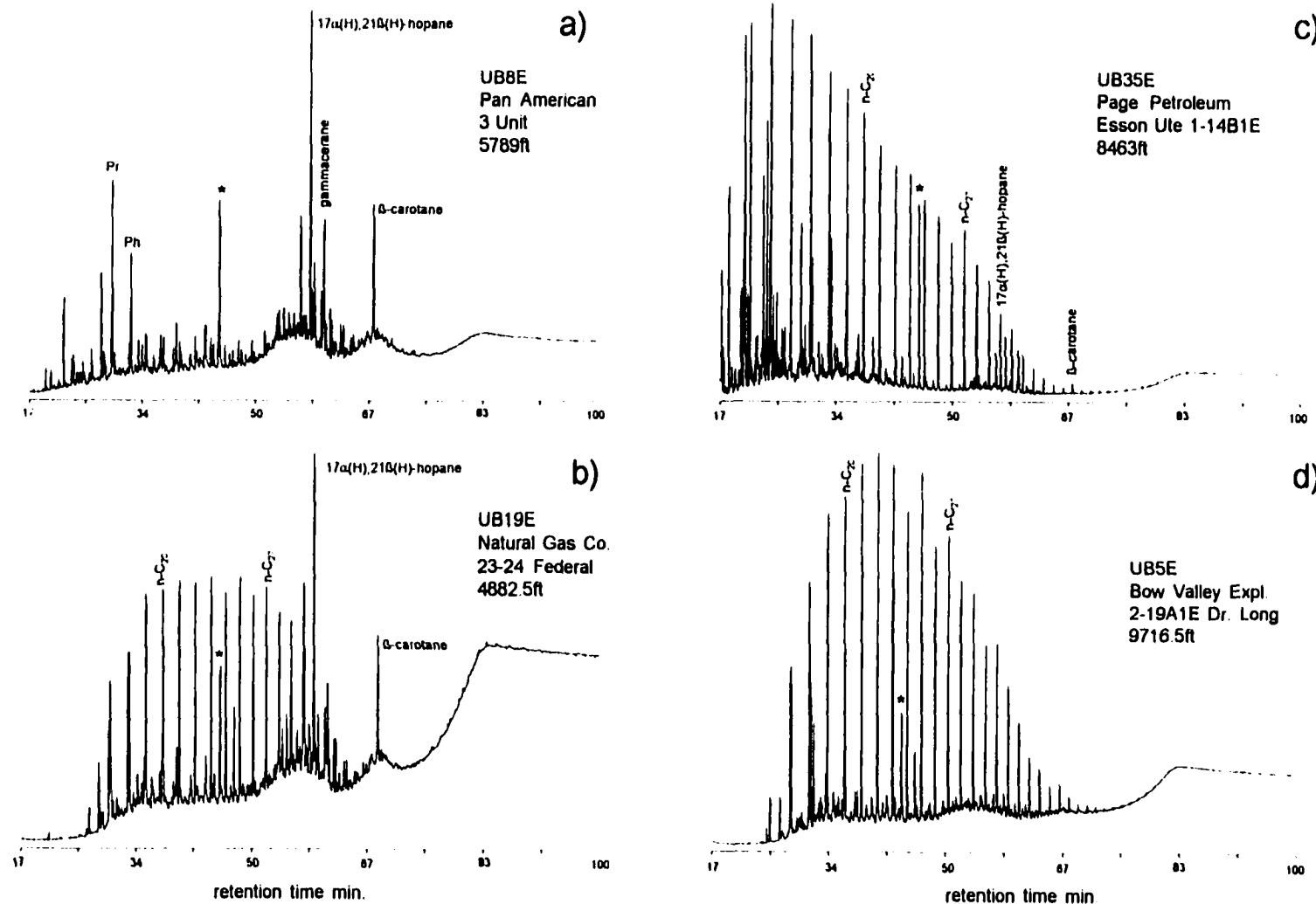


**Figure 13:** Representative high-temperature gas chromatograms of source rock extract saturated hydrocarbon fractions (oil-shale type (a and b) and regular type (c and d)). Samples in (b) and (d) show possible evaporative loss of lower molecular weight fractions. \* = Internal standard  $\text{C}_{24}\text{D}_{50}$ .

The second type of source rock displays a dominant and homologous series of *n*-alkanes (Fig. 13c and d) with varying carbon number range and carbon preference patterns (CPI > 1.0 for *n*-alkanes >*n*-C<sub>25</sub>). A number of samples display an even predominance between *n*-C<sub>19</sub> and *n*-C<sub>23</sub>, possibly characteristic for bacterial organic matter (see Hunt (1996) for review). However, hypersalinity, as suggested by R22 >> 1.5 (ten Haven *et al.*, 1988; definition in Appendix 1.1) is not indicated in any sample. Still, in most samples R22 ranges between 1.0 and 1.5, suggesting elevated *n*-C<sub>22</sub> concentrations. Some of the samples show minor traces of triterpanes and  $\beta$ -carotanes (see Fig. 13c). In general, TOC and HI are lower in these samples compared to oil-shale type samples. Maturity ranges appear similar, although sample plots in Figure 12b suggest generally slightly higher maturities based on T<sub>max</sub>. Besides the problems associated with T<sub>max</sub> as described above, its suppression at high HI is also a known phenomenon (*e.g.* Snowdon, 1995) and the interpretation requires some caution.

Lithologic and macroscopic/microscopic petrographic analysis (thin sections were available at the USGS core library) of the core samples shows that, although oil-shale type samples are laminated dolomiticrites, there is no apparent general sedimentological criteria which would separate oil-shale and regular source rock types. It appears that the absence of lamination (except in streaked and babbly type of oil-shales described from the Piceance Creek Basin by Cole (1984)) excludes oil-shale type geochemical composition.

A third type of potential source rock comprises the coaly samples (UB26E, UB42E, UB45E), distinguished by their physical appearance and high TOC coupled with a comparatively high HI. Samples UB26E and UB42E show high Pr/Ph-values, high *n*-alkane concentrations, recognizable triterpane peaks but no  $\beta$ -carotane. The GC trace of UB45E (Appendix 6-1) on the other hand would qualify this sample as an oil-shale type. Ruble (1996) investigated a coal sample from the black shale facies of the lower Green River Formation (sample UB42E in this study) and

considered paludal coals as a potential hydrocarbon generative facies.

### 6.1.2. Gas Chromatography-Mass Spectrometry (GC-MS) Analysis

General observations made during GC-MS analysis of the branched and cyclic fractions of source rock extracts and implications of the biomarkers which were identified are briefly discussed below. For easier reference interpretations for all biomarkers detected in GC and GC-MS analysis are summarized in Table 4. Biomarkers in the aromatic fractions were not investigated.

Exploratory inter-sample comparisons are subsequently made based on multivariate statistical analysis, which provides a first means to identify composition and genetic differences of the source rocks, in addition to their separation into oil-shale type, regular and coal source rocks as described in the previous chapter.

Compound	Interpretation - source/depositional environment
n-alkanes relative abundance, distribution and carbon-number range	algae ( $n\text{-C}_{16}$ - $n\text{-C}_{24}$ ) particularly $n\text{-C}_{15}$ , $n\text{-C}_{17}$ , $n\text{-C}_{19}$ bacteria ( $n\text{-C}_{15}$ - $n\text{-C}_{17}$ ) higher plants ( $n\text{-C}_{25}$ - $n\text{-C}_{31}$ )
$\beta$ -carotane	algae, phototrophic bacteria, hypersaline and/or reducing environments
pristane	chlorophyll
phytane	chlorophyll, also in methanogenic bacteria and archaeabacteria
tricyclic terpanes	algae (Tasmanites), bacteria
pentacyclic terpanes (hopanes)	bacteria, archaeabacteria
methyl hopanes	methylotrophic bacteria
diahopanes	clay-catalyzed rearrangement of regular hopanes
gammacerane	halophilic protozoa, bacterivorous ciliates
oleananes	angiosperms
desmethyl-steranes	higher plants (particularly C <sub>29</sub> ), phyto- and zooplankton (particularly C <sub>27</sub> )
diasteranes	clay-catalyzed rearrangement of regular steranes
methyl steranes	phytoplankton, dinoflagellates
sesquiterpanes	bacteria associated with oxic decomposition of higher plant material degradation of regular hopanoids
diterpanes	higher plant resins
monoaromatic steroids	diagenetic transformation of desmethyl steranes

**Table 4:** Brief summary of biomarker interpretations described in Chapter 6.1.; after Peters and Moldowan (1993), Fu Jiamo *et al.* (1990) and references listed in the text.

### 6.1.2.1 Biomarker Distributions in the Source Rock Extracts

Representative examples of biomarker distributions detected in the branched and cyclic fractions of source rock extracts are illustrated in Figures 14-17, 19, 20 and 21 and provide examples for some of the geochemical differences discussed in the following chapter. The branched and cyclic fractions are generally dominated by relative amounts of isoprenoids, sesquiterpanes, diterpanes and triterpanes, including gammacerane. Steroidal biomarkers are generally less abundant (Fig. 14). It should be noted that relative biomarker distributions are modified during thermal maturation by thermal destruction or the release of compounds from the kerogen matrix. However, since the maturity of the most samples ranges from immature to early mature (see Chapter 6.2), it is assumed that diagenetic composition of the organic matter is still preserved and recognizable in the extracts .

### TRICYCLIC TERPANES

Tricyclic terpanes (Fig. 15) were determined to extend from carbon number C<sub>19</sub> to C<sub>31</sub> based on GC-MS/MS data. A number of components occurring between 17 $\alpha$ (H),21 $\beta$ (H)-hopane and 17 $\alpha$ (H),21 $\beta$ (H)-bishomohopane could not be positively identified. Some of these compounds may represent extended tricyclic terpanes (*e.g.* de Grande *et al.*, 1993) which alternate, or coelute, with extended moretanes and methyl hopanes. Relative amounts of tricyclic terpanes vary considerably from barely detectable to dominating over the pentacyclic hopanes. The concentrations of tricyclic terpanes increase relative to pentacyclic terpanes with increasing maturity (Aquino Neto *et al.*, 1981), but due to the low maturity of most samples, relative abundances are assumed to mostly reflect differences in source input. Although synthesized by prokaryotes (Orrison *et al.*, 1982), the occurrence of tricyclic terpanes is usually associated with contribution of algal material to the sedimentary organic matter (Aquino Neto *et al.*, 1981;

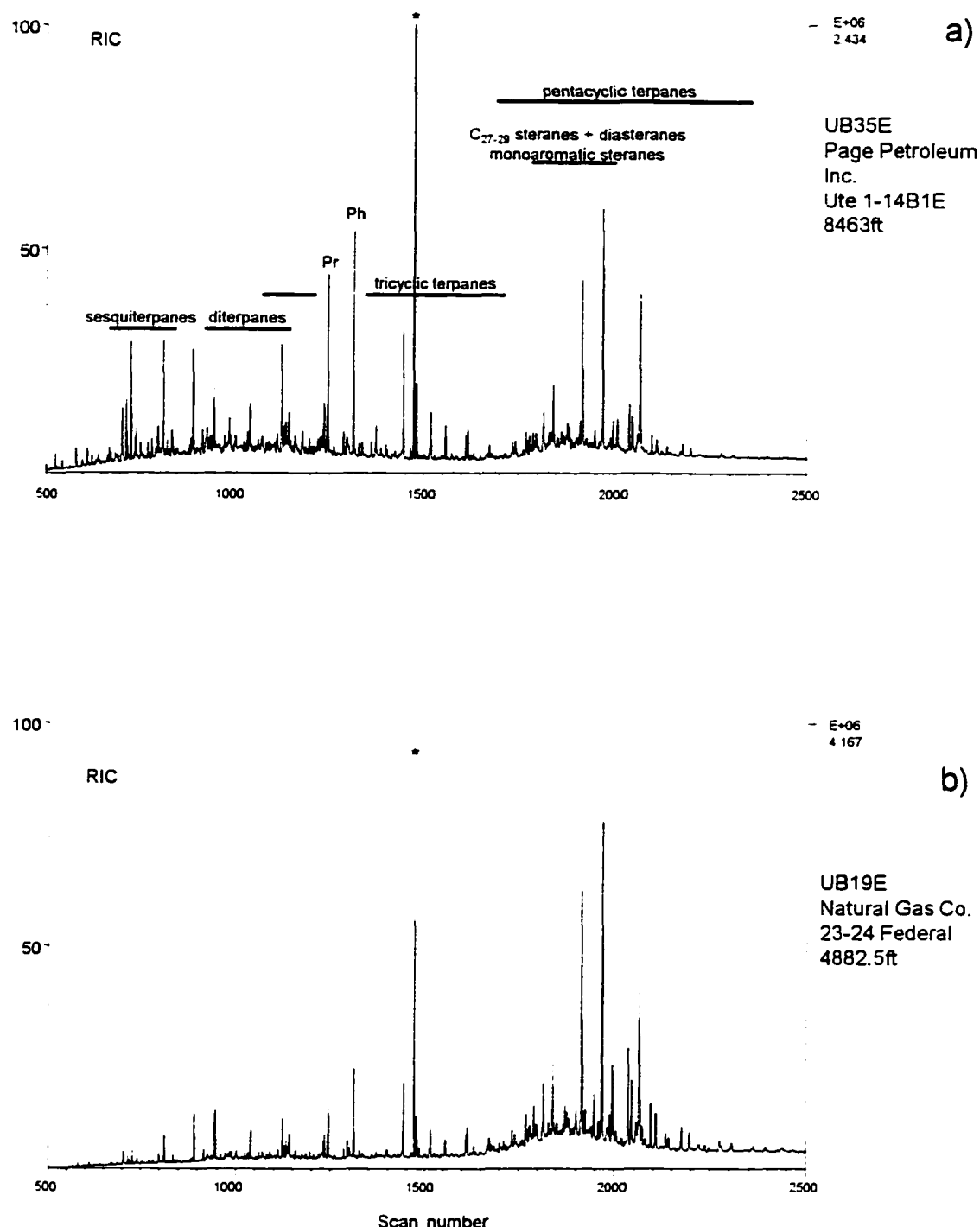


**Figure 14:** Representative reconstructed ion current chromatograms of source rock extract branched and cyclic fraction obtained with MID GC-MS. Regular type source rock in (a), oil shale type source rock in (b). \*=Internal standard C<sub>24</sub>D<sub>50</sub> (approx. 287 ppm); Pr=pristane, Ph=phytane.

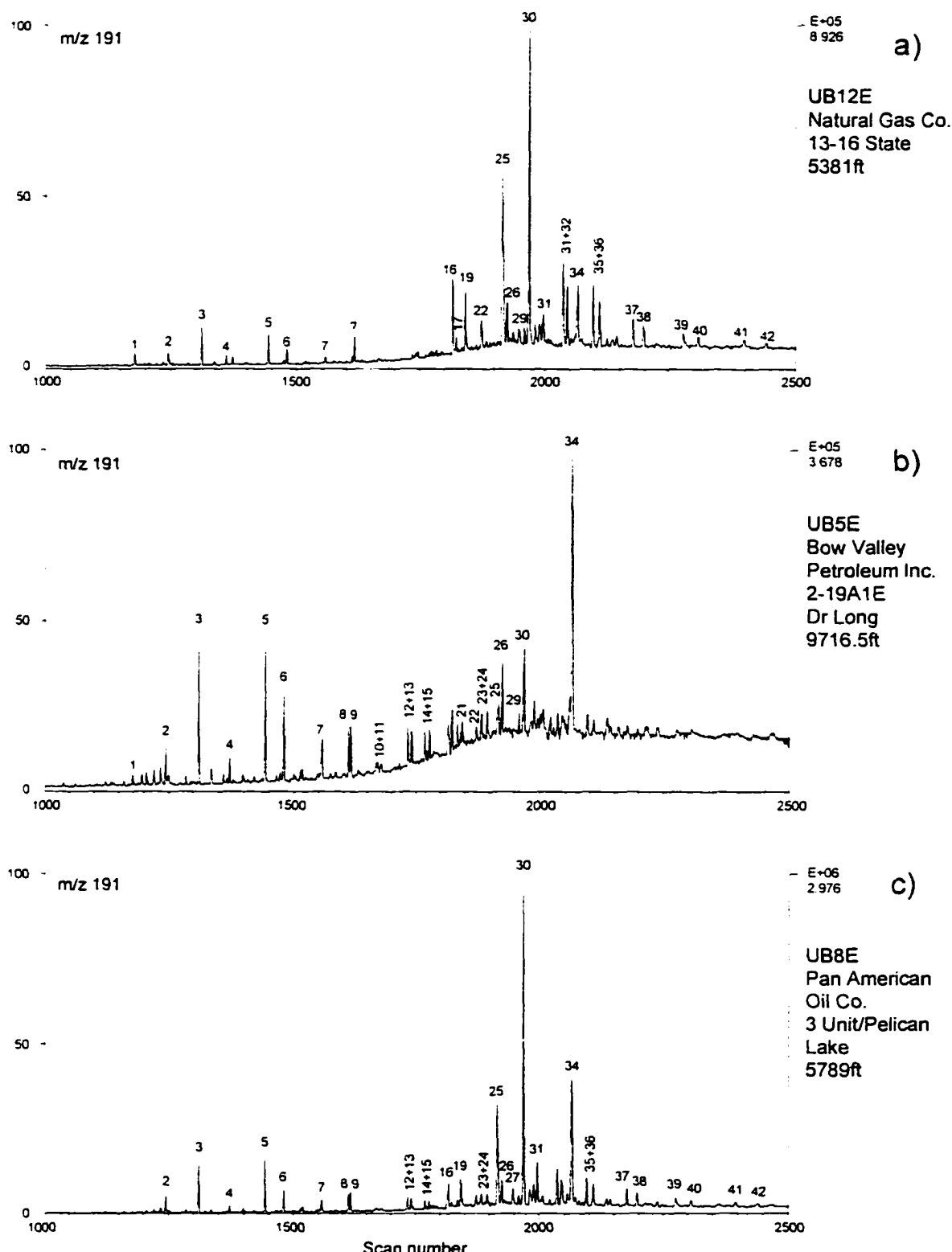


**Figure 15:** Representative mass-chromatograms  $m/z$  191 of source rock extracts branched and cyclic fractions. Peak labels refer to compounds listed in Appendix 1.2. Chromatogram (a) and (b) show regular type source rock, (c) is oil-shale type; peak labeled ? in (a) is possibly  $C_{24}$ -tetracyclic terpane.

Volkman *et al.*, 1989).

## HOPANOIDS

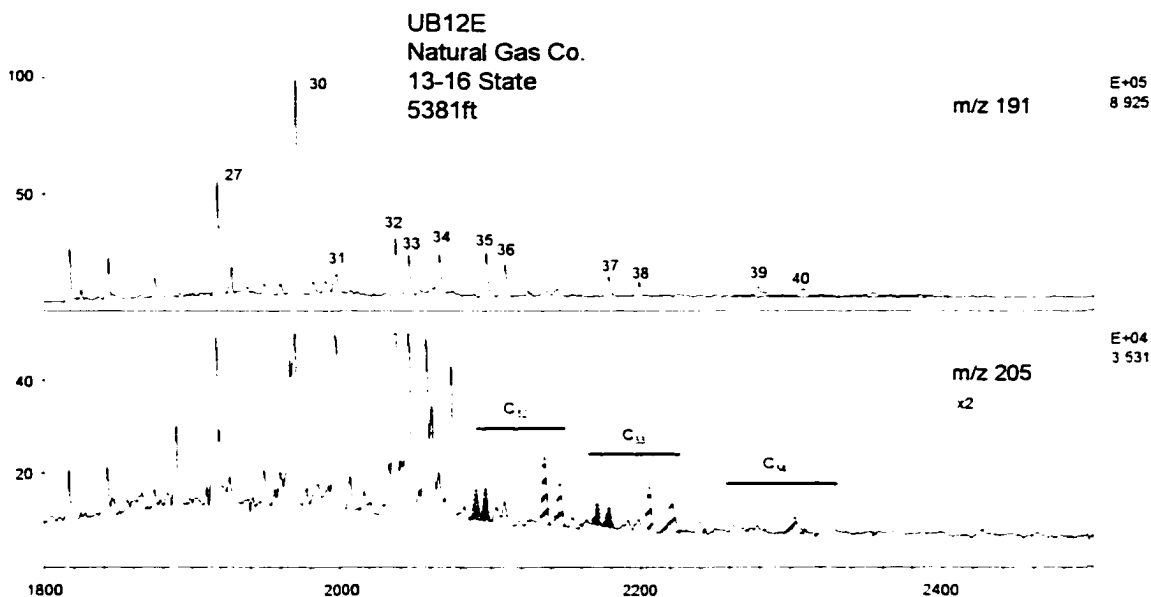
In many samples pentacyclic terpanes dominate the terpane fraction relative to tricyclic terpanes. In most of the chromatograms three peaks were present which could not be identified to any degree of certainty. The unknown compounds represented by peaks 17 and 22 (Fig. 15) may be diahopanes and/or norhopanes; peak 22 may be a bisnorhopane. Other terpanes detected include  $17\beta(H),21\alpha(H)$ -22,29,30-trisnormoretane (peak 21, Fig. 15b), a compound also identified in immature oils from China (Hong *et al.*, 1986). The thermally more stable  $17\alpha(H),21\beta(H)$ -22,29,30-trisnorhopane (Tm) is present along with  $18\alpha(H),21\beta(H)$ -22,29,30-trisnorhopane (Ts) and permitted calculation of the Ts/Tm ratios for nearly all samples (Appendix 5). Also identified was a C<sub>30</sub> diahopane ( $17\alpha(H)$ -15 $\alpha$ -methyl-27-norhopane; peak 26; Fig. 15a and b), as confirmed by GC-MS/MS m/z 412 to 191 metastable ion transition monitoring and comparison of analyses published by Moldowan *et al.* (1991). Formation of this compound through clay-catalyzed, diagenetic transformation of regular hopanes has been proposed but partial oxidation of  $17\alpha(H)$ -hopanes may provide an alternative origin (Moldowan *et al.*, 1991). The suspiciously broad peak of  $17\alpha(H),21\beta(H)$ -norhopane in many m/z 191 traces is caused by coelution of this compound with C<sub>29</sub>-Ts ( $18\alpha(H)$ -30-norneohopane; e.g. Fig. 15a). This coelution is one of the reasons why peak-heights were reported for analysis as opposed to the usually more reliable peak-areas. The two identified norneohopanes indicate that a homologous series of these compounds (Moldowan *et al.*, 1991) may be present in the samples. The C<sub>29</sub>-Ts has been shown to be thermally stable (e.g. Fowler and Brooks, 1990) and is suspected to originate from diplotene or diplopterol (Moldowan *et al.*, 1991). With no exception, extended homohopanes show a regular decrease of the relative abundance with increasing carbon number. Peters and Moldowan (1991)

suggested that, as a result of low sulfur in lacustrine settings, the sequestration and preservation of C<sub>35</sub>-homohopane in anaerobic environments is inefficient, thus enhanced concentration of extended hopanes rarely occurs.

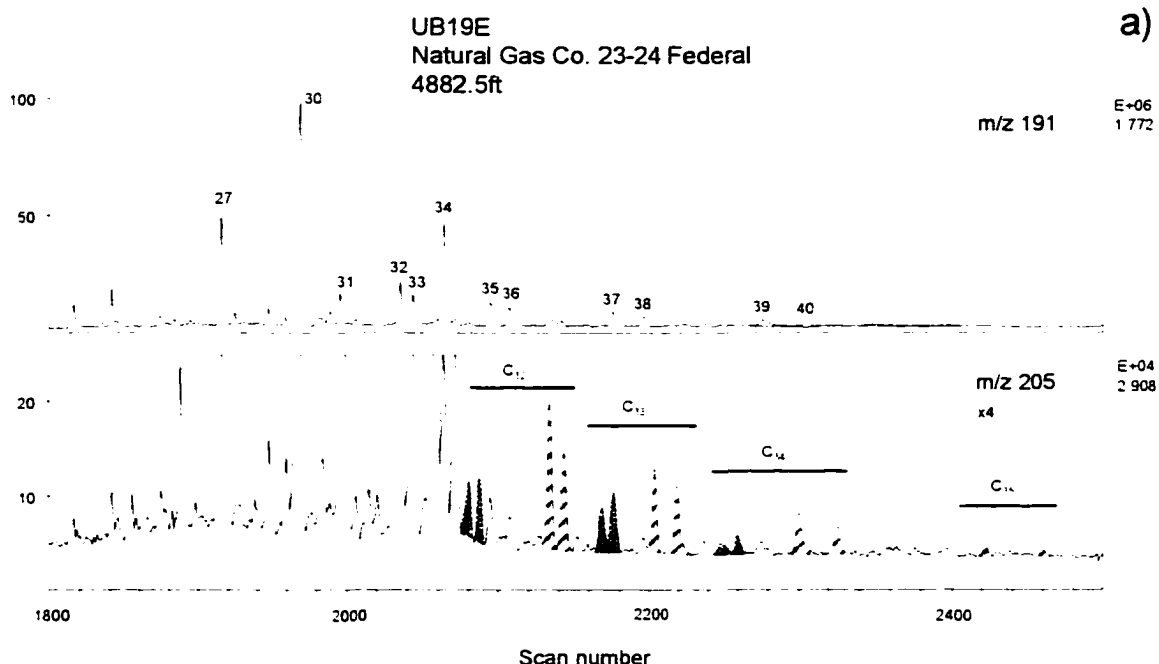
A C<sub>24</sub>-tetracyclic terpane was tentatively identified in a number of samples (e.g. Fig. 15a), but was not integrated into the GC-MS data matrix because of coelution with C<sub>26</sub> tricyclic terpane 20R. The compound was found in samples from peripheral areas of the basin and was not identified in oil-shale type extracts. Its presence is qualitatively indicated in Appendix 5. The C<sub>24</sub>-tetracyclic terpane is considered to be a thermocatalytic degradation product of regular pentacyclic terpanes (Ekwezor *et al.*, 1981). Philp and Gilbert (1986) report the compound in terrigenous Australian oils and its occurrence was recently found to be more closely related to oxic, paludal environments (Philp, 1994). A C<sub>24</sub> tetracyclic terpane was also identified in oils derived from carbonate and evaporite environments and related to microbial degradation of hopanes (e.g. Clark and Philp, 1989).

In the extended hopane region of the chromatograms of some samples, a series of methyl hopanes is present based on comparison of m/z 191 and 205 chromatograms (Fig. 16) and their relative abundances compared to regular hopanes are qualitatively indicated in Appendix 5. The series found in the source rock extracts examined in this study were tentatively identified as 2 $\alpha$ -methyl and 3 $\beta$ -methyl hopanes. Ruble and Philp (1991) described a series of 3 $\beta$ -methyl hopanes in their investigation of Uinta Basin solid bitumens. Methyl hopanes are present in most samples but appear to be more abundant in regular type source rock extracts. Methyl hopanes are interpreted to originate from aerobic methylotrophic bacteria (Summons and Jahnke, 1990), which, in turn, implicate the activity of obligate anaerobic methanogenic bacteria in the anaerobic hypolimnion or surface sediments of the lake (Killops and Killops, 1993). Schoell *et al.* (1994) and Ruble *et al.*

b)



a)

2 $\alpha$ (Me)-hopanes3 $\beta$ (Me)-hopanes

**Figure 16:** Methyl hopanes (shaded peaks) in two representative source rock extract branched and cyclic fractions. Chromatogram (a) shows regular source rock type, chromatogram (b) shows oil shale type sample; peak identification in Appendix 1.2

(1994) interpreted the  $\delta^{13}\text{C}$ -depleted methyl hopanes in Uinta Basin gilsonites, which are generated from mahogany zone oil-shales, as a product of methylotrophic bacteria living above an oxic/anoxic interface in Lake Uinta.

## NON-HOPANOID TERPANES

Minor traces of  $18\alpha(\text{H})$ -oleanane, eluting immediately before  $17\alpha(\text{H}),21\beta(\text{H})$ -hopane, were tentatively identified in many extracts (e.g. Fig. 15a and b). Although metastable ion transition of m/z 412 $\rightarrow$ 191 confirmed oleanane, the general low concentration in the branched and cyclic fractions did not allow the verifications suggested by Peters and Moldowan (1993). Relatively high oleanane-indices in Appendix 5 (samples UB5E, UB30E and UB47E) are due to low C<sub>30</sub>-hopanes abundances. The presence of oleanane may indicate a constant "background" of angiosperm-derived organic matter (ten Haven and Rullkötter, 1988), although its preservation and concentration also depends on diagenetic conditions (Murray *et al.*, 1997). Oleanane was generally present in very low concentration relative to  $17\alpha(\text{H}),21\beta(\text{H})$ -hopane in oil-shale type samples.

Gammacerane is present in highly variable relative concentrations. It should be noted that gammacerane and  $17\alpha(\text{H}),21\beta(\text{H})$ -hopane fragment into two ions with m/z 191 during GC-MS operation, thus overestimating the abundance of these compounds (Peters and Moldowan, 1993). Gammacerane is interpreted as a marker indicating hypersalinity and anoxic environments (ten Haven *et al.*, 1988) and is also present in highly variable absolute concentrations in the extracts (Appendix 5). The biological precursor of gammacerane, tetrahymanol, is a lipid in protozoan membranes and in phototrophic bacteria (Peters and Moldowan, 1993, and references therein). Recent reports indicate that tetrahymanol is also a neutral lipid in marine bacterivorous ciliate species, and has been proposed as a principal marker for these organisms in marine sediments (Harvey and McManus, 1991). Sinnighe Damsté *et al.* (1995) proposed gammacerane as a marker

for water stratification, since its occurrence is not restricted to sediments deposited under hypersaline conditions. Water density interfaces were shown to be locations of extensive microbial activity by Wakeham (1990) which provides a substrate for ciliates. Schoell *et al.* (1994) interpreted gammacerane as a marker for the stable density stratification in Lake Uinta during mahogany oil-shale deposition, and not as a marker for hypersalinity. Similar interpretations involving gammacerane and biomarker carbon-isotopic composition were recently made by Santos Neto *et al.* (1998) for lacustrine source rocks of the Poitugar Basin, Brazil.

### DESMETHYL STERANES

The m/z 217 chromatograms are dominated by regular desmethyl steranes and highly variable relative concentrations of diasteranes (Fig. 17). The distribution of C<sub>27</sub>-, C<sub>28</sub>- and C<sub>29</sub>-desmethyl steranes in Figure 18 is irregular and no trend associated with location or source rock type is apparent. The scatter of the samples is caused by the multiple sources that contribute desmethyl steranes to sedimentary organic matter within a lacustrine environment (*e.g.* Volkman, 1986). Note also the wide scatter of sterane distributions in the oil-shale type samples. As will be shown in the statistical analysis of the data, positive correlation of steranes and hopanes may indicate that both biomarker groups in part may be synthesized by organisms feeding on primary organic matter, *i.e.* bacteria in the case of the hopanes and possibly herbivorous zooplanton in the case of the steranes.

Compounds tentatively identified as C<sub>21</sub>- and C<sub>22</sub>-steranes (diginane and homodiginane; Requejo *et al.*, 1997) and minor concentrations of possibly other lower molecular weight steranes are present in a number of samples (Fig. 17a and b), most notably in those from deeper stratigraphic sections. Except for traces in samples UB2E and UB19E, lower molecular weight steranes do not occur in oil-shale type samples. The C<sub>21</sub>- and C<sub>22</sub>-steranes are interpreted as

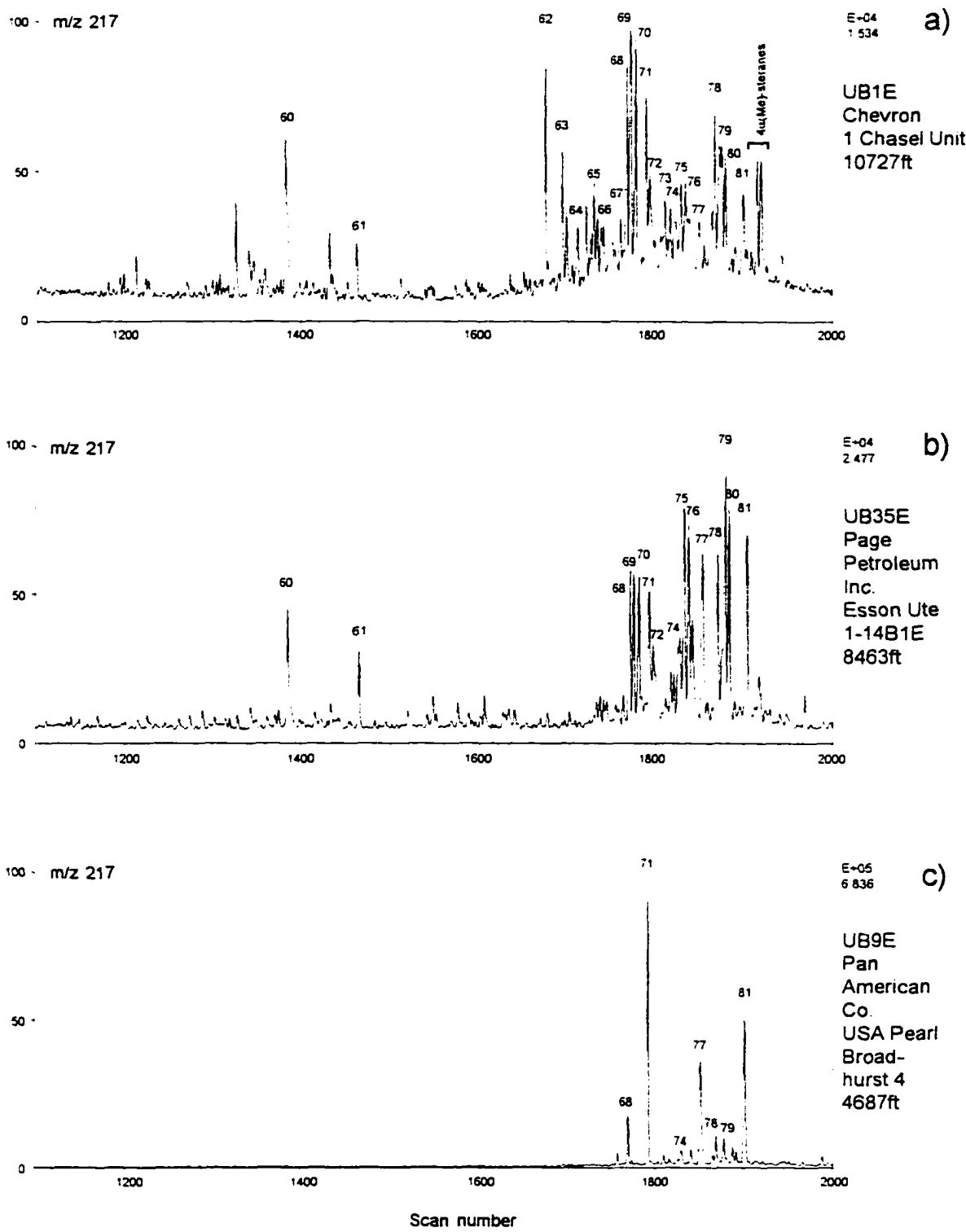


**Figure 17:** Representative mass-chromatograms m/z 217 of source rock extract branched and cyclic fraction ((a and b) regular type, (c) oil-shale type). Peak labels refer to compounds listed in Appendix 1.2. 4 $\alpha$ (Me)-steranes refer to 4 $\alpha$ (Me)-24-ethyl-14 $\beta$ (H),17 $\beta$ (H),20S+R-cholestanes.

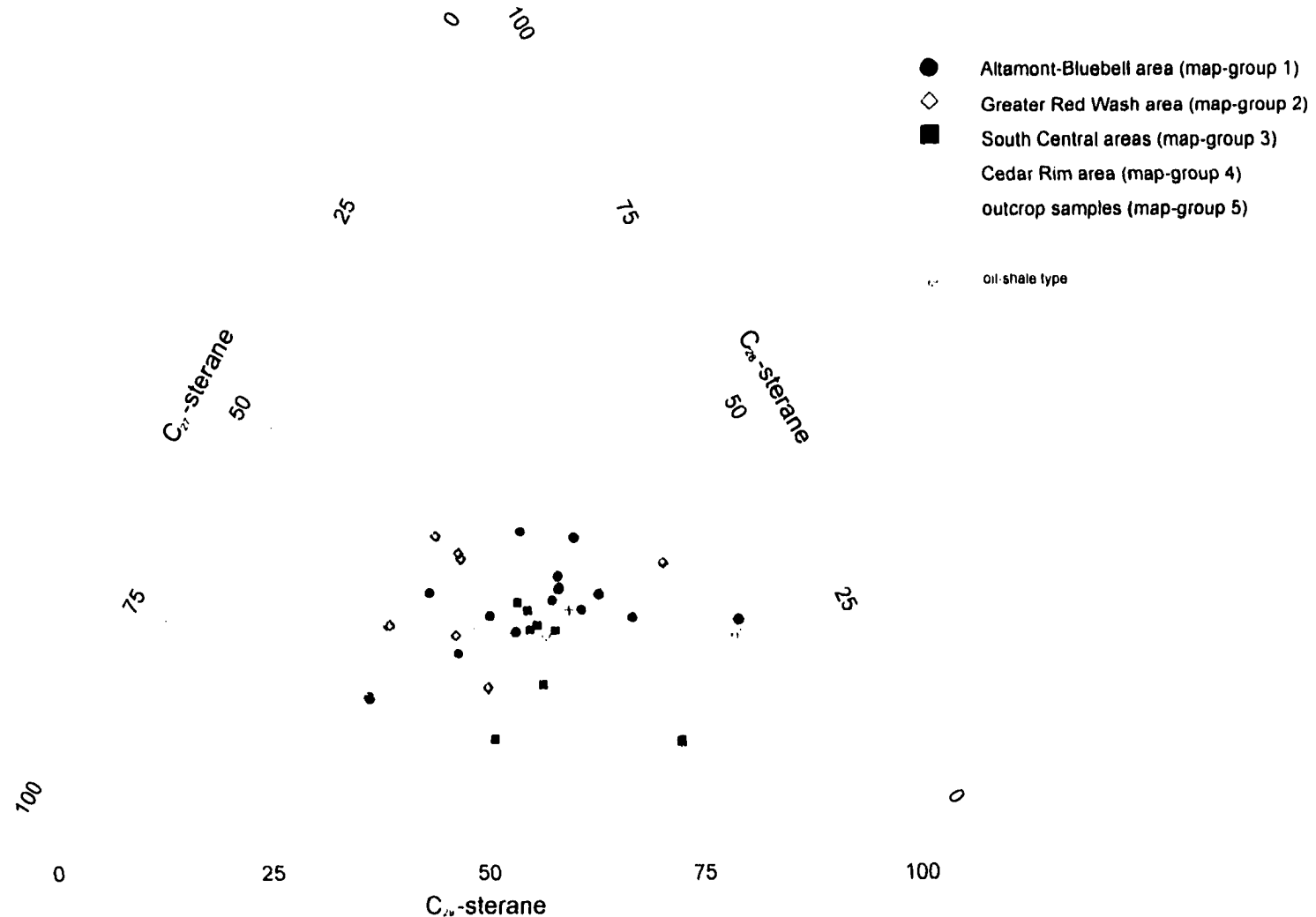


**Figure 18:** Ternary diagram of desmethyl sterane distribution (using 14 $\alpha$ (H),17 $\alpha$ (H),20R isomers) in Uinta Basin source rock extracts. Graph differentiates between map-groups and oil-shale vs. regular type extracts. Samples and % sterane values listed in Appendix 5.

indicators of elevated salinity (Wingert and Pomerantz, 1986), but a number of other possible origins have been suggested by Matveeva and Petrov (1997).

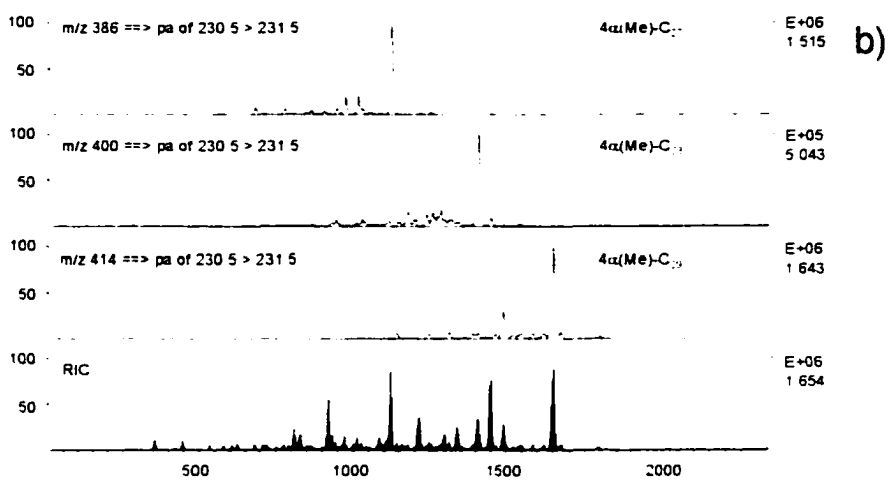
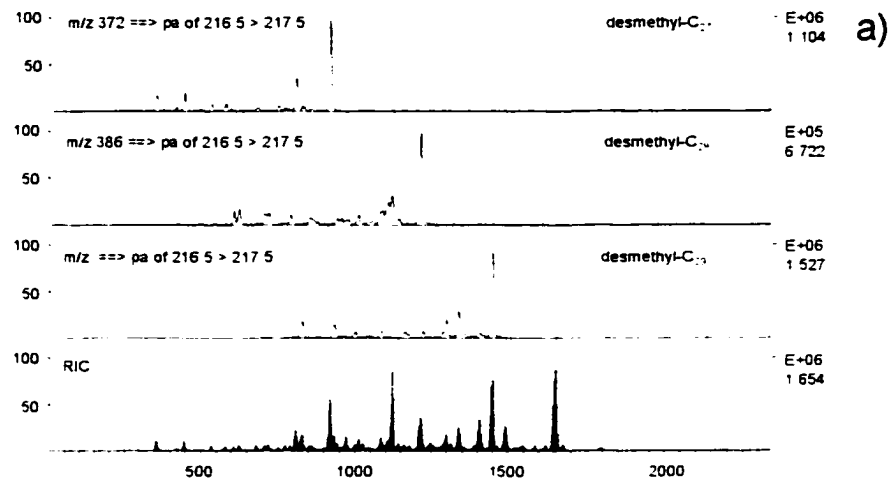
## DIASTERANES

Diasteranes are more abundant in stratigraphically lower, regular type source rock samples, which may be partly due to the higher thermal stability of diasteranes (Peters *et al.*, 1990). However, since the samples involved are generally of low maturity, it is assumed that the diasterane-index (definition in Appendix 1.1.: Appendix 5) reflects primarily the depositional environment. It has been proposed that diasteranes are formed via clay-catalysis in clastic-rich depositional environments (Sieskind *et al.*, 1979), although their occurrence has also been related to low pH, high Eh environments (Moldowan *et al.*, 1992). Lower molecular weight ( $C_{21}$  and  $C_{22}$ ) diasteranes have been described recently by Requejo *et al.* (1997) and may be present as well. No clear correlation could be found between diasteranes and  $C_{30}$  diahopanes.

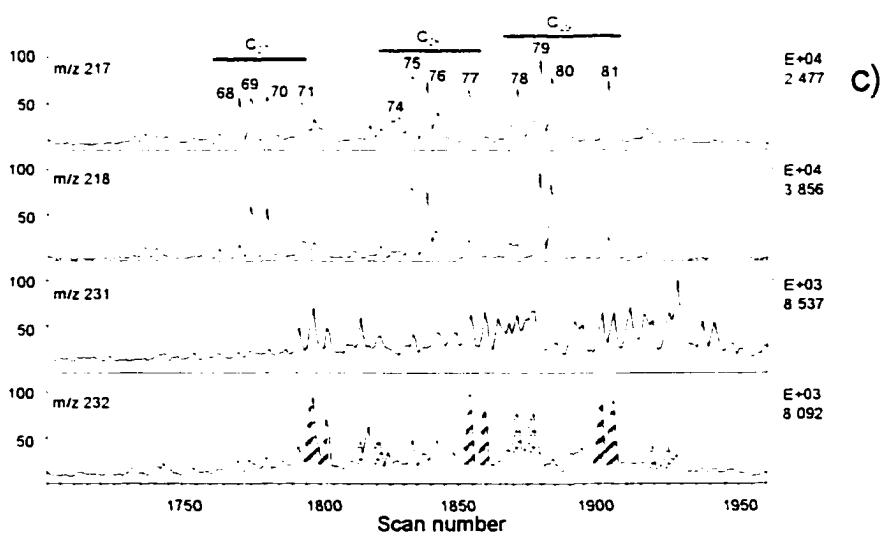
## METHYL STERANES

Methyl steranes are present in a number of samples and have been identified in GC-MS/MS experiments (Fig. 19) and by comparison with published chromatograms (e.g. Wolff *et al.*, 1985; Summons and Capon, 1991; Peters and Moldowan, 1993). The GC-MS/MS metastable ion transitions allowed identification of abundant  $4\alpha(Me)$ -steranes in the black shale facies outcrop sample from Indian Canyon (Fig. 19a). These compounds were not positively identified in mahogany zone shales and are rare or not present in other oil-shale type source rocks. Interestingly, Horsfield *et al.* (1994) found  $4\alpha(Me)$ -steranes to be the dominant steranes in Green River Formation oil-shales collected from the Luman Tongue and Laney Member of the Washaki Basin, Wyoming. In most cases when methyl steranes have been found, it appears that a series of  $3\beta(Me)$ -

UB41E  
black shale facies  
outcrop sample



UB35E  
Page Petroleum Inc.  
Esson Ute 1-14B1E  
8464ft



- 3β(Me)-steranes  
ββ-isomers
- 4α(Me)-steranes  
ββ-isomers

**Figure 19:** Methyl sterane identification in representative source rock extracts. Chromatograms (a) and (b) show metastable ion transitions, (c) compares characteristic ions obtained from MID GC-MS analysis. Note the distinct pattern of 3β(Me)- and 4α(Me) ββ-isomers in m/z 232. Labels refer to compounds listed in Appendix 1.2.

steranes is present (Fig. 19c), which has been identified by comparison of m/z 217, 218, 231, and 232. The  $14\beta(H),17\beta(H)$ -isomers of the  $3\beta(Me)$ -and  $4\alpha(Me)$ -steranes form a characteristic sequence of doublets apparent in the m/z 232 chromatograms but otherwise coelute with regular desmethyl and diasteranes in the chromatograms of the other ions (Fig. 19c). The  $2\alpha(Me)$ -steranes elute closer to the desmethyl counterparts than either  $3\beta(Me)$ - and  $4\alpha(Me)$ -steranes (Summons and Capon, 1988; Wang and Philp, 1997) and were not identified in any of the samples. Unequivocal methyl sterane identification was not possible in many cases and coelution problems, often also caused by fragments of the dominant hopane series, prevented incorporation of methyl steranes into the GC-MS data matrix. A qualitative indication of the abundance of methyl steranes relative to desmethyl steranes and diasteranes in m/z 217 is given in Appendix 5. The occurrence and abundance of methyl steranes is rather erratic in the lower Green River Formation samples and they are rare or do not occur in most of the oil-shale type samples of the upper Green River Formation. In cases when the  $4\alpha(Me)$ -steranes are present in oil-shale type samples, they are by no means as significant as in samples of the lower Green River Formation. Although not as diagnostic as dinosteranes, their abundance is viewed as indicative for the presence of dinoflagellates (Robinson *et al.*, 1984). However, other algae possibly synthesize these compounds (Goodwin *et al.*, 1988). Less diagnostic are the  $3\beta(Me)$ -steranes, which may be formed from sterols *via* bacterial rearrangement processes (Summons and Capon, 1991) but their occurrence may also be related to the depositional environment (Dahl *et al.*, 1992).

## MONOAROMATIC STEROIDS

Monoaromatic steroids (m/z 253) were present in many of the samples (Fig. 20), their abundance apparently related to the maturity of the samples. Oil-shale type samples show distinct m/z 253 responses while monoaromatic steroids in regular source rock type samples are often

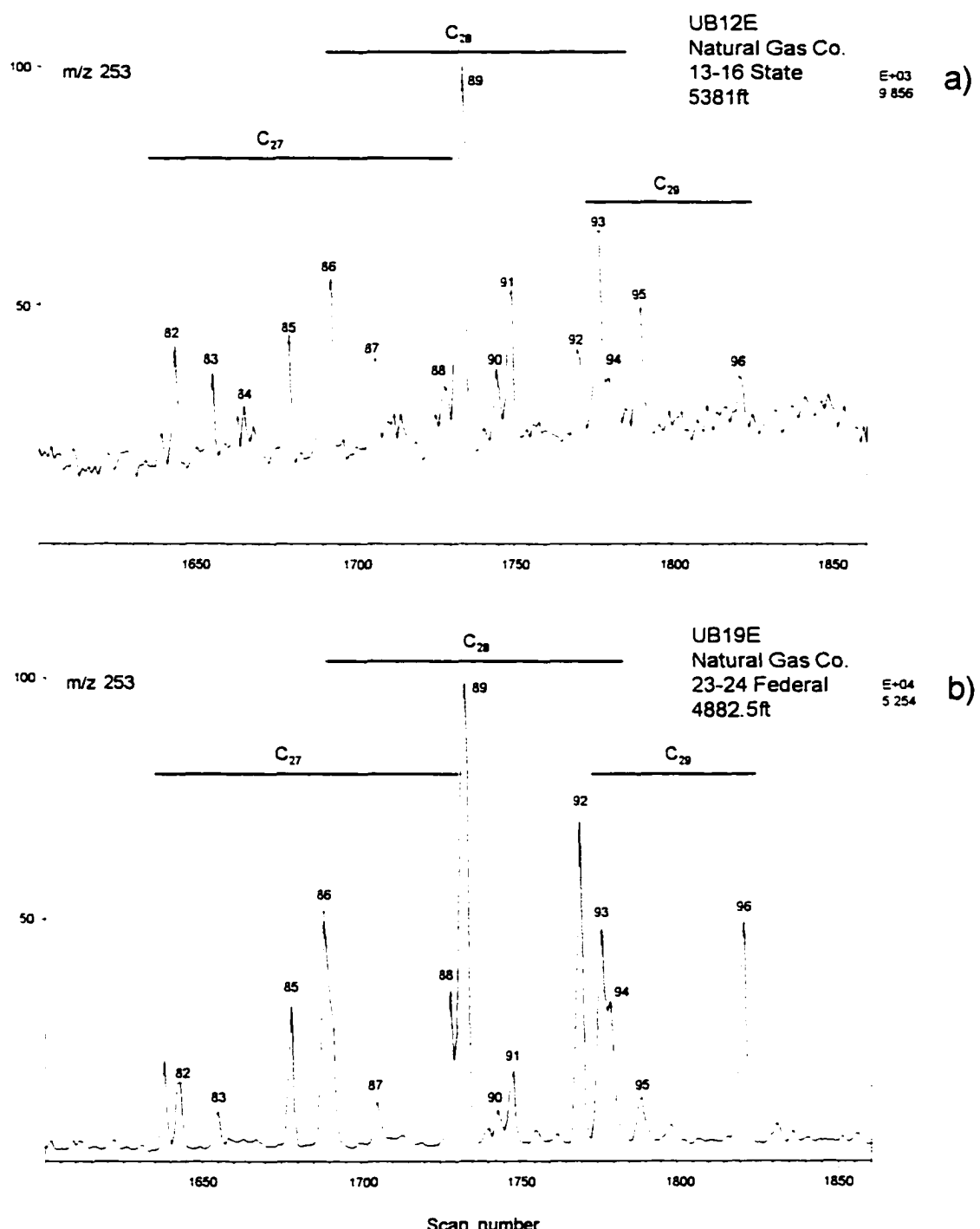


**Figure 20:** Representative chromatograms of monoaromatic steroids in the saturate fractions of Uinta Basin source rock extracts. Sample in (a) is a regular source rock type, sample (b) shows the  $m/z$  253 chromatogram of an oil-shale type sample. Peak identification is tentative because of coelution of a number of compounds; peak labels refer to compounds listed in Appendix 1.2

obliterated by isoprenoid fragments. Identification of compounds is tentative and based on standard and published chromatograms (e.g. Seifert *et al.*, 1981). However, the separation capacity of the column used in GC-MS analysis was not sufficient to resolve all peaks and rendered peak identification difficult. Therefore, peaks are only identified according to carbon number. Monoaromatic steroids are early diagenetic products derived from sterols with side chain double bonds (Riolo *et al.*, 1986) and may be more specific for their precursors than steranes (Peters and Moldowan, 1993).

## SESQUITERPANES AND DITERPANES

Investigation of bicyclic sesquiterpanes and diterpanes with ion m/z 123 showed high variations in the distribution of the identified compounds and also relative to other biomarkers (Fig. 14). Evaporative loss of sesquiterpanes during sample preparation may have altered the relative sesquiterpane abundance in some samples, and their distribution has to be interpreted with caution. Sesqui- and diterpanes are related to the contribution of bacterial organic matter (Alexander *et al.*, 1984) and higher plant (conifer) resins, respectively (e.g. Alexander *et al.*, 1987). The dominant components were tentatively identified as drimane and homodrimane (peaks 45 and 49), an unidentified diterpane (peak 53), norisoprimarane (peak 54) and 16 $\beta$ (H)-phyllocladane (peak 59). Eudesmane could not be identified unequivocally in the samples. Identification was performed using GC-MS/MS parent to m/z 123 transitions, standard chromatograms and comparison to published chromatograms (e.g. Weston *et al.*, 1989; Oung and Philp, 1994). Representative examples for sesqui- and diterpane distributions are shown in Figure 21.

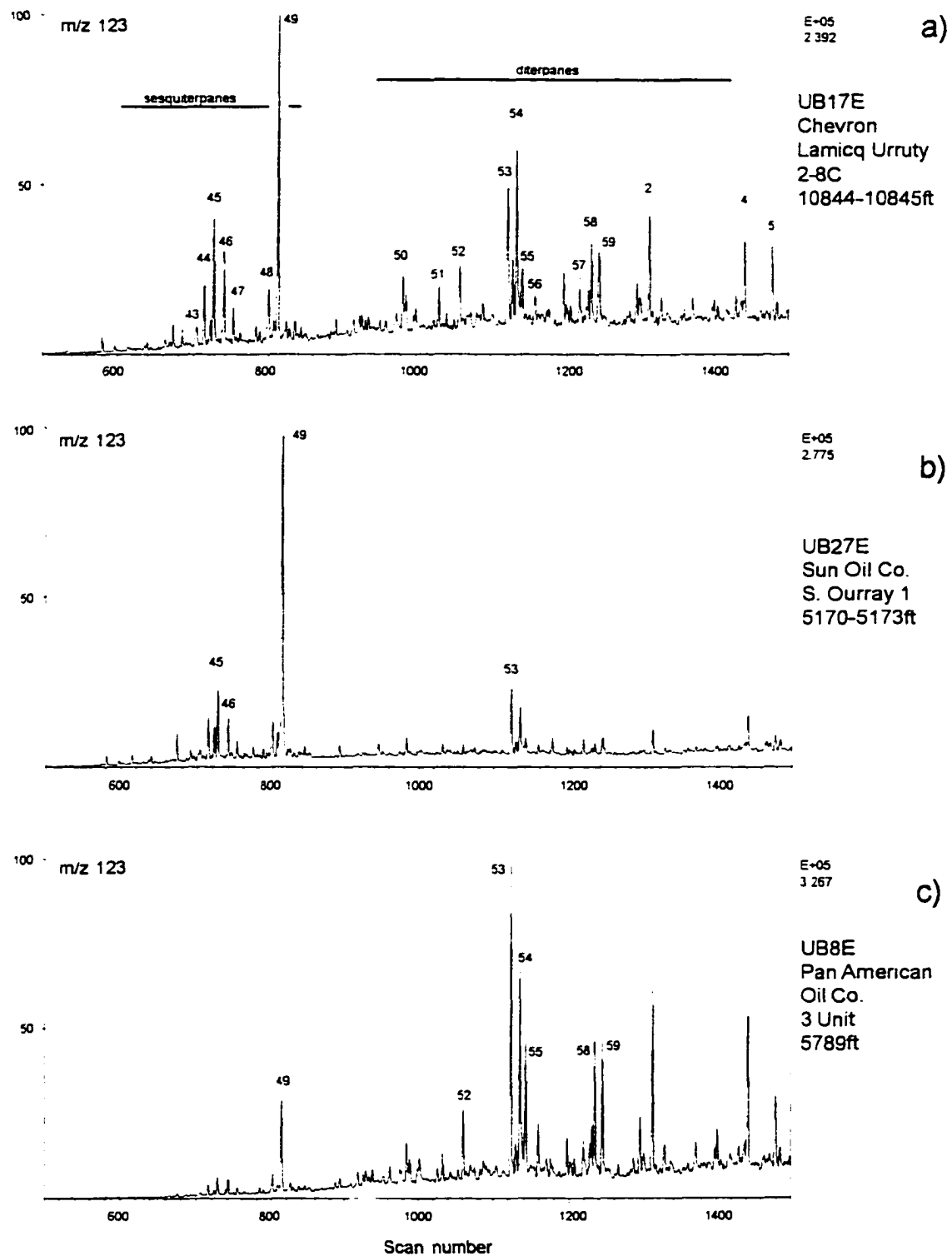


**Figure 21:** Representative examples for sesquiterpane and diterpane distributions in Uinta Basin source rock extract branched and cyclic fractions, determined with MID GC-MS. Chromatogram (a and b) are from regular type source rocks, (c) is an oil-shale type source rock. Peak labels refer to compounds listed in Appendix 1.2.

### 6.1.2.2 Principal Component Analysis (PCA) of Source Rock Extract GC-MS data

The PCA of the first principal components (PC) based on variance-covariance matrices using 96 ( $m=96$ ; peak heights are listed Appendix 4)) and 20 ( $m=20$ ) selected variables of the same data set (peaks for PCA with  $m=20$  are listed in Table 2) and 35 source rock samples are reported in Table 4a and b. Additionally, a PCA using a correlation matrix with  $m=20$  is provided in Table 4c for comparison of PCA performance. Samples of very high maturity (UB33E, UB34E and UB46E) and a sample with potential contamination based on Rock-Eval PI (UB32E) have been excluded from the analysis.

m=96, variance-covariance matrix					
a)	PC	Eigenvalue	% Variance	Cumulative % variance	Broken-stick eigenvalue
1	3.785	41.4	41.4	0.491	
2	1.625	17.8	59.2	0.395	
3	1.045	11.4	70.6	0.348	
4	0.607	6.6	77.2	0.316	
5	0.499	5.5	82.6	0.292	
6	0.358	3.9	86.5	0.273	
7	0.319	3.5	90.0	0.257	
8	0.203	2.2	92.2	0.243	

m=20, variance covariance matrix					
b)	PC	Eigenvalue	% Variance	Cumulative % variance	Broken-stick eigenvalue
1	3.877	46.6	46.6	1.497	
2	1.655	19.9	66.5	1.081	
3	0.974	11.7	78.2	0.873	
4	0.594	7.1	85.3	0.734	
5	0.425	5.1	90.4	0.630	

m=20, correlation matrix					
c)	PC	Eigenvalue	% Variance	Cumulative % variance	Broken-stick eigenvalue
1	8.113	40.6	40.6	3.598	
2	3.356	16.8	57.4	2.598	
3	2.363	11.8	69.2	2.098	
4	1.317	6.6	75.8	1.764	
5	1.065	5.3	81.1	1.514	

**Table 5:** Principal component analysis results (using 96 variables in (a) and 20 variables in (b)), based on the variance-covariance matrix of GC-MS peak-heights obtained from the analysis of the branched and cyclic fractions of source rock extracts. Results of the PCA using a correlation matrix with 20 variables ( $m=20$ ) are shown in (c).

According to the broken-stick model PC1 to 7 comprise more variance than explicable by chance alone when using 96 variables and the variance-covariance matrix (Table 4a). Thus the dimensionality of the data set is not reduced sufficiently. Restricting the number of variables to  $m=20$  shows that the dimensionality in this analysis can be reduced to 3 significant principal components which comprise 78.2% of the total variance (Table 4b). A similar result is obtained in the PCA of the correlation matrix of 20 variables, although the first 3 principal components are associated with a reduced portion of the total variance (69.2%; Table 4c).

#### *6.1.2.2.1 Principal Component Loadings - Source Rock Extract Analysis*

The first step in the PCA is the interpretation of the variables which influence the individual principal components. In Figure 22 bar diagrams of the first three principal components obtained from the variance-covariance based PCA using 96 variables (Fig.22a) and 20 variables (Fig.22b) are shown. Comparison of the loadings of variables used in both analyses show similar patterns and magnitudes. Although many variables in the first analysis have to be considered insignificant, the bar diagram in Figure 22a indicates a well defined separation of biomarker groups in the analysis. Loadings distribution and signs obtained for PC1 of the correlation matrix based PCA ( $m=20$ ) in Figure 22c are comparable to the results of the variance-covariance analysis in Figure 22b. However, the patterns of the loadings of PC2 and PC3 in Figure 22c are difficult to interpret, e.g. the high loadings and significance of C31 hopane S+R (peaks 32 and 33) could not be verified by inspection of the raw data. The relative abundance of gammacerane as expressed by PC2 (Figure 22b) in the PCA of the variance-covariance matrix on the other hand was found to be most useful in the characterization and differentiation of the extract samples. Therefore, and for reasons given in Chapter 5.5, the results of the variance-covariance based PCA with 20 variables are used in the exploratory analysis of the source rock extracts GC-MS analysis. The input matrix

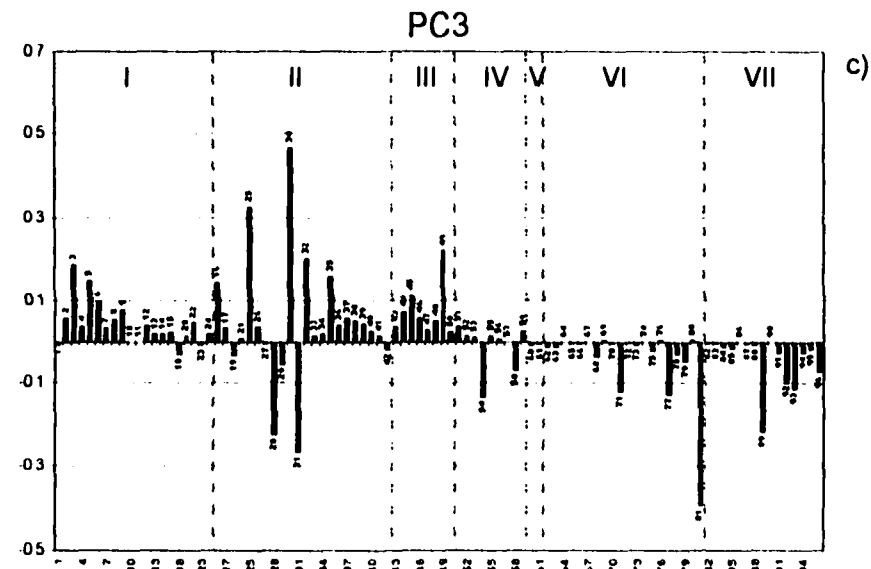
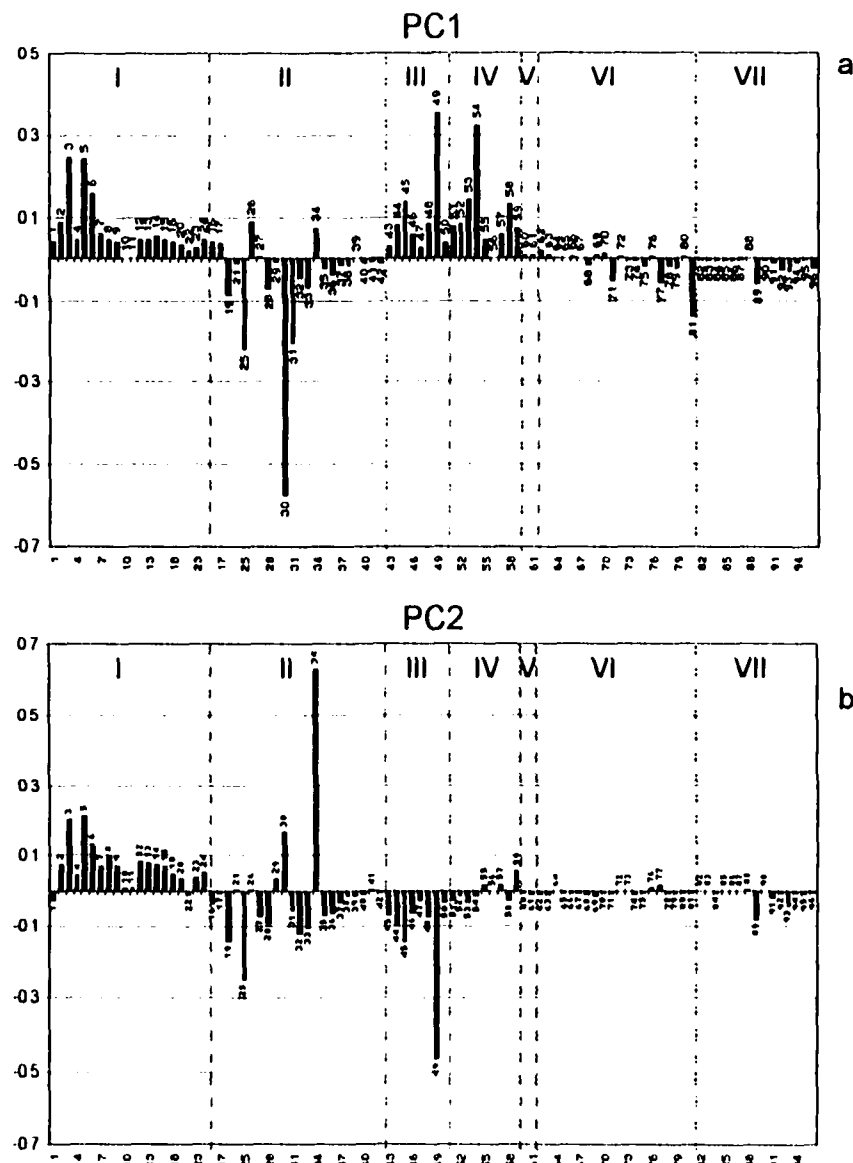
of normalized peak heights is given in Table 6, which also lists the original variance associated with each variable. The complete results of this PCA are given in Appendix 4.2.

#### VARIANCE-COVARIANCE BASED PCA (m=20) - PC1

The PC1 is dominated by the high absolute magnitude of C<sub>30</sub> hopane (peak 30), which is negatively loaded with other hopanes (Figure 22a and b) and the C<sub>29</sub>  $\alpha\alpha$  20R desmethyl steranes (C<sub>27</sub> and C<sub>28</sub> sterane fall below the suggested cutoff value of |0.118|; Appendix 4.2). These compounds are negatively correlated to the tricyclic terpanes, sesquiterpanes, diterpanes and C<sub>30</sub> diahopane. This PC appears to represent the relative proportions of bacterial and primary organic matter derived from algae and higher plants. Bacterial biomarkers both may represent primary organic matter (*e.g.* derived from autotrophs such as cyanobacteria) or prokaryotes reworking primary organic matter. Bacterial production is generally high in lacustrine systems (Kelts, 1988), although bacterial reworking of organic matter proceeds at the expense of primary organic matter with no net addition of organic carbon (Meyer and Ishiwatari, 1993). The sesquiterpanes are also derived from bacterial sources through degradation of hopanoids (Alexander *et al.*, 1984), but recent interpretations associate these compounds with the degradation of higher plant material in oxic environments (Philp, 1994). The positive correlation of hopanes/morettanes and C<sub>29</sub>  $\alpha\alpha$  20R desmethyl sterane in this PC is possibly related to variance introduced by maturity variations between samples and does not represent source differences. Maturity related variance may also be the cause for the positive loading of C<sub>30</sub> diahopane, considering the high thermal stability of this compound (Moldowan *et al.*, 1991). Maturity also influences the relative abundance of tricyclic terpanes, sesquiterpanes and diterpanes and PC1 has to be used with caution. However, the maturity of the 35 samples included in the analysis ranges from immature to early mature (see Chapter 6.2) such that the biomarker distributions and PC1 are assumed to represent mainly source

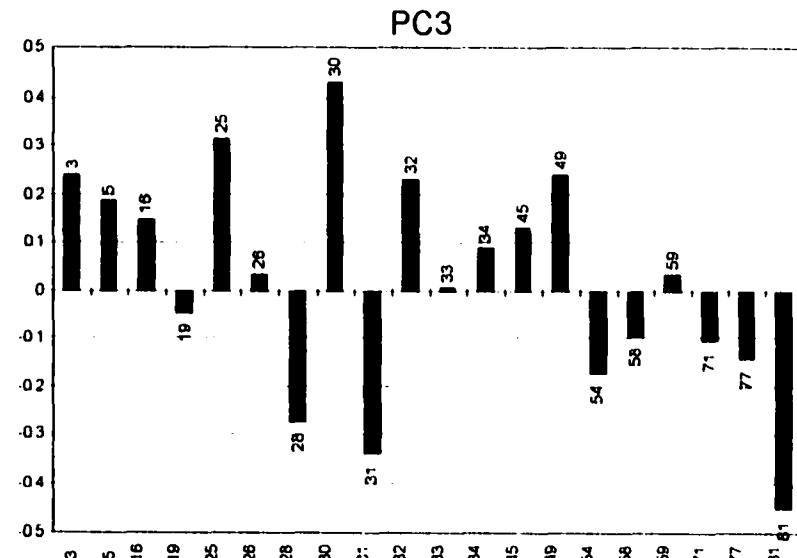
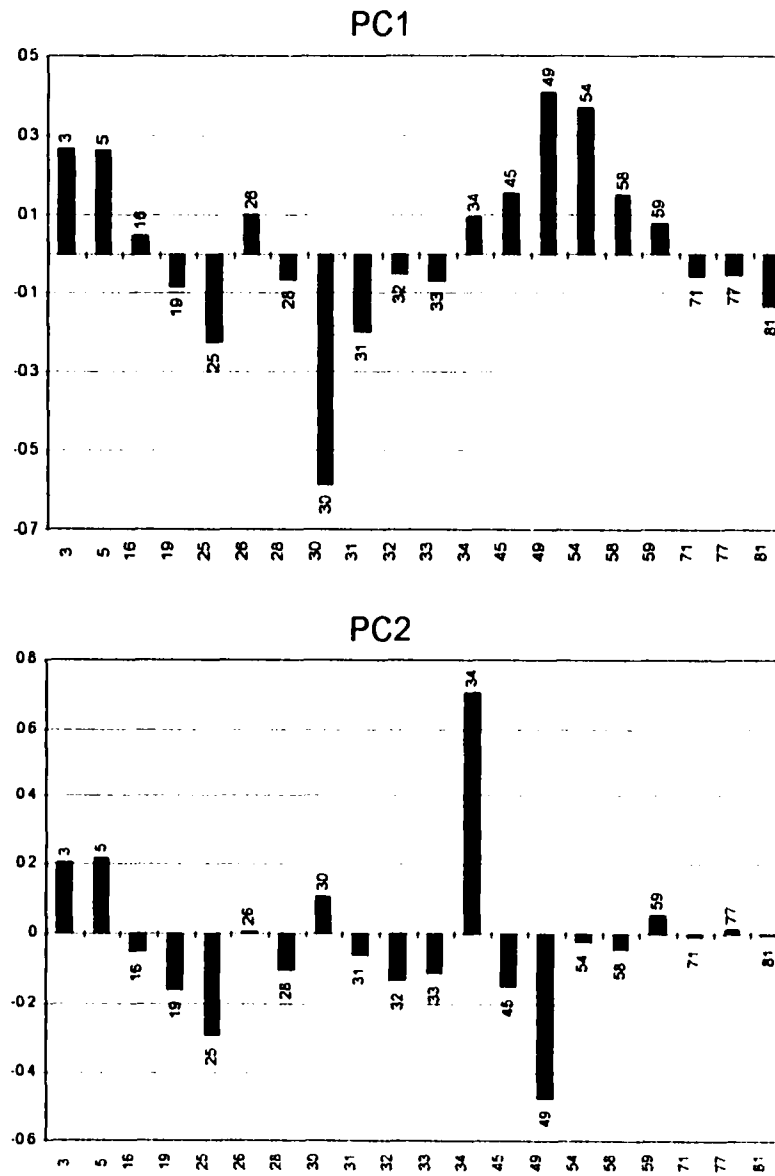
	3	5	16	19	25	26	28	30	31	32	33	34	45	49	54	58	59	71	77	81
UB5E	0.38466	0.37469	0.07918	0.02735	0.0734	0.19931	0.02578	0.20902	0.02646	0.06656	0.04098	0.84437	0.08479	0.27698	0.31105	0.06877	0.08723	0.00903	0.00449	0.0078
UB1E	0.38495	0.3098	0.10855	0.05339	0.09455	0.07553	0.07553	0.19801	0	0.06673	0.06498	0.12075	0.19717	0.70429	0.3238	0.10557	0.0562	0.03931	0.01051	0.02005
UB2E	0.19399	0.15743	0.03446	0.18961	0.3772	0.01871	0.05268	0.82626	0.19006	0.11516	0.09805	0.11749	0.00458	0.02338	0.04053	0.00898	0.04242	0.02377	0.02511	0.03791
UB3E	0.11876	0.11826	0.02636	0.16568	0.56519	0.01485	0.06419	0.74843	0.10644	0.13284	0.06676	0.13342	0.00686	0.014	0.00386	0.00371	0.01268	0.00853	0.02492	0.06637
UB4E	0.20324	0.19914	0.08575	0.12187	0.41415	0.04423	0.03739	0.78474	0.08595	0.13217	0.09241	0.23185	0.05572	0.10247	0.05982	0.02208	0.03717	0.00384	0.00264	0.00267
UB47E	0.23936	0.35193	0.04375	0.03691	0.10084	0.16511	0.02123	0.30836	0.04109	0.10193	0.07687	0.72685	0	0.22735	0.2818	0.04702	0.05544	0.00434	0.00412	0.00855
UB36E	0.46377	0.36613	0.04411	0.1222	0.30951	0.02274	0.02831	0.63798	0.0684	0.10026	0.07487	0.23908	0.01092	0.01854	0.05405	0.05609	0.21487	0.00284	0.00325	0.00456
UB17E	0.3004	0.3155	0.13788	0.08084	0.23005	0.1335	0.02271	0.67606	0.07385	0.14346	0.06813	0.26043	0.12559	0.31037	0.17839	0.04872	0.08181	0.00684	0.00476	0.00688
UB18E	0.28859	0.28805	0.14509	0.07188	0.27289	0.18009	0.03344	0.69008	0.07787	0.15951	0.12748	0.2809	0.15481	0.21865	0.15154	0.03453	0.08229	0.00388	0.00258	0.00458
UB37E	0.08635	0.07827	0.01083	0.11904	0.33785	0.00598	0.05458	0.70443	0.32127	0.07323	0.06284	0.49003	0.00283	0	0.00306	0.00299	0.00758	0.02941	0.03584	0.06208
UB38E	0.10781	0.10301	0.1078	0.04754	0.22492	0.09985	0.04023	0.88807	0.09586	0.13557	0.10608	0.2222	0.03347	0.1306	0.07132	0.02446	0.02698	0.01103	0.00527	0.00921
UB35E	0.451	0.28389	0.08941	0.08232	0.24312	0.01238	0.02006	0.4609	0.04025	0.07356	0.05687	0.40624	0.338	0.36378	0.04888	0.03183	0.09029	0.00652	0.01037	0.01233
UB16E	0.31534	0.2897	0.10932	0.05728	0.20907	0.14766	0.02283	0.76882	0.07865	0.14721	0.08411	0.24952	0.05342	0.12984	0.14588	0.03587	0.07592	0.0024	0.0031	0.00303
UB22E	0.08065	0.01986	0.00495	0.10825	0.1881	0.00253	0.09182	0.60212	0.38978	0.07704	0.10536	0.16871	0.01749	0.00926	0.00354	0.00341	0.01025	0.06818	0.18183	0.27014
UB10E	0.18258	0.1489	0.1184	0.06964	0.29658	0.08542	0.04237	0.84126	0.09104	0.17193	0.10856	0.23445	0.0239	0.09732	0.06807	0.01874	0.03908	0.01065	0.00523	0.0057
UB11E	0.3	0.23382	0.07417	0.13338	0.33639	0.04455	0.07038	0.71773	0.13199	0.17987	0.12522	0.31381	0.02759	0.08854	0.06682	0.01445	0.06512	0.06833	0.04767	0.09387
UB19E	0.17228	0.15418	0.08329	0.12948	0.38121	0.04012	0.08259	0.76842	0.11509	0.1518	0.10329	0.33922	0.04301	0.09682	0.04658	0.00941	0.04349	0.03819	0.01965	0.0297
UB20E	0.26393	0.24802	0.03629	0.05656	0.15698	0.03642	0.02877	0.54543	0.0678	0.07057	0.05826	0.70358	0.04953	0.11246	0.09082	0.02171	0.05788	0.04857	0.0283	0.04351
UB7E	0.08885	0.10748	0.03044	0.07029	0.1598	0.02148	0.04102	0.88858	0.10163	0.05398	0.04514	0.23504	0.01688	0.03871	0.08018	0.01463	0.04509	0.18911	0.07362	0.18818
UB8E	0.12388	0.12359	0.08509	0.09353	0.25379	0.05514	0.0498	0.86081	0.10406	0.06824	0.06729	0.33634	0	0.01876	0.06439	0.01225	0.04689	0.0148	0.01368	0.01005
UB8E	0.14128	0.15238	0.08587	0.0742	0.26379	0.08338	0.04165	0.85717	0.10523	0.0948	0.06318	0.32754	0.00832	0.02563	0.05549	0.00977	0.03564	0.01324	0.0121	0.01075
UB9E	0.05887	0.03383	0.02014	0.095	0.25515	0.00881	0.13884	0.90158	0.24869	0.06978	0.07727	0.1225	0.01309	0.01381	0.01957	0.00887	0.02209	0.02023	0.01803	0.01689
UB29E	0.15008	0.12312	0.09487	0.12651	0.34478	0.09887	0.04809	0.70208	0.11119	0.20282	0.1429	0.35738	0.08972	0.31075	0.07281	0.01321	0.0317	0.01673	0.01258	0.02252
UB14E	0.24581	0.18118	0.19166	0.14752	0.43088	0.18934	0.05031	0.63008	0.0948	0.21715	0.14063	0.1189	0.08348	0.2731	0.21501	0.11582	0.05568	0.00878	0.00413	0.01188
UB21E	0.22915	0.20317	0.05852	0.03849	0.08223	0.07247	0.02906	0.13905	0.04008	0.051	0.0288	0.02677	0.29295	0.74076	0.43501	0.18634	0.08931	0	0	0
UB13E	0.20854	0.21469	0.03991	0.06396	0.29551	0.12827	0.03792	0.73509	0.11145	0.29581	0.1771	0.2628	0.02781	0.21559	0.08262	0.01809	0.03861	0.0305	0.02511	0.03666
UB12E	0.08888	0.07311	0.17158	0.14688	0.36438	0.09095	0.03119	0.6847	0.06084	0.19072	0.13313	0.13151	0.23195	0.43197	0.07837	0.02513	0.02616	0.00486	0.00377	0.00733
UB25E	0.07281	0.04686	0.10318	0.18871	0.36808	0.07839	0.04248	0.69065	0.13683	0.18035	0.13142	0.10163	0.1089	0.46435	0.05855	0.01813	0.02032	0.00857	0.00808	0.01102
UB26E	0.0309	0.02558	0.02526	0.26528	0.54342	0.05479	0.13385	0.52633	0.21263	0.28982	0.18384	0.06201	0.07728	0.39773	0.03547	0	0	0.01369	0.00581	0.04042
UB27E	0.01202	0.009525	0.07359	0.17104	0.51525	0.07759	0.09008	0.71408	0.11132	0.19942	0.13351	0.06371	0.07563	0.29033	0.03844	0.01227	0.00909	0.0201	0.0045	0.02071
UB30E	0.32243	0.37388	0.09258	0.10782	0.08347	0.21068	0.077	0.08	0	0	0	0.10463	0.06048	0.1872	0.68743	0.35125	0.18144	0.01286	0.01228	0.02164
UB42E	0.03038	0.02802	0.03284	0.25765	0.39822	0.05524	0.14015	0.71552	0.23041	0.22934	0.17996	0.12413	0	0.08112	0.02409	0	0.01075	0.22441	0.06801	0.14784
UB41E	0.0424	0.03878	0.05011	0.1817	0.43725	0.0423	0.09122	0.74788	0.17559	0.12854	0.14781	0.1554	0.0092	0.02258	0.01968	0	0.01573	0.18897	0.12043	0.23659
UB39E	0.04318	0.01175	0.00804	0.08798	0.08125	0.005	0.07318	0.78844	0.19811	0.02307	0.03598	0.48087	0.00333	0.00229	0.00853	0.00115	0.00558	0.04348	0.10418	0.30564
UB45E	0.00747	0.00991	0.02753	0.1989	0.27184	0.08744	0.40798	0.52852	0.45032	0.05189	0.23555	0.05729	0	0.00182	0.01145	0.00305	0.00514	0.02761	0.07671	0.4041
Mean	0.18412	0.16803	0.07041	0.11326	0.2843	0.07448	0.06618	0.8504	0.12837	0.1278	0.09983	0.25548	0.06648	0.18392	0.11241	0.0384	0.04816	0.03479	0.02745	0.06225
Var	0.0162	0.0134	0.0021	0.0035	0.0185	0.0033	0.0046	0.0485	0.0102	0.0049	0.0025	0.0318	0.0071	0.0370	0.0205	0.0044	0.0019	0.0030	0.0014	0.0098
Std dev	0.1272	0.1158	0.0463	0.0584	0.1359	0.0579	0.0678	0.2203	0.1011	0.0697	0.0499	0.1784	0.0841	0.1923	0.1432	0.0687	0.0440	0.0545	0.0380	0.0982

Table 6: Normalized peak-heights of 20 GC-MS peaks used in the PCA (m=20), source rock extracts; peak (variable) numbers are listed in Appendix 1 2  
var = variance; std.dev. = standard deviation



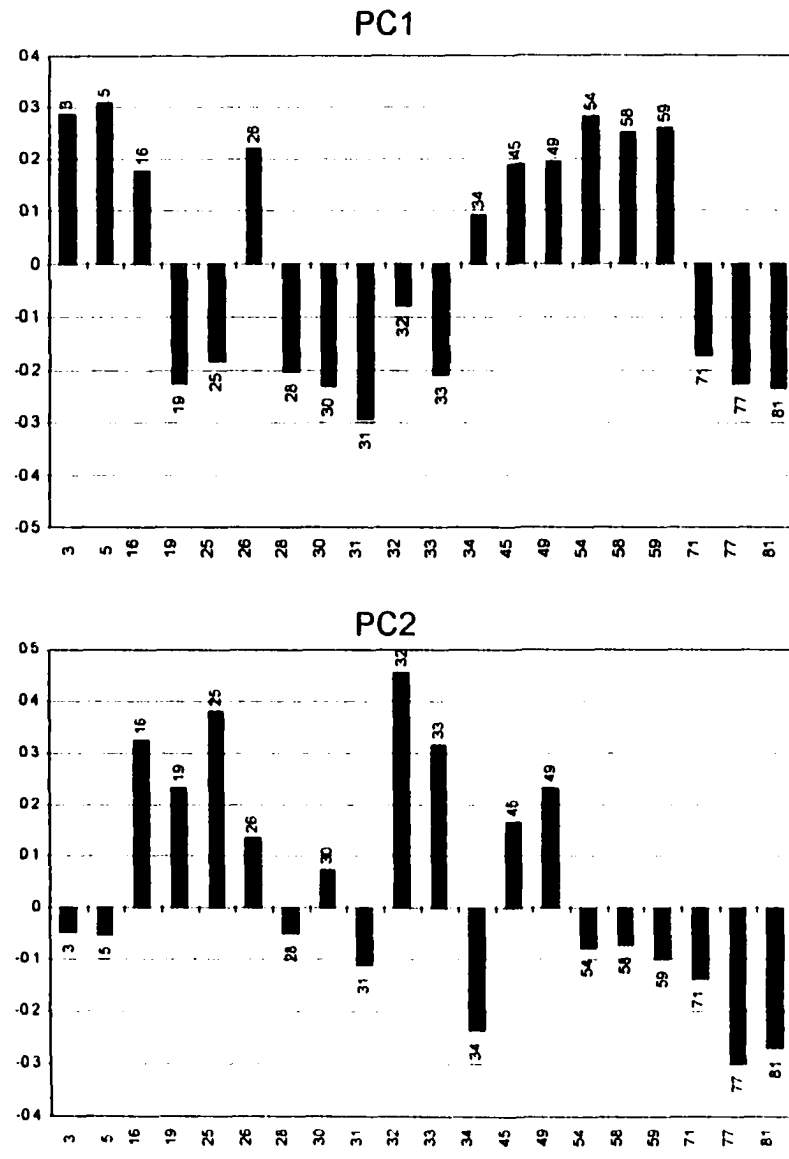
- I: Tricyclic terpanes
- II: Pentacyclic terpanes
- III: Sesquiterpanes
- IV: Diterpanes
- V: Pregnanes
- VI: Steranes, diasteranes
- VII: Monoaromatic steranes

**Figure 22a:** Loadings on principal components PC1 (a), PC2 (b) and PC3 (c), source rock extract GC-MS analysis; m=96, variance-covariance matrix based PCA. Bar labels and numbers on x-axis are the variables and refer to peak numbers listed in Appendix 1.2.



peak no	compound	ion m/e	peak no	compound	ion m/e
3	C <sub>n</sub> tricyclic terpane	191	33	17 $\alpha$ (H)-21 $\beta$ (H)-22R-30-homotripane	191
5	C <sub>n</sub> tricyclic terpane	191	34	gammacerane	191
16	18 $\alpha$ (H)-22,29,30-homotripane (T <sub>1</sub> )	191	48	86(H) diterpane	123
19	17 $\alpha$ (H)-22,29,30-trisnorhopane (T <sub>m</sub> )	191	49	86(H)-9-norhopane	123
25	17 $\alpha$ (H)-21 $\beta$ (H)-30-norhopane	191	54	48(H)-19-norhopane	123
26	C <sub>n</sub> diterpane	191	56	9-pristane	123
28	17 $\alpha$ (H)-21 $\alpha$ (H)-30-norhopane	191	59	16 $\beta$ (H)-phytadiene	123
30	17 $\alpha$ (H)-21 $\beta$ (H)-hopane	191	71	14 $\alpha$ (H)-17 $\alpha$ (H)-20R-cholestane	211
31	17 $\alpha$ (H)-21 $\alpha$ (H)-hopane	191	77	26-methyl-14 $\alpha$ (H)-17 $\alpha$ (H)-20R-cholestane	211
32	17 $\alpha$ (H)-21 $\beta$ (H)-22S-30-homotripane	191	81	24-ethy-14 $\alpha$ (H)-17 $\alpha$ (H)-20R-cholestane	211

**Figure 22b:** Loadings on principal components PC1 (a), PC2 (b) and PC3 (c), source rock extract GC-MS analysis;  $m=20$ , variance-covariance matrix based PCA. Bar labels and numbers on x-axis are the variables and refer to peaks listed in the accompanying table. This PCA method has been used to characterize source rock biomarker composition.



peak no	compound	lon m/z	peak no	compound	lon m/z
3	C <sub>18</sub> tricyclic terpane	191	33	17 $\alpha$ (H)-21 $\beta$ (H)-22R-30-norhopane	191
5	C <sub>22</sub> tricyclic terpane	191	34	gammacerane	191
16	18 $\alpha$ (H)-22,29,30-norhopane (Ts)	191	48	8 $\beta$ (H) diene	123
19	17 $\alpha$ (H)-22,29,30-trisnorphane (Trm)	191	49	8 $\beta$ (H)-19-norhopane	123
25	17 $\alpha$ (H)-21 $\beta$ (H)-30-norhopane	191	54	48 $\beta$ (H)-19-norhopane	123
26	C <sub>20</sub> diastereope	191	56	heptamane	123
28	17 $\beta$ (H)-21 $\alpha$ (H)-30-norhopane	191	59	16 $\beta$ (H)-phytadiene	123
30	17 $\alpha$ (H)-21 $\beta$ (H)-heptane	191	71	14 $\alpha$ (H)-17 $\beta$ (H)-20R-cholostenane	217
31	17 $\beta$ (H)-21 $\alpha$ (H)-heptane	191	77	24-methyl-14 $\alpha$ (H)-17 $\beta$ (H)-20R-cholostenane	217
32	17 $\alpha$ (H)-21 $\beta$ (H)-22S-30-norhopane	191	81	24-ethyl-14 $\alpha$ (H)-17 $\beta$ (H)-20R-cholostenane	217

**Figure 22c:** Loadings on principal components PC1 (a), PC2 (b) and PC3 (c), source rock extract GC-MS analysis; m=20, correlation matrix based PCA. Bar labels and numbers on x-axis are the variables and refer to peak numbers listed in Appendix 1.2.

differences in the extracts. A negative correlation is indicated between tricyclic terpanes and desmethyl steranes, although both are reportedly synthesized by algae and phytoplankton (Volkman, 1986). They may simply represent different types of algae but positive correlation to hopanes suggests herbivorous zooplankton as a potential source for desmethyl steranes. These organisms are known to synthesize C<sub>27</sub> steranes and may also have contributed a portion of the C<sub>28</sub> and C<sub>29</sub> steranes (see Kilops and Kilops, 1993, for review). Negative correlation to diterpanes similarly can indicate that C<sub>29</sub> steranes, which are often interpreted as markers for higher plant input (Huang and Meinschein, 1979), have a different source.

#### VARIANCE-COVARIANCE BASED PCA (n=20) - PC2

The PC2 in Figure 22b is clearly controlled by the relative abundance of gammacerane and to a lesser degree by the tricyclic terpanes. The loadings of most other variables fall below the suggested cut-off value of |0.141| (Appendix 4.2). A positive correlation to C<sub>29</sub> norhopane (peak 25) and homodrimane (peak 49) is indicated. Visual inspection of the chromatograms identified gammacerane as a useful compound for the characterization of extract samples. The gammacerane concentration was quantified and correlated to the source rock samples of different map-groups in Figure 23. Gammacerane concentrations and PC2 show similar trends, although extremely high concentrations do not coincide with high PC2 scores. However, the graph supports the interpretation of PC2 as representing the abundance of gammacerane in the samples. As outlined in Chapter 6.1.2.1, gammacerane is considered a marker for hypersaline conditions, and recently has also been related to the presence of bacterivorous ciliates living at density interfaces of water columns (Sinninghe Damsté *et al.*, 1995).

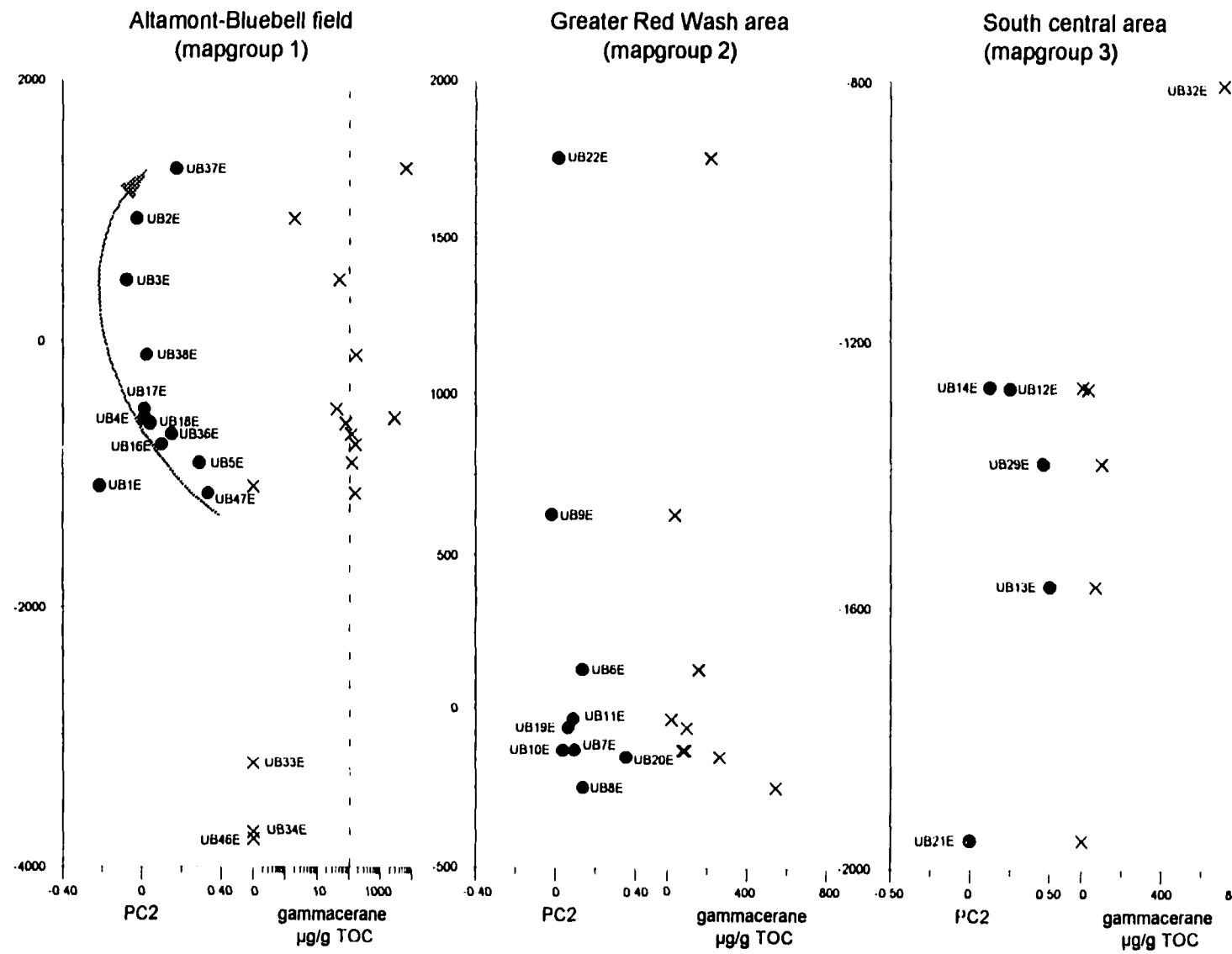


**Figure 23:** Comparison of PC2 and absolute gammacerane concentration vs. depth relative to a datum in map-groups 1-3 of the Uinta Basin.  
Note logarithmic scale for gammacerane concentration in the Altamont-Bluebell field (left panel) and the varying depth scales.

### VARIANCE-COVARIANCE BASED PCA (m=20) - PC3

The moretanes (peaks 28, 31) and  $\alpha\alpha$  20R desmethyl steranes (peaks 71, 77 and 81) are negatively loaded on PC3, suggesting that PC3 is partly determined by the relative abundance of thermally less stable compounds, thus represents thermal maturity (Fig. 22c). However, positive correlation of these compounds with diterpanes suggests that there is also a source component determining PC3.

#### **6.1.2.2 Source Rock Extract Principal Component Scores**

The second aspect of PCA is to use the loadings above as coefficients in a set of simultaneous equations and calculate sample scores as combinations of data values and eigenvector elements (see Chapter 5.5). Cross plotting scores on individual PCs can reveal compositional and therefore genetic differences between samples. The inversion of sample scores permits the interpretation of depositional environment, source and maturity of the samples (depending on PC loading interpretations). Relating PC1 and PC2 of the Uinta Basin source rock extract data, for example, results in isolation of variance caused by source and depositional environment from a portion of those variances introduced by maturity differences (PC3) into the data.

Sample associations are shown in score cross plots in Figure 24 with annotated PC interpretations in Figure 24a, as described in the preceding chapter. The samples have been separated into map-groups (see Fig. 8) to facilitate identification of spatial relations, and were also distinguished based on GC responses into oil-shale type and regular type samples. Samples plotting close to zero of either PC are unweighted toward the respective PC, i.e. there is a balance between opposite loadings characterizing the PC. Sample UB25E from the Ouray/Natural Buttes area (Fig. 8 and 9) illustrates the approach of interpreting scores on PCA cross plots and relevant chromatograms are given in Figure 25. The sample is unweighted on PC1, i.e. opposite loadings compensate. The RIC trace confirms high relative abundances of sesquiterpanes and pentacyclic hopanes, explaining PC1 scores close to zero (Fig. 25b). High negative PC2 score indicates relatively insignificant or absent tricyclic terpanes and/or gammacerane, and high sesquiterpanes (Fig. 25e). The cross plot of PC1 and PC3 reveals that immature biomarkers are insignificant (e.g. moretanes), and that sample composition is determined by hopanes and sesquiterpanes with no or only minor gammacerane (Fig. 25c). The sample can be interpreted to have a mature biomarker composition dominated by bacterial derived organic material. These bacteria were probably

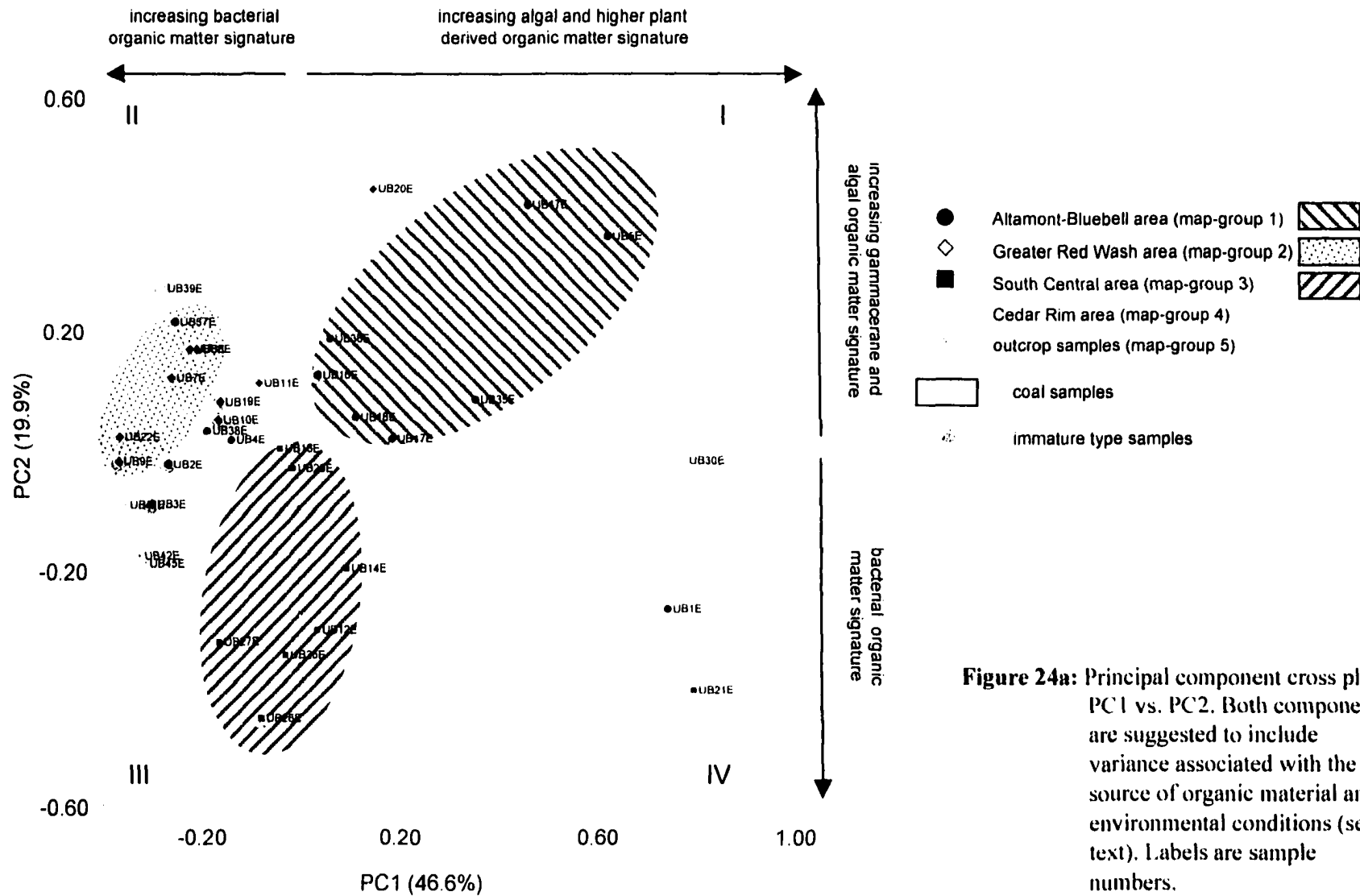


**Figure 24a:** Principal component cross plot PC1 vs. PC2. Both components are suggested to include variance associated with the source of organic material and environmental conditions (see text). Labels are sample numbers.

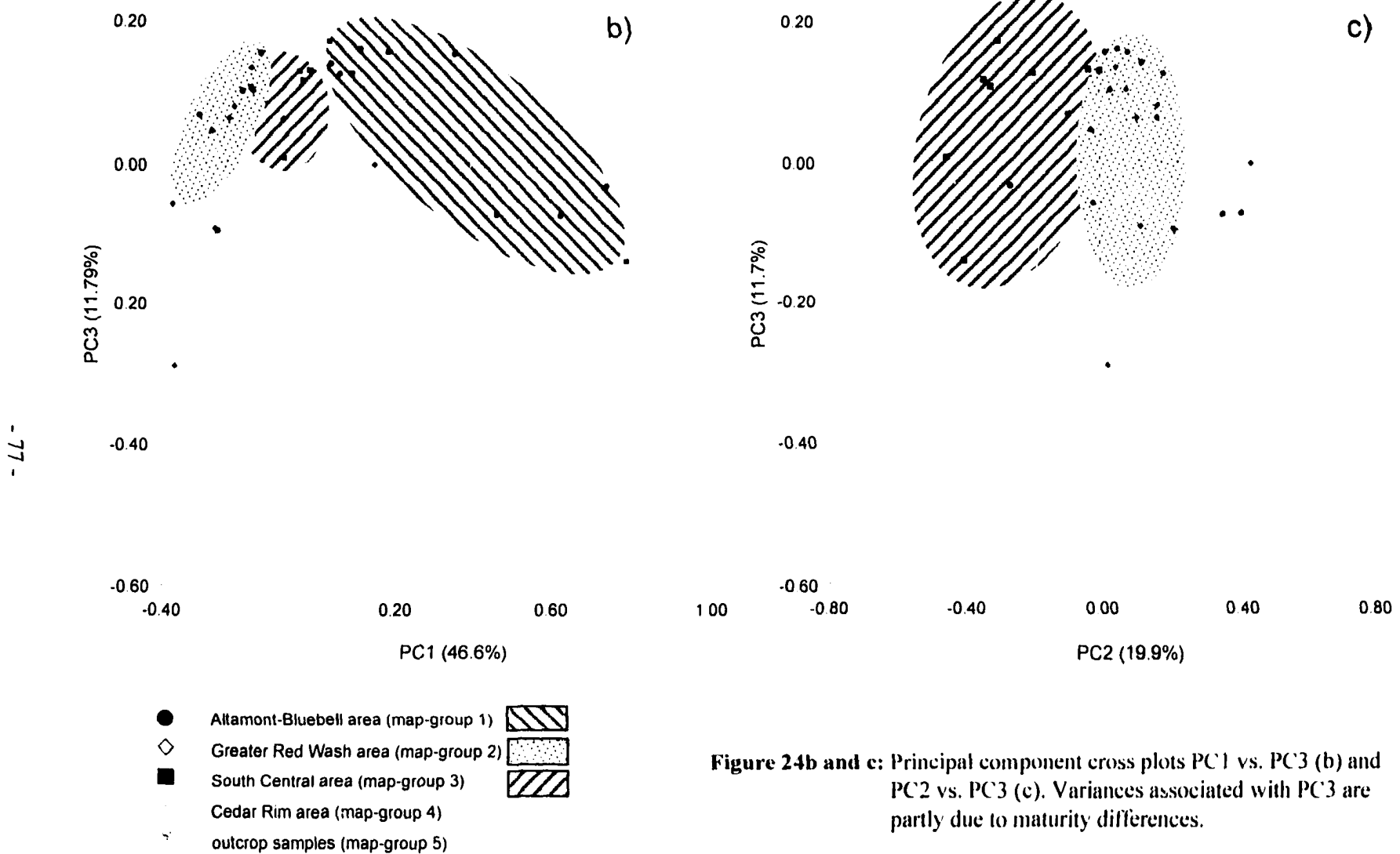


**Figure 24b and c:** Principal component cross plots PC1 vs. PC3 (b) and PC2 vs. PC3 (c). Variances associated with PC3 are partly due to maturity differences.

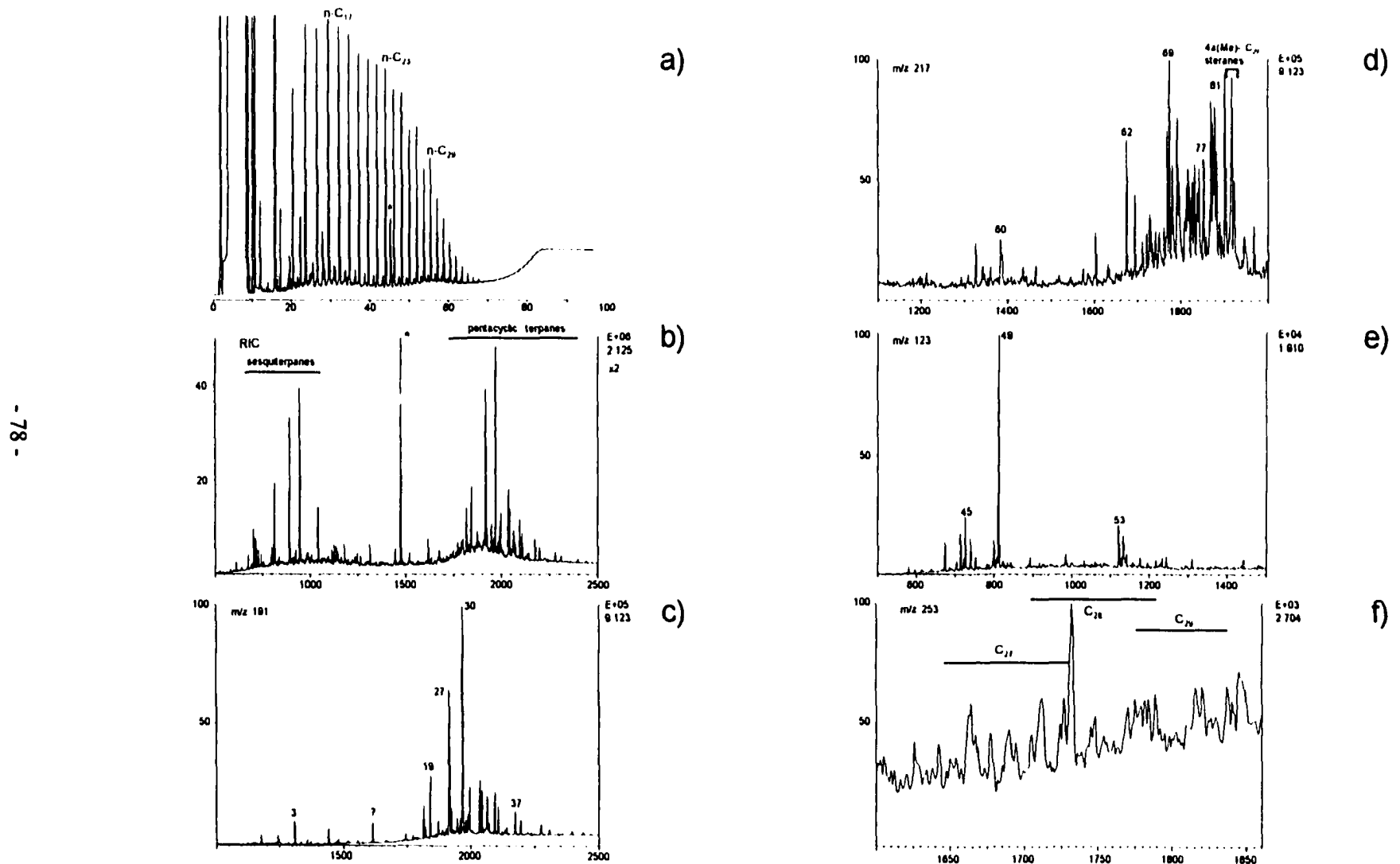


**Figure 25:** PCA interpretation illustrated with sample UB25E as an example. Refer to Figures 24a-c for location of the sample within PC ordination. (a) is the HTGC trace, (b) to (e) show the RIC,  $m/z$  191, 217, 123 and 253 MID chromatograms. Peak labels refer to compounds listed in Appendix 1.2. \* = internal standard  $C_{24}D_{50}$

mainly herbivorous protozoa reworking the primary organic matter, since autotrophic bacteria require extreme conditions (e.g. hypersaline or anoxic (Killops and Killops, 1993)) not indicated by other biomarkers. However, the example in Figure 25 also shows non-unique PCA results since, e.g. no definite conclusions can be drawn regarding the diterpane distribution. Balanced PC1 scores can be caused by either high sesquiterpane, tricyclic terpane and/or diterpanes vs. hopane relative concentrations, and inspection of other cross plots does not definitely exclude one or the other.

It is obvious, however, that the cross plots facilitate the visualization of sample relationships and recognition of unusual sample compositions (outliers in Figures 24). In this context it should be noted that PCA is constrained by variances introduced by outliers and does not model non-linear relations well (James and McCulloch, 1990). It appears that samples obtained from the south-central part of the basin (map-group 3) plot in a fairly well defined and separated region (Fig. 24a), with the exception of sample UB35E and 21E. Both samples have very low TOC values. The PC interpretation indicates dominance of bacterial derived organic material, low relative concentrations of gammacerane and tricyclic terpanes, and relative high maturity. Oil-shale type samples also plot consistently in quadrants II and III on PC1 and PC2 cross plots (Fig. 24a). However, the fact that samples show opposite signs on PC2 confirms that there are significant differences in the composition of oil-shale type samples, notably in the gammacerane abundance. All oil-shale type samples (except UB16E) have high relative hopane concentrations and an example for the terpane distribution is given in Figure 15c. Their dominance is also obvious in the RIC trace example of Figure 14b and GC trace in Figure 13b. Within the field of oil-shale type source rocks, samples obtained from the Greater Red Wash area (map-group 2, Fig. 9) cluster in a well defined area in Figure 24a. They appear to be similar in biomarker composition to the mahogany zone outcrop sample (UB39E), with the exception of sample UB20E. This sample,

unlike the other oil-shale type samples from the area, has a TOC < 1.0%. Samples obtained from the Altamont-Bluebell area (map-group 1) scatter over the entire cross plot, a fact which is interpreted to reflect the larger stratigraphic range represented by the samples. However, samples from deeper stratigraphic intervals (see also Chapter 6.2) cluster in quadrant I, whilst samples from higher stratigraphic levels plot close to the samples from the Greater Red Wash area.

A similar sample distribution pattern results in a cross plot of PC1 vs. PC3 (Fig. 24b), in which south-central and Greater Red Wash area samples cluster closely together. However, maturity variations appear to cause a large spread in the oil-shale type samples along PC3. Because of the relatively low total variance included, PC2 vs. PC3 shows a large scatter (Fig. 24c) and is useful only for verification of score interpretations made based on PC1 vs. PC2 and PC3, respectively.

#### **6.1.2.2.3 Correlation of PCA Sample Scores and other Geochemical Parameters**

The original idea of employing PCA to gain insight into the data matrix created by GC-MS analysis was to use it as a means to compare variations associated with certain biomarker groups and develop an initial interpretative model for source rock composition. Comparison with geochemical parameters derived from other methods (GC and Rock-Eval) can be integrated into the interpretation by simply correlating the PC scores of samples and the interpretation of the individual PCs as described above. The correlation coefficients (Pearson's correlation coefficient  $r$ ) are shown in Table 7. Correlation coefficients of  $r \geq |0.45|$  are arbitrarily considered to imply significant covariation. Statistical significance at levels of significance levels of  $p=0.05$  is indicated for  $r > |0.34|$ .

The correlation of PC1 to HI suggests that this PC is related to the type of organic matter. Positive PC1 scores apparently coincide with decreasing hydrogen content, which can be attributed to increasing proportions of terrestrial organic matter. The positive correlation of PC1 to GC parameters reflecting the distribution of *n*-alkanes ( $C_{21}/C_{22}$  and  $C_{21}+C_{22}/C_{28}+C_{29}$ ; definition in Appendix 1.1) and to the oleanane-index supports the interpretation of PC1 as a source parameter. Algae are known to synthesize mostly low molecular weight *n*-alkanes (*n*-C<sub>15</sub> to *n*-C<sub>21</sub>) while higher molecular weight *n*-alkanes (*n*-C<sub>13</sub> to *n*-C<sub>35</sub>) are typical for higher plant input (for review of *n*-alkane distributions see Collister *et al.*, 1994). Oleanane is a compound related to the occurrence of angiosperms (ten Haven and Rullötter, 1988). Correlation to Pr/*n*-C<sub>17</sub> may be reflecting the transformation of phytol side chains to pristane in oxic environments, but the restricted use of pristane (and phytane) as environmental indicators (ten Haven *et al.*, 1987), possible multiple sources (e.g. Goosens *et al.*, 1984) and sensitivity to maturity (e.g. Peters and Moldowan, 1993) make this interpretation less definitive. All parameters correlating with PC1 are sensitive to changes in maturity and, since some of the variance associated with PC1 appears to be maturity

	Pt/Ph	Pt/n-C <sub>11</sub>	Pt/n-C <sub>13</sub>	C <sub>21-22</sub> /C <sub>23-24</sub>	C <sub>7</sub> /C <sub>22</sub>	Betacarotane µg/g TOC	Pt+n-C <sub>11</sub> /Pt+n-C <sub>13</sub>	R22	CPI	T <sub>max</sub> °C	S1	S2	S3	PI	TOC	H	O	PC1	PC2	PC3	Gammacerane µg/g TOC	Dihopane-index	Oleanane-index	Diasterane-index	22S/(22S+22R) C <sub>11</sub> : Hopane	20S/(20S+20R) C <sub>11</sub> :	$\alpha\beta/(\alpha\beta+\alpha\alpha)$ C <sub>11</sub>	
Pt/Ph	1																											
Pt/n-C <sub>11</sub>	0.258	1																										
Ph/n-C <sub>13</sub>	-0.221	0.494	1																									
C <sub>21-22</sub> /C <sub>23-24</sub>	-0.069	-0.572	-0.478	1																								
C <sub>21</sub> /C <sub>22</sub>	0.220	-0.290	-0.234	0.616	1																							
Betacarotane µg/g TOC	-0.245	0.298	0.958	-0.392	-0.206	1																						
Pt+n-C <sub>11</sub> /Ph+n-C <sub>13</sub>	0.860	0.555	-0.034	-0.231	0.151	-0.132	1																					
R22	-0.246	-0.141	-0.397	0.207	-0.137	-0.378	-0.183	1																				
CPI	0.092	0.310	0.753	-0.474	0.195	0.743	0.150	-0.609	1																			
T <sub>max</sub> °C	0.155	0.041	0.012	0.168	0.215	0.020	0.180	0.087	-0.009	1																		
S1	0.252	0.148	0.035	-0.174	-0.265	0.038	0.184	-0.129	0.045	0.109	1																	
S2	0.328	0.103	-0.023	-0.100	-0.139	-0.038	0.315	-0.145	0.255	0.184	0.472	1																
S3	0.365	0.138	-0.047	-0.305	-0.182	-0.064	0.304	-0.287	0.625	0.007	0.070	0.499	1															
PI	-0.226	-0.121	-0.080	-0.062	-0.168	-0.047	-0.303	-0.177	-0.118	-0.708	0.176	0.445	0.143	1														
TOC	0.593	0.144	-0.113	-0.206	-0.129	-0.126	0.518	-0.289	0.382	0.104	0.415	0.843	0.800	-0.307	1													
HI	-0.339	0.337	0.413	-0.180	-0.318	0.349	-0.138	0.294	0.115	0.225	-0.012	0.223	-0.238	-0.418	-0.176	1												
OI	-0.154	0.076	0.111	-0.335	-0.244	0.064	-0.201	-0.317	0.285	-0.499	0.157	-0.233	0.349	0.729	0.004	-0.303	1											
PC1	-0.044	-0.500	-0.355	0.603	0.554	-0.304	-0.205	-0.152	-0.334	-0.280	-0.247	-0.358	-0.239	0.412	-0.261	-0.582	0.046	1										
PC2	-0.569	0.138	0.186	-0.208	-0.428	0.129	-0.359	0.260	-0.106	-0.039	-0.101	-0.247	-0.198	0.162	-0.363	0.230	0.079	1										
PC3	-0.079	-0.157	-0.326	0.430	0.046	-0.282	-0.088	0.475	-0.635	0.435	0.213	-0.110	-0.615	-0.187	-0.345	0.233	-0.513	1										
Gammacerane µg/g TOC	-0.157	0.330	0.264	0.169	0.231	0.196	-0.152	-0.134	0.112	0.013	0.311	0.155	-0.033	0.293	-0.137	0.084	0.488	-0.180	0.220	0.038	1							
Dihopane-index	-0.168	-0.280	-0.206	0.240	0.118	-0.175	-0.236	0.006	-0.185	-0.487	-0.205	-0.378	-0.112	0.556	-0.247	-0.442	0.232	0.773	0.209	0.284	0.158	1.000						
Oleanane-index	-0.124	-0.250	-0.196	0.012	0.018	-0.181	-0.207	-0.081	-0.123	-0.702	-0.270	-0.319	0.003	0.638	-0.179	-0.431	0.352	0.610	0.133	-0.487	0.154	0.786	1.000					
Diasterane-index	-0.095	-0.248	-0.173	0.225	-0.200	-0.074	-0.264	0.035	-0.131	-0.279	0.082	-0.240	-0.120	0.397	-0.185	-0.220	0.125	0.242	0.021	0.053	0.309	0.432	0.212	1.000				
22S/(22S+22R) C <sub>11</sub>	0.082	-0.011	-0.131	0.338	0.293	-0.110	0.125	0.321	-0.423	0.783	0.158	-0.090	-0.488	-0.451	-0.253	0.184	-0.584	-0.058	0.061	0.787	0.038	-0.288	-0.594	0.109	1.000			
20S/(20S+20R) C <sub>11</sub>	0.003	-0.157	-0.278	0.233	-0.140	-0.216	-0.106	0.275	-0.601	0.105	0.238	-0.187	-0.388	0.132	-0.221	-0.015	0.213	0.211	0.043	0.663	-0.089	0.131	-0.082	0.163	0.341	1.000		
$\alpha\beta/(\alpha\beta+\alpha\alpha)$ C <sub>11</sub>	-0.072	-0.346	-0.359	0.373	-0.202	-0.266	-0.215	0.175	-0.441	0.043	0.138	-0.188	-0.281	0.256	-0.210	-0.171	0.199	0.335	0.189	0.598	0.119	0.318	0.130	0.622	0.212	0.714	1.000	

Table 7: Correlation coefficient matrix (Pearson's correlation coefficient r) relating source rock principal components and other parameters obtained from GC and Rock-Eval analysis;  $r > |0.45|$  highlighted.

related, the correlations have to be interpreted with caution.

A high negative correlation between PC2 and Pr/Ph ( $r=-0.599$ ) supports the interpretation that PC2 represents the relative abundance of gammaceranes which, in turn, can be related to salinity and/or redox potential of the lake environment. A common source for pristane and phytane has been interpreted based on compound  $\delta^{13}\text{C}$  ratios by Schoell *et al.* (1994) for Uinta Basin gilsonites, which are derived from mahogany zone oil-shales. However, the Pr/Ph value is only in the Mahogany zone outcrop sample UB39E (Appendix 5) distinctly smaller than 1, which would be expected for hypersaline systems (ten Haven *et al.*, 1988).

The high correlations of maturity parameters to PC3 support the hypothesis that this component is associated with the variance introduced by maturity differences between the samples. The CPI (Marzi *et al.*, 1993) and R22 (ten Haven *et al.*, 1987; for definition see Appendix 1.1) appear to be maturity dependent, as is the oxygen content measured as S3 and OI, respectively. A decrease in the latter two parameters and a convergence of CPI and R22 to 1 in association with a positive PC3 score (*i.e.* a decrease of the relative concentration of thermally unstable isomers), indicates a relatively higher maturity level of the sample under consideration. Conventional molecular maturity parameters have been included into the correlation coefficient matrix of Table 7 and show positive correlation to PC3. Lack of correlation of other maturity sensitive parameters such as Pr/n-C<sub>17</sub> may indicate that these ratios reflect primarily a source signal.

None of the PC's show a definite relationship to the absolute  $\beta$ -carotane concentration in the samples, but there is a correlation of  $\beta$ -carotane to CPI and Pr/n-C<sub>17</sub>. Both  $\beta$ -carotane and phytane are indicators of hypersalinity (*e.g.* Fu Jiamo *et al.*, 1990). Lack of correlation of  $\beta$ -carotane to gammacerane and PC2 may indicate that gammacerane is not necessarily dependent on the occurrence of hypersalinity alone and can indeed also be a marker for water column stratification (Sinnighe Damsté *et al.*, 1995) when other salinity indicators are not present or

present only in minor abundance. The  $\beta$ -carotane concentration varies extensively (Appendix 5; see also Table 3), but is generally highest in some oil-shale type samples. The Pearson's correlation coefficient is sensitive to outliers (Rock, 1988) and the lack of correlation may thus also be caused by the number of extreme outliers in the analysis. Based on compound specific  $\delta^{13}\text{C}$  measurements Schoell *et al.* (1994) interpreted  $\beta$ -carotane in Uinta Basin gilsonite (which is generated from the mahogany zone) as a compound synthesized by halophilic algae or photosynthetic bacteria living at or near a halocline. In this study, isotopic similarity to pristane and phytane was interpreted as an indication that the  $\beta$ -carotane synthesizing organisms also lived in the photic zone of the lake.

## **6.2 Stratigraphic and Facies Related Aspects of the Source Rock Geochemistry**

In order to permit further source rock interpretations within a geological framework, samples were divided into three map-groups depending on well locations (Fig. 8) and, where possible, related to a common subsurface datum within their group. The depth of the datum used in each well are listed in Appendix 2. The subsurface datum are lithostratigraphic markers and were obtained from published structure maps. The temporal relationship between these markers and the spatial and stratigraphic association of the map-groups are illustrated schematically in Figure 26. Fouch (1981) published a cross section correlating the southwestern and north-central part of the basin and regional correlations based on wells and outcrop data exist for the southern part of the basin (*e.g.* Johnson, 1989; Franczyk and Pitman, 1989). No subsurface correlation between the north-central and the eastern part of the basin has been published. However, the approximate temporal relationship between the markers is known (see Ryder *et al.*, 1976) and the stratigraphic association shown in Figure 26 is useful as an approximation. Some of the samples included into the geochemical analysis could not be integrated into the map-groups because of lack of well information or well position outside published structure map areas. The gas chromatograms of these samples are shown in Appendix 6.

Relative biomarker abundances and many organic geochemical parameters are sensitive to thermal maturity. Thermal maturation may modify or obliterate geochemical signals representing source input or depositional environment, thus the maturity assessment must be also considered in terms of potential interference with source and environmental interpretations. As described below, the maturity of the samples integrated into the different map-groups ranges from immature to early mature and it is assumed that the extracts still carry the diagenetic signal of the organic matter. In this context, Tissot *et al.* (1978) reported that hydrocarbon generation for Uinta Basin source rocks occurs at higher maturity levels ( $>0.7 R_o\%$ ) than for other source rock types.

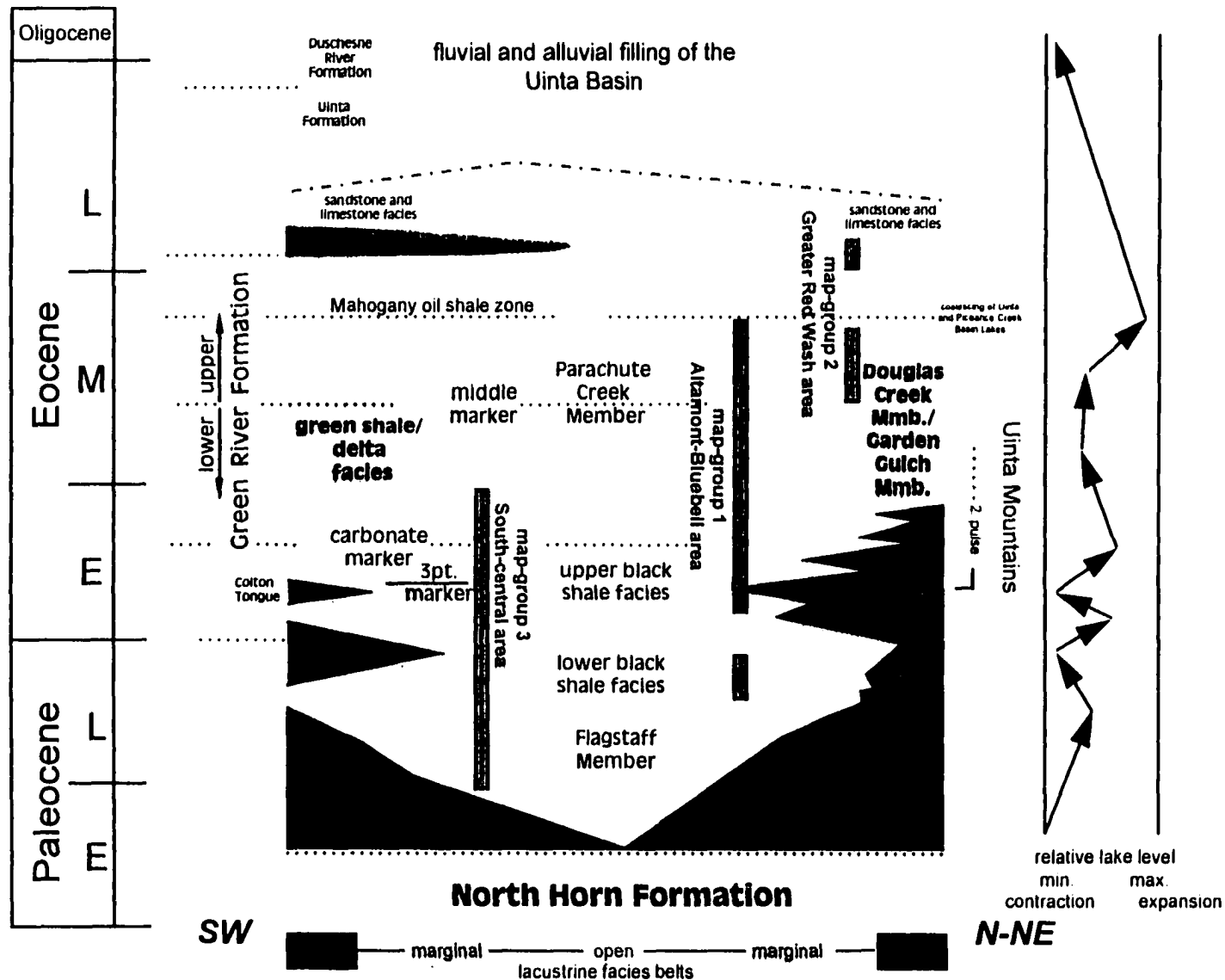


Figure 26: Schematic overview over the approximate relative stratigraphic positions of the cores summarized into map-groups 1 to 3.

### **6.2.1 Altamont-Bluebell Area - Map-group 1**

An attempt to reference samples from the Altamont-Bluebell area to the middle marker datum was made using structure maps published by Peterson (1973) and Morgan and Tripp (1996). Peterson (1973) used a log marker in the lower Green River Formation but structural equivalency and interpolation permitted estimation of the depth difference to the middle marker for the well included in this map (Appendix 2). The wells are located in T1S-R2W and T1S-R1W and the cores comprise an estimated total section of about 4,800 ft (Fig.27 and 28). A large sample gap exists between the upper and lower black shale facies, leaving the Colton Tongue and equivalent open lacustrine strata uncovered. Sample UB35E (Appendix 2 and 5) is interpreted to originate from this interval, but the well is located outside the datum control area. According to Fouch's (1975) and Ryder's *et al.* (1976) facies maps (see also Fig.5), the area was close to or located within the open lacustrine core during the existence of Lake Uinta. Because of the large stratigraphic section covered and the significance of the middle datum as a lithostratigraphic marker, there is little stratigraphic control over the relative position of samples from different wells representing only short depth intervals. Although the stratigraphic associations of samples at relatively small scales is only approximate, the stratigraphic ranking on a large scale is consistent and the samples can be separated into a lower black shale facies, upper black shale facies/green shale facies and upper Green River Formation section. The stratigraphic framework for map-group 1 was derived from Fouch's (1981) assignment in well Mapco George E Fisher (API no. 43-013-30131-00; SW NE-Sec7-T1S-R3W) located approximately 3 mi west of map-group 3. The top of the Colton was identified in well Chasel Unit Flying 1 (Appendix 3.1-7) but otherwise the locations and boundaries between the units are also only rough approximations.

## THERMAL MATURITY

Selected maturity parameters *vs.* depth are shown in Figure 28a to assess the maturity range represented in the samples. The plots permit evaluation of systematic maturity trends and facies dependence of maturity parameters. Systematic depth trends are visible for C<sub>29</sub> sterane isomerization at C20 and  $\alpha\alpha$ - *vs.*  $\beta\beta$ -isomerization. The sterane isomerization parameters show higher variability than the hopane C22-isomerization. The slope for the hopane C22-isomerization slightly increases with depth and it appears that equilibrium for this reaction has been attained in the samples at the base of the black shale facies/green shale facies interval. The hopane C22-isomerization equilibrium occurs earlier than the equilibrium of other isomerization reactions. Reversal of isomerization reactions at higher maturity levels has been reported (Moldowan *et al.*, 1991) and a reversal is suspected to occur in the sterane C20- and  $\alpha\alpha$ - *vs.*  $\beta\beta$ -isomerization of the stratigraphically deepest samples (UB33E, UB46E). This reversal is an indication that the peak generation maturity level presently occurs above the lower black shale facies, probably within the Colton Tongue of this area. No, or very low concentrations of biomarker were detected in sample UB34E due to thermal degradation of biomarker compounds. Thermal degradation of biomarkers, extremely low HI, EOM, T<sub>max</sub>, and *n*-alkane distributions suggest high thermal maturity of the samples beyond the maximum generative stage (Fig.27; Fig.28a). Although irregularities in sterane and terpane isomerization parameters have been reported for hypersaline sediments (ten Haven *et al.*, 1986), elevated salinities are unlikely to have occurred before the deposition of laminated oil-shale facies (see Chapter 3.4) and only thermal control on isomerization is assumed. The use of moretane/hopane values as maturity indicators has been suggested by Seifert and Moldowan (1980). This parameter shows an exponential decay trend *vs.* depth. Equilibrium is reached before hopane C22-isomerization equilibrium and, according to Peters and Moldowan (1993), invariance of the ratio is equivalent to maturity levels of R<sub>o</sub>≈0.7%. Not surprising is the scatter of T<sub>max</sub> data

points *vs.* depth, although this parameter may be more useful at maturity stages beyond biomarker isomerization equilibrium. The ratio of Ts and Tm showed considerable scatter *vs.* depth and was not useful for the assessment of thermal maturity (Appendix 5). Variation of Ts/Tm values depending on source rock facies has been reported by Moldowan *et al.* (1986). The parameters controlling Tm *vs.* Ts are speculative and may be related to lithology (*e.g.* McKirdy *et al.*, 1984), salinity (Rulkötter and Marzi, 1988) and Eh (Moldowan *et al.*, 1986), any of which may have had major influence during deposition of the Green River Formation in the Uinta Basin. A distinct depth trend is displayed by PC3 which drops sharply with thermal conversion of moretanes and may thus be a measure for the suggested equilibrium at  $R_s \approx 0.7\%$ .

## GEOCHEMICAL INTERPRETATION OF SOURCE ROCKS

Gas chromatograms of the samples included in map-group 1 are shown with their interpreted stratigraphic association in Figure 27. Increasing thermal maturity with depth has probably modified the diagenetic distribution of compounds, but it is assumed that the variation in the relative abundance of *n*-alkanes, isoprenoids, terpanes and  $\beta$ -carotane visible in the chromatograms primarily reflects source input. Samples UB17E and UB18E taken from the same core about 100 ft apart support this assumption. Both samples show similar TOC and HI but UB18E shows relative higher abundances of isoprenoids, terpanes and  $\beta$ -carotane relative to the *n*-alkanes, although both have approximately similar maturity. The stratigraphically deepest samples (UB33E, UB34E, UB46E) are thermally mature or overmature, as indicated by the low HI,  $T_{max}$  and the distribution of *n*-alkanes. Samples from the stratigraphically highest section show oil-shale type composition (UB2E, UB3E, UB37E). Sample UB16E obtained from sections below the middle marker also displays oil-shale type signature and is compositionally similar to a carbonate marker outcrop sample analyzed by Ruble (1996). Other samples from this section are dominated

by *n*-alkanes with variable distributions and preference patterns. Because of high  $T_{max}$  values of samples UB5E and UB36E and particularly UB1E it was suspected that these samples originate from stratigraphically deeper, thermally more mature sections. However, the samples show distinct *n*-alkane distributions (UB1E), clear preference patterns (UB5E) and relatively high HI values interpreted to reflect source differences.

Depth profiles of parameters related to source input and depositional environment based on the stratigraphic ranking of the samples are shown in Figure 28b and c. A distinct trend of PC1 vs. depth (Fig.28b) suggests a high relative proportion of primary organic matter derived from algae and higher plants in samples from the upper black shale facies/green shale facies section beneath the middle marker. Odd carbon number preference of the *n*-alkanes (Fig.27), high % diterpane and oleanane-indices (Fig.28c) also suggest higher plant contribution in this section. The presence of methyl steranes in a number of samples (Appendix 5) also suggests algal contribution, possible from dinoflagellates. The relatively high influence of clastic material is indicated by high diahopane- and diasterane-indices. Reduced  $\beta$ -carotane concentrations in this section may be a consequence of the elevated maturity of the samples, but the variability is preserved and may reflect fluctuations in lake water salinity. The plots of PC2 vs. depth (Fig.28b) also show a systematic trend, roughly paralleled by the absolute gammacerane concentration (Fig.23). Although often interpreted as a marker for hypersalinity, the lack of correlation with  $\beta$ -carotane and Pr/Ph values in samples beneath the middle marker suggests other controls on gammacerane abundance. The presence of water column stratification in relatively fresh water and origin of gammacerane from bacterivorous ciliates living along the density interface as proposed by Sinnighe Damsté *et al.* (1995) provides an alternative interpretation for the presence of this compound.

Lithofacies observations (Appendix 3.1) suggest that samples UB1E, UB5E and UB47E are derived from open lacustrine sediments, based on the of laminated dark brown to black shales,

mudstones and packstones. Shallow water structures such as algal lamination, syneresis cracks, cross- and flaser-bedding characteristic for marginal lacustrine rocks were identified in these cores and suggest rapid facies changes, which is apparently also reflected in the variable source rock geochemistry. This agrees with the interpretation of the black shale facies and green shale facies as deposits of a phase of lake transgression and subsequent contraction associated with expansion of marginal lacustrine and deltaic facies (see Chapter 3.4). The sediments of the other cores from the black shale facies/green shale facies section also represent marginal lacustrine facies ranging from light colored mudstones and packstones (Hiko Bell 1) to medium sandstones with basal lag conglomerates in Lamicq Urruty 2-8C (Appendix 3.1) and exhibit dominantly flaser- and lenticular bedding.

The sign of the PC1 scores changes up section and oil-shale type samples are characterized by the dominance of bacterial derived biomarkers. The organic matter is also dominated by variable proportions of terpanes, isoprenoids and  $\beta$ -carotane, with minor contribution of *n*-alkanes. Parameters representing the input of allochthonous inorganic and organic material decrease, also suggesting a change in the dominant source of the organic matter. Decreasing PC2 in the oil-shale type samples UB2E and UB3E and reversal to high positive scores in UB37E indicate differences in the source and depositional environment of the organic matter in these sediments. Low  $\beta$ -carotane and variations in Pr/Ph support this conclusion and argue for saline water conditions during the deposition of the oil-shales represented by samples UB2E and UB3E. These samples possibly originate from the low grade oil shale zones beneath the mahogany zone (Johnson, 1989). Sample UB37E is geochemically similar to the mahogany shale sample UB39E (compare PCA cross plot in Fig. 24a), although it has much lower TOC and HI values and less distinctly low Pr/Ph ratio. Extremely high  $\beta$ -carotane in UB37E and dominance of hypersaline markers in the mahogany shales (UB39E) indicate increasing saline conditions relative to the lean oil-shale zone.

Lithofacies of the cores from which samples UB2E and UB3E were obtained indicate shallow water, marginal lacustrine deposition (flaser-bedding, bioturbation, dewatering and desiccation structures, syneresis cracks, algal boundstones *etc.*) interrupted by the deposition of laminated oil-shales (Appendix 3.1-1). Planar lamination of UB2E and UB3E suggests lack of bioturbation, possibly due to anoxicity or possibly salinity of the bottom water. Possibly, these oil-shales were deposited during short term transgressive periods, when marginal lacustrine areas were inundated by water sufficiently anoxic and/or saline to preserve sediment lamination and organic matter.

Well Blanchard 1-33-3 is the longest, most complete section available for the area and is interpreted to cover parts of the uppermost black shale facies/green shale facies transition to oil-shale facies. This section therefore represents the development of the lake system from stratified, fresh-water, through shallow, fluctuating alkaline and hypersaline lake systems. It is therefore instructive to observe changes in bulk geochemical parameters derived from Rock-Eval analysis with depth and lithofacies (Fig. 29). The upper section (black shale facies/green shale facies and lean oil-shale facies) is generally more TOC- and hydrocarbon-rich (9,360-9,480 ft), although TOC varies considerably. Source rock units, however, appear to be thinner and alternate frequently with organic-lean sand-, silt- and limestones. The lower section beneath the middle marker (below 10,320 ft core depth) is distinguished by a uniform mudstone to packstone sequence with relative invariant TOC and HI. Rock-Eval PI is constant at 0.2 to <0.4 and in combination with  $T_{max}$  (430-435°C) supports that this section is entering the hydrocarbon generation stage. The dark mudstones and shales of lower Green River Formation (upper black shale - green shale facies section) represent organic facies deposited after the first major lake expansion and are more organic-lean and lower in hydrogen concentration. However, constant TOC values around 1.0% indicate consistent sedimentation of organic matter, unlike in the upper Green River Formation (8,940-9,180 ft), which shows erratic episodes of high quality source rock deposition.

---

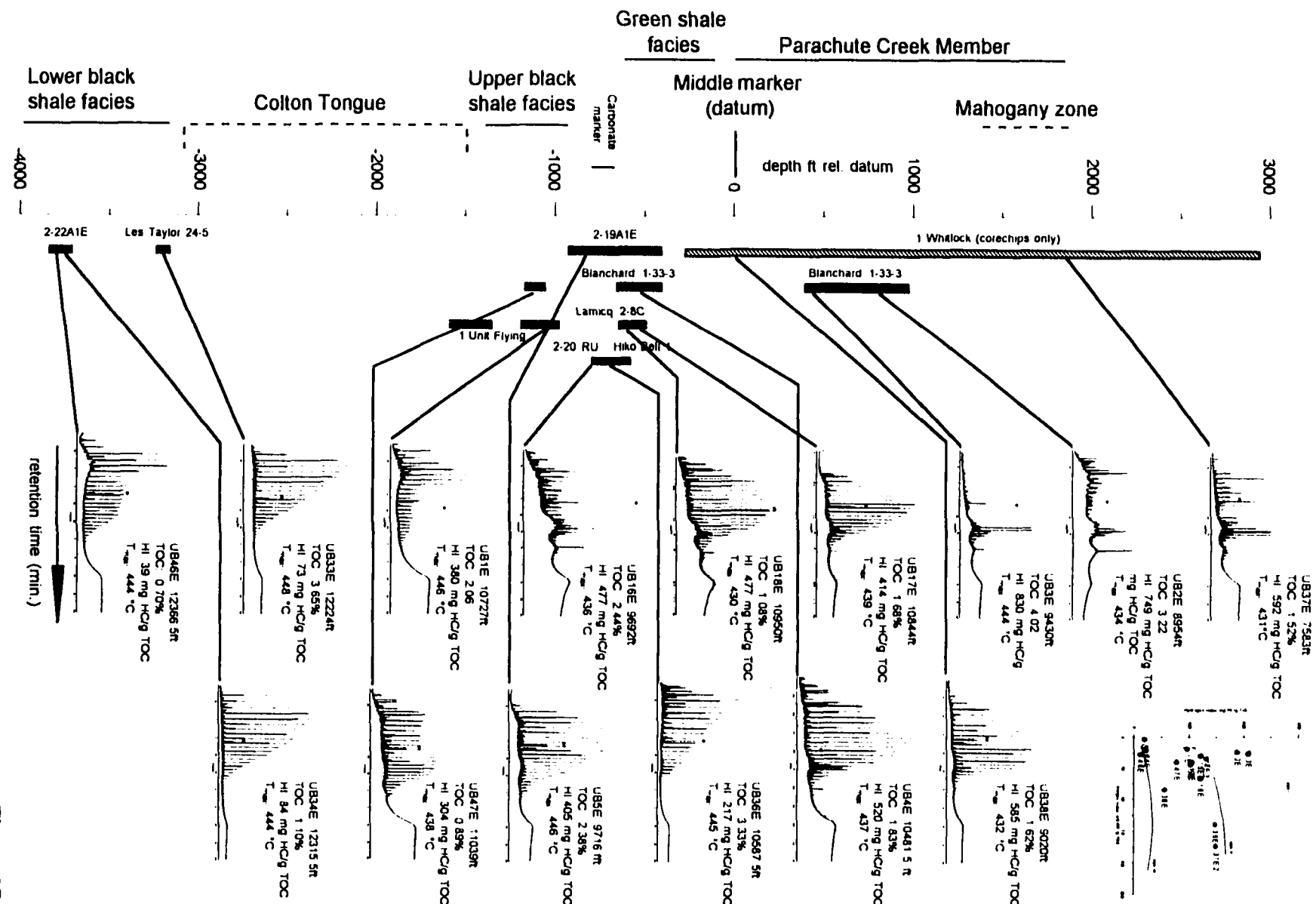
Captions (next 4 pages)

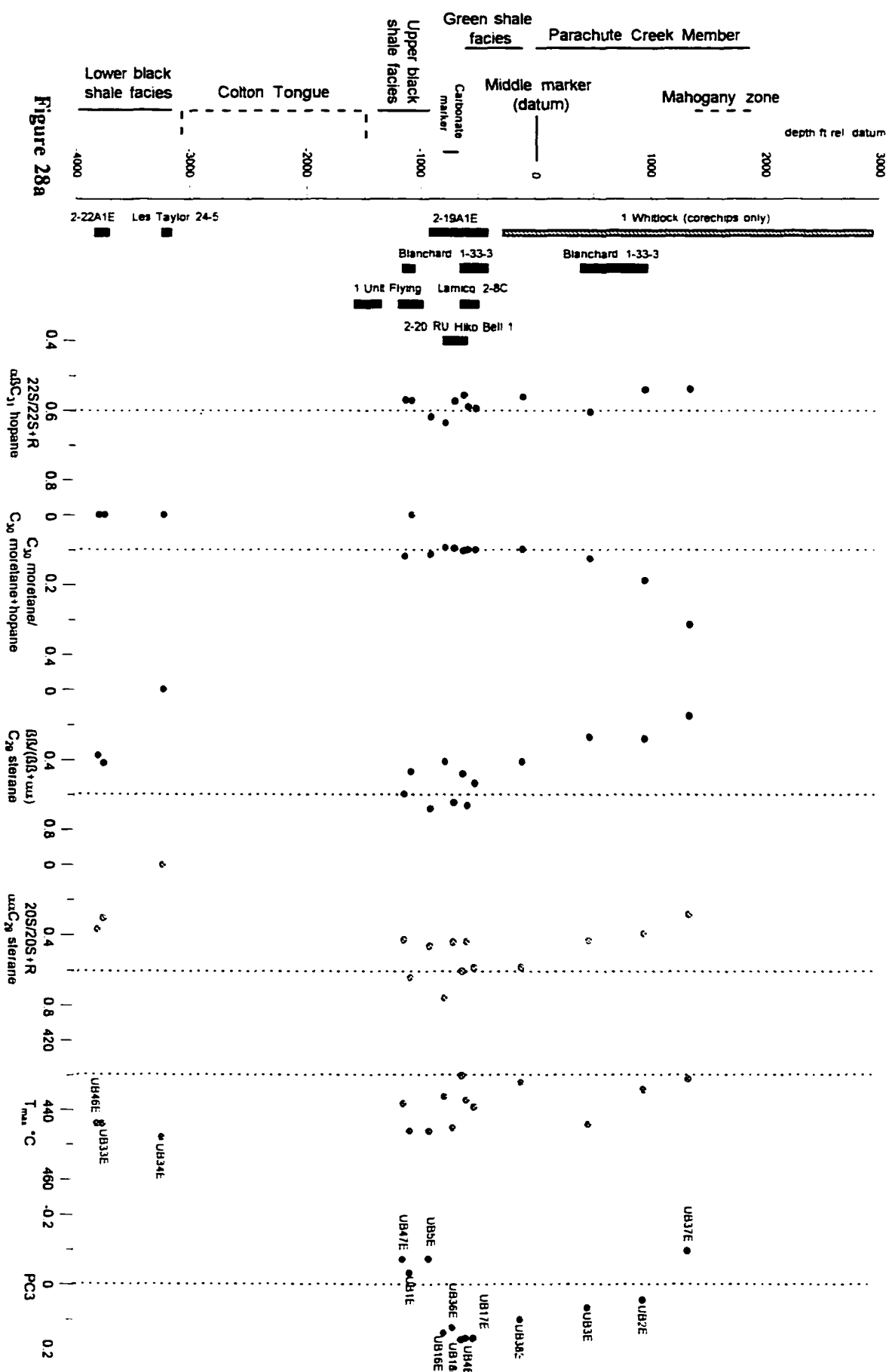
**Figure 27:** HTGC analysis of source rock extract saturated fractions from cores of the Altamont-Bluebell area (map-group 1). Sample depths are referenced to the middle marker datum (see text); stratigraphy adopted from well Mapco George E Fisher (SW NE, Sec7-T1S-R3W) published by Fouch (1981). Sample information includes sample number, depth of sample in well and Rock-Eval bulk data. \*= Internal standard C<sub>24</sub>D<sub>50</sub>; black rectangles=cores, hatched rectangles=core chips.

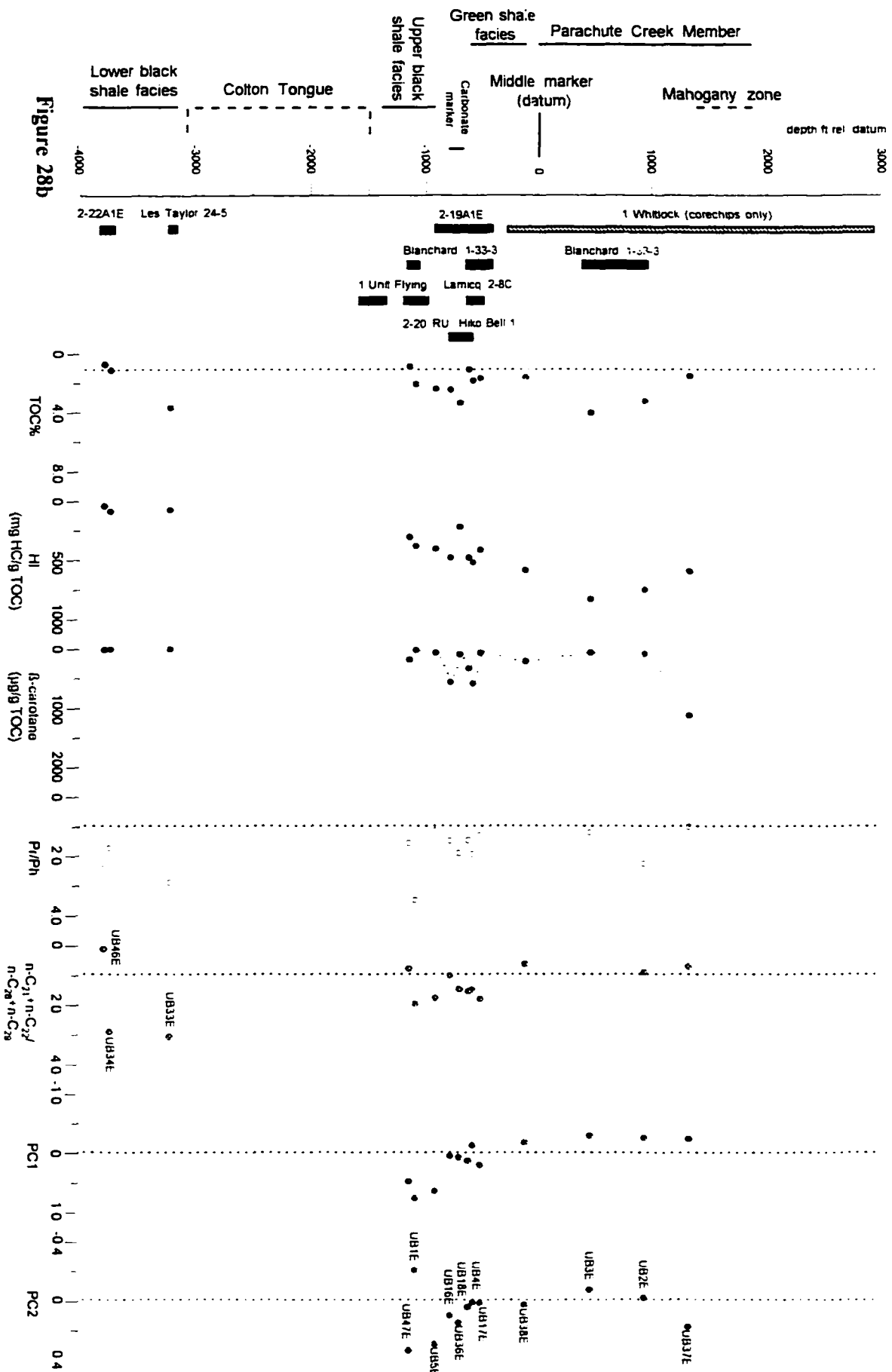
**Figure 28a:** Maturity related biomarker indices and principal component 3 vs. depth in the Altamont-Bluebell area (map-group 1). Sample depth datum is the middle marker (see text); stratigraphy adopted from well Mapco George E Fisher (SW NE, Sec7-T1S-R3W) published by Fouch (1981); abbreviations and ratios are explained in Appendix 1.1.; black rectangles=cores, hatched rectangles=core chips.

**Figure 28b:** Biomarkers and principal components 1 and 2 vs. depth in the Altamont-Bluebell area (map-group 1). Sample depth datum is the middle marker (see text); stratigraphy adopted from well Mapco George E Fisher (SW NE, Sec7-T1S-R3W) published by Fouch (1981); abbreviations and ratios are explained in Appendix 1.1.; black rectangles=cores, hatched rectangles=core chips.

**Figure 28c:** Biomarker ratios as proxies for clastic and higher plant organic matter input vs. depth in the Altamont-Bluebell area (map-group 1). Sample depth datum is the middle marker (see text); stratigraphy adopted from well Mapco George E Fisher (SW NE, Sec7-T1S-R3W) published by Fouch (1981); abbreviations and ratios are explained in Appendix 1.1; black rectangles=cores, hatched rectangles=core chips.







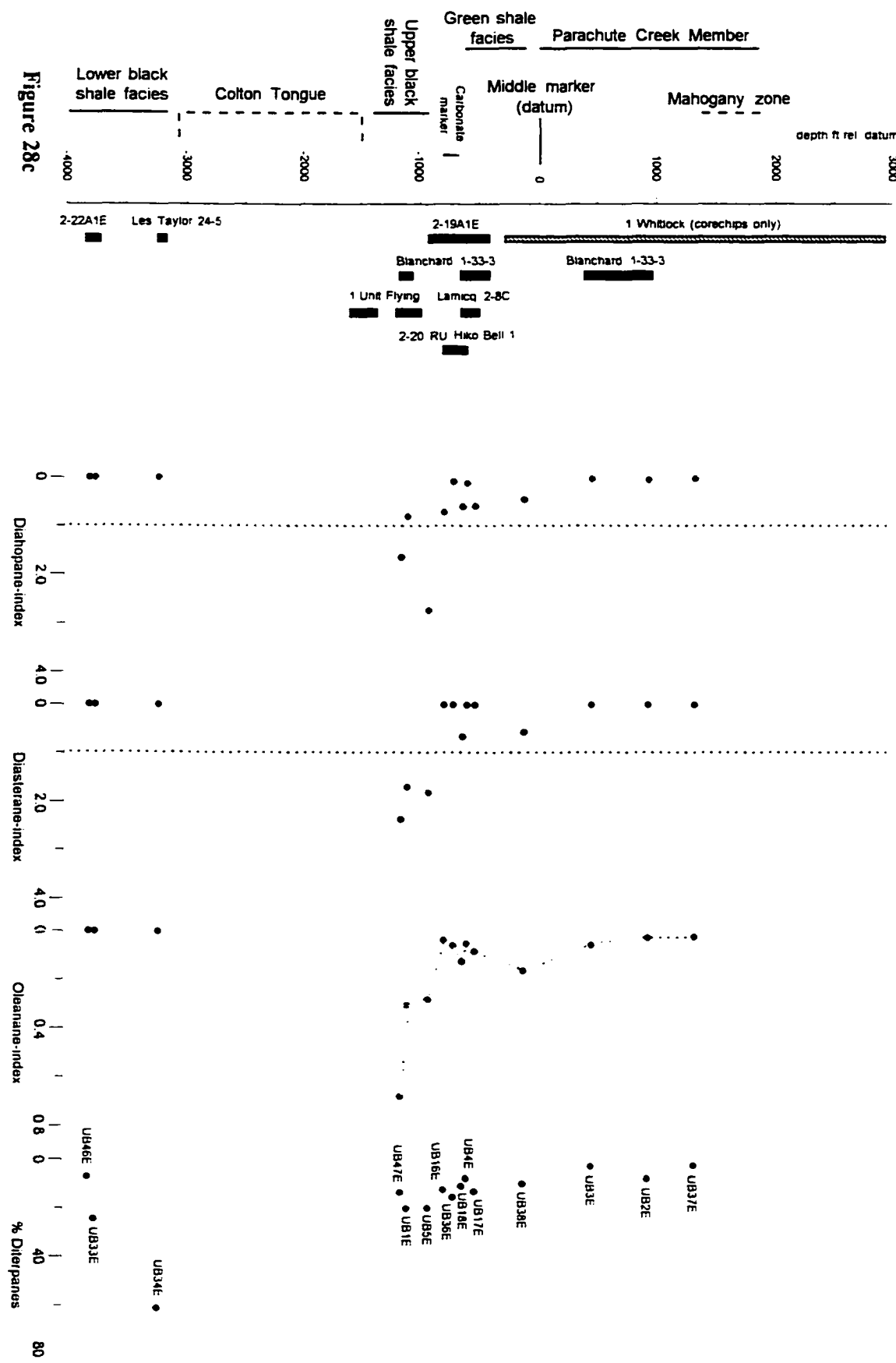
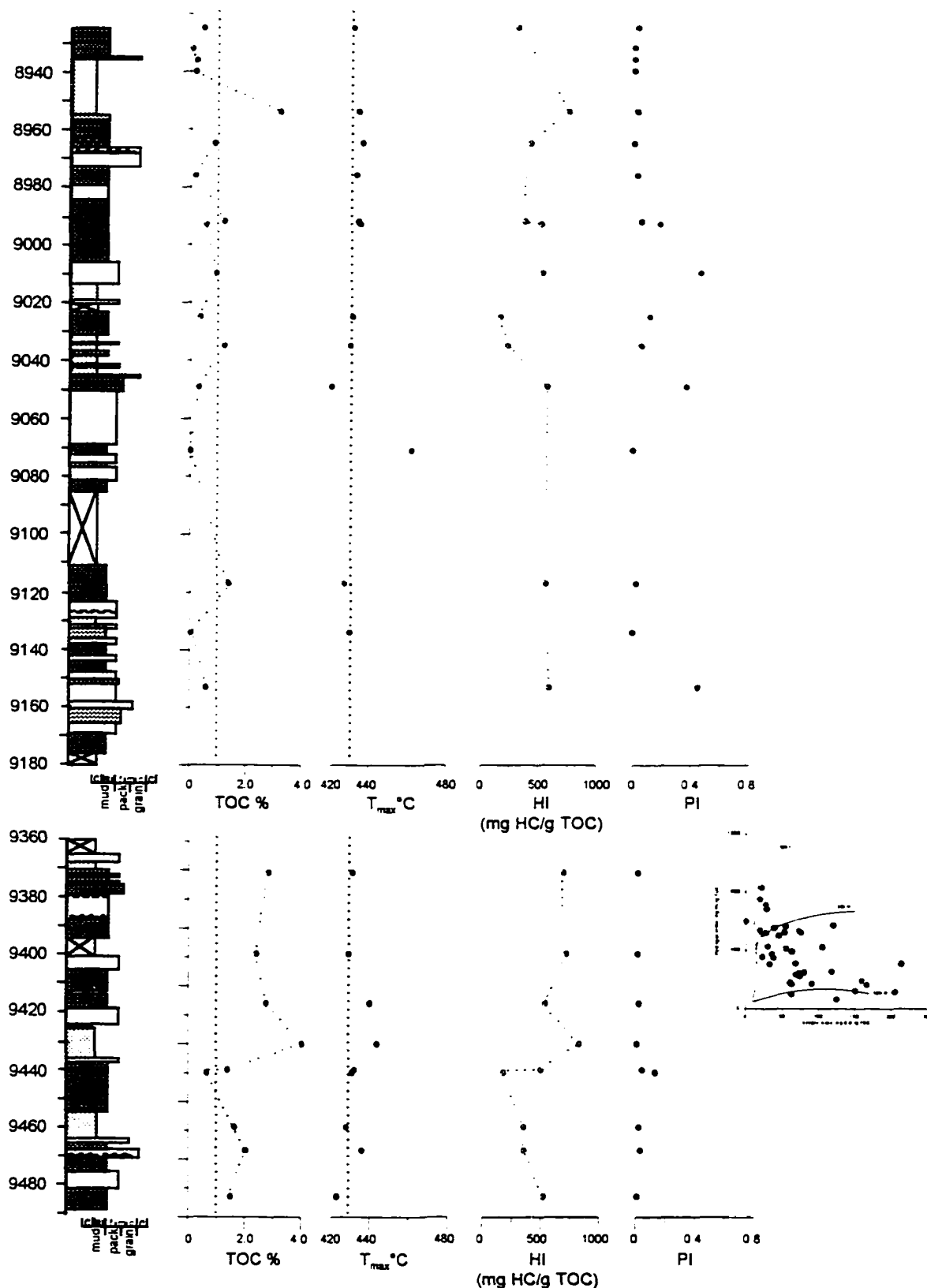
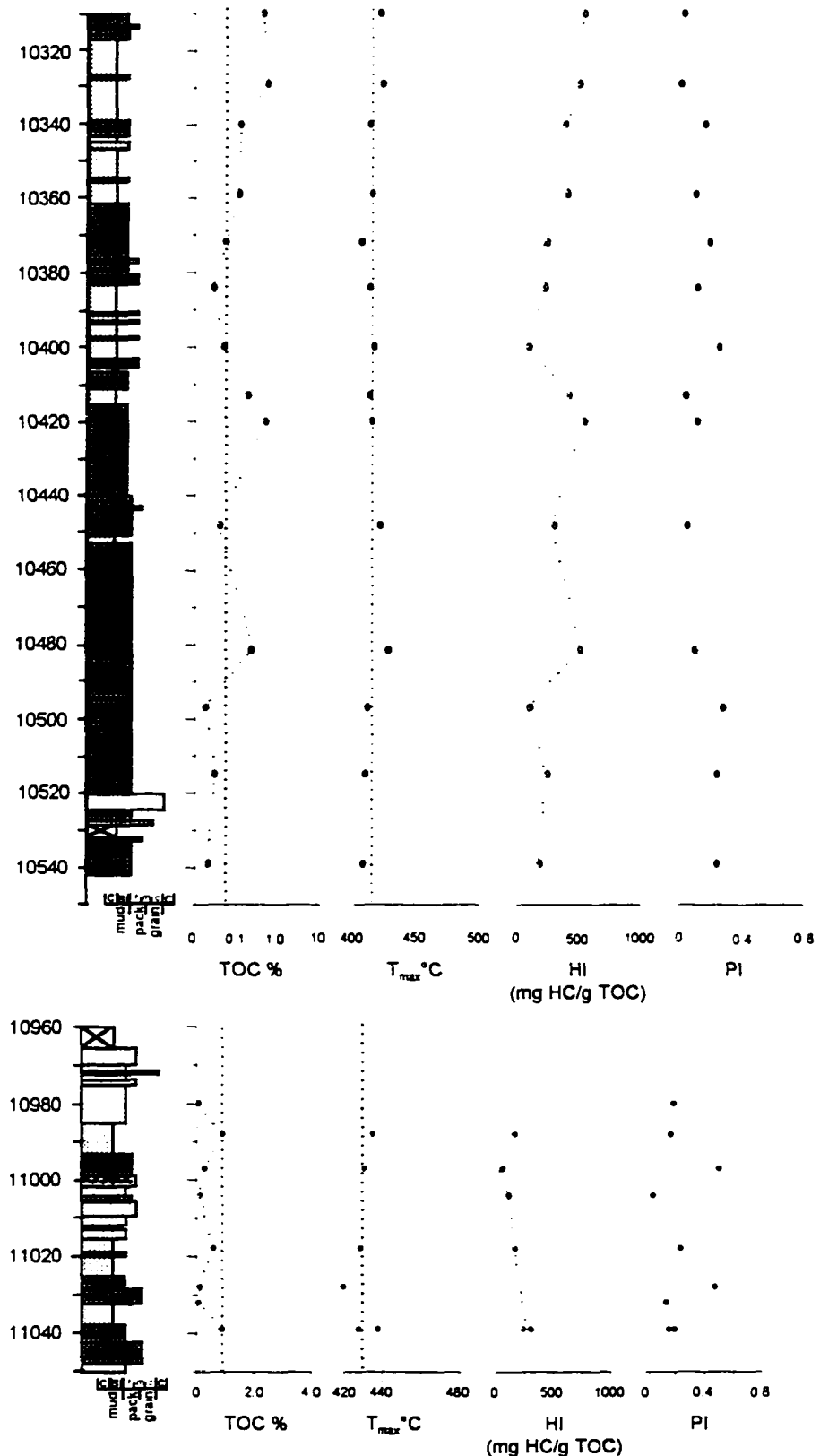


Figure 28c

### Chevron Blanchard 1-33-3



**Figure 29:** Rock-Eval vs. depth profile from well Blanchard 1-33-3 from the Altamont Bluebell area. Core comprises mostly the green shale facies and Parachute Creek Member below the mahogany zone. Legend in Appendix 3.



**Figure 29: cont.**

### **6.2.2 Greater Red Wash Area - Map-group 2**

Similar to the procedure described for the Altamont-Bluebell field, samples from the Greater Red Wash area were referenced to the top of the Douglas Creek Member (Red Wash K-marker) based on structure maps published by Castle (1990) and Kelly and Castle (1990). The wells cover a large area (T9-10S, R21-23E) and stratigraphic associations of the samples to each other are only very approximate. The section covered comprises approximately 1,200 ft. including the upper marginal lacustrine Douglas Creek and lower to middle Parachute Creek Member. Lateral stratigraphic equivalency to the Altamont-Bluebell area is only speculative but the sections of map-group 2 probably correlate to upper part of the green shale facies to Parachute Creek Member below the mahogany zone, based on correlations of Johnson (1989). Most of the samples therefore cover the oil-shale intervals R4-R6 of Johnson (1989) and, in terms of lake evolution, the transitional period between the black shale facies/green shale facies and mahogany zone (equivalent to samples UB3E and UB2E in the Altamont-Bluebell area). Sample UB22E of well Red Wash 32 was obtained from shallow drilling depths and probably represent saline facies equivalent oil-shales.

### **THERMAL MATURITY**

Plots of the GCs of extract saturated fractions (Fig.30) and thermal maturity parameters vs. depth (Fig. 31a) confirm the results of Anders *et al.* (1992) that the organic matter of the source rocks in the Greater Red Wash area is at or near the beginning of the oil generation stage, *i.e.* still too immature for significant hydrocarbon generation. The sterane C<sub>29</sub>  $\alpha\alpha$ 20R and  $\alpha\alpha$ - and  $\beta\beta$ -sterane isomerization indices indicate considerable variations related to source and depositional environment control on these parameters. As mentioned before, processes other than thermal maturation may generate geologic isomers of steranes and terpanes in hypersaline environments

(ten Haven *et al.*, 1986) and the erratic trends may be attributed to changes in lake water and/or sediment pore water chemistry. Moretanes and homohopane stereoisomers appear to be less influenced by these factors and apparently most closely reflect thermal maturity. The geochemical variability of the source rock extracts, despite the similar maturity levels of the samples, supports the assumption that the relative abundance of biomarkers reflect primarily source input or depositional environment.

## GEOCHEMICAL INTERPRETATION OF SOURCE ROCKS

As in the case of the oil-shale type samples in the Altamont-Bluebell field, the organic matter of the Greater Red Wash area is composed mostly of bacterial and algal organic material (Fig.30 and PC1 in Fig.31b). Relative abundances of *n*-alkanes are variable and odd carbon number predominance points to varying degrees of higher plant input. Low relative abundance of rearranged compounds, oleanane and diterpanes indicates reduced influence of clastic and allochthonous organic matter (Fig.31c), although the presence of diterpanes suggests conifers as contributors to the organic matter (Alexander *et al.*, 1987). High molecular weight alkanes in UB7E and UB11E are possibly biopolymers derived from algal cell walls (Tegelaar *et al.*, 1989).  $\beta$ -Carotane is present in variable absolute concentrations in all samples but was detected in all cases significantly below the concentration measured in the mahogany zone sample UB39E (Fig.31b, Appendix 5). Gammacerane is present in low absolute concentration (Fig.24; Appendix 5) and relative abundance as represented by PC2 (Fig.31b). Sample UB20E shows high gammacerane abundance relative to pentacyclic terpanes, but the sample has a low TOC and is also unusual comparing the HI and the compound distribution in the other samples. Sample UB11E has a regular source rock type *n*-alkane distribution and its geochemical composition does not resemble the other samples analyzed from this area (Fig.30). The high relative abundance of *n*-

alkanes in sample UB11E indicates that their presence is a source related feature of the organic matter. The TOC and HI values indicate that this sample represents a viable source facies. Overall, the geochemistry of map-group 2 samples supports the correlation to similar samples in the Altamont-Bluebell area (UB2E, UB3E), and represent a relatively shallow, alkaline lake environment with a productive algal and bacterial population. It is likely that the bacterial biomass in this case at least partially represent autotrophic bacteria, which flourished in the saline lake water. It appears again, though, that the water was less saline than the during the deposition of the mahogany oil-shales, based on the lower concentration of hypersaline markers in the samples. This is also suggested by low absolute gammacerane concentrations (Fig.23), with the exception of sample UB8E. This sample is compositionally related to the Mahogany zone outcrop sample UB39E (compare plot of sample points on PC1 vs. PC2 in Fig.24a), but has different Pr/Ph values and β-carotane concentration. Similar to the lean oil-shales of the Altamont-Bluebell area, the sediments are interpreted to have been deposited in a marginal lacustrine setting. These areas were inundated by frequent, short term lake expansions which resulted in saline shallow lacustrine environments possibly with anoxic bottom water. The lithology of the cores consist of variable light brown-gray siltstones, occasional sandstones in addition to dark shales and mudstones which often exhibit lamination. Sedimentary structures (frequent cross-, flaser- and lenticular-bedding) also suggest marginal lacustrine setting (Appendix 3.2).

Well 23-24 Federal comprises a 120 ft thick interval composed mostly of shales and dolomite/dolomitic limestone in which algal and shallow water sedimentary structures have been identified (Appendix 3.2.-1). However, exceptionally TOC-rich shales are present (UB19E), indicating that this type of setting is also conducive to the deposition of thick, organic-rich source units. Figure 32 shows a Rock-Eval depth profile of this core. Thickness and pervasive lamination of shales with variable colors and TOC content are interpreted as products of transitional distal

marginal lacustrine and open lacustrine deposition. However, algal boundstones in addition to the facies context and the geochemistry of TOC-rich beds in other wells of this area indicate that they are deposits of probably short term open lacustrine incursions with extremely high productivity (possibly algal blooms) and/or preservation potential. Lamination indicates the absence of bottom feeding scavengers and burrowers, thus also providing evidence for lake bottom water anoxicity and/or salinity.

---

Captions (next 4 pages)

**Figure 30:** HTGC analysis of source rockextract saturated fractions from cores of the Greater Red Wash area. Sample depths relative to top of Douglas Creek Member (K-marker) datum (see text). Sample information includes sample number, depth of sample in well and Rock-Eval bulk data. \*=Internal standard C<sub>24</sub>D<sub>50</sub>; abbreviations and ratios are explained in Appendix 1.1; black rectangles=cores, hatched rectangles=core chips.

**Figure 31a:** Maturity related biomarker indices and principal component 3 vs. depth in the Greater Red Wash area (map-group 2). Sample depth datum is the top of the Douglas Creek Member (see text); black rectangles=cores, hatched rectangles=core chips.

**Figure 31b:** Selected biomarkers and principal components 1 and 2 vs. depth in the Greater Red Wash area (map-group 2). Sample depth datum is the top of the Douglas Creek Member (see text). Sample information includes sample number, depth of sample in well and Rock-Eval bulk data; abbreviations and ratios are explained in Appendix 1.1; black rectangles=cores, hatched rectangles=core chips.

**Figure 31c:** Biomarker ratios as proxies for clastic and higher plant organic matter input vs. depth in the Greater Red Wash area (map-group 2). Sample depth datum is the top of the Douglas Creek Member (see text); abbreviations and ratios are explained in Appendix 1.1.; black rectangles=cores, hatched rectangles=core chips.

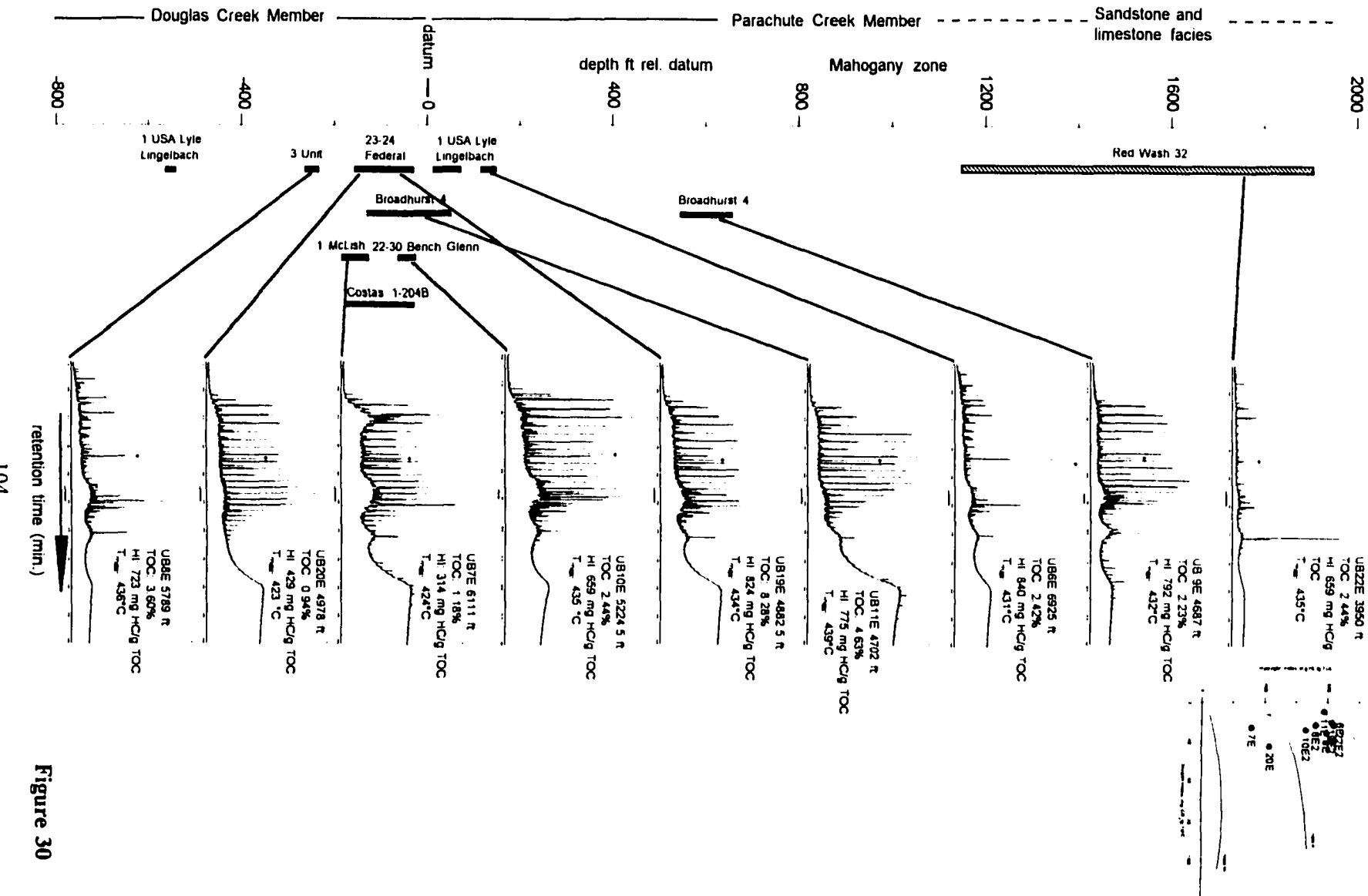


Figure 30

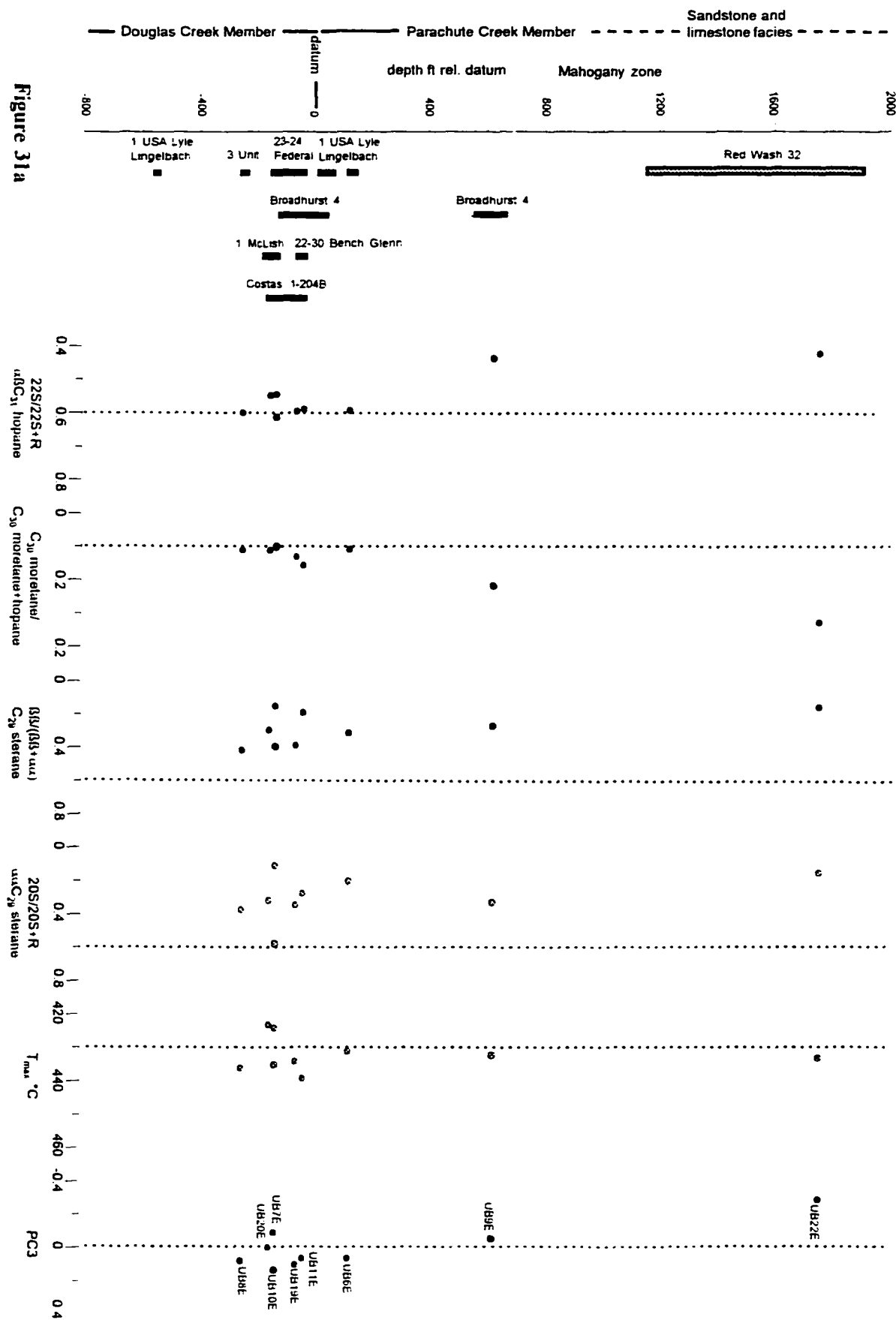
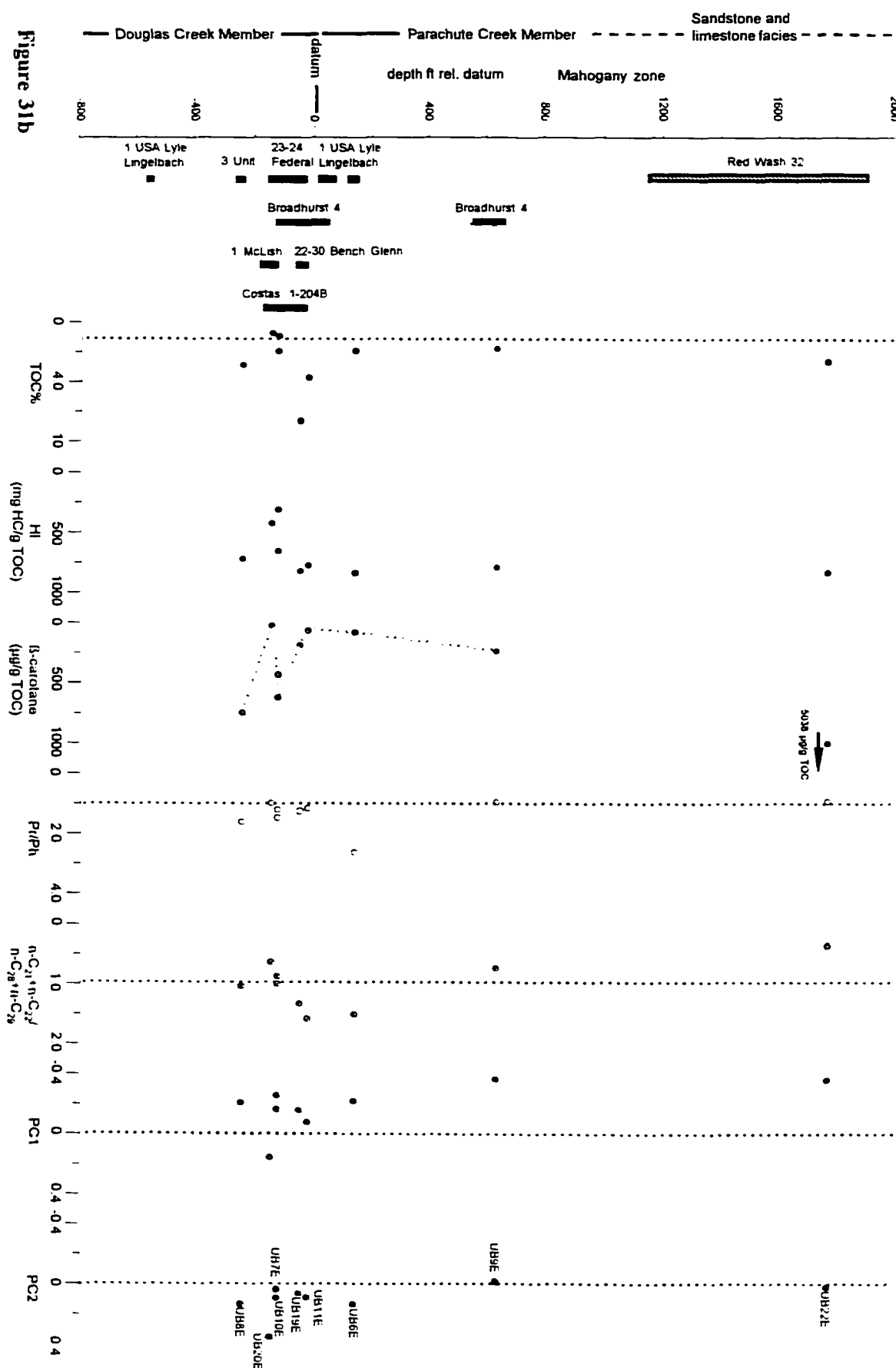


Figure 31a



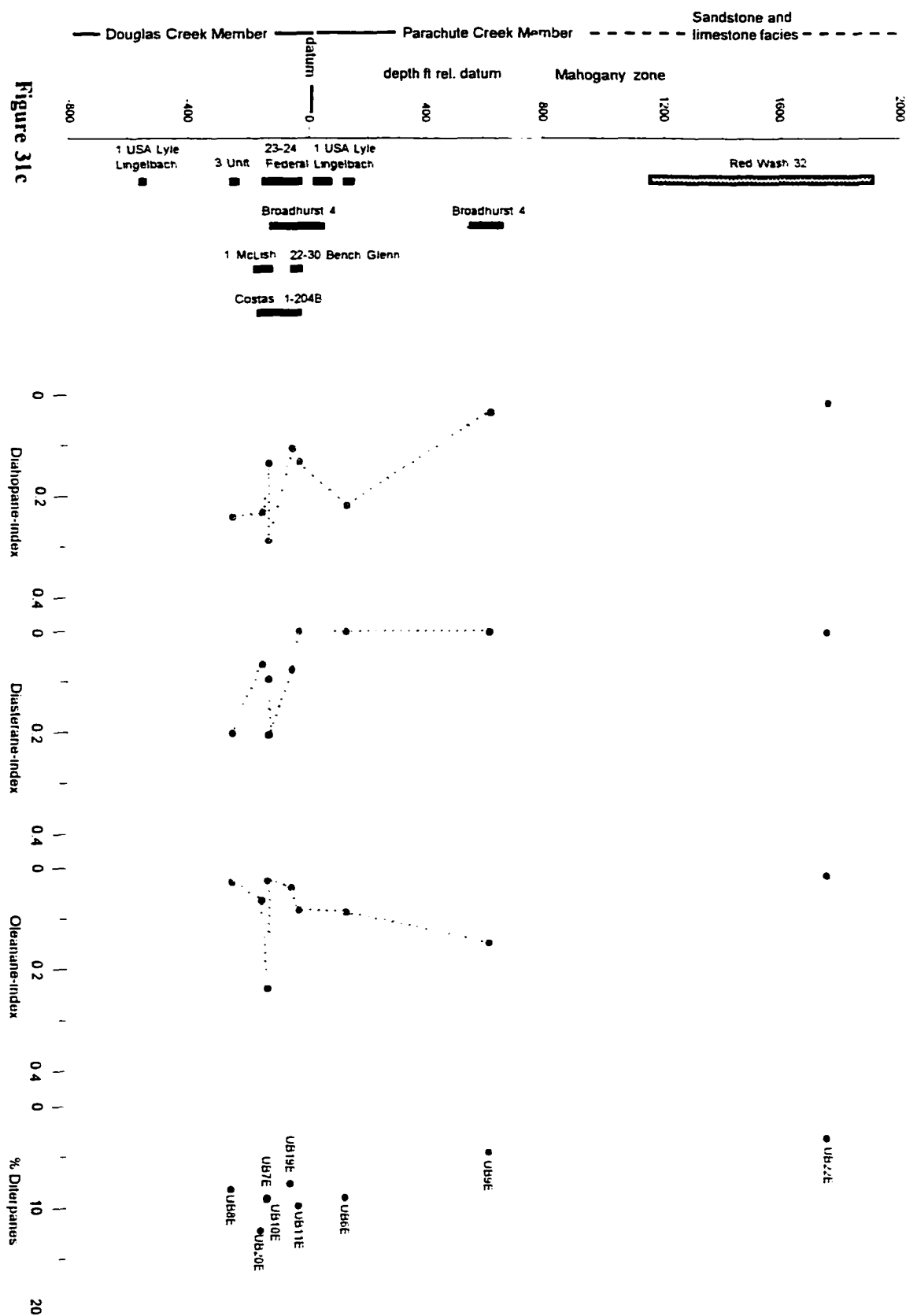
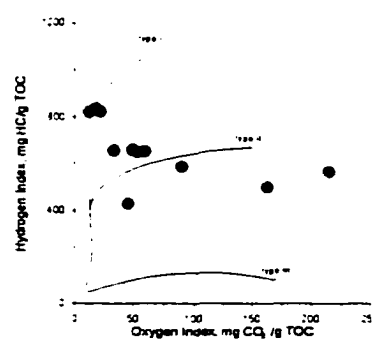
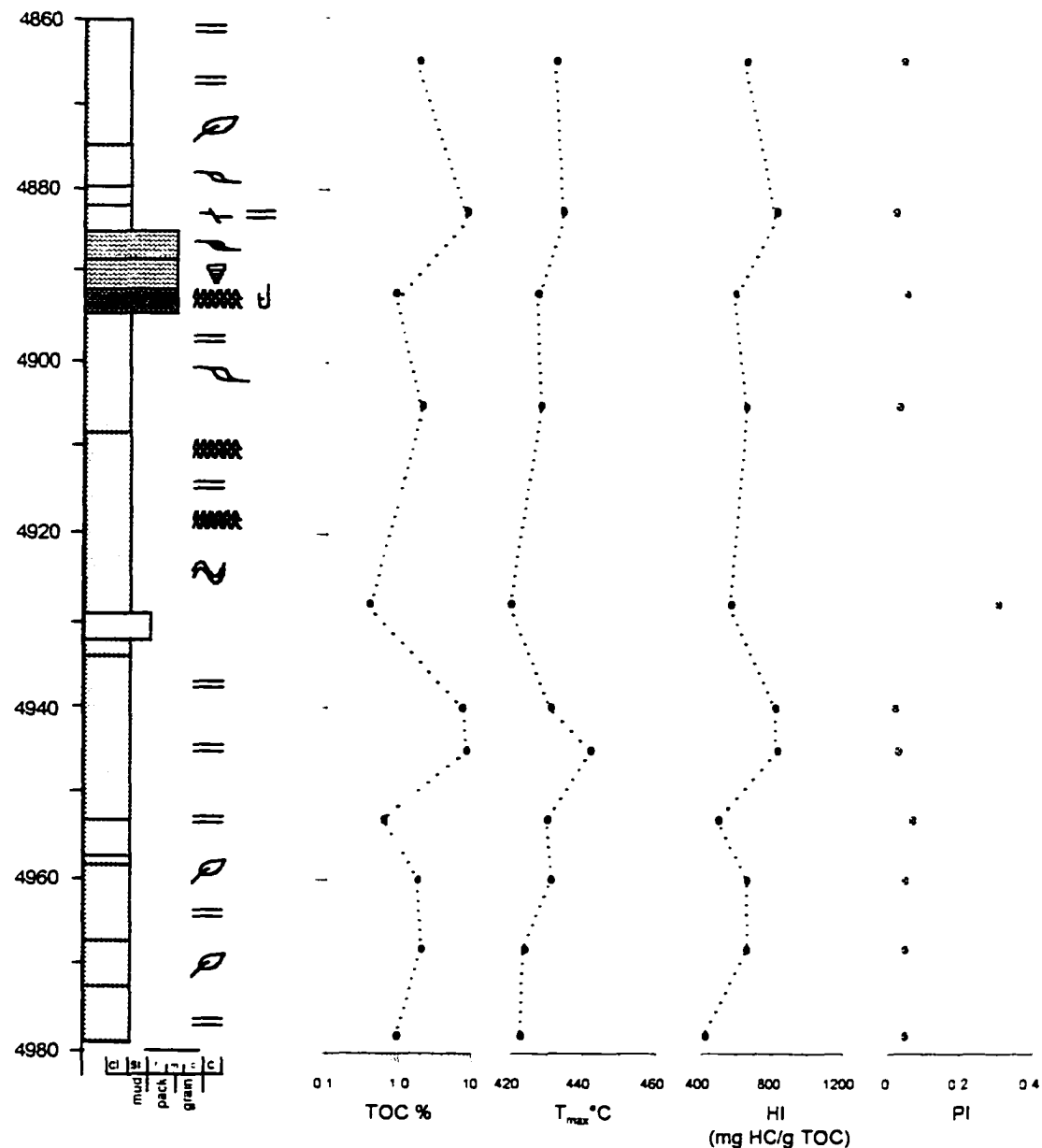


Figure 31c



**Figure 32:** Rock-Eval vs. depth profile for well 23-24 Federal from the Greater Red Wash area. Rocks are from the upper Douglas Creek Member. Legend in Appendix 3.

### 6.2.3 South-Central Area - Map-group 3

A datum for reference of wells in the south-central area of the basin was provided by Colburn *et al.* (1985). Based on their structure map, samples were referenced to the 3pt. marker in the green shale facies, a consistent log marker for the area some 150-200 ft below the middle marker. The sections covered by the cores therefore are interpreted to range from the lower Green River Formation (upper and lower black shale facies to green shale facies). Similar to the markers of map-groups 1 and 2, the 3pt. marker has only lithostratigraphic significance and the stratigraphic association of the samples within this group is only very approximate. According to the cross section published by Colburn *et al.* (1985), the Colton Tongue is present only in the southernmost part of the area and the black shale facies forms a continuous section to the top of the Wasatch Formation some 1,800 ft below the 3pt. marker. Based on this interpretation, the lowermost sample (UB21E) may be located in the Wasatch Formation-black shale facies transition. Sample UB32E has a high Rock-Eval PI and is probably stained by migrated bitumen. All other samples originate from sections below the carbonate marker and thus represent, together with the stratigraphically deepest samples from the Altamont-Bluebell area (UB33E, UB34E, UB46E), the stratigraphically lowest sections of the Green River Formation. These source rocks represent organic facies from the early stages of Lake Uinta.

### THERMAL MATURITY

Thermal maturity parameters show an early mature stage of the source rocks. The dominance of *n*-alkanes in the GCs of the extracts (Fig. 33) is a source related feature. Ruble (1996) suggested that  $T_{max}$  is a reliable maturity parameter for the black shale facies, and the samples show a  $T_{max}$  of around 440°C (Fig. 34a). The scores on PC3 are positive except for UB21E, which indicates the presence of thermally labile moretanes and dominance of  $\alpha\alpha20R$ .

sterane isomers. Sterane isomer ratios were measured below the suggested equilibrium values (Fig. 34a). The low TOC content of sample UB21E renders the maturity measurements on this sample less reliable, as is also suggested by comparison of maturity parameters measured in sample take from higher stratigraphic levels. Organic-rich samples at similar depths may therefore be in the late early to beginning peak generation stage. Frequent oilstained sand- and silt-units intercalated between organic-rich sections, however, indicate that hydrocarbon generation may be occurring. It has also been suggested that isomerization reactions of molecular thermal maturity indicators (sterane and hopane/morepane isomerization) in Tertiary source rocks and oils are often incomplete due to the lack of sufficient time for the reactions to occur (Grantham *et al.*, 1986). It is therefore possible, that the biomarker maturity ratios presented in Figure 34a underestimate the maturity of the samples.

## GEOCHEMICAL INTERPRETATION OF SOURCE ROCKS

The difference compared to the upper Green River samples of the Bluebell-Altamont area and the Greater Red Wash area becomes apparent in the stratigraphically ranked GC plots of Figure 33. The samples display abundant *n*-alkanes and only minor traces of  $\beta$ -carotane are recognizable in two samples (UB13E and UB32E). Samples are more or less indifferent to PC1 vs. depth (Fig. 34b), suggesting that inversely correlated variables have similar influence on this PC and compensate each other. In combination with observation of PC2 an abundance of bacterial organic matter in these samples is apparent. Surprisingly, diterpanes and oleananes are present in low relative concentrations, suggesting low input of conifer resins and angiosperms compared to the upper black shale facies analyzed in the Altamont-Bluebell area. Rearranged hopane and sterane-indices are also relatively low, possibly due to the lack of clastic sediment input (Fig. 34c). The portion of terrestrial organic matter, however, is significant, as is obvious from the high

relative concentration of *n*-alkanes  $\geq n\text{-C}_{25}$  and distinct odd predominance displayed in the samples of Figure 33 (except for UB21E). This can indicate that the surrounding flora of higher plants was different from the upper Green River Formation, possibly related to climatic changes occurring during the Early to Middle Eocene (Chapter 3.4). Methyl steranes are ubiquitous in the organic-rich samples providing evidence for the presence of dinoflagellates in the photic epilimnion. The samples have no or only minor  $\beta$ -carotane concentrations, confirming that the synthesizing organisms were not abundant during the early stages of Lake Uinta. Low absolute and relative gammacerane concentrations (Fig.24; Fig.34b) also suggests minor contribution from bacterivorous ciliates or other tetrahymanol-synthesizing prokaryotes. Low concentrations of  $\beta$ -carotane and gammacerane indicate that the lake was indeed in a freshwater stage, perhaps thermally stratified, which did not support a fauna and flora of organisms requiring higher salinities. However, organic carbon production and preservation was sufficient for the deposition of viable source rocks. Two samples (UB29E, UB12E) are massive pelecypod packstones, a facies type that has been interpreted as nearshore open lacustrine (Wiggins and Harris, 1994). The sedimentary facies of cores and the location of the area in marginal lacustrine settings during the initial stage of Lake Uinta (compare Fig.5d for facies distributions) also suggest that the organic-rich rocks represent nearshore to marginal lacustrine, littoral source rocks and are not of profundal open lacustrine origin. Organic-leaner samples apparently originate from silt- and sand-rich proximal facies. The core from well Island Unit 16 (sample UB29E, Appendix 3.3.-2) records approximately 125 ft of open lacustrine facies in the lower Green River/black shale facies, in which massive and laminated shales with occasional gastropods and pelecypods are interrupted by partly organic-rich fossiliferous or oolitic packstones. The pelecypod and gastropod fauna has also been interpreted as evidence for freshwater lacustrine deposition (LaRoque, 1960).

---

Captions (next 4 pages)

**Figure 33:** HTGC analysis of source rock extract saturated fractions from cores of the South-central area (map-group 3). Sample depths relative to the 3pt. marker datum Colburn *et al.* (1985). Sample information includes sample number, depth of sample in well and Rock-Eval data. \*=Internal standard C<sub>24</sub>D<sub>50</sub>; black rectangles=cores.

**Figure 34a:** Maturity related biomarker indices and principal component 3 vs. depth in the south-central area (map-group 2) of the Uinta Basin. Sample depth datum is the 3pt. marker of Colburn *et al.* (1985); black rectangles=cores.

**Figure 34b:** Selected biomarkers and principal components 1 and 2 vs. depth in the south-central area (map-group 3) of the Uinta Basin. Sample depth datum is the 3pt. marker of Colburn *et al.* (1985); black rectangles=cores.

**Figure 34c:** Biomarker ratios as proxies for clastic and higher plant organic matter input vs. depth in the south-central area of the Uinta Basin (map-group 3). Sample depth datum is the 3pt. marker of Colburn *et al.* (1985; see text); ratios are explained in Appendix 1.1.; black rectangles=cores.

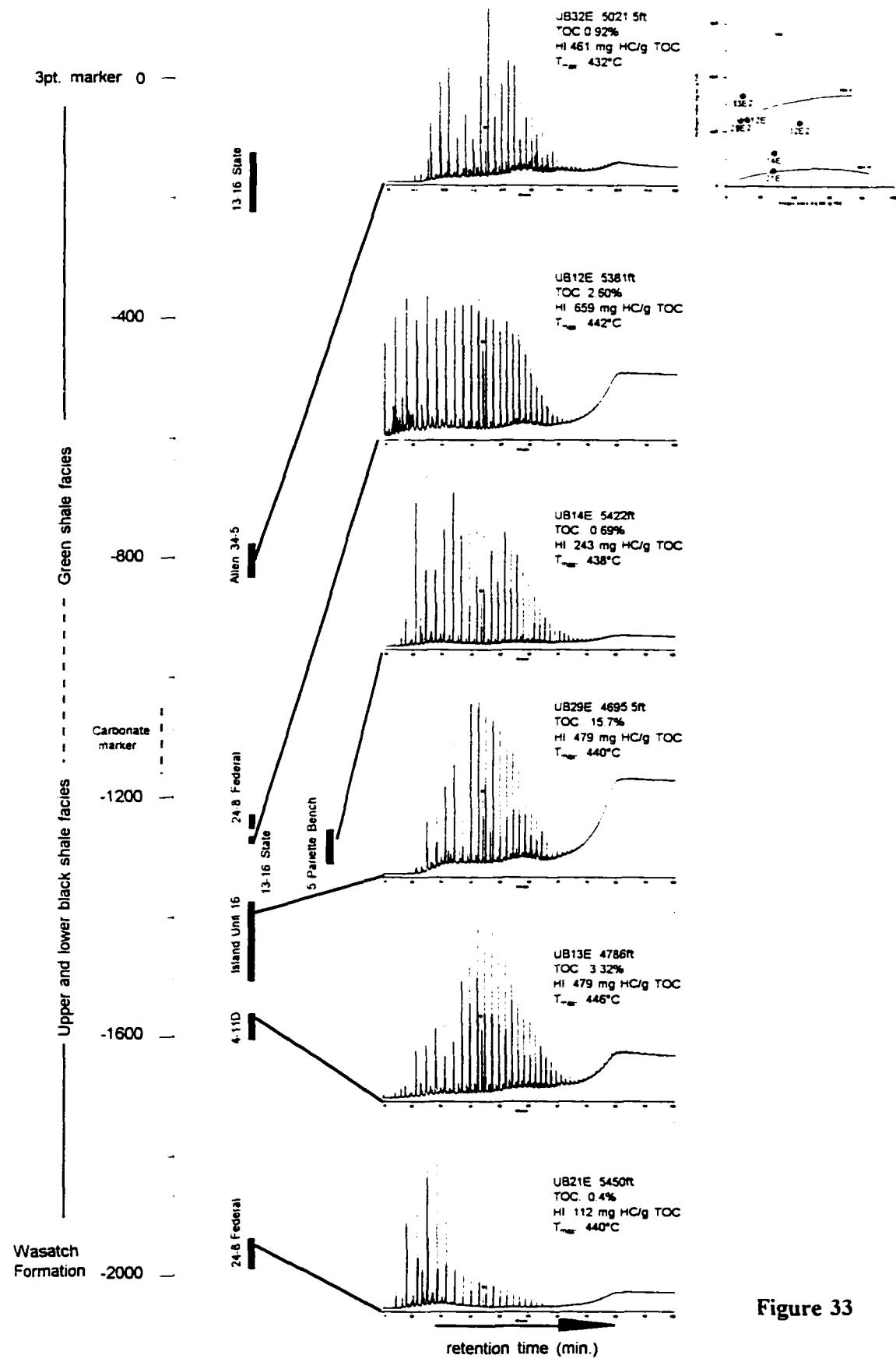


Figure 33

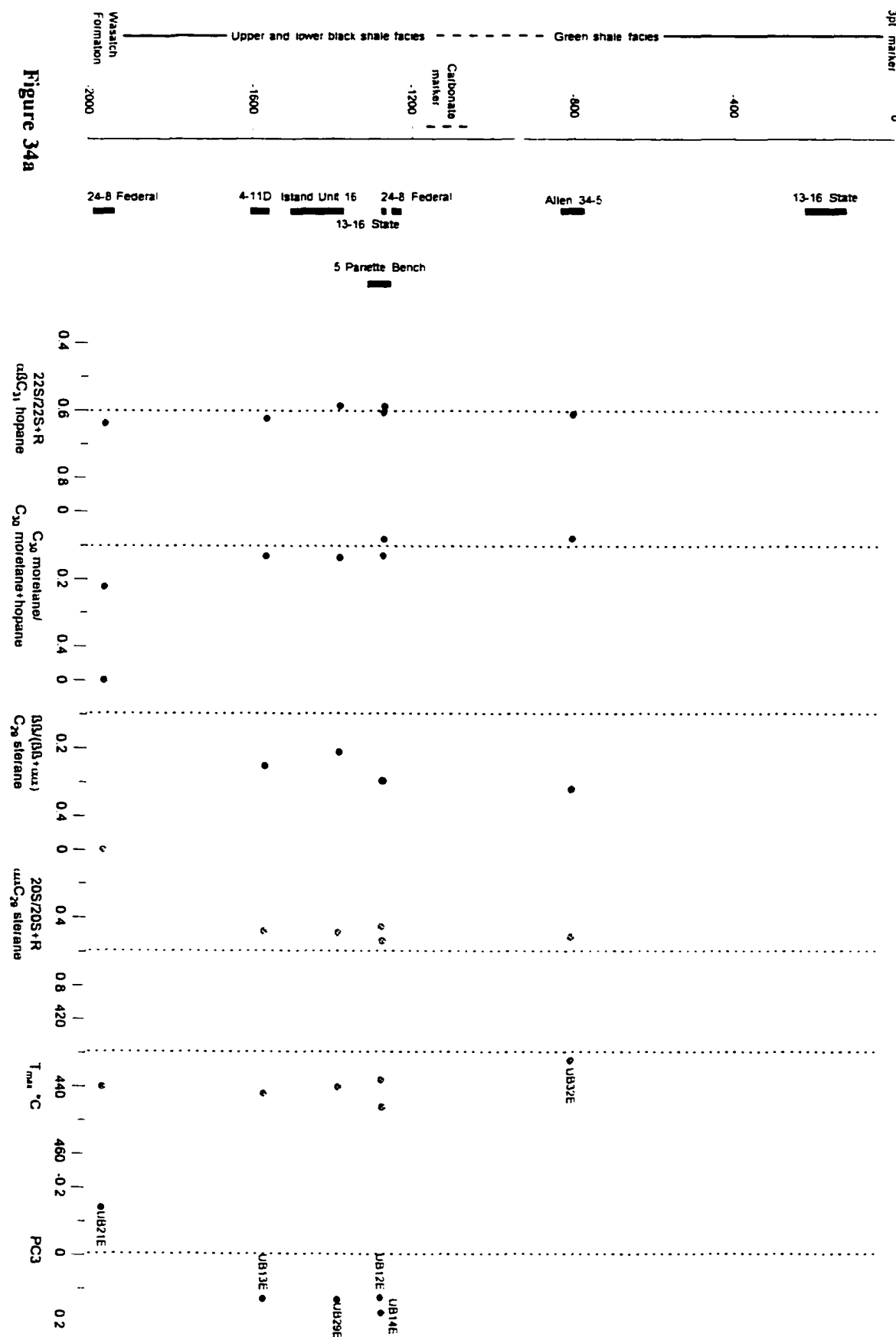


Figure 34a

- S11 -

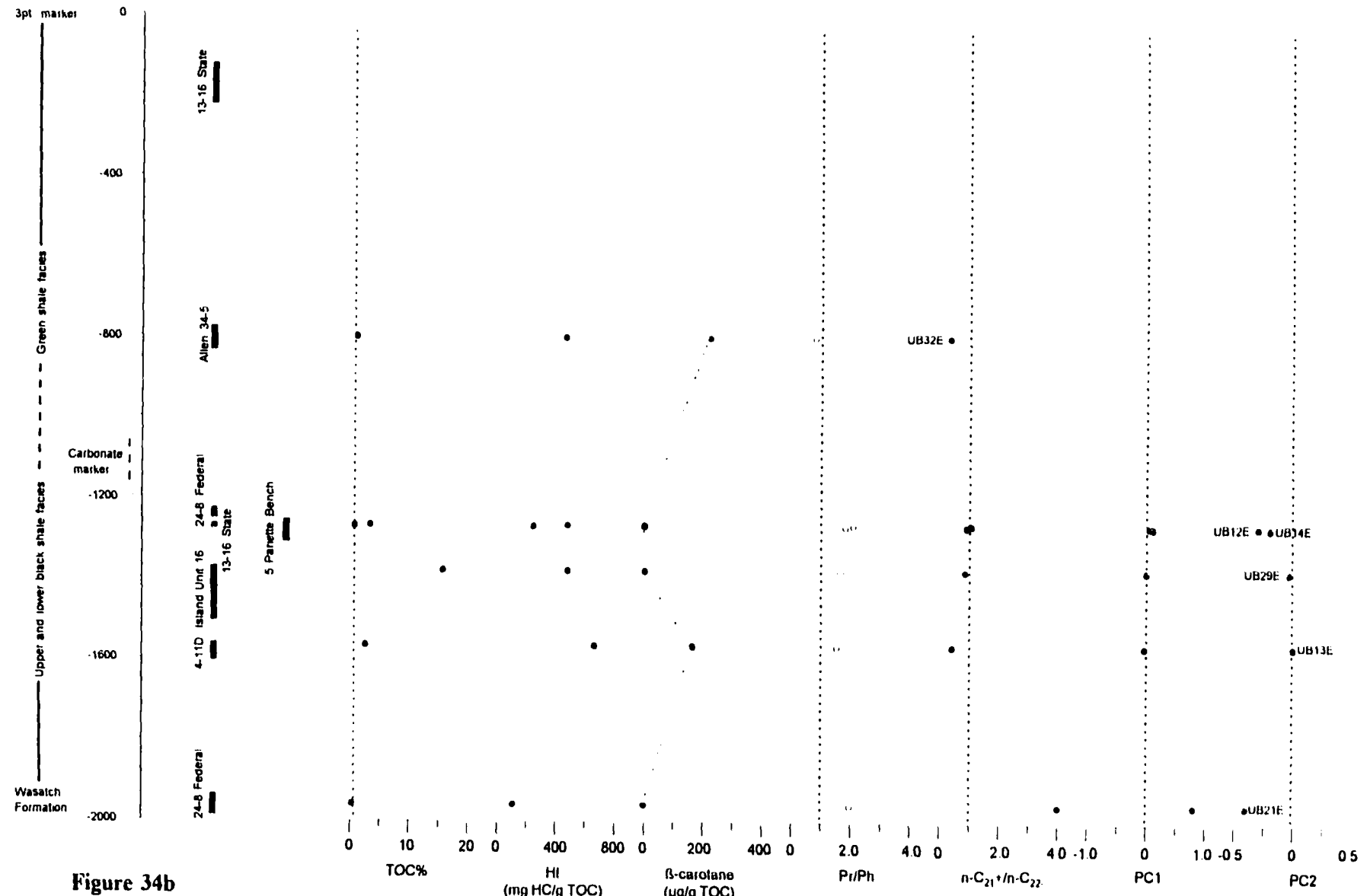


Figure 34b

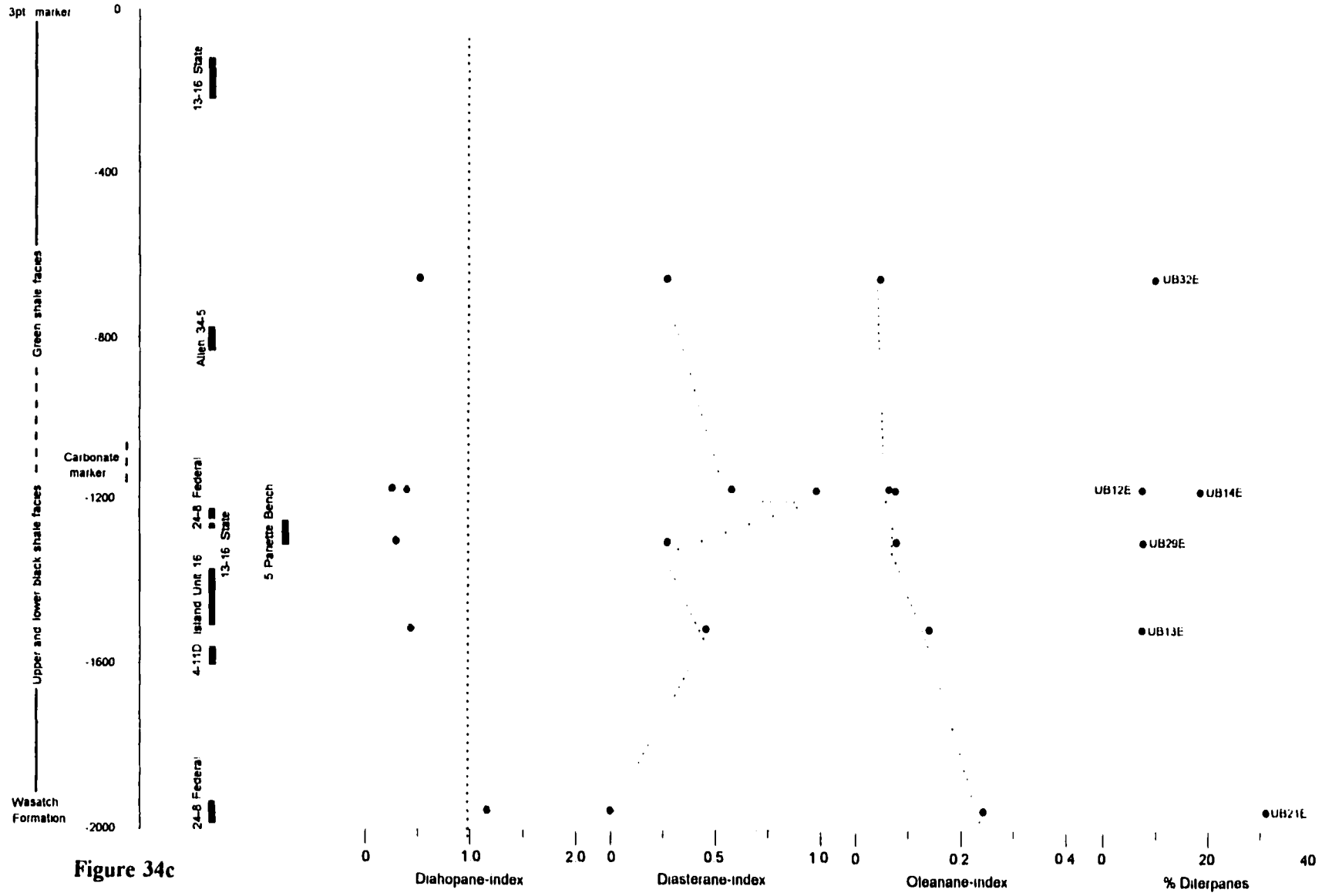


Figure 34c

### **6.3 Crude Oil Analysis**

After the geochemical characterization of the source rocks and documentation of the relationships between extract composition and stratigraphic position, the question is how the variability in source rock composition affects the geochemistry of crude oils in the Uinta Basin. An attempt was made to define this stratigraphic control by analyzing 52 crude oil samples from various fields in the basin (see Appendix 7 for well data). Samples from all major fields were obtained, except for the Red Wash field. All oils are separated into map-groups based on well location (Fig. 10) and appear non-degraded, although some samples may have lost lower molecular weight alkanes and possibly sesquiterpanes through evaporation during sample preparation. Otherwise no signs of severe secondary alterations were recognizable. Except for the Altamont-Bluebell, Cedar Rim and Brennan Bottom/Horseshoe Bend areas, the wells in the individual fields produce approximately from the same stratigraphic interval such that lateral variations in oil composition between the fields are expected to be larger than vertical variations within a field. Reservoir descriptions (Chapter 3.5; see Fouch *et al.*, 1994 for review) indicated that, except in the deep Altamont-Bluebell and Cedar Rim areas, the reservoirs are generally thin (maximum thickness 10's of ft), unfractured and consist of individual reservoir compartments with stratigraphic closure (see also Table 1, and references therein).

#### **6.3.1 General Observations**

Similar to the source rock analyses, it is convenient to first describe common features observed in the sample set before describing the details of the geochemical composition. The API gravity of Uinta Basin crude oils varies considerably (22° to 54°; Table 1), but are mostly ~31°. Generally, the oils are viscous to solid at STP, low in sulfur (Fouch *et al.*, 1994) and vary in color from black to greenish brown and yellow.

The crude oils can be differentiated into an immature type (see also Ruble, 1996) and a more frequently occurring regular oil-type based on GC analysis in a similar manner to the source rock extracts (see Appendix 10 for gas chromatograms of the oils analyzed). A third group is the green to yellow colored waxy oils from the deep reservoirs of the Altamont-Bluebell and Cedar Rim areas. A ternary plot describing the relative amounts of fractions for the three oil-types is shown in Figure 35a, in which the oil-types are fairly well separated. Immature oil-types are characterized by relatively high aromatic and polar fractions, waxy oils consist almost purely of saturated compounds. Samples of the regular type show a wide scatter, indicating that there is a larger compositional heterogeneity inherent to this group. Representative high temperature gas chromatograms of the different oil-types are shown in Figure 36, and average parameters obtained from fractionation and GC analysis are listed in Table 8. The differentiation of crude oil types is based on relative abundance of *n*-alkanes other compounds such as isoprenoids and  $\beta$ -carotane in the chromatograms.

Oil-type		%ASPH	%SAT	%POL	%bran.	$\beta$ -caro-tane ( $\mu\text{g/g oil}$ )	Pr/Ph	Pr/ <i>n</i> -C <sub>17</sub>	C <sub>21+22/C</sub> 28-29	CPI
waxy <i>n</i> =5	avg.	6.9	91.6	3.9	43.1	0	3.93	0.26	1.54	0.99
	range	3.3-13.1	86.9-97.2	1.6-6.8	20.1-60.8	0	2.3-6.6	0.14-0.32	1.24-1.90	0.96-1.02
	std.dev.	4.0	3.8	2.2	15.0	0	2.1	0.07	0.30	0.02
immature <i>n</i> =8	avg.	11.9	69.3	15.2	80.8	1332	1.44	2.97	0.84	1.27
	range	1.2-53.0	61.1-78.9	8.1-24.3	76.4-88.3	550-3287	0.97-2.12	1.74-6.43	0.55-1.24	1.08-1.54
	std.dev.	16.8	7.8	5.8	4.4	944	0.39	1.67	0.21	0.17
regular <i>n</i> =39	avg.	7.4	77.6	8.5	69.1	316	1.18	0.72	1.07	1.04
	range	2.5-28.3	50.3-88.8	3.8-19.8	50.7-94.2	0-968	0.65-2.07	0.07-2.47	0.52-1.90	0.97-1.11
	std.dev.	4.4	7.3	3.4	8.3	222	0.39	0.44	0.11	0.03

**Table 8:** Averages and ranges of selected geochemical parameters for waxy, immature, and regular oil types produced in the Uinta Basin (*n*=number of samples, avg.= average, std.dev.=standard deviation).

A more differentiated picture arises when comparing relative amounts of *n*-alkanes, branched and cyclic and aromatic+polar fractions shown in Figure 35b (after Tissot and Welte,

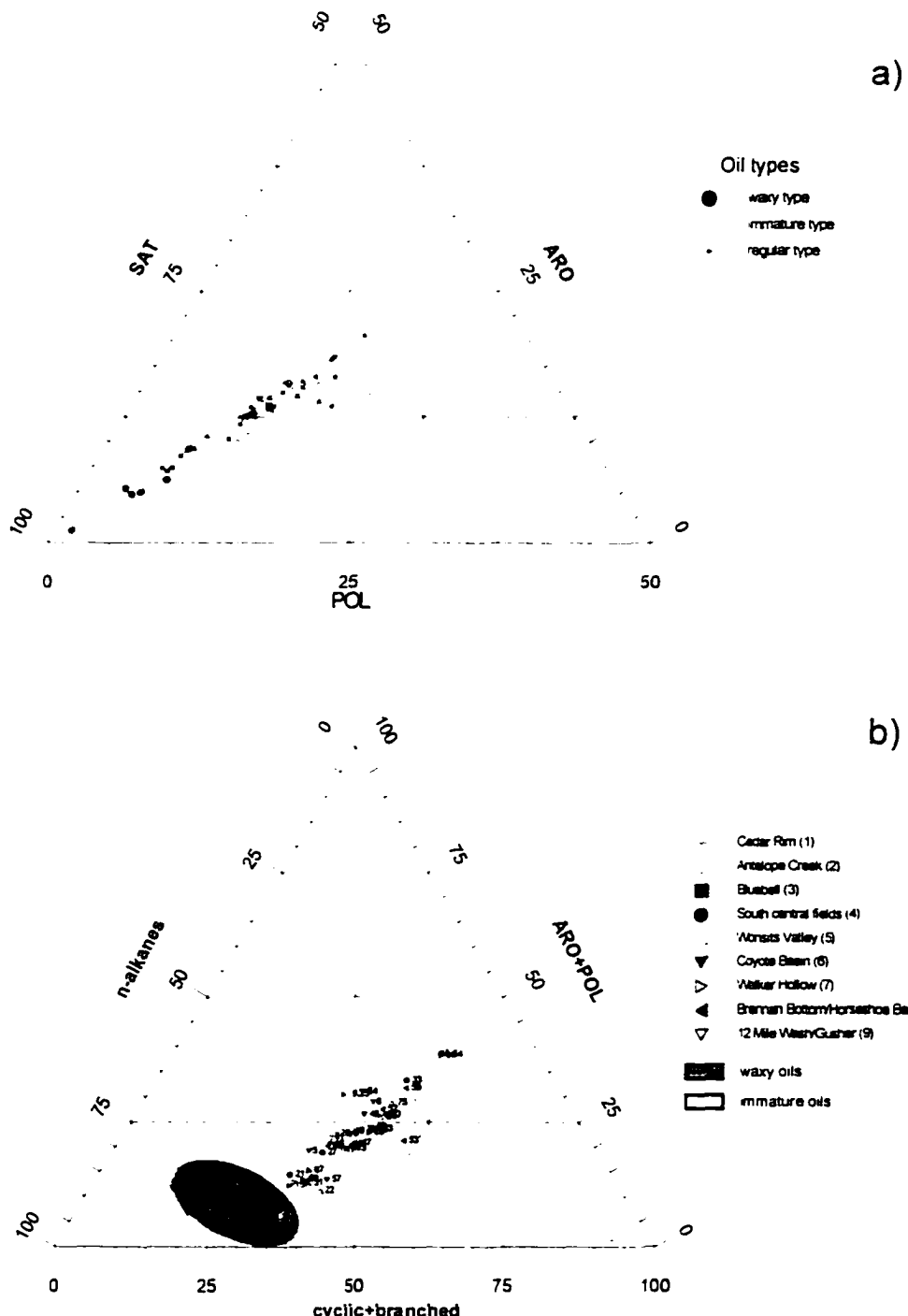


**Figure 35:** Ternary diagrams of crude oil saturated, aromatic and polar fractions in the three different oil types (a) (note axis scales); n-alkanes, aromatics+polars and cyclic & branched fractions of samples separated into map-groups (labels indicate sample numbers) (b). Based on classification suggested by Tissot and Welte (1984) oils are paraffinic and napthenic crudes.

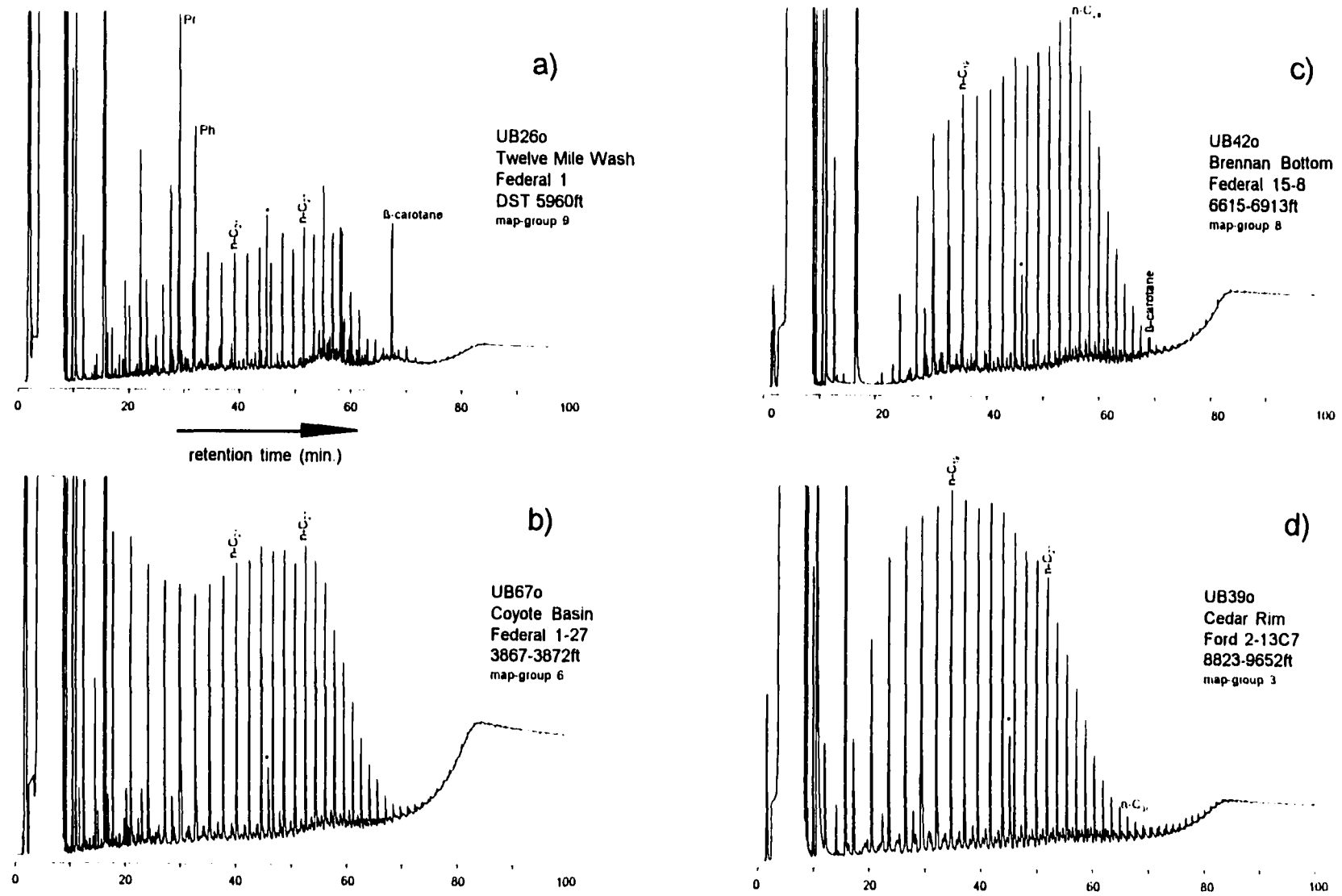


**Figure 36:** HTGC of representative samples of oils produced in the Uinta Basin. Chromatogram in (a) is an immature type oil, (b) and (c) are regular type oils and (d) is a waxy (yellow) crude oil sample. \* = Internal standard  $\text{C}_{24}\text{D}_{50}$ .

1984). Waxy oils have the highest *n*-alkane concentrations and, due to incomplete separation of high molecular weight compounds during fractionation, it can be expected that some waxy compounds eluted in the aromatic or polar fractions. Immature samples plot at the opposite side of the diagram with high concentrations of branched and cyclic compounds and relatively high aromatic and polar fractions. Some regular type oils plot close to the immature types, indicating that both types are transitional and there is no clear separation (e.g. sample UB75o, Appendix 10.5-1). Waxy oils are characterized by the dominance of *n*-alkanes extending to >*n*-C<sub>45</sub> (Figure 36d). No biomarkers were detected in the branched and cyclic fractions, and isoprenoids (pristane, phytane) are present in minor concentrations only. In the high temperature region of the oils a new homologous series of monocyclic and branched compounds (Carlson *et al.*, 1993) dominates over *n*-alkanes. Two regular oil type samples are shown in Figure 36b and c to illustrate the variability within this group. Both unimodal and bimodal distributions are present and most unimodal samples are skewed towards the high molecular weight *n*-alkanes. A distinct odd carbon number predominance between *n*-C<sub>25</sub> and *n*-C<sub>30</sub> is characteristic of most samples. However, a slight predominance of even numbered homologues between *n*-C<sub>19</sub> and *n*-C<sub>23</sub> is also frequently present. An elevated *n*-C<sub>22</sub> concentration (Appendix 8) was described as characteristic for source rocks deposited in hypersaline environments but the R22 ratio (Appendix 1.1) never exceeded the suggested limit of >> 1.5 (ten Haven *et al.* 1988). Small peaks of high molecular weight compounds were visible in the high temperature range of the chromatograms. A few samples in this group displayed a distinct β-carotane peak (e.g. Fig. 36c). Sample UB26o in Figure 36a illustrates the typically high isoprenoid, terpane and β-carotane dominance over the distinctly odd predominated *n*-alkane series in immature oils. The compound distribution is comparable to the composition of mahogany zone extracts described in Chapter 6.1 (compare sample UB39E in Appendix 6-1). Similar to the source rock extracts the differentiation between immature and

regular types is somewhat artificial and their geochemical properties are transitional. Samples UB33o and UB9o from shallow reservoirs in the Altamont-Bluebell and Coyote Basin area, respectively, are very immature and show properties of both groups (Appendix 10.4-1 and 10.6-1).

### **6.3.2 Crude Oil Biomarker Composition - GC-MS Analysis**

The variety of biomarkers detected in the branched and cyclic fractions of the crude oil samples is similar to those described for the branched and cyclic fractions of the source rock extracts. The geochemical implications of biomarker occurrences and distributions are summarized in Chapter 6.1.2.1 and Table 4. In most cases the hopane series with regular extended hopanes dominate in the crude oils, which also show varying abundance of gammacerane and tricyclic terpanes. Methyl hopanes ( $2\alpha$ (Me)- and  $3\beta$ (Me)-hopane series) and C<sub>24</sub>-tetracyclic terpanes were detected in minor concentrations in a number of samples (Appendix 9). Desmethyl steranes are present in higher relative abundances in the oils than in the extracts. Methyl steranes were detected as  $3\beta$ (Me) and  $4\alpha$ (Me)-sterane series, and their presence confirmed by GC-MS/MS. Sesquiterpanes, diterpanes and monoaromatic steroids were also detected with compound distributions comparable to the source rock extracts. The sesquiterpanes and diterpanes in the m/z 123 chromatograms show high variabilities in their distributions and relative abundance compared to other biomarkers. While conventional oil-source rock correlations often rely on the presence and absence of compounds, the biomarker fractions of source rock and crude oil samples investigated in this study qualitatively show the same range of composition. Differences between the oils and genetic relationships to the source rocks are detectable by comparing the relative abundances of individual compounds or biomarker groups.

### 6.3.2.1 Principal Component Analysis of Crude Oil GC-MS Data

Similar to the evaluation of GC-MS data obtained from the analysis of branched and cyclic fractions of source rock extracts the peak-heights for the 20 compounds (Table 2) detected in the m/z 191, 217 and 123 mass-chromatograms of 52 crude oil branched and cyclic fractions were determined (Appendix 8.1). Using the same variables for the PCA facilitates the comparison of oil and extract composition. Some rare compounds detected in the extracts were not present in the oils (e.g. some low molecular weight steranes). The peak-height table was arranged in matrix form, normalized to the response total (Table 10) and the variance-covariance matrix calculated. Eigenanalysis was performed as described in Chapter 5.5, after testing various data transformations and input data combinations similar to the source rock analysis. The use of the original untransformed data again provided the most consistent results and facilitated the PCA interpretation. The apparently very mature waxy crude oil samples (UB2o, UB4o, UB11o, UB38o, UB39o), in which most biomarker concentrations were below the detection limits, were not included in the analysis. The results obtained from the PCA are listed in Table 9 and Appendix 8.2.

m=20, variance covariance matrix

PC	Eigenvalue	% Variance	Cumulative % variance	Broken-stick eigenvalue
1	3.497	59.2	59.2	1.063
2	1.172	19.8	79.0	0.768
3	0.419	7.1	86.1	0.620
4	0.242	4.1	90.2	0.521
5	0.181	3.1	93.3	0.448

**Table 9:** Principal component analysis results using 20 variables, based on the variance-covariance matrix of GC-MS peak-heights obtained from the analysis of the saturated fractions of 47 crude oil samples.

The first two PCs represent 79.0% of the total variance associated with the data set, with PC1 alone incorporating 59.2%. According to the broken-stick model, only these two PCs

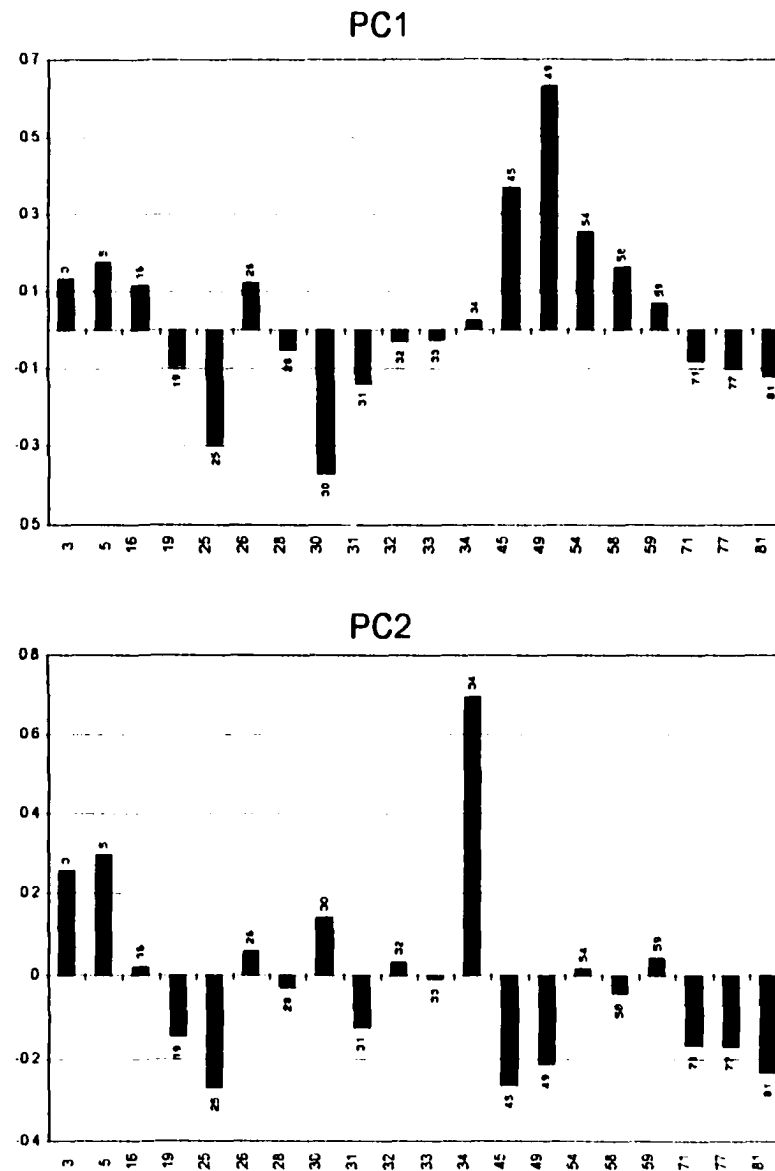
	3	5	16	19	25	26	28	30	31	32	33	34	45	49	54	58	59	71	77	81
UB14o	0.05325	0.04178	0.00885	0.18047	0.48918	0	0.06837	0.73965	0.25114	0.15762	0.11068	0.19978	0.0354	0.05328	0.00777	0.00821	0.00699	0.04495	0.15023	0.14818
UB15o	0.05349	0.03809	0.01262	0.15364	0.40995	0	0.05272	0.79375	0.1719	0.13938	0.12057	0.25879	0.04558	0.07843	0.00845	0.00642	0.00683	0.03679	0.1407	0.10498
UB21o	0.27568	0.28828	0.12173	0.03722	0.10845	0.0958	0.02558	0.3189	0.04598	0.09348	0.05304	0.3235	0.40711	0.55025	0.25872	0.20715	0.09154	0.00548	0.00788	0.01193
UB33o	0.058	0.0777	0.02558	0.17718	0.43803	0.03223	0.03302	0.67557	0.06267	0.18798	0.10497	0.17322	0.17078	0.13589	0	0.01794	0	0.14573	0.23275	0.32599
UB27o	0.34795	0.34567	0.07049	0.06438	0.23043	0.08594	0.02151	0.60259	0.06353	0.10423	0.07249	0.26074	0.32156	0.32537	0.14855	0.04964	0.08769	0.00725	0.00609	0.0132
UB73o	0.11327	0.12584	0.05988	0.09438	0.37683	0.04645	0.03814	0.81122	0.11015	0.17348	0.13178	0.30659	0.00488	0.00687	0.00275	0.00125	0.00237	0.02096	0.01753	0.0298
UB16o	0.22516	0.30192	0.11696	0.05081	0.20567	0.1332	0.02633	0.59019	0.05029	0.1404	0.09878	0.56384	0.12518	0.24239	0.07152	0.06183	0.03119	0.01156	0.01282	0.01583
UB31o	0.2176	0.27144	0.09111	0.07667	0.11518	0.15151	0	0.24785	0	0.0821	0.03997	0.30607	0.39905	0.58139	0.32223	0.24209	0.07716	0.0118	0.00763	0.0118
UB51o	0.22329	0.25065	0.09956	0.05449	0.26572	0.11018	0.02213	0.71508	0.06488	0.15384	0.0913	0.48275	0.0183	0.08745	0.00028	0.02548	0.03141	0.01234	0.01197	0.01489
UB22o	0.27026	0.31887	0.09903	0.06088	0.21233	0.08005	0	0.52311	0.06393	0.09185	0.0577	0.44882	0.20343	0.38507	0.00082	0.15335	0.0839	0.00851	0.0147	0.00837
UB76o	0.20393	0.15231	0.07289	0.06401	0.16484	0.07335	0.01822	0.74994	0.07714	0.13568	0.0877	0.50287	0.1184	0.18982	0.03751	0.02308	0	0.02377	0.01169	0.02948
UB70o	0.22182	0.22505	0.11798	0.0559	0.23486	0.11135	0.01872	0.65927	0.06818	0.18344	0.010674	0.4391	0.12583	0.32223	0.13002	0.07186	0.05538	0.01018	0.00679	0.0113
UB46o	0.1708	0.19409	0.09188	0.06554	0.24471	0.07897	0.02595	0.6819	0.07129	0.13079	0.06987	0.38564	0.20855	0.38635	0.11053	0.05525	0.05078	0.0083	0.00724	0.01147
UB74o	0.05835	0.04899	0.01789	0.15502	0.49391	0.01079	0.06818	0.75228	0.22306	0.15853	0.10671	0.18164	0.00231	0.00302	0.00035	0.0004	0.00065	0.06925	0.08914	0.17412
UB75o	0.08463	0.05386	0.01918	0.15257	0.49737	0.01108	0.07127	0.72889	0.23539	0.14246	0.1451	0.17899	0.0388	0.00354	0.00047	0.00057	0.0077	0.08286	0.11801	0.19122
UB20o	0.14138	0.14918	0.06181	0.06481	0.26628	0.06163	0.03199	0.7868	0.08044	0.14636	0.08077	0.39785	0.12381	0.20913	0.0422	0.01871	0.03307	0.01143	0.0117	0.01805
UB84o	0.14881	0.17448	0.05085	0.07494	0.26144	0.08972	0.03027	0.7182	0.09042	0.17209	0.10783	0.54579	0	0	0	0	0	0.02988	0.01683	0.02651
UB86o	0.2093	0.20432	0.09518	0.07311	0.24621	0.08704	0	0.71573	0.07426	0.14921	0.10921	0.38687	0.16283	0.29802	0.09273	0.04586	0.05835	0.02024	0.00793	0.01719
UB55o	0.23881	0.23267	0.08394	0.06618	0.24032	0.08511	0.02398	0.71505	0.06863	0.14243	0.0938	0.3757	0.11252	0.29819	0.12639	0.05084	0.07787	0.01159	0.00915	0.01704
UB71o	0.2113	0.22142	0.09288	0.07826	0.2861	0.10672	0.02531	0.69889	0.08961	0.16508	0.12487	0.42408	0.13725	0.2389	0.09836	0.0387	0.05809	0.01477	0.01059	0.01908
UB83o	0.17487	0.17578	0.1047	0.05583	0.18545	0.08749	0.02529	0.73417	0.08004	0.18772	0.11061	0.46551	0.08935	0.23634	0.10077	0.04002	0.04078	0.00842	0.00578	0.01017
UB24o	0.18238	0.20548	0.0585	0.09118	0.35785	0.02381	0.03484	0.75712	0.08214	0.14982	0.09593	0.34267	0.14156	0.17159	0.02428	0.0185	0.04069	0.02267	0.02298	0.0323
UB56o	0.12035	0.1204	0.1263d	0.07335	0.18602	0.16708	0	0.49366	0.0978	0.14817	0.12851	0.11213	0.41994	0.0171	0.11881	0.09175	0.04278	0.02827	0.01046	0.02747
UB89o	0.13883	0.17073	0.18083	0.08928	0.2784	0.14338	0.02637	0.61708	0.07512	0.18034	0.11787	0.16334	0.22524	0.51307	0.14557	0.1004	0.03558	0.0404	0.01387	0.02696
UB15o	0.11001	0.14718	0.16248	0.06866	0.21105	0.11895	0	0.50818	0.05156	0.13825	0.11057	0.12732	0.33791	0.04527	0.14939	0.11083	0.03222	0.03369	0.01101	0.03334
UB87o	0.17034	0.21726	0.20907	0.10553	0.31349	0.19275	0.0327	0.60474	0.0788	0.20058	0.14583	0.19888	0.21377	0.41583	0.15198	0.10888	0.0532	0.03945	0.01394	0.03327
UB89o	0.05347	0.08192	0.039	0.09889	0.28145	0.01211	0.05753	0.64545	0.08828	0.07438	0.08857	0.28791	0.01785	0.03395	0.03977	0.00881	0.03468	0.05773	0.11931	0.18788
UB34o	0.13543	0.15925	0.13408	0.0778	0.23587	0.11846	0.01557	0.5828	0.07646	0.15224	0.10825	0.14254	0.36413	0.53257	0.18827	0.07426	0.03011	0.05378	0.019	0.03828
UB23o	0.19374	0.21472	0.0687	0.08592	0.31217	0	0.03924	0.76548	0.10876	0.15402	0.10925	0.3475	0.07708	0.18497	0.07273	0.02207	0.05273	0.03357	0.02364	0.03712
UB52o	0.22716	0.224	0.06318	0.0759	0.34348	0.05485	0.04721	0.74847	0.10454	0.15538	0.10823	0.34263	0.08977	0.14584	0	0.01285	0.05544	0.03941	0.03108	0.04849
UB59o	0.19185	0.19112	0.075	0.08686	0.35318	0.05979	0.04308	0.77585	0.11042	0.18933	0.11158	0.33978	0.02218	0.08182	0.05066	0.01496	0.03508	0.02487	0.01832	0.02338
UB53o	0.22728	0.23	0.07288	0.07663	0.28698	0.05803	0.04078	0.79973	0.09599	0.18618	0.09478	0.25097	0.07326	0.1817	0.07026	0.01864	0.05552	0.02374	0.01945	0.03259
UB54o	0.19888	0.23448	0.05693	0.09365	0.31713	0.05733	0.04361	0.7645	0.12138	0.15754	0.12374	0.33095	0.08386	0.14789	0.08347	0.01982	0.05582	0.03364	0.01719	0.03225
UB60o	0.16042	0.17051	0.08928	0.09269	0.32056	0.01401	0.04843	0.61089	0.128	0.15634	0.14262	0.31075	0.04655	0.09619	0.05239	0.01526	0.03642	0.02178	0.01759	0.02852
UB68o	0.20108	0.25614	0.07418	0.11008	0.25081	0.13242	0.0409	0.65034	0.08877	0.23058	0.18972	0.4027	0.09822	0.29575	0.11625	0.03598	0.03828	0.05457	0.01413	0.04033
UB42o	0.26531	0.27157	0.07842	0.08634	0.2382	0.08143	0.0413	0.5912	0.05768	0.13553	0.113	0.29748	0.24284	0.46198	0.14973	0.05098	0.05622	0.05121	0.01824	0.0256
UB13o	0.23768	0.26442	0.08832	0.04809	0.16939	0.04065	0.00708	0.51883	0.05926	0.13857	0.07835	0.5958	0.07596	0.35657	0.18645	0.04141	0.07773	0.01513	0.01135	0.0138
UB57o	0.21441	0.25734	0.0957	0.10718	0.27703	0.14124	0.02988	0.72154	0.08438	0.2206	0.15915	0.40386	0.01187	0.04153	0.01551	0.00465	0.00604	0.03754	0.02949	
UB88o	0.17811	0.17275	0.05217	0.07158	0.24531	0.03548	0.0323	0.62803	0.0882	0.11842	0.08501	0.23821	0.16748	0.24106	0.08043	0.02845	0.05832	0.01573	0.01282	0.01645
UB47o	0.27018	0.28503	0.08401	0.04444	0.22789	0.10055	0.02535	0.58582	0.03027	0.13025	0.09167	0.30207	0.26823	0.43826	0.19353	0.07282	0.08319	0.01409	0.01122	0.0188
UB48o	0.27855	0.3055	0.09418	0.06755	0.23478	0.08059	0.03457	0.61589	0.07849	0.15737	0.09283	0.35453	0.15271	0.3878	0.19175	0.06478	0.08287	0.01662	0.01015	0.01766
UB26o	0.16897	0.11015	0.01472	0.18417	0.52225	0.00485	0.05868	0.71791	0.19158	0.09419	0.07541	0.21314	0.13375	0.07527	0.00901	0.00899	0.02048	0.03669	0.05908	0.09028
UB7o	0.16239	0.12526																		

represent more variance than can be explained by chance. However, it needs to be emphasized again that the first principal component in this analysis reflects the weight of the variable with the highest absolute variance in the data.

#### *6.3.2.1.1 Principal Component Loadings - Crude Oil Analysis*

PC1 is influenced mostly by the relative abundance of C<sub>29</sub> and C<sub>30</sub> hopanes vs. sesquiterpanes and diterpanes (Fig. 37), similar to PC1 in the source rock extract analysis. As noted in the extracts, Tm and C<sub>30</sub> diahopane are inversely correlated to hopanes, although the Tm coefficient falls below the cut-off value of |0.126| (Appendix 8.2). The similarity between PC1 loadings of the source rock extract and crude oil PCA is conceivable considering their general genetic relation, and the comparable covariations determined between biomarker groups and individual biomarkers. Because of obvious similarities of PC1, implications are similar to those derived from the source rock extract analysis. Thus, PC1 is considered to represent the relative proportions of primary (higher plants and associated bacterial fauna, algal material) and bacterial organic matter either generated by herbivorous or autotrophic prokaryotes in the respective source rocks. However, unlike in extract PC1 a maturity influence cannot be clearly identified (compare moretanes in Fig. 37 and Fig. 22), since only the loading of C<sub>30</sub> moretane exceeds the suggested cut-off. Also, a distinct negative correlation appears to exists between C<sub>27</sub> to C<sub>29</sub> steranes and the tricyclic terpanes.

The PC2 of the crude oil analysis also shows similarities to PC2 obtained from the source rock extract analysis, and is determined by the relative abundance of gammacerane. A positive correlation to tricyclic terpanes, and negative association to certain hopanes, sesquiterpanes are visible in Figure 37b. The steranes again display a positive correlation to hopanes. PC2 of the crude oil GC-MS analysis bears the same implication as PC2 derived from the source rock extract



peak no	compound	ion m/z	peak no	compound	ion m/z
3	C <sub>15</sub> tricyclic terpene	191	33	17 $\alpha$ (H)-21 $\beta$ (H)-22R-30-hemispane	191
6	C <sub>15</sub> bicyclic terpene	191	34	gem-mecane	191
16	18 $\alpha$ (H)-22,29,30-norhopane (Ts)	191	45	88(H)-dimane	123
19	17 $\alpha$ (H)-22,29,30-ketanopane (Tm)	191	49	88(H)-hexadimane	123
26	17 $\alpha$ (H)-21,8(0)-30-norhopane	191	54	48(H)-19-norhopane	123
28	C <sub>15</sub> diethopane	191	58	Isoprimane	123
29	17 $\beta$ (H)-21 $\alpha$ (H)-30-normecane	191	61	168(H)-propylcetane	123
30	17 $\alpha$ (H)-21,8(0)-hepane	191	71	14 $\alpha$ (H)-17 $\alpha$ (H)-20R-chestane	217
31	17 $\beta$ (H)-21 $\alpha$ (H)-mecane	191	77	24-methyl-14 $\alpha$ (H)-17 $\alpha$ (H)-20R-chestane	217
32	17 $\alpha$ (H)-21,8(0)-22S-30-hemispane	191	81	24-ethyl-14 $\alpha$ (H)-17 $\alpha$ (H)-20R-chestane	217

**Figure 37:** Loadings on principal components PC1 (a), PC2 (b), crude oil GC-MS analysis;  $m=20$ , variance-covariance matrix based PCA. Bar labels and numbers on x-axis are the variables and refer to peaks listed in the accompanying table. Only PC1 and PC2 are retained according to the broken-stick model.

analysis, thus representing a second source of primary organic matter input (halophilic protozoa and/or ciliates, algae) in addition to the organic matter sources represented by PC1.

#### *6.3.2.1.2 Principal Component Scores of the Crude Oil Analysis - Correlation to Source Rocks*

After establishing the significance of the loadings in the statistical analysis, principal component cross plots are used to reveal biomarker distributions and compositional similarities between samples. Sample clustering in different areas of the cross plot implies genetic differences, which can be attributed to variations in the composition of source rocks, as described in Chapter 6.2. A cross plot of PC1 and PC2 is shown in Figure 38, and reveals separation of oils into distinct groups more or less associated with the map-groups into which the samples have been divided.

Differences in relative biomarker distribution are illustrated using five representative samples from map-groups 4, 5, 6, and 7 as well as one immature type oil from the Cedar Rim area (UB1o) in Figure 39.1-4. Inspection of the chromatograms also visualizes the potential problems associated with recognizing subtle geochemical differences in 47 samples if no statistical evaluation is employed. This is illustrated by the similarity between hopane distributions of samples from map-groups 4, 5, 6 and 7 in Figure 39.1b-e. More distinct variations are recognizable in the relative abundance of tricyclic terpanes and particularly gammacerane. Differences in geochemical composition also become more apparent when comparing sterane (Fig.39.2) and sesquiterpane (Fig.39.3) distributions, although caution needs to be exercised when interpreting sesquiterpanes, due to the potential evaporative loss of these compounds during sample preparation. The immature oil-type sample (UB1o, Figures 40.1-4a) is easily distinguishable based on the absence of tricyclic terpanes, C<sub>28</sub>-sterane dominance, low diterpane content and characteristic monoaromatic sterane distributions.

Source rock - oil correlation is problematic because of the heterogeneity of organic matter,

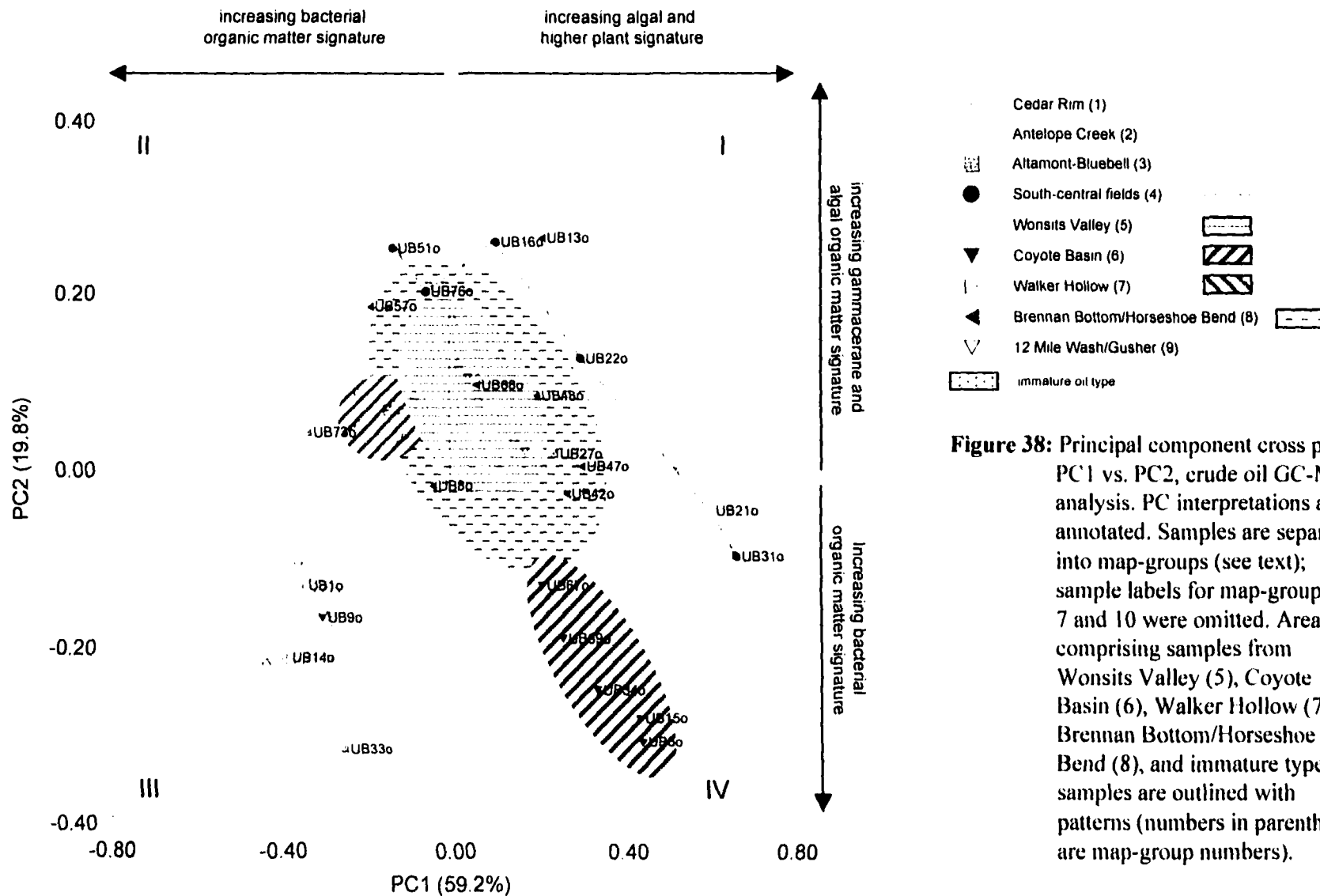


**Figure 38:** Principal component cross plot PC1 vs. PC2, crude oil GC-MS analysis. PC interpretations are annotated. Samples are separated into map-groups (see text); sample labels for map-groups 5, 7 and 10 were omitted. Areas comprising samples from Wonsits Valley (5), Coyote Basin (6), Walker Hollow (7), Brennan Bottom/Horseshoe Bend (8), and immature type samples are outlined with patterns (numbers in parenthesis are map-group numbers).

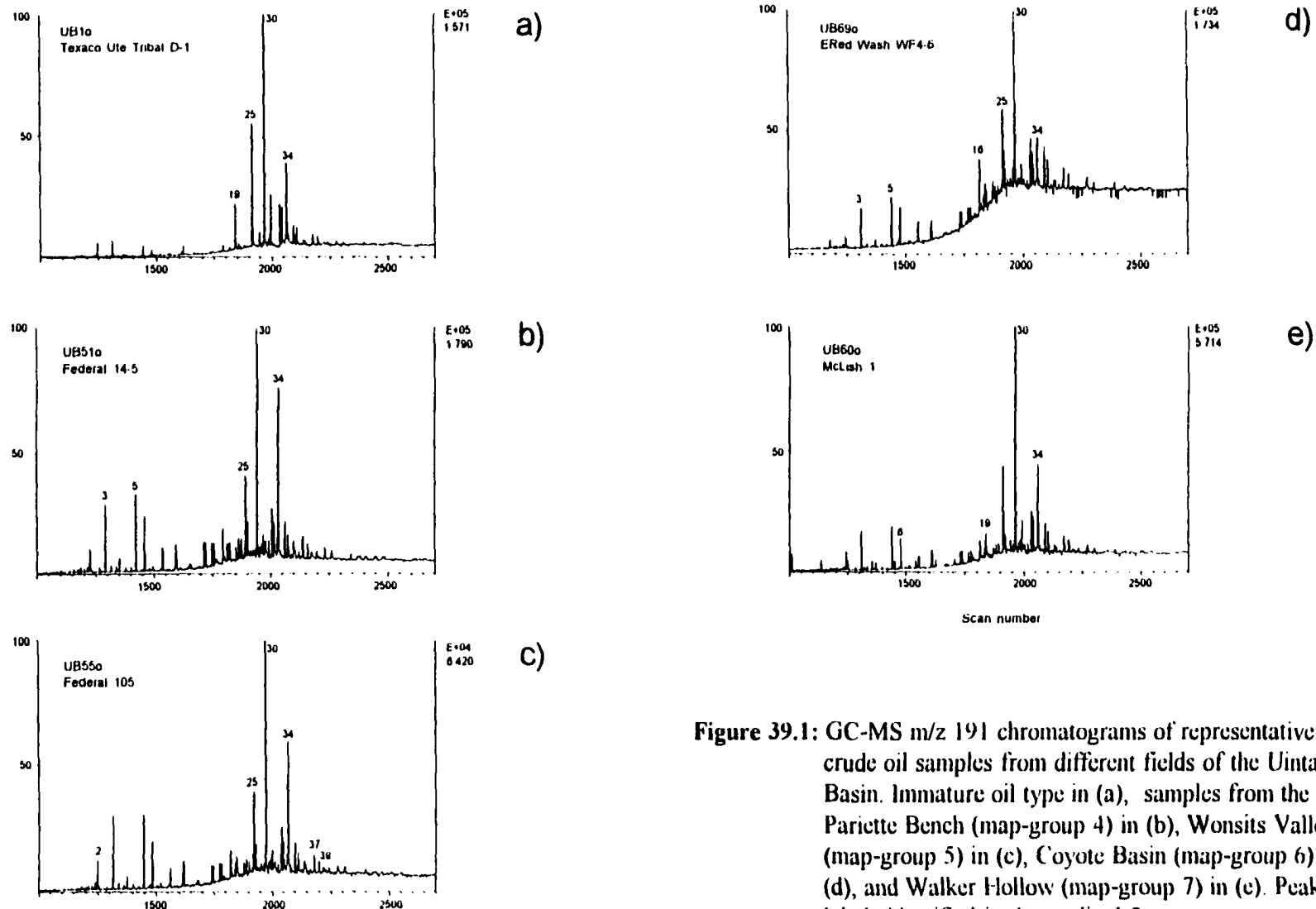


**Figure 39.1:** GC-MS  $m/z$  191 chromatograms of representative crude oil samples from different fields of the Uinta Basin. Immature oil type in (a), samples from the Pariette Bench (map-group 4) in (b), Wonsits Valley (map-group 5) in (c), Coyote Basin (map-group 6) in (d), and Walker Hollow (map-group 7) in (e). Peak labels identified in Appendix 1.2.

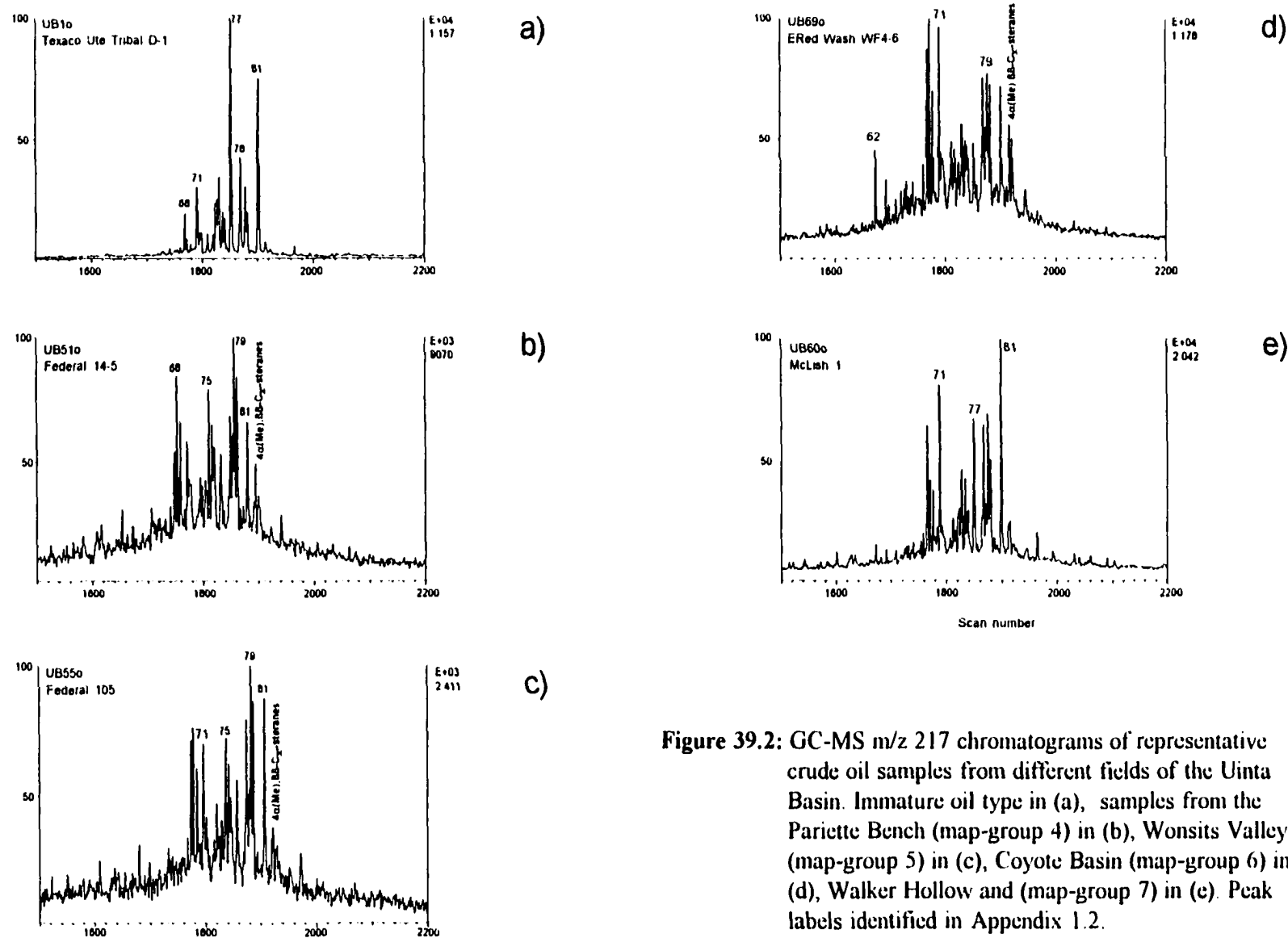


**Figure 39.2:** GC-MS  $m/z$  217 chromatograms of representative crude oil samples from different fields of the Uinta Basin. Immature oil type in (a), samples from the Pariette Bench (map-group 4) in (b), Wonsits Valley (map-group 5) in (c), Coyote Basin (map-group 6) in (d), Walker Hollow and (map-group 7) in (e). Peak labels identified in Appendix 1.2.

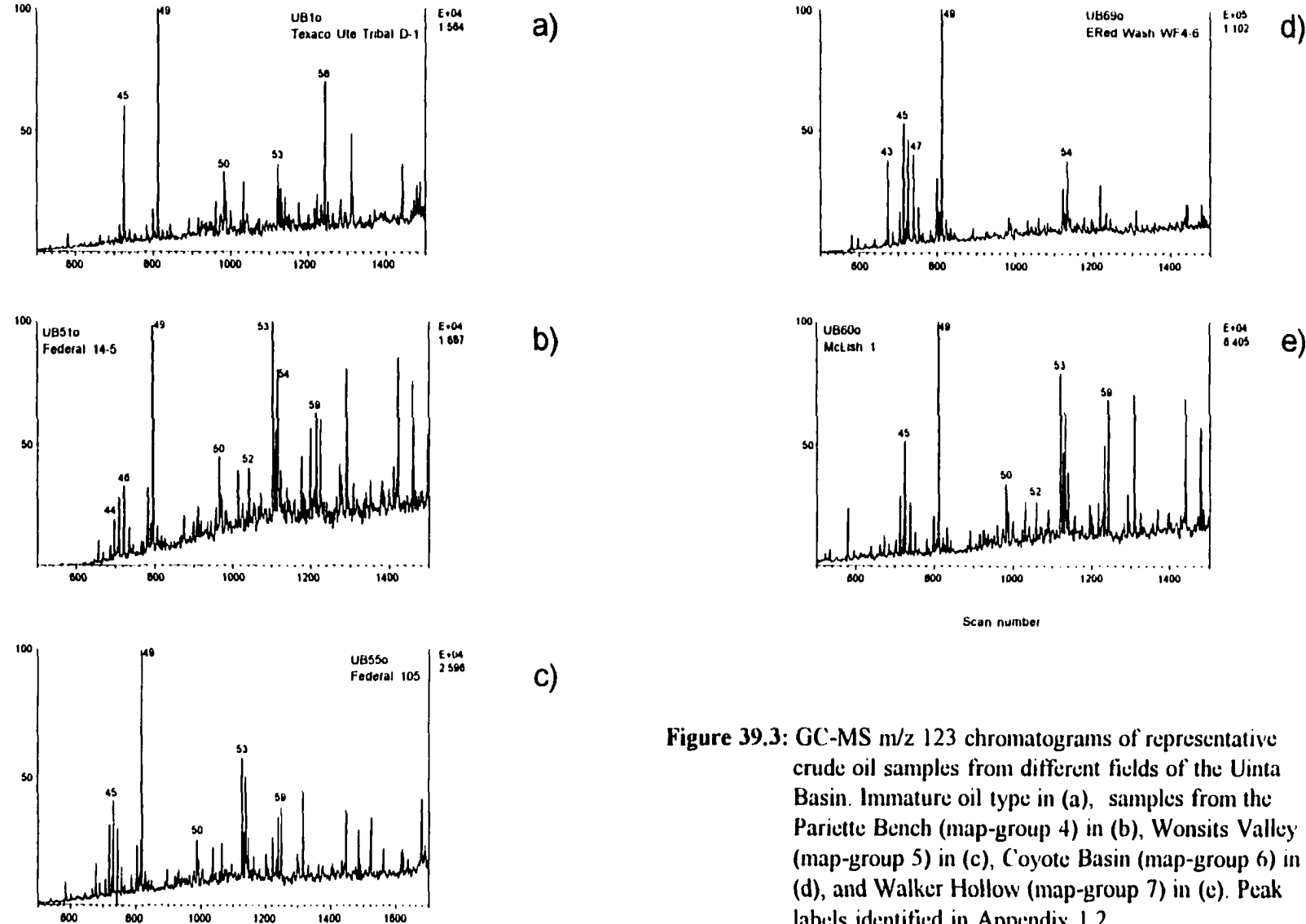
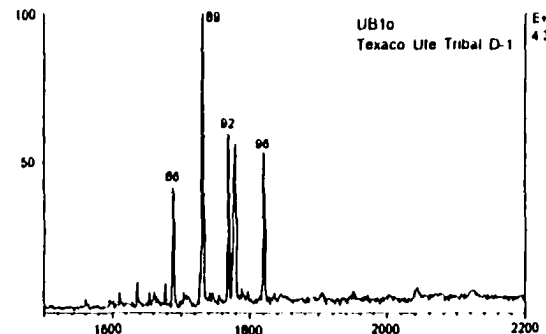
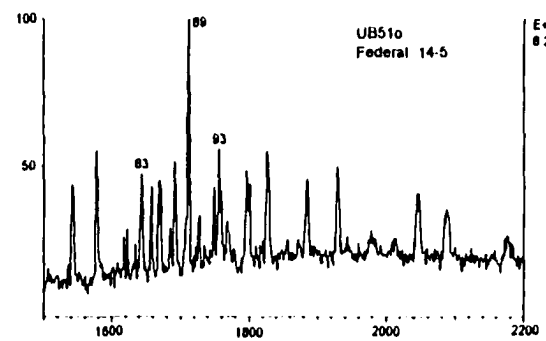


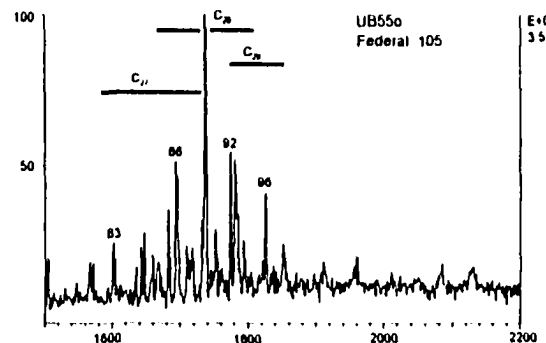
**Figure 39.3:** GC-MS  $m/z$  123 chromatograms of representative crude oil samples from different fields of the Uinta Basin. Immature oil type in (a), samples from the Pariette Bench (map-group 4) in (b), Wonsits Valley (map-group 5) in (c), Coyote Basin (map-group 6) in (d), and Walker Hollow (map-group 7) in (e). Peak labels identified in Appendix 1.2.



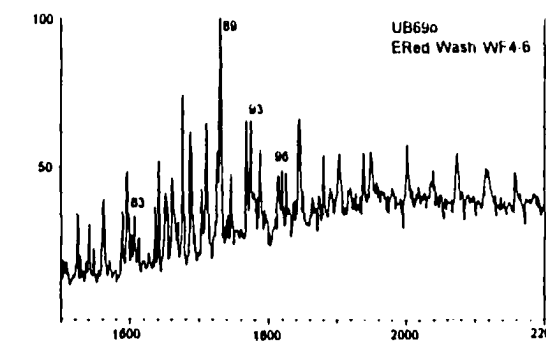
a)



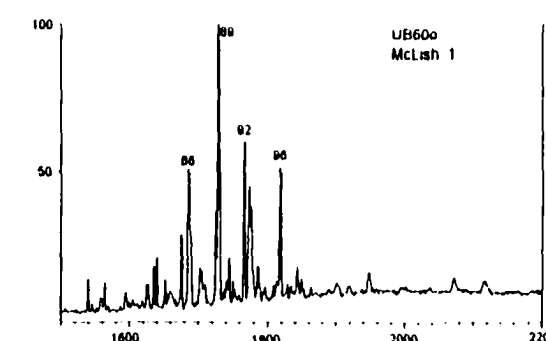
b)



c)



d)



e)

**Figure 39.4:** GC-MS m/z 253 chromatograms of representative crude oil samples from different fields of the Uinta Basin. Immature oil type in (a), samples from the Pariette Bench (map-group 4) in (b), Walker Hollow (map-group 5) in (c), Coyote Basin (map-group 6) in (d), and Wonsits Valley (map-group 7) in (e). Peak labels identified in Appendix 1.2.

different expulsion rates and efficiencies for different compounds, geochromatographic effects during migration and other secondary alteration processes (e.g. Curiale, 1993). Correlations often rely on qualitative (presence or absence) identification of compounds in source rock extracts and crude oils. The samples in the investigation contain a similar suite of compounds and the primary distinguishing factor is their relative abundances of these compounds. Multivariate analysis using PCA is ideal for exploratory comparison of biomarker distributions and relative abundances since this method presents an unweighted combination of all variables included.

Cross plots of PC1 vs. PC2 (Figure 38) distinguish samples from the Wonsits Valley, Coyote Basin and Walker Hollow area (map-groups 5, 6, 7). The cluster of samples in quadrant III are immature crude oils and a regular type sample from the Altamont-Bluebell field (UB33o) with biomarker distributions obviously different from other samples of regular oil type group. Although the immature samples originate from different fields, their comparable composition suggests a similar source. The Coyote Basin samples (map-group 6) are distinguished from other samples by enhanced relative concentrations of sesquiterpanes and compounds derived from higher plants and algae. Low gammacerane, C<sub>28</sub>-sterane and β-carotane suggest source rocks from the basal stratigraphic sections of the Green River Formation. Comparison of scores from extract cross plots (Fig. 24) implies source rocks similar to those analyzed from the south-central area of the basin (map-group 3 in the source rock extract analysis). The higher PC1 scores of the Coyote Basin oil samples indicate higher relative abundance of compounds representing primary organic matter derived from algae and higher plants in the respective source rocks. Source rock samples analyzed from the south-central area are more or less indifferent to PC1.

Only rather subtle differences in relative biomarker concentrations differentiate the Wonsits Valley and Walker Hollow crude oil samples, mostly related to variations in the signature

of sesquiterpanes, C<sub>29</sub>-steranes and diterpanes. Also, the relative abundance of gammacerane compared to hopanes appears lower in the Walker Hollow (group 7) samples, as is visible in the m/z 191 chromatograms of Figure 39.1c and e. Some overlap along the PC1 axis also indicates mixing and/or related sources for the oils. The tight clustering, particularly for the Walker Hollow samples, suggests geochemical homogeneity of the group, whilst the wider radius of the Wonsits Valley envelope reveals a higher degree of heterogeneity (assuming no sampling bias). Comparing the chromatograms of Walker Hollow samples (map-group 7), however, imply distinct compositional differences between the oils (see Appendix 10.7-1), based on relative *n*-alkane concentrations. Significant maturity differences exist between oil samples of map-group 5 and 7 (Wonsits Valley and Walker Hollow) as is obvious from the sterane isomer and monoaromatic sterane distributions (Figure 39.2c and e, Figure 39.4c and e, respectively). Sterane isomerization values for the Walker Hollow samples indicate that these oils are generally less mature than those of the Wonsits Valley and other areas (Table 11). The Walker Hollow oils are immature based on sterane isomerization scales published for Chinese non-marine basins (Huang Difan *et al.*, 1988). The Wonsits Valley wells (map-group 5) reportedly produce from stratigraphically lower reservoirs than those of the Walker Hollow area (see Table 1). The geochemical differences between the oils appear to be mostly related to the relative proportions of higher plant and algal biomarkers and bacterial derived compounds (which are lower in the Walker Hollow samples) as described by PC1. A change in relative concentrations of compound groups defining these two organic matter types in source rocks was found in the upper black shale facies/green shale facies to lean oil-shale zone transition of the Altamont-Bluebell cores and, considering the low oil maturity, these stratigraphic sections are interpreted to be the source of the Walker Hollow oils. Sources for the Wonsits Valley oils are suspected to be upper black shale facies sediments, probably open lacustrine equivalents of the Colton Tongue. Sample UB35E, obtained from a well drilled

a)

Mapgroup		Pr/Ph	$\beta$ -Carotane ( $\mu\text{g/g oil}$ )	$C_{23}$ tric. terp/C <sub>30</sub> hopane	Dia- hopane- index	Olea- nane- Index	Dia- sterane- index	Gamma- cerane- index	Gamma- cerane ( $\mu\text{g/g oil}$ )	Drimane/ phylo- cladane	20S/ 20S+R $\alpha\alpha C_{29}$	$\beta\beta/\beta\beta+\alpha\alpha$ $C_{29}$ steranes	22S/22S+R $C_{30}$ hopane
Bluebell (3) n=3	avg.	1.07	321	0.28	0.16	0.07	0.19	0.36	1232	0.82	0.47	0.52	0.60
	range	0.65-1.34	62-618	0.12-0.57	0.07-0.29	0.03-0.11	0.02-0.47	0.26-0.43	336-2823	0.67-1.00	0.47	0.47-0.58	0.57-0.64
South Central (4) n=5	avg.	1.08	157	0.55	0.58	0.03	0.25	0.88	1501	0.74	0.47	0.62	0.61
	range	0.90-1.30	68-290	0.20-1.10	0.38-1.00	0-0.06	0-0.49	0.67-1.23	221-3258	0.34-1.00	0.39-0.60	0.49-0.67	0.58-0.63
Wonsits Valley (5) n=8	avg.	1.08	437	0.29	0.34	0.04	0.27	0.59	917	0.62	0.45	0.51	0.60
	range	0.75-1.43	224-754	0.24-0.34	0.07-0.53	0.02-0.06	0.02-0.47	0.45-0.76	538-1858	0-0.80	0.35-0.48	0.31-0.63	0.57-0.61
Coyote Basin (6) n=6	avg.	1.55	131	0.29	0.51	0.10	0.45	0.30	318	0.91	0.45	0.46	0.57
	range	1.04-2.07	0-329	0.24-0.36	0-0.90	0.05-0.14	0-0.76	0.29-0.45	85-1318	0.88-0.91	0.36-0.50	0.40-0.50	0.53-0.61
Walker Hollow (7) n=4	avg.	1.55	574	0.27	0.11	0.05	0.06	0.41	945	0.55	0.36	0.37	0.59
	range	1.03-1.11	301-466	0.21-0.30	0-0.20	0.04-0.05	0-0.11	0.31-0.46	554-1330	0.39-0.62	0.33-0.40	0.31-0.41	0.56-0.64
Brennan Bottom (8) n=7	avg.	1.30	277	0.42	0.42	0.09	0.55	0.60	612	0.69	0.45	0.48	0.59
	range	1.02-1.90	144-625	0.21-0.51	0.14-0.62	0.04-0.17	0-0.87	0.29-1.15	247-1487	0.49-0.81	0.38-0.54	0.39-0.56	0.55-0.64
Gusher (9) n=2	avg.	1.07	237	0.38	0.28	0.06	0.15	0.49	378.5	0.77	0.44	0.52	0.55
	range	1.05-1.09	234-240	0.37-0.38	0.27-0.29	0.05-0.07	0-0.30	0.48-0.50	317-438	0.73-0.81	0.39-0.48	0.46-0.58	0.54-0.56

b)

Mapgroup		Pr/Ph	$\beta$ - Carotane ( $\mu\text{g/g oil}$ )	$C_{23}$ tric. terp/C <sub>30</sub> hopane	Dia- hopane- index	Olea- nane- Index	Dia- sterane- index	Gamma- cerane- index	Gamma- cerane ( $\mu\text{g/g oil}$ )	Drimane/ phylo- cladane	20S/ 20S+R $\alpha\alpha C_{29}$	$\beta\beta/\beta\beta+\alpha\alpha$ $C_{29}$ steranes	22S/22S+R $C_{30}$ hopane
immature type n=8	avg.	1.44	1332	0.13	0.03	0.02	0.02	0.29	1486	0.79	0.35	0.29	0.57
	range	0.97-2.12	360-3287	0.05-0.31	0-0.18	0-0.04	0-0.12	0.21-0.43	0-3670	0.53-0.88	0.30-0.45	0.19-0.42	0.50-0.62
regular type n=39	avg.	1.18	316	0.35	0.37	0.06	0.24	0.54	767	0.70	0.44	0.48	0.59
	range	0.65-2.07	0-906	0.12-1.10	0-1.00	0-0.17	0.02-0.47	0.23-1.23	0-3258	0-1.00	0.20-0.60	0.16-0.67	0.46-0.64

**Table 11:** Comparison of averages and ranges of biomarker ratios and parameters between different mapgroups (a) and immature vs. regular type oils (b). Abbreviations and ratio formulas are listed in Appendix 1.1.

southeast of the core sample map-group 1 (Appendix 3.1-10, chromatogram in Appendix 6-2), and the organic-leaner samples UB17E and UB18E are representatives of this facies.

Considerable scatter of sample points of crude oils produced from the Brennan Bottom/Horseshoe Bend fields (map-group 8) are visible in Figure 38. The spread of sample points indicate heterogeneous composition within the group, in which most samples are related to oils from the Wonsits Valley area, and some appear associated with oils from the Walker Hollow field. Regular type samples from the Gusher area (map-group 9) appear to have similar biomarker compositions. These oils are produced from reservoirs approximately 200-300 ft deeper than those which produce immature type oils (samples UB7o, UB10o and UB26o). The rather minor differences in PC-scores and the close clustering of samples from map-groups 5, 8, and 9 suggest similar, if not the same source based on the biomarkers integrated in the statistical analysis.

The consistent wide scatter of map-group 4 samples from the south-central fields in Figure 38 strongly suggests that significant geochemical differences exist within the group and also compared to oils of other groups. Exceptions are samples UB22o and UB76o, which appear to have biomarker compositions similar to the Walker Hollow and Wonsits Valley oils, respectively. The appearance of the chromatograms from samples of this map-group in Appendix 10.2-1 and 10.4-1 does not necessarily imply the same conclusions, and rather suggests that partly similar organic matter composition in the respective source rocks. This is also indicated by generally low  $\beta$ -carotane concentrations, presence and odd predominance patterns, and carbon number range  $>C_{30}$  in the south-central oils. The abundance of gammacerane is variable, but generally high relative to  $C_{30}$  hopane. Rearranged compounds are inconsistent as a correlation tool for samples of map-group 4 (Table 11; Appendix 9). The partly rather unique composition of samples UB16o, UB21o, UB22o, UB31o, and UB51o and their occurrence in small fields suggests multiple small, local pods of generating source rocks, possibly adjacent to the reservoirs. Integration of GC data

into the analysis indicates mixing of sources for some oils. The GC of sample UB76o (Appendix 10.4-1) shows a distinctly different *n*-alkane profile compared to the Wonsits Valley (map-group 5) crude oils to which the sample plots close in the PC cross plot (Fig.38), which is not explicable by evaporative loss in the Wonsits Valley sample. Samples UB16o and UB51o fall adjacent to the Wonsits Valley and Brennan Bottom/Horseshoe Bend sample clusters in quadrants I and II of Figure 38, but comparison of GC-MS chromatograms confirmed differences (namely elevated gammacerane concentrations in UB16o and 51o; see also Appendix 9). In general it is not possible to clearly relate map-group 4 oils to any of the source rock samples analyzed. Comparison of PCA scores of samples UB31o and UB21o to extract PCA scores suggest a similarity to an unusual, algal organic matter rich source rock comparable to sample UB1E from the upper black shale facies interval (Figure 24 and Figure 38). Direct comparison of GC-MS data of these samples, however, showed significant differences.

The Altamont-Bluebell crude oil samples are similarly unrelated to each other (UB27o, UB33o, UB73o) based on their biomarker composition, and strongly suggest stratigraphic control on composition. There are only three samples out of an area with several hundred producing wells, and the samples cannot be regarded as representative. The distinct geochemical signature of the samples (Appendix 10.3-1) verify the hypothesis that individual source rock units generate crude oils with characteristic compositions. The score plot of samples UB27o and UB73o close to the samples of the Wonsits Valley and Walker Hollow areas (Figure 38) reveals interesting genetic relations. These samples are possibly an equivalent oil generated from the same stratigraphic intervals located in the deeper north-central part of the basin but which have been trapped closer to the source. Depths of production (Appendix 7) suggest an upper black shale facies/green shale facies source at the initial phase of oil generation, as they have been identified in cores from the Altamont-Bluebell area described in Chapter 6.2.1.

Samples UB9o and UB33o from the Coyote Basin and Altamont-Bluebell areas plot close to the immature samples in Figure 39a. Chromatograms in Appendix 10.6-1 and 10.3-1 also suggest a rather unique composition. Oil UB9o is very immature (Appendix 9), possibly originating from generation processes other than thermal maturation. The GC analysis of other immature oils (UB1o, UB14o, UB74o, UB74o) compares these to mahogany type oil-shale extracts, but inspection of the PC cross plots in Figures 24 and 38 indicates differences in biomarker distribution not explicable by varying maturity levels for oils and extracts. The differences are interpreted to be a result of the heterogeneous nature of the organic matter in oil-shales from different stratigraphic intervals (*i.e.* lean oil-shales *vs.* mahogany zone oil-shales). These generate immature oils simultaneously which causes oil mixing. This interpretation is also supported by the occurrence of methyl steranes in the oils, which have been detected in the lean oil-shales but not in the mahogany shales.

#### 6.3.2.1.3 Other Geochemical Data of the Crude Oils

The interpretation of GC-MS data from compositionally different oil-types using PCA has to be supported by additional geochemical data. Since PCA confirmed the validity of separating the crude oil samples according to their location in the basin, it is convenient to compare averages and ranges of selected biomarker ratios in the different sample groups (Table 11a). The parameter selection is based in part on the evaluation of the PCA loadings and the selection of the parameters in the source rock extract analysis. For comparison, averages and ranges of the same parameters for regular and immature type oils are given in Table 11b. A correlation coefficient matrix comparing principal components and parameters derived from GC analysis is shown in Table 12. Correlations between a number of GC parameters,  $\beta$ -carotane and absolute gammacerane concentrations with PC1 was found, possibly due to the high total variance represented by PC1.

	Pr/Ph	Pr+n-C <sub>17</sub> /Ph+n-C <sub>18</sub>	Beta-carotene µg/g oil	C <sub>21+22</sub> /C <sub>28+29</sub>	C <sub>21</sub> /C <sub>22</sub>	Pr/n-C <sub>17</sub>	Pr/n-C <sub>18</sub>	R22	CPI	Gammacerane µg/g oil	Diahopane-Index	Oleanane-Index	Diasterane-Index	22S/(22S+22R) C <sub>31</sub> , Hopane	20S/(20S+20R) ααC <sub>29</sub>	ββ/(ββ+αα) C <sub>29</sub>	PC1	PC2
Pr/Ph	1																	
Pr+n-C <sub>17</sub> /Ph+n-C <sub>18</sub>	<b>0.6888</b>	1																
Beta-carotene µg/g oil	0.2914	<b>0.7252</b>	1															
C <sub>21+22</sub> /C <sub>28+29</sub>	-0.0707	-0.3243	-0.4391	1														
C <sub>21</sub> /C <sub>22</sub>	0.3080	0.2899	-0.0530	0.3679	1													
Pr/n-C <sub>17</sub>	0.0438	0.2211	<b>0.4591</b>	-0.3552	-0.2794	1												
Ph/n-C <sub>18</sub>	0.3712	<b>0.8099</b>	<b>0.8333</b>	-0.4338	0.0069	<b>0.5760</b>	1											
R22	-0.2233	<b>-0.4866</b>	-0.3008	<b>0.4775</b>	-0.1198	-0.1927	-0.3501	1										
CPI	0.3944	<b>0.6385</b>	<b>0.7259</b>	<b>-0.4696</b>	0.0504	0.4133	<b>0.7585</b>	<b>-0.6562</b>	1									
Gammacerane µg/g oil	-0.1846	-0.0876	0.1291	-0.1493	0.0871	0.1169	-0.0214	-0.0564	0.1205	1								
Diahopane-Index	0.0969	-0.2353	<b>-0.5407</b>	<b>0.5332</b>	<b>0.5347</b>	<b>-0.5076</b>	-0.4442	0.1373	<b>-0.4782</b>	-0.3083	1							
Oleanane-Index	0.3568	0.3100	0.1866	-0.1560	0.1900	-0.1599	0.3030	-0.0572	-0.0112	-0.2937	0.1196	1						
Diasterane-Index	-0.1392	-0.0571	-0.1277	0.0559	0.3148	-0.1014	-0.0703	0.0651	-0.0956	0.0049	0.0998	-0.0413	1					
22S/(22S+22R) C <sub>31</sub> , Hopane	-0.1555	-0.0699	-0.0561	0.3476	0.1242	-0.1078	-0.0865	0.3866	-0.1833	-0.1437	0.1937	-0.2220	0.0978	1				
20S/(20S+20R) ααC <sub>29</sub>	0.1010	-0.2221	-0.3452	0.3891	0.2819	-0.4407	-0.4291	0.3061	-0.4463	-0.1885	<b>0.5309</b>	0.0525	-0.0145	0.3915	1			
ββ/(ββ+αα) C <sub>29</sub>	-0.2535	<b>-0.4515</b>	<b>-0.5884</b>	<b>0.6090</b>	0.3051	<b>-0.4814</b>	<b>-0.5425</b>	0.3968	<b>-0.5858</b>	-0.1686	<b>0.6707</b>	-0.1501	0.0672	<b>0.4890</b>	<b>0.7147</b>	1		
PC1	0.1517	-0.2823	<b>-0.6602</b>	<b>0.5079</b>	0.2894	<b>-0.5021</b>	<b>-0.4696</b>	0.3032	<b>-0.6271</b>	<b>-0.6036</b>	<b>0.8495</b>	0.0823	-0.0056	0.1681	<b>0.5527</b>	<b>0.6545</b>	1	
PC2	-0.4081	-0.3105	-0.2806	0.1368	-0.0460	-0.1405	-0.2818	0.1300	-0.3259	0.0929	0.1386	-0.3182	0.1952	0.3178	0.1972	0.4156	<b>0.6693</b>	1

Table 12: Correlation coefficient matrix (Pearson's correlation coefficient r) relating crude oil principal components to other parameters obtained by GC analysis;  $|r| > 0.45$  are highlighted.

High correlations to sterane isomerization ratios reflect the maturity related variance associated with PC1, similar to the PC1 obtained from the source rock extract analysis. A correlation between PC2 and Pr/Ph values and  $\beta\beta/\beta\beta+\alpha\alpha$  C<sub>29</sub> sterane ratios also appears to exist, which was also found for Pr/Ph in the source rock extract analysis. Some of the biomarkers ratios in Table 11a relate the oils to specific source intervals, such as rearranged hopanes and steranes, and the oleanane-index. High diahopane indices for the south-central fields and Coyote Basin (map-groups 4 and 6) samples compare to high ratios in lower Green River Formation extracts, therefore also suggesting basal Green River Formation as potential source rocks. However, the diahopane-index shows correlation to maturity sensitive parameters in Table 12 which also indicates that this parameter is not only related to source and depositional environment. Significantly different gammacerane-indices and absolute gammacerane concentrations appear to exclude a common source within the basal Green River Formation. The ranges for the ratios of the south-central samples are large, confirming that this map-group comprises different oil-types. Higher  $\beta$ -carotane suggests stratigraphically younger source rock intervals for the Wonsits Valley and Walker Hollow oils (map-group 5 and 7). Low rearranged sterane and hopane indices characterize samples from the Altamont-Bluebell area (map-group 3). Selected biomarker parameters of Table 11a are displayed graphically in Figure 40 for representative oil samples (samples in Figures 39.1-4) to illustrate the geochemical differences between the samples with conventional biomarker ratios.

A frequently used technique to distinguish oil groups and establish correlations is the use of the distribution of C<sub>27</sub>, C<sub>28</sub> and C<sub>29</sub> desmethyl steranes shown in a ternary diagram in Figure 41. Some separation of map-groups is recognizable, such as map-group 6 samples have relatively high concentration of C<sub>27</sub>-sterane. Immature samples are distinguished on the plot as well, again indicating similar sources irrespective of the location (e.g. map-group 12). Most other samples

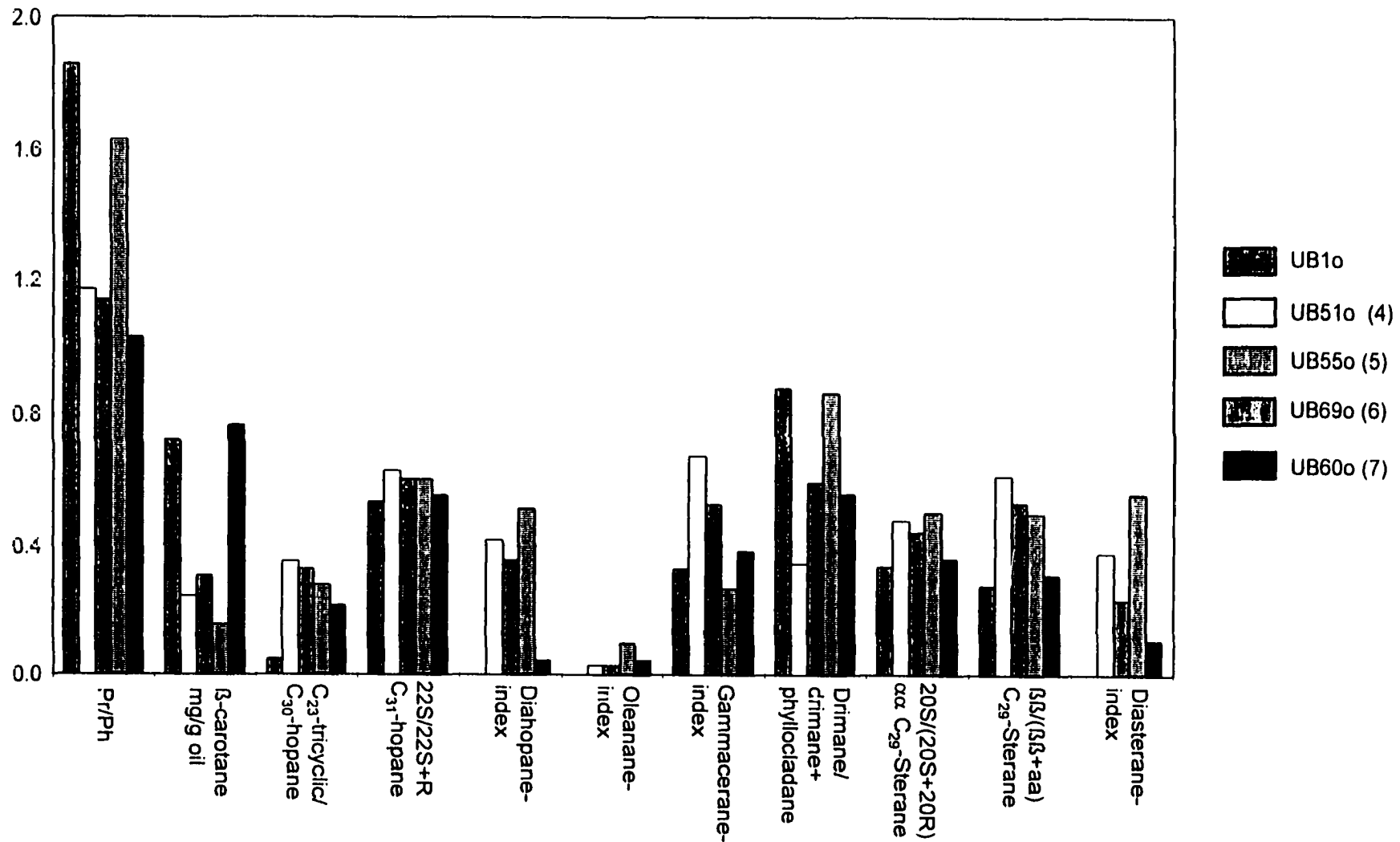


**Figure 40:** Comparison of biomarker ratios of representative samples from mapgroups 4-7 (GC-MS chromatograms for the samples are shown in Fig.39.1-4). Sample UB1o is an immature sample from the Cedar Rim area (map-group 1). Numbers in parenthesis in legend are the map-group numbers. Indices are explained in Appendix 1.1; numerical values in Appendix 8.1.

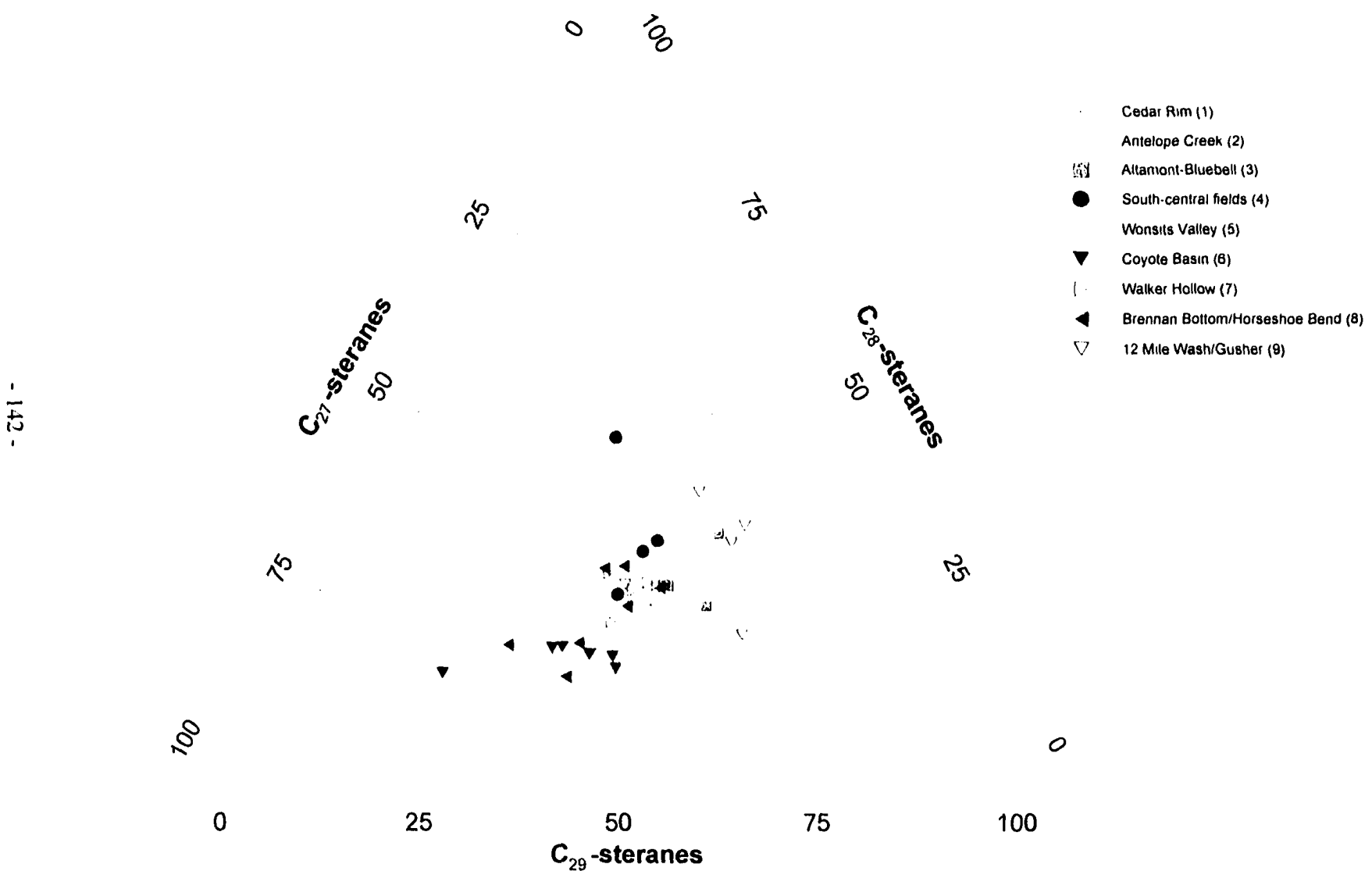


**Figure 41:** Ternary diagram of sterane distributions in crude oil samples from the Uinta Basin. Samples are separated into map-groups (numbers in legend, see text).

from the Greater Red Wash area and Brennan Bottom/Horseshoe Bend cluster around the same area on the plot. South-central samples (map-group 4) generally tend to higher C<sub>28</sub>-sterane concentrations.

Comparison of molecular maturity indicators listed in Table 11a show some maturity differences between the oil map-groups. Maturity parameters indicate that samples from the Gusher (map-group 9) and Walker Hollow (map-group 7) areas are the least mature, apparently the hopane isomerization has not reached equilibrium in the Gusher samples. The ranges in other samples are at the proposed equilibrium equilibrium of 0.57-0.62 (Peters and Moldowan, 1993). Hopane and moretane maturity indicators were found to be most reliable in the source rock analysis, *i.e.* they displayed a reasonable depth trend with little scatter. However, they are only useful parameters for the beginning and early stages of oil generation (Peters and Moldowan, 1993). Sterane isomerization maturity parameters fall below the equilibrium values and suggest that the oils represent relatively early generation products from their respective source rocks. Maturity differences are also seen in the relative amounts and distribution of monoaromatic steroids (Figure 39.4). The mature samples (Pariette Bench (Fig.39.4b) and Coyote Basin (Fig.39.4d)) show low monoaromatic steroid concentrations and interference with isoprenoid peaks. Maturity parameters for immature and regular type oils in Table 11b support the suggested distinction between the two groups and indicate that immature type oils are indeed early generation products. Considering the ranges of ratios in the regular oil type samples, it is apparent that some samples in this group are also early generation products, but do not show the typical low *n*-alkane, high isoprenoid, terpane and  $\beta$ -carotane pattern of other immature oils. Examples are samples UB9o (Appendix 10.6-1) and UB20o (Appendix 10.4-1). In sample UB9o, a second homologous series of compounds, proposed to represent monomethyl-branched compounds (Carroll, 1998) elutes close to the *n*-alkane peaks.

## **7. Synthesis of the Source Rock and Crude Oil Geochemistry and Implications for the Petroleum System of the Uinta Basin**

### **7.1 Green River Formation Source Rocks in the Uinta Basin**

The geochemical analysis of source rocks within the stratigraphic framework of the Tertiary Uinta Basin indicates that changes in the lacustrine depositional environment are reflected in the composition of the organic matter preserved in the sediments. Some biological markers are proxies for specific processes or conditions, e.g. the abundance of gammacerane can be related to water salinity or lake water stratification if other salinity indicators are not present or present in minor concentration. Higher plant biomarkers, in combination with compounds modified by clay-catalyzed structural rearrangement, monitor the proportion of allochthonous sedimentary material and also suggest changes in the type of vegetation surrounding the basin. Specific markers such as  $\beta$ -carotane and their concentration correlate with the salinity of the lake water and indicate mass-occurrence of specific algae or bacteria. Other markers such as methyl steranes, tricyclic terpanes and isoprenoids reflect the development of phytoplankton living in the epilimnion of the lake.

Basal Green River Formation source rocks (black shale facies) were encountered in the south-central area of the basin and represent littoral nearshore open lacustrine to marginal lacustrine facies. Equivalent open lacustrine rocks are probably present in the deep, high maturity sections at depths >11,000 ft in the Bluebell -Altamont area. Low absolute  $\beta$ -carotane and gammacerane concentrations indicate low salinity, and the presence of gammacerane may be related to water density stratification (possibly thermally induced as is typical for low latitude lakes (Talbot and Allen, 1997)), which created a temporary dys- or anoxic hypolimnion. Anoxia is evidenced by preservation of lamination in the organic-rich sediments and ubiquity of methanogenic bacteria on one hand, but is not expressed in low Pr/Ph values. Proportions of algal and higher plant derived biomarkers and bacterial biomarkers are balanced, and a comparatively

low input of clastic material in regards to the upper black shale facies is interpreted. Extracts of the upper black shale facies are unique in terms of their relatively high amount of allochthonous material as manifested by high relative concentrations of rearranged steranes and hopanes and other biomarkers indicating higher plant organic matter. Lake conditions were similar to the lower black shale facies, with low salinity, temporal stratification and lake bottom water anoxia. The upper black shale facies/green shale facies section is characterized by fluctuating biomarker composition of the organic matter. The variable composition of source rocks is interpreted to indicate rapid changes in lake conditions, possibly with an overall shallowing and episodes of elevated salinity in the lake water.

Composition and lithofacies association of the low grade oil-shales located above the middle marker show evidence for shallow and saline water conditions. The high abundance of hopanoid biomarkers indicate the activity of possibly autotrophic bacteria. Preservation of lamination was possible due to anoxia and/or salinity of the lake bottom water, which permitted the preservation of hydrogen-rich organic matter. Preservation of similar rocks in the Greater Red Wash area and their facies relation record episodes of short term lake expansion towards the east and southeast over vast, flat marginal lacustrine areas. High  $\beta$ -carotane and gammacerane concentrations in mahogany zone oil-shales coupled with low terrestrial input indicate a high level of production of autochthonous organic matter, but, due to high salinity, a low diversity biosphere in the lake system. The lake water salinity during the deposition of the mahogany zone oil-shales was probably higher than during the deposition of the underlying lean oil-shales, based on the Pr/Ph values and absolute concentrations of  $\beta$ -carotane and gammacerane.

The variations in lake conditions summarized above and determined on the basis of geochemical data and supporting sedimentological observations, lead to the deposition of various source rock types. All of these are generally TOC- and hydrocarbon-rich and geochemical

variability is expressed in the relative abundances of biomarker compounds. No compounds which could be classified as unique and characteristic of only a few samples were detected, and the range of biomarkers is generally similar in all of the samples examined.

Thermal maturation parameters suggest that the beginning of the oil generation window is presently located at approximately the upper black shale facies section in the Altamont-Bluebell area. The peak oil generation window is expected to be located in the Colton Tongue and stratigraphically equivalent open lacustrine facies. Organic-rich sediments beneath this alluvial section have already lost most of their generative potential. The same parameters confirmed the immature stage of Greater Red Wash area samples. Samples from the south-central area representing source rocks deposited in the initial freshwater stage of Lake Uinta are in the late early generation stage to beginning peak generation stage.

## **7.2 Uinta Basin Crude Oils and their Correlation to Source Rocks**

Significant variations in the biomarker distribution of crude oils suggest distinct sources for a number of oils and aids in refining the initial GC analysis based grouping into immature, regular and waxy type oils. Several additional subgroups within the regular oil types have been identified using a combination of statistical evaluation of GC-MS data and parameters obtained from GC analysis. Immature samples can be subdivided into two subgroups, the regular type samples into four subgroups. For the most part, genetic separation is equivalent to geographical separation, *i.e.* specific oil groups occur in specific fields. A direct correlation of source rock extract and crude oil compositions based on PCA is possible because of the similar loadings on PC1 and PC2 (Fig.42). An overlay of PC1 vs. PC2 obtained from the PCA of source rocks extract and crude oil GC-MS data permits a direct comparison of biomarker composition (Figure 43). Since the loadings are similar but not identical, this technique can only be a rough guide but

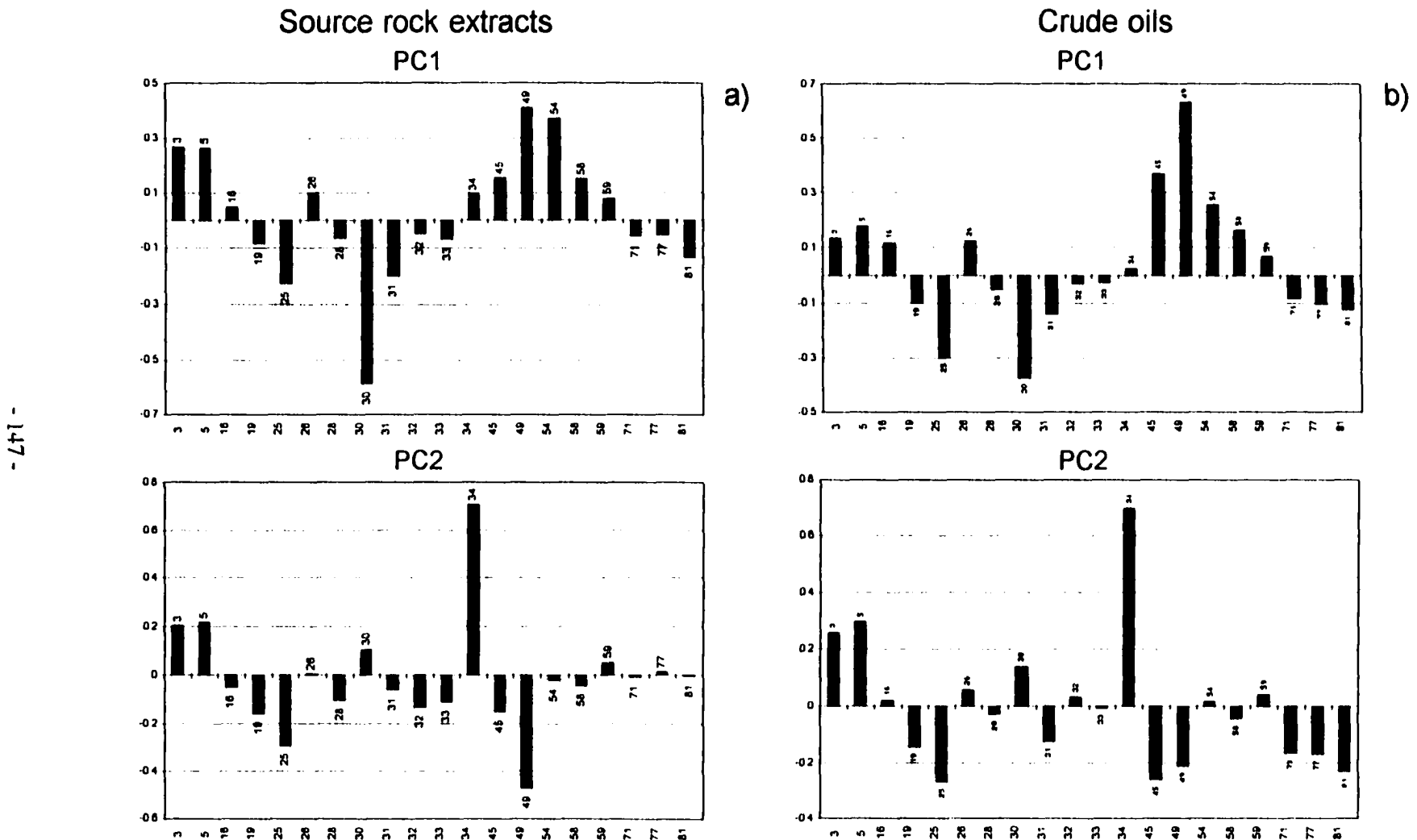


**Figure 42:** Comparison of the loadings on principal components PC1 and PC2, source rock extract (a) and crude oil (b) GC-MS analysis;  $m=20$ , variance-covariance matrix based PCA. Bar labels and numbers on x-axis are the variables and refer to peak numbers listed in Appendix 1.2.

nevertheless provides a means to rapidly compare source rock and oil analyses for correlation purposes. Several crude oil-types have been identified and correlated to source rock intervals:

- i) Immature oils with dominant isoprenoid, terpane and  $\beta$ -carotane signatures, which can be correlated to mahogany zone and lean oil-shale source rocks.
- ii) Unusual oils with regular oil-type *n*-alkane distribution, both relatively mature (UB33o) and immature (UB9o, UB20o), derived from unknown sources.
- iii) Regular type oils with common dominance of homologous *n*-alkane series and which can be subdivided into the following subgroups:
  - a) Walker Hollow immature oils derived from shallow stratigraphic intervals of the green shale facies to lean oil-shale zone and possible contribution or migration dissolution from organic matter of the mahogany zone;
  - b) Wonsits Valley, Brennan Bottom, Horseshoe Bend, Gusher and shallow Bluebell-Altamont oils; probable source rock intervals are upper black shale facies sections occurring in open lacustrine facies equivalents of the Colton Tongue to the south and southeast of the Altamont-Bluebell area;
  - c) Coyote Basin oils, generated from the stratigraphically lowest source rock intervals similar in composition to those rock samples investigated from the south-central area; geochemical differences point to more distal and profundal sources to the north.
  - d) South-central oil fields (Monument Butte (UB31o), Antelope Creek (UB21o), Pleasant Valley (UB22o), Eight Mile Wash (UB16o), Pariette Bench (UB51o), West Willow Creek (UB76o)). The small fields in the south-central area of the basin were charged from local, unidentified sources with, in some cases, a possible contribution from upper black shale facies sources. Oil samples from other fields of this area do not show any relation to

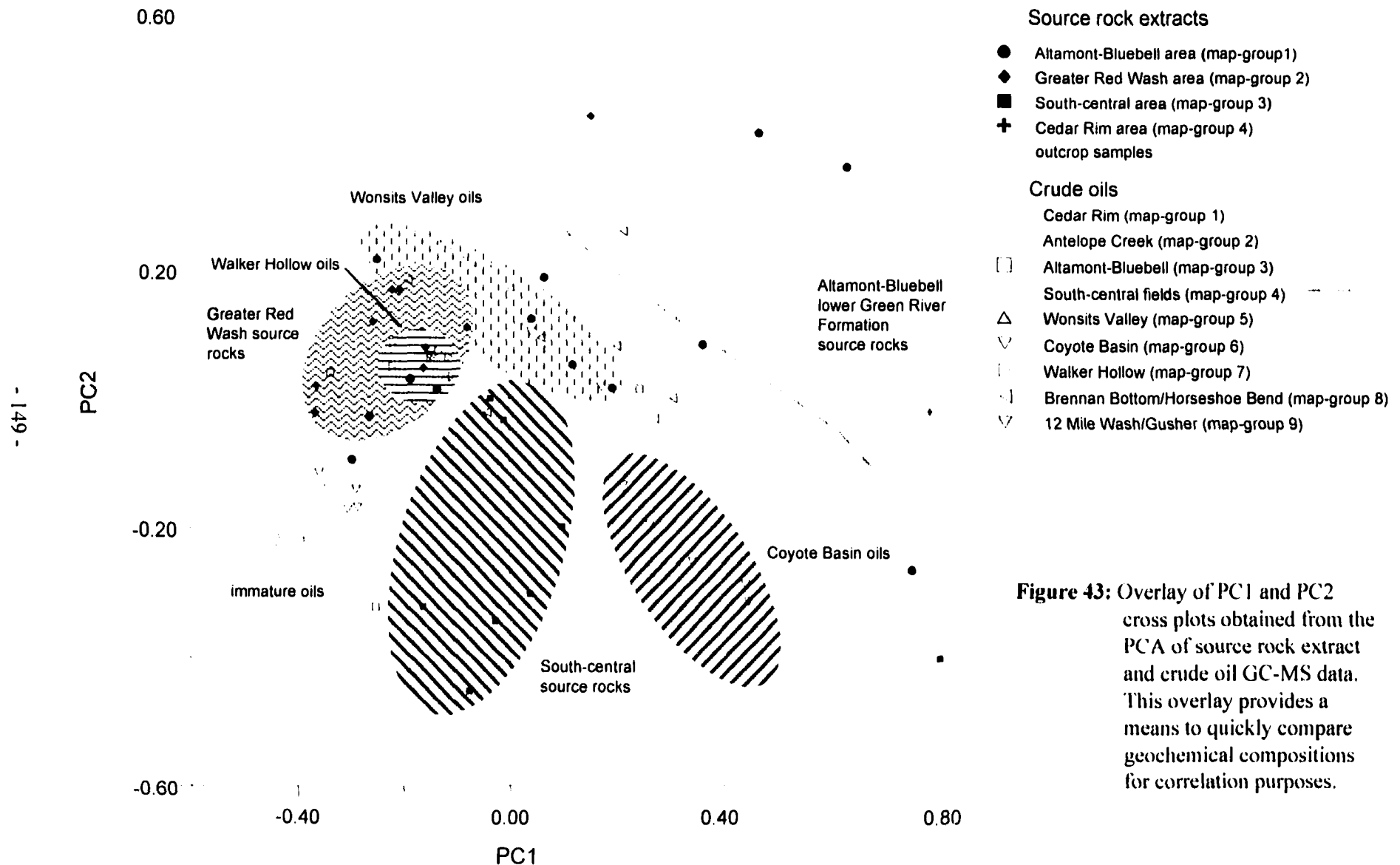


**Figure 43:** Overlay of PC1 and PC2 cross plots obtained from the PCA of source rock extract and crude oil GC-MS data. This overlay provides a means to quickly compare geochemical compositions for correlation purposes.

nearshore open lacustrine to marginal lacustrine source facies found in cores from the same area.

iv) Waxy, high maturity oils from the deep reservoirs in the Altamont-Bluebell area.

A comparison of two examples for the source rock - oil correlation based on PCA are shown in Figure 44. The examples show how differences in the relative abundance of gammacerane, triterpanes, sesquiterpanes and diterpanes can be used to separate samples and establish correlations. Other compounds such as methyl steranes in samples UB12E and UB67o (Fig. 44b) support the correlation.

### **7.3 Secondary Migration**

The presence of geochemically distinct crude oils in various reservoirs and their spatial distribution suggest complex generation and migration pathways in the basin. Although there is probably mixing of oils, particularly in the Altamont-Bluebell area with reservoirs close to the sources, geochemical signatures of oils in the peripheral fields can be used to trace subsurface fluid flow and migration patterns. The oils migrated through hydrodynamic and buoyancy driven flow to the southeast (see fluid flow models of McPherson, 1996), possibly also being forced by the continuous generation of hydrocarbons from successively younger source rock intervals. The sequential generation and expulsion is a possible explanation for the minor mixing of oils and preservation of their geochemical signatures which they inherited from the source rocks.

The oils of the Coyote Basin field originate from the stratigraphically oldest source rocks, which have generated oils early during the subsidence of the Uinta Basin. They are interpreted to have migrated from structurally deeper locations to the northeast of the reservoirs, probably those sections of the lower black shale facies and Flagstaff Formation which are presently beyond the

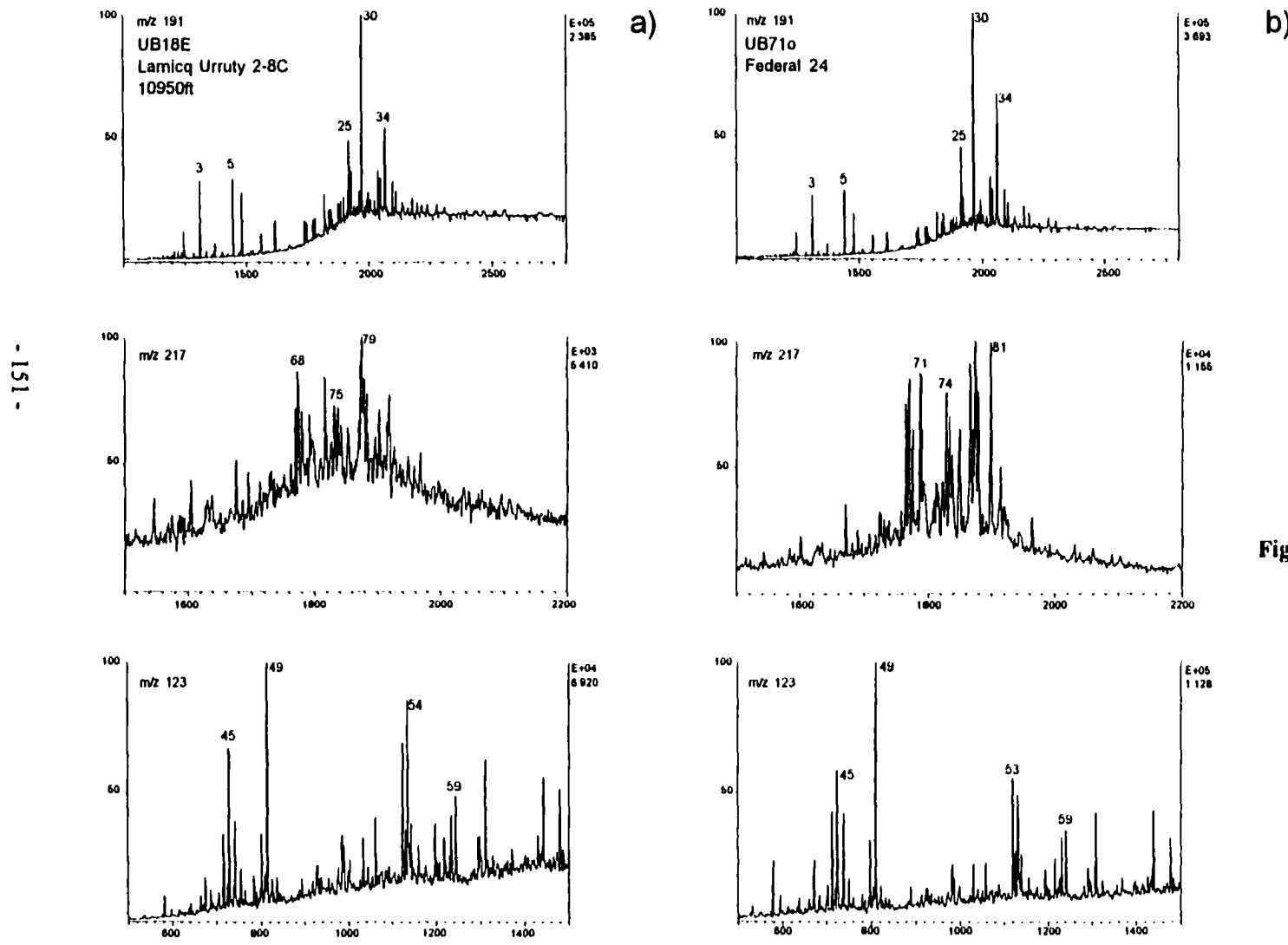


**Figure 44a:** Examples for PCA based source rock and crude oil correlation. Source rock UB18E (a) was obtained from lower black shale facies/green shale facies sediments in the Altamont-Bluebell area (source rock map-group 1). Crude oil sample UB71o is a representative sample oil for map-group 5 (Wonsits Valley). Peak labels identified in Appendix 1.2.

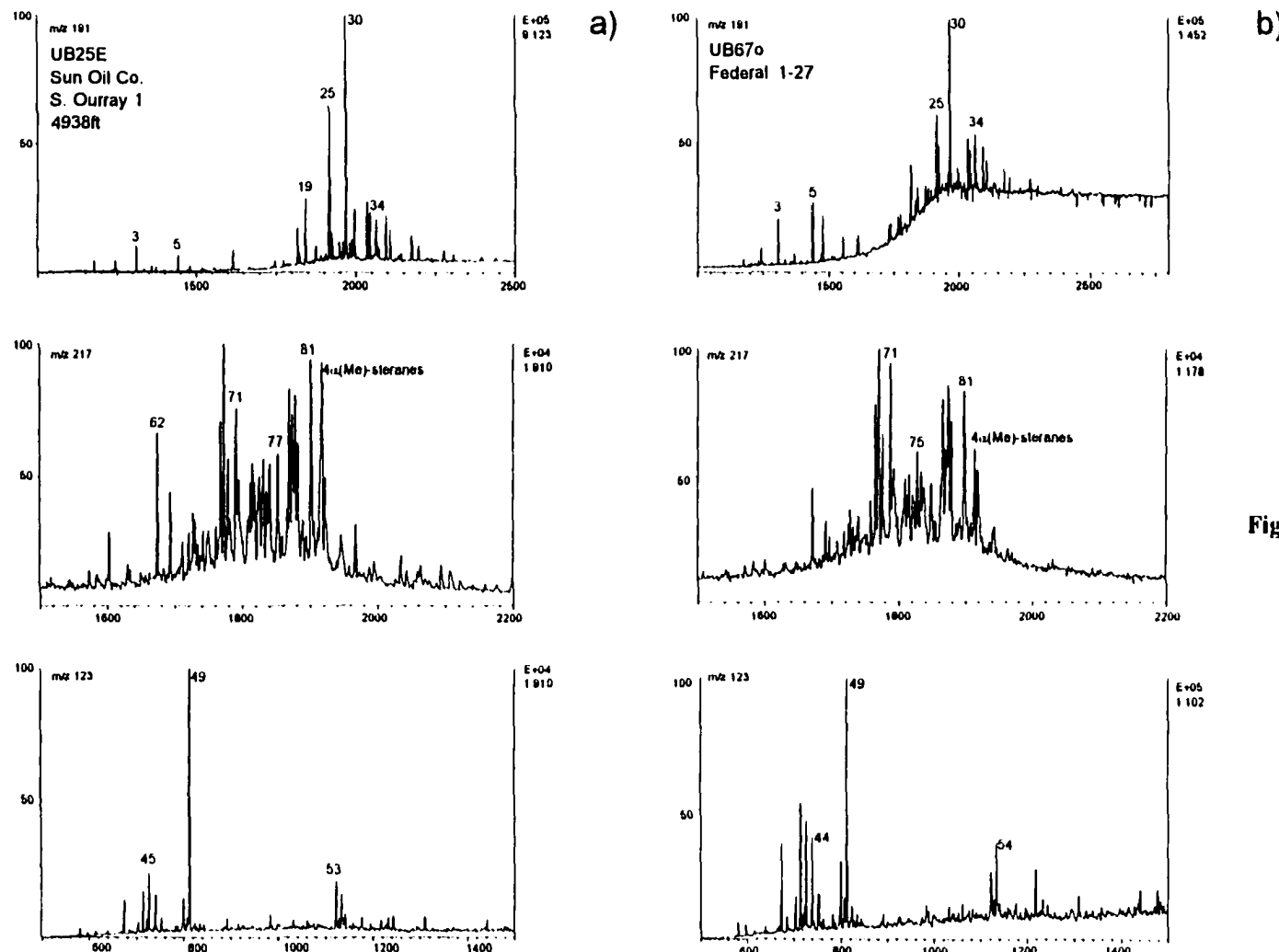


**Figure 44b:** Examples for PCA based source rock and crude oil correlation. Source rock UB12E (a) was obtained from basal Green River Formation sediments (lower black shale facies) in the south-central area (source rock map-group 3). Crude oil sample UB67o is a representative sample oil for map-group 7 (Coyote Basin). Peak labels identified in Appendix 1.2.

main generative stage. Oils generated from younger source rock units are trapped in the reservoirs of the Wonsits Valley, Brennan Bottom, Horseshoe Bend and Gusher fields, and lastly those of the Walker Hollow area. An alternative explanation for the spatial pattern is the simultaneous generation and expulsion of oils from a thick source rock section and secondary migration along stratigraphically equivalent carrier beds into the reservoirs. However, this would result in oil mixing and oils similar to those in the Coyote Basin should be present in the deep reservoirs of the Brennan Bottom, Horseshoe Bend Wonsits Valley, and Walker Hollow areas. The south-central fields apparently are not located along the primary north-southeast directed migration routes described above, otherwise geochemically similar oils would be expected to be present. Only local sources with some contribution from the main generative sections supply hydrocarbon charges to the fields, thus significantly reducing the amount of reserves which can be expected. The migration model is illustrated in Figure 45 and agrees with fluid flow models published in Bredehoeft *et al.* (1994) and McPherson (1997).

Another source of crude oils are apparently extremely rich but immature oil-shales, which generate entirely different oils than those described above by means other than thermal maturity. Warren (1986), for example, described the conversion of gypsum to anhydrite and similar diagenetic dewatering of hydrous evaporite minerals in organic-rich-rocks and simultaneous flushing of hydrocarbons as a potential mechanism. In Chinese immature lacustrine shales, liquid hydrocarbons were generated directly from specific organic matter components (such as dinoflagellates) instead of the kerogen (Quiang and McCabe, 1998).

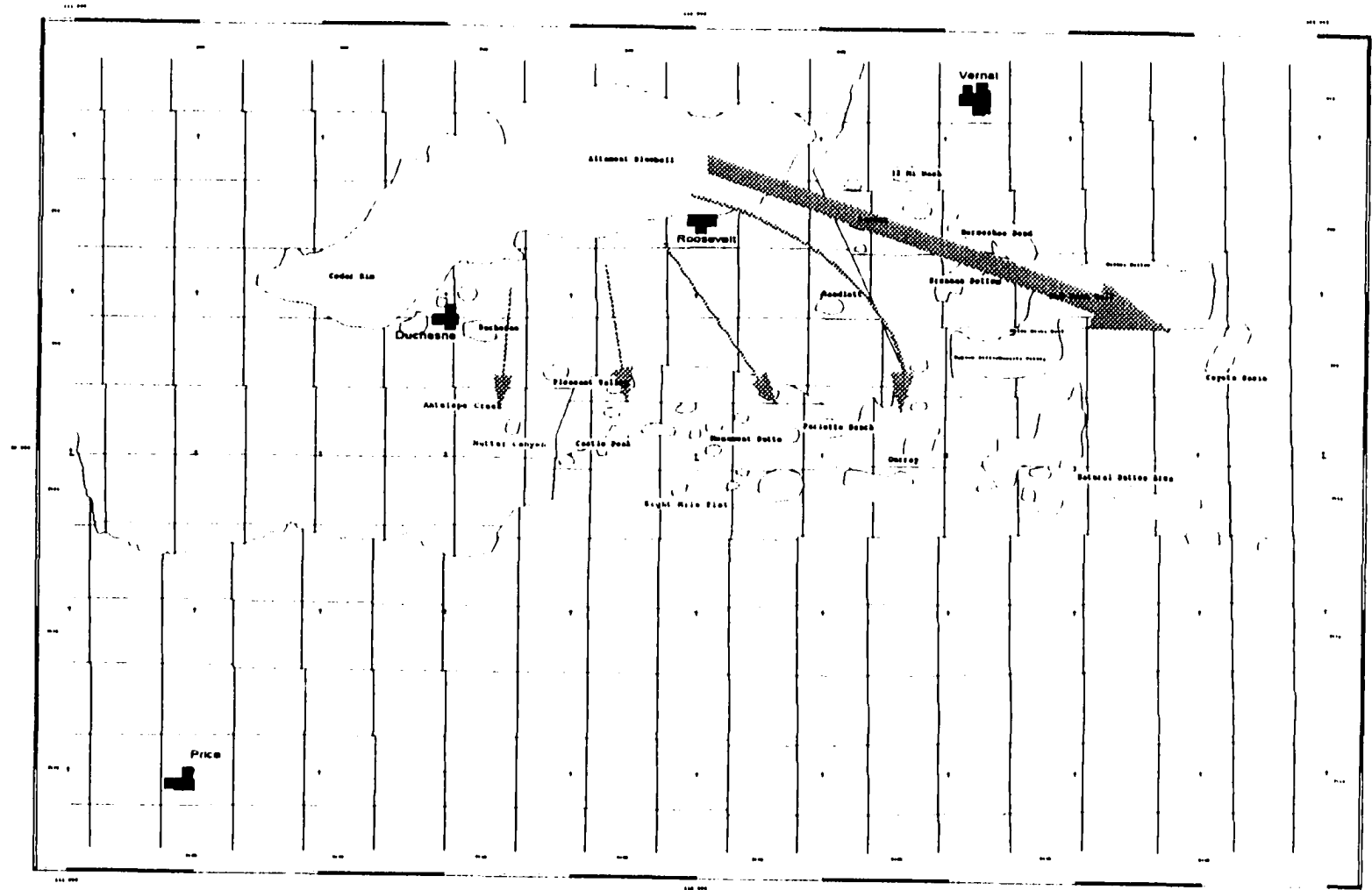


**Figure 45:** Conceptual interpretation of migration patterns in the Tertiary petroleum system of the Uinta Basin, based on geochemical analysis of source rocks and oils, and geographic distribution of crude oils. Size of arrows symbolizes quantity of migrating hydrocarbons.

## **8. Conclusions**

Organic matter composition and biomarker analysis of source rocks can be closely related to the evolution of the Uinta Basin lacustrine depositional system from freshwater to saline and hypersaline during the Paleogene. Biological markers, considered as molecular fossils, can support interpretations regarding environmental conditions and changes thereof through time. Prerequisite is the analysis and interpretation of source rocks in a stratigraphic framework. Changes in lake conditions caused deposition of compositionally variable source rocks, identifiable by monitoring overall biomarker distributions and specific compounds in source rock extracts. Multivariate statistical analysis significantly facilitates the evaluation of these geochemical variations. Analysis of thermal maturity parameters suggests that the oil generation window is presently located approximately between 10,000-12,000 ft depth in the deep north-central part of the basin (Colton Tongue and stratigraphically equivalent intervals).

Crude oils in the basin inherited the stratigraphic signature of the source rock geochemistry and allow detailed correlation to specific sources. Based on this correlation, 6 different oil-groups in addition to the waxy oils from the deepest reservoirs of the Altamont-Bluebell area have been identified. Similar to source rock analysis, compositional differences and similarities can be revealed using simple multivariate statistical techniques, and genetic relationships of source rocks and crude oils can be directly compared based on PCA results.

Distribution of oil-types and geographical location of oil fields permit inferences of migration patterns in the basin. The main migration routes from the north-central area is to the southeast, and oils from the stratigraphically oldest source rock are trapped farthest away from the source. Smaller pools in the central part of the basin receive charges from distinct sources, in some cases with contribution from hydrocarbon charges of the main migration pathway.

## 9. References

- Abbott, W., 1957, Tertiary of the Uinta Basin. In Geology of the Uinta Basin, International Association of Petroleum Geologists Guidebook, 8th Annual Field Conference, pp. 102-109.
- Alexander, R., Kagi, R., Noble, R.A., Volkman, J.K. (1984) Identification of some bicyclic alkanes in petroleum. In P.A. Schenck, J.W. de Leeuw, Lijmbach, G.W.M., eds., Advances in Organic Geochemistry 1983, Pergamon Press, Oxford, pp. 63-70.
- Alexander, R., Noble, R.A., Kagi, R.J. (1987) Fossil resin biomarkers and their application in oil to source-rock correlation, Gippsland Basin, Australia. APEA Journ. 27, 63-72.
- Anders, D.E., Gerrild, P.M. (1984) Hydrocarbon generation in lacustrine rocks of Tertiary age, Uinta Basin. Utah-Organic carbon, pyrolysis yield, and light hydrocarbons. In J. Woodward, F.F. Meissner, J.L. Clayton, eds., Hydrocarbon Source Rocks of the Greater Rocky Mountain Region, Rocky Mtn. Assoc. Geol. Denver, pp. 513-529.
- Anders, D.E., Palacas, J.G., Johnson, R.C. (1992) Thermal maturity of rocks and hydrocarbon deposits, Uinta Basin, Utah. In T.D. Fouch, V.F. Nuccio, T.C. Chidsey, Jr., eds., Hydrocarbon Resources of the Uinta Basin, Utah and Colorado, Utah Geol. Assoc. Guidebook 20, pp. 53-76.
- Anderson, T.W. (1963) Asymptotic theory for principal component analysis. Ann. math. statist. 34, 122-148
- Aquino Neto, F.R., Trendel, J.M., Restle, A., Connan, J., Albrecht, P.A. (1981) Occurrence and formation of tricyclic and tetracyclic terpanes in sediments and petroleum. In M. Bjorøy *et al.*, Advances in Organic Geochemistry, pp. 659-667.
- Baer, J.L. (1969) Paleoecology of cyclic sediments of the lower Green River Formation, central Utah. Brigham Young Univ. Geol. Stud. 16, Salt Lake City, 95 p.
- Barron, E.J., Moore, G.T. (1994) Climate model application in paleoenvironmental analysis, Soc. Econ. Paleont. Mineral. Short Course No. 33, 339 p.
- Bass, N.W. (1964) Relationship of crude oils to depositional environment of source rocks in the Uinta Basin. In Guidebook to the Geology and Mineral Resources of the Uinta Basin, 13th Ann. Field Conf., Intermtn. Assoc. Petrol. Geol., pp. 201-206.
- Borer, J., McPherson, M.L. (1996) High-resolution stratigraphy of the Green River Formation, NE Uinta Basin; implications for Red Wash reservoir compartmentalization (abstr.) Am. Assoc. Petrol. Geol. Annual Conv., San Diego, May 19-22, 1996, A18.
- Boyer, B.W. (1982) Green River laminites: Does the playa-lake model really invalidate the stratified-lake model? Geology 10, 321-324.

Bradley, M.D. (1995) Timing of the Laramide rise of the Uinta Mountains, Utah and Colorado. Wyoming Geol. Assoc., 1995 Field Conf. Guidebook, pp.31-44.

Bradley, W. (1929) The warves and climate of the Green River Epoch. U.S.Geo. Surv. Prof. Paper 158, 87-110.

Bradley, W.H. (1931) Origin and microfossils of the oil shale of the Green River Formation of Colorado and Utah. U.S.Geo. Surv. Prof. Paper 168, 58 p.

Bradley, W.H., Eugster, H.P. (1969) Geochemistry and paleoclimatology of the trona deposits and associated authigenic minerals of the Green River Formation of Wyoming. USGS Prof. Paper 496-B, 71 p.

Bredehoeft, J.D., Wesley, J.B., Fouch, T.D. (1994) Simulation of the origin of fluid pressure, fracture generation and the movement of fluids in the Uinta Basin, Utah. Am. Assoc. Petrol. Geol. Bull. 78, 1729-1747.

Brobst, D.A., Tucker, J.D. (1973) X-ray mineralogy of the Parachute Creek Member, Green River Formation, in the northern Piceance Creek Basin, Colorado. U.S.Geo. Surv. Prof. Paper 803, 53 p.

Bryant, B., Naeser, C.W., Marvin, R.F., Mehnert, H.H. (1989) Upper Cretaceous and Paleogene sedimentary rocks and isotopic ages of Paleogene tuffs, Uinta Basin, Utah. U.S.Geo. Surv. Bull. 1787, J1-J20.

Buchheim, H.P. (1994) Eocene Fossil Lake, Green River Formation, Wyoming: A history of fluctuating salinity. In Sedimentology and Geochemistry of Modern and Ancient Saline Lakes. Soc. Econ. Paleont. Mineral. Spec. Publ. 50, 239-247.

Burnham, A.K., Carlson, S.E., Singleton, M.F., Wong, C.M., Crawford, R.W. (1982) Biological markers from Green River kerogen decomposition. Geochim. Cosmochim. Acta 46, 1243-1251.

Cashion, W.B. (1967) Geology and fuel resources of the Green River Formation, southeastern Uinta Basin, Utah and Colorado. U.S.Geo. Surv. Prof. Paper 548, 48 p.

Carlson, R.M.K., Teerman, S.C., Moldowan, J.M., Jacobson, S.R., Chan, E.I., Dorrough, K.S., Seetoo, W.C., Mertani, B. (1993) High temperature gas chromatography of high-wax oils. Proceedings of the Indonesian Petroleum Association, 20th Annual Convention, 483-504.

Carroll, A., Brassell, S.C., Graham, S.A. (1992) Upper Permian lacustrine oil shales, southern Juggar Basin, northwest China. Am. Assoc. Petrol. Geol. Bull. 76, 1874-1902.

Carroll, A. (1998) Upper Permian lacustrine organic facies evolution, southern Juggar Basin, northwest China. Org. Geochem. 28, 649-667.

- Castle, J.W. (1990) Sedimentation in Eocene Lake Uinta (Lower Green River Formation). northeastern Uinta Basin, Utah. In B.J. Katz, ed., Lacustrine Basin Exploration - Case Studies and Modern Analogs, Am. Assoc. Petrol. Geol. Mem. 50, pp. 243-263.
- Chatfield, L., Collins, A.J. (1980) Introduction to multivariate analysis. Chapman and Hall, London, 246 p.
- Chidsey, T.C. Jr. (1993) Uinta Basin plays - overview. In Atlas of Major Rocky Mountain Gas Reservoirs, New Mexico Bureau of Mines and Mineral Resources, pp. 83.
- Clark, J.P., Philp, R.P. (1989) Geochemical characterization of evaporitic and carbonate depositional environments and correlation of associated crude oils in the Black Creek Basin, Alberta. Canad. Petrol. Geol. Bull. 37, 401-416.
- Clem, K. (1985) Oil and gas production summary of the Uinta Basin. In M.D. Picard, ed., Geology and Energy Resources of Utah, Utah Geol. Assoc. Publ. 12, pp. 159-168.
- Colburn, J.A., Bereskin, S.R., McGinley, D.C., Schiller, D.M. (1985) Lower Green River Formation in the Pleasant Valley producing area, Duchesne and Uinta Counties, Utah. In M.D. Picard, ed., Coal and Energy Resources, Uinta Basin, Utah Geol. Assoc. 12, pp. 177-186.
- Cole, R.D. (1984) Sedimentological, mineralogical and geochemical definition of oil shale facies in the lower Parachute Creek Member of the Green River Formation, Colorado. In J.H. Gary, ed., Proc. 17th Oil Shale Sympos., pp. 143-158, Colorado School of Mines.
- Collister, J.W., Lichtfouse, E., Hieshima, G., Hayes, J.M. (1994) Partial resolution of sources of *n*-alkanes in the saline portion of the Parachute Creek Member, Green River Formation (Piceance Creek Basin, Colorado). Org. Geochem. 21, 645-659.
- Curiale, J.A. (1993) Oil to source rock correlation: Concepts and case studies. In M.H. Engel, A.S. Macko, eds., Organic Geochemistry-Principles and Applications, Plenum Press, N.Y., pp. 473-490.
- Dahl, J., Moldowan, J.M., McCaffrey, M.A., Lipton, P.A. (1992) 3-Alkyl steranes in petroleum. Evidence for a new class of natural products. Nature 355, 154-157.
- Dane, C.H. (1954) Stratigraphic and facies relationships of upper part of Green River Formation and the lower part of Uinta Formation in Duchesne, Uintah, and Wasatch Counties, Utah, USGS Oil and Gas Investigations, Chart OC-52.
- Davis, J.C. (1986) Statistics and data analysis in geology. 2nd ed., Wiley and Sons, New York., 646 p.
- Dean, W.E., Anders, D.E. (1991) Effects of source, depositional environment, and diagenesis on characteristics of organic matter in oil shale from the Green River Formation, Wyoming, Utah, and Colorado. U.S. Geol. Surv. Bull. 1973, F1-16.

- Desborough, G.A. (1978) A biogenic-chemical stratified lake model for the origin of oil shale of the Green River Formation - An alternative to the playa-lake model. *Geol. Soc. Am. Bull.* 89, 961-971.
- Dickinson, W.E., Klute, M.A., Hayes, M.J., Janecke, S.U., Lundin, E.R., McKittrick, M.A., Olivares, M.D. (1988) Paleogeographic and paleotectonic setting of Laramide sedimentary basins in the central Rocky Mountain region. *Geol. Soc. Am. Bull.* 100, 1023-1039.
- Dunham, R.J. (1962) Classification of carbonate rocks according to depositional texture. In W.E. Hamm, ed., *Classification of Carbonate Rocks*, Am. Assoc. Petrol. Geol. Memoir 1, pp. 108-121.
- Dyni, J.R., Milton, C., Cashion, W.R. (1985) The saline facies of the upper part of the Green River Formation near Duchesne, Utah. In M.D. Picard, ed., *Geology and Energy Resources of Utah*, Utah Geol. Assoc. Publ. 12, pp. 51-60.
- Ekweozor, C.M., Okogun, J.I., Ekong, D.E.U., Maxwell, J.R. (1981) C<sub>24</sub>-C<sub>27</sub> degraded triterpanes in Nigerian petroleum: Novel molecular markers of source/input or organic maturation? *Journ. Geochem. Exploration* 15, 653-662.
- Engel, M.H., Imbus, S.W., Zumberge, J.E. (1988) Organic geochemical correlation of Oklahoma crude oils using R- and Q-mode factor analysis. *Org. Geochem.* 12, 157-170.
- Espitalié, J. (1986) Use of T<sub>max</sub> as a maturation index for different types of organic matter. Comparison with vitrinite reflectance. In J. Burrus, ed., *Thermal Modeling in Sedimentary Basins*, 1st Inst. Fr. Pet. Explor. Res. Conf., Editions Technip, Paris, pp. 475-496.
- Eugster, H.P., Surdam, R.C. (1973) Depositional environment of the Green River Formation of Wyoming: A preliminary report. *Geol. Soc. Am. Bull.* 84, 1115-1120.
- Fouch, T. D. (1975) Lithofacies and related hydrocarbon accumulations in Tertiary strata of the western and central Uinta Basin, Utah. In D. W. Boylard, ed., *Rocky Mountain Association of Petroleum Geologists Symposium on Deep Drilling Frontiers of the Central Rocky Mountains*, pp. 163-174.
- Fouch, T.D. (1976) Revision of the lower part of the Tertiary system in the central and western Uinta basin, Utah. *U.S. Geol. Surv. Bull.* 1405-C, 7 p.
- Fouch, T.D., Hanley, J.H. (1977) Interdisciplinary analysis of some petroleum source rocks in east-central Utah - implications for hydrocarbon exploration in nonmarine rocks of western United States (abstr.). *Am. Assoc. Petrol. Geol. Bull.* 61, 1377-1378.
- Fouch, T.D., Cashion, W.B. (1979) Distribution of rock types, lithologic groups, and depositional environments for some Lower Tertiary and Upper Cretaceous, and Upper and Middle Jurassic rocks in the subsurface between Altamont oil field and San Arroyo gas field, northcentral and northeastern Uinta Basin, Utah. *U.S. Geol. Surv. Open File Report*, pp. 79-365.

- Fouch, T.D. (1981) Distribution of rock types, lithologic groups, and interpreted depositional environments for some lower Tertiary and Upper Cretaceous rocks from outcrops at Willow Creek-Indian Canyon through the subsurface of Duchesne and Altamont oil fields, southwest to north central part of the Uinta Basin, Utah. U.S. Geol. Surv. Oil and GAS Investigation Chart OC-81, 2 charts
- Fouch, T.D., Nuccio, V.F., Osmond, J.C., MacMillan, L., Cashion, W.B., Wandrey, C.J. (1992) Oil and gas in the uppermost Cretaceous and Tertiary rocks, Uinta Basin, Utah. In T.D. Fouch, V.F. Nuccio, T.C. Chidsey, Jr., eds., Hydrocarbon Resources of the Uinta Basin, Utah and Colorado, Utah Geol. Assoc. Guidebook 20, pp. 9-47.
- Fouch, T.D., Nuccio, V.F., Anders, D.E., Dudley, D.R., Pitman, J.K., Mast, R.F. (1994), Green River(!) Petroleum System, Uinta Basin, Utah, USA. In Magoon, L.B. and Dow, W.G., eds., The Petroleum System - from source to trap, Am. Assoc. Petrol. Geol. Mem. 60, pp. 399-421.
- Fowler, M.G., Brooks, P.W. (1990) Organic geochemistry as an aid in the interpretation of the history of oil migration into different reservoirs at the Hibernia K-18 and Ben Naris 1-45 wells, Jeanne d'Arc Basin, offshore Eastern Canada. Org. Geochem. 16, 461-475.
- Franczyk, K.J., Pitman, J.K. (1989) Evolution of resource rich foreland and intermontane basins in eastern Utah and western Colorado. 28th Intern. Geol. Congress, Field Trip Guidebook T324, Salt Lake City, 53 p.
- Franczyk, K.J., Fouch, T.D., Johnson, R.C., Molenaar, C.M., Cobban, W.A. (1992) Cretaceous and Tertiary paleogeographic reconstruction for the Uinta-Piceance Creek Basin study area, Colorado and Utah. U.S. Geol. Surv. Bull. 1787, Q1-37.
- Fu Jiamo, Sheng Guoying, Xu Jiayon, Eglington, G., Gowar, A.P., Jia Rongfen, Fan Shanfa, Peng Pingan (1990) Application of biological markers in the assessment of paleoenvironments of Chinese non-marine sediments. Org. Geochem. 16, 769-779.
- Glenn, C.R., Kelts, K. (1991) Sedimentary rythms in lake deposits. In G., Einsele, A., Seilacher, eds., Cycles and Event Stratigraphy, Springer, Berlin, pp.188-221.
- Goodwin, N.S., de Leeuw, S.W., Püttmann, W., Tegelaar, E.W. (1988) Structure and significance of C<sub>30</sub> 4-methyl steranes in lacustrine shales and oils. Org. Geochem. 12, 495-506.
- Goosens, H., de Leeuw, J.W., Schenck, P.A., Brassell, S.C. (1984) Tocopherol as likely precursor of pristane in ancient sediments and crude oils. Nature 312, 440-442.
- Gower, J.C. (1966) Some distance properties of latent root and vector methods in multivariate analysis. Biometrika 53, 325-338.
- de Grande J.M.B., Aquino Neto, F.R., Mello, M.R. (1993) Extended tricyclic terpanes in sediments and petroleums. Org. Geochem. 20, 1039-1047.
- Grantham, P.J. (1986) Sterane isomerization and morteane/hopane ratios in crude oils derived from Tertiary source rocks. Org. Geochem. 9, 293-304.

- Grossman, G.D., Nickerson, D.M., Freeman, M.C. (1991) Principal component analysis of assemblage structure data: Utility of tests based on eigenvalues. *Ecology* 72, 341-347.
- Harvey, H.R., McManus, G.B. (1991) Marine ciliates as a widespread source of tetrahymanol and hopan-3 $\beta$ -ol in sediments. *Geochim. Cosmochim. Acta* 55, 3387-3390.
- Hang, Z.H., Li, H.-X., Rullkötter, J., Mackenzie, A.S. (1986) Geochemical application of steranes and triterpane biological marker compounds in the Linyi Basin. *Org. Geochem.* 10, 433-439.
- ten Haven, H.L., de Leeuw, J.W., Peakman, T.M., Maxwell, J.R. (1986) Anomalies in steroid and hopanoid maturity indices. *Geochim. Cosmochim. Acta* 50, 853-855.
- ten Haven, H.L., de Leeuw, J.W., Rullkötter, J., Sinnighe Damsté, J.S. (1987) Restricted utility of the pristane/phytane ratio as a paleoenvironmental indicator. *Nature* 330, 641-643.
- ten Haven, H.L., Rullkötter, J. (1988) The diagenetic fate of taraxer-14-ene and oleanane isomers. *Geochim. Cosmochim. Acta* 52, 1977-1987.
- ten Haven, H.L., de Leeuw, J.W., Sinnighe Damsté, J.S., Schenck, P.A., Palmer, S.E., Zumberge, J.E. (1988) Application of biological markers in the recognition of paleo-hypersaline environments. In A.J. Fleet, K. Kelts, M.R. Talbot, eds., *Lacustrine Petroleum Source Rocks*. Geol. Soc. Spec. Publ. 40, pp. 123-130.
- Hill, B.G., Bereskin, S.R. (1993) Oil and gas fields of Utah. *Utah Geol. Assoc. Publ.* 22, Salt Lake City, 168 p.
- Hills, I.R., Whitehead, E.V., Anders, D.E., Cummins, J.J., Robinson, W.E. (1966) An optically active triterpane, gammacerane in Green River, Colorado, oil shale bitumen. *J. Chem. Soc., Chem. Commun.*, 752-754.
- Hintze, L.F. (1980) Geologic Map of Utah. *Utah Geologic and Mineral Survey*. 1:500,000.
- Hong Zhi-Hua, Li Hui-Xiang, Rullkötter, J., Mackenzie, A.S. (1986) Geochemical application of sterane and triterpane biological marker compounds in the Linyi Basin. *Org. Geochem.* 10, 433-439.
- Horsfield, B., Curry, D.J., Bohacs, K., Littke, R., Rullkötter, J., Schenck, H.J., Radke, M., Schaefer, R.G., Carroll, A.R., Isaaksen, G., Witte, E.G. (1994) Organic geochemistry of freshwater and alkaline lacustrine sediments in the Green River Formation of the Washakie Basin, Wyoming, U.S.A. *Org. Geochem.* 22, 415-440.
- Huang, W.Y., Meinschein, W.G. (1979) Sterols as source indicators of organic materials in sediments. *Geochim. Cosmochim. Acta* 43, 739-745.
- Huang Difan, Li Jinchao, Zang Daqiang (1990) Maturation sequence of continental crude oils in hydrocarbon basins in China and its significance. *Org. Geochem.* 16, 521-529.

- Huizinger, B.J., Aizenshtat, Z.A., Peters, K.E. (1988) Programmed pyrolysis-gas chromatography of artificially matured Green River kerogen. *Energy & Fuels* 2, 74-81.
- Hunt, J.M. (1996) Petroleum Geochemistry and Geology, 2nd ed., Freeman, N.Y., 743p.
- Irwin, H., Meyer, T. (1990) Lacustrine organic facies. A biomarker study using multivariate statistical analysis. *Org. Geochem.* 16, 197-210.
- Jackson, D. (1993) Stopping rules in principal component analysis: A comparison of heuristic and statistical approaches. *Ecology* 74, 2204-2214.
- James, F.C., McCulloch, C.E. (1990) Multivariate analysis in ecology and systematics: Pangea or Pandora's box? *Ann. Rev. Ecol. Syst.* 21, 129-166.
- Jiang, Z.S., Fowler, M.G. (1986) Carotenoid-derived alkanes in oils from northwestern China. *Org. Geochem.* 10, 831-839.
- Johnson, R.C., Finn, T.M. (1976) Cretaceous through Holocene history of the Douglas Creek Arch, Colorado and Utah. In *New Interpretations of Northwest Colorado Geology*, Rocky Mtn. Assoc. Geol., pp. 77-96.
- Johnson, R.C. (1981) Stratigraphic evidence for a deep Eocene Lake Uinta, Piceance Creek Basin, Colorado. *Geology* 9, 55-62.
- Johnson, R.C. (1985) Early Cenozoic history of the Uinta Basin and Piceance Creek Basins, Utah and Colorado, with special reference to the development of Eocene Lake Uinta. In R.M. Flores, S.S. Kaplan, eds., *Cenozoic Paleogeography of the West-Central United States*, Soc. Econ. Paleont. Mineral., Denver, pp. 247-276.
- Johnson, R.C. (1988) Early Cenozoic history of the Uinta and Piceance Creek basins, Colorado and Utah. In L.L. Sloss, ed., *Sedimentary Cover - North American Craton*, Geol. Soc. Am. Geology of North America, v. D-2, pp. 144-154.
- Johnson, R.C. (1989) Detailed cross section correlating Upper Cretaceous and Lower Tertiary rocks between the Uinta Basin of eastern Utah and western Colorado and the Piceance Creek Basin of western Colorado. *Utah Geol. Surv. Misc. Invest. Series Map 1-1974*.
- Johnson, S.Y. (1992) Phanerozoic evolution of sedimentary basins in the Uinta-Piceance Basin region, northwestern Colorado and northeaster Utah. *U.S. Geol. Surv. Bull.* 1787, FF1-38.
- Katz, B. (1995) The Green River shale: an Eocene carbonate lacustrine source rock. In B.J. Katz, ed., *Petroleum Source Rocks*, Springer, Berlin, pp. 209-324.
- Kelly, J.M., Castle, J.W. (1990) Red Wash Field-USA, Uinta Basin, Utah. In N.H. Foster, E.A. Beaumont, Am. Assoc. Petrol. Geol. Treatise of Petroleum Geology, Stratigraphic Traps IV, Atlas of Oil and Gas Fields, pp. 231-255.

- Kelts, K. (1988) Environments of deposition of lacustrine petroleum source rocks: an introduction. In A.J. Fleet, K. Kelts, M.R. Talbot, *Lacustrine Petroleum Source Rocks*, Geol. Soc. Spec. Publ., pp 3-26.
- Killops, S.D., Killops, V.J. (1993) An introduction to organic geochemistry. Longman Scientific and Technical, N.Y., 265 p.
- Koesomatinada, R.P. (1970) Stratigraphy and Petroleum occurrence, Green River Formation, Red Wash field, Utah. Quarterly of the Colorado School of Mines 65, 77 p.
- LaRoque, A. (1960) Molluscan faunas of the Flagstaff Formation in central Utah. Geol. Soc. Amer. Mem. 78, 100 p.
- Legendre, L., Legendre, P. (1983) Numerical Ecology. Developments in environmental modeling 3. Elsevier, Amsterdam, 419 p.
- LeMaitre, R.W. (1982) Numerical petrology. Developments in Petrology 8, Elsevier, Amsterdam. 281 p.
- Leopold, E.B., MacGinitie, H.D. (1972) Development and affinities of Tertiary floras in the Rocky Mountains. In A. Graham, ed., *Floristics and Paleofloristics of Asia and eastern North America*, Elsevier, Amsterdam, pp 147-200.
- Lewan, M. D. (1993) Laboratory simulation of petroleum formation-hydrous pyrolysis. In M.H. Engel, A.S. Macko, eds., *Organic Geochemistry-Principles and Applications*, Plenum Press, N.Y., pp. 419-442.
- Lundell, I.L., Surdam, R.C. (1975) Playa-lake deposition: Green River Formation, Piceance Creek Basin, Colorado. Geol. 3, 493-497.
- Marzi, R., Torkelson, B.E., Olson, R.K. (1993) A revised carbon preference index. Org. Geochem. 20, 1303-1306.
- Matveeva, I.A., Petrov, A.A. (1997) Geochemical implications of C<sub>21</sub>-C<sub>22</sub> steranes. Geochem. Internat. 35, 398-402.
- Mauger, R.L. (1977) K-Ar ages of biotites from tuffs in Eocene rocks of the Green River, Washaki, and Uinta basins, Utah, Wyoming, and Colorado. Contrib. to Geol., Univ. of Wyoming 15, 17-41.
- MacGinitie, H.D. (1969) The Eocene Green River flora of northwestern Colorado and northeastern Utah. Calif. Pubs. Geol. Sci. 83, 203 p.
- McDonald, T.J. and Mahlon, C.K. (1992) Fractionation of crude oils by HPLC and quantitative determination of aliphatic and aromatic biological markers by GC-MS with selected ion monitoring. LC \* GC 10, 935-938.

- McKirdy, D.M., Kantsler, A.J., Emmett, J.K., Aldridge, A.K. (1984) Hydrocarbon genesis and organic facies in Cambrian carbonates of the Eastern Officer Basin, South Australia. In J.G. Palacas, ed., Petroleum Geochemistry and Source Rock Potential of Carbonate Rocks. Am. Assoc. Petrol. Geol. Studies in Geology 18, pp. 13-31.
- McPherson (1996) A three-dimensional model of the geologic and hydrodynamic history of the Uinta Basin, Utah: Analysis of overpressure and migration. Unpubl. PhD. thesis, Dept. of Geol. and Geophys., University of Utah. 119 p.
- Mello, M.R., Telnaes, N., Gagliamone, P.C., Chicarelli, M.I., Brassell, S.C., Maxwell, J.R. (1988) Organic geochemical characterization of depositional paleoenvironments of source rocks and oils in Brazilian margin basins. *Organic Geochemistry* 13, 31-45.
- Mello, M.R., Maxwell, J.R. (1990) Organic geochemical and biological characterization of source rocks and oils derived from lacustrine environments in the Brazilian Continental margin. In B.J. Katz, Lacustrine Basin Exploration: Case Studies and Modern Analogs, Am. Assoc. Petrol. Geol. Mem. 50, p. 77-97.
- Meyer, P.A., Ishiwatari, R. (1993) The early diagenesis of organic matter in lacustrine sediments. In M.H. Engel, A.S. Macko, *Organic Geochemistry-Principles and Applications*, Plenum Press, N.Y., p.185-209
- Moldowan, J.M., Sundararaman, P., Schoell, M. (1986) Sensitivity of biomarker properties to depositional environment and/or source input in the Lower Toarcian of S.W. Germany. *Org. Geochem.* 10, 915-926.
- Moldowan, J.M., Fago, F.S., Carlson, R.M.K., Young, D.C., Duyne, G.V., Clardy, J., Schoell, M., Pillinger, C.T., Watt, D.S. (1991) Rearranged hopanes in sediments and petroleum. *Geochim. Cosmochim. Acta* 55, 3333-3353.
- Moldowan, J.M., Sundararaman, P., Salvatori, T., Alajbeg, A., Gjukic, B., Lee, C.Y., Demaison, G.J. (1992) Source correlation and maturity assessment of select oils and rocks from the central Adriatic Basin (Italy and Yugoslavia). In J.M. Moldowan, P., Albrecht, R.P., Philp, eds., *Biological markers in Sediments and Petroleum*. Prentice Hall, Englewood & Cliffs, pp. 370-401.
- Moncure, G., Surdam, R.C. (1980) Depositional environment of the Green River Formation in the vicinity of the Douglas Creek Arch, Colorado and Utah, Univ. of Wyoming Contrib. Geol. 19, 9-24.
- Montgomery, S.L., Morgan, C.D. (1998) Bluebell field, Uinta Basin: Reservoir characterization for improved well completion and oil recovery. *Am. Assoc. Petrol. Geol. Bull.* 82, 1113-1132.
- Morgan, C.D., Tripp, C.N. (1996) Formation evaluation and mapping. In M.L. Allison and C.D. Morgan, eds., *Increased oil production and reserves from improved completion techniques in the Bluebell field, Uinta Basin, Utah*. U.S. National Technical Information Service

DOE/BC/14953-14. Ann. Report for the period October 1, 1994, to September 30, 1995. pp. 6-11.

Morgan, C.D., Hill, B.G., Jarvis, D.J. (1998) Secondary oil recovery (water flood) from the lower Green River Formation, Central Uinta Basin, Utah. In J.K. Pitman, A.R. Carroll, eds., Modern and Ancient Lake Systems, Utah Geol. Assoc. Guidebook 26, pp. 277-288.

Mueller, E., Philp, R.P. (1998) Extraction of high molecular weight hydrocarbons from source rocks: an example from the Green River Formation, Uinta Basin, Utah. Org. Geochem. 28, 625-631.

Murphy, M.T.J., McCormick, A., Eglinton, G. (1967) Perhydro- $\beta$ -carotene in Green River shale. Science 157, 1040-1042.

Murray, A.P., Sosrowidjojo, I.B., Alexander, R., Kagi, R.I., Norgata, C.M., Summons, R.E. (1997) Oleananes in oils and sediments-Evidence of marine influence during early diagenesis. Geochim. Cosmochim. Acta 61, 1261-1276.

Osborne, M.J., Swarbrick, R.E. (1997) Mechanisms for generating overpressure in sedimentary basins: a reevaluation. Am. Assoc. Petrol. Geol. Bull. 81, 1023-1041.

Osmond, J.C. (1964) Tectonic history of the Uinta Basin, Utah. In E.F. Sabatka, ed., Guidebook to the Geology and Mineral Resources of the Uinta Basin, 13th Annual Field Conference. Intermountain Assoc. Petroleum Geologists, pp.47-58.

Osmond, J.C. (1992) Greater Natural Buttes gas field, Uintah County, Utah. In T.D. Fouch, V.F. Nuccio, T.C. Chidsey, Jr., eds., Hydrocarbon Resources of the Uinta Basin, Utah and Colorado, Utah Geol. Assoc. Guidebook 20, pp. 143-163.

Oung, J.-N., Philp, R.P. (1994) Geochemical characteristics of oils from Taiwan. Journ. SE Asian Earth Sci. 9, 193-206.

Ourisson, G., Albrecht, P., Rohmer, M. (1982) Predictive microbial biochemistry from molecular fossils to prokaryotic membranes. Trends in Biochemical Sciences, Vol.7, 236-239.

Peters, K.E. (1986) Guidelines for evaluating petroleum source rocks using programmed pyrolysis. Am. Assoc. Petrol. Geol. Bull. 70, 318-329.

Peters, K.E., Moldowan, J.M., Sundararaman, P. (1990) Effects of hydrous pyrolysis on biomarker thermal maturity parameters. Monterey Phosphatic and Siliceous members. Org. Geochem. 15, 249-265

Peters, K.E., Moldowan, J.M. (1991) Effects of source, thermal maturity and biodegradation on the distribution and isomerization of homohopanes in petroleum. Org. Geochem 17, 47-61.

Peters, K.E., Moldowan, J.M. (1993) The biomarker guide. Prentice Hall, N.J., 363 p.

- Peterson, P.R. (1973) Bluebell Field. Oil and Gas Field Studies No. 12, Utah Geologic and Mineral Survey. 4pp.
- Picard, M.D. (1953) Marlstone - a misnomer as used in the Uinta Basin, Utah. Am. Assoc. Petrol. Geol. Bull. 37, 1075-1077.
- Picard, M.D. (1955) Subsurface stratigraphy and lithology of Green River Formation in Uinta Basin, Utah. Am. Assoc. Petrol. Geol. Bull. 39, 75-102.
- Picard, M.D. (1957) Green River and lower Uinta Formation subsurface stratigraphy in western Uinta Basin, Utah. In N.C. Williams, ed., Guidebook to the Geology of the Wasatch and Uinta Mountains Transition Area, 10th Annual Field Conf., Intermountain Asso. Petrol. Geol., pp. 129-149.
- Picard, D.M., Thompson, W.D. and Williamson, C.R. (1973) Petrology, geochemistry and stratigraphy of black shale facies of Green River Formation (Eocene), Uinta Basin, Utah: Utah Geological Survey Bulletin 100, pp.50.
- Picard, M.D. (1985) Hypothesis of oil-shale genesis, Green River Formation, northeast Utah, northwest Colorado, and southwest Wyoming. In M.D. Picard, ed., Geology and Energy Resources, Uinta Basin of Utah, Utah Geol. Assoc., Salt Lake City, pp. 193-210.
- Pitman, J.K., Fouch, T.D., Goldhaber, M.B. (1982) Depositional setting and diagenetic evolution of some Tertiary unconventional reservoir rocks, Uinta Basin, Utah. Am. Assoc. Petrol. Geol. Bull. 66, 1581-1596.
- Philp, R.P., Gilbert, T.D. (1986) Biomarker distributions in oils predominantly derived from terrigenous source material. Org. Geochem. 10, 73-84.
- Philp, R.P. (1994) Geochemical characteristics of oils derived predominately from terrigenous materials. In A.C. Scott, A.J. Fleet, eds., Coal and Coal-bearing strata as Oil-prone Source Rocks? Geological Society Special Publication 77, pp. 71-91.
- Powell, T.G. (1986) Petroleum geochemistry and depositional setting of lacustrine source rocks. Marine Petrol. Geol. 18, 137-148.
- Quiang, J., McCabe, P.J. (1998) Genetic features of petroleum systems in rift basins of eastern China. Marine Petrol. Geol. 15, 343-358.
- Reed, W.E., Henderson, W. (1972) Proposed stratigraphic control on the composition of crude oils reservoirs in the Green River Formation, Uinta Basin, Utah. In Adv. Org. Geochem., Pergamon, Oxford, 499-515.
- Remy, R.R. (1992) Stratigraphy of the Eocene part of the Green River Formation in the south-central part of the Uinta Basin, Utah. U.S. Geol. Surv. Bull. 1787, BB1-79.

- Requejo, A.G., Wielchowski, C.C., Klosterman, M.J., Sassen, R. (1994) Geochemical characterization of lithofacies and organic facies in Cretaceous organic-rich rocks from Trinidad, East Venezuela Basin. *Org. Geochem.* 22, 441-459.
- Requejo, A.G., Hieshima, G.B., Hsu, C.S. McDonald, T.J., Sassen, R. (1997) Short-chain (C21 and C22) diasteranes in petroleum and source rocks as indicators of maturity and depositional environment. *Geochim. Cosmochim. Acta* 61, 2653-2667.
- Rice, D.D., Fouch, T.D. Johnson, R.C. (1992) Influence of source rock type, thermal maturity and migration on composition and distribution of natural gases, Uinta Basin, Utah. In T.D. Fouch, V.F. Nuccio, T.C. Chidsey, Jr., eds., *Hydrocarbon Resources of the Uinta Basin, Utah and Colorado*, Utah Geol. Assoc. Guidebook 20, pp. 95-109.
- Richman, M. B., Gong, X. (1999) Relationship between the definition of the hyperplane width to the fidelity of PC loading patterns. *Journ. Climate*, in print.
- Riolo, J., Hussler, G., Albrechts, P., Connan, J. (1986) Distribution of aromatic steroids in geological samples: Their evaluation as geochemical parameters. *Org. Geochem.* 10, 981-990.
- Robinson, N., Eglinton, G., Brassell, S.C., Cranwell, P.A. (1984) Dinoflagellate origin for sedimentary 4 $\alpha$ -methyl steroids and 5 $\alpha$ -stanols. *Nature* 308, 439-441.
- Robinson, W.E. (1979) The origin, deposition, and alteration of the organic material in the Green River shale. *Org. Geochem.* 6, 205-218.
- Rock, N.M.S. (1988) Numerical geology. Lecture Notes in Earth Sciences No. 18, Springer, Berlin, 427 p.
- Roehler, H.W. (1993) Eocene climates, depositional environments, and geography, Greater Green River Basin, Wyoming, Utah, and Colorado. U.S. Geol. Surv. Prof. Paper 1506-F, F1-74.
- Ruble, T.E., Philp, R.P. (1991) Geochemical investigation of mature bitumens from the Uinta Basin, Utah, U.S.A. *The Compass* 68, 135-150.
- Ruble, T.E., Bakel, A.J., Philp, R.P. (1994) Compound specific isotopic variability in Uinta Basin native bitumens: plaeoenvironmental implications. *Org. Geochem.* 21, 661-671.
- Ruble, T.E. (1996) Geochemical investigation of the mechanism of hydrocarbon generation and accumulation in the Uinta Basin, Utah, Ph.D. dissertation, University of Oklahoma, 304 p.
- Ruble, T.E., Philp, R.P. (1998) Stratigraphy, depositional environments and organic geochemistry of source rocks in the Green River Petroleum system, Uinta Basin, Utah. In J.K. Pitman, A.R. Carroll, eds., *Modern and Ancient Lake Systems*, Utah Geol. Assoc. Guidebook 26, pp.289-320.
- Rullkötter, J., Marzi, R. (1988) Natural and artificial maturation of biological markers in a Toarcian shale from northern Germany, *Org. Geochem.* 13, 639-645.

Ryder, R. T., Fouch, T.D. and Elison, J.H. (1976) Early Tertiary sedimentation in the western Uinta Basin, Utah: Geol. Soc. Am. Bull. 87, 496-512

dos Santos Neto, E., Hayes, J.M., Takaki, T., (1998) Isotopic biogeochemistry of the Neocomian lacustrine and Upper Aptian marine-evaporitic sediments of the Potiguar Basin, northeastern Brasil. Org. Geochem. 28, 361-381.

Schoell, M., Hwang, R.J., Carlson, R.M.K., Welton, J.E. (1994) Carbon isotopic compositions of individual biomarkers in gilsonites (Utah). Org. Geochem. 21, 673-683.

Seifert, W.K., Moldowan, J.M. (1980) The effect of thermal stress on source rock quality as measured by hopane geochemistry. In A.G. Douglas, J.R. Maxwell, eds., Advances in Organic Geochem. 1979, Pergamon Press, Oxford, pp. 229-237.

Seifert, W.K., Carlson, R.M.K., Moldowan, J.M., (1981) Geomimetic synthesis, structure assignments, and geochemical correlation of monoaromatized petroleum steroids. Adv. Org. Geochem. 1981, pp. 710-724.

Sieskind, O., Yoly, G., Albrecht, P. (1979) Simulation of the geochemical transformation of sterols: Supraacid effects of clay minerals. Geochim. Cosmochim. Acta 43, 1675-1679.

Sinninghe Damsté, J.S., Kenig, F., Koopmans, M.P., Köster, J., Schouten, S., Hayes, J.M., de Leeuw, J.W. (1995) Evidence for gammacerane as an indicator for water column stratification. Geochim. Cosmochim. Acta 59, 1895-1900.

Snowdon, R.W. (1995) Rock-Eval  $T_{max}$  suppression: Documentation and amelioration. Am. Assoc. Petrol. Geol. Bull. 79, 1337-1348.

Spencer, C.W. (1987) Hydrocarbon generation as a mechanism for overpressuring in Rocky Mountain Region. Am. Assoc. Petrol. Geol. Bull. 71, 368-388.

Stanley, K.O., Collinson, J.W. (1979) Depositional history of Paleocene-lower Eocene Flagstaff limestone and coeval rocks, central Utah. Am. Assoc. Petrol. Geol. Bull. 63, 311-323.

Summons, R.E., Capon, R.J. (1988) Fossil steranes with unprecedented methylation in ring A. Geochim. Cosmochim. Acta 52, 2733-2736.

Summons, R.E., Jahnke, L.L. (1990) Identification of the methyl hopanes in sediments and petroleum. Geochim. Cosmochim. Acta 54, 247-251.

Summons, R.E., Capon, R.J. (1991) Identification and significance of  $3\beta$ -ethyl steranes in sediments and petroleum. Geochim. Cosmochim. Acta 55, 1232-1239.

Surdam, R.C. Stanley, K.O. (1979) Lacustrine sedimentation during the culminating phase of Eocene Lake Gosiute, Wyoming (Green River Formation), GSA Bull. 90, 93-110.

- Surdam, R.C., Stanley, K.O. (1980) Effects of changes in drainage basin boundaries on sedimentation in Eocene Lakes Gosiute and Uinta of Wyoming, Utah, and Colorado. *Geol.* 8, 135-139.
- Surdam, K.O., Wolfbauer, C.A. (1975) Green River Formation, Wyoming: A playa lake complex. *GSA Bull.* 86, 335-345.
- Sweeney, J.J., Burnham, A.K., Braun, R.L., (1987) A model of hydrocarbon generation from type I kerogen: Application to Uinta Basin, Utah. *Am. Assoc. Petrol. Geol. Bull.* 71, 967-985.
- Talbot, M.R., Allen, P.A. (1996) Lakes. In H.G. Reading, ed., *Sedimentary Environments: Processes, Facies and Stratigraphy*. Blackwell Sciences, Oxford, pp.83-124.
- Tegelaar, E.W., Matthezing, R.M., Jansen, J.B.H., Horsfield, B., de Leeuw, J.W. (1989) Possible origin of n-alkanes in high-wax crude oils. *Nature* 342, 529-531.
- Telnaes, N., Dahl, B. (1985) Oil-oil correlation using multivariate techniques. *Org. Geochem.* 10, 425-432
- Telnaes, N., Cooper, B.S. (1991) Oil-source correlation using biological markers, Norwegian continental shelf. *Marine Petrol. Geol.* 8, 302-310.
- Tissot, B., Deroo, G., Hood, A. (1978) Geochemical study of the Uinta Basin: formation of petroleum from the Green River Formation. *Geochim. Cosmochim. Acta* 42, 1469-1485
- Tissot, B., Welte, D. (1984) Petroleum formation and occurrence. 2nd ed., Springer, Berlin, 699 p.
- Tissot, B.P., Pelet, R., Ungerer, P.H. (1987) Thermal history of sedimentary basins, maturation indices and kinetics of oil and gas generation. *Am. Assoc. Petrol. Geol. Bull.* 71, 1445-1466.
- Tuttle, M.L. (1991) Geochemical, biogeochemical, and sedimentological studies of the Green River Formation, Wyoming, Utah, and Colorado-Introduction. *U.S. Geol. Surv. Bull.* 1973, A1-11.
- Volkman, J.K. (1986) A review of sterol markers for marine and terrigenous organic matter. *Org. Geochem.* 9, 83-99.
- Volkman, S.K., Banks, M.R., Denwer, K., Aquino Neto, F.R. (1989) Biomarker composition and depositional setting of Tasmanite rich oil-shale from northern Tasmania, Australia. 14th Internat. Mtg. on Org. Geochem., Paris, Sept. 18-22, 1989, Abstract No. 168.
- Wakeham, S.G. (1990) Algal and bacterial hydrocarbons in particulate matter and interfacial sediments of the Cariaco Trench. *Geochim. Cosmochim. Acta* 54, 1325-1336.
- Wang, H.D., Philp, R.P. (1997) Geochemical study of potential source rocks and crude oils in the Anadarko Basin, Oklahoma. *Am. Assoc. Petrol. Geol. Bull.* 81, 249-275.
- Waples, D.W., Machihara, T. (1990) Application of sterane and triterpane biomarkers in petroleum exploration. *Bull. Canad. Petrol. Geol.* 38, 357-380

- Warren, J.K. (1986) Shallow-water evaporitic environments and their source rock potential. *Journ. Sed. Petrol.* 56, 442-454.
- West, N., Alexander, R., Kagi, R.I. (1990) The use of silicalite for rapid of branched and cyclic alkane fractions of petroleum. *Org. Geochem.* 15, 499-501.
- Weston, R.J., Philp, R.P., Sheppard, C.M., Woolhouse, A.D. (1989) Sesquiterpanes, diterpanes and other higher terpanes in oils from the Taranaki Basin of New Zealand. *Org. Geochem.* 14, 405-421.
- Wiggins, W.D., Harris, P.M. (1994) Lithofacies , depositional cycles, and stratigraphy of the lower Green River Formation, southwestern Uinta Basin, Utah. In A.J. Lomando, C.B., Schreiber, P.M., Harris, eds., *Lacustrine Reservoirs and Depositional Systems*, Soc. Econ. Paleont. Mineral. Core Workshop No. 19, pp.105-141.
- Wing, S.L., Bown, T.M., Obradovich, J.D. (1991) Early Eocene biotic and climatic change in interior western United States. *Geol.* 19, 1189-1192
- Wingert, W.S., Pomerantz, M. (1986) Structure and significance of some 21 and 22 carbon petroleum steranes. *Geochim. Cosmochim. Acta* 50, 2763-2769.
- Wolff, G.A., Lamb, N.A., Maxwell, J.R. (1985) The origin and fate of 4-methyl steroid hydrocarbons. I Diagenesis of 4-methyl steranes. *Geochim. Cosmochim. Acta* 50, 335-342.
- Wolfbauer, C.A., Surdam, R.C. (1974) Origin of nonmarine dolomite in Eocene Lake Gosiute, Green River Basin, Wyoming. *Geol. Soc. Am. Bull.* 85, 1733-1740.

## APPENDIX 1.1

### Abbreviations and formulas used in the text and appendices.

EOM	Extractable organic matter
%ASHP	% Asphaltenes after deasphalting
%Malt.	% Maltenes after deasphalting
%SAT	% Saturated fraction in maltenes
%ARO	% Aromatic fraction in maltenes
%POL	% Polar fraction in maltenes
%bran.	% Branched and cyclic compounds after molecular sieving
Pr/Ph	Pristane/phytane ratio (2,6,10,14 tetramethylpentadecane/ 2,6,10,14tetramethylhexadecane)
Pr/n-C <sub>17</sub>	Pristane/n-C <sub>17</sub> ratio
Ph/n-C <sub>18</sub>	Phytane/n-C <sub>18</sub> ratio
Pr+n-C <sub>17</sub> /Ph-nC <sub>18</sub>	Pristane+n-C <sub>17</sub> /phytane+n-C <sub>18</sub> ratio
C <sub>21+22</sub> /C <sub>28+29</sub>	Ratio of n-C <sub>21</sub> +n-C <sub>22</sub> /n-C <sub>28</sub> +n-C <sub>29</sub> ratio
C <sub>21</sub> /C <sub>22+</sub>	Ratio of n-alkanes with carbon numbers ≤ 21 vs. n-alkanes ≥ 22 (range n-C <sub>15</sub> to n-C <sub>35</sub> )
R22	(2*n-C <sub>22</sub> )/(n-C <sub>21</sub> +n-C <sub>23</sub> ) ten Haven et al. (1987)
CPI	Carbon preference index after Marzi et al. (1993)
	$\frac{n\text{-}C_{23}+n\text{-}C_{25}+n\text{-}C_{27})+(n\text{-}C_{25}+n\text{-}C_{27}+n\text{-}C_{29})}{2 * (n\text{-}C_{24}+n\text{-}C_{26}+n\text{-}C_{28})}$
22S/(22S+R) C <sub>31</sub> hopanes	Ratio of 17α(H),21β(H),22S and 22R bishomohopanes
Ts/Ts+Tm	Ratio of 18α(H)-22,29,30-normeohopane (Ts)/17α(H)- 22,29,30-norhopane (Tm)
Diahopane-index	Ratio of C <sub>30</sub> -diahopane/17α(H),21β(H)-30-norhopane
Oleanane-index	Ratio of 18α(H)-Oleanane/17α(H),21β(H)-hopane
C <sub>30</sub> Moretane/ Moretane+hopane	Ratio of 17β(H),21α(H)-moretane and 17α(H),21β(H)- hopane
Tricyclic/pentacyclic	Ratio of sum of tricyclic and pentacyclic terpane peaks detected in m/z191 chromatogram
Gammacerane-index	Ratio of gammacerane/17α(H),21β(H)-hopane
C <sub>29</sub> /C <sub>30</sub> -Hopane	Ratio of 17α(H),21β(H)-30-norhopane/17α(H),21β(H)- hopane
C <sub>23</sub> tricyclic/C <sub>30</sub> hopane	Ratio of C <sub>23</sub> tricyclic terpane/17α(H),21β(H)-hopane

$C_{34}S/C_{31}S$ $\alpha\beta$ hopane	Ratio of $17\alpha(H),21\beta(H)$ -tetrakishomohopane 20Sand $17\alpha(H),21\beta(H)$ -homohopane 20S
Unknown terpane/ $C_{29}$ $17\alpha$ hopane	Ratio of unknown terpane 3 at scan number 1935/ $17\alpha(H),21\beta(H)$ -30-norhopane
Sesquit./sesquit.+diterpane	Ratio of sum of sesquiterpanes and diterpanes detected in m/z 123 chromatograms
Sesquit./sesquit.+pentac.terpanes	Ratio of sum of sesquiterpanes and diterpanes and pentacyclic terpanes detected in m/z 123 and m/z 191 chromatograms
Sesquit./sesquiter.+steranes	Ratio of sum of sesquiterpanes and diterpanes and pregnanes, steranes and diasteranes detected in m/z 123 and m/z 217 chromatograms
Diterpanes/ diterpanes+pentacycl. terpanes	Ratio of sum of sesquiterpanes and diterpanes and pentacyclic terpanes detected in m/z 123 and m/z 191 chromatograms
Diterpanes/diterpanes+steranes	Ratio of sum of sesquiterpanes and diterpanes and pregnanes, steranes and diasteranes detected in m/z 123 and m/z 217 chromatograms
$20S/20S+R\ \alpha\alpha C_{29}$	Ratio of $14\alpha(H),17\alpha(H),20S$ and $20R$ desmethyl-ethyl-cholestanes
$\beta\beta/\beta\beta+\alpha\alpha\ C_{29}$	Ratio of $14\beta(H),17\beta(H),20S+20R/14\alpha(H),17\alpha(H),20S+20R$ desmethyl-ethyl-cholestanes
Steranes/terpanes	Ratio of sum of peaks of steranes/terpanes
Pregnanes/steranes	Ratio of pregnanes and $C_{27}\text{-}C_{29}$ -steranes+diasteranes detected in m/z 217 chromatograms
Methyl-steranes $4\alpha(Me)$ -steranes $3\beta(Me)$ steranes methyl hopanes	Qualitative indicator for the presence of $3\beta$ -methyl steranes and $4\alpha$ -methyl steranes; $3\beta$ -methyl steranes (relative abundance in m/z 217); methyl hopanes in m/z 191 - not present, + present, ++ abundant, +++ very abundant
% Sesquiterpanes, % diterpanes, %tricyclic terpanes, %pentacyclic terpanes, %steranes+diasteranes, %diginane+homodiginane	Relative abundance of biomarker group to the sum of detected peaks in m/z 191, 217 and 123 chromatograms
% $C_{27}$ , % $C_{28}$ , % $C_{29}$	Relative abundances of $14\alpha(H),17\alpha(H),20R$ -cholestane, methyl- and ethyl-cholestanes

T <sub>max</sub>	Temperature of maximum hydrocarbon generation (S2) during Rock-Eval pyrolysis °C
PI	Production index (S1/S1+S2)
TOC	% Total organic carbon
HI	Hydrocarbon index
OI	Oxygen index
Maximum carbon number in GC	Qualitative indication of the highest molecular weight compound discernable in high temperature gas chromatograms
Maximum peak in GC	Qualitative indication of the most intense peak in high temperature gas chromatograms
modal	Modality in high temperature gas chromatograms
n.a.	not available
n.d.	not detected
MID	Multiple ion detection
DTD	Drilled total depth
KB	Kelly bushing
GR/GL	Ground level
ML	Map level (elevation read from topographic map 1:10.000)
DF	Derrick floor
s.l.	Sea level
API	Crude oil gravity °API
STP	Standard temperature and pressure

## APPENDIX 1.2

Peakno.	Compound	Peak no.	Compound
	<b>Tricyclic terpanes</b>		<b>Diterpanes</b>
1	Tricyclic terpane C <sub>19</sub>	51	C17-tricyclane
2	Tricyclic terpane C <sub>20</sub>	52	C18-tricyclane
3	Tricyclic terpane C <sub>21</sub>	53	unknown diterpane
4	Tricyclic terpane C <sub>22</sub>	54	4 $\beta$ (H)-19-norisopimarane
5	Tricyclic terpane C <sub>23</sub>	55	C17 tricyclane
6	Tricyclic terpane C <sub>24</sub>	56	C19 tricyclane
7	Tricyclic terpane C <sub>25</sub>	57	17-nortetracyclic diterpane
8	Tricyclic terpane C <sub>26</sub> 22S	58	isopimarane
9	Tricyclic terpane C <sub>26</sub> 22R	59	16 $\beta$ (H)-phylocladane
10	Tricyclic terpane C <sub>27</sub> 22S		<b>Short-chain steranes</b>
11	Tricyclic terpane C <sub>27</sub> 22R	60	5 $\alpha$ (H),14 $\beta$ (H),17 $\beta$ (H)-diginane
12	Tricyclic terpane C <sub>28</sub> 22S	61	5 $\alpha$ (H),14 $\beta$ (H),17 $\beta$ (H)-homodiginane
13	Tricyclic terpane C <sub>28</sub> 22R		<b>Steranes, diasteranes</b>
14	Tricyclic terpane C <sub>29</sub> 22S	62	13 $\beta$ (H),17 $\alpha$ (H),20S-diacholestanate
15	Tricyclic terpane C <sub>29</sub> 22R	63	13 $\beta$ (H),17 $\alpha$ (H),20R-diacholestanate
18	Tricyclic terpane C <sub>30</sub> 22S	64	13 $\alpha$ (H),17 $\beta$ (H),20S-diacholestanate
20	Tricyclic terpane C <sub>30</sub> 22R	65	13 $\alpha$ (H),17 $\beta$ (H),20R-diacholestanate
23	Tricyclic terpane C <sub>31</sub> 22S	66	24-methyl-13 $\beta$ (H),17 $\alpha$ (H),20S-diacholestanate
24	Tricyclic terpane C <sub>31</sub> 22R	67	24-methyl-13 $\beta$ (H),17 $\alpha$ (H),20R-diacholestanate
	<b>Pentacyclic terpanes</b>	68	24-methyl-13 $\alpha$ (H),17 $\beta$ (H),20S-diacholestanate + 14 $\alpha$ (H),17 $\alpha$ (H),20S-cholestane
16	18 $\alpha$ (H)-22,29,30-nomechopane (Ts)		
17	1. unknown terpane	69	24-ethyl-13 $\alpha$ (H),17 $\beta$ (H),20S-diacholestanate + 14 $\beta$ (H),17 $\beta$ (H),20R-cholestane
19	17 $\alpha$ (H)-22,29,30-irisnorhopane (Tm)		
21	17 $\beta$ (H)-22,29,30-irisnormoretane	70	24-methyl-13 $\alpha$ (H),17 $\beta$ (H),20R-diacholestanate + 14 $\beta$ (H),17 $\beta$ (H),20S-cholestane
22	2. unknown terpane		
25	17 $\alpha$ (H),21 $\beta$ (H)-30-norhopane	71	14 $\alpha$ (H),17 $\alpha$ (H),20R-cholestane
26	C <sub>30</sub> diahopane	72	24-ethyl-13 $\beta$ (H),17 $\alpha$ (H),20R-diacholestanate
27	3. unknown terpane	73	24-ethyl-13 $\beta$ (H),17 $\alpha$ (H),20S-diacholestanate
28	17 $\beta$ (H),21 $\alpha$ (H)-30-normoretane	74	24-methyl-14 $\alpha$ (H),17 $\alpha$ (H),20S-cholestane
29	18 $\alpha$ (H)-oleanane	75	24-ethyl-13 $\alpha$ (H),17 $\beta$ (H),20R-diacholestanate + 24-methyl-14 $\beta$ (H),17 $\beta$ (H),20R-cholestane
30	17 $\alpha$ (H),21 $\beta$ (H)-hopane		
31	17 $\beta$ (H),21 $\alpha$ (H)-morethane	76	24-methyl-14 $\beta$ (H),17 $\beta$ (H),20S-cholestane
32	17 $\alpha$ (H),21 $\beta$ (H),22S-30-homohopane	77	24-methyl-14 $\alpha$ (H),17 $\alpha$ (H),20R-cholestane
33	17 $\alpha$ (H),21 $\beta$ (H),22R-30-homohopane	78	24-ethyl-14 $\alpha$ (H),17 $\alpha$ (H),20S-cholestane
34	gammacerane	79	24-ethyl-14 $\beta$ (H),17 $\beta$ (H),20R-cholestane
35	17 $\alpha$ (H),21 $\beta$ (H),22S-30,31-bishomohopane	80	24-ethyl-14 $\beta$ (H),17 $\beta$ (H),20S-cholestane
36	17 $\alpha$ (H),21 $\beta$ (H),22R-30,31-bishomohopane	81	24-ethyl-14 $\alpha$ (H),17 $\alpha$ (H),20R-cholestane
37	17 $\alpha$ (H),21 $\beta$ (H),22S-30,31,32-trishomohopane		<b>Monoaromatic sterane</b>
38	17 $\alpha$ (H),21 $\beta$ (H),22R-30,31,32-trishomohopane	82	monoaromatic sterane C <sub>27</sub>
39	17 $\alpha$ (H),21 $\beta$ (H),22S-tetrakishomohopane	83	monoaromatic sterane C <sub>27</sub>
40	17 $\alpha$ (H),21 $\beta$ (H),22R-tetrakishomohopane	84	monoaromatic sterane C <sub>27</sub>
41	17 $\alpha$ (H),21 $\beta$ (H),22S-pentakishomohopane	85	monoaromatic sterane C <sub>27</sub>
42	17 $\alpha$ (H),21 $\beta$ (H),22R-pentakishomohopane	86	monoaromatic sterane C <sub>27</sub> +C <sub>28</sub>
	<b>Sesquiterpanes</b>	87	monoaromatic sterane C <sub>27</sub> +C <sub>28</sub>
43	C15-bicyclane	88	monoaromatic sterane C <sub>27</sub> +C <sub>28</sub>
44	C15-bicyclane	89	monoaromatic sterane C <sub>27</sub> +C <sub>28</sub>
45	8 $\beta$ (H)-drimane	90	monoaromatic sterane C <sub>27</sub> +C <sub>28</sub>
46	C15-bicyclane	91	monoaromatic sterane C <sub>27</sub> +C <sub>28</sub>
47	C15-bicyclane	92	monoaromatic sterane C <sub>28</sub> +C <sub>29</sub>
48	C16-bicyclane	93	monoaromatic sterane C <sub>28</sub> +C <sub>29</sub>
49	8 $\beta$ (H)-homodrimane	94	monoaromatic sterane C <sub>28</sub> +C <sub>29</sub>
50	C17-bicyclane	95	monoaromatic sterane C <sub>29</sub>
		96	monoaromatic sterane C <sub>29</sub>

## APPENDIX 2

### Core Well Data

No.	Lib. no.	Operator	Well Name	core depths [ft]		location	API
				Min	Max		
1	D304	Chevron Oil Co.	1 Chasel Unit Flying	10630 11001	10827 11222	SE NW NE 18 1S 1W	43 13 30030
2	R693	Chevron Oil Co.	1-33-3 Blanchard	8924 9023 9112 9366 10310 10965	9020 9085 9174 9485 10540 11053	NW SE 3 1S 2W	43 13 20316
3	D400	Bow Valley Exploration	2-19 A1E Dr Long	9213 9628	9216 9720	SW SE 19 1S 1E	43 47 31470
4	A690	PanAm Petroleum	1 USA Lyle Lingelbach	6910 6988 7600	6937 7040 7616	NW SE SE 29 6S 21E	43 47 10869
5	A690	PanAm Petroleum	1 McIish Unit	6110	6160	SW SE 34 6S 22E	43 47 10870
6	A689	PanAm Petroleum	3 Unit/Pelicane Lake Unit	5777	5799	NW SE 34 7S 21E	43 47 10876
7	A679	PanAm Petroleum	4 USA Pearl Broadhurst	4661 5269	4764 5417	SW SE 9 7S 23E	43 47 15694
8	B592	Gulf Oil Co.	1-20-4B Costas	5215 5242	5237 5262	NE SW 20 8S 21E	43 47 31006
9	D257	Natural Gas Co.	22-30 Bench Glen	4700	4730	NW SE NW 30 8S 22E	43 47 31260
10	C703	Diamond Shamrock	24-8 Pariette Federal	4724 5434	4739 5478	SE SE SW 8 9S 17E	43 13 30675
11	E202	Natural Gas Co.	13-16 State	4238 5350	4328 5385	NE NW SW 16 9S 19E	43 47 31128
12	D172	Mapco Inc.	4-11 D River Bend Unit	4783	4821	SE NW NW 11 10S 18E	43 47 30718
13	A687	Davis Oil Co.	5 Pariette Bench Unit	5407 5435 5450	5423 5445 5457	SE SE 9 9S 18E	43 47 10298
14	S050	Coors Energy	3-10D Ute Tribal	6205	6280	10 4S 4W	
15	D209	Rio Bravo Oil Co.	20-2 RU	9678	9696	SE SE SW 17 1S 1E	43 47 31422
16	E109	Chevron Oil Co.	(2-8C) Lamiq Urruty 1-8-A2	10824 10846	10845 10964	NW SW 8 1S 2W	43 13 30036
17	D273	Natural Gas Co.	23-24 Federal	4859 4902	4899 4978	NE SW 24 8S 21E	43 47 31253
18	1823	California Oil Co.	Red Wash 32	3800 5259 7753 8873 9252 9989 10183	4553 5599 7795 9249 9986 10259 10802	SW SW NE 22 7S 22E	43 47 15159
19	1373	Sun Oil Co.	South Ouray No 1/Unit 1	3228 3540	3535 5346	NE NE 22 9S 20E	43 47 11162
20	n.a.	Celsius Energy Co. /Wexpro Co	Island Unit 16	4690 4746	4738 4815	NW NE SW 11 10S 18E	43 47 31505

No.	Lib. no.	Operator	Well Name	core depths (ft)		location	
				Min	Max	1/4 Sec.-Sec.-Twn-Rng	API
21	1891	Carter Oil	Joseph Smith 1	8551	8560	16 3S 5W	43 13 10491
22	92	Mountain Fuel Supply	Cedar Rim 3	7890	7910	SW NE 19 3S 6W	43 13 30040
				8166	8186		
				8220	8240		
				8487	8508		
23	206	Diamond Shamrock Co.	Allen 34-5	4995	5044	NW SW SE 5 9S 17E	43 13 30721
24	2723	Quinex Energy Co.	Leslie Taylor 24-5	12180	12193	24 1S 1W	43 47 31828
				12195	12238		
25	n.a.	Bow Valley Petroleum Inc.	Ute 2-22A1E	12297	12407	NE SW NE 22 1S 1E	43 47 31265
26	2272	Page Petroleum Inc.	Page Esson Ute 1-14B1E	8446	8518	SE NW NE 14 2S 1E	43 47 30774
27		Chevron Oil Co.	Hiko Bell Unit 1/ 1 Walker	10480	10627	NE SW NE 12 1S 2W	43 13 30031
28		Gulf Oil Co.	1 Whitlock/1 Lynn Whitlock	5969	9179	10 1S 1E	43 47 05727
29		outcrop	Indian Canyon - mahogany zone			NE NE 2 7S 8W	
30		outcrop	Gate Canyon - mahogany zone			NW SE 17 11S 15E	
31		outcrop	Indian Canyon - black shale facies			NE NW 26 11S 10E	
32		outcrop	Indian Canyon - black shale facies coal			NW SW 26 11S 10E	
33		outcrop	Raven Ridge - lower Green River coal			SW SW 12 2N 04W	

datum 1: lower Green River Formation log marker after

Peterson (1973); map-group 1

datum 2: middle marker after Morgan and Tripp (1994);

map-group 1

datum 3: Top Douglas Creek Member (K-marker) after Castle

(1990) and Kelly and Castle (1990), map-group 2 and

Kelly and Castle (1990), map-group 2

datum 4: 3pt. marker (green shale facies) after Coburn et al.

(1985), map-group 3

## APPENDIX 2

### Core Well Data

No.	Lib. no.	Operator	Well Name	core depths [ft]		dates		samples	No.
				Min	Max	spud	completion		
1	D304	Chevron Oil Co.	1 Chasel Unit Flv. 1g	10630 11001	10827 11222	11/27/70	12/13/70	10727	1E
2	R693	Chevron Oil Co.	1-33-3 Blanchard	8924	9020	10/22/67	3/31/68	8954	2E
				9023	9085			8992	3E
				9112	9174			9056.2	4E
				9366	9485			9393.5	47E
				10310 10965	10540 11053				
3	D400	Bow Valley Exploration	2-19 A1E Dr Long	9213	9216	5/5/84	7/2/84	9716.5	5E
				9628	9720				
4	A690	PanAm Petroleum	1 USA Lyle Lingelbach	6910	6937	10/5/63	2/8/64	6925	6E
				6988	7040				
				7600	7616				
5	A690	PanAm Petroleum	1 McIish Unit	6110	6160	2/12/64	3/13/64	6111	7E
6	A689	PanAm Petroleum	3 Unit/Pelican Lake Unit	5777	5799	5/30/64	6/26/64	5789	8E
7	A679	PanAm Petroleum	4 USA Pearl Broadhurst	4661	4764	3/30/64	7/7/64	4687	9E
				5269	5417				
8	B592	Gulf Oil Co.	1-20-4B Costas	5215	5237	7/3/81	9/26/81	5224.5	10E
				5242	5262				
9	D257	Natural Gas Co.	22-30 Bench Glen	4700	4730	11/1/82	12/18/82	4702 4703	11E
10	C703	Diamond Shamrock	24-8 Pariette Federal	4724	4739	8/18/83	7/4/83	5450 5452	21E
				5434	5478				
11	E202	Natural Gas Co.	13-16 State	4238	4328	1/16/82	4/30/82	5381 5382	12E
				5350	5385				
12	D172	Mapco Inc.	4-11 D River Bend Unit	4783	4821	11/9/80	4/4/81	4786 4787	13E
13	A687	Davis Oil Co.	5 Pariette Bench Unit	5407	5423	2/29/64	5/5/64	5422 5422.5	14E
				5435	5445				
				5450	5457				
14	S050	Coors Energy	3-10D Ute Tribal	6205	6280			6272.8 6273.5	48E
15	D209	Rio Bravo Oil Co.	20-2 RU	9678	9696	12/30/83	6/1/84	9692 9693	16E
16	E109	Chevron Oil Co.	(2-8C) Lamiq Urrutty 1-8-A2	10824	10845			10844 10845	17E
				10846	10964	3/25/74	6/6/74	10950	18E
17	D273	Natural Gas Co.	23-24 Federal	4859	4899	10/23/82	11/12/82	4882.5 4978	19E
				4902	4978			4978.5	20E
18	1823	California Oil Co.	Red Wash 32	3800	4553	9/27/54	6/16/55	3950 9745	22E
				5259	5599			9751	23E
				7753	7795				
				8873	9249				
				9252	9986				
				9989	10259				
				10183	10802				
19	1373	Sun Oil Co.	South Ouray No.1/Unit 1	3228	3535	6/25/51	10/25/51	4938 4955	25E
				3540	5346			4955 5170	26E
				4746	4815			5173	27E
20	n.a.	Celsius Energy Co. Wexpro Co	Island Unit 16	4690	4738	7/28/84	2/7/85	4695.5 4696	29E

No.	Lib. no.	Operator	Well Name	core depths (ft)		dates		samples		No.
				Min	Max	spud	completion	depth ft from - to ft		
21	1891	Carter Oil	Joseph Smith 1	8551	8560	7/5/52	12/4/52	8551	8560	30E
22	92	Mountain Fuel Supply	Cedar Rim 3	7890	7910	6/3/70	11/10/70	8507		31E
				8166	8186					
				8220	8240					
				8487	8508					
23	206	Diamond Shamrock Co.	Allen 34-5	4995	5044	9/11/83	11/28/83	5021.5		32E
24	2723	Quinex Energy Co.	Leslie Taylor 24-5	12180	12193	5/3/88		12224		33E
				12195	12238					
25	n.a.	Bow Valley Petroleum Inc.	Ute 2-22A1E	12297	12407	9/24/82	1/16/83	12315.5		34E
								12366.5		46E
26	2272	Page Petroleum Inc.	Page Esson Ute 1-14B1E	8446	8518	10/7/80	10/26/81	8463		35E
27		Chevron Oil Co.	Hiko Bell Unit 1/1 Walker	10480	10627	1/18/70	5/7/70	10587.4		36E
28		Gulf Oil Co.	1 Whitlock/1 Lynn Whitlock	5969	9179	8/15/52		7583		37E
								9020		38E
29		outcrop	Indian Canyon - mahogany zone							39E
30		outcrop	Gate Canyon - mahogany zone							40E
31		outcrop	Indian Canyon - black shale facies							41E
32		outcrop	Indian Canyon - black shale facies coal							42E
33		outcrop	Raven Ridge - lower Green River coal							45E

datum 1: lower Green River Formation log marker after

Peterson (1973); map-group 1

datum 2: middle marker after Morgan and Tripp (1994);

map-group 1

datum 3: Top Douglas Creek Member (K-marker) after Castle

(1990) and Kelly and Castle (1990), map-group 2 and

Kelly and Castle (1990), map-group 2

datum 4: 3pt. marker (green shale facies) after Coburn et al

(1985), map-group 3

## APPENDIX 2

### Core Well Data

No.	Lib. no.	Operator	Well Name	core depths [ft]		DTD	KB	GR/GL	DF	datum	depth of datum to s.l. (ft)
				Min	Max						
1	D304	Chevron Oil Co.	1 Chasel Unit Flying	10630 11001	10827 11222	11376	5686	5672		1	-4471
2	R693	Chevron Oil Co.	1-33-3 Blanchard	8924 9023 9085 9112 9174 9366 9485 10310 10540 10965 11053	9020 9112 9174 9366 9485 10310 10540 10965 11053	11190	5863	5851		1	-4551
3	D400	Bow Valley Exploration	2-19 A1E Dr Long	9213 9628	9216 9720	10655		5430		2	-3354
4	A690	PanAm Petroleum	1 USA Lyle Lingelbach	6910 6988 7040 7600	6937 7040 7616	8102	4904	4892	4900	3	-2150
5	A690	PanAm Petroleum	1 McIish Unit	6110	6160	6600	5129	5117	5125	3	-850
6	A689	PanAm Petroleum	3 Unit/Pelican Lake Unit	5777	5799	6175		4773	4783	3	-750
7	A679	PanAm Petroleum	4 USA Pearl Broadhurst	4661 5269	4764 5417	5900	5192	5190	5180	3	-120
8	B592	Gulf Oil Co.	1-20-4B Costas	5215 5242	5237 5262	5425	4693	4679		3	-400
9	D257	Natural Gas Co.	22-30 Bench Glen	4700	4730	5501		4756	4769	3	100
10	C703	Diamond Shamrock	24-8 Pariette Federal	4724 5434	4739 5478	7475	4712	4705		4	1220
11	E202	Natural Gas Co.	13-16 State	4238 5350	4328 5385	7475	4712	4705		4	600
12	D172	Mapco Inc.	4-11 D River Bend Unit	4783	4821	4893	4980	4971	4979	4	1760
13	A687	Davis Oil Co.	5 Pariette Bench Unit	5407 5435 5450	5423 5445 5457	5998	4990	4978	4987	4	840
14	S050	Coors Energy	3-10D Ute Tribal	6205	6280		5741 map			n.a.	
15	D209	Rio Bravo Oil Co.	20-2 RU	9678	9696	10690	5522	5474		2	-3385
16	E109	Chevron Oil Co.	(2-8C) Lamiq Urruty 1-8-A2	10824 10846	10845 10964	15300		6153		1	-4675
17	D273	Natural Gas Co.	23-24 Federal	4859 4902	4899 4978	5864	4835	4819		3	10
18	1823	California Oil Co.	Red Wash 32	3800 5259 7753 8873 9252 9989 10183	4553 5599 7795 9249 9986 10259 10802	11288		5270		3	-420
19	1373	Sun Oil Co.	South Curray No.1/Unit 1	3228 3540	3535 5346	8457	4832	4820		n.a.	
20	n.a.	Celsius Energy Co. Wexpro Co	Island Unit 16	4690 4746	4738 4815	5000	5094	5079	5093	4	1780

No.	L.b. no.	Operator	Well Name	core depths (ft)		DTD	KB	GR/GL	DF	datum	depth of datum to s.l. (ft)
				Min	Max						
21	1891	Carter Oil	Joseph Smith 1	8551	8560	9103		5694		2	-3487
22	92	Mountain Fuel Supply	Cedar Rim 3	7890	7910	9738	6304	6286		n.a.	
				8166	8186						
				8220	8240						
				8487	8508						
23	206	Diamond Shamrock Co.	Allen 34-5	4995	5044	6067	5216	5205	5215	4	1000
24	2723	Quinex Energy Co.	Leslie Taylor 24-5	12180	12193	14016	5518	5497		2	-3487
				12195	12238						
25	n.a.	Bow Valley Petroleum Inc.	Ute 2-22A1E	12297	12407	13640		5354		2	-3204
26	2272	Page Petroleum Inc.	Page Esson Ute 1-14B1E	8446	8518	11843	5079	5068		n.a.	
27		Chevron Oil Co.	Hiko Bell Unit 1/1 Walker	10480	10627	11745	5925	5908	5917	1	-4478
28		Gulf Oil Co.	1 Whitlock/1 Lynn Whitlock	5969	9179	9660		5464		2	-3430
29		outcrop	Indian Canyon - mahogany zone								
30		outcrop	Gate Canyon - mahogany zone								
31		outcrop	Indian Canyon - black shale facies								
32		outcrop	Indian Canyon - black shale facies coal								
33		outcrop	Raven Ridge - lower Green River coal								

datum 1: lower Green River Formation log marker after

Peterson (1973); map-group 1

datum 2: middle marker after Morgan and Tripp (1994);

map-group 1

datum 3: Top Douglas Creek Member (K-marker) after Castle

(1990) and Kelly and Castle (1990), map-group 2 and

Kelly and Castle (1990), map-group 2

datum 4: 3pt. marker (green shale facies) after Coburn *et al.*

(1985), map-group 3

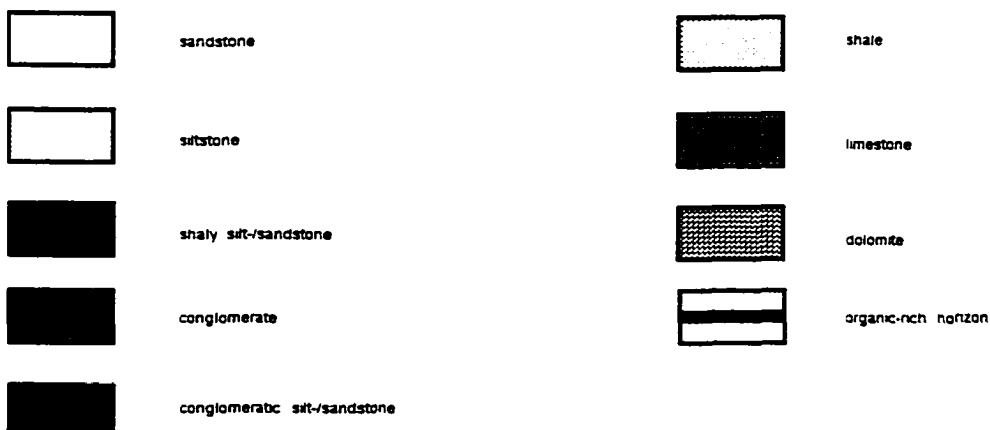
### **Appendix 3: Core description**

## LEGEND

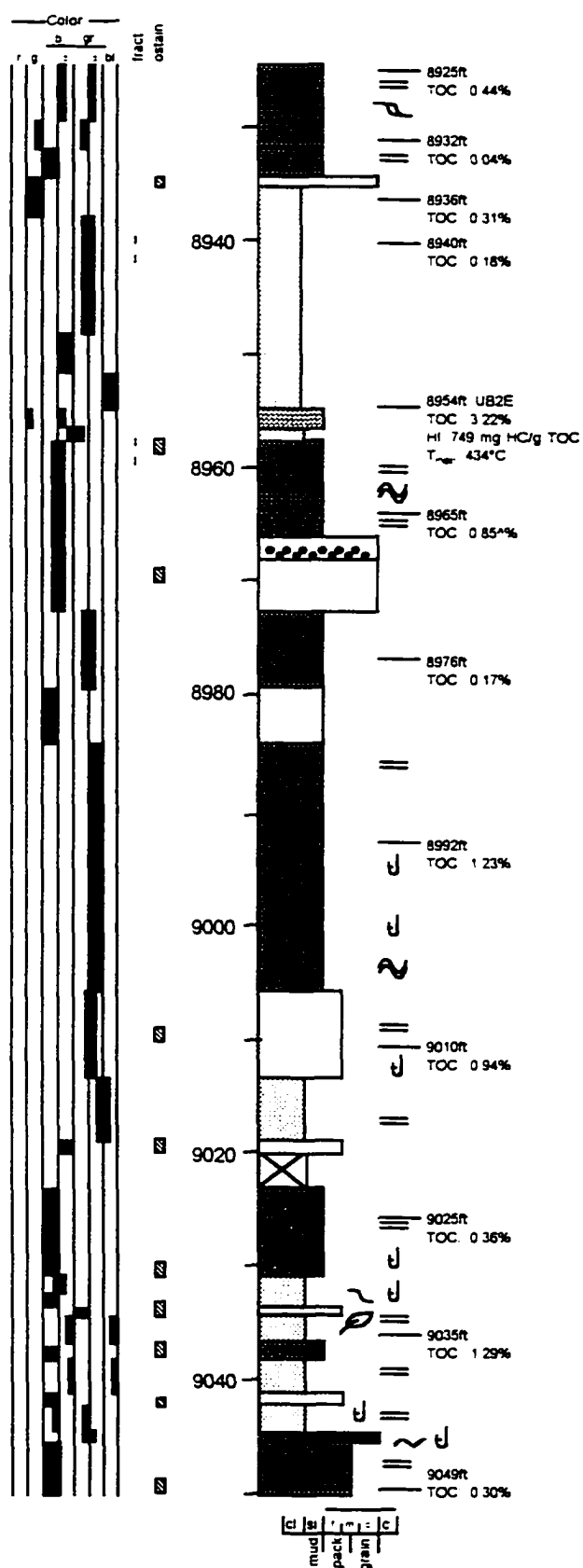
	pelecypod shells		mudcracks		
	abundant pelecypod shells		rough cross bedding		
	gastropods		synsedimentary faults		
	abundant gastropods		loop structures		
	shell hash		current ripples		
	ostracodes		horizontal lamination		
	ostracodes abundant		mud drapes/wavy bedding		
	algal filaments/algal boundstone		lenticular bedding		
	plant/organic debris		flaser bedding		
	bioturbation		synsedimentary deformation		
	ooids		syneresis/diastasis (?) cracks		
	peloids		gradation		
	nODULES		root structures		
	clasts		stylolites		
estimated grainsize					
sand		coarsening upward			
clastic	cl si ri mi cl				
carbonate	mud pack grain	fining upward			
mud=mudstone pack=wacke-/packstone grain=grainstone					
carbonate classification after Dunham (1962)					

color:  
r=red  
g=green  
b=brown l=light d=dark  
gr=grey l=light d=dark  
bl=black

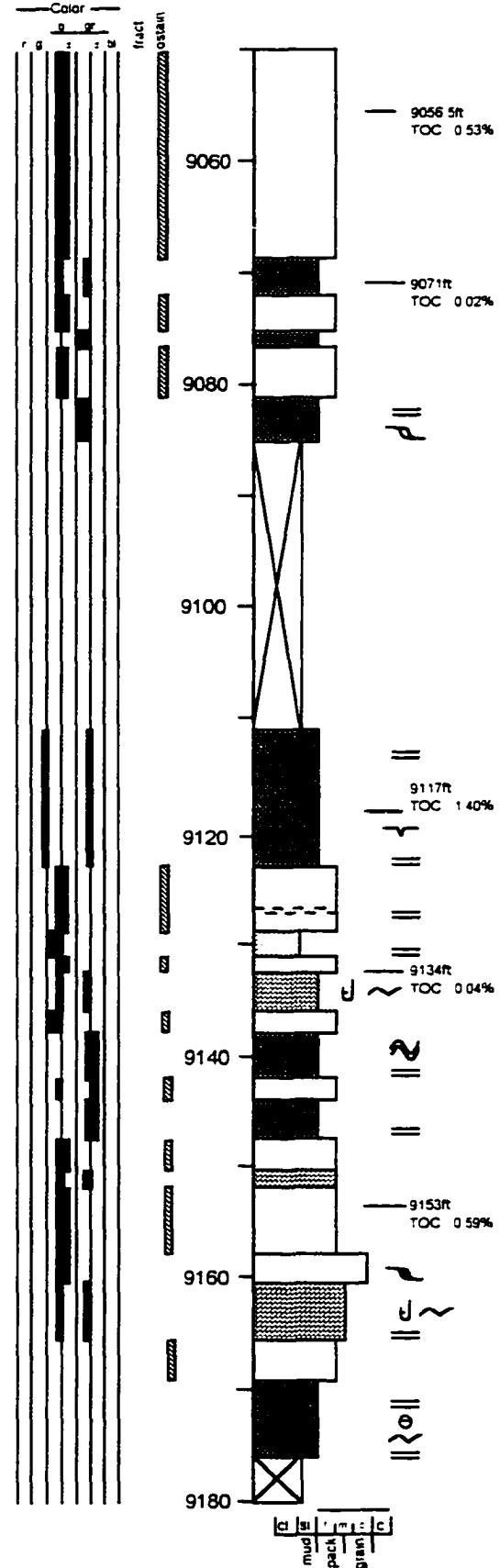
mud=mudstone  
pack=wacke-/packstone  
grain=grainstone  
carbonate classification after Dunham (1962)



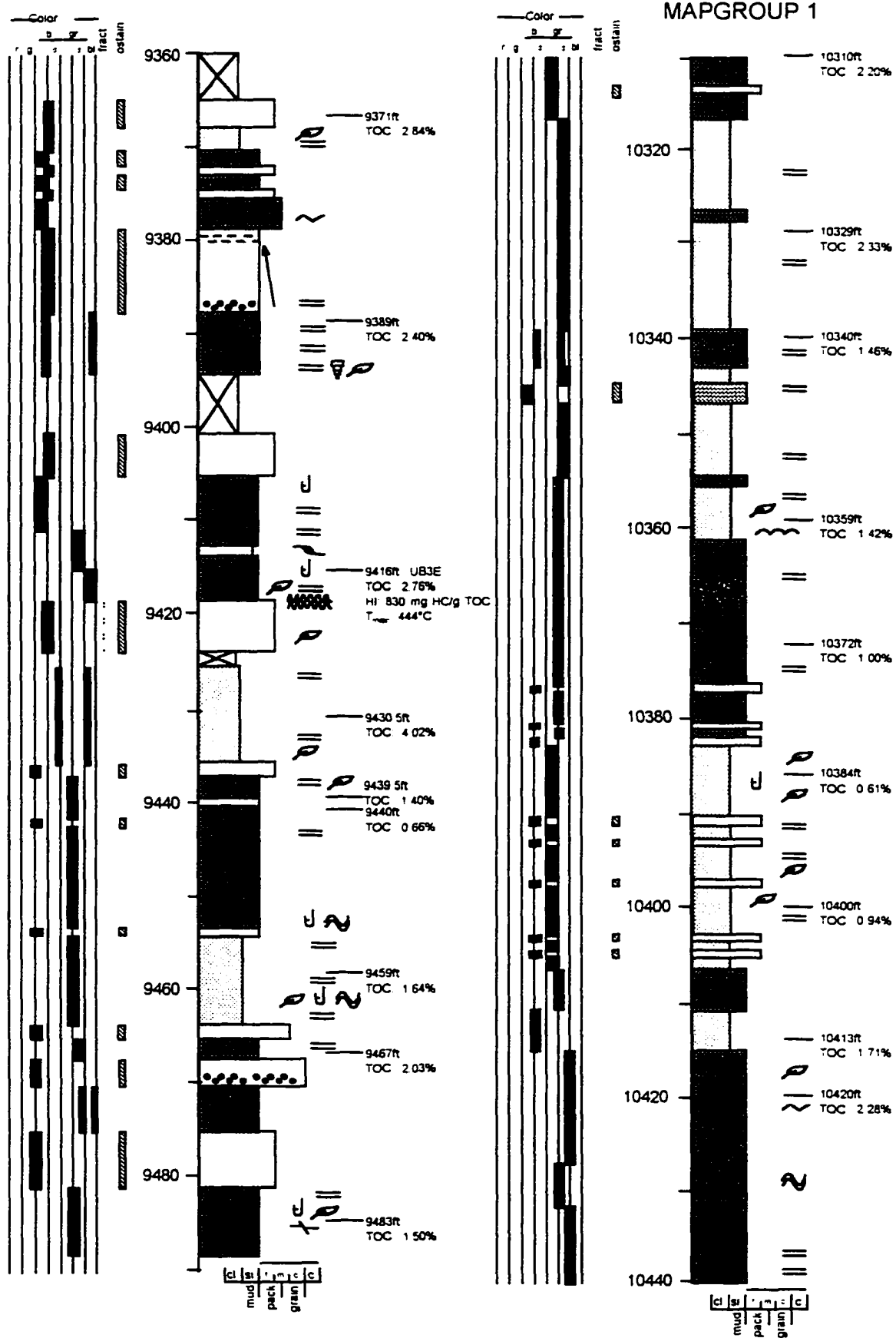
Chevron  
 Blanchard 1-33-3  
 NWSE 3-R2W-T1S  
 5863FT KB



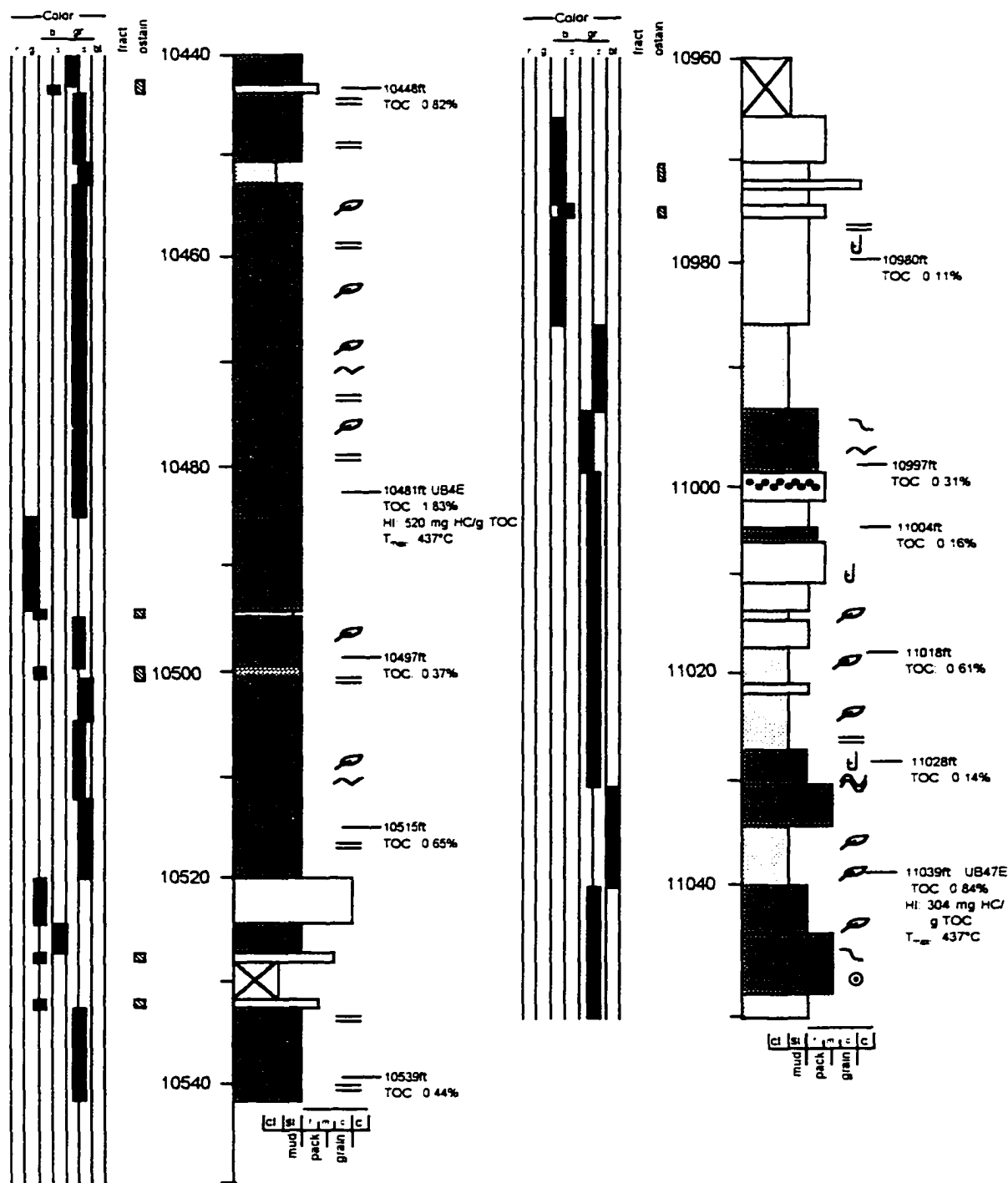
MAPGROUP 1



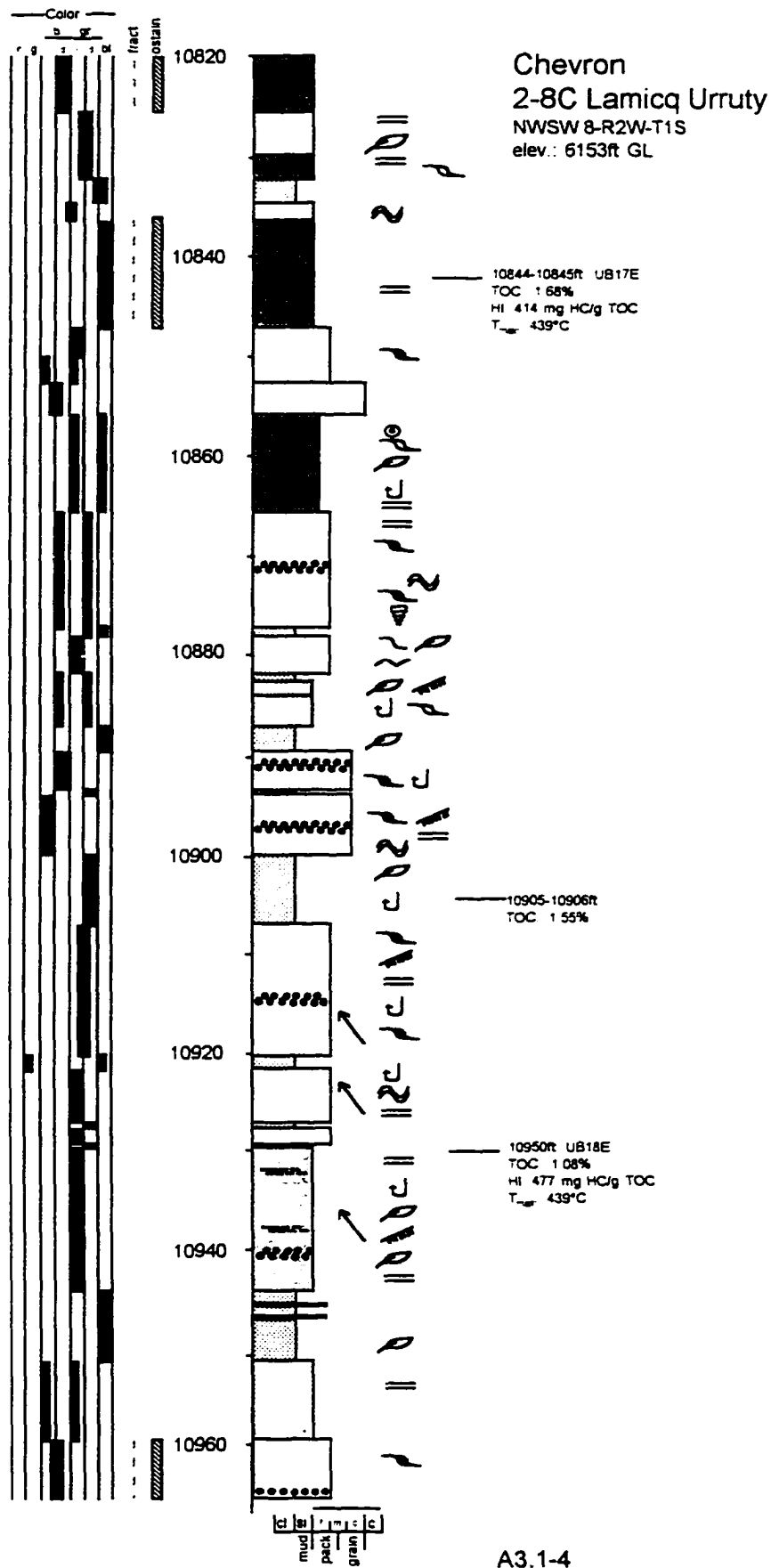
A3.1-1



# MAPGROUP 1

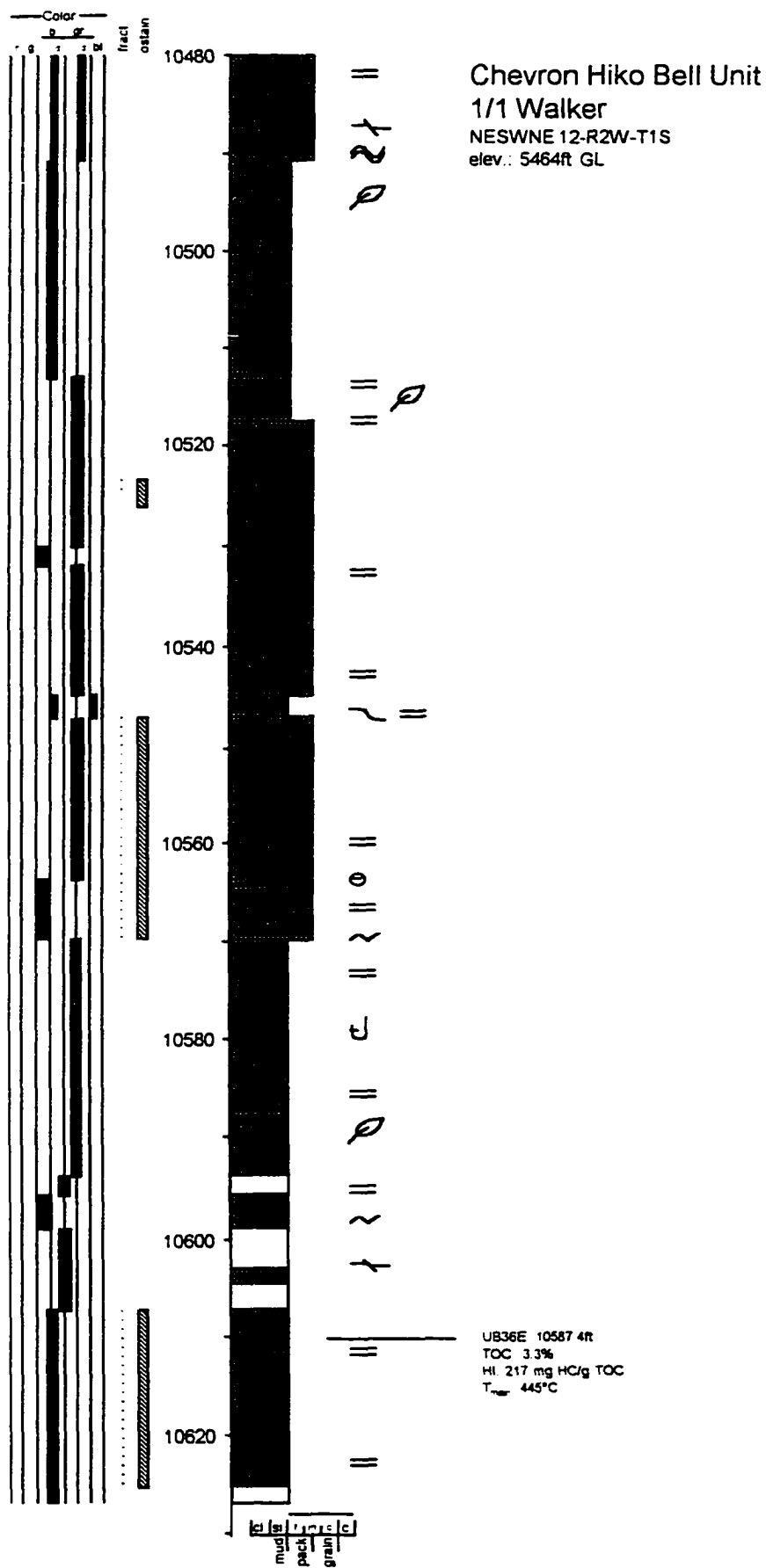


MAPGROUP 1

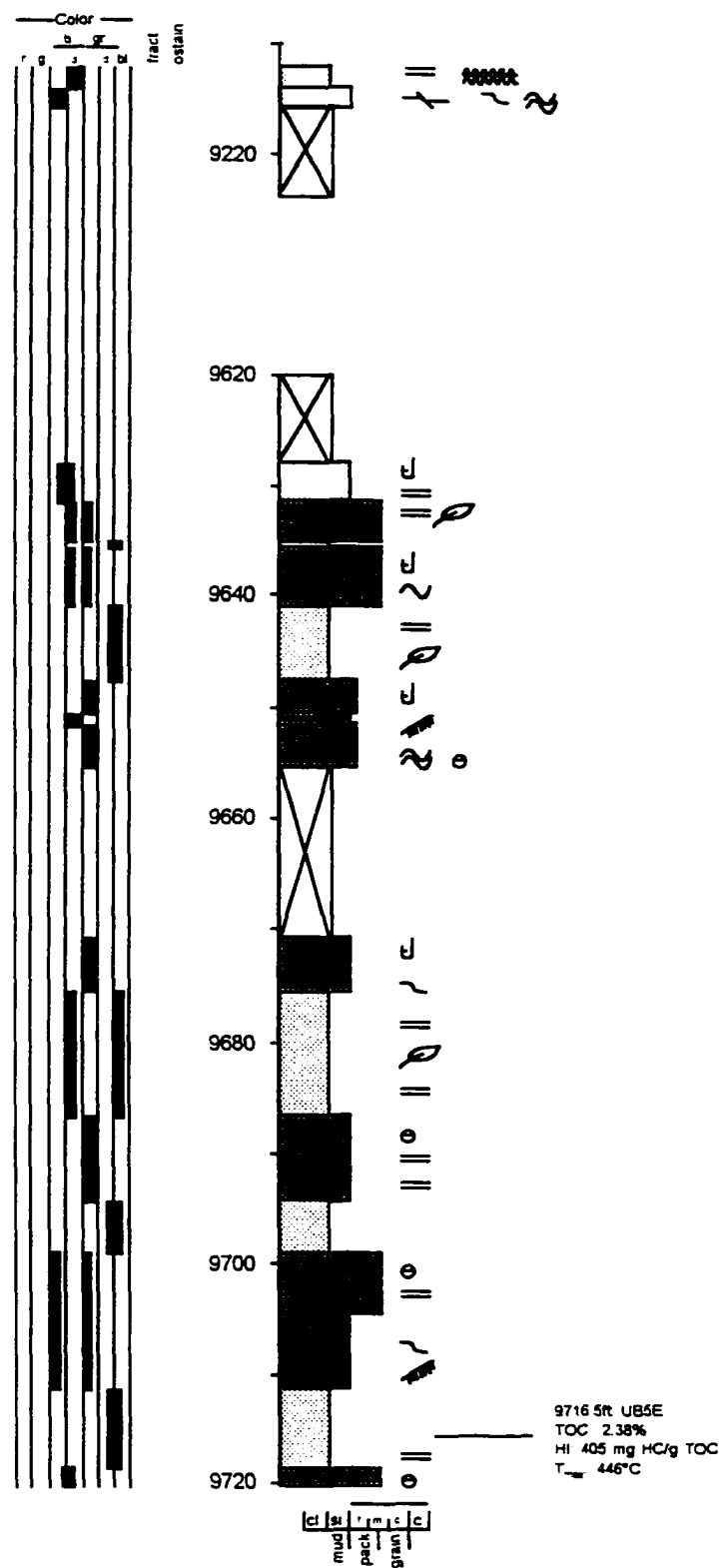


A3, 1-4

MAPGROUP 1

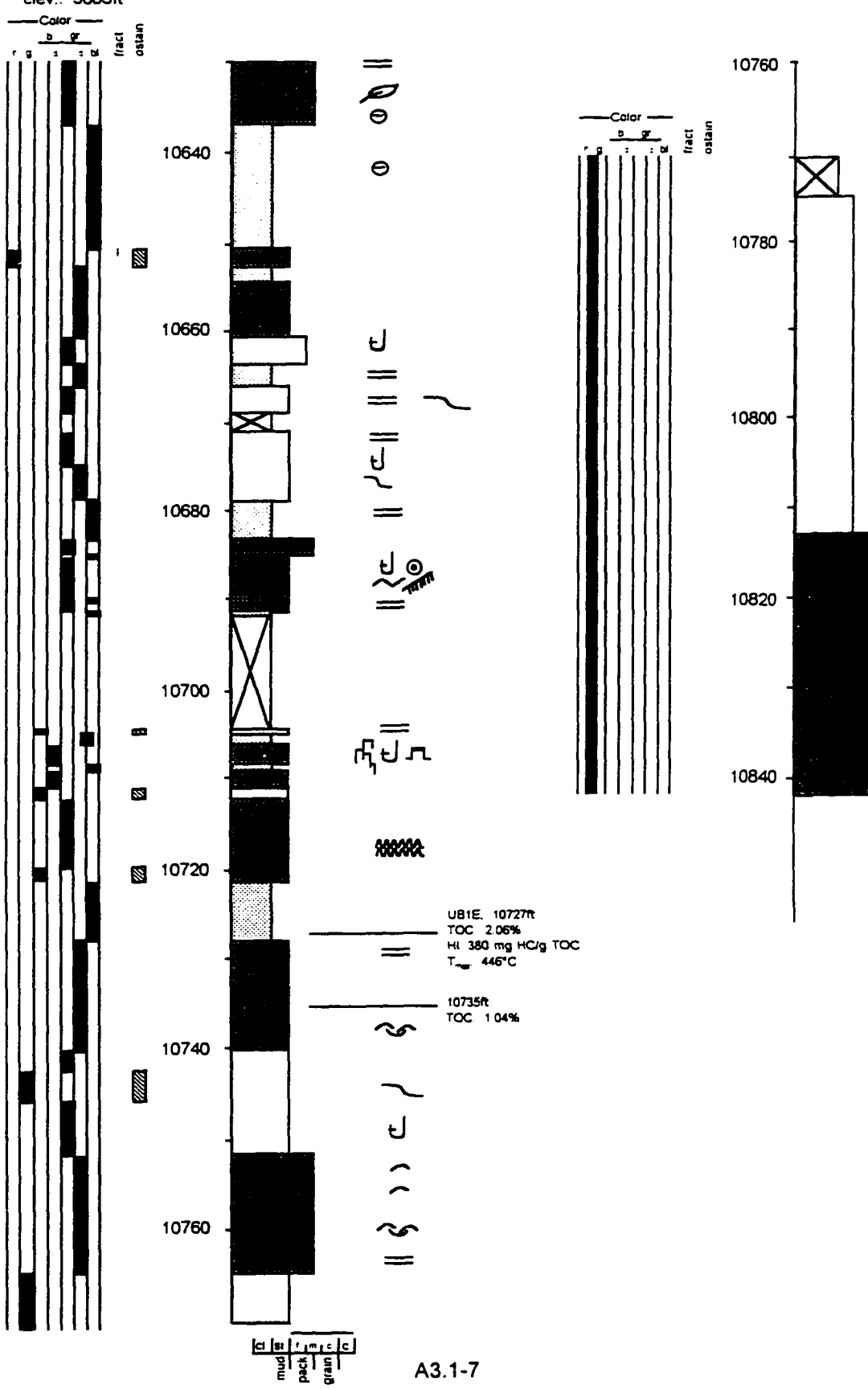


**Bow Valley Inc.  
2-19A1E Dr Long  
SWSE 19-R1E-T1S  
elev.: 5430ft GR**

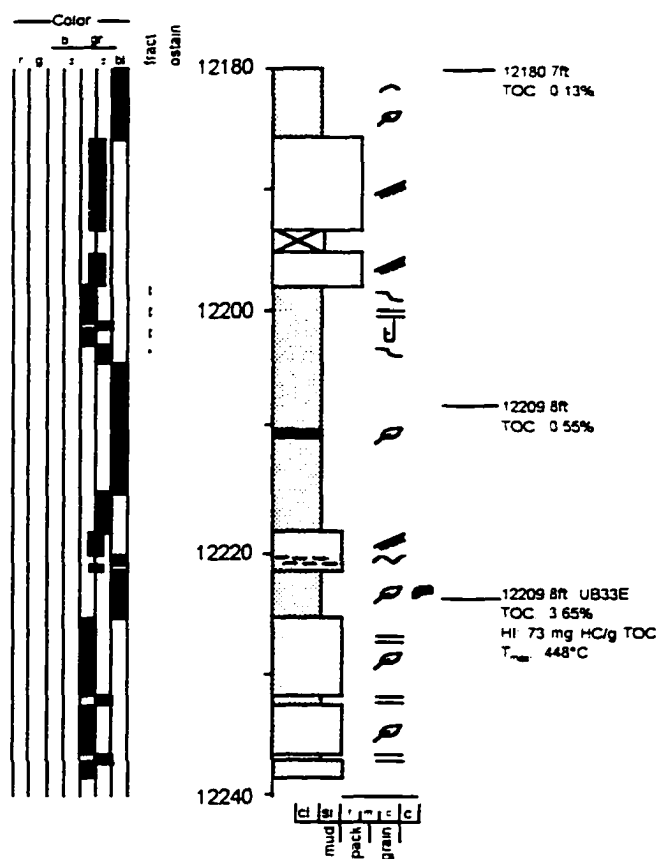


Chevron  
1 Chasel Unit  
SENWNE 18-R2W-T1S  
elev.: 5683ft

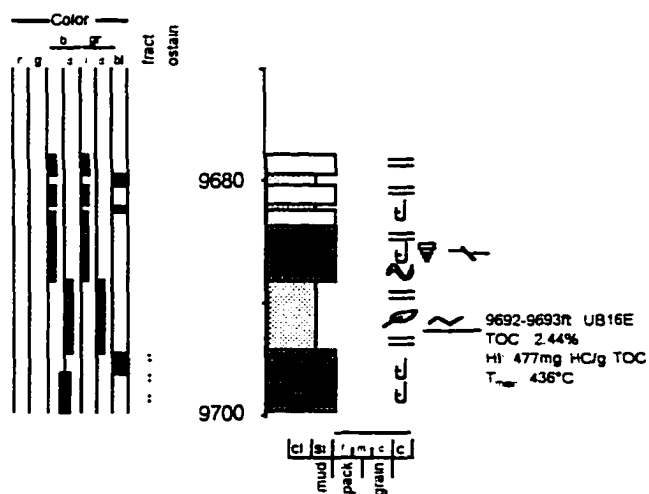
MAPGROUP 1



Quinex Energy Inc.  
 Leslie Taylor 24-5  
 24-R1W-T1S  
 elev.: 5518ft KB

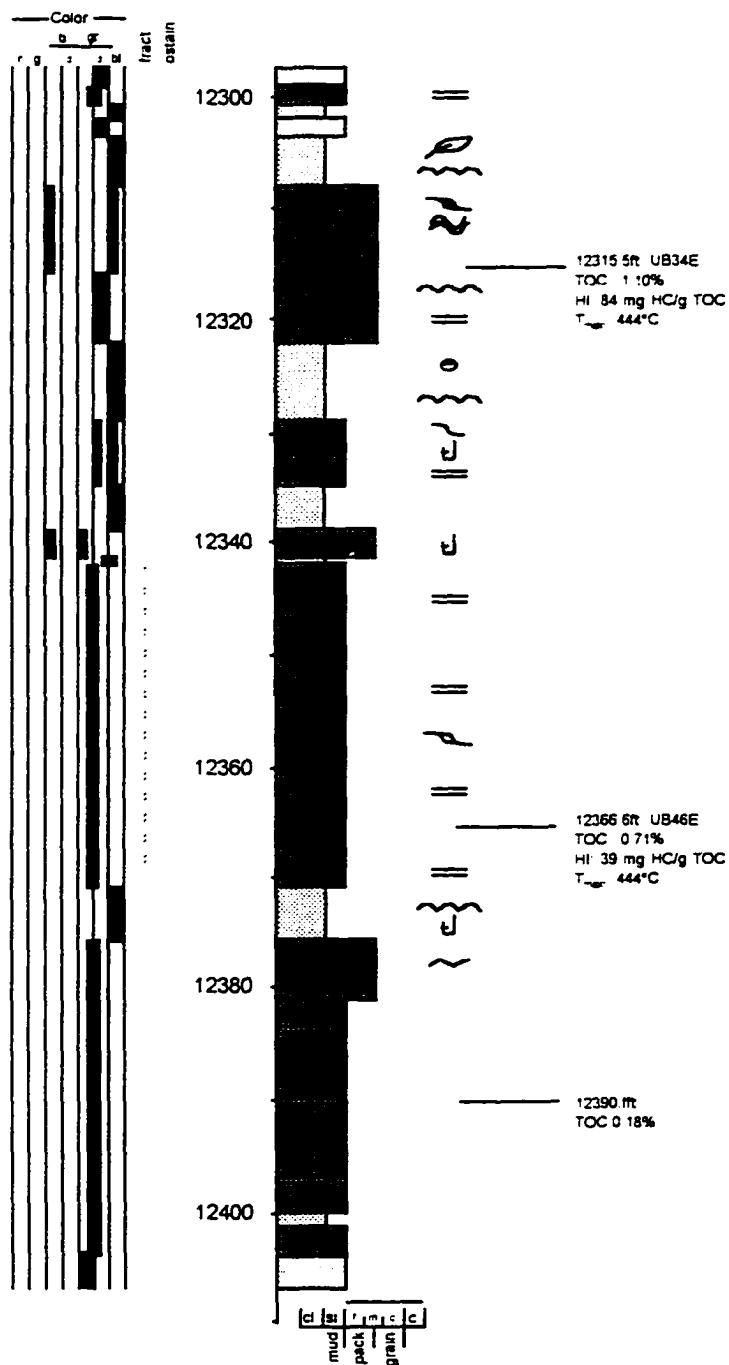


Rio Bravo  
 20-2 RU  
 SESESW 17-R1E-T1S  
 elev.: 5522ft



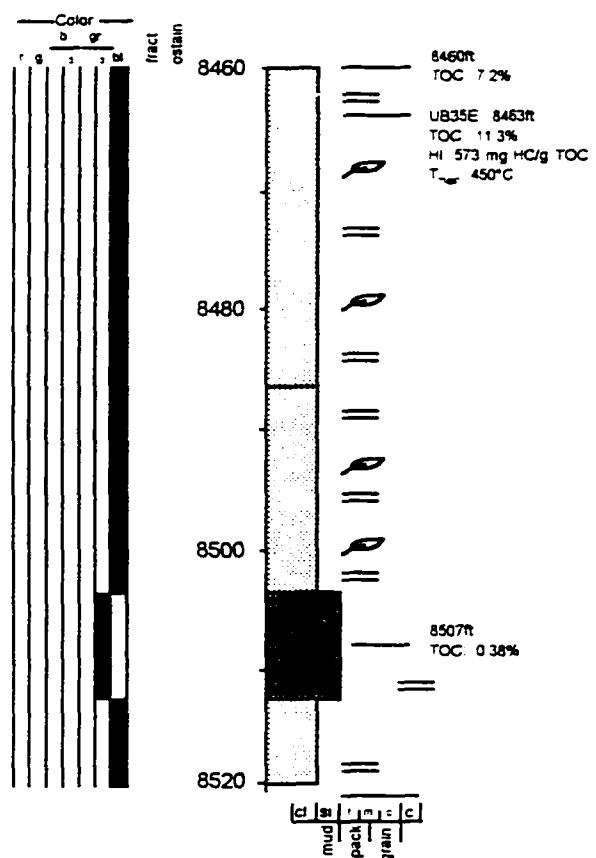
MAPGROUP 1

**Bow Valley Petroleum Inc.**  
**Ute 2-22A1E**  
**22-R1E-T1S**  
**elev.: 5354ft GR**



Altamont-Bluebell area  
well outside mapgroup 1

Page Petroleum Inc.  
Esson Ute 1-14B1E  
SENWNE 14-R2S-T1E  
elev.: 5079ft KB

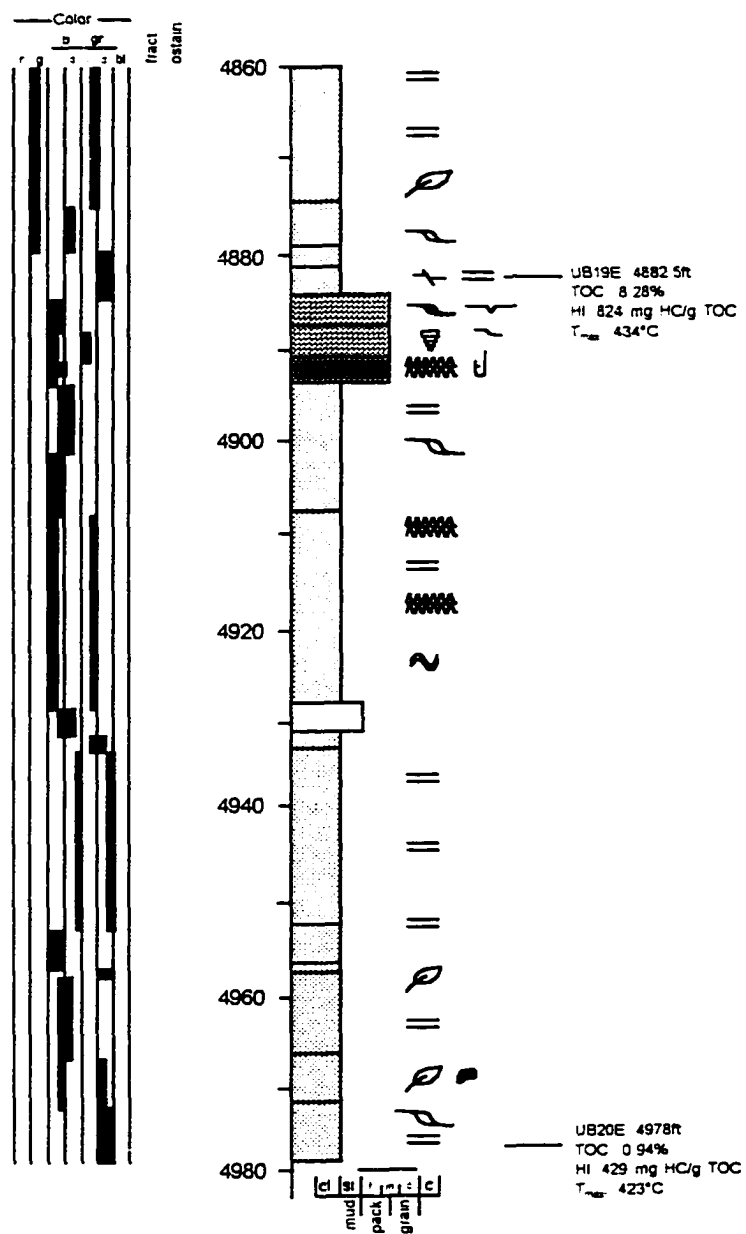


Natural Gas Co.

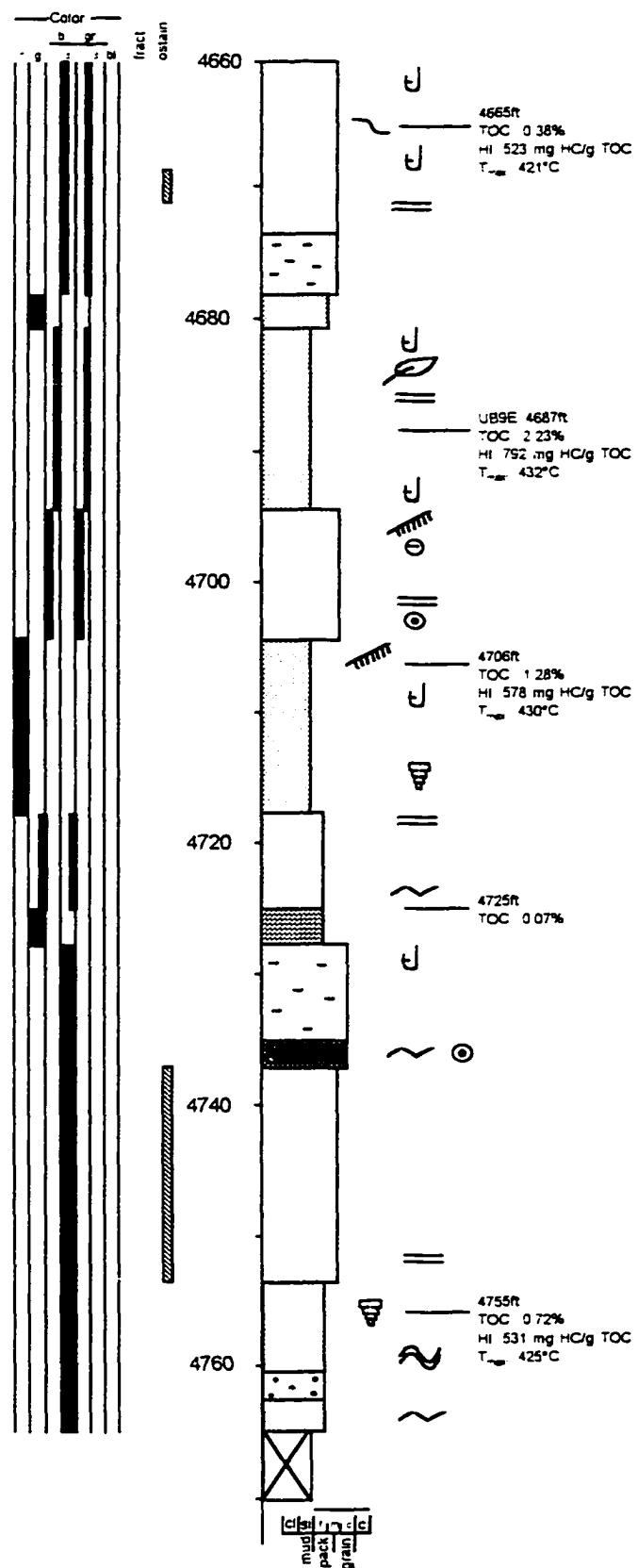
23-24 Federal

NESW 24-R21E-T8S

elev.: 4835ft KB



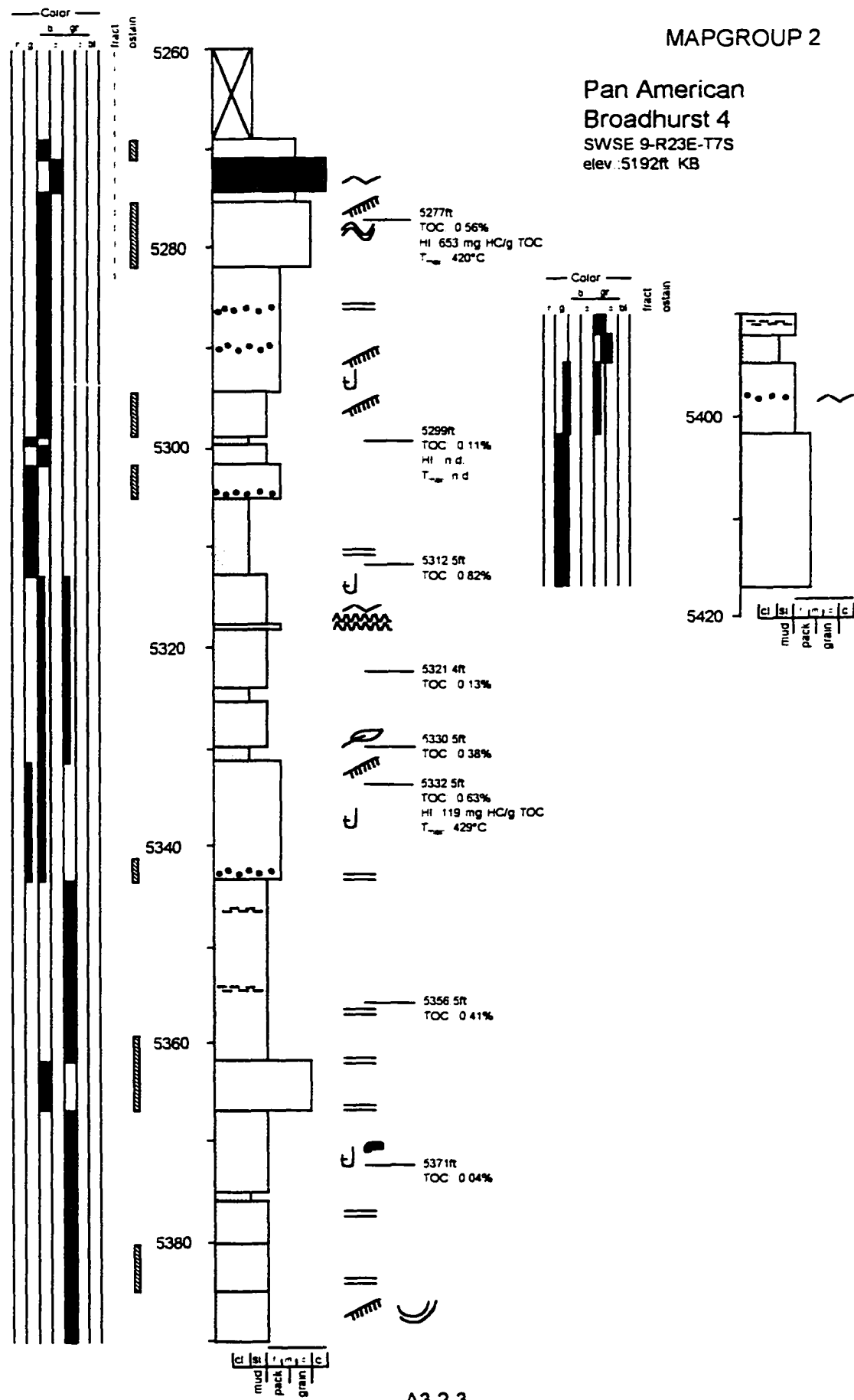
MAPGROUP 2



Pan American  
Broadhurst 4  
SWSE 9-R23E-T7S  
elev. 5192ft KB

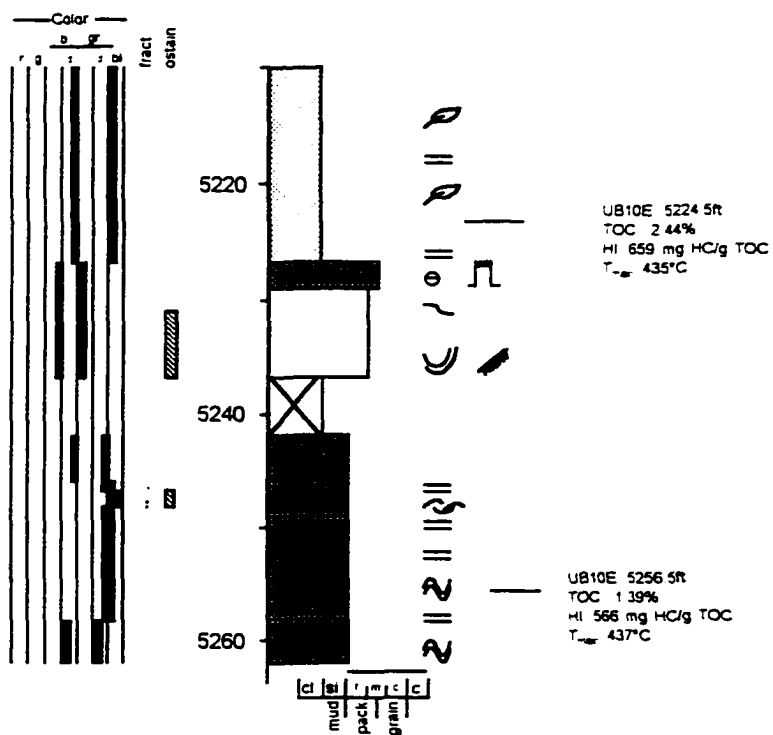
MAPGROUP 2

Pan American  
Broadhurst 4  
SWSE 9-R23E-T7S  
elev. 5192ft KB

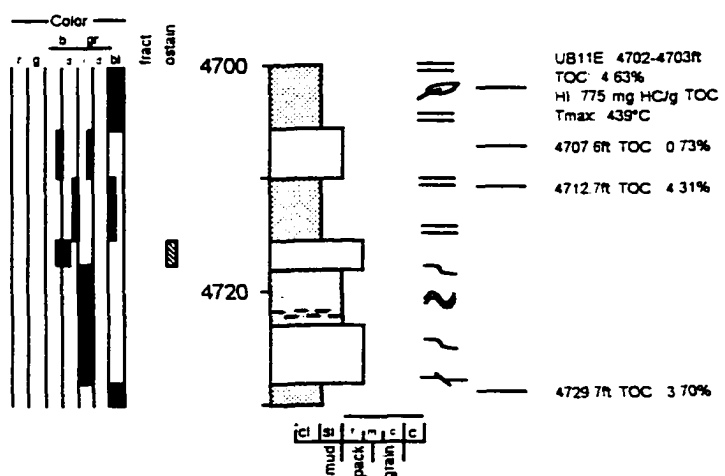


Gulf Oil  
 1-20-4B Costas Federal  
 NESW 20-R21E-T8S  
 elev.: 4693ft KB

MAPGROUP 2

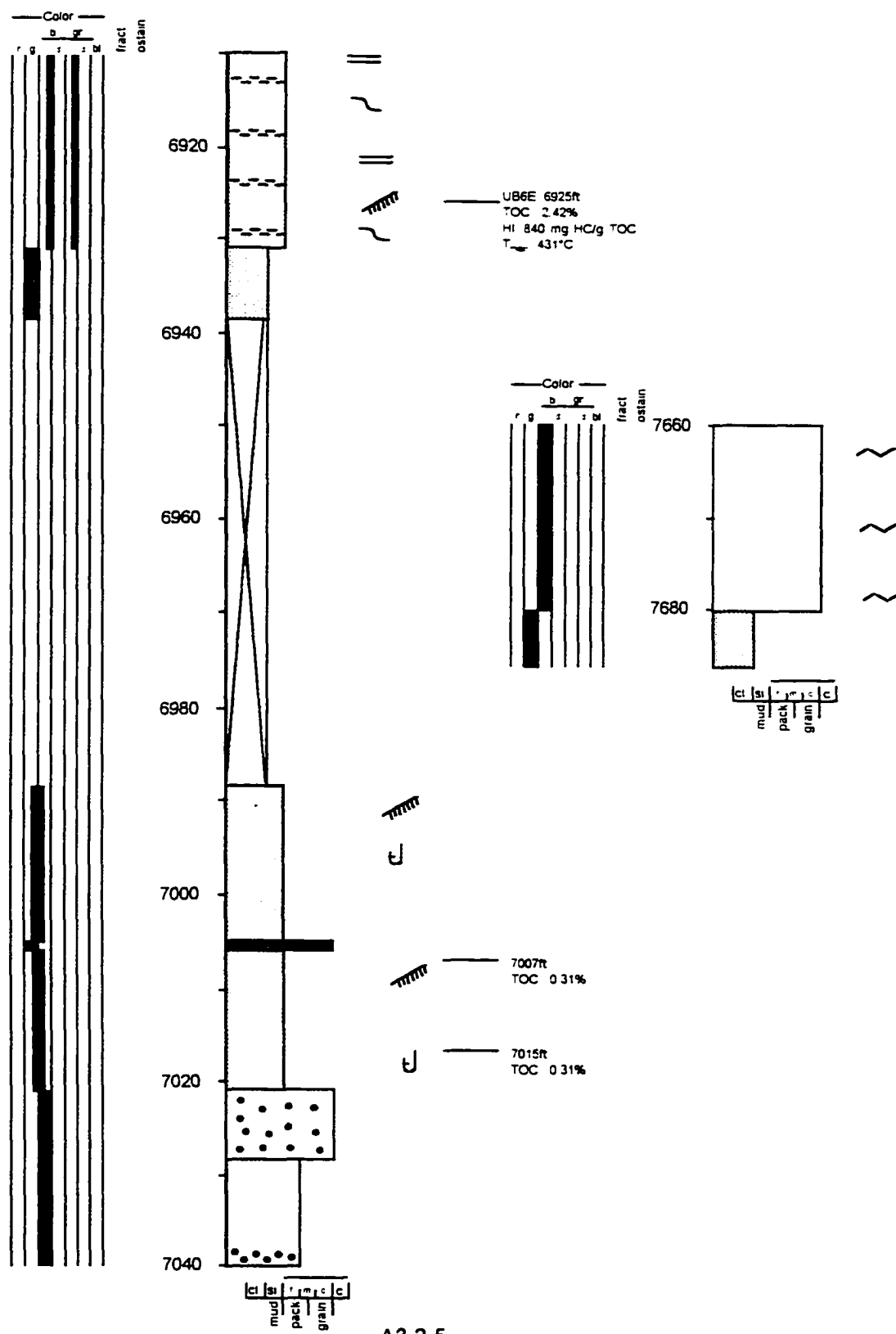


Natural Gas Co.  
 22-30 Bench Glenn  
 NWSENW 30-R22E-T8S  
 ELEV.: 4756ft GL

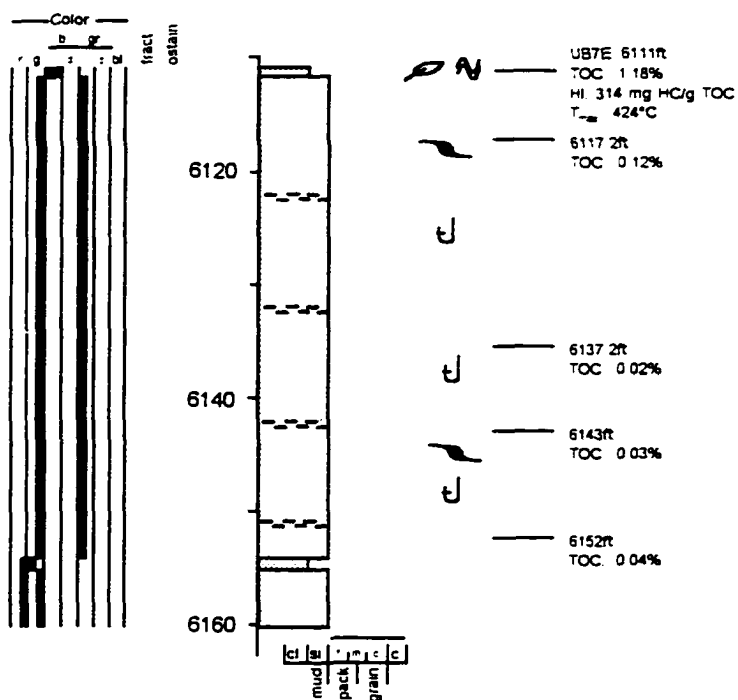


MAPGROUP 2

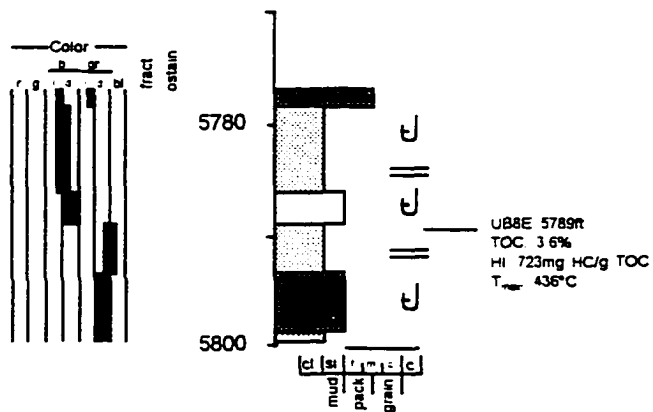
Pan American  
Lyle Lingelbach 1  
NWSESE 29-R21E-T6S  
elev.: 4904ft



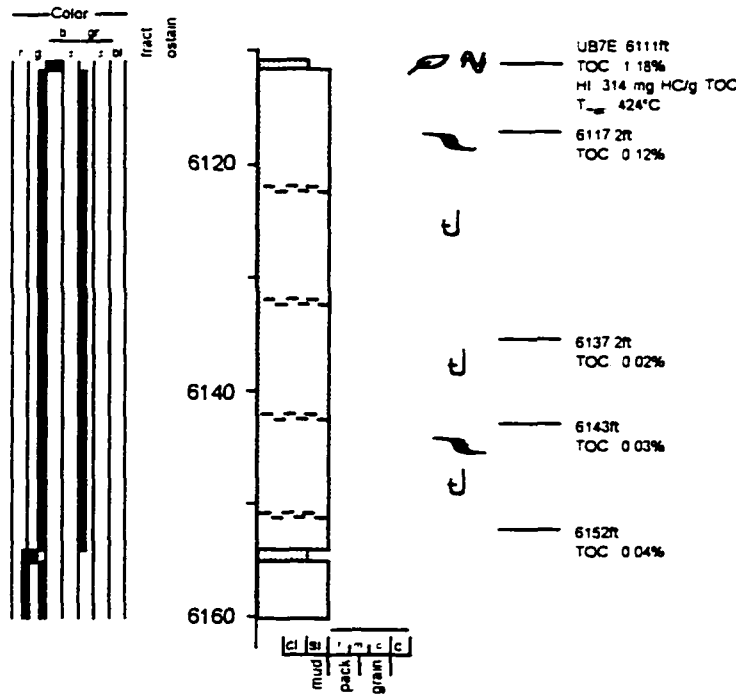
Pan American  
McLish 1 Unit  
SWSE 34-R22E-T6S  
elev.: 5129ft



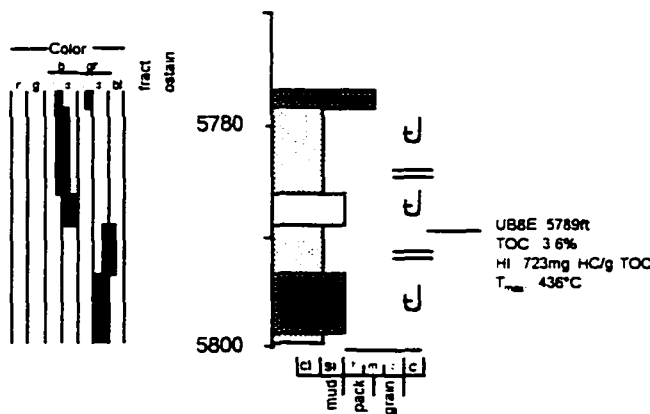
Pan American  
#3 Pelican Lake/3Unit  
NWSE 34-R21E-T7S  
elev.: 4773ft GL

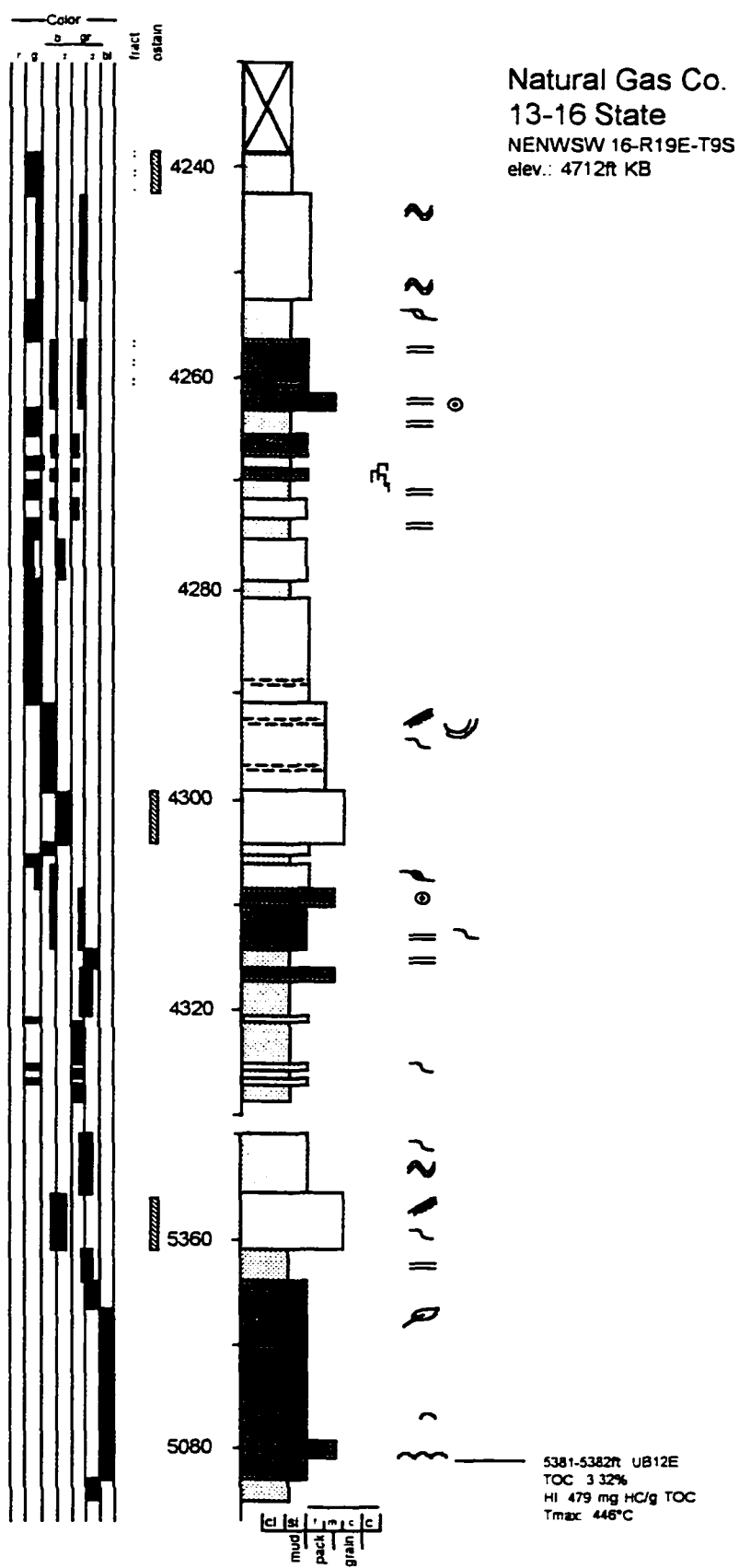


Pan American  
McLish 1Unit  
SWSE 34-R22E-T6S  
elev.: 5129ft



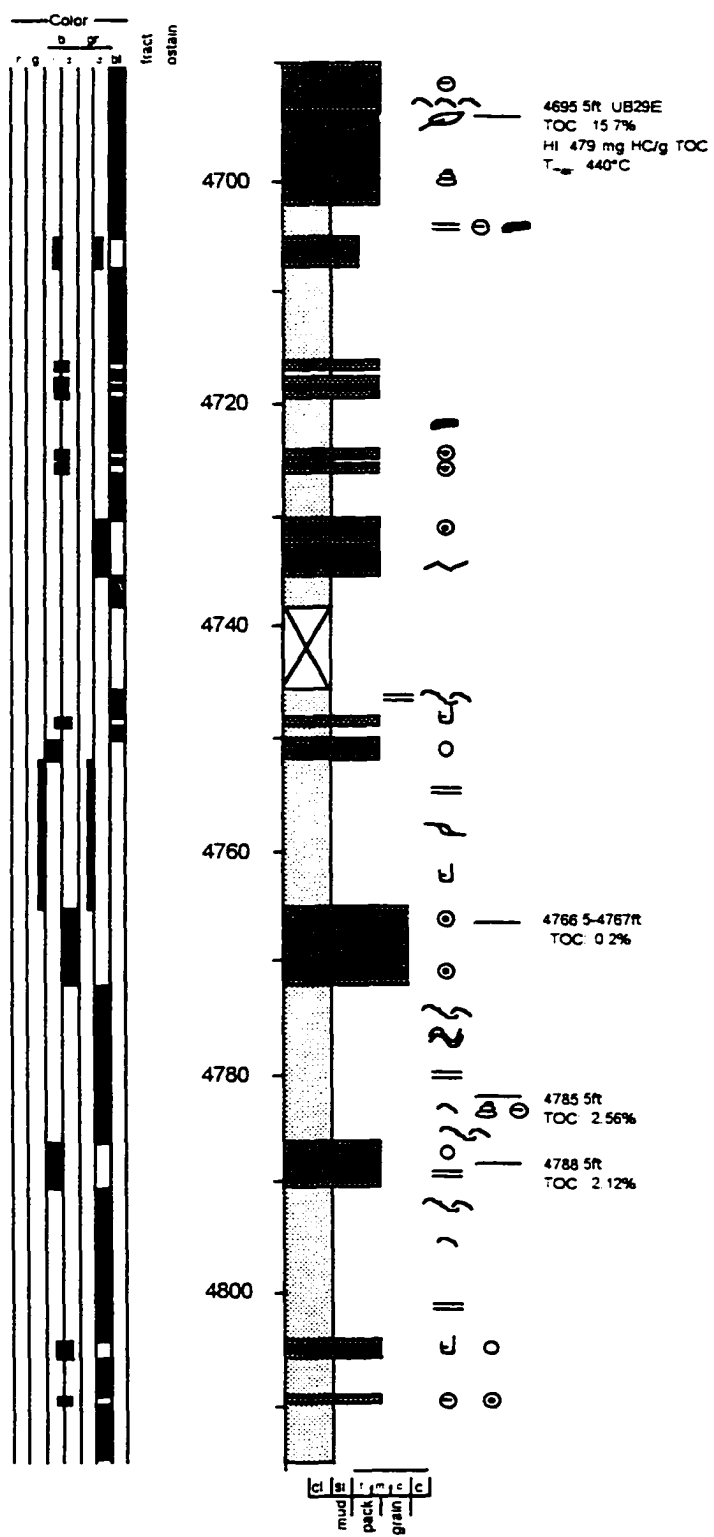
Pan American  
#3 Pelican Lake/3Unit  
NWSE 34-R21E-T7S  
elev.: 4773ft GL

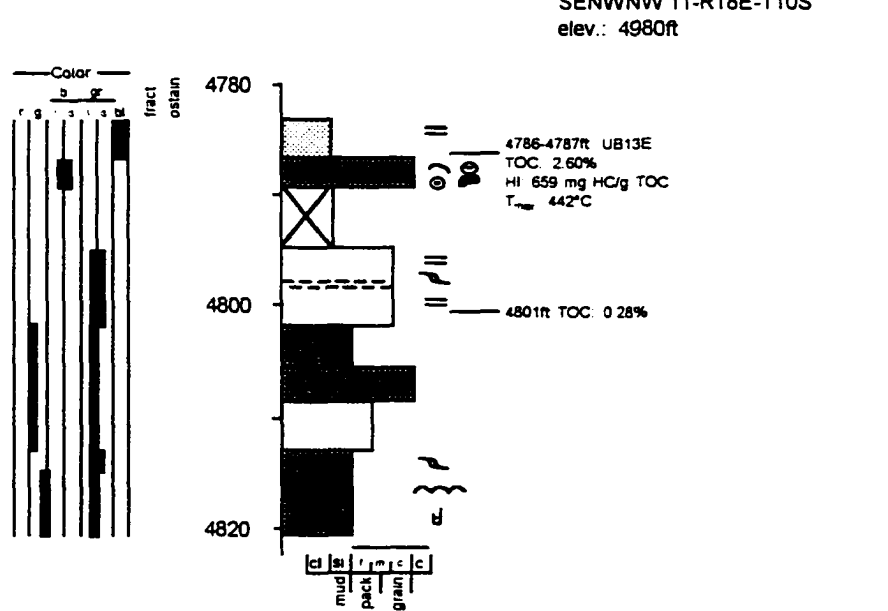
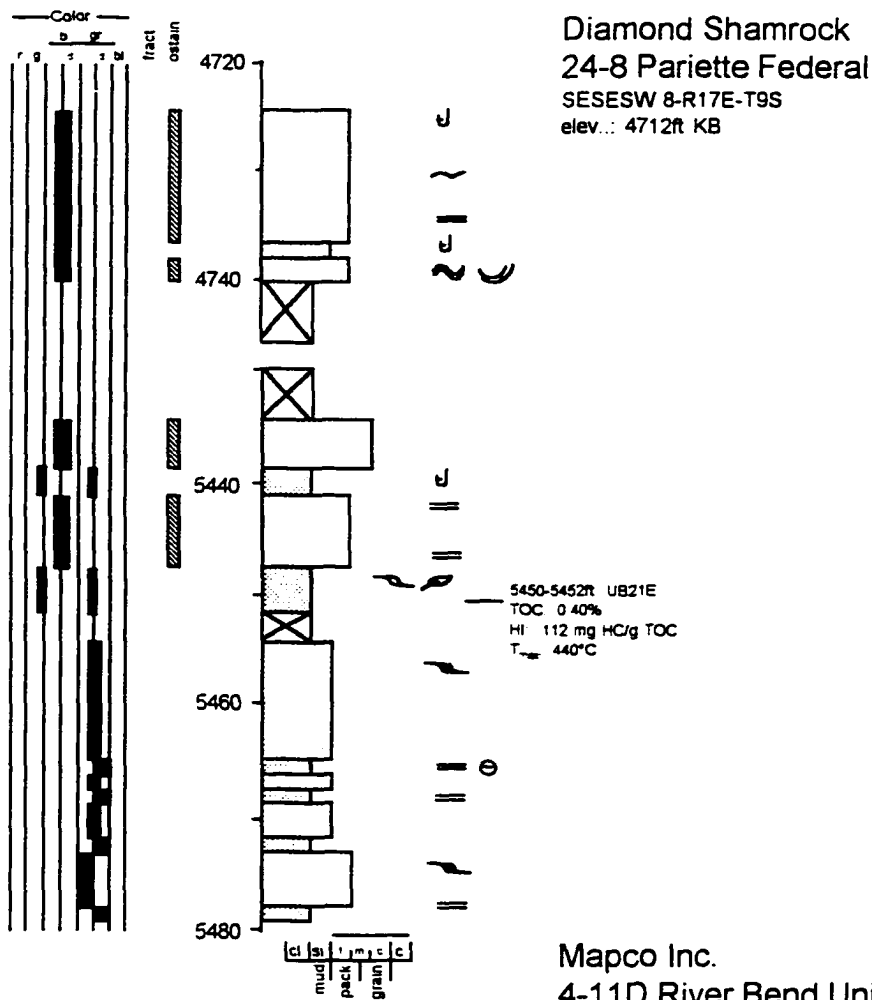




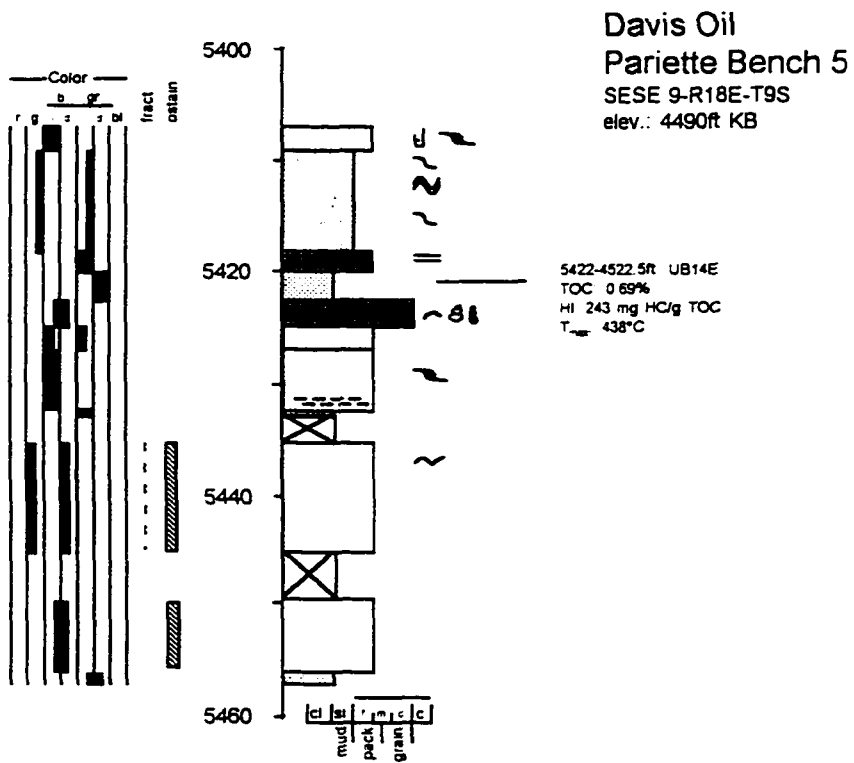
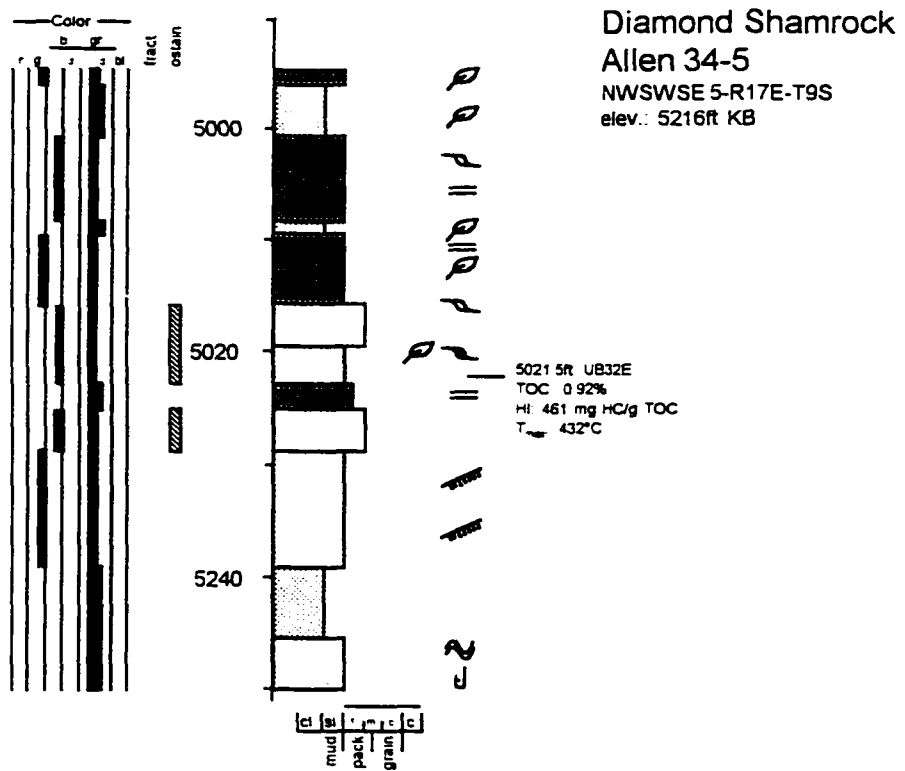
A3.3-1

Celsius Energy Inc.  
Island Unit 16  
NWNESW 11-R18E-T10S  
elev.: 5094ft KB





MAPGROUP 3



## APPENDIX 4.1

### Source Rock Extracts - GC-MS Peak Heights [µV]

Peak #	Compound	UB1E	UB2E	UB3E	UB4E	UB5E	UB6E	UB7E	UB8E	UB9E	UB10E
<b>Terpanes m/z 191</b>											
1	Tricyclic terpane C <sub>18</sub>	12735	9331	12677	9950	9978	2000	8000	6000	7000	
2	Tricyclic terpane C <sub>20</sub>	32317	323212	393721	139489	43722	59187	54152	171090	73330	
3	Tricyclic terpane C <sub>21</sub>	85172	386324	500867	305654	165332	171476	143883	477225	123498	
4	Tricyclic terpane C <sub>22</sub>	14292	53585	99745	54608	30918	16375	11068	69500	0	
5	Tricyclic terpane C <sub>23</sub>	68545	313516	498776	299499	161047	171080	174419	514630	70972	
6	Tricyclic terpane C <sub>24</sub>	49121	139150	290299	346209	98318	70378	124873	209590	90532	
7	Tricyclic terpane C <sub>25</sub>	21491	47587	127743	71717	38349	41329	54631	107668	28710	
8	Tricyclic terpane C <sub>26</sub> 22S	15674	59303	172548	91792	51266	73376	77647	158792	41594	
9	Tricyclic terpane C <sub>26</sub> 22R	18422	81528	219198	97227	52515	79770	85390	180241	70905	
10	Tricyclic terpane C <sub>27</sub> 22S	0	0	0	9170	8789	0	32569	28882	0	
11	Tricyclic terpane C <sub>27</sub> 22R	0	0	0	12710	10407	0	12008	24313	0	
12	Tricyclic terpane C <sub>28</sub> 22S	13516	50605	123878	83865	42719	52029	41416	120801	15018	
13	Tricyclic terpane C <sub>28</sub> 22R	10217	42586	94865	57990	33578	46416	33038	100642	17238	
14	Tricyclic terpane C <sub>29</sub> 22S	16890	31885	105602	74926	35245	43523	43659	80928	24133	
15	Tricyclic terpane C <sub>29</sub> 22R	15760	33801	108300	78290	32022	45337	46306	73481	24379	
16	18a(H)-22,29,30-normethopane (Ts)	24018	68665	111151	128965	34031	90102	49409	222482	42256	
17	1 unknown terpane	0	0	0	0	45534	15416	0	44944	14738	
18	Tricyclic terpane C30 22S	11689	22290	63886	55652	24867	27565	32858	65234	18118	
19	17a(H)-22,29,30-trisnorhopane (Tm)	11813	337773	698749	183292	11754	129466	114085	250623	199298	
20	Tricyclic terpane C <sub>30</sub> 22R	12903	11552	49453	57000	24833	0	0	0	0	
21	17b(H)-22,29,30-trisnormorethane	0	28675	76800	24032	0	17063	26268	27170	30952	
22	2 unknown terpane	0	20394	40697	40113	14591	40850	52149	107883	0	
23	Tricyclic terpane C <sub>31</sub> 22S	0	40837	104924	68691	27052	52019	34359	94626	0	
24	Tricyclic terpane C <sub>31</sub> 22R	11044	36304	88274	64114	32246	37626	32108	101195	0	
25	17a(H),21b(H)-30-normopane	20919	751167	2383682	622850	31548	351297	259370	891016	535273	
26	C <sub>30</sub> diaphopane	16711	37252	62639	66524	85668	76327	34863	214011	18055	
27	3 unknown terpane	0	0	0	28487	0	9568	0	0	0	
28	17b(H),21a(H)-30-normorethane	16711	104877	270719	56239	11080	68658	66578	140683	291269	
29	18a(H)-oleanane	12981	41898	169887	56417	24781	102417	341987	80950	276195	
30	17a(H),21 b(H)-hopane	43369	1645436	3156458	1180201	89842	1191547	1442191	2895318	1891403	
31	17b(H),21a(H)-morethane	0	378484	448908	129260	11375	144045	164955	355429	521731	
32	17a(H),21 b(H),22S-30-homohopane	19190	229337	560232	198773	28608	135983	87615	320217	125406	
33	17a(H),21 b(H),22R-30-homohopane	14378	195268	365905	138986	17613	93142	73267	213413	162111	
34	gammacerane	26716	233980	562696	348388	276960	465567	381481	1105337	257000	
35	17a(H),21b(H),22S-30 31-bishomohopane	14162	143247	391403	132216	21299	93357	58288	252166	75211	
36	17a(H),21b(H),22R-30,31-bishomohopane	12646	108872	262230	86571	14062	70076	73503	198417	154225	
37	17a(H),21b(H),22S-30,31,32-trishomohopane	9103	66073	194738	60617	11942	44433	23202	160578	36762	
38	17a(H),21b(H),22R-30,31,32-trishomohopane	0	53342	135436	43159	9981	35038	27793	118452	55382	
39	17a(H),21b(H),22S-tetrakishomohopane	0	18943	71034	21744	7887	16135	13291	72092	40365	
40	17a(H),21b(H),22R-tetrakishomohopane	0	17274	54824	23124	0	0	24640	54079	13009	
41	17a(H),21b(H),22S-pentakishomohopane	0	9742	21720	13249	0	6858	13201	41245	8998	
42	17a(H),21b(H),22R-pentakishomohopane	0	9853	35717	8428	0	12733	14987	30396	0	
<b>Sesqui-, Diterpanes m/z 123</b>											
43	C <sub>15</sub> bicyclane	0	0	0	0	21608	0	0	0	0	
44	C <sub>15</sub> bicyclane	16488	0	0	16663	32431	0	12624	11323	8202	
45	8G(H)-dnmane	43625	9118	28927	83800	36446	0	30516	21352	27456	
46	C <sub>15</sub> bicyclane	13833	0	0	18208	24688	4134	13626	17182	7681	
47	C <sub>15</sub> bicyclane	8450	0	0	10232	9762	0	0	6343	0	
48	C <sub>16</sub> bicyclane	19188	3997	6492	25564	36259	4070	10360	17415	18158	
49	8G(H)-homodnmane	155827	46554	59059	154102	119043	25973	59583	86571	28963	
50	C <sub>17</sub> , bicyclane	11106	8618	7493	12970	10485	0	11023	10358	0	
51	C <sub>17</sub> , bicyclane	26717	40270	36800	45125	26007	16892	21934	41080	16396	
52	C <sub>18</sub> , bicyclane	26770	27940	25563	35008	25197	13067	20355	25423	21679	
53	unknown diterpane	54337	164139	132244	99371	87379	109884	165385	292892	75045	
54	4G(H)-19-nonsopnmarane	71643	80710	16289	89962	133694	89136	130132	187416	41065	
55	C <sub>19</sub> , bicyclane	11776	86346	40010	45602	33626	48755	54630	115105	34304	
56	C <sub>19</sub> , bicyclane	0	0	0	0	0	0	0	0	0	
57	17-nortetracyclic diterpane	8209	10969	5158	26418	39633	20027	18470	42716	0	
58	isopnmarane	23358	17882	15631	33210	29558	16955	24074	32984	14419	
59	16G(H)-phytiocladiadane	12435	84470	53478	55906	37495	64900	73191	120389	46346	

Peak #	Compound	UB1E	UB2E	UB3E	UB4E	UB5E	UB6E	UB7E	UB8E	UB9E	UB10E
<b>Steranes, diasteranes m/z 217</b>											
60	5a(H)-14 $\beta$ (H)-17 $\beta$ (H)-diginnane	2058	0	0	0	0	0	0	0	0	0
61	5a(H)-14 $\beta$ (H)-17 $\beta$ (H)-homodiginnane	2927	2573	0	0	0	0	0	0	0	0
62	13 $\beta$ (H)-17 $\alpha$ (H)-20S-diacholestanane	13191	0	0	0	6588	0	16513	6852	0	0
63	13 $\alpha$ (H)-17 $\alpha$ (H)-20R-diacholestanane	7516	0	0	0	4310	0	16011	4801	0	0
64	13 $\alpha$ (H)-17 $\beta$ (H)-20S-diacholestanane	3432	0	0	0	1886	0	0	3125	0	0
65	13 $\alpha$ (H)-17 $\beta$ (H)-20R-diacholestanane	3790	0	0	0	0	0	0	2763	0	0
66	24-methyl-13 $\beta$ (H)-17 $\alpha$ (H)-20S-diacholestanane	4458	0	0	0	4160	0	0	3341	0	0
67	24-methyl-13 $\beta$ (H)-17 $\alpha$ (H)-20R-diacholestanane	2571	5723	10978	3352	2319	0	0	4665	4298	0
68	24-C <sub>28</sub> - $\alpha\beta$ dia 20S+ $\alpha\beta$ C <sub>27</sub> -20S	11006	31918	39178	5918	3232	9967	73123	28933	27305	0
69	24-C <sub>28</sub> - $\alpha\beta$ dia 20S- $\beta\beta$ C <sub>27</sub> -20R	11706	16497	19042	6596	10948	8897	30891	23645	0	0
70	24-C <sub>28</sub> - $\alpha\beta$ dia 20R+ $\alpha\beta$ C <sub>27</sub> -20S	11560	13755	13162	5723	4576	6482	13320	17417	15855	0
71	14a(H),17a(H)-20R-cholestane	8698	47345	35967	5930	3882	20481	306935	44715	42446	0
72	24-ethyl-13 $\beta$ (H)-17 $\alpha$ (H)-20R-diacholestanane	3810	5734	23758	1947	0	0	0	0	0	0
73	24-ethyl-13 $\beta$ (H)-17 $\alpha$ (H)-20S-diacholestanane	3605	4197	9983	0	2858	0	10502	4786	0	0
74	24-methyl-14 $\alpha$ (H)-17 $\alpha$ (H)-20S-cholestane	2780	19574	47429	2184	3377	3986	15711	15715	12920	0
75	24-C <sub>28</sub> - $\alpha\beta$ dia 20R-C <sub>28</sub> - $\beta\beta$ 20R	3660	22908	69845	4661	4087	10038	42256	31789	29130	0
76	24-methyl-14 $\beta$ (H)-17 $\beta$ (H)-20S-cholestane	3677	17336	47000	3094	2845	7335	10459	23510	21990	0
77	24-methyl-14 $\alpha$ (H)-17 $\alpha$ (H)-20R-cholestane	2325	49998	105095	3963	1931	19179	119486	40887	37824	0
78	24-ethyl-14 $\alpha$ (H)-17 $\alpha$ (H)-20S-cholestane	7866	48456	213101	3129	2795	3535	37207	21518	17015	0
79	24-ethyl-14 $\beta$ (H)-17 $\beta$ (H)-20R-cholestane	5724	29109	175196	9448	6656	4911	60870	23915	19085	0
80	24-ethyl-14 $\beta$ (H)-17 $\beta$ (H)-20S-cholestane	5060	19000	8001	4308	6068	2988	0	17249	0	0
81	24-ethyl-14 $\alpha$ (H)-17 $\alpha$ (H)-20R-cholestane	4437	75488	279931	4023	3265	13906	305431	36295	35007	0
<b>Monoaromatic steroids m/z 253</b>											
82	monoaromatic sterane C <sub>27</sub>	0	3235	3173	602	0	1867	7649	5620	2077	0
83	monoaromatic sterane C <sub>27</sub>	0	646	995	418	442	2141	8444	5313	288	0
84	monoaromatic sterane C <sub>27</sub>	420	1128	5557	471	388	879	5082	3048	603	0
85	monoaromatic sterane C <sub>27</sub>	756	2302	2339	1029	777	3269	15259	8550	3996	0
86	monoaromatic sterane C <sub>27</sub> +C <sub>28</sub>	601	8901	9494	928	427	4018	15507	12367	6963	0
87	monoaromatic sterane C <sub>27</sub> +C <sub>28</sub>	0	1150	1627	299	0	1624	7055	6537	482	0
88	monoaromatic sterane C <sub>27</sub> +C <sub>28</sub>	406	3601	2672	469	1102	1312	7573	4083	5796	0
89	monoaromatic sterane C <sub>27</sub> +C <sub>28</sub>	490	15918	36399	1633	1114	8278	48646	31872	10899	0
90	monoaromatic sterane C <sub>27</sub> +C <sub>28</sub>	0	763	878	0	0	832	3992	2730	0	0
91	monoaromatic sterane C <sub>27</sub> +C <sub>28</sub>	0	1346	6203	0	0	682	13989	4049	0	0
92	monoaromatic sterane C <sub>28</sub> +C <sub>29</sub>	288	14741	37848	393	0	2763	16544	10057	7516	0
93	monoaromatic sterane C <sub>28</sub> +C <sub>29</sub>	0	6124	13890	1158	0	2511	34792	12241	5882	0
94	monoaromatic sterane C <sub>28</sub> +C <sub>29</sub>	0	8097	14455	804	340	3257	2605	9377	4500	0
95	monoaromatic sterane C <sub>29</sub>	0	793	2710	609	524	489	11714	3118	0	0
96	monoaromatic sterane C <sub>29</sub>	0	9325	27796	757	0	1906	15472	7613	7034	0

oil-shale type sample

coal sample

regular type sample

## APPENDIX 4.1

Peak #	Compound	UB10E	UB11E	UB12E	UB13E	UB14E	UB15E	UB16E	UB17E	UB18E	UB19E
<b>Terpanes m/z 191</b>											
1	Tricyclic terpane C <sub>18</sub>	4000	8000	32673	5000	13713	0	8514	13828	3000	12433
2	Tricyclic terpane C <sub>20</sub>	90571	86802	39452	15481	31318	0	91355	64774	27162	192983
3	Tricyclic terpane C <sub>21</sub>	238996	190025	112595	52128	59502	0	263099	214216	74878	365512
4	Tricyclic terpane C <sub>22</sub>	37702	21497	20651	11188	0	0	52066	44362	13525	50901
5	Tricyclic terpane C <sub>23</sub>	194913	148104	83256	63962	43893	0	241702	224983	74218	327113
6	Tricyclic terpane C <sub>24</sub>	118700	50948	39117	36177	25706	0	143196	154398	51450	181596
7	Tricyclic terpane C <sub>25</sub>	52144	29219	18831	27439	9520	0	57763	50281	18315	62889
8	Tricyclic terpane C <sub>26</sub> 22S	86854	39647	18529	15339	0	0	79764	59472	28622	79902
9	Tricyclic terpane C <sub>26</sub> 22R	95019	43593	67371	19923	17497	0	90096	68119	30334	110008
10	Tricyclic terpane C <sub>27</sub> 22S	0	0	0	0	0	0	0	0	0	14132
11	Tricyclic terpane C <sub>27</sub> 22R	0	0	0	0	0	0	0	0	0	10964
12	Tricyclic terpane C <sub>28</sub> 22S	68033	30098	10124	15242	0	0	66606	54434	22909	62995
13	Tricyclic terpane C <sub>28</sub> 22R	50165	26068	12942	14044	0	0	57383	52218	19410	52123
14	Tricyclic terpane C <sub>29</sub> 22S	49039	18703	10380	14688	0	0	55913	43234	22088	52671
15	Tricyclic terpane C <sub>29</sub> 22R	47172	20237	10758	14478	0	0	52649	39303	21902	49951
16	18a(H)-22,29,30-normethopane (Ts)	152371	46980	195387	11891	46432	0	91206	98180	37646	176712
17	1 unknown terpane	11605	0	39639	24994	21356	0	12398	21700	18497	0
18	Tricyclic terpane C30 22S	41876	20476	10237	13901	0	0	30523	31144	18887	33011
19	17a(H)-22,29,30-trisnorhopane (Tm)	91151	84470	167259	19054	35738	0	47789	57644	18592	274712
20	Tricyclic terpane C <sub>30</sub> 22R	38245	20502	0	12857	0	0	0	32333	18000	0
21	17b(H)-22,29,30-trisnorhopane	12314	18072	10395	0	0	0	0	0	18914	25230
22	2 unknown terpane	63395	18072	70496	7430	20486	0	45829	45509	18592	68048
23	Tricyclic terpane C <sub>11</sub> 22S	53534	23187	15236	8218	10110	0	53985	35846	21561	45446
24	Tricyclic terpane C <sub>11</sub> 22R	55884	23002	14277	0	0	0	59915	40456	25553	36991
25	17a(H),21b(H)-30-norhopane	388211	213079	414939	88041	104386	0	174434	164053	70751	808776
26	C <sub>16</sub> diahopane	111819	28217	103568	38216	41030	0	123193	95197	41536	85126
27	3 unknown terpane	12963	0	28238	0	0	0	31988	13946	9579	0
28	17b(H),21a(H)-30-normorethane	55459	44580	35515	11297	12189	0	19045	16197	9677	132781
29	18a(H)-oceanane	28083	37548	47640	30302	11249	0	21702	37701	21847	61941
30	17a(H),21 b(H)-hopane	1101188	454625	779703	219002	152640	0	640927	482105	179046	1632392
31	17d(H),21a(H)-morethane	119172	83608	69284	33204	22917	0	65616	52660	20203	244171
32	17a(H) 21 b(H) 22S-30-homohopane	225058	113934	217178	88130	52606	0	122822	102304	41387	322062
33	17a(H) 21 b(H) 22R-30-homohopane	142107	79314	151600	52763	34069	0	70177	69979	33071	219136
34	gammacerane	306886	198649	149753	78295	28805	0	208179	185713	75477	719679
35	17a(H),21b(H) 22S-30 31-bishomohopane	138620	66236	163652	72220	38049	0	89744	77038	30741	171233
36	17a(H) 21b(H) 22R-30 31-bishomohopane	89299	52217	114013	48039	25029	0	58085	48912	19833	132348
37	17a(H),21b(H),22S-30,31,32-trishomohopane	87566	40166	70205	43516	16382	0	46837	34071	16287	103320
38	17a(H),21b(H),22R-30,31,32-trishomohopane	59137	35918	58100	30545	12595	0	37160	23640	11160	65572
39	17a(H),21b(H),22S-tetrakishomohopane	29862	16453	30511	27056	12589	0	18791	14044	9894	30488
40	17a(H),21b(H),22R-tetrakishomohopane	15305	17552	20957	17628	9591	0	13893	15057	4675	33702
41	17a(H),21b(H),22S-pentakishomohopane	12346	8357	7866	18382	0	0	9240	7723	4189	15148
42	17a(H),21b(H),22R-pentakishomohopane	10950	6762	7776	10554	0	0	9761	4057	3021	13413
<b>Sesqui-, Diterpanes m/z 123</b>											
43	C <sub>15</sub> bicyclane	8568	0	87915	3753	15713	29738	5830	23596	7946	11354
44	C <sub>15</sub> bicyclane	14194	6045	205659	5938	13888	6786	22812	50671	19330	38374
45	Bb(H)-dnmane	31287	17477	264132	8284	20224	0	44567	89559	40193	91248
46	C <sub>15</sub> bicyclane	34136	10548	113015	5327	8385	0	23103	58174	19655	45495
47	C <sub>15</sub> bicyclane	11364	0	53678	0	4388	0	11898	28221	8373	18679
48	C <sub>15</sub> bicyclane	27827	7565	108608	9330	19875	8161	26057	39169	15298	26382
49	Bb(H)-homodimane	127395	56085	491905	64230	66161	0	108327	221325	56211	205421
50	C <sub>15</sub> , bicyclane	11910	5244	25493	4596	11979	5932	9106	13427	5238	17894
51	C <sub>15</sub> , bicyclane	38801	22328	27108	12424	22673	10139	30710	41033	11208	47346
52	C <sub>15</sub> , bicyclane	22945	11352	19832	12074	23354	0	30918	30854	12771	32026
53	unknown diterpane	141323	101326	86241	28717	55397	9144	107295	97750	32460	192278
54	4b(H)-19-nonsopimarane	89104	42325	89239	24616	52088	20613	121712	127214	39317	98821
55	C <sub>15</sub> , bicyclane	46188	37012	25208	10519	12131	0	31728	32732	12375	74466
56	C <sub>15</sub> , bicyclane	0	0	17035	0	8007	0	0	0	0	0
57	17-nortetracyclic diterpane	35486	8089	17515	4776	12166	25018	36204	37488	13309	15408
58	isopimarane	24528	9152	28617	5390	28010	12615	29758	33315	8960	19969
59	16b(H)-phylocladane	51154	41249	29785	11503	13484	0	63346	58339	16162	92275

peak #	Compound	UB10E	UB11E	UB12E	UB13E	UB14E	UB15E	UB16E	UB17E	UB18E	UB19E
<b>Steranes, diasteranes m/z 217</b>											
60	5 $\alpha$ (H).14 $\beta$ (H).17 $\beta$ (H)-dignane	0	0	0	0	0	0	0	0	0	0
61	5 $\alpha$ (H).14 $\beta$ (H).17 $\beta$ (H)-homodiglane	0	0	2916	0	1018	0	0	0	0	3107
62	13 $\beta$ (H).17 $\alpha$ (H).20S-diacholestan e	3597	0	7083	5805	3212	0	0	0	1074	4141
63	13 $\beta$ (H).17 $\alpha$ (H).20R-diacholestan e	0	0	3195	3771	1951	0	0	0	873	3099
54	13 $\alpha$ (H).17 $\beta$ (H).20S-diacholestan e	0	0	2177	1894	935	0	0	0	0	2120
65	13 $\alpha$ (H).17 $\beta$ (H).20R-diacholestan e	0	0	1764	1785	892	0	0	0	0	0
66	24-methyl-13 $\beta$ (H).17 $\alpha$ (H).20S-diacholestan e	0	0	2944	3960	1634	0	0	0	0	1911
67	24-methyl-13 $\beta$ (H).17 $\alpha$ (H).20R-diacholestan e	0	1881	4588	2223	1220	0	0	0	0	4057
68	24-C <sub>28</sub> $\alpha\beta$ dia 20S+ $\alpha\alpha$ C <sub>27</sub> .20S	13006	19422	6127	9671	2400	0	3214	5897	1787	34034
69	24-C <sub>28</sub> $\alpha\beta$ dia 20S+ $\beta\beta$ C <sub>27</sub> .20R	12263	7581	16175	13140	5924	0	4130	7508	2358	20423
70	24-C <sub>28</sub> $\alpha\beta$ dia 20R+ $\beta\beta$ C <sub>27</sub> .20S	10688	4838	6559	5592	2995	0	3147	6915	1328	13324
71	14 $\alpha$ (H).17 $\alpha$ (H).20R-cholestane	13941	42017	5538	9088	2126	0	2000	4949	1007	76772
72	24-ethynyl-13 $\beta$ (H).17 $\alpha$ (H).20R-diacholestan e	0	0	0	0	0	0	0	0	0	0
73	24-ethyl-13 $\beta$ (H).17 $\alpha$ (H).20S-diacholestan e	8561	0	0	1690	1962	0	0	0	0	2866
74	24-methyl-14 $\alpha$ (H).17 $\alpha$ (H).20S-cholestane	0	0	4377	5311	1558	0	0	0	0	12177
75	24-C <sub>28</sub> $\alpha\beta$ dia 20R+C <sub>28</sub> $\beta\beta$ 20R	6892	10049	8389	8896	2004	0	4774	6393	0	21575
76	24-methyl-14 $\beta$ (H).17 $\beta$ (H).20S-cholestane	4334	6208	0	6374	1632	0	4457	5162	0	14796
77	24-methyl-14 $\alpha$ (H).17 $\beta$ (H).20R-cholestane	6849	30193	4293	7480	1000	0	2589	3396	670	41690
78	24-ethyl-14 $\alpha$ (H).17 $\alpha$ (H).20S-cholestane	10090	21876	9609	10205	2416	0	7862	6964	1803	32759
79	24-ethyl-14 $\beta$ (H).17 $\beta$ (H).20R-cholestane	5991	16932	13910	11771	4037	0	4127	7457	1173	28716
80	24-ethyl-14 $\beta$ (H).17 $\beta$ (H).20S-cholestane	5356	2592	11991	9594	3629	0	3098	6048	1557	32000
81	24-ethyl-14 $\alpha$ (H).17 $\alpha$ (H).20R-cholestane	7463	59457	8343	10923	2878	0	2529	4974	1189	63016
<b>Monoaromatic steroids m/z 253</b>											
82	monoaromatic sterane C <sub>27</sub>	1938	4288	613	1243	0	88	0	284	0	9610
83	monoaromatic sterane C <sub>27</sub>	4426	3156	2439	3146	0	97	282	683	0	6964
84	monoaromatic sterane C <sub>27</sub>	1665	1730	1689	2458	0	119	0	1098	212	3699
85	monoaromatic sterane C <sub>27</sub>	5135	7057	2501	3831	0	382	521	1075	175	15318
86	monoaromatic sterane C <sub>27</sub> +C <sub>28</sub>	5028	9638	2921	4370	459	0	0	458	0	23389
87	monoaromatic sterane C <sub>27</sub> +C <sub>28</sub>	2438	1991	1683	4795	0	149	379	331	243	3974
88	monoaromatic sterane C <sub>27</sub> +C <sub>28</sub>	2055	4321	809	665	0	0	261	1723	0	11084
89	monoaromatic sterane C <sub>27</sub> +C <sub>28</sub>	7781	22321	7575	8206	0	0	1328	0	0	42848
90	monoaromatic sterane C <sub>27</sub> +C <sub>28</sub>	806	1198	1290	2571	0	0	335	401	531	2775
91	monoaromatic sterane C <sub>27</sub> +C <sub>28</sub>	1765	3228	2822	5662	0	0	221	463	207	7326
92	monoaromatic sterane C <sub>28</sub> +C <sub>28</sub>	2967	16440	1712	1844	0	0	0	1321	360	34563
93	monoaromatic sterane C <sub>28</sub> +C <sub>28</sub>	3665	10595	3488	4139	1127	480	843	498	204	20425
94	monoaromatic sterane C <sub>28</sub> +C <sub>28</sub>	2439	7577	0	0	801	0	798	250	0	12211
95	monoaromatic sterane C <sub>28</sub>	816	1589	2393	4172	0	881	144	288	0	3917
96	monoaromatic sterane C <sub>28</sub>	1871	11667	1023	1259	0	0	0	397	203	23168

oil-shale type sample

coal sample

regular type sample

## APPENDIX 4.1

peak no	Compound	UB20E	UB21E	UB22E	UB25E	UB26E	UB27E	UB29E	UB30E	UB31E	UB32E
<b>Terpanes m/z 191</b>											
1	Tricyclic terpane C <sub>19</sub>	4000	14070	1000	37920	0	13385	14615	6707	0	4000
2	Tricyclic terpane C <sub>20</sub>	97117	29029	321880	38177	0	58433	39710	14048	0	18813
3	Tricyclic terpane C <sub>21</sub>	219401	54173	236500	88954	11960	10840	110119	22508	0	51652
4	Tricyclic terpane C <sub>22</sub>	43838	8035	7475	15856	0	0	19228	3260	0	10495
5	Tricyclic terpane C <sub>23</sub>	206175	48031	57661	59815	9891	85907	90338	26100	0	51729
6	Tricyclic terpane C <sub>24</sub>	75223	21079	35232	21527	0	35688	37482	17912	0	45781
7	Tricyclic terpane C <sub>25</sub>	57156	0	16072	10941	0	26197	27345	8352	0	26904
8	Tricyclic terpane C <sub>26</sub> 22S	76661	0	46455	12376	9188	12346	16057	5688	0	28669
9	Tricyclic terpane C <sub>26</sub> 22R	76936	0	50926	78466	0	29418	55449	7244	0	27767
10	Tricyclic terpane C <sub>27</sub> 22S	0	0	0	0	0	0	0	0	0	0
11	Tricyclic terpane C <sub>27</sub> 22R	0	0	0	0	0	0	0	0	0	0
12	Tricyclic terpane C <sub>28</sub> 22S	49437	0	11771	0	0	14412	13592	6188	0	26239
13	Tricyclic terpane C <sub>28</sub> 22R	52058	0	11119	0	0	12429	10604	7263	0	31069
14	Tricyclic terpane C <sub>29</sub> 22S	37497	0	10309	0	0	13879	10083	7541	0	33544
15	Tricyclic terpane C <sub>29</sub> 22R	36672	0	10933	0	0	14108	12028	6563	0	31150
16	18a(H)-22,29 30-normehopane (Ts)	30166	13362	14528	126063	9775	66371	59612	6463	0	27711
17	1 unknown terpane	0	13565	0	44511	9226	36106	27511	0	0	0
18	Tricyclic terpane C30 22S	32987	0	8153	0	0	7503	12155	9442	0	26196
19	17a(H)-22,29,30-trisnorhopane (Tm)	47016	9099	311575	228106	102673	154262	92828	7513	0	15435
20	Tricyclic terpane C <sub>30</sub> 22R	33000	7393	0	0	0	0	0	0	0	27229
21	17b(H)-22,29,30-trisnormorethane	0	0	11870	10023	0	8188	5850	0	0	0
22	2 unknown terpane	9570	8000	0	56338	0	40339	28582	4525	0	15440
23	Tricyclic terpane C <sub>1</sub> , 22S	31885	4500	7591	0	0	20917	7539	8107	0	24417
24	Tricyclic terpane C <sub>1</sub> , 22R	40426	5000	21506	0	0	65747	6492	8755	0	24528
25	17a(H),21b(H)-30-norhopane	130490	14712	492959	486362	210326	464701	252960	5827	0	72498
26	C <sub>30</sub> diahopane	30271	17132	7421	93326	21207	69977	72546	14706	0	37227
27	3 unknown terpane	0	0	0	12842	95550	17354	0	5158	0	10636
28	17b(H),21a(H)-30-normorethane	23915	6869	268677	51903	51805	81247	33818	5375	0	7567
29	18a(H)-olethane	28724	7989	27671	59921	0	36709	39130	5107	0	9342
30	17a(H),21 b(H)-hopane	453396	32874	2352180	843799	203712	644002	515131	5585	0	213021
31	17b(H),21a(H)-morethane	56362	9470	1142949	167175	82295	100396	81581	0	0	18275
32	17a(H),21 b(H) 22S-30-homohopane	58663	12057	225904	195901	112171	179859	148820	0	0	43325
33	17a(H),21 b(H),22R-30-homohopane	48426	6808	308954	160562	71155	120408	104849	0	0	27436
34	gammacerane	584864	6328	494738	124163	24000	57461	262205	7304	0	180739
35	17a(H),21b(H),22S-30,31-bishomohopane	64979	8023	41293	156473	59046	111653	117538	0	0	27747
36	17a(H),21b(H),22R-30,31-bishomohopane	48862	6532	48601	99233	39965	73546	78712	0	0	18923
37	17a(H),21b(H),22S-30,31,32-trishomohopane	37801	7206	17378	83696	24315	54452	53370	0	0	21113
38	17a(H),21b(H),22R-30,31,32-trishomohopane	32519	5785	17974	53837	20914	41024	37515	0	0	12870
39	17a(H),21b(H),22S-tetrakishomohopane	17488	7086	0	36577	9765	25505	22564	0	0	8675
40	17a(H),21b(H),22R-tetrakishomohopane	16069	0	0	24202	10166	17575	17459	0	0	8364
41	17a(H),21b(H),22S-pentakishomohopane	8759	0-Jan-00	7433	13653	0	15151	14081	0	0	7679
42	17a(H),21b(H),22R-pentakishomohopane	8229	0	8734	7652	0	9939	7719	0	0	0
<b>Sesqui-, Diterpanes m/z 123</b>											
43	C <sub>15</sub> bicyclane	8824	31256	0	77979	16006	22832	27822	0	66763	3538
44	C <sub>15</sub> bicyclane	17257	55289	7146	95442	23066	37240	42202	0	41125	7424
45	8b(H)-drimane	41177	69256	51287	133043	29911	68208	65829	4222	24911	12216
46	C <sub>15</sub> bicyclane	27866	38795	0	81926	19357	34209	26677	0	7448	10175
47	C <sub>15</sub> bicyclane	10318	15040	0	34835	7497	13146	12813	0	0	3814
48	C <sub>15</sub> bicyclane	17481	50678	14495	72987	15317	34390	28901	0	15337	11116
49	8b(H)-homodrimane	93481	175124	27159	567317	153939	261844	228006	13068	29876	33710
50	C <sub>17</sub> bicyclane	10630	29738	0	28818	5187	10795	12916	0	6776	3222
51	C <sub>17</sub> bicyclane	31181	46826	16138	34373	0	16567	15929	0	0	11782
52	C <sub>18</sub> bicyclane	17283	40008	21289	19064	0	8237	13837	5143	0	12039
53	unknown diterpane	117296	58697	145725	105006	22924	60879	68499	21599	21410	26271
54	4b(H)-19-norsoprinarane	75498	102842	10370	69093	13730	34673	53425	47988	0	24514
55	C <sub>17</sub> bicyclane	43742	20409	17398	29473	4578	10310	24830	6786	0	5135
56	C <sub>18</sub> bicyclane	0	0	0	7649	0	0	0	0	0	0
57	17-nortetracyclic diterpene	18218	17283	0	16039	0	7951	6864	6728	20828	9735
58	isopimarane	18049	44052	9999	22155	0	11068	9692	24520	6540	22614
59	16b(H)-phylocladane	48094	21113	30062	24831	0	8200	23260	11270	0	11908

Peak #	Compound	UB20E	UB21E	UB22E	UB25E	UB26E	UB27E	UB29E	UB30E	UB31E	UB32E
<b>Steranes, diasteranes m/z 217</b>											
60	5a(H) 14a(H) 17a(H)-diginane	0	5192	0	0	0	0	0	1306	0	0
61	5a(H) 14a(H) 17a(H)-homodiginane	0	6752	0	0	0	0	0	0	0	0
62	13a(H),17a(H),20S-diacholestanane	3415	3198	0	6382	1945	14347	5244	2061	0	1432
63	13a(H),17a(H),20R-diacholestanane	0	2048	0	2557	1456	3692	3387	1350	0	0
64	13a(H),17a(H) 20S-diacholestanane	0	0	0	2880	0	4189	1628	0	0	0
65	13a(H),17a(H) 20R-diacholestanane	0	0	0	0	0	5082	2064	0	0	0
66	24-methyl-13a(H) 17a(H) 20S-diacholestanane	0	0	0	4044	2221	6127	3169	1076	0	0
67	24-methyl-13a(H) 17a(H) 20R-diacholestanane	2881	0	3426	2825	1573	3754	3404	0	0	0
68	24-C <sub>28</sub> aβ dia 20S+αα C <sub>27</sub> , 20S	23405	0	71339	9837	1921	9164	13015	0	0	2901
69	24-C <sub>28</sub> aβ dia 20S+ ββ C <sub>27</sub> , 20R	10562	0	6363	15403	12331	34232	15517	1136	0	4313
70	24-C <sub>28</sub> aβ dia 20R+ ββ C <sub>27</sub> , 20S	7878	0	4474	7260	2102	8260	7821	2884	0	2930
71	14a(H),17a(H) 20R-cholestane	38713	0	199934	10470	5297	18125	12275	898	0	2089
72	24-ethyl-13a(H) 17a(H) 20R-diacholestanane	0	0	0	0	0	0	0	1148	0	0
73	24-ethyl-13a(H) 17a(H) 20S-diacholestanane	0	0	0	3590	0	3979	7348	0	0	0
74	24-methyl-14a(H) 17a(H) 20S-cholestane	5239	0	21067	5451	6249	12219	6115	0	0	0
75	24-C <sub>28</sub> aβ dia 20R+ C <sub>28</sub> ββ 20R	11637	0	65904	6883	1979	5603	9166	0	0	3793
76	24-methyl-14a(H) 17a(H) 20S-cholestane	8714	0	18821	4723	0	0	7377	1061	0	3232
77	24-methyl-14a(H) 17a(H) 20R-cholestane	23524	0	474571	7434	2250	4060	9228	856	0	1686
78	24-ethyl-14a(H) 17a(H) 20S-cholestane	16465	0	143414	10352	12460	13473	15800	905	0	2764
79	24-ethyl-14a(H) 17a(H) 20R-cholestane	13396	0	177765	9144	7159	15662	13131	1122	0	5354
80	24-ethyl-14a(H) 17a(H) 20S-cholestane	8700	0	0	6676	4095	13997	10420	1078	0	4154
81	24-ethyl-14a(H) 17a(H) 20R-cholestane	36166	0	792163	13464	15644	18680	16524	1511	0	2666
<b>Monoaromatic steroids m/z 253</b>											
82	monoaromatic sterane C <sub>27</sub>	4201	767	748	150	0	415	2063	0	0	0
83	monoaromatic sterane C <sub>27</sub>	5784	558	0	393	1713	1861	7144	0	0	0
84	monoaromatic sterane C <sub>27</sub>	2491	101	379	157	1950	836	4958	0	291	0
85	monoaromatic sterane C <sub>27</sub>	9947	1215	1143	457	1118	1693	7283	741	0	720
86	monoaromatic sterane C <sub>27</sub> +C <sub>28</sub>	12222	977	5291	273	6279	1953	9686	148	0	565
87	monoaromatic sterane C <sub>27</sub> +C <sub>28</sub>	3614	0	291	3549	1613	9201	0	0	0	209
88	monoaromatic sterane C <sub>27</sub> +C <sub>28</sub>	6696	703	1310	474	650	1582	789	933	536	91
89	monoaromatic sterane C <sub>27</sub> +C <sub>28</sub>	26486	1628	19364	1518	20390	8140	17578	0	3	1137
90	monoaromatic sterane C <sub>27</sub> +C <sub>28</sub>	2480	0	0	162	0	0	3758	0	0	154
91	monoaromatic sterane C <sub>27</sub> +C <sub>28</sub>	3910	0	232	338	10348	2716	10115	0	0	296
92	monoaromatic sterane C <sub>28</sub> +C <sub>28</sub>	13604	329	20819	300	2076	1454	4142	1131	0	247
93	monoaromatic sterane C <sub>28</sub> +C <sub>28</sub>	10631	133	16685	249	11399	4035	9359	0	0	333
94	monoaromatic sterane C <sub>28</sub> +C <sub>28</sub>	8038	382	12820	201	2094	2798	1317	0	248	107
95	monoaromatic sterane C <sub>28</sub>	2923	295	184	441	5487	2116	6914	950	312	258
96	monoaromatic sterane C <sub>28</sub>	10062	202	27811	396	1973	1004	3166	0	0	320

oil-shale type sample

coal sample

regular type sample

## APPENDIX 4.1

Peak #	Compound	UB33E	UB34E	UB35E	UB36E	UB37E	UB38E	UB39E	UB40E	UB41E
<b>Terpanes m/z 191</b>										
1	Tricyclic terpane C <sub>19</sub>	0	0	34522	12386	2000	5000	0	0	4000
2	Tricyclic terpane C <sub>20</sub>	0	0	358478	237633	326677	22841	156475	0	22970
3	Tricyclic terpane C <sub>21</sub>	0	0	587484	382061	348647	56129	155792	0	30648
4	Tricyclic terpane C <sub>22</sub>	0	0	93828	50447	44931	11710	0	0	0
5	Tricyclic terpane C <sub>23</sub>	0	0	369803	301625	316021	63183	42420	0	26568
6	Tricyclic terpane C <sub>24</sub>	0	0	207849	198523	98614	50579	32751	0	12100
7	Tricyclic terpane C <sub>25</sub>	0	0	84637	62225	57351	18342	14419	0	8760
8	Tricyclic terpane C <sub>26</sub> 22S	0	0	64098	89383	77613	33445	39267	0	0
9	Tricyclic terpane C <sub>26</sub> 22R	0	0	68038	96454	100019	33745	47896	0	24682
10	Tricyclic terpane C <sub>27</sub> 22S	0	0	0	0	0	0	0	0	0
11	Tricyclic terpane C <sub>27</sub> 22R	0	0	0	0	0	0	0	0	0
12	Tricyclic terpane C <sub>28</sub> 22S	0	0	39299	72695	72801	22776	9641	0	0
13	Tricyclic terpane C <sub>28</sub> 22R	0	0	34711	62949	50443	28112	0	0	0
14	Tricyclic terpane C <sub>29</sub> 22S	0	0	31979	48595	38950	27110	12713	0	0
15	Tricyclic terpane C <sub>29</sub> 22R	0	0	30476	55002	44536	26737	13917	0	0
16	18a(H)-22,29,30-normethopane (Ts)	0	0	90410	36340	42922	66125	21801	0	36219
17	1 unknown terpane	0	0	0	0	0	0	0	0	0
18	Tricyclic terpane C <sub>30</sub> 22S	0	0	23503	40550	36919	20585	1660	0	8705
19	17a(H)-22,29,30-trisnormopane (Tm)	0	0	107238	100670	480635	29163	317590	0	131325
20	Tricyclic terpane C <sub>30</sub> 22R	0	0	0	41000	0	21549	0	0	0
21	17b(H)-22,29,30-trisnormorethane	0	0	16574	11759	47185	0	13908	0	14387
22	2 unknown terpane	0	0	0	9988	0	23975	0	0	0
23	Tricyclic terpane C <sub>31</sub> 22S	0	0	11921	49999	0	32140	0	0	0
24	Tricyclic terpane C <sub>31</sub> 22R	0	0	0	63186	52103	33077	31497	0	0
25	17a(H),21b(H)-30-norhopane	0	0	316703	254977	1364124	137967	293292	0	316026
26	C <sub>30</sub> diahopane	0	0	16103	18736	24158	61247	18040	0	30572
27	3 unknown terpane	0	0	0	9953	11334	0	0	0	0
28	17b(H),21a(H)-30-normorethane	0	0	26137	23320	220373	24678	264183	0	65927
29	18a(H)-oceanane	0	0	13449	28955	58848	86517	13449	0	79069
30	17a(H),21 b(H)-hopane	0	0	500384	525577	2844222	544736	2838966	0	540537
31	17b(H),21a(H)-morethane	0	0	52430	54699	1297165	58860	715150	0	126912
32	17a(H) 21 b(H),22S-30-homohopane	0	0	95820	82597	295671	83157	83292	0	92906
33	17a(H),21 b(H),22R-30-homohopane	0	0	73820	61516	253727	65067	129873	0	105684
34	gammacerane	0	0	529183	196554	1978573	136297	1663697	0	112314
35	17a(H),21b(H),22S-30,31-bishomohopane	0	0	49804	53955	163832	69700	20752	0	97549
36	17a(H),21b(H),22R-30,31-bishomohopane	0	0	39000	31768	138262	47557	49924	0	112687
37	17a(H),21b(H),22S-30,31,32-trishomohopane	0	0	18714	20519	91588	36698	68688	0	41193
38	17a(H),21b(H),22R-30,31,32-trishomohopane	0	0	21280	17472	80858	26623	17849	0	43621
39	17a(H),21b(H),22S-tetraakis(homohopane)	0	0	10553	0	34398	12154	0	0	22205
40	17a(H),21b(H),22R-tetraakis(homohopane)	0	0	6558	0	32107	14183	0	0	29783
41	17a(H),21b(H),22S-pentaakis(homohopane)	0	0	0	0	10233	7688	0	0	23831
42	17a(H),21b(H),22R-pentaakis(homohopane)	0	0	0	0	24163	3793	0	0	26152
<b>Sesqui-, Diterpanes m/z 123</b>										
43	C <sub>15</sub> bicyclane	29672	12275	23205	5269	0	6780	0	0	0
44	C <sub>15</sub> bicyclane	0	10165	131022	65411	0	11036	1728	2980	0
45	8b(H)-dihmane	15335	8406	437582	8992	11428	20530	12003	18377	6651
46	C <sub>15</sub> bicyclane	0	0	114013	4508	0	22341	0	0	0
47	C <sub>15</sub> bicyclane	18429	0	44839	20856	0	8695	0	0	3232
48	C <sub>16</sub> bicyclane	2841	7062	85956	103972	2850	19638	7584	7019	0
49	8b(H)-homodihmane	0	36419	473848	15274	0	80107	8257	13933	16317
50	C <sub>15</sub> bicyclane	14583	0	46259	62574	0	7862	0	0	0
51	C <sub>15</sub> bicyclane	0	0	100844	51908	16519	30252	3871	7373	5493
52	C <sub>15</sub> bicyclane	71209	0	81767	126144	15435	17994	13653	13706	7910
53	unknown diterpane	0	0	302979	51169	100232	58048	98519	136563	42011
54	4b(H)-19-nonsopnmarane	0	7590	63420	44530	12341	43748	30802	13041	14222
55	C <sub>15</sub> bicyclane	0	0	65409	0	30819	16046	22463	33240	8663
56	C <sub>15</sub> bicyclane	11081	0	0	18306	0	0	26680	0	0
57	17-nortetracyclic diterpane	0	0	18739	32467	0	16219	0	0	0
58	isopimarane	8107	17642	41454	46208	12087	15001	4168	5600	0
59	16b(H)-phyllocladiene	0	0	117619	176849	30588	16552	20071	33961	11369

Peak #	Compound	UB33E	UB34E	UB35E	UB36E	UB37E	UB38E	UB39E	UB40E	UB41E
<b>Steranes, diasteranes m/z 217</b>										
60	5 $\alpha$ (H) 14 $\beta$ (H) 17 $\beta$ (H)-digirane	0	0	1678	0	1867	0	0	0	0
61	5 $\alpha$ (H) 14 $\beta$ (H) 17 $\beta$ (H)-homodigirane	0	0	7093	0	0	0	0	0	0
62	13 $\beta$ (H) 17 $\alpha$ (H) 20S-diacholestanate	0	0	0	0	0	5157	0	0	0
63	13 $\beta$ (H) 17 $\alpha$ (H) 20R-diacholestanate	0	0	0	0	0	2437	0	0	0
64	13 $\alpha$ (H) 17 $\beta$ (H) 20S-diacholestanate	0	0	0	0	0	0	0	0	0
65	13 $\alpha$ (H) 17 $\beta$ (H) 20R-diacholestanate	0	0	0	0	0	0	0	0	5373
66	24-methyl-13 $\beta$ (H) 17 $\alpha$ (H) 20S-diacholestanate	0	0	0	0	0	0	1668	0	5024
67	24-methyl-13 $\beta$ (H) 17 $\alpha$ (H) 20R-diacholestanate	0	0	0	0	0	1881	5584	0	5333
68	24-C <sub>28</sub> $\alpha\beta$ dia 20S+ $\alpha\alpha$ C <sub>27</sub> , 20S	0	0	12130	3276	59083	8862	31969	0	57481
69	24-C <sub>28</sub> $\alpha\beta$ dia 20S+ $\alpha\alpha$ C <sub>27</sub> , 20R	0	0	11620	3934	9662	10808	7613	0	21807
70	24-C <sub>28</sub> $\alpha\beta$ dia 20R+ $\alpha\alpha$ C <sub>27</sub> , 20S	0	0	12326	3425	7268	6257	3813	0	5617
71	14 $\alpha$ (H), 17 $\alpha$ (H), 20R-cholestane	0	403	8492	2342	118752	6764	156898	0	136579
72	24-ethyl-13 $\beta$ (H) 17 $\alpha$ (H) 20R-diacholestanate	0	0	3171	0	8030	0	0	0	0
73	24-ethyl-13 $\beta$ (H) 17 $\alpha$ (H) 20S-diacholestanate	0	0	1344	0	11251	0	44812	0	19907
74	24-methyl-14 $\alpha$ (H), 17 $\alpha$ (H) 20S-cholestane	0	210	4645	1674	0	0	0	0	15757
75	24-C <sub>28</sub> $\alpha\beta$ dia 20R+C <sub>28</sub> 20R	0	163	15904	4516	28298	5573	53664	0	94916
76	24-methyl-14 $\beta$ (H) 17 $\beta$ (H) 20S-cholestane	0	0	15601	3782	14001	3871	14604	0	0
77	24-methyl-14 $\alpha$ (H) 17 $\alpha$ (H) 20R-cholestane	0	492	13503	2681	145105	3230	376064	0	87045
78	24-ethyl-14 $\alpha$ (H) 17 $\beta$ (H) 20S-cholestane	0	463	13268	2947	98701	7822	167342	0	41231
79	24-ethyl-14 $\beta$ (H) 17 $\beta$ (H) 20R-cholestane	0	665	20578	7064	50486	5007	164865	0	50369
80	24-ethyl-14 $\beta$ (H) 17 $\beta$ (H) 20S-cholestane	0	423	15986	4927	11250	4350	0	0	9395
81	24-ethyl-14 $\alpha$ (H) 17 $\alpha$ (H) 20R-cholestane	0	1049	16057	3755	250563	5649	1103335	0	170998
<b>Monoaromatic steroids m/z 253</b>										
82	monoaromatic sterane C <sub>27</sub>	0	0	434	0	3711	534	3212	4145	9228
83	monoaromatic sterane C <sub>27</sub>	0	0	495	0	0	1756	0	0	7340
84	monoaromatic sterane C <sub>27</sub>	0	0	437	0	979	639	2827	1573	7214
85	monoaromatic sterane C <sub>27</sub>	0	166	846	0	3082	1499	3459	5336	15392
86	monoaromatic sterane C <sub>27</sub> +C <sub>28</sub>	0	0	939	293	11682	1304	24595	25100	18514
87	monoaromatic sterane C <sub>27</sub> +C <sub>28</sub>	0	75	312	0	275	706	289	523	5219
88	monoaromatic sterane C <sub>27</sub> +C <sub>28</sub>	978	277	308	133	6373	435	5508	7811	4364
89	monoaromatic sterane C <sub>27</sub> +C <sub>28</sub>	276	637	2465	393	22421	2494	108520	96415	85891
90	monoaromatic sterane C <sub>27</sub> +C <sub>28</sub>	0	0	193	110	480	234	533	1873	2757
91	monoaromatic sterane C <sub>27</sub> +C <sub>28</sub>	0	78	387	106	849	502	1814	3059	13103
92	monoaromatic sterane C <sub>28</sub> +C <sub>28</sub>	205	381	743	0	20805	708	302179	162865	34450
93	monoaromatic sterane C <sub>28</sub> +C <sub>28</sub>	184	0	1047	394	6000	1303	67423	40000	0
94	monoaromatic sterane C <sub>28</sub> +C <sub>28</sub>	175	544	540	158	12178	944	75478	62249	46296
95	monoaromatic sterane C <sub>28</sub>	906	609	141	0	560	552	1060	2150	6903
96	monoaromatic sterane C <sub>28</sub>	294	633	527	130	16107	414	263645	164088	28219

oil-shale type sample

coal sample

regular type sample

## APPENDIX 4.1

Peak #	Compound	m/z 191	UB46E	UB47E
<b>Terpanes m/z 191</b>				
1	Triyclic terpane C <sub>29</sub>	3000	8040	585
2	Triyclic terpane C <sub>29</sub>	9847	6247	1701
3	Triyclic terpane C <sub>29</sub>	17245	8783	2953
4	Triyclic terpane C <sub>29</sub>	0	0	5337
5	Triyclic terpane C <sub>29</sub>	15907	11653	3156
6	Triyclic terpane C <sub>29</sub>	6866	12432	0
7	Triyclic terpane C <sub>29</sub>	0	0	48204
8	Triyclic terpane C <sub>29</sub> 22S	0	0	29659
9	Triyclic terpane C <sub>29</sub> 22R	1198	15025	753
10	Triyclic terpane C <sub>29</sub> 22S	0	0	0
11	Triyclic terpane C <sub>29</sub> 22R	0	0	0
12	Triyclic terpane C <sub>29</sub> 22S	0	0	22457
13	Triyclic terpane C <sub>29</sub> 22R	8043	9133	0
14	Triyclic terpane C <sub>29</sub> 22S	0	0	23932
15	Triyclic terpane C <sub>29</sub> 22R	0	0	30395
16	18a(H)-22,29,30-normethopane (1S)	18641	32372	0
17	1 unknown terpane	8655	0	9756
18	Triyclic terpane C <sub>29</sub> 22S	0	71120	0
19	17a(H)-22,29,30-trimethopane (1M)	146262	233855	0
20	Triyclic terpane C <sub>29</sub> 22R	7196	11523	0
21	17a(H)-22,29,30-trimethopane	8942	23752	0
22	2 unknown terpane	36046	0	8461
23	Triyclic terpane C <sub>29</sub> 22S	86754	0	16064
24	Triyclic terpane C <sub>29</sub> 22R	9815	0	15675
25	17a(H)-21a(H)-30-homotripane	226651	319376	8552
26	C <sub>29</sub> diaphane	31360	79289	0
27	3 unknown terpane	13495	28223	0
28	17a(H)-21a(H)-30-homotripane	79558	479677	0
29	18a(H)-olefane	52261	124258	0
30	17a(H)-21a(H)-olefane	426184	622581	19620
31	17a(H)-21a(H)-methylene	130797	529460	0
32	17a(H)-21a(H)-22S-30-homotripane	130193	61006	0
33	17a(H)-21a(H)-22R-30-homotripane	102159	276943	2113
34	gammasecane	70467	67353	1142
35	17a(H)-21a(H)-22S-30,31-dishomotripane	80670	28098	3117
36	17a(H)-21a(H)-22R-30,31-dishomotripane	63494	139615	0
37	17a(H)-21a(H)-22S-30,31-dishomotripane	25048	83198	9212
38	17a(H)-21a(H)-22R-30,31,32-dishomotripane	21394	31012	0
39	17a(H)-21a(H)-22S-tertbutylhomotripane	5988	0	8747
40	17a(H)-21a(H)-22R-tertbutylhomotripane	12797	11377	0
41	17a(H)-21a(H)-22S-pentylhomotripane	1281	0	4310
42	17a(H)-21a(H)-22R-pentylhomotripane	48469	17401	0
<b>Sesqui-, Diterpanes m/z 123</b>				
43	C <sub>19</sub> bicyclane	0	0	0
44	C <sub>19</sub> bicyclane	0	0	6859
45	8a(H)-deutane	0	0	0
46	C <sub>19</sub> bicyclane	0	0	4803
47	C <sub>19</sub> bicyclane	0	0	0
48	C <sub>19</sub> bicyclane	0	0	7231
49	8a(H)-homotripane	46052	2145	6077
50	C <sub>19</sub> bicyclane	0	0	50694
51	C <sub>19</sub> bicyclane	2243	0	0
52	C <sub>19</sub> bicyclane	3088	0	12314
53	unknown diterpane	39612	74272	0
54	4a(H)-19-norbornane	13678	13457	2604
55	C <sub>19</sub> bicyclane	0	3377	0
56	C <sub>19</sub> bicyclane	0	0	9663
57	17-norbornacyclic diterpane	0	2478	0
58	isopimarane	0	3584	1831
59	16a(H)-phylladiene	6102	6049	0
		12362		

Peak #	Compound		UB46E	UB47E
<b>Steranes, diasteranes m/z 217</b>				
60	5 $\alpha$ (H),14 $\beta$ (H),17 $\beta$ (H)-digrene	0	0	0
61	5 $\alpha$ (H),14 $\beta$ (H),17 $\beta$ (H)-homodigrene	0	2971	0
62	13 $\beta$ (H),17 $\alpha$ (H),20S-diacholestane	13855	2384	0
63	13 $\beta$ (H),17 $\alpha$ (H),20R-diacholestane	12833	3667	0
64	13 $\alpha$ (H),17 $\beta$ (H),20S-diacholestane	6920	0	791
65	13 $\alpha$ (H),17 $\beta$ (H),20R-diacholestane	7099	0	1320
66	24-methyl-13 $\beta$ (H),17 $\alpha$ (H),20S-diacholestane	5852	0	1815
67	24-methyl-13 $\beta$ (H),17 $\alpha$ (H),20R-diacholestane	6352	2286	0
68	24-C <sub>28</sub> $\alpha\beta$ dia 20S+ $\alpha\alpha$ C <sub>27</sub> , 20S	66727	9127	421
69	24-C <sub>28</sub> $\alpha\beta$ dia 20S+ $\beta\beta$ C <sub>27</sub> , 20R	26018	0	653
70	24-C <sub>28</sub> $\alpha\beta$ dia 20R+ $\beta\beta$ C <sub>27</sub> , 20S	7861	5078	0
71	14 $\alpha$ (H),17 $\alpha$ (H),20R-cholestane	127395	32457	976
72	24-ethyl-13 $\beta$ (H),17 $\alpha$ (H),20R-diacholestane	0	0	0
73	24-ethyl-13 $\beta$ (H),17 $\alpha$ (H),20S-diacholestane	6605	3557	0
74	24-methyl-14 $\alpha$ (H),17 $\alpha$ (H),20S-cholestane	14578	0	0
75	24-C <sub>28</sub> $\alpha\beta$ dia 20R+C <sub>28</sub> $\beta\beta$ 20R	24047	0	372
76	24-methyl-14 $\beta$ (H),17 $\beta$ (H),20S-cholestane	0	0	240
77	24-methyl-14 $\alpha$ (H),17 $\alpha$ (H),20R-cholestane	38608	90197	984
78	24-ethyl-14 $\beta$ (H),17 $\beta$ (H),20S-cholestane	24784	20363	1040
79	24-ethyl-14 $\beta$ (H),17 $\beta$ (H),20R-cholestane	19841	52154	1028
80	24-ethyl-14 $\beta$ (H),17 $\beta$ (H),20S-cholestane	3044	16905	664
81	24-ethyl-14 $\alpha$ (H),17 $\alpha$ (H),20R-cholestane	83925	475119	1783
				1460
<b>Monoaromatic steroids m/z 253</b>				
82	monoaromatic sterane C <sub>27</sub>	9733	577	0
83	monoaromatic sterane C <sub>27</sub>	18887	922	0
84	monoaromatic sterane C <sub>27</sub>	13725	13851	0
85	monoaromatic sterane C <sub>27</sub>	25827	1810	0
86	monoaromatic sterane C <sub>27</sub> +C <sub>28</sub>	0	3190	0
87	monoaromatic sterane C <sub>27</sub> +C <sub>28</sub>	16192	551	0
88	monoaromatic sterane C <sub>27</sub> +C <sub>28</sub>	7612	1671	0
89	monoaromatic sterane C <sub>27</sub> +C <sub>28</sub>	411615	51598	0
90	monoaromatic sterane C <sub>27</sub> +C <sub>28</sub>	8409	0	0
91	monoaromatic sterane C <sub>27</sub> +C <sub>28</sub>	62957	5739	0
92	monoaromatic sterane C <sub>28</sub> +C <sub>29</sub>	103600	52911	0
93	monoaromatic sterane C <sub>28</sub> +C <sub>29</sub>	231317	29219	0
94	monoaromatic sterane C <sub>28</sub> +C <sub>29</sub>	25186	9072	0
95	monoaromatic sterane C <sub>29</sub>	38071	3103	0
96	monoaromatic sterane C <sub>29</sub>	81368	40211	0
				136

 oil-shale type sample

 coal sample

 regular type sample

## APPENDIX 4.2

PCA Results, Source Rock Analysis GC-MS Data

### PCA, 20 variables, normalized, variance-covariance matrix

Variance extracted, first 10 axis

AXIS	Eigenvalue	% variance	cum. %var.	broken-stick
1	3.877	46.6	46.6	1.497
2	1.655	19.9	66.5	1.081
3	0.974	11.7	78.2	0.873
4	0.594	7.1	85.3	0.734
5	0.425	5.1	90.4	0.63
6	0.275	3.3	93.7	0.547
7	0.155	1.9	95.6	0.478
8	0.128	1.5	97.1	0.418
9	0.072	0.9	98.0	0.366
10	0.05	0.6	98.6	0.32

First 6 eigenvector loadings

Peak n°	attribut	Eigenvector					
		1	2	3	4	5	6
3	#1310	0.2665	0.2023	0.2395	-0.2515	-0.0976	-0.6082
5	#1441	0.2623	0.2141	0.1852	-0.265	-0.1569	-0.1992
16	#1816	0.0481	-0.0488	0.1476	-0.0616	0.0442	0.0683
19	#1841	-0.0843	-0.1562	-0.0478	0.0024	-0.2815	-0.0095
25	#1915	-0.2266	-0.2887	0.3133	-0.0315	-0.6438	0.0568
26	#1924	0.1016	0.0064	0.033	-0.0955	-0.0725	0.2771
28	#1947	-0.0654	-0.1006	-0.275	0.0073	-0.1468	-0.1292
30	#1967	-0.5882	0.1029	0.4304	-0.144	0.4643	0.0393
31	#1995	-0.2008	-0.0606	-0.339	0.1224	-0.078	-0.1861
32	#2034	-0.0504	-0.1326	0.2279	0.0724	-0.2207	0.1271
33	#2043	-0.0688	-0.1093	0.0044	0.0687	-0.1754	-0.0382
34	#2063	0.0955	0.7064	0.0889	0.5528	-0.2065	0.1924
45	#727	0.1554	-0.1478	0.1313	0.1791	0.1744	-0.2966
49	#814	0.4099	-0.4723	0.2376	0.499	0.2422	-0.023
54	#1134	0.3705	-0.0222	-0.175	-0.3475	0.0727	0.4444
58	#1219	0.1505	-0.0405	-0.0961	-0.2403	0.0277	0.1489
59	#1234	0.0798	0.0531	0.0317	-0.1768	-0.025	-0.141
71	#1791	-0.0577	-0.0057	-0.1063	0.0104	0.0147	0.0061
77	#1852	-0.0539	0.0151	-0.143	0.0291	0.0479	-0.0795
81	#1901	-0.1324	-0.0022	-0.4507	0.0977	0.0368	-0.2526
	cut-off:	0.118	0.141	0.09			

Coordinates (scores) of source rock samples

No.	samples	map-group	Axis (Component)					
			1	2	3	4	5	6
1	UB5E	1	0.635	0.3633	-0.0754	0.1062	-0.1118	0.0322
2	UB1E	1	0.7536	-0.2648	-0.0341	0.0727	0.1029	-0.1185
3	UB2E	1	-0.2637	-0.0269	0.0445	-0.1508	-0.0189	-0.0551
4	UB3E	1	-0.2969	-0.0942	0.0669	-0.0985	-0.165	0.0036
5	UB4E	1	-0.1367	0.0147	0.1542	-0.0786	-0.0442	-0.007
6	UB47E	1	0.4709	0.4165	-0.0738	0.1725	-0.1277	0.1501
7	UB36E	1	0.066	0.188	0.1239	-0.2484	-0.1175	-0.2243
8	UB17E	1	0.192	0.0163	0.1548	-0.0469	0.0682	-0.0411
9	UB18E	1	0.119	0.0528	0.159	-0.0481	0.0175	-0.0293
10	UB37E	1	-0.2486	0.2173	-0.0966	0.1466	-0.0916	0.0389
11	UB38E	1	-0.186	0.0305	0.1003	-0.0396	0.17	0.088
12	UB35E	1	0.3629	0.0832	0.1528	0.1506	-0.0089	-0.2715
13	UB16E	1	0.042	0.1243	0.1389	-0.1507	0.0758	-0.031
14	UB22E	2	-0.364	0.0197	-0.2931	0.0206	0.1427	-0.1004
15	UB10E	2	-0.1614	0.0477	0.1332	-0.0745	0.0614	0.04
16	UB11E	2	-0.079	0.1104	0.0612	-0.049	-0.0878	-0.0925
17	UB19E	2	-0.1574	0.0792	0.1007	0.0152	-0.0592	0.0182
18	UB20E	2	0.1553	0.4435	-0.0037	0.1859	-0.0554	0.0064
19	UB7E	2	-0.2559	0.1196	-0.0922	-0.056	0.2218	0.018
20	UB6E	2	-0.2188	0.1696	0.0615	-0.0398	0.0781	0.0788
21	UB8E	2	-0.205	0.17	0.0781	-0.0476	0.0753	0.0595
22	UB9E	2	-0.3658	-0.0218	-0.0583	-0.0784	0.1429	0.0141
23	UB29E	3	-0.0117	-0.0337	0.1302	0.1555	-0.0207	0.059
24	UB14E	3	0.0975	-0.1987	0.1251	-0.1214	-0.0862	0.057
25	UB21E	3	0.805	-0.4016	-0.1405	0.0692	0.2019	-0.0004
26	UB13E	3	-0.0374	0	0.1285	0.008	-0.0184	0.0222
27	UB12E	3	0.0376	-0.3008	0.1703	0.1272	0.0807	0.0346
28	UB25E	3	-0.0284	-0.3426	0.1152	0.1394	0.0455	0.0479
29	UB26E	3	-0.0782	-0.452	0.0061	0.1625	-0.2115	0.0431
30	UB27E	3	-0.1633	-0.3209	0.1058	0.0341	-0.0722	0.0822
31	UB30E	4	0.7882	-0.0201	-0.3358	-0.4295	-0.0586	0.1606
32	UB42E	5	-0.3247	-0.1775	-0.1349	0.0155	-0.1104	0.0359
33	UB41E	5	-0.3529	-0.0955	-0.1423	-0.0122	-0.0748	0.0088
34	UB39E	5	-0.2744	0.2755	-0.2624	0.1612	0.1771	0.0117
35	UB45E	5	-0.3146	-0.1911	-0.5683	0.027	-0.121	-0.1397

## APPENDIX 5

### Source Rock Extracts - Rock-Eval, GC and GC-MS Parameters

Well	depth ft	Sample no	Mapgroup	Extraction								GC			
				ECOM ppm	ASP	%Mai	%SAT	%ARO	%POL	%bran	P/ $\mu$ Ph	P/ $\mu$ nC <sub>11</sub>	P/ $\mu$ nC <sub>12</sub>	P/ $\mu$ nC <sub>13</sub>	C <sub>11</sub> /C <sub>12</sub>
Chevron 1 Chasel Unit Flying	10727 0	1E	1	176	17.4	82.6	59.6	23.6	16.8	74.1	3.47	0.74	0.28	1.78	1.95
Chevron Blanchard 1-33-3	8954 0	2E	1	1007	30.1	69.9	1.2	41.1	57.6	85.9	2.25	5.55	3.37	2.33	0.89
Chevron Blanchard 1-33-3	9430 0	3E	1	267	14.6	85.4	49.8	23.8	26.4	93.6	1.19	na	na	1.19	na
Chevron Blanchard 1-33-3	10481 5	4E3	1	91	11.6	88.4	57.6	21.7	20.7	80.4	1.93	1.22	0.54	1.23	1.48
Chevron Blanchard 1-33-3	11039 0	47E	1	266	16.0	84.0	85.2	20.7	14.1	72.9	1.56	2.21	1.66	1.41	0.77
Bow Valley 2-19A1E Dr Long	9716 5	5E	1	601	17.2	82.8	63.1	21.6	15.3	72.5	1.13	0.65	0.64	1.12	1.76
PanAm 1 USA Lyle Lingebach	6925 0	6E	2	834	23.1	76.9	27.6	33.1	39.2	87.2	2.63	3.65	2.50	2.25	1.51
PanAm 1 McLish Unit	8111 0	7E	2	278	34.8	65.2	39.0	26.2	34.8	68.9	1.49	1.38	1.35	1.48	0.88
PanAm 3 Unit/Pelican Lake	5789 0	8E	2	1517	23.0	77.0	39.7	29.0	31.2	94.6	1.83	5.40	4.12	1.56	1.04
PanAm 4 USA Pearl Broadhurst	4887 0	9E	2	400	22.4	77.6	29.7	23.1	47.2	81.4	0.96	2.61	2.68	0.96	0.73
Gulf Oil 1-20-4B Costas	5224 5	10E	2	1470	20.5	79.5	42.0	27.9	30.1	81.9	1.22	1.54	1.57	1.23	1
Natural Gas Co 22-30 Bench Glenn	4702 0	11E	2	473	13.0	87.0	33.9	29.0	37.2	79.5	1.17	0.68	0.57	1.05	1.58
Natural Gas Co 13-16 State	5381 0	12E	3	353	26.8	73.2	63.5	23.4	13.1	40.3	2.06	0.26	0.14	1.20	1.47
Mapco 4-11 D River Bent	4786 0	13E	3	666	3.6	98.4	65.9	16.9	17.2	64.3	1.51	0.78	0.45	1.07	1.89
Davis Oil 5 Panette Bench	5422 0	14E	3	275	13.5	88.5	69.3	17.3	13.4	48.5	1.80	0.41	0.22	1.12	1.46
Coors Ute Tribal 13-10D	6272 8	15E	4	112	8.9	91.1	80.0	4.4	15.6	89.4	1.59	0.91	0.67	1.34	2.19
Rio Bravo Oil 20-2 RU	9692 0	16E	1	1078	23.1	76.9	54.1	27.6	18.3	91.0	1.48	3.10	2.71	1.43	1.00
Chevron Lamicq Urury 2-8C	10844 0	17E	1	260	27.4	72.6	52.1	26.4	21.4	75.3	1.28	0.70	0.49	1.02	1.79
Chevron Lamicq Urury 2-8C	10950 0	18E	1	552	27.5	72.5	51.1	28.1	20.8	83.0	1.47	1.20	0.73	1.14	1.52
Natural Gas Co 23-24 Federal	4882.5	19E	2	651	18.7	81.3	41.4	22.0	36.6	80.8	1.26	1.28	0.96	1.11	1.33
Natural Gas Co 23-24 Federal	4978 0	20E	2	197	8.1	91.9	48.8	20.2	31.0	79.0	1.00	1.21	1.64	1.13	0.64
Diamond Shamrock 24-8 Paiute Federal	5450 0	21E	3	70	11.5	88.5	68.8	17.7	13.5	59.7	1.97	0.38	0.24	1.39	2.28
California Oil Red Wash 32	3850 0	22E	2	946	27.3	72.7	42.6	18.8	38.6	90.1	0.93	3.11	17.67	1.17	0.35
California Oil Red Wash 32	9745 0	23E	2	122	40.9	59.1	na	na	na	na	na	na	na	na	na
Sun Oil Co South Ouray No 1/Unit 1	4938 0	25E	3	193	18.6	81.4	63.4	19.7	17.0	28.6	1.52	0.83	0.58	1.20	1.88
Sun Oil Co South Ouray No 1/Unit 1	4955 0	26E	3	2245	43.5	58.5	38.3	41.4	22.3	53.1	5.37	3.81	0.88	3.18	0.72
Sun Oil Co South Ouray No 1/Unit 1	5170 0	27E	3	2330	32.4	87.6	47.0	32.3	20.8	87.5	3.48	2.33	0.65	1.97	1.02
Celsius Energy Co Island 18	4895 5	29E	3	2684	44.6	55.4	60.0	25.6	14.3	83.8	1.64	0.36	0.24	1.19	1.65
Carter Oil Josep Smith 1	8551 0	30E	4	224	2.6	97.4	74.7	11.8	13.5	54.3	0.91	0.55	0.42	0.76	1.24
Mountain Fuel Supply Cedar Rim 3	8507 0	31E	4	195	11.2	88.8	57.2	33.7	9.1	58.4	2.89	0.52	0.18	1.31	2.48
Diamond Shamrock Allen 34 5	5021 5	32E	3	745	6.9	93.1	69.2	15.1	15.7	68.4	0.77	0.77	0.68	0.72	1.11
Quinex Energy Leslie Taylor 24-5	12224 0	33E	1	190	27.0	73.0	58.0	34.5	9.5	63.4	2.88	0.28	0.10	1.17	3.07

Well	depth ft	Sample no	Map group	Extraction										GC			
				EOM ppm	ASP	%Mai	%SAT	%ARO	%POL	%bran	Pi/Ph	Pi/n-C <sub>11</sub>	Pi/n-C <sub>12</sub>	Pi+n-C <sub>13</sub> /Pi+n-C <sub>12</sub>	C <sub>11</sub> ,/C <sub>12</sub>		
Bow Valley Petroleum Ute 2-22A1E	12315.5	34E	1	67	5.8	94.2	87.2	18.5	14.3	43.2	1.73	0.08	0.04	1.03	2.90		
Bow Valley Petroleum Ute 2-22A1E	12368.5	46E	1	71	54.0	46.0	32.8	52.3	14.9	272.5	2.42	0.44	0.23	1.50	0.11		
Page Petroleum Inc Page Esson Ute 1-14B1E	8463.0	35E	1	343	24.0	76.0	46.2	31.1	22.7	67.3	0.99	0.46	0.56	1.11	2.16		
Chevron Hiko Bell Unit 1/Walker	10587.4	36E	1	839	34.4	65.6	60.3	25.5	14.1	79.2	1.89	1.24	0.78	1.50	1.46		
Gulf Oil 1 Whidlock	7583.0	35E	1	1840	24.7	75.3	60.1	15.1	24.9	80.5	0.99	4.62	6.70	1.05	0.70		
Gulf Oil 1 Whidlock	9020.0	36E	1	705	34.6	65.4	62.1	21.2	16.7	58.9	1.63	1.51	0.97	1.33	0.62		
Outcrop sample Indian Canyon 980714-2			5	2486	19.4	80.6	39.7	20.8	39.5	80.9	0.59	1.21	1.34	n.a.	n.a.		
Outcrop sample Gate Canyon 980714-1			5	2262	11.1	88.9	40.7	18.2	41.0	67.9	1.02	4.92	9.30	1.11	1.13		
Outcrop sample Black Shale Facies 930922-1		41E	5	882	32.9	67.1	44.9	17.8	37.3	55.2	1.53	1.13	0.79	1.27	0.60		
Outcrop sample Black Shale coal TR1928			5	13484	60.6	39.4	39.5	27.3	33.2	45.4	3.61	4.81	0.90	n.a.	0.60		
Outcrop sample EM-RR8			5	3492	75.0	25.0	31.8	15.1	53.1	74.3	3.38	2.67	0.80	2.05	0.51		

oil-shale type sample



coal sample



regular type sample



## APPENDIX 5

Well	depth ft	Sample no	GC					GC-MS terpanes								
			C <sub>11</sub> /C <sub>12</sub>	δ-caradane µg/g TOC	R22	CPI	C <sub>19</sub> /C <sub>18</sub> Tricyclic terpanes	22S/(22S+22R) C <sub>19</sub> hopane	Tm + Tm	Dihopane index	Quaternane index	Morepane/(morepane + hopane)	C <sub>18</sub>	Triacyclics	Gammacerane index	Gammacene µg/g TOC
Chevron 1 Chaset Unit Flying	10727.0	1E	2.65	13	0.93	1	0.19	0.57	0.67	0.80	0.30	0.00	1.90	0.62	4	
Chevron Blanchard 1-33-3	8954.0	2E	1.05	79	0.98	1.23	0.03	0.54	0.17	0.05	0.03	0.19	0.39	0.14	2	
Chevron Blanchard 1-33-3	9430.0	3E	n.a.	59	0.50	n.a.	0.03	0.60	0.14	0.03	0.05	0.12	0.32	0.18	51	
Chevron Blanchard 1-33-3	10481.5	4E3	0.49	581	1.02	1.02	0.03	0.59	0.41	0.11	0.05	0.10	0.61	0.30	2791	
Chevron Blanchard 1-33-3	11039.0	47E	0.48	174	0.97	0.98	0.05	0.57	0.54	1.64	0.68	0.12	1.28	2.36	157	
Bow Valley 2-19A1E Dr Long	9718.5	5E	0.86	60	1.04	1.09	0.06	0.62	0.74	2.72	0.28	0.11	1.96	3.08	125	
PanAm 1 USA Lyle Lingelbach	6925.0	6E	1.09	85	1.16	1.10	0.01	0.59	0.41	0.22	0.09	0.11	0.36	0.39	157	
PanAm 1 McLish Unit	6111.0	7E	1.03	438	1.09	1.01	0.05	0.54	0.30	0.13	0.24	0.10	0.35	0.26	89	
PanAm 3 Unit/Pelican Lake	5789.0	8E	0.42	753	1.00	1.03	0.01	0.60	0.47	0.24	0.03	0.11	0.39	0.38	543	
PanAm 4 USA Pearl Broadhurst	4687.0	9E	0.54	238	1.06	1.09	0.10	0.44	0.17	0.03	0.15	0.22	0.13	0.14	38	
Gulf Oil 1-20-4B Costas	5224.5	10E	1.08	623	1.10	1.10	0.02	0.61	0.63	0.29	0.03	0.10	0.45	0.28	77	
Natural Gas Co 22-30 Bench Glenn	4702.0	11E	0.81	67	1.03	0.98	0.05	0.59	0.38	0.13	0.08	0.18	0.55	0.44	19	
Natural Gas Co 13-16 State	5381.0	12E	1.06	0	1.03	1.03	0.39	0.59	0.54	0.25	0.06	0.08	0.18	0.19	4	
Mapco 4-11 D River Bent	4786.0	13E	0.40	187	1.18	1.03	0.08	0.63	0.38	0.43	0.14	0.13	0.39	0.36	87	
Davis Oil 5 Panette Bench	5422.0	14E	0.90	0	0.95	1.06	0.31	0.61	0.57	0.39	0.07	0.13	0.32	0.19	32	
Coors Ute Tribal 13-10D	6272.6	15E	1.12	74	0.99	1.01	0.00	0.00	0.00	0.00	0.00	0.00	0.00	0.00	0	
Rio Bravo Oil 20-2 RU	9692.0	16E	0.70	558	1.14	0.75	0.04	0.64	0.66	0.71	0.03	0.09	0.80	0.32	162	
Chevron Lamicq Urury 2-8C	10844.0	17E	0.65	61	1.07	0.95	0.06	0.59	0.63	0.58	0.08	0.10	0.83	0.39	41	
Chevron Lamicq Urury 2-8C	10950.0	18E	0.58	327	1.05	1.07	0.04	0.56	0.67	0.59	0.12	0.10	0.79	0.42	79	
Natural Gas Co 23-24 Federal	4882.5	19E	0.80	189	1.05	0.95	0.04	0.60	0.39	0.11	0.04	0.13	0.38	0.44	97	
Natural Gas Co 23-24 Federal	4978.0	20E	0.58	30	1.00	1.17	0.02	0.55	0.39	0.23	0.06	0.11	1.02	1.29	284	
Diamond Shamrock 24-8 Paiute Federal	5450.0	21E	4.01	0	0.96	1.08	0.29	0.64	0.58	1.18	0.24	0.22	1.03	0.19	0	
California Oil Red Wash 32	3950.0	22E	0.40	5038	0.83	2.64	0.02	0.42	0.04	0.02	0.01	0.33	0.16	0.21	218	
California Oil Red Wash 32	9745.0	23E	n.a.	n.a.	n.a.	n.a.	n.a.	n.a.	n.a.	n.a.	n.a.	n.a.	n.a.	n.a.	n.a.	
Sun Oil Co South Ouray No 1/Unit 1	4938.0	25E	1.24	10	1.00	1.12	0.63	0.55	0.38	0.19	0.07	0.17	0.12	0.15	28	
Sun Oil Co South Ouray No 1/Unit 1	4955.0	26E	1.01	0	0.92	1.24	0.00	0.61	0.08	0.10	0.00	0.29	0.03	0.12	3	
Sun Oil Co South Ouray No 1/Unit 1	5170.0	27E	0.52	0	1.00	1.16	0.16	0.60	0.30	0.15	0.06	0.13	0.18	0.09	20	
Celsius Energy Co Island 16	4695.5	29E	0.86	0	1.05	1.00	0.16	0.59	0.43	0.29	0.06	0.14	0.26	0.51	99	
Carter Oil Josep Smith 1	8551.0	30E	0.36	0	0.98	1.04	0.26	0.00	0.46	2.52	0.91	0.00	2.75	1.31	0	
Mountain Fuel Supply Cedar Rim 3	8507.0	31E	1.78	0	0.98	0.98	0.00	0.00	0.00	0.00	0.00	0.00	0.00	0.00	0	
Diamond Shamrock Allen 34 S	5021.5	32E	0.34	218	0.98	1.10	0.08	0.61	0.64	0.51	0.04	0.08	0.81	0.65	713	
Quinex Energy Leslie Taylor 24-5	12224.0	33E	1.62	0	0.99	1.03	0.00	0.00	0.00	0.00	0.00	0.00	0.00	0.00	0	

Well	depth ft	Sample no	GC						GC-MS terpanes								
			C <sub>1</sub> /C <sub>2</sub>	% carbonate µg/g TOC	R22	CPI	C <sub>19</sub> C <sub>21</sub> Tricyclic terpanes	22S(22S+22R) C <sub>19</sub> hopane	Ts/Ts+Tr	Dahopane index	Cleanane index	Moreane/(moreane+hopane)	C <sub>2</sub>	Tricyclic/pentacyclics	Gammacerane index	Gammaconene µg/g TOC	
Bow Valley Petroleum Ute 2-22A1E	12315.5	34E	1.40	0	0.99	1.00	0.00	0.00	0.00	0.00	0.00	0.00	0.00	0.00	0.00	0.00	
Bow Valley Petroleum Ute 2-22A1E	12366.5	46E	1.01	4	1.07	1.00	0.19	0.00	0.00	0.00	0.00	0.00	0.00	0.27	0.57	0	
Page Petroleum Inc Page Esson Ute 1-14B1E	8463.0	35E	1.49	2	0.95	1.06	0.09	0.56	0.46	0.05	0.02	0.08	1.31	0.88	42		
Chevron Hike Bell Unit 1/Walker	10587.4	38E	1.07	87	0.98	1.04	0.04	0.57	0.27	0.07	0.08	0.09	1.39	0.37	119		
Gulf Oil 1 Whitlock	7583.0	██████	0.17	1118	0.95	1.42	0.01	0.54	0.08	0.02	0.02	0.31	0.22	0.70	6472		
Gulf Oil 1 Whitlock	9020.0	38E	0.32	206	1.00	1.05	0.08	0.56	0.69	0.44	0.16	0.10	0.37	0.25	166		
Outcrop sample Indian Canyon 980714-2		██████	n.a.	2470	n.a.	n.a.	0.00	0.39	0.06	0.08	0.00	0.20	0.11	0.59	745		
Outcrop sample Gate Canyon 980714-1		██████	0.42	749	0.62	2.50	0.00	0.00	0.00	0.00	0.00	0.00	0.00	0.00	0.00	96	
Outcrop sample Black Shale Facies 930922-1		41E	0.52	57	1.05	1.10	0.15	0.47	0.22	0.10	0.15	0.19	0.07	0.21	47		
Outcrop sample Black Shale coal TR1928		██████	0.47	0	n.a.	n.a.	0.19	0.56	0.11	0.14	0.13	0.24	0.11	0.17	14		
Outcrop sample EM-RR8		██████	0.28	0	0.91	2.11	0.69	0.18	0.12	0.25	0.20	0.46	0.05	0.11	6		

oil-shale type sample



coal sample



regular type sample



## APPENDIX 5

Well	depth ft	Sample no	GC-MS				Sesquiterpanes and diterpanes									
			C <sub>19</sub> C <sub>20</sub> 17 $\alpha$ hopanes	Methyl hopanes	C <sub>19</sub> Tetracyclic terpane	C <sub>19</sub> SIC <sub>20</sub> Sub-hopane	Unknown terpane/C <sub>20</sub> 14 hopane	Sesqui / sesqui + diterpanes	Sesqui / sesqui + pentac terpanes	Sesqui / sesqui + steranes	Diterpanes/ diterpanes + pentac terpanes	Diterpanes/ diterpanes + steranes	Diterpanes/ diterpanes + steranes	Diquat dimethane/ Diquat + dimethane + homodimethane	Isopimarane/ isopimarane + phytocadinane	Homodimethane/ homodimethane + isopimarane
Chevron 1 Chasel Unit Flying	10727 0	1E	0.48	+	-	0	0	0.51	0.544	0.68	0.533	0.671	0.219	0.65	0.87	
Chevron Blanchard 1-33-3	8954 0	2E	0.48	+	-	0.08	0.00	0.10	0.01	0.13	0.11	0.56	0.16	0.17	0.72	
Chevron Blanchard 1-33-3	9430 0	3E	0.78	+	-	0.13	0.00	0.22	0.01	0.08	0.03	0.23	0.33	0.23	0.79	
Chevron Blanchard 1-33-3	10481 5	4E3	0.53	+	-	0.11	0.05	0.41	0.09	0.83	0.12	0.87	0.35	0.37	0.82	
Chevron Blanchard 1-33-3	11039 0	47E	0.33	-	-	0.28	0.00	0.34	0.17	0.70	0.28	0.82	0.00	0.46	0.83	
Bow Valley 2-19A1E Dr Long	9718 5	5E	0.35	-	-	0.28	0.00	0.40	0.37	0.79	0.47	0.85	0.23	0.44	0.80	
PanAm 1 USA Lyle Lingelbach	8925 0	6E	0.29	+	-	0.12	0.03	0.08	0.01	0.23	0.12	0.77	0.00	0.21	0.61	
PanAm 1 McLish Unit	8111 0	7E	0.18	+	-	0.15	0.00	0.20	0.04	0.11	0.15	0.33	0.34	0.25	0.71	
PanAm 3 Unit/Pelican Lake	5789 0	8E	0.31	-	-	0.23	0.00	0.18	0.02	0.31	0.11	0.71	0.20	0.22	0.72	
PanAm 4 USA Pearl Broadhurst	4687 0	9E	0.28	+	+	0.32	0.00	0.27	0.02	0.26	0.05	0.49	0.49	0.24	0.67	
Gulf Oil 1-20-4B Costas	5224 5	10E	0.35	+	-	0.13	0.03	0.36	0.08	0.70	0.13	0.81	0.20	0.32	0.84	
Natural Gas Co 22-30 Bench Glenn	4702 0	11E	0.47	+	-	0.14	0.00	0.26	0.06	0.30	0.16	0.55	0.24	0.18	0.86	
Natural Gas Co 13-16 State	5381 0	12E	0.53	-	++	0.14	0.07	0.78	0.32	0.92	0.12	0.76	0.35	0.49	0.95	
Mapco 4-11 D River Bent	4786 0	13E	0.40	+	+	0.31	0.00	0.46	0.10	0.43	0.11	0.47	0.11	0.32	0.92	
Davis Oil 5 Panetta Bench	5422 0	14E	0.68	-	++	0.24	0.00	0.38	0.18	0.77	0.26	0.84	0.23	0.68	0.70	
Coors Ute Tribal 13-10D	8272 8	15E	0.00	-	-	0.00	0.00	0.35	1.00	1.00	1.00	1.00	0.00	1.00	0.00	
Rio Bravo Oil 20-2 RU	9692 0	16E	0.27	+	-	0.15	0.18	0.35	0.12	0.85	0.21	0.92	0.29	0.32	0.78	
Chevron Lamicq Urury 2-8C	10844 0	17E	0.34	+	-	0.14	0.09	0.52	0.26	0.89	0.24	0.88	0.29	0.36	0.87	
Chevron Lamicq Urury 2-8C	10950 0	18E	0.40	-	-	0.24	0.14	0.52	0.21	0.92	0.19	0.91	0.42	0.38	0.86	
Natural Gas Co 23-24 Federal	4882 5	19E	0.50	+	+	0.08	0.00	0.43	0.09	0.52	0.11	0.59	0.31	0.18	0.91	
Natural Gas Co 23-24 Federal	4978 0	20E	0.29	+	-	0.30	0.00	0.38	0.16	0.51	0.25	0.84	0.31	0.27	0.84	
Diamond Shamrock 24-8 Pault Federal	5450 0	21E	0.45	-	+	0.59	0.00	0.54	0.70	0.99	0.67	0.99	0.28	0.68	0.80	
California Oil Red Wash 32	3950 0	22E	0.21	+	-	0.00	0.00	0.29	0.02	0.05	0.05	0.11	0.65	0.25	0.73	
California Oil Red Wash 32	9745 0	23E	n.a.	n.a.	n.a.	n.a.	n.a.	n.a.	n.a.	n.a.	n.a.	n.a.	n.a.	n.a.	n.a.	
Sun Oil Co South Ouray No 1/Unit 1	4938 0	25E	0.58	-	++	0.19	0.03	0.75	0.26	0.89	0.11	0.73	0.19	0.47	0.96	
Sun Oil Co South Ouray No 1/Unit 1	4955 0	26E	1.03	-	+	0.09	0.45	0.85	0.19	0.77	0.04	0.37	0.16	0.00	1.00	
Sun Oil Co South Ouray No 1/Unit 1	5170 0	27E	0.72	-	+	0.14	0.04	0.74	0.17	0.70	0.07	0.48	0.21	0.57	0.96	
Celsius Energy Co Island 16	4895 5	29E	0.49	+	++	0.15	0.00	0.65	0.19	0.73	0.11	0.58	0.22	0.29	0.96	
Carter Oil Josep Smith 1	8551 0	30E	1.04	-	-	0.00	0.89	0.12	0.22	0.50	0.67	0.88	0.24	0.69	0.35	
Mountain Fuel Supply Cedar Rim 3	8507 0	31E	0.00	-	-	0.00	0.00	0.77	1.00	1.00	1.00	1.00	0.45	1.00	0.82	
Diamond Shamrock Allen 34 5	5021 5	32E	0.34	+	++	0.20	0.15	0.39	0.12	0.69	0.17	0.77	0.27	0.66	0.80	
Quinex Energy Leslie Taylor 24-5	12224 0	33E	0.00	-	-	0.00	0.00	0.39	1.00	1.00	1.00	1.00	1.00	1.00	0.00	

Well	depth ft	Sample no	GC-MS					Sesquiterpanes and diterpanes								
			C <sub>n</sub> C <sub>n+1</sub> hopanes	Methyl hopanes	C <sub>n</sub> Tetracyclic terpane	C <sub>n</sub> SIC <sub>n+1</sub> Sub hopane	Unknown terpane/C <sub>n+1</sub> hopane	Sesqui / sesquit + diterpanes	Sesqui / sesquit + pentac terpanes	Sesqui / sesquit + steranes	Diterpanes/ diterpanes + pentac terpanes	Diterpanes/ diterpanes + steranes	BQ(H)-dimethyl/BQ(H)-dimane/homodimane	Isopimarane/ isoprimalane + phyllocladane	Homodimane/ homodimane/isoprimalane	
Bow Valley Petroleum Ute 2-22A1E	12315.5	34E	0.00	-	-	0.00	0.00	0.75	1.00	0.95	1.00	0.87	0.19	1.00	0.67	
Bow Valley Petroleum Ute 2-22A1E	12366.5	46E	0.44	-	-	0.00	0.00	0.58	0.15	0.43	0.12	0.35	0.00	1.00	0.77	
Page Petroleum Inc Page Esson Ute 1-14B1E	8463.0	35E	0.53	+	-	0.11	0.00	0.61	0.48	0.89	0.35	0.84	0.48	0.26	0.92	
Chevron Hiko Bell Unit 1/Walker	10587.4	38E	0.49	+	+	0.00	0.04	0.27	0.14	0.83	0.31	0.93	0.37	0.21	0.25	
Gulf Oil 1 Whirlpool	7583.0		0.48	+	-	0.12	0.01	0.06	0.00	0.02	0.03	0.21	1.00	0.28	0.00	
Gulf Oil 1 Whirlpool	9020.0	38E	0.25	+	-	0.15	0.00	0.43	0.11	0.69	0.14	0.74	0.20	0.48	0.84	
Outcrop sample Indian Canyon 980714-2			0.10	+	-	0.00	0.00	0.12	0.01	0.01	0.04	0.09	0.59	0.17	0.66	
Outcrop sample Gate Canyon 980714-1			0.00	+	-	0.00	0.00	0.15	1.00	1.00	1.00	1.00	0.57	0.14	0.71	
Outcrop sample Black Shale Facies 930922-1		41E	0.58	+	+	0.24	0.00	0.23	0.01	0.03	0.04	0.11	0.29	0.00	1.00	
Outcrop sample Black Shale coal TR1928			0.56	+	+	0.05	0.06	0.42	0.03	0.08	0.04	0.11	0.00	0.00	1.00	
Outcrop sample EM-RR8			0.51	-	-	0.00	0.09	0.02	0.00	0.00	0.03	0.13	0.00	0.37	0.37	

oil-shale type sample



coal sample



regular type sample



## APPENDIX 5

Well	depth ft	Sample no	Steranes, diginanes								% biomarkers		
			Dimane/ dimane+phylocladane	20S/(20S+20R) n.d. C <sub>29</sub>	29/(29S+29R) C <sub>29</sub>	Diginanes/steranes	Sterane/terpanes	Methyl steranes	Diasterane-index	% Sesquiterpanes	% Diterpanes	% Tricyclic terpanes	% Hopanes
Chevron 1 Chase Unit Flying	10727 0	1E	0.78	0.64	0.47	0.04	0.19	+++	1.68	20.5	19.6	32.6	17.2
Chevron Blanchard 1-33-3	8954 0	1E	0.10	0.39	0.28	0.01	0.07	-	0.00	0.9	7.5	24.3	61.5
Chevron Blanchard 1-33-3	9430 0	2E	0.35	0.43	0.27	0.00	0.08	-	0.00	0.7	2.4	21.4	67.8
Chevron Blanchard 1-33-3	10481 5	4E3	0.60	0.44	0.68	0.00	0.01	-	0.00	5.1	7.3	32.6	53.7
Chevron Blanchard 1-33-3	11039 0	47E	0.00	0.43	0.58	0.00	0.03	+	2.38	8.7	13.0	43.5	33.9
Bow Valley 2-19A1E Dr Long	9716 5	5E	0.49	0.46	0.68	0.00	0.05	-	1.80	12.9	19.5	42.5	21.7
PanAm 1 USA Lyle Lingelbach	6925 0	5E	0.00	0.20	0.31	0.00	0.03	-	0.00	0.8	8.9	23.2	64.4
PanAm 1 McLish Unit	8111 0	5E	0.29	0.11	0.15	0.00	0.24	-	0.09	2.2	9.1	18.3	51.9
PanAm 3 Unit/Pelican Lake	5789 0	5E	0.15	0.37	0.42	0.00	0.03	-	0.02	1.5	8.1	24.2	62.8
PanAm 4 USA Pearl Broadhurst	4687 0	5E	0.37	0.33	0.27	0.00	0.05	+	0.00	1.6	4.4	10.6	78.8
Gulf Oil 1-20-4B Costas	5224 5	5E	0.38	0.57	0.39	0.00	0.02	-	0.20	5.0	9.0	26.1	57.8
Natural Gas Co 22-30 Bench Glenn	4702 0	11E	0.30	0.27	0.19	0.00	0.09	-	0.00	3.4	9.7	27.9	51.2
Natural Gas Co 13-18 State	5381 0	12E	0.90	0.54	0.59	0.02	0.03	++	0.57	25.8	7.1	10.1	54.6
Mapco 4-11 D River Bent	4786 0	13E	0.42	0.48	0.50	0.00	0.10	+	0.05	6.1	7.2	22.1	56.4
Davis Oil 5 Panette Bench	5422 0	14E	0.60	0.46	0.59	0.02	0.05	++	0.98	11.3	18.2	18.1	50.9
Coors Ute Tribal 13-10D	6272 8	15E	0.00	0.00	0.00	0.00	0.00	n.a.	n.a.	34.9	85.1	0.0	0.0
Rio Bravo Oil 20-2 RU	9692 0	5E	0.41	0.78	0.41	0.00	0.01	-	0.00	6.2	11.8	36.0	44.9
Chevron Lamicq Urury 2-8C	10844 0	17E	0.81	0.58	0.53	0.00	0.02	-	0.00	13.6	12.6	32.6	39.5
Chevron Lamicq Urury 2-8C	10850 0	18E	0.71	0.60	0.48	0.00	0.01	-	0.65	11.3	10.3	34.1	43.3
Natural Gas Co 23-24 Federal	4882.5	5E	0.50	0.34	0.39	0.01	0.06	-	0.08	5.6	7.6	22.3	59.2
Natural Gas Co 23-24 Federal	4978 0	20E	0.48	0.31	0.30	0.00	0.07	+	0.08	6.9	12.1	37.4	38.8
Diamond Shamrock 24-8 Paito Federal	5450 0	21E	0.77	0.00	0.00	2.28	0.01	+	n.a.	38.5	31.2	15.7	15.3
California Oil Red Wash 32	3950 0	22E	0.63	0.15	0.16	0.00	0.30	-	0.00	1.2	3.0	10.1	82.5
California Oil Red Wash 32	9745 0	23E	n.a.	n.a.	n.a.	n.a.	n.a.	n.a.	n.a.	n.a.	n.a.	n.a.	n.a.
Sun Oil Co. South Ouray No 1/Unit 1	4938 0	25E	0.84	0.43	0.40	0.00	0.04	+	0.38	21.6	7.2	7.4	81.2
Sun Oil Co. South Ouray No 1/Unit 1	4955 0	26E	1.00	0.44	0.29	0.00	0.07	-	0.12	17.0	3.0	2.0	72.9
Sun Oil Co. South Ouray No 1/Unit 1	5170 0	27E	0.89	0.42	0.48	0.00	0.07	++	0.75	13.0	4.6	11.6	85.2
Celsius Energy Co Island 18	4895 5	29E	0.74	0.49	0.42	0.00	0.06	++	0.27	13.8	7.3	15.4	58.2
Carter Oil Josep Smith 1	8551 0	30E	0.27	0.37	0.48	0.08	0.07	+	0.41	4.5	32.2	43.0	15.8
Mountain Fuel Supply Cedar Rim 3	8507 0	31E	1.00	0.00	0.00	0.00	0.00	n.a.	n.a.	76.9	23.1	0.0	0.0
Diamond Shamrock Allen 34 5	5021 5	32E	0.51	0.51	0.64	0.00	0.03	+	0.26	8.1	9.5	36.6	45.0
Quinex Energy Leslie Taylor 24-S	12224 0	33E	1.00	0.00	0.00	0.00	0.00	n.a.	n.a.	38.7	81.3	0.0	0.0

Well	depth ft	Sample no	Steranes, diginanes								% biomarkers			
			Dumane/ dumane+phyllodadane	20S/(20S+20R) $\mu\text{C}_{27}$	$\Delta D/(D_0 + D_1)$ C <sub>28</sub>	Diginane/Steranes	Sterane/Sterpanes	Methyl steranes	Diasterane index	% Sequiterpanes	% Diterpanes	% Tricyclic terpanes	% Hopanes	
Bow Valley Petroleum Ute 2-22A1E	12315.5	34E	1.00	0.31	0.42	0.00	0.00	-	0.00	71.9	24.4	0.0	0.0	
Bow Valley Petroleum Ute 2-22A1E	12368.5	46E	0.00	0.37	0.37	0.00	0.15	-	0.00	9.9	7.2	14.9	54.6	
Page Petroleum Inc Page Esson Ute 1-14B1E	8463.0	35E	0.79	0.45	0.55	0.05	0.04	-	0.00	22.1	14.2	34.5	26.3	
Chevron Hiko Bell Unit 1/Walker	10587.4	36E	0.05	0.44	0.64	0.00	0.01	--	0.00	5.5	14.9	45.6	32.9	
Gulf Oil 1 Whitlock	7583.0	[Hatched]	0.27	0.28	0.15	0.00	0.07	-	0.00	0.1	2.1	18.4	73.4	
Gulf Oil 1 Whitlock	9020.0	38E	0.55	0.58	0.41	0.00	0.04	--	0.56	7.1	9.3	21.7	58.7	
Outcrop sample Indian Canyon 980714-2		[Hatched]	0.37	0.13	0.11	0.00	0.30	+	0.00	0.4	2.8	7.2	62.3	
Outcrop sample Gate Canyon 980714-1		[Hatched]	0.35	0.00	0.00	0.00	0.00	-	n.a.	14.8	85.2	0.0	0.0	
Outcrop sample Black Shale Facies 930922-1		41E	0.37	0.19	0.22	0.00	0.33	+++	0.00	0.9	3.1	4.7	66.4	
Outcrop sample Black Shale coal TR1928		[Hatched]	0.00	0.23	0.17	0.00	0.26	+++	0.25	1.9	2.6	7.2	68.0	
Outcrop sample EM-RR8		[Hatched]	0.00	0.04	0.12	0.00	0.21	-	0.01	0.1	2.5	3.8	76.2	

oil-shale type sample      [Hatched]  
 coal sample      [Horizontal lines]  
 regular type sample      [Empty box]

## APPENDIX 5

Well	depth ft	Sample no	$\alpha\alpha 20R$ steranes						Rock-Eval									
			% Steranes + dia steranes	% Dignane + homodignane	% C <sub>27</sub>	% C <sub>29</sub>	% C <sub>30</sub>	T <sub>max</sub>	C	S1	S2	S3	P1	S2/S3	TOC %	H/I (mg HC/g TOC)		
Chevron 1 Chase Unit Flying	10727.0	1E	9.6	0.4	58.3	15.0	28.7	448	0.20	7.8	0.31	0.02	25.3	2.06	38.0			
Chevron Blanchard 1-33-3	8954.0		5.9	0.0	27.4	28.9	43.7	434	0.48	24.1	0.63	0.02	38.3	3.22	74.9			
Chevron Blanchard 1-33-3	9430.0		7.8	0.0	8.5	25.0	68.5	444	0.24	33.4	0.88	0.01	38.0	4.02	83.0			
Chevron Blanchard 1-33-3	10481.5	4E3	1.1	0.0	42.6	28.5	28.9	437	1.19	9.5	0.51	0.11	18.7	1.83	52.0			
Chevron Blanchard 1-33-3	11039.0	47E	2.9	0.0	28.9	27.5	43.6	438	0.51	2.7	0.29	0.16	9.34	0.89	30.4			
Bow Valley 2-19A1E Dr Long	9718.5	5E	3.5	0.0	42.8	21.3	38.0	448	0.90	9.7	0.84	0.08	11.5	2.38	40.5			
PanAm 1 USA Lyle Linglebach	6925.0		2.6	0.0	38.2	35.8	26.0	431	0.29	20.3	0.60	0.01	33.9	2.42	84.0			
PanAm 1 McLish Unit	6111.0		18.5	0.0	41.9	18.3	41.7	424	0.09	3.7	0.31	0.02	12.0	1.18	31.4			
PanAm 3 Unit/Pelican Lake	5789.0		3.3	0.0	38.7	33.5	29.8	436	1.02	28.0	0.87	0.04	29.9	3.60	72.3			
PanAm 4 USA Pearl Broadhurst	4687.0		4.6	0.0	38.8	32.6	30.4	432	0.13	17.7	0.73	0.01	24.2	2.23	79.2			
Gulf Oil 1-20-4B Costas	5224.5		2.1	0.0	49.3	24.2	26.4	435	1.22	18.1	0.73	0.07	22.0	2.44	65.9			
Natural Gas Co 22-30 Bench Glenn	4702.0	11E	7.8	0.0	31.9	22.9	45.2	439	0.29	35.9	0.48	0.01	74.8	4.63	77.5			
Natural Gas Co 13-18 State	5381.0	12E	2.3	0.1	30.5	23.6	45.9	446	0.97	15.9	0.83	0.06	19.2	3.32	47.9			
Mapco 4-11 D River Bent	4786.0	13E	8.2	0.0	33.1	27.2	39.7	442	0.83	17.1	0.51	0.05	33.6	2.60	65.9			
Davis Oil 5 Panette Bench	5422.0	14E	3.4	0.1	35.4	16.7	47.9	436	0.22	1.7	0.39	0.12	4.3	0.69	24.3			
Coors Ute Tribal 13-10D	6272.8	15E	0.0	0.0	0.0	0.0	0.0	445	0.11	1.2	0.37	0.08	3.29	0.65	18.7			
Rio Bravo Oil 20-2 RU	9892.0		11.1	0.0	28.1	36.4	35.5	436	0.77	11.7	0.60	0.08	19.4	2.44	47.7			
Chevron Lamicq Urury 2-8C	10844.0	17E	1.7	0.0	37.2	25.5	37.3	439	0.28	7.0	0.55	0.04	12.7	1.68	41.4			
Chevron Lamicq Urury 2-8C	10950.0	18E	1.0	0.0	35.1	23.4	41.5	430	0.42	5.2	0.58	0.08	8.89	1.08	47.7			
Natural Gas Co 23-24 Federal	4882.5		5.3	0.0	42.3	23.0	34.7	434	1.10	68.3	1.74	0.02	39.2	8.28	82.4			
Natural Gas Co 23-24 Federal	4978.0	20E	6.7	0.0	39.3	23.9	36.8	423	0.19	4.0	0.43	0.05	9.39	0.94	42.9			
Diamond Shamrock 24-8 Paiute Federal	5450.0	21E	0.4	1.0	0.0	0.0	0.0	440	0.05	0.5	0.22	0.10	2.04	0.40	11.2			
California Oil Red Wash 32	3950.0		23.3	0.0	13.6	32.4	54.0	433	0.90	27.8	1.34	0.03	20.7	3.32	83.8			
California Oil Red Wash 32	9745.0	23E	n.a.	n.a.	n.a.	n.a.	n.a.	440	0.03	1.3	0.18	0.02	7.44	1.37	9.7			
Sun Oil Co South Ouray No 1/Unit 1	4938.0	25E	2.6	0.0	33.4	23.7	42.9	445	0.38	14.0	0.68	0.03	20.6	2.24	62.4			
Sun Oil Co South Ouray No 1/Unit 1	4955.0		5.1	0.0	22.8	9.7	67.5	432	2.35	58.3	4.05	0.04	13.9	21.3	28.4			
Sun Oil Co South Ouray No 1/Unit 1	5170.0	27E	5.5	0.0	44.4	9.9	45.7	436	2.75	50.9	2.58	0.05	19.7	13.2	38.7			
Celsius Energy Co Island 16	4895.5	29E	5.2	0.0	32.3	24.3	43.5	440	3.40	75.1	2.76	0.04	27.0	15.7	47.9			
Carter Oil Josep Smith 1	8551.0	30E	4.4	0.3	27.5	26.2	46.3	291	0.48	0.7	0.38	0.42	1.76	0.31	21.6			
Mountain Fuel Supply Cedar Rim 3	8507.0	31E	0.0	0.0	0.0	0.0	0.0	463	0.91	6.4	0.39	0.12	16.5	6.32	10.1			
Diamond Shamrock Allen 34 S	5021.5	32E	2.8	0.0	32.4	26.2	41.4	432	1.41	4.3	0.80	0.25	5.31	0.92	48.1			
Quinex Energy Leslie Taylor 24-5	12224.0	33E	0.0	0.0	0.0	0.0	0.0	448	0.39	2.7	0.14	0.13	19.1	3.85	7.3			

Well	depth ft	Sample no	% Steranes+staeranes	% Diginane+homodiginate	$\alpha\alpha 20R$ steranes				Rock-Eval								
					% C <sub>27</sub>	% C <sub>28</sub>	% C <sub>29</sub>	T <sub>10</sub> °C	S1	S2	S3	PI	S2/S3	TOC %	H (mg HC/g TOC)		
Bow Valley Petroleum Ute 2-22A1E	12315.5	34E	3.7	0.0	20.7	25.3	54.0	444	0.06	0.9	0.17	0.06	5.47	1.10	84		
Bow Valley Petroleum Ute 2-22A1E	12368.5	46E	13.3	0.2	26.1	26.3	47.6	444	0.05	0.3	0.16	0.16	1.8	0.71	39.0		
Page Petroleum Inc Page Esson Ute 1-1481E	8483.0	35E	2.8	0.1	22.3	35.5	42.2	450	1.34	65.0	1.24	0.02	52.4	11.3	573		
Chevron Hiko Bell Unit 1/Walker	10587.4	36E	1.1	0.0	26.7	30.5	42.8	445	1.55	7.2	2.26	0.18	3.19	3.33	217		
Gulf Oil 1 Whitlock	7583.0		7.9	0.0	23.1	28.2	48.7	431	2.43	9.0	2.12	0.21	4.25	1.52	582		
Gulf Oil 1 Whitlock	9020.0	38E	3.3	0.0	43.2	20.8	38.1	432	2.62	9.5	1.80	0.22	5.27	1.62	585		
Outcrop sample Indian Canyon 980714-2			27.3	0.0	9.6	23.0	87.4	435	2.94	138	4.27	0.02	32.4	13.6	1020		
Outcrop sample Gate Canyon 980714-1			0.0	0.0	0.0	0.0	0.0	441	1.85	142	2.82	0.01	50.2	15.8	898		
Outcrop sample Black Shale Facies 930922-1		41E	24.9	0.0	34.6	22.1	43.3	438	0.65	43.0	2.73	0.01	15.8	5.88	734		
Outcrop sample Black Shale coal TR1928			20.3	0.0	51.0	15.4	33.6	417	8.06	399	9.36	0.02	42.6	67.7	589		
Outcrop sample EM-RR8			17.4	0.1	5.4	15.1	79.5	430	0.68	74.2	33.2	0.01	2.2	32.2	230		

oil-shale type sample



coal sample



regular type sample



## APPENDIX 5

Well	depth ft	Sample no	GC qualitative					
			OI (mg CO <sub>2</sub> /g TOC)	S1/S2	Maximum carbon number in GC	Maximum peak in GC	Modal	lithology
Chevron 1 Chase Unit Flying	10727 0	1E	15	8.03	41	n-C <sub>17</sub>	1	black claystone (massive)
Chevron Blanchard 1-33-3	8954 0	2E	19	24.6	35	Pr	2	shale, black
Chevron Blanchard 1-33-3	9430 0	3E	21	33.6	n.a.	β-carot.	-	laminated black calc. shale, abund. org. clasts, above noncalc. shale, rootlike features
Chevron Blanchard 1-33-3	10481 5	4E3	27	10.7	37	n-C <sub>24</sub>	1	laminated black mudstone, coal clasts, thick sequence
Chevron Blanchard 1-33-3	11039 0	47E	32	3.22	39	Pr	2	black shale, org. clasts
Bow Valley 2-19A1E Dr Long	9716 5	5E	35	10.6	39	n-C <sub>22</sub>	1	black-dark brown laminated shale, v. fissile
PanAm 1 USA Lyle Lingelbach	8925 0	6E	24	20.6	35	Pr	2	grey-dark grey siltst., calc. cemented, shale drapes
PanAm 1 McLish Unit	8111 0	7E	26	3.8	47	n-C <sub>17</sub>	2	light brown siltst., contorted, w/ syneresis/bioturb., alternat. w/ calc. shale w/ large org BW21 clasts
PanAm 3 Unit/Pelican Lake	5789 0	8E	24	27.1	32	β-carot.	2	dark, laminated-bedded shale, small syneresis/bioturb.
PanAm 4 USA Pearl Broadhurst	4887 0	9E	32	17.8	48	n-C <sub>27</sub>	2	laminated grey brown mudst. w/ siltbeds, syneresis
Gulf Oil 1-20-4B Costas	5224 5	10E	29	17.3	38	Pr	2	laminated black-brown claystone, coal clasts
Natural Gas Co 22-30 Bench Glenn	4702 0	11E	10	36.2	57	n-C <sub>22</sub>	1	black brown shaly mudstone (massive), finely laminated, coal clasts abundant
Natural Gas Co 13-16 State	5381 0	12E	25	18.9	42	n-C <sub>17</sub>	1	black massive mudst., rare large pelecypode shells, fract.
Mapco 4-11 D River Bent	4786 0	13E	19	18.6	54	n-C <sub>22</sub>	1	dark brown ostracode grainstone, shells
Davis Oil 5 Panette Bench	5422 0	14E	56	1.9	55	n-C <sub>18</sub>	1	dark grey shale, flaser-laminated, syneresis
Coors Utz Trbal 13-10D	8272 8	15E	56	1.33	39	n-C <sub>17</sub>	1	thin brown-black shale, laminated, org. clasts
Rio Bravo Oil 20-2 RU	9692 0	16E	24	12.4	37	gammac.	2	laminated black shale, large and abundant org. clasts
Chevron Lamicq Urruty 2-8C	10844 0	17E	32	7.25	53	n-C <sub>22</sub>	1	black shaly mudstone, stained fract., faint lamination
Chevron Lamicq Urruty 2-8C	10950 0	18E	53	5.58	40	n-C <sub>22</sub>	1	black calc. shale, org. clasts, lenticular bed
Natural Gas Co 23-24 Federal	4882.5	19E	21	89.4	36	gammac.	1	noncalc. black-brown shale, laminated synsed. faults
Natural Gas Co 23-24 Federal	4978 0	20E	45	4.23	40	Pr	2	dark grey laminated shale, org. clasts
Diamond Shamrock 24-8 Pauute Federal	5450 0	21E	55	0.5	42	n-C <sub>17</sub>	1	grey greenish laminated to flaser shale, org. clasts
California Oil Red Wash 32	3950 0	22E	40	28.7	40	β-carot.	1	laminated brown-black shale
California Oil Red Wash 32	9745 0	23E	13	1.37				dark shales, org. fragments
Sun Oil Co South Ourray No 1/Unit 1	4938 0	25E	30	14.4	37	n-C <sub>17</sub>	1	black massive mudstones, pelecypode shells
Sun Oil Co South Ourray No 1/Unit 1	4955 0	26E	19	58.6	35	Pr	1	black shale, coal
Sun Oil Co South Ourray No 1/Unit 1	5170 0	27E	19	53.7	51	Pr	1	coaly black shale
Cessus Energy Co Island 16	4895 5	29E	17	78.5	38	n-C <sub>22</sub>	1	black shale-mudstone, silt beds, laminaton, Unionid/pelecypode shells (shell hash)
Carter Oil Josep Smith 1	8551 0	30E	122	1.15	50	n-C <sub>22</sub>	1	dark grey-black mudstone, contorted+BW22
Mountain Fuel Supply Cedar Rim 3	8507 0	31E	6	7.33	38	n-C <sub>18</sub>	1	black coaly shale, laminated, above black shale w/ pelecypode shells
Diamond Shamrock Allen 34 5	5021 5	32E	86	5.66	45	n-C <sub>25</sub>	1	dark impregnated siltstone, shale drapes, above grey green shales
Quinex Energy Leslie Taylor 24-5	12224 0	33E	3	3.07	38	n-C <sub>18</sub>	1	black claystone, coaly beds, ostracodes

Well	depth ft	Sample no	OI (mg CO/g TOC)	GC qualitative				lithology
				S1+S2	Maximum carbon number in GC	Maximum peak in GC	Modal	
Bow Valley Petroleum Ute 2-22A1E	12315.5	34E	15 0.99	43	n-C <sub>17</sub>	1	dark gray mudstone, pelecypoda hash bedded, dewatering, mudstone w/ thin shale sequence	
Bow Valley Petroleum Ute 2-22A1E	12366.5	46E	22.0 0.33	40	n-C <sub>17</sub>	1	grey mudstone (calc siltstone), some lamination, fract.	
Page Petroleum Inc Page Esson Ute 1-14B1E	8483.0	35E	10 66.3	37	n-C <sub>17</sub>	1	laminated to bedded black shale, large org. clasts	
Chevron Hiko Bell Unit 1/Walker	10587.4	38E	87 8.78	37	Pr	1	dark laminated mudstone, oilstained fract., org. clasts/coal	
Gulf Oil 1 Whitlock	7583.0	██████	139 11.4	39	gammac	1	black laminated shale, org. clasts	
Gulf Oil 1 Whitlock	9020.0	38E	111 12.1	47	n-C <sub>19</sub>	1	black laminated shale, org. clasts	
Outcrop sample Indian Canyon 960714-2		██████	31 141	37	β-carot		laminated oil shale	
Outcrop sample Gate Canyon 960714-1		██████	17 143	39	Pr	2	laminated oil shale	
Outcrop sample Black Shale Facies 930922-1		41E	48 43.7	49	n-C <sub>17</sub>	2	black shale	
Outcrop sample Black Shale coal TR1928		██████	13 1205	49	Pr	1	coal	
Outcrop sample EM-RR8		██████	103 74.9	34	n-C <sub>27</sub>	1	coaly shale	

oil-shale type sample



coal sample

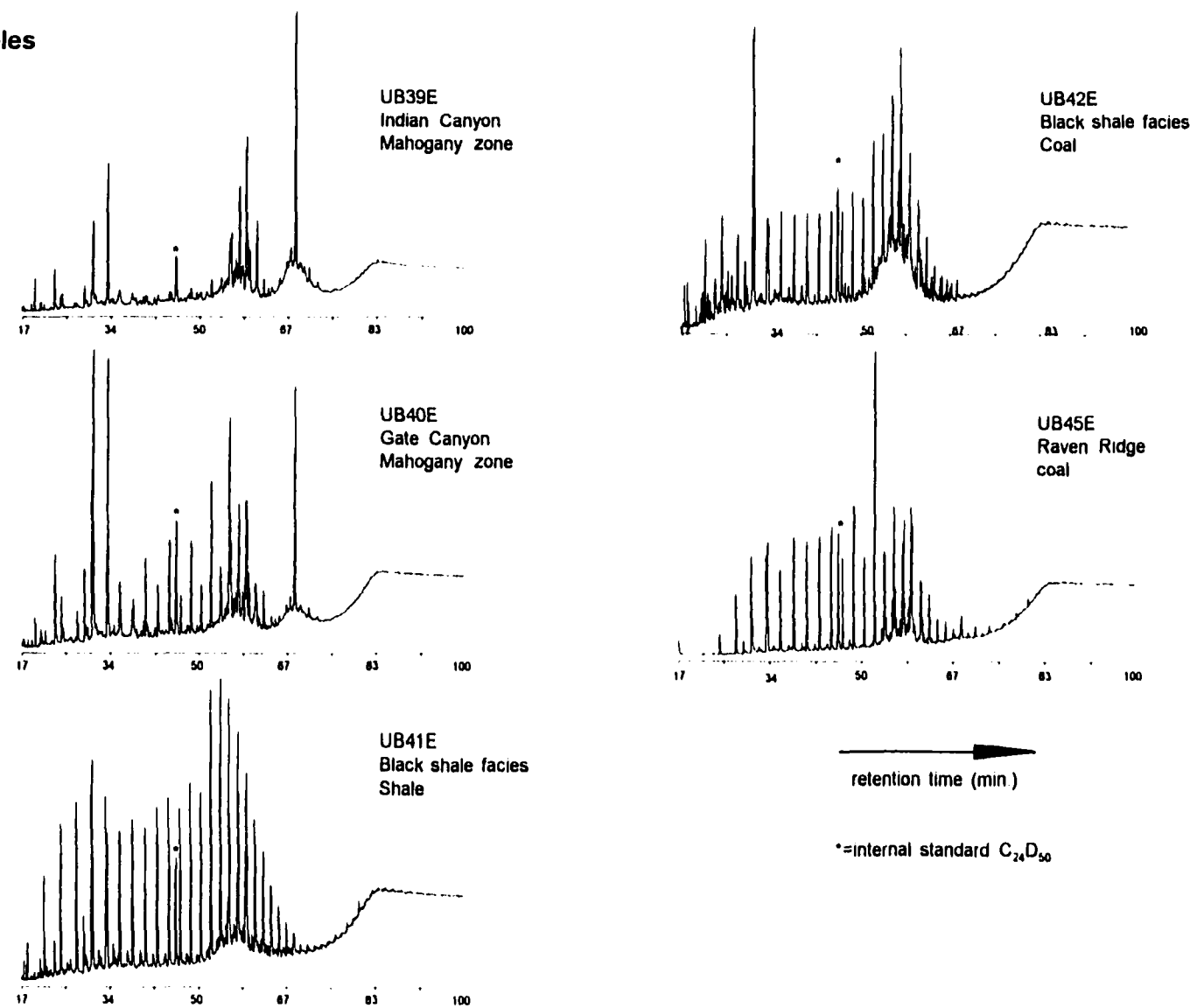


regular type sample



**APPENDIX 6**  
**Outcrop samples**

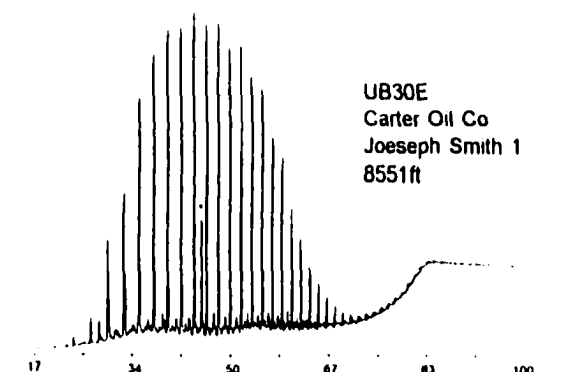
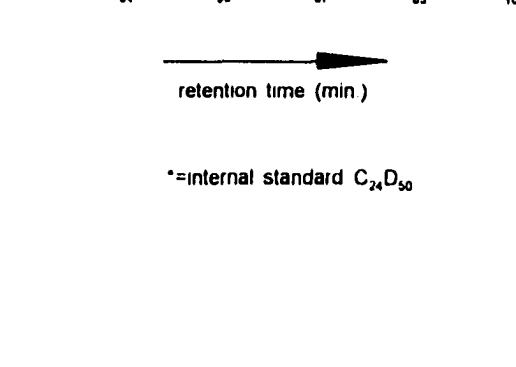
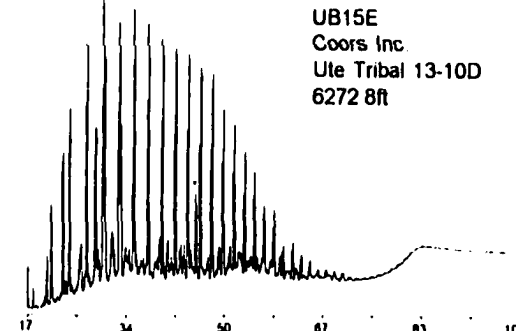
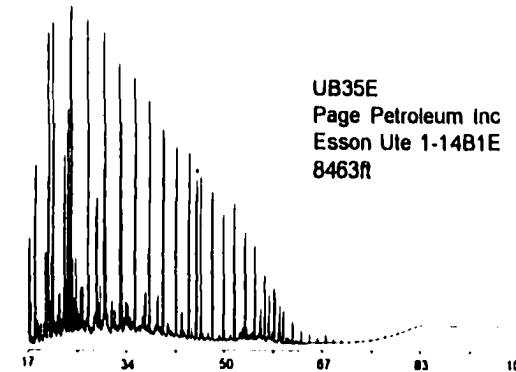
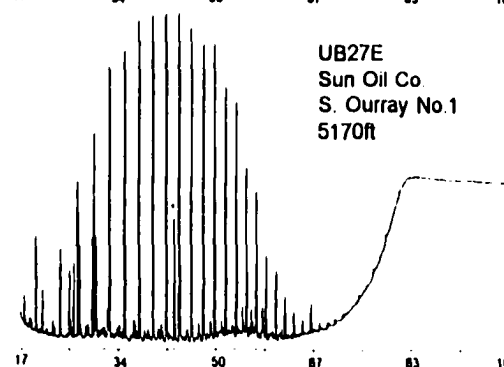
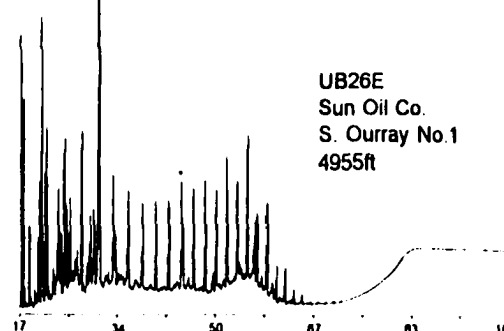
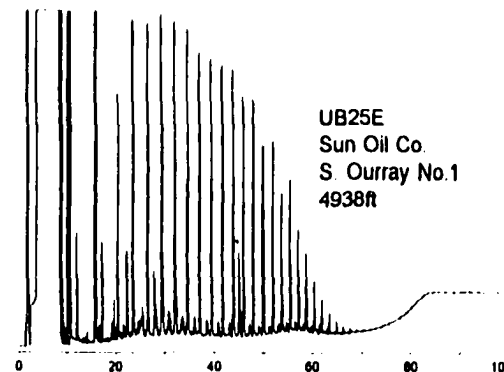
A6-1



## APPENDIX 6

### Core samples from wells outside areas with datum control

A6-2



— retention time (min.)

\*=internal standard C<sub>24</sub>D<sub>50</sub>

**APPENDIX 7 Crude Oils - Well Locations and Sample Data**

Sample	No	API	Field	map group	Operator	Sec	Twn		Rng	Spot		
Texaco D-1 Ute Tribal 4700ft	1	430133056	Cedar Rim	1	Texaco	14	3	S	6	W		
Texaco D-1 Ute Tribal 9251ft	2	430133056	Cedar Rim	1								
Red Wash Whole Field 5900ft	3		Red Wash	-	Chevron	7	S	22	E			
Bluebell Freston 2-8B1	4		Bluebell	3	Pennzoil	8	2	S	1	W	SW	NE
Coyote Basin E Red Wash 1-5	5		Coyote Basin	6	Maxus	5	8	S	25	E	SE	NW
Wonsits Valley 133&71	6		Wonsits Valley (Red Wash)	5	Chevron	15	8	S	21	E		
Twelve Mile Wash Fed 1	7		12 Mile Wash	9								
Horseshoe Bend 2/22-34 Fed	8		Horseshoe Bend	8								
E Red Wash 1/91-28C(State 1-41-36C)	9	4304715128	Walker Hollow	6	-	36	7	S	24	E	NE	NE
Twelve Mile Wash Fed 1	10	4304720281	12 Mile Wash	9	-	2	5	S	20	E		
Antelope Creek Ute Tribal 1-5 (05-07)	11	4301330785	Antelope Creek	2	Petroglyph Operating	5	5	S	3	W	SE	SW
Brennan Bottom Federal 2-20	13	4304731275	Brennan Bottom	8	Lomax Exploration	20	7	S	21	E	SE	NW
Cedar Rim Ute Tribal 2-2C8	14	4301330531	Cedar Rim	1	Page Petroleum	2	3	S	6	W	NW	SW
Coyote Basin Federal 12-13	15	4304731266	Coyote Basin	6	-	13	8	S	24	E	SE	NW
Eight Mile Wash State 33-52D (33-32)	16	4304731116	Eight Mile Flat N (Monument Butte)	4	Natural Gas Co	32	8	S	18	E	SE	NW
Natural Buttes Old Squaws Crossing 4A	20	4304730122	Orray (Natural Buttes)	4	-	37	9	S	20	E		
Nutter Canyon Ute Tribal 10-21	21	4301331283	Nutter Canyon	2	Zink & Trumbo	21	5	S	4	W	SW	NE
Pleasant Valley Federal 24 15-H	22	4301330681	Pleasant Valley	4	Natural Gas of California	15	9	S	17	E	S2	SE
Walker Hollow Broadhurst 21	23	4304730942	Walker Hollow (Red Wash)	7	Energy Reserves Group	9	7	S	23	E	NE	SE
Wonsits Valley Whiton Valley 1-19-3C	24	4304731085	Wonsits Valley (Red Wash)	5	Gulf Oil	19	8	S	21	E	C	SE
Twelve Mile Wash DST 5960' Federal 1	25	4304720281	12 Mile Wash	9	Tenneco	27	5	S	20	E		SW
Bluebell Fay Mecham Fee Federal 1	27	4301330001	Bluebell	3	Chevron	2	1	S	2	W	SE	NW
Gusher Gusher 3	30			9								
Monument Butte (Treaty Boundary?) Federal 15-20	31	4301330687	Monument Butte	4	Lomax Energy	20	8	S	17	E	SE	SE
Bluebell 1-33A1 Lit Pack	33		Bluebell	3								
Red Wash 20 1 32-28C	34	4304715302	Walker Hollow	6	Chevron	28	7	S	24	E		SW
Cedar Rim Ute Tribal 2-24C7	36	4301331028	Cedar Rim	1	Linmar Energy	24	3	S	7	W	SW	NE
Cedar Rim Ford 2-13C7	38	4301331082	Cedar Rim	1	Linmar Energy	13	3	S	7	W	E2	SW
Brennan Bottom Federal 15-8	42	4304731272	Brennan Bottom	8	Lomax Exploration	8	7	S	21	E	SE	SW
Gypsum Hills Federal 3	46	4307420002	Gypsum Hills (Red Wash)	5	Gulf Oil	20	8	S	21	E	NE	NE
Horseshoe Bend Federal 4 2-F	47	4304731853	Horseshoe Bend	8	Alta Energy	4	7	S	21	E	SW	SE
Horseshoe Bend Federal 5 SH	48	4304731903	Horseshoe Bend	8	Phoenix Hydrocarbons	5	7	S	21	E	SE	SE
Panette Bench Federal 14-5	51	4304731123	Panette Bench	4	Diamond Shamrock	5	9	S	19	E	SW	SW
Walker Hollow Pearl Broadhurst 1	52	4304715692	Walker Hollow (Red Wash)	7	Pan American	9	7	S	23	E	NE	SE
Walker Hollow Pearl Broadhurst 15	53	4304730901	Walker Hollow (Red Wash)	7	Energy Reserves Group	9	7	S	23	E	SE	SE

Sample	No	API	Field	map group	Operator	Sec	Twn		Rng	Spot		
Walker Hollow Pearl Broadhurst 18	54	4304730939	Walker Hollow (Red Wash)	7	Energy Reserves Group	9	7	S	23	E	NW NW NE	
Wonsits Valley Federal 105	55	4304730023	Wonsits Valley (Red Wash)	5	Gulf Oil	10	8	S	21	E	NW SE SE	
Brennan Bottom Federal 6	57	4304730109	Brennan Bottom	8	Gulf Oil	19	7	S	21	E	SW NW NW	
Walker Hollow Pearl Broadhurst 12	59	4304730841	Walker Hollow (Red Wash)	7	Energy Reserves Group	10	7	S	23	E	SW NW NW	
Walker Hollow Unit 1	60	4304720280	Walker Hollow (Red Wash)	7	McLish	8	7	S	23	E	SW SW	
Gusher Gov 4-14	61	4004730155	Gusher E	9	Flying Diamond	14	6	S	20	E	SW NW NW	
Wonsits Valley Unit 88-2	63	4304731048	Wonsits Valley (Red Wash)	5	Gulf Oil	12	8	S	21	E	SW NW SW	
White River Unit 47-10	64	4304731561	White River (Red Wash)	5	Belico Development	10	8	S	22	E	SW SW SW	
Federal 1-27	67	4304731847	Coyote Wash	8	Gilmore Oil & Gas	27	8	S	24	E	NE SE SW	
Brennan Bottom Federal 1	68		Brennan Bottom	8								
Coyote Basin E Red Wash Fed 4-6	69	4304720281	Coyote Basin	8	Shamrock Oil&Gas	6	8	S	25	E	SW NE	
Gypsum Hills Costas Federal 2 20-3b	70	4304715454	Gypsum Hills (Red Wash)	5	Gulf Oil							
Wonsits Valley Federal 24	71	4304715454	Wonsits Valley (Red Wash)	5	Gulf Oil	1	8	S	21	E	SW SW	
Chevron Blanchard 1-33-3	73	4301320316	Bluebell	3	Chevron	3	1	S	2	W	NW SE	
Conoco Tnbal 31-55A	74		Orray (Natural Buttes)	5	Conoco	31	8	S	22	E	SW SW	
Conoco Tnbal 35-51	75		Orray (Natural Buttes)	5	Conoco	35	8	S	21	E	SW SE	
CNG 3-25B	76	4304732417	West Willow Creek	4	CNG	25	9	S	19	E	SW NE NW	

waxy type



immature type



regular type



## APPENDIX 7

Sample	No.	perforation/sample depth [ft]	elev [ft]	sample description
				appearance
Texaco D-1 Ute Tribal 4700ft	1	4700	5893	KB black fluid
Texaco D-1 Ute Tribal 9251ft	2	9251		dark yellow solid
Red Wash Whole Field 5900ft	3	5900		black viscous
Bluebell Freston 2-BB1	4	11232-11720	5105	GI <sup>a</sup> dark yellow, solid
Coyote Basin E Red Wash 1-5	5	4495-4501		black viscous
Wonsits Valley 133&71	6	5192-5223 (71) 5202-5217 (133)	4810	GI <sup>a</sup> black, viscous
Twelve Mile Wash Fed 1	7	6958-6960	5250	KB black fluid
Horseshoe Bend 2/22-34 Fed	8	6870-6890	5000	ML black, viscous
E Red Wash 1/91- 26C (State 1-41-38C)	9	4936-4971	5758	KB black, viscous
Twelve Mile Wash Fed 1	10	7386-7426	5250	KB black fluid
Antelope Creek Ute Tribal 1-5 (05-07)	11	6329-6338, 6552-6555, 6590- 6592, 6729-6732	6024	GR black, viscous
Brennan Bottom Federal 2- 20	13	6890-6711	4759	GR black, viscous
Cedar Rim Ute Tribal 2- 2C8	14	8594-9914	6137	KB black fluid
Coyote Basin Federal 12- 13	15	4200-4213	5404	KB black, viscous
Eight Mile Wash State 33- 52D (33-32)	16	5130-5582	4943	KB black, viscous
Natural Buttes Old Squaws Crossing 4A	20	n a	4725	ML black, viscous
Nutter Canyon Ute Tribal 10-21	21	4593-5402	6519	KB black, viscous
Pleasant Valley Federal 24 15-H	22	4435-5288	5296	KB black, viscous
Walker Hollow Broadhurst 21	23	5312-5419	5194	KB black, viscous
Wonsits Valley Whinton Valley 1-19-3C	24	5253-5286	4693	KB black, viscous
Twelve Mile Wash DST 5960' Federal 1	25	6958-6980	5250	KB black, viscous
Bluebell Fay Mecham Fee Federal 1	27	10395-10407, 10414- 10418, 10440-10449, 10450- 10451	5916	KB black, fluid
Gusher Gusher 3	30	7748-7995		black, viscous
Monument Butte (Treaty Boundary?) Federal 15-20	31	5789-5848	5288	KB black, viscous
Bluebell 1-33A1 Lili Pack	33	8272-8276		black, solid asphalt
Red Wash 20 1-32-28C	34	5160-5233	5688	KB black, viscous
Cedar Rim Ute Tribal 2- 24C7	38	8595-10500	6555	KB light brown, viscous
Cedar Rim Ford 2-13C7	39	8823-9652	6502	KB light brown, viscous
Brennan Bottom Federal 15-8	42	6815-6913	4808	KB black, viscous
Gypsum Hills Federal 3	46	5241	4705	KB black, viscous
Horseshoe Bend Federal 4 2-F	47	6808-6876, 6929-7053	4972	KB black, viscous
Horseshoe Bend Federal 5 5H	48	6907-7098	4894	GR black, viscous
Panette Bench Federal 14- 5	51	4858-5075	4725	KB black, viscous
Walker Hollow Pearl Broadhurst 1	52	4770-4800, 5300-5407	5195	KB black, viscous
Walker Hollow Pearl Broadhurst 15	53	5199-5358	5195	KB black, fluid

Sample	No	perforation/sample depth [ft]	elev [ft]	sample description appearance
Walker Hollow Pearl Broadhurst 18	54	5379-5409	5091	KB black, fluid
Wonsits Valley Federal 105	55	5268-5402	4877	DF black, viscous
Brennan Bottom Federal 6	57	6542-6792	4691	KB black, viscous
Walker Hollow Pearl Broadhurst 12	59	5382-5423	5155	KB black, fluid
Walker Hollow Unit 1	60	5642-5898, 5717-5742	5373	KB black, viscous
Gusher Gov 4-14	61	7690-7697, 7708-7732	4961	GR black, viscous
Wonsits Valley Unit 88-2	63	5491-5503	4983	KB black, fluid
White River Unit 47-10	64	5445-5458	4945	KB black-dark brown, viscous
Federal 1-27	67	3867-3872	5340	KB black, viscous
Brennan Bottom Federal 1	68	n a		black, viscous
Coyote Basin E Red Wash Fed 4-6	69	4443-4449	5582	KB black, viscous
Gypsum Hills Costas Federal 2 20-3b	70	n a		black, viscous
Wonsits Valley Federal 24	71	4571-4582, 5858-5881 (Pl)	5017	KB black, medium viscous
Chevron Blanchard 1-33-3	73	9039-9056 (10388-10410)	5863	KB black, medium viscous-fluid
Conoco Tribal 31-55A	74	3150-3154	4695	ML black, medium viscous-fluid
Conoco Tribal 35-51	75	3180-3180	4690	ML black, medium viscous-fluid
CNG 3-25B	78	4740-4795	4740	KB black, medium viscous-fluid

waxy type

immature type

regular type

## APPENDIX 8.1

## Crude Oils - GC-MS Peak Heights [μV]

Peak no.		UB1o	UB2o	UB3o	UB4o	UB5o	UB6o	UB7o	UB8o	UB9o	UB10o	UB11o
<b>Terpanes m/z 191</b>												
1	Tricyclic terpane C <sub>18</sub>	790	0	500	0	365	700	500	1376	2500	500	0
2	Tricyclic terpane C <sub>20</sub>	8439	0	3258	0	487	3094	37937	5877	5018	34531	0
3	Tricyclic terpane C <sub>21</sub>	9827	0	8316	0	2256	8864	43335	15561	8063	40166	0
4	Tricyclic terpane C <sub>22</sub>	1251	0	1239	0	0	1400	5253	1835	1167	4968	0
5	Tricyclic terpane C <sub>23</sub>	6999	0	7825	0	2257	8653	33424	15093	12354	28770	0
6	Tricyclic terpane C <sub>24</sub>	3535	0	5201	0	1744	5792	23739	8650	6607	19241	0
7	Tricyclic terpane C <sub>25</sub>	1135	0	2384	0	888	2664	6730	4145	4253	5162	0
8	Tricyclic terpane C <sub>26</sub> 22S	1842	0	3273	0	630	3110	6585	6155	3494	7479	0
9	Tricyclic terpane C <sub>26</sub> 22R	5950	0	3364	0	1029	3433	9975	5525	4818	9318	0
10	Tricyclic terpane C <sub>27</sub> 22S	0	0	0	0	0	0	0	0	0	0	0
11	Tricyclic terpane C <sub>27</sub> 22R	0	0	0	0	0	0	0	0	0	0	0
12	Tricyclic terpane C <sub>28</sub> 22S	1129	0	2362	0	722	2566	6120	3807	2572	5263	0
13	Tricyclic terpane C <sub>28</sub> 22R	986	0	2261	0	1718	2525	5905	4231	2536	4093	0
14	Tricyclic terpane C <sub>29</sub> 22S	0	0	2596	0	787	2408	4336	3031	3466	3722	0
15	Tricyclic terpane C <sub>29</sub> 22R	799	0	2383	0	865	2545	4321	4480	2582	4418	0
16	18a(H)-22,29,30-normethopane (Ts)	2318	0	2986	0	2369	4031	4205	4558	5882	3349	0
17	1 unknown terpane	0	0	0	0	625	0	0	0	0	0	0
18	Tricyclic terpane C <sub>30</sub> 22S	774	0	1517	0	716	1596	3339	3837	2184	2859	0
19	17a(H)-22,29,30-trisnorhopane (Tm)	28229	0	4325	0	1375	3096	46936	6252	15064	39259	0
20	Tricyclic terpane C <sub>30</sub> 22R	0	0	1375	0	536	1820	3458	3022	0	4107	0
21	17b(H)-22,29,30-trisnormorethane	3434	0	0	0	0	0	4643	0	2655	4107	0
22	2 unknown terpane	0	0	1135	0	0	0	0	0	1553	0	0
23	Tricyclic terpane C <sub>31</sub> 22S	0	0	1545	0	576	2075	7395	0	0	2987	0
24	Tricyclic terpane C <sub>31</sub> 22R	0	0	1435	0	576	1546	3311	3000	0	4107	0
25	17a(H),21b(H)-30-norhopane	75321	0	13879	0	3487	10427	123784	21432	42443	107400	0
26	C <sub>30</sub> diaphopane	0	0	2485	0	3132	3686	1789	3100	1826	0	0
27	3. unknown terpane	0	0	457	0	658	0	0	0	0	0	0
28	17b(H),21a(H)-30-normorethane	9687	0	1753	0	0	0	14241	2822	8676	10502	0
29	18a(H)-olethane	0	0	1926	0	1122	1007	3347	3000	10003	3347	0
30	17a(H),21 b(H)-hopane	145837	0	39076	0	9254	30311	206940	72342	97335	180641	0
31	17b(H),21a(H)-morethane	31583	0	4730	0	1833	3145	50276	7531	13011	39664	0
32	17a(H),21 b(H),22S-30-homohopane	25608	0	5895	0	2740	6319	29788	10171	11217	24425	0
33	17a(H),21 b(H),22R-30-homohopane	22153	0	4840	0	2409	4625	18456	7427	13357	15208	0
34	gammacerane	47547	0	17870	0	2102	16384	52381	20812	40401	46767	0
35	17a(H),21 b(H),22S-30,31-bishomohopane	11692	0	4812	0	2473	4188	13673	5589	10543	11377	0
36	17a(H),21 b(H),22R-30,31-bishomohopane	10666	0	3320	0	1318	2689	9919	3864	10813	8729	0
37	17a(H),21 b(H),22S-30,31,32-trishomohopane	6770	0	2604	0	1074	2779	8676	2623	3414	7539	0
38	17a(H),21 b(H),22R-30,31,32-trishomohopane	5106	0	2018	0	511	2235	6758	2572	4279	4954	0
39	17a(H),21 b(H),22S-tetrakishomohopane	2134	0	1558	0	480	920	3656	1670	1462	2108	0
40	17a(H),21 b(H),22R-tetrakishomohopane	1129	0	581	0	0	698	2583	993	3165	1484	0
41	17a(H),21 b(H),22S-pentakishomohopane	1702	0	513	0	0	266	941	0	2416	611	0
42	17a(H),21 b(H),22R-pentakishomohopane	612	0	535	0	0	265	1172	0	2444	475	0
<b>Di-, Sesquiterpanes m/z 123</b>												
43	C <sub>15</sub> bicyclane	0	2374	744	9595	5381	2328	0	3496	0	0	872
44	C <sub>15</sub> bicyclane	1101	1120	1898	4892	7306	5410	1427	8183	1554	2297	951
45	80(H)-drimane	8375	0	3751	1950	7872	6896	16998	14632	2662	24057	940
46	C <sub>15</sub> bicyclane	678	0	2033	947	5453	4127	1730	6605	1209	1718	523
47	C <sub>15</sub> bicyclane	0	0	613	0	2201	1573	0	2681	1391	730	0
48	C <sub>15</sub> bicyclane	1784	280	1573	1571	3760	3415	0	4530	941	2604	831
49	80(H)-homodrimane	14410	0	7380	2053	11568	12621	0	21061	5120	19552	2021
50	C <sub>17</sub> bicyclane	1058	0	598	0	721	885	1513	1490	706	2557	0
51	C <sub>17</sub> bicyclane	3715	0	1946	0	590	1721	9866	3774	1824	6042	0
52	C <sub>18</sub> bicyclane	3122	0	1361	0	567	1760	5879	3002	2578	6185	351
53	unknown diterpane	3553	799	4680	1300	1581	5151	19527	10418	10954	18653	2206
54	40(H)-19-norisopimarane	1552	1330	3464	3322	2246	3927	2408	7027	5998	2231	2506

Peak no.		UB1o	UB2o	UB3o	UB4o	UB5o	UB6o	UB7o	UB8o	UB9o	UB10o	UB11o
55	C <sub>17</sub> -bicyclane	1821	0	1772	0	0	1394	6427	3420	3497	5820	0
56	C <sub>18</sub> -bicyclane	0	0	0	0	0	0	0	0	0	0	0
57	17-nortetracyclic diterpane	0	0	982	611	497	1332	0	2228	570	314	454
58	isoprinarane	1180	0	1184	598	1720	1942	3158	2486	1328	1770	1425
59	16 $\beta$ (H)-phytadiene	1158	0	1974	0	802	2471	6619	5095	5230	4421	572
	<b>Steranes, diasteranes m/z 217</b>											
60	5 $\alpha$ (H),14 $\beta$ (H),17 $\beta$ (H)-dignane	0	0	0	0	0	0	0	0	0	0	0
61	5 $\alpha$ (H),14 $\beta$ (H),17 $\beta$ (H)-homodignane	0	0	0	0	0	0	0	0	0	0	0
62	13 $\beta$ (H),17 $\alpha$ (H),20S-diacholestan e	0	0	0	0	368	374	0	0	2512	0	0
63	13 $\beta$ (H),17 $\alpha$ (H),20R-diacholestan e	0	0	219	0	363	0	0	0	1998	0	0
64	13 $\alpha$ (H),17 $\beta$ (H),20S-diacholestan e	0	0	0	0	0	270	0	0	1298	0	0
65	13 $\alpha$ (H),17 $\beta$ (H),20R-diacholestan e	0	0	0	0	217	185	0	0	2716	0	0
66	24-methyl-13 $\beta$ (H),17 $\alpha$ (H),20S-diacholestan e	0	0	235	0	151	0	0	0	469	0	0
67	24-methyl-13 $\beta$ (H),17 $\alpha$ (H),20R-diacholestan e	0	0	251	0	206	0	0	0	1843	0	0
68	24-C <sub>29</sub> $\alpha\beta$ dia 20S+ $\alpha\alpha$ C <sub>27</sub> ,20S	4400	0	1349	0	449	710	6344	1481	31728	5919	0
69	24-C <sub>29</sub> $\alpha\beta$ dia 20S+ $\beta\beta$ C <sub>27</sub> ,20R	1614	0	793	0	757	726	2052	1055	2676	1764	0
70	24-C <sub>29</sub> $\alpha\beta$ dia 20R+ $\beta\beta$ C <sub>27</sub> ,20S	0	0	585	0	444	0	1750	725	1276	1332	0
71	14 $\beta$ (H),17 $\alpha$ (H),20R-cholestan e	6760	0	2545	0	530	857	9516	1374	87047	8037	0
72	24-ethyl-13 $\beta$ (H),17 $\alpha$ (H),20R-diacholestan e	1937	0	295	0	382	187	2053	0	2199	2086	0
73	24-ethyl-13 $\beta$ (H),17 $\alpha$ (H),20S-diacholestan e	2044	0	316	0	0	306	1831	0	1404	1550	0
74	24-methyl-14 $\alpha$ (H),17 $\alpha$ (H),20S-cholestan e	5446	0	401	0	0	417	6116	274	1768	5805	0
75	24-C <sub>29</sub> $\alpha\beta$ dia 20R+C <sub>27</sub> ,20R	7990	0	652	0	352	549	7650	655	10452	6774	0
76	24-methyl-14 $\beta$ (H),17 $\beta$ (H),20S-cholestan e	3930	0	494	0	257	713	5205	728	476	5134	0
77	24-methyl-14 $\alpha$ (H),17 $\alpha$ (H),20R-cholestan e	25850	0	1639	0	196	336	18349	1120	17992	16313	0
78	24-ethyl-14 $\alpha$ (H),17 $\alpha$ (H),20S-cholestan e	9699	0	1316	0	451	653	15737	965	7223	14446	0
79	24-ethyl-14 $\beta$ (H),17 $\beta$ (H),20R-cholestan e	6884	0	1281	0	269	753	11538	825	6196	9915	0
80	24-ethyl-14 $\beta$ (H),17 $\beta$ (H),20S-cholestan e	3930	0	804	0	500	661	7655	721	444	5900	0
81	24-ethyl-14 $\alpha$ (H),17 $\alpha$ (H),20R-cholestan e	19288	0	2904	0	515	728	19265	1437	28332	23418	0
	<b>Monoaromatic steroids m/z 253</b>											
82	monoaromatic sterane C <sub>27</sub>	834	0	551	0	0	353	932	313	4940	745	0
83	monoaromatic sterane C <sub>27</sub>	70	0	344	0	180	322	74	538	1337	83	0
84	monoaromatic sterane C <sub>27</sub>	414	0	151	0	177	220	322	254	1603	188	0
85	monoaromatic sterane C <sub>27</sub>	807	0	765	0	264	438	693	589	7066	530	0
86	monoaromatic sterane C <sub>27</sub> +C <sub>28</sub>	3942	0	1199	0	273	684	2868	791	11890	2333	0
87	monoaromatic sterane C <sub>27</sub> +C <sub>28</sub>	339	0	247	0	24	250	139	370	557	128	0
88	monoaromatic sterane C <sub>27</sub> +C <sub>28</sub>	485	0	623	0	115	227	657	331	9012	659	0
89	monoaromatic sterane C <sub>27</sub> +C <sub>28</sub>	9643	0	2235	0	552	1311	8359	2313	19955	7153	0
90	monoaromatic sterane C <sub>27</sub> +C <sub>28</sub>	268	0	209	0	220	136	266	68	575	309	0
91	monoaromatic sterane C <sub>27</sub> +C <sub>28</sub>	276	0	370	0	311	240	268	164	765	475	0
92	monoaromatic sterane C <sub>27</sub> +C <sub>28</sub>	6188	0	1734	0	177	788	6918	1085	16461	5803	0
93	monoaromatic sterane C <sub>27</sub> +C <sub>28</sub>	2500	0	1215	0	216	489	2600	0	11077	2296	0
94	monoaromatic sterane C <sub>27</sub> +C <sub>28</sub>	5144	0	891	0	55	278	4422	663	8555	3330	0
95	monoaromatic sterane C <sub>27</sub>	324	0	198	0	97	214	202	210	116	150	0
96	monoaromatic sterane C <sub>27</sub>	5165	0	1256	0	53	369	4844	702	12413	4394	0

waxy type

immature type

regular type

## APPENDIX 8.1

Peak no.		UB13o	UB14o	UB15o	UB16o	UB20o	UB21o	UB22o	UB23o	UB24o	UB26o	UB27o
<b>Terpanes m/z 191</b>												
1	Tricyclic terpane C <sub>19</sub>	550	903	546	1653	165	500	500	1494	500	1244	533
2	Tricyclic terpane C <sub>20</sub>	3635	12262	845	7098	3435	1620	2136	5975	9424	26725	8251
3	Tricyclic terpane C <sub>21</sub>	13086	11787	2168	20057	8892	5177	5682	12783	17632	32232	9186
4	Tricyclic terpane C <sub>22</sub>	2915	1349	0	5349	1647	890	1027	2576	3575	3343	2925
5	Tricyclic terpane C <sub>23</sub>	14559	9244	2900	26895	9382	5376	6725	14167	19868	21012	9060
6	Tricyclic terpane C <sub>24</sub>	7410	4260	2310	22637	5579	4377	5928	10035	14404	14326	14897
7	Tricyclic terpane C <sub>25</sub>	3912	1438	1029	9144	2718	1797	2094	4011	6536	4725	4863
8	Tricyclic terpane C <sub>26</sub> 22S	2660	2364	794	9712	3083	2086	1845	3660	5893	6367	6318
9	Tricyclic terpane C <sub>27</sub> 22R	3532	7781	1205	11199	3345	1863	2185	4838	7041	7401	6980
10	Tricyclic terpane C <sub>27</sub> 22S	0	0	0	1593	0	0	0	0	0	0	0
11	Tricyclic terpane C <sub>27</sub> 22R	0	0	0	1381	0	0	0	0	0	0	0
12	Tricyclic terpane C <sub>28</sub> 22S	3163	1280	529	8724	2463	1591	2258	3875	6349	3626	5086
13	Tricyclic terpane C <sub>28</sub> 22R	2555	803	771	8711	2363	1407	1841	3505	4374	4326	4502
14	Tricyclic terpane C <sub>29</sub> 22S	2438	912	1170	10345	2505	2037	1658	2608	5385	4043	4959
15	Tricyclic terpane C <sub>29</sub> 22R	2614	968	897	10051	2607	2001	1954	2881	5283	3193	4780
16	18a(H)-22,29,30-nomechopane (Ts)	3762	1960	3202	10419	3875	2286	2082	4401	5444	2807	3887
17	1 unknown terpane	1312	0	502	0	0	556	0	0	0	0	0
18	Tricyclic terpane C <sub>30</sub> 22S	2086	931	878	7224	2303	1348	1557	2068	4554	2056	4216
19	17a(H)-22,29,30-trisnorhopane (Tm)	2648	39952	1353	4526	4076	699	1280	5669	8816	35132	3550
20	Tricyclic terpane C <sub>30</sub> 22R	2545	0	786	6406	2148	1226	1426	3000	3725	0	3300
21	17 $\beta$ (H)-22,29,30-trisnormethane	0	3685	0	0	0	0	0	0	1243	4124	0
22	2 unknown terpane	1520	0	1192	4236	1652	674	0	1862	1505	0	1316
23	Tricyclic terpane C <sub>31</sub> 22S	1772	4326	872	7792	2369	1121	1456	2253	3629	2840	2258
24	Tricyclic terpane C <sub>31</sub> 22R	1807	1197	525	7793	2020	1574	1266	2404	3686	1968	4384
25	17a(H),21 $\beta$ (H)-30-normopane	9327	103863	4159	18321	16747	1999	4464	20597	34600	99621	12706
26	C <sub>30</sub> diaphopane	5762	0	2344	11865	3876	1799	1683	0	2283	925	3638
27	3 unknown terpane	0	0	0	2406	569	617	0	0	785	0	0
28	17 $\beta$ (H),21 $\alpha$ (H)-30-normetane	390	15135	0	2345	2012	480	0	2589	3369	10809	1186
29	18a(H)-oleane	1671	3719	1144	1639	1286	0	564	2352	1552	2793	2496
30	17a(H),21 $\beta$ (H)-norpene	28457	163738	10014	52573	49471	5951	10998	50506	73205	136944	33227
31	17 $\beta$ (H),21 $\alpha$ (H)-metane	3263	55596	1016	4480	5059	863	1344	7044	7942	36541	3503
32	17a(H),21 $\beta$ (H),22S-30-homopane	7630	34892	2685	11940	9205	1755	1931	10162	14486	17967	5747
33	17a(H),21 $\beta$ (H),22R-30-homopane	4314	24496	2179	8799	5080	996	1213	7208	9275	14385	3997
34	gammacerane	32805	44226	2509	50208	25009	6075	9436	22928	33132	40658	14377
35	17a(H),21 $\beta$ (H),22S-30,31-bishomopane	6226	11899	2173	8812	7463	852	1084	7088	8719	10738	4045
36	17a(H),21 $\beta$ (H),22R-30,31-bishomopane	4278	10077	1430	5210	4361	663	1125	4432	6329	7714	2523
37	17a(H),21 $\beta$ (H),22S-30,31,32-trishomopane	3184	6240	889	4627	3667	654	716	4066	4904	6504	2136
38	17a(H),21 $\beta$ (H),22R-30,31,32-trishomopane	2262	5195	960	4170	765	503	689	2544	3402	4305	1466
39	17a(H),21 $\beta$ (H),22S-tetrakishomopane	1289	1848	735	2630	2512	0	334	1246	1771	2286	635
40	17a(H),21 $\beta$ (H),22R-tetrakishomopane	827	663	546	1961	1200	0	959	865	1535	2072	1308
41	17a(H),21 $\beta$ (H),22S-pentakishomopane	849	1364	382	1306	607	511	0	483	984	1870	363
42	17a(H),21 $\beta$ (H),22R-pentakishomopane	919	436	0	808	483	0	0	471	615	576	541
<b>Di-, Sesquiterpanes m/z 123</b>												
43	C <sub>15</sub> bicycane	1433	0	4854	6444	2314	5510	1300	1125	1086	0	2670
44	C <sub>15</sub> bicycane	3160	637	6346	10286	4777	7185	2895	2603	3633	2426	6128
45	8 $\beta$ (H)-anmane	4184	7836	6659	11151	7774	7645	4277	5086	13687	25514	17731
46	C <sub>15</sub> bicycane	2444	620	5263	8685	4001	5977	2515	3019	3725	2065	5577
47	C <sub>15</sub> bicycane	1438	0	2254	3439	1468	1695	1141	1212	1509	589	1967
48	C <sub>15</sub> bicycane	2028	1761	3812	7153	2942	3946	1937	1684	2194	2267	4964
49	8 $\beta$ (H)-homodimane	19633	11795	12716	21592	13153	10333	8306	12204	16591	14359	17941
50	C <sub>17</sub> bicycane	1182	1238	757	1561	915	923	858	765	1839	1861	1401
51	C <sub>17</sub> bicycane	2704	2963	885	3373	2439	1325	1328	2645	3433	5769	3660
52	C <sub>18</sub> bicycane	2373	4128	864	2913	1891	1233	1815	1518	3323	4845	3943
53	unknown diterpane	8125	5801	2343	6420	5830	4796	3740	6731	8380	13240	10362
54	4 $\beta$ (H)-19-norsopimarane	10266	1720	2944	6371	2654	4821	4222	4799	2348	1719	8081

Peak no.		UB13o	UB14o	UB15o	UB16o	UB20o	UB21o	UB22o	UB23o	UB24o	UB25o	UB26o	UB27o
55	C <sub>17</sub> -bicyclane	3119	2792	583	862	1335	808	749	2626	2361	4371	3563	
56	C <sub>18</sub> -bicyclane	465	0	0	704	0	0	0	0	552	0	0	
57	17-nortetracyclic diterpane	1501	0	597	1717	894	1251	1180	1307	736	0	2912	
58	isopimarane	2280	1818	2184	5517	1051	3890	3224	1456	1789	1714	2737	
59	16 $\beta$ (H)-phylocladane	4280	1547	635	2778	2080	1719	1764	3479	3934	3902	4835	
	<b>Steranes, diasteranes m/z 217</b>												
60	5 $\alpha$ (H),14 $\beta$ (H),17 $\beta$ (H)-diguanane	801	0	0	0	0	0	0	0	0	406	0	
61	5 $\alpha$ (H),14 $\beta$ (H),17 $\beta$ (H)-homodiguanane	710	0	0	0	0	0	0	0	107	203	0	
62	13 $\beta$ (H),17 $\alpha$ (H),20S-diacholestan e	731	0	400	0	286	124	107	0	143	0	374	
63	13 $\beta$ (H),17 $\alpha$ (H),20R-diacholestan e	345	0	0	0	140	0	107	0	0	0	270	
64	13 $\alpha$ (H),17 $\beta$ (H),20S-diacholestan e	0	0	0	0	163	0	102	0	145	0	0	
65	13 $\alpha$ (H),17 $\beta$ (H),20R-diacholestan e	311	0	0	0	0	0	0	0	129	0	0	
66	24-methyl-13 $\beta$ (H),17 $\alpha$ (H),20S-diacholestan e	298	0	0	0	0	0	121	0	168	0	0	
67	24-methyl-13 $\beta$ (H),17 $\alpha$ (H),20R-diacholestan e	300	0	300	0	273	0	111	0	425	395	0	
68	24-C <sub>28</sub> $\alpha\beta$ dia 20S+ $\alpha\alpha$ C <sub>27</sub> , 20S	947	5687	737	1177	871	198	154	1245	2096	4369	710	
69	24-C <sub>28</sub> $\alpha\beta$ dia 20S+ $\beta\beta$ C <sub>27</sub> , 20R	1503	1751	806	2355	820	333	409	1211	1628	1524	726	
70	24-C <sub>28</sub> $\alpha\beta$ dia 20R+ $\beta\beta$ C <sub>27</sub> , 20S	1164	1093	431	1463	398	255	312	1000	1574	1059	570	
71	14 $\alpha$ (H),17 $\alpha$ (H),20R-cholestan e	833	9951	664	1030	719	103	179	2215	2192	6999	400	
72	24-ethyl-13 $\beta$ (H),17 $\alpha$ (H),20R-diacholestan e	306	2951	199	473	0	105	0	252	578	1605	187	
73	24-ethyl-13 $\beta$ (H),17 $\alpha$ (H),20S-diacholestan e	0	2777	178	499	145	191	0	175	126	1409	417	
74	24-methyl-14 $\alpha$ (H),17 $\alpha$ (H),20S-cholestan e	358	9303	0	327	316	0	0	435	662	4619	0	
75	24-C <sub>28</sub> $\alpha\beta$ dia 20R+C <sub>28</sub> $\beta\beta$ 20R	919	9034	375	1536	691	246	199	1023	2041	5381	549	
76	24-methyl-14 $\beta$ (H),17 $\beta$ (H),20S-cholestan e	761	4668	288	1264	571	303	290	749	1833	3415	713	
77	24-methyl-14 $\alpha$ (H),17 $\alpha$ (H),20R-cholestan e	625	33256	217	1142	736	148	309	1560	2222	11270	336	
78	24-ethyl-14 $\alpha$ (H),17 $\alpha$ (H),20S-cholestan e	588	15413	553	1287	840	285	264	1400	2632	11465	653	
79	24-ethyl-14 $\beta$ (H),17 $\beta$ (H),20R-cholestan e	931	10510	639	2999	922	327	456	1347	3172	8002	753	
80	24-ethyl-14 $\beta$ (H),17 $\beta$ (H),20S-cholestan e	802	569	480	2348	754	301	384	1269	2613	466	661	
81	24-ethyl-14 $\alpha$ (H),17 $\alpha$ (H),20R-cholestan e	760	32804	657	1392	1135	224	176	2449	3123	17222	728	
	<b>Monoaromatic steroids m/z 253</b>												
82	monoaromatic sterane C <sub>27</sub>	368	821	0	1296	394	0	0	614	641	521	203	
83	monoaromatic sterane C <sub>27</sub>	574	71	264	0	769	0	0	554	435	59	134	
84	monoaromatic sterane C <sub>27</sub>	445	193	125	0	274	0	0	324	424	196	149	
85	monoaromatic sterane C <sub>27</sub>	885	857	338	0	908	114	0	1199	639	466	244	
86	monoaromatic sterane C <sub>27</sub> +C <sub>28</sub>	756	5973	255	0	872	0	0	1554	1670	2254	275	
87	monoaromatic sterane C <sub>27</sub> +C <sub>28</sub>	459	339	191	0	403	104	0	613	286	138	122	
88	monoaromatic sterane C <sub>27</sub> +C <sub>28</sub>	152	731	100	0	303	90	0	722	703	918	77	
89	monoaromatic sterane C <sub>27</sub> +C <sub>28</sub>	1372	13045	596	0	2726	75	191	3107	3825	5772	486	
90	monoaromatic sterane C <sub>27</sub> +C <sub>28</sub>	160	355	135	826	233	105	0	150	107	79	80	
91	monoaromatic sterane C <sub>27</sub> +C <sub>28</sub>	255	361	189	0	521	110	110	465	546	272	108	
92	monoaromatic sterane C <sub>27</sub> +C <sub>28</sub>	519	10216	155	0	1139	0	0	1995	2245	5323	171	
93	monoaromatic sterane C <sub>27</sub> +C <sub>28</sub>	682	3500	203	0	1432	71	0	1309	1312	2459	300	
94	monoaromatic sterane C <sub>27</sub> +C <sub>28</sub>	255	7897	64	214	400	0	103	940	1123	3418	198	
95	monoaromatic sterane C <sub>27</sub>	366	83	0	0	301	98	0	299	260	101	132	
96	monoaromatic sterane C <sub>27</sub>	490	7310	216	300	941	100	0	1509	1756	3483	114	

waxy type

immature type

regular type

## APPENDIX 8.1

Peak no.		UB30o	UB31o	UB33o	UB34o	UB38o	UB39o	UB42o	UB46o	UB47o	UB48o
<b>Terpanes m/z 191</b>											
1	Tricyclic terpane C <sub>19</sub>	300	370	1290	450	0	0	400	506	474	538
2	Tricyclic terpane C <sub>20</sub>	2204	913	4174	767	0	0	2468	1735	2499	2965
3	Tricyclic terpane C <sub>21</sub>	5794	3136	4549	2609	0	0	7419	5490	6596	8783
4	Tricyclic terpane C <sub>22</sub>	950	768	1071	542	0	0	1194	1041	1423	1670
5	Tricyclic terpane C <sub>23</sub>	5156	3912	6094	3068	0	0	7594	6246	6959	9633
6	Tricyclic terpane C <sub>24</sub>	3776	3565	2848	2098	0	0	3976	4271	5512	5751
7	Tricyclic terpane C <sub>25</sub>	1841	777	1403	1541	0	0	2637	2077	2117	2507
8	Tricyclic terpane C <sub>26</sub> 22S	1826	1251	1793	878	0	0	2115	2146	1947	2607
9	Tricyclic terpane C <sub>26</sub> 22R	2377	1523	5007	1087	0	0	2663	2248	2443	3161
10	Tricyclic terpane C <sub>27</sub> 22S	0	0	0	0	0	0	0	0	0	0
11	Tricyclic terpane C <sub>27</sub> 22R	0	0	0	0	0	0	0	0	0	0
12	Tricyclic terpane C <sub>28</sub> 22S	1514	1686	1314	1030	0	0	1976	1661	2141	2891
13	Tricyclic terpane C <sub>28</sub> 22R	1741	1124	1161	962	0	0	1837	1762	1887	2069
14	Tricyclic terpane C <sub>29</sub> 22S	1781	1267	1065	1304	0	0	2157	1721	1457	2074
15	Tricyclic terpane C <sub>29</sub> 22R	1452	1234	796	1154	0	0	2222	1891	1490	2138
16	18a(H)-22,29-30-norneohopane (Ts)	1542	1313	2005	2583	0	0	2193	2956	2051	2969
17	1 unknown terpane	0	0	0	657	0	0	0	540	0	0
18	Tricyclic terpane C <sub>30</sub> 22S	1097	1083	482	868	0	0	1378	1180	1338	1699
19	17a(H)-22,29,30-Insnorhopane (Tm)	1562	1105	13895	1495	0	0	2750	2109	1085	2130
20	Tricyclic terpane C <sub>30</sub> 22R	877	0	785	697	0	0	1554	1205	1408	1312
21	17a(H)-22,29,30-Insnomorpane	466	0	2153	0	0	0	0	448	0	0
22	2 unknown terpane	835	656	0	1152	0	0	772	1385	682	988
23	Tricyclic terpane C <sub>31</sub> 22S	1236	666	1325	644	0	0	1316	1212	1205	1705
24	Tricyclic terpane C <sub>31</sub> 22R	1218	1216	0	514	0	0	1064	1159	1269	1594
25	17a(H),21a(H)-30-normopane	5108	1660	34199	4544	0	0	5661	7875	5559	7403
26	C <sub>30</sub> diahopane	1358	1659	2528	2244	0	0	2277	2477	2455	2541
27	3 unknown terpane	348	0	749	0	0	0	0	502	0	0
28	17β(H),21a(H)-30-normorpane	480	0	2590	300	0	0	400	835	619	1090
29	18a(H)-oleane	712	0	5814	1133	0	0	1580	630	851	1243
30	17a(H),21 β(H)-hopane	13805	3572	52987	11224	0	0	16532	21944	14305	19420
31	17β(H),21a(H)-moratane	1566	0	4915	1473	0	0	1613	2294	739	2475
32	17a(H),21 β(H),22S-30-homohopane	2229	895	14744	2933	0	0	3790	4209	3180	4962
33	17a(H),21 β(H),22R-30-homohopane	1898	576	8233	2047	0	0	3160	2892	2238	2912
34	gammacerane	6631	4411	13586	2746	0	0	8318	12410	7375	11179
35	17a(H),21 β(H),22S-30,31-bishomohopane	1566	401	8299	2163	0	0	3244	3041	2299	3913
36	17a(H),21 β(H),22R-30,31-bishomohopane	1425	346	5201	1618	0	0	1764	2282	1633	2516
37	17a(H),21 β(H),22S-30,31,32-trishomohopane	681	346	4623	1325	0	0	1727	1688	1021	1799
38	17a(H),21 β(H),22R-30,31,32-trishomohopane	691	666	2984	680	0	0	1198	1259	528	1158
39	17a(H),21 β(H),22S-tetrakishomohopane	522	553	3152	569	0	0	526	934	498	1134
40	17a(H),21 β(H),22R-tetrakishomohopane	323	0	1791	256	0	0	469	763	341	472
41	17a(H),21 β(H),22S-pentakishomohopane	0	0	1325	445	0	0	3895	0	297	0
42	17a(H),21 β(H),22R-pentakishomohopane	0	0	751	315	0	0	483	0	0	0
<b>Di-, Sesquiterpanes m/z 123</b>											
43	C <sub>15</sub> bicyclane	1393	4454	0	4291	3625	7197	2665	3236	2668	2318
44	C <sub>15</sub> bicyclane	3341	6327	0	7567	973	2523	4382	5231	4414	3672
45	8β(H)-anidriane	5942	5751	13393	7015	512	711	6785	6647	6500	4957
46	C <sub>15</sub> bicyclane	2829	3992	0	4711	0	862	2509	4937	3472	3362
47	C <sub>15</sub> bicyclane	828	1659	0	1639	0	0	1383	1721	1159	1532
48	C <sub>16</sub> bicyclane	1925	2909	898	3102	236	812	1953	3799	2050	2290
49	8β(H)-homodrimane	6575	8523	10658	10260	0	622	12918	12433	10700	11591
50	C <sub>17</sub> bicyclane	445	828	1705	912	0	0	832	616	627	614
51	C <sub>17</sub> bicyclane	1517	719	3948	733	0	0	1649	1566	1567	1751
52	C <sub>18</sub> bicyclane	1511	1000	3575	735	0	0	1663	1350	1335	1276
53	unknown diterpane	3464	2192	1509	2372	0	661	4111	3591	3509	5818
54	40(H)-19-nonsopimarane	3099	4644	0	3627	446	827	4187	3557	4725	5046

Peak no.		UB30o	UB31o	UB33o	UB34o	UB38o	UB39o	UB42o	UB46o	UB47o	UB48o
55	C <sub>17</sub> bicyclane	839	472	1027	385	0	0	1340	791	1156	1704
56	C <sub>18</sub> bicyclane	0	0	1903	0	0	0	0	0	0	0
57	17-nortetracyclic diterpane	940	1041	527	708	0	0	1007	1330	1085	1227
58	isoprimarane	1631	3489	1407	1431	0	0	1425	1778	1778	2042
59	16 $\beta$ (H)-phylocladane	1422	1112	0	580	0	0	1572	1634	2031	2613
	<b>Steranes, diasteranes m/z 217</b>										
60	5 $\alpha$ (H),14 $\beta$ (H),17 $\beta$ (H)-dignane	0	0	1999	1384	0	0	208	0	0	149
61	5 $\alpha$ (H),14 $\beta$ (H),17 $\beta$ (H)-homodignane	0	0	1858	0	0	0	127	0	0	0
62	13 $\beta$ (H),17 $\alpha$ (H),20S-diacholestan e	0	0	545	444	0	0	834	229	146	99
63	13 $\beta$ (H),17 $\alpha$ (H),20R-diacholestan e	0	0	539	257	0	0	533	0	150	139
64	13 $\alpha$ (H),17 $\beta$ (H),20S-diacholestan e	0	0	0	90	0	0	283	75	0	93
65	13 $\alpha$ (H),17 $\beta$ (H),20R-diacholestan e	0	0	318	146	0	0	146	0	124	110
66	24-methyl-13 $\beta$ (H),17 $\alpha$ (H),20S-diacholestan e	165	0	2777	250	0	0	150	122	122	99
67	24-methyl-13 $\beta$ (H),17 $\alpha$ (H),20R-diacholestan e	0	0	3377	243	0	0	506	156	143	166
68	24-C <sub>28</sub> $\alpha\beta$ dia 20S+ $\alpha\alpha$ C <sub>27</sub> 20S	378	122	14842	939	0	0	1637	358	340	424
69	24-C <sub>28</sub> $\alpha\beta$ dia 20S+ $\beta\beta$ C <sub>27</sub> 20R	394	281	13771	979	0	0	1548	458	680	714
70	24-C <sub>28</sub> $\alpha\beta$ dia 20R+ $\beta\beta$ C <sub>27</sub> 20S	279	221	12384	527	0	0	1019	450	243	418
71	14 $\alpha$ (H),17 $\alpha$ (H),20R-cholestane	176	170	11430	1036	0	0	1432	267	344	524
72	24-ethyl-13 $\beta$ (H),17 $\alpha$ (H),20R-diacholestan e	0	87	7154	168	0	0	247	0	98	0
73	24-ethyl-13 $\beta$ (H),17 $\alpha$ (H),20S-diacholestan e	0	0	2578	164	0	0	137	116	117	135
74	24-methyl-14 $\alpha$ (H),17 $\alpha$ (H),20S-cholestane	0	108	8047	299	0	0	294	0	187	165
75	24-C <sub>28</sub> $\alpha\beta$ dia 20R+C <sub>28</sub> $\beta\beta$ 20R	227	285	29043	527	0	0	716	367	285	336
76	24-methyl-14 $\beta$ (H),17 $\beta$ (H),20S-cholestane	258	130	24308	266	0	0	614	314	184	348
77	24-methyl-14 $\alpha$ (H),17 $\alpha$ (H),20R-cholestane	133	110	18255	366	0	0	454	233	274	320
78	24-ethyl-14 $\alpha$ (H),17 $\alpha$ (H),20S-cholestane	258	109	22613	578	0	0	857	345	321	337
79	24-ethyl-14 $\beta$ (H),17 $\beta$ (H),20R-cholestane	271	303	35214	492	0	0	576	377	406	550
80	24-ethyl-14 $\beta$ (H),17 $\beta$ (H),20S-cholestane	290	263	30246	502	0	0	665	319	370	507
81	24-ethyl-14 $\alpha$ (H),17 $\alpha$ (H),20R-cholestane	398	170	25568	737	0	0	716	369	459	557
	<b>Monoaromatic steroids m/z 253</b>										
82	monoaromatic sterane C <sub>27</sub>	150	0	227	190	0	0	295	99	78	189
83	monoaromatic sterane C <sub>27</sub>	137	60	0	353	0	0	516	159	181	434
84	monoaromatic sterane C <sub>27</sub>	87	109	30	229	0	0	341	140	134	153
85	monoaromatic sterane C <sub>27</sub>	214	0	194	494	0	0	673	402	216	450
86	monoaromatic sterane C <sub>27</sub> +C <sub>28</sub>	306	0	497	412	0	0	589	358	286	533
87	monoaromatic sterane C <sub>27</sub> +C <sub>28</sub>	49	0	0	242	0	0	172	145	167	265
88	monoaromatic sterane C <sub>27</sub> +C <sub>28</sub>	112	0	169	89	0	0	260	73	152	128
89	monoaromatic sterane C <sub>27</sub> +C <sub>28</sub>	525	61	882	821	0	0	855	705	749	805
90	monoaromatic sterane C <sub>27</sub> +C <sub>28</sub>	0	0	0	221	0	0	68	0	78	184
91	monoaromatic sterane C <sub>27</sub> +C <sub>28</sub>	0	0	104	211	0	0	150	140	88	241
92	monoaromatic sterane C <sub>28</sub> +C <sub>28</sub>	319	0	303	240	0	0	401	408	177	369
93	monoaromatic sterane C <sub>28</sub> +C <sub>28</sub>	256	0	383	331	0	0	424	275	230	411
94	monoaromatic sterane C <sub>28</sub> +C <sub>28</sub>	140	63	377	76	0	0	50	120	93	187
95	monoaromatic sterane C <sub>28</sub>	149	62	0	135	0	0	279	99	168	196
96	monoaromatic sterane C <sub>28</sub>	254	0	313	120	0	0	168	212	250	490

waxy type

immature type

regular type

## APPENDIX 8.1

Peak no.		UB51o	UB52o	UB53o	<b>UB54o</b>	UB55o	UB57o	UB59o	UB60o	UB61o	UB63o
<b>Terpanes m/z 191</b>											
1	Tricyclic terpane C <sub>29</sub>	3263	332	200	300	745	3508	8000	1835	4520	5564
2	Tricyclic terpane C <sub>28</sub>	16583	7970	5073	7703	7125	15569	70953	45153	31124	25137
3	Tricyclic terpane C <sub>27</sub>	49145	17609	12400	16989	18897	52051	167418	98459	85112	78058
4	Tricyclic terpane C <sub>26</sub>	10390	2650	2139	3136	3729	11312	24329	18350	13558	16513
5	Tricyclic terpane C <sub>25</sub>	55167	17364	12548	20031	18567	62473	166783	104648	88734	78455
6	Tricyclic terpane C <sub>24</sub>	41367	11039	7405	12762	11947	46993	110540	74466	67597	51411
7	Tricyclic terpane C <sub>23</sub>	17476	4222	3318	4944	4639	24869	40376	29462	27979	26169
8	Tricyclic terpane C <sub>28</sub> -22S	16788	5433	3946	4920	5554	16528	54577	42619	35098	32230
9	Tricyclic terpane C <sub>28</sub> -22R	18262	6014	4533	6148	6315	20005	64140	43125	37453	34423
10	Tricyclic terpane C <sub>27</sub> -22S	2702	0	0	0	905	0	8700	0	5736	0
11	Tricyclic terpane C <sub>27</sub> -22R	3253	0	0	0	541	0	8302	0	5343	0
12	Tricyclic terpane C <sub>28</sub> -22S	18007	4435	2258	5308	4791	17962	50697	31960	35819	29991
13	Tricyclic terpane C <sub>28</sub> -22R	18351	3789	2865	5331	4105	21682	50827	34251	28570	23642
14	Tricyclic terpane C <sub>28</sub> -22S	17133	3338	2806	3776	4335	24687	36269	30473	25384	25046
15	Tricyclic terpane C <sub>28</sub> -22R	17322	4056	2853	4110	4294	24688	38264	31370	27907	25845
16	18a(H)-22,29,30-normethopane (Ts)	21912	4896	3975	4864	6698	23232	65450	42509	32493	46735
17	1 unknown terpane	3236	0	0	0	0	7774	0	0	0	10817
18	Tricyclic terpane C <sub>30</sub> -22S	13286	2660	2291	2999	3277	19771	29290	25322	23533	21394
19	17a(H)-22,29,30-trisnorhopane (Tm)	11994	7434	4181	8001	5281	26020	75576	56886	19577	24831
20	Tricyclic terpane C <sub>30</sub> -22R	12871	2600	2200	2900	3500	0	30000	25000	22562	21452
21	17β(H)-22,29,30-trisnormorethane	0	665	0	1045	498	0	0	0	0	0
22	2. unknown terpane	9973	1779	1338	2507	2961	9754	27013	18508	9389	21400
23	Tricyclic terpane C <sub>31</sub> -22S	15038	3243	2435	3156	3398	15264	41746	26088	24500	21900
24	Tricyclic terpane C <sub>31</sub> -22R	15144	2949	524	3289	3669	14758	42507	26430	21804	19863
25	17a(H),21a(H)-30-norhopane	58484	26626	15657	27094	19177	67253	308192	196740	88385	82781
26	C <sub>30</sub> diahopane	24249	4252	3057	4898	6792	34288	52177	8601	25841	43520
27	3. unknown terpane	4710	769	884	1526	930	7402	9977	0	4792	11568
28	17β(H),21a(H)-30-normorethane	4871	3660	2224	3726	1912	7253	37595	29726	7809	11291
29	18a(H)-olefane	4396	2977	1743	2672	1718	20445	30991	21622	16688	12281
30	17a(H),21 β(H)-hopane	157385	58020	43631	65314	57124	175166	677060	497554	230645	327721
31	17β(H),21a(H)-morethane	14279	8104	5237	10370	5450	20484	96360	75368	24216	35729
32	17a(H),21 β(H),22S-30-homohopane	33860	12045	9065	13459	11366	53603	147766	95951	45175	74866
33	17a(H),21 β(H),22R-30-homohopane	20094	8390	5171	10572	7469	38636	97369	76487	35166	49374
34	gammacerane	106251	26560	13692	28274	29981	98043	296515	190718	114554	207796
35	17a(H),21 β(H),22S-30,31-bishomohopane	25137	6902	5256	8831	7384	45262	72998	65862	36624	55368
36	17a(H),21 β(H),22R-30,31-bishomohopane	14473	5174	4167	6566	4712	34709	64342	52636	24212	33427
37	17a(H),21 β(H),22S-30,31,32-trishomohopane	15558	4446	3179	5286	4254	23278	52597	39502	16588	26797
38	17a(H),21 β(H),22R-30,31,32-trishomohopane	12081	3064	2640	3408	2605	16593	38414	30198	12998	23080
39	17a(H),21 β(H),22S-tetrahomohopane	7839	1494	1723	1711	1473	14083	21576	23214	6611	13714
40	17a(H),21 β(H),22R-tetrahomohopane	5683	1197	1376	1661	1303	9125	17611	12826	6613	9373
41	17a(H),21 β(H),22S-pentakishomohopane	3943	176	518	1013	981	12313	12454	0	6187	6128
42	17a(H),21 β(H),22R-pentakishomohopane	2198	347	389	394	237	6326	9642	0	6672	7831
<b>Di-, Sesquiterpanes m/z 123</b>											
43	C <sub>15</sub> bicyclane	1281	1143	885	1043	3495	1178	4132	5821	18701	18569
44	C <sub>15</sub> bicyclane	2616	3226	2195	2451	7128	1825	10623	15246	30279	32834
45	8β(H)-dimane	3587	6959	3997	5439	8979	2832	19354	29799	45630	39885
46	C <sub>15</sub> bicyclane	4586	3047	2150	3537	7099	1421	14929	13873	24535	29584
47	C <sub>15</sub> bicyclane	1783	1171	931	1287	2663	802	6026	5672	11929	13075
48	C <sub>16</sub> bicyclane	4131	1609	1530	2607	4428	1156	13362	9240	19978	20800
49	8β(H)-homodimane	14846	11305	9913	12635	23636	10082	71225	59038	76919	105500
50	C <sub>17</sub> bicyclane	1470	859	828	971	1784	723	5622	5007	5342	5955
51	C <sub>17</sub> bicyclane	4356	1966	1920	3633	3726	1264	23321	14067	16522	14703
52	C <sub>18</sub> bicyclane	3732	2424	1774	2119	3490	1394	14463	10667	13620	11055
53	unknown diterpane	1131	8963	6049	9346	10927	3712	73897	41960	38381	37463
54	4β(H)-19-nonsopimarane	13268	0	3833	7131	10086	3766	44206	32155	39618	44984

Peak no.		UB51o	UB52o	UB53o	<b>UB54o</b>	UB55o	UB57o	UB59o	UB60o	UB61o	UB63o
55	C <sub>17</sub> bicyclane	8896	0	2332	3962	3803	875	26638	15613	9737	11732
56	C <sub>18</sub> bicyclane	2500	3869	0	0	0	0	0	0	0	0
57	17-nortetracyclic sterpane	4103	1228	1058	1978	2417	590	14391	8422	11865	13398
58	soprinarane	5608	996	1017	1693	4057	1130	13051	9381	18034	17865
59	16 $\beta$ (H)-phylocladane	6914	4298	3029	4769	6198	1466	30613	23577	17099	18205
	<b>Steranes, diasteranes m/z 217</b>										
60	5 $\alpha$ (H),14 $\beta$ (H),17 $\beta$ (H)-digirane	0	0	0	0	0	1549	687	0	703	0
61	5 $\alpha$ (H),14 $\beta$ (H),17 $\beta$ (H)-homodigirane	0	0	0	0	0	0	866	0	0	0
62	13 $\beta$ (H),17 $\alpha$ (H) 20S-diacholestane	1449	227	154	310	341	6234	1621	1671	1263	2418
63	13 $\beta$ (H),17 $\alpha$ (H),20R-diacholestane	902	136	0	165	224	3464	1301	1198	807	1453
64	13 $\alpha$ (H),17 $\beta$ (H) 20S-diacholestane	357	0	122	225	82	1896	1098	1115	0	0
65	13 $\alpha$ (H),17 $\beta$ (H),20R-diacholestane	237	0	0	0	0	2497	1112	0	0	0
66	24-methyl-13 $\beta$ (H),17 $\alpha$ (H) 20S-diacholestane	1368	167	134	228	163	1789	0	608	0	932
67	24-methyl-13 $\beta$ (H),17 $\alpha$ (H),20R-diacholestane	1239	244	222	281	269	2644	2127	2152	1046	1545
68	24-C <sub>28</sub> αβ dia 20S+αα C <sub>27</sub> 20S	2649	2007	1279	1385	1117	10851	12775	10850	3399	4955
69	24-C <sub>28</sub> αβ dia 20S+ ββ C <sub>27</sub> 20R	5318	1011	642	1335	1093	12074	10212	5187	4990	5659
70	24-C <sub>28</sub> αδ dia 20R+ββ C <sub>27</sub> 20S	3646	676	627	738	800	8118	7087	5439	4028	4674
71	14 $\alpha$ (H),17 $\alpha$ (H),20R-cholestane	2717	3055	1295	2874	925	9113	21705	13366	3342	3757
72	24-ethyl-13 $\beta$ (H),17 $\alpha$ (H),20R-diacholestane	857	206	141	0	243	979	988	886	0	1356
73	24-ethyl-13 $\beta$ (H),17 $\alpha$ (H),20S-diacholestane	1355	265	269	169	482	3022	3614	916	1187	948
74	24-methyl-14 $\alpha$ (H),17 $\alpha$ (H),20S-cholestane	1654	538	357	690	376	1694	4459	2674	1024	1608
75	24-C <sub>28</sub> αδ dia 20R+C <sub>28</sub> ββ 20R	4787	755	505	1088	926	4923	8679	6494	3712	3584
76	24-methyl-14 $\beta$ (H),17 $\beta$ (H),20S-cholestane	2732	813	553	643	802	3887	7475	6038	2264	3373
77	24-methyl-14 $\alpha$ (H),17 $\alpha$ (H),20R-cholestane	2635	2409	1061	1469	730	3493	15989	10795	2392	2580
78	24-ethyl-14 $\alpha$ (H),17 $\alpha$ (H),20S-cholestane	2985	1879	1005	1170	1065	7430	13378	9762	3282	3867
79	24-ethyl-14 $\beta$ (H),17 $\beta$ (H),20R-cholestane	5129	1774	1189	1586	1498	6995	14074	10827	4457	7132
80	24-ethyl-14 $\beta$ (H),17 $\beta$ (H),20S-cholestane	4676	1110	762	1213	1186	5369	8600	1153	4920	5421
81	24-ethyl-14 $\alpha$ (H),17 $\alpha$ (H),20R-cholestane	3278	3759	1778	2755	1360	7160	20401	17506	3519	4540
	<b>Monoaromatic steroids m/z 253</b>										
82	monoaromatic sterane C <sub>27</sub>	1014	951	406	1042	525	2118	5146	3092	1147	1297
83	monoaromatic sterane C <sub>27</sub>	1170	759	334	908	697	3837	4629	3642	1176	2088
84	monoaromatic sterane C <sub>27</sub>	703	301	315	1645	117	2457	1962	1844	519	1181
85	monoaromatic sterane C <sub>27</sub>	1837	1709	999	2326	918	4461	7954	5142	1985	2584
86	monoaromatic sterane C <sub>27</sub> +C <sub>28</sub>	2635	2657	1380	744	1339	4136	12599	9036	2287	3039
87	monoaromatic sterane C <sub>27</sub> +C <sub>28</sub>	985	448	498	1087	1173	2273	3284	2360	693	1589
88	monoaromatic sterane C <sub>27</sub> +C <sub>28</sub>	290	1269	585	4391	446	2235	6131	4498	860	849
89	monoaromatic sterane C <sub>27</sub> +C <sub>28</sub>	5990	5546	2552	111	490	5900	24680	19014	4480	7769
90	monoaromatic sterane C <sub>27</sub> +C <sub>28</sub>	423	294	220	346	2768	1001	1757	931	249	669
91	monoaromatic sterane C <sub>27</sub> +C <sub>28</sub>	1261	821	540	537	100	1632	4051	2834	633	1925
92	monoaromatic sterane C <sub>28</sub> +C <sub>28</sub>	2010	3519	1624	2501	611	2373	17365	11772	2442	3076
93	monoaromatic sterane C <sub>28</sub> +C <sub>28</sub>	2281	2241	1372	2243	1573	2825	12125	7726	2139	3514
94	monoaromatic sterane C <sub>28</sub> +C <sub>28</sub>	728	1754	975	1539	1264	372	8006	5248	1436	1470
95	monoaromatic sterane C <sub>28</sub>	769	596	301	533	440	1483	2302	2237	1322	1949
96	monoaromatic sterane C <sub>28</sub>	1370	2529	1193	2397	966	1252	10467	8795	1828	2088

waxy type

immature type

regular type

## APPENDIX 8.1

Peak no.		UB64o	UB67o	UB68o	UB69o	UB70o	UB71o	UB73o	UB74o	UB75o	UB76o
<b>Terpanes m/z 191</b>											
1	Tricyclic terpane C <sub>19</sub>	3500	500	4800	5542	6081	6410	5000	6452	6513	164
2	Tricyclic terpane C <sub>20</sub>	29988	9536	15579	8154	20614	34683	44191	100861	101268	951
3	Tricyclic terpane C <sub>21</sub>	86716	26049	54479	27501	70579	91646	88660	121158	117813	2678
4	Tricyclic terpane C <sub>22</sub>	16448	5813	14403	5108	13387	19230	15915	18431	18651	487
5	Tricyclic terpane C <sub>23</sub>	101805	33223	69396	33820	71607	96035	98500	101731	98187	2006
6	Tricyclic terpane C <sub>24</sub>	48658	26487	50072	26470	53444	63727	70408	61088	64059	1118
7	Tricyclic terpane C <sub>25</sub>	25920	12328	28665	14226	24965	26678	26384	24706	23666	891
8	Tricyclic terpane C <sub>26</sub> 22S	21096	8577	19165	11486	27216	27818	29606	29754	25744	591
9	Tricyclic terpane C <sub>26</sub> 22R	28280	11560	20617	13906	30928	29845	37300	59265	57237	756
10	Tricyclic terpane C <sub>27</sub> 22S	0	0	0	0	4740	0	5437	0	0	135
11	Tricyclic terpane C <sub>27</sub> 22R	0	0	0	0	5148	0	5617	0	0	86
12	Tricyclic terpane C <sub>28</sub> 22S	22209	9608	18242	12263	24872	23155	36234	30557	29447	727
13	Tricyclic terpane C <sub>28</sub> 22R	22853	10212	21320	10583	22201	28796	33110	27130	28475	564
14	Tricyclic terpane C <sub>29</sub> 22S	20463	10782	27174	10644	20758	27251	28582	22364	23469	792
15	Tricyclic terpane C <sub>29</sub> 22R	19370	11821	23875	3590	3597	26284	33235	26600	22950	682
16	18a(H)-22,29,30-normethopane (T's)	29673	31971	20098	37763	37534	40195	46866	37153	34985	960
17	1 unknown terpane	11009	0	11676	4859	7969	6911	0	0	0	0
18	Tricyclic terpane C <sub>10</sub> 22S	15662	9955	19554	10041	18114	21846	28396	21153	16731	487
19	17a(H)-22,29,30-trisnorhopane (Tm)	43727	16138	29820	17682	17786	33073	73876	321897	278115	843
20	Tricyclic terpane C <sub>10</sub> 22R	15000	9608	18354	11000	13080	18339	29000	0	0	685
21	17b(H)-22,29,30-trisnormorethane	0	0	0	2895	0	0	8763	34913	34357	0
22	2 unknown terpane	13930	12343	7795	14263	15458	20877	13794	7578	10051	448
23	Tricyclic terpane C <sub>11</sub> 22S	18578	9029	11849	11275	18630	25379	29181	27711	26143	348
24	Tricyclic terpane C <sub>11</sub> 22R	15954	6474	9925	10792	16374	20678	28214	25547	24867	466
25	17a(H),21b(H)-30-normopane	152555	47938	67952	55149	74729	115411	294955	1025601	906656	2171
26	C <sub>29</sub> diahopane	40683	29475	35878	28403	35431	46284	36356	22398	20203	966
27	3 unknown terpane	0	7424	0	11419	7123	7475	6606	0	6861	0
28	17b(H),21a(H)-30-normorethane	17664	5000	11080	5224	5955	10979	28290	137387	129912	240
29	18a(H)-oleaneane	23921	13117	29125	12050	8667	12437	21733	54304	58158	346
30	17a(H),21 b(H)-hopane	419091	92477	176198	122235	209772	303034	634958	1562118	1328327	9877
31	17b(H),21a(H)-morethane	52765	12020	24050	14881	21695	38866	86220	463187	429094	1016
32	17a(H),21 b(H),22S-30-homopopane	100419	30672	62471	35725	52004	71589	135769	329189	259683	1787
33	17a(H),21 b(H),22R-30-homopopane	62920	22269	45984	23309	33964	54158	103146	221583	264500	1155
34	gammacerane	318482	30532	109104	32357	139716	183928	239971	335649	322642	6623
35	17a(H),21 b(H),22S-30,31-bishomopopane	72089	24620	63261	29973	38649	53824	93200	173855	173046	1389
36	17a(H),21 b(H),22R-30,31-bishomopopane	47889	15865	42312	18476	25315	38774	53574	132444	122203	1027
37	17a(H),21 b(H),22S-30,31,32-trishomopopane	43346	12703	28679	13676	23018	31102	42664	97211	98228	905
38	17a(H),21 b(H),22R-30,31,32-trishomopopane	29858	11882	20993	10791	15773	20800	30848	68538	71369	659
39	17a(H),21 b(H),22S-tetraakis homopopane	18797	10363	17353	7703	12514	13205	17245	40290	35664	28
40	17a(H),21 b(H),22R-tetraakis homopopane	16055	5853	12081	5224	7889	13918	16263	29224	29848	393
41	17a(H),21 b(H),22S-pentaakis homopopane	11461	2901	16595	5050	4089	6094	10481	21678	20668	102
42	17a(H),21 b(H),22R-pentaakis homopopane	8815	1789	7649	4621	2257	6183	8115	17420	13390	112
<b>Di-, Sesquiterpanes m/z 123</b>											
43	C <sub>15</sub> bicyclane	0	24492	9348	37789	18506	21876	1056	0	0	774
44	C <sub>15</sub> bicyclane	0	32960	16786	54177	36111	42629	1493	615	887	1214
45	8b(H)-dnmane	0	32689	25612	44618	39975	59527	3807	4804	7083	1533
46	C <sub>15</sub> bicyclane	0	26855	10033	37632	30080	40264	1251	401	580	942
47	C <sub>15</sub> bicyclane	0	10572	3850	15195	12613	13458	349	0	0	311
48	C <sub>16</sub> bicyclane	0	20198	11873	26906	23730	29095	963	776	830	524
49	8b(H)-homodrimane	0	63589	80621	101635	102529	102747	5378	6281	6452	2234
50	C <sub>17</sub> bicyclane	0	4380	5514	4510	6667	7853	431	656	588	0
51	C <sub>17</sub> bicyclane	0	5943	10498	7386	16214	15599	1013	1189	1438	287
52	C <sub>18</sub> bicyclane	0	5217	11732	6077	11987	15975	872	899	1044	178
53	unknown diterpane	0	17885	25789	17682	33720	48917	3071	3395	4483	714
54	4b(H)-19-nonsopimarane	0	23237	31496	28837	41370	42659	2151	726	861	494

Peak no.		UB64o	UB67o	UB68o	UB69o	UB70o	UB71o	UB73o	UB74o	UB75o	UB76o
55	C <sub>17</sub> bicyclane	0.00	4659	9546	3941	8298	15794	905	1200	958	216
56	C <sub>18</sub> bicyclane	0.00	0	2541	1888	3368	1779	0	0	0	0
57	17-nortracyclic diterpane	0.00	4121	4090	5806	13156	11299	386	0	0	130
58	isopimarane	0.00	16650	9743	19889	22801	16785	980	825	1038	304
59	16 $\beta$ (H)-phylladiene	0.00	8135	10372	7049	17621	25194	1857	1360	1405	0
	<b>Steranes, diasteranes m/z 217</b>										
60	5 $\alpha$ (H),14 $\beta$ (H),17 $\beta$ (H)-diginane	893	1334	1992	1373	884	934	1646	4035	3992	0
61	5 $\alpha$ (H),14 $\beta$ (H),17 $\beta$ (H)-homodiginane	0	0	786	700	753	450	1294	4555	4156	0
62	13 $\beta$ (H),17 $\alpha$ (H),20S-diacholestan e	2927	3054	11533	3742	1940	2348	1842	0	0	164
63	13 $\beta$ (H),17 $\alpha$ (H),20R-diacholestan e	1775	1526	7091	2241	1217	1153	1116	0	0	90
64	13 $\alpha$ (H),17 $\beta$ (H),20S-diacholestan e	1134	670	3348	1141	0	898	832	0	0	75
65	13 $\alpha$ (H),17 $\beta$ (H),20R-diacholestan e	1458	987	3825	1249	0	0	0	0	0	66
66	24-methyl-13 $\beta$ (H),17 $\alpha$ (H),20S-diacholestan e	1801	799	2161	1099	902	1519	1141	0	0	63
67	24-methyl-13 $\beta$ (H),17 $\alpha$ (H),20R-diacholestan e	2312	1886	5129	2452	1055	1332	2796	0	0	36
68	24-C <sub>28</sub> $\alpha\beta$ dia 20S+ $\alpha\alpha$ C <sub>27</sub> ,20S	8682	5015	18827	7568	3338	5885	15561	80310	79691	409
69	24-C <sub>28</sub> $\alpha\beta$ dia 20S+ $\beta\beta$ C <sub>27</sub> ,20R	8628	7123	18995	9132	5866	7011	11770	30853	35632	459
70	24-C <sub>28</sub> $\alpha\beta$ dia 20R+ $\beta\beta$ C <sub>27</sub> ,20S	5026	3893	12085	5358	4184	4607	8567	27255	25826	300
71	14 $\beta$ (H),17 $\alpha$ (H),20R-cholestan e	17436	6032	14786	8002	3240	6407	16402	143795	151043	313
72	24-ethyl-13 $\beta$ (H),17 $\alpha$ (H),20R-diacholestan e	1282	1817	1417	1592	1741	738	3371	16403	18626	0
73	24-ethyl-13 $\beta$ (H),17 $\alpha$ (H),20S-diacholestan e	1384	1883	5387	2345	963	992	1955	22525	24200	0
74	24-methyl-14 $\alpha$ (H),17 $\alpha$ (H),20S-cholestan e	5025	1630	4108	1827	1207	1997	5772	35748	43585	69
75	24-C <sub>28</sub> $\alpha\beta$ dia 20R+C <sub>28</sub> $\beta\beta$ 20R	6694	2868	7529	3634	4435	5872	12661	72008	53855	237
76	24-methyl-14 $\beta$ (H),17 $\beta$ (H),20S-cholestan e	3488	1865	5076	2885	3385	4779	10298	57302	42831	144
77	24-methyl-14 $\alpha$ (H),17 $\alpha$ (H),20R-cholestan e	9702	2131	3829	2747	2161	4592	13718	185092	216950	154
78	24-ethyl-14 $\alpha$ (H),17 $\alpha$ (H),20S-cholestan e	9299	4093	10789	5397	3179	6574	20607	155289	156658	258
79	24-ethyl-14 $\beta$ (H),17 $\beta$ (H),20R-cholestan e	7202	4699	9251	5429	5864	7038	20533	127466	105285	283
80	24-ethyl-14 $\beta$ (H),17 $\beta$ (H),20S-cholestan e	4618	3931	8907	5220	5784	5266	17986	73000	80000	336
81	24-ethyl-14 $\alpha$ (H),17 $\alpha$ (H),20R-cholestan e	17222	5088	10926	5340	3594	8276	23171	361552	348578	388
	<b>Monocyclic steroids m/z 253</b>										
82	monoaromatic sterane C <sub>27</sub>	3666	690	2507	1216	648	1805	1472	4637	4579	99
83	monoaromatic sterane C <sub>27</sub>	4582	1402	7609	2253	1203	2289	1183	839	656	0
84	monoaromatic sterane C <sub>27</sub>	2392	1003	4255	1241	648	990	695	1670	1177	0
85	monoaromatic sterane C <sub>27</sub>	8284	2500	8875	3378	1631	3522	2346	4239	4388	134
86	monoaromatic sterane C <sub>27</sub> +C <sub>28</sub>	8853	1591	6098	2315	1824	4444	3083	14499	14328	200
87	monoaromatic sterane C <sub>27</sub> +C <sub>28</sub>	4348	818	3692	1237	878	1334	862	698	1031	44
88	monoaromatic sterane C <sub>27</sub> +C <sub>28</sub>	3500	660	2450	982	409	2128	782	5002	5619	0
89	monoaromatic sterane C <sub>27</sub> +C <sub>28</sub>	19794	3699	10048	4031	4236	8126	7265	30925	35516	289
90	monoaromatic sterane C <sub>27</sub> +C <sub>28</sub>	2411	223	1545	422	474	602	524	1287	936	0
91	monoaromatic sterane C <sub>27</sub> +C <sub>28</sub>	3992	1092	3714	1351	1290	1724	1268	2097	2158	0
92	monoaromatic sterane C <sub>27</sub> +C <sub>28</sub>	10035	1978	2904	2251	1645	4575	4429	35653	39755	47
93	monoaromatic sterane C <sub>27</sub> +C <sub>28</sub>	10417	1419	5238	1755	1821	4201	3945	16834	18758	30
94	monoaromatic sterane C <sub>27</sub> +C <sub>28</sub>	5245	206	401	451	826	2371	1629	15251	19409	0
95	monoaromatic sterane C <sub>27</sub>	2798	1702	2653	1419	936	1231	1349	1189	1156	0
96	monoaromatic sterane C <sub>27</sub>	7063	720	1795	1065	1226	2876	3169	31549	31224	67

- waxy type
- immature type
- regular type

## APPENDIX 8.2

### PCA Results, Crude Oil Analysis GC-MS Data

#### PCA, 20 variables, normalized, variance-covariance matrix

Variance extracted, first 10 axis

AXIS	Eigenvalue	% variance	cum. %var.	broken-stick
1	3.497	59.161	59.161	1.063
2	1.172	19.824	78.984	0.768
3	0.419	7.087	86.071	0.62
4	0.242	4.094	90.165	0.521
5	0.181	3.07	93.236	0.448
6	0.12	2.032	95.268	0.388
7	0.077	1.309	96.577	0.339
8	0.066	1.114	97.691	0.297
9	0.038	0.646	98.337	0.26
10	0.028	0.478	98.815	0.227

First 6 eigenvector loadings

Peak no	attribut	Eigenvector					
		1	2	3	4	5	6
3	#1310	0.1345	0.2584	0.1571	0.3653	-0.3859	-0.1409
5	#1441	0.1767	0.2951	0.0631	0.2851	-0.3207	-0.4017
16	#1816	0.1148	0.0208	0.0569	-0.2515	0.0376	-0.3101
19	#1841	-0.0934	-0.1438	0.0152	0.1447	0.1039	-0.0843
25	#1915	-0.2935	-0.2682	0.1996	0.3195	0.1134	-0.2831
26	#1924	0.1244	0.0592	0.0095	-0.227	0.1636	-0.3825
28	#1947	-0.0524	-0.0275	-0.003	0.0408	-0.0205	-0.0531
30	#1967	-0.3711	0.1379	0.4692	-0.4229	-0.3843	0.2102
31	#1995	-0.1403	-0.1231	0.1044	0.1355	0.1613	-0.0123
32	#2034	-0.029	0.0349	0.0987	-0.2239	0.1618	-0.3681
33	#2043	-0.0263	-0.0045	0.0492	-0.1912	0.0754	-0.2726
34	#2063	0.0227	0.6969	-0.2869	-0.0114	0.3477	0.2278
45	#727	0.3681	-0.26	0.1237	0.1476	-0.1525	0.3876
49	#814	0.6336	-0.2136	0.1507	-0.3242	0.0795	0.0154
54	#1134	0.2554	0.0179	-0.0597	0.1455	-0.0569	-0.1029
58	#1219	0.1633	-0.0407	-0.0697	0.1493	0.1053	-0.0198
59	#1234	0.068	0.0427	0.014	0.092	-0.1655	-0.019
71	#1791	-0.0819	-0.1661	-0.679	-0.2575	-0.5234	-0.1229
77	#1852	-0.0969	-0.1682	-0.17	0.0958	0.121	0.0413
81	#1901	-0.1242	-0.2341	-0.2566	0.087	0.0982	-0.0398
	cut-off	0.127	0.139				

Coordinates (scores) of crude oil samples

No.	samples	map-group	Axis (Component)					
			1	2	3	4	5	6
1	UB14o	1	-0.3869	-0.2171	0.0025	0.0487	0.1047	0.0104
2	UB1o	1	-0.3473	-0.1351	0.0125	-0.0182	0.0807	0.0669
3	UB21o	2	0.6125	-0.0496	-0.0994	0.1383	0.0285	0.0323
4	UB33o	3	-0.2503	-0.3217	-0.1385	0.0231	0.0465	0.0009
5	UB27o	3	0.2454	0.0147	0.0653	0.1406	-0.1494	0.0022
6	UB73o	3	-0.3347	0.0391	0.0509	-0.0388	0.0225	-0.0104
7	UB16o	4	0.1078	0.2576	-0.0871	0.0184	0.0723	-0.0159
8	UB31o	4	0.6731	-0.1014	-0.1501	0.1535	0.0738	0.0309
9	UB51o	4	-0.1344	0.2506	-0.0317	0.0125	0.0201	-0.0386
10	UB22o	4	0.3076	0.126	-0.0592	0.1076	0.0151	-0.0013
11	UB76o	4	-0.0562	0.2015	-0.0355	-0.0739	0.0288	0.1148
12	UB70o	5	0.1206	0.1327	-0.0021	-0.038	0.0366	-0.017
13	UB46o	5	0.1507	0.0335	0.0335	-0.0584	0.0223	0.0641
14	UB74o	5	-0.4358	-0.2176	-0.0008	0.0426	0.064	-0.029
15	UB75o	5	-0.4333	-0.2219	-0.0311	0.0555	0.0748	-0.0401
16	UB20o	5	-0.0825	0.0838	0.0412	-0.0806	0.0147	0.0893
17	UB64o	5	-0.248	0.2554	-0.087	-0.0178	0.0913	0.033
18	UB6o	5	0.0662	0.0793	0.033	-0.0493	-0.0075	0.0271
19	UB55o	5	0.0673	0.1051	0.0355	-0.0231	-0.0294	-0.001
20	UB71o	5	0.0204	0.1218	0.0142	-0.0198	0.0185	-0.01
21	UB63o	5	0.0064	0.1741	-0.0059	-0.098	0.0455	0.0402
22	UB24o	5	-0.1176	0.0338	0.0568	0.0158	-0.0272	0.0312
23	UB5o	6	0.451	-0.3134	0.0483	-0.1108	0.0449	0.0363
24	UB69o	6	0.2633	-0.1947	0.0694	-0.1224	0.0193	-0.0791
25	UB15o	6	0.4442	-0.286	0.0363	-0.1205	0.0401	0.0077
26	UB67o	6	0.2132	-0.1347	0.0558	-0.0698	0.0226	-0.1552
27	UB9o	6	-0.3032	-0.1717	-0.4951	-0.1082	-0.2001	-0.0041
28	UB34o	6	0.3452	-0.2531	0.0491	-0.0849	-0.0164	0.0173
29	UB23o	7	-0.1125	0.0649	0.0388	-0.001	-0.0384	0.0106
30	UB52o	7	-0.1466	0.0633	0.0372	0.0239	-0.0397	-0.0216
31	UB59o	7	-0.2166	0.0871	0.0449	0.0016	-0.0126	-0.0416
32	UB53o	7	-0.1055	0.0341	0.0919	-0.0212	-0.0944	-0.031
33	UB54o	7	-0.1319	0.0733	0.0435	0.0083	-0.0413	-0.0356
34	UB60o	7	-0.2181	0.05	0.0631	-0.0246	-0.0288	0.011
35	UB68o	8	0.0618	0.0945	-0.0265	-0.0499	0.0357	-0.0985
36	UB42o	8	0.2732	-0.0304	0.0143	0.0123	-0.0545	-0.0196
37	UB13o	8	0.2162	0.2625	-0.1364	0.0254	0.107	0.0006
38	UB57o	8	-0.189	0.1845	-0.0139	-0.0197	0.0138	-0.1191
39	UB8o	8	-0.0417	-0.0215	0.1114	-0.0623	-0.0998	0.0875
40	UB47o	8	0.308	0.0007	0.0286	0.037	-0.0596	-0.0119
41	UB48o	8	0.2026	0.0819	0.0154	0.0454	-0.0416	-0.057
42	UB26o	9	-0.2856	-0.1689	0.0593	0.1441	0.0083	0.018
43	UB7o	9	-0.3583	-0.1147	0.064	0.1125	-0.023	0.0056
44	UB10o	9	-0.2887	-0.1412	0.0698	0.0958	-0.0255	0.0305
45	UB61o	9	0.0423	0.1042	0.0509	0.0264	-0.0579	-0.0304
46	UB30o	9	0.1742	0.0178	0.0559	0.0646	-0.0774	0.05
47	UB3o	9	-0.1488	0.0669	0.0067	-0.0426	-0.0276	0.0496

## APPENDIX 9

### Crude Oils - Fractionation, GC and GC-MS Parameters

Sample	No.	Map-group	Fractionation						GC	$P_{nC_1}/P_{nC_{11}}$	$P_{nC_{11}}/P_{nC_{12}}$	$P_{nC_{12}}/P_{nC_{13}}$	$C_{11}/C_{12}/C_{13}$	
			%ASPH	%Mait	%SAT	%ARO	%POL	%bran						
Texaco D-1 Ute Tribal 4700ft	1a	1	53.0	47.0	61.1	14.5	24.3	84.7	1.86	1.84	3.09	2.17	0.70	
Texaco D-1 Ute Tribal 9251ft	2a	1	33	96.7	92.7	5.4	1.8	41.3	2.30	0.14	0.60	1.06	1.48	
Cedar Rim Ute Tribal 2-2C8	24a	1	9.3	90.7	81.7	15.8	22.5	84.3	2.12	1.74	12.98	3.11	0.55	
Cedar Rim Ute Tribal 2-24C7	38a	1	13.1	86.9	97.2	1.2	1.6	80.8	5.73	0.28	0.05	1.20	1.30	
Cedar Rim Ford 2-13C7	39a	1	6.5	93.5	91.2	4.6	4.0	43.3	6.64	0.32	0.05	1.23	1.80	
Antelope Creek Ute Tribal 1-5 (05-07)	11a	2	7.9	92.1	89.9	5.1	5.1	50.1	2.42	0.26	0.09	0.98	1.90	
Nutter Canyon Ute Tribal 10-21	21a	2	6.0	94.0	85.5	9.3	5.1	57.19	1.18	0.18	0.24	1.05	1.32	
Bluebell Preston 2-8B1	4a	3	3.8	96.2	86.9	6.3	6.8	20.1	2.58	0.28	0.11	1.16	1.24	
Bluebell Fay Mecham Fee Federal 1	27a	3	7.9	92.1	81.1	12.5	6.4	63.1	1.34	0.84	0.82	1.12	1.13	
Bluebell 1-33A1 Lili Pack	33a	3	28.3	71.7	88.6	13.5	19.8	78.6	0.65	0.88	1.31	0.79	1.08	
Chevron Blanchard 1-33-3	73a	3	3.4	98.6	80.4	11.8	7.9	74.1	1.23	0.68	0.57	1.10	0.90	
Eight Mile Wash State 33-52D (33-32)	18a	4	7.5	92.5	80.1	12.7	7.2	70.8	1.30	0.39	0.31	1.10	1.30	
Natural Buttes Old Squaws Crossing 4A	20a	4	9.1	90.9	77.4	13.8	9.0	82.4	2.35	1.44	0.99	1.01	0.76	
Pleasant Valley Federal 24-15-H	22a	4	8.6	91.4	88.8	7.4	3.8	73.7	0.92	0.44	0.47	0.96	1.02	
Monument Butte Federal 15-20	31a	4	7.3	92.7	87.2	7.5	5.3	87.1	1.13	0.29	0.25	1.02	1.40	
Panette Bench Federal 14-5	51a	4	9.3	90.7	78.0	14.4	7.8	60.9	1.17	0.58	0.49	1.08	1.15	
CNG 3-25B	78a	4	9.1	90	50.3	n.a.	n.a.	62.1	0.90	0.48	0.55	1.02	1.11	
Wonsits Valley 133&71	6a	5	4.9	95.1	77.4	13.7	8.9	69.3	1.11	0.52	0.48	1.03	0.97	
Wonsits Valley Whiton Valley 1-19-3C	24a	5	5.9	94.1	68.9	18.5	14.8	58.8	0.75	0.88	0.18	0.86	0.72	
Gypsum Hills Federal 3	46a	5	7.5	92.5	76.9	15.9	7.2	87.7	1.03	0.47	0.44	0.98	0.98	
Wonsits Valley Federal 105	55a	5	18.3	81.7	76.1	15.8	8.3	76.1	1.14	0.64	0.54	1.02	1.12	
Wonsits Valley Unit 88-2	63a	5	4.1	95.9	76.3	14.9	8.7	79.3	1.04	0.53	0.52	1.04	1.51	
White River Unit 47-10	84a	5	6.1	93.9	74.0	16.0	10.0	77.0	1.43	1.14	0.89	1.27	0.87	
Wonsits Valley Federal 24	71a	5	7.8	92.2	80.3	13.5	6.2	72.1	1.03	0.54	0.52	1.00	1.17	
Conoco Tribal 31-55A	74a	5	4.5	95.5	76.1	15.6	8.1	76.4	1.11	1.78	1.87	1.13	0.93	
Conoco Tribal 35-51	75a	5	4.6	95.4	71.1	15.6	13.3	77.3	1.11	1.88	2.09	1.15	0.90	
Gypsum Hills Costas Federal 2-20-3b	70a	5	10.0	90.0	76.6	13.6	9.9	69.7	1.11	0.47	0.43	1.05	1.16	
Coyote Basin E Red Wash 1-5	5a	6	4.1	95.9	80.8	10.3	9.0	58.9	1.64	0.46	0.27	1.11	1.02	
Coyote Basin Federal 12-13	15a	6	5.7	94.3	87.7	7.1	5.2	60.6	2.07	0.07	0.31	1.21	0.93	
Red Wash 20 1-32-28C	34a	6	7.2	92.6	87.0	8.6	4.3	61.3	1.65	0.35	0.24	1.24	1.15	
Federal 1-27	67a	6	6.2	93.8	84.7	10.6	4.7	63.4	1.27	0.71	0.60	1.14	1.08	
Coyote Basin E Red Wash Fed 4-6	89a	6	6.6	93.4	88.5	9.4	4.1	64.0	1.63	0.38	0.25	1.19	1.90	
E Red Wash 1-81-28C (State 1-41-36C)	9a	6	3.7	96.3	69.4	14.0	16.6	50.7	0.68	0.78	1.47	0.92	0.52	

Sample	No	Map-group	Fractionation						GC	P/nC <sub>11</sub>	P/nC <sub>12</sub>	P+nC <sub>11</sub> /P+nC <sub>12</sub>	C <sub>11</sub> ,n/C <sub>12</sub> ,n
			%ASPH	%Malt	%SAT	%ARO	%POL	%bran					
Walker Hollow	23a	7	3.8	96.2	77.1	13.4	9.6	76.7	1.04	1.02	0.78	0.90	0.94
Pearl Broadhurst 21													
Walker Hollow	52a	7	3.5	96.5	72.4	16.5	11.1	75.1	1.05	1.34	1.90	0.95	1.15
Pearl Broadhurst 1													
Walker Hollow	53a	7	2.5	97.5	78.7	12.6	8.8	94.2	1.04	0.97	0.81	0.95	1.24
Pearl Broadhurst 15													
Walker Hollow	54a	7	1.2	98.8	81.4	24.1	14.5	88.3	0.97	6.43	5.64	0.95	0.94
Pearl Broadhurst 18													
Walker Hollow	59a	7	5.3	94.7	88.1	20.6	11.3	78.9	1.11	2.47	1.89	1.02	0.91
Pearl Broadhurst 12													
Walker Hollow Unit 1	60a	7	8.6	91.4	73.5	15.4	11.1	78.0	1.03	1.26	0.98	0.92	0.87
Horseshoe Bend													
2/22-34 Federal	8a	8	7.6	92.4	71.0	18.5	10.5	68.0	1.41	1.60	1.22	1.28	0.98
Brennan Bottom Federal 2-20	13a	8	4.3	95.7	79.4	14.3	6.3	63.3	1.08	0.51	0.58	1.13	0.93
Brennan Bottom Federal 15-8	42a	8	7.5	92.5	79.5	13.2	7.3	73.0	1.90	0.56	0.50	1.00	0.90
Horseshoe Bend Federal 4-2-F	47a	8	7.6	92.4	79.2	12.7	8.0	74.7	1.19	0.58	0.48	1.04	1.14
Horseshoe Bend Federal 5-5H	48a	8	9.7	90.3	73.5	14.5	12.0	68.2	1.17	0.59	0.51	1.06	1.28
Brennan Bottom Federal 6	57a	8	8.3	91.7	86.6	9.2	4.3	73.3	1.02	0.47	0.44	0.98	0.93
Brennan Bottom Federal 1	68a	8	8.9	91.1	79.8	14.4	5.9	63.0	1.35	1.36	1.10	1.23	0.85
Twelve Mile Wash Fed 1	73a	9	6.4	93.6	65.6	17.1	17.3	77.0	1.45	2.51	3.11	1.53	1.24
6956-6960ft													
Twelve Mile Wash Federal 1	7398-7428ft	9	8.8	91.2	78.9	9.9	11.1	78.5	1.42	4.31	3.97	1.39	0.68
Twelve Mile Wash Federal 1	7456	9	7.6	92.4	78.3	11.1	10.6	80.0	1.47	3.25	2.71	1.40	0.77
DST 5960ft													
Gusher Gov 4-14	81a	9	6.0	94.0	76.9	13.4	9.7	78.7	1.09	0.59	0.51	0.99	1.21
Gusher Gusher 3	30a	9	4.9	95.1	80.0	12.5	7.5	71.5	1.05	0.57	0.50	0.99	1.12
Red Wash Whole Field	3a	-	4.8	95.2	71.3	18.2	10.5	62.6	1.04	0.99	0.97	1.03	1.12

waxy type

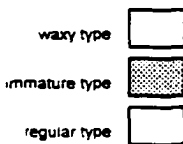
immature type

regular type

## APPENDIX 9

Sample	No.	Map-group	GC				Terpanes							
			C <sub>11</sub> /C <sub>12</sub>	B-carbonate (ug/gTOC)	R <sub>22</sub>	CPI	C <sub>19</sub> C <sub>11</sub> Tricyclic terpanes	22S/(22S+22R) C <sub>19</sub> hopane	T <sub>1</sub> /T <sub>1m</sub>	Dihopane index	Cleanane index	Mantane/(mantane+hopane) C <sub>2</sub>	Tricyclics/pentacyclics	Gammacerane index
Texaco D-1 Ute Tribal 4700ft	1a	1	0.64	723	0.73	1.54	0.11	0.54	0.08	0.00	0.00	0.18	0.11	0.33
Texaco D-1 Ute Tribal 9251ft	2a	1	1.40	0	0.99	1.02	0.00	0.00	0.00	0.00	0.00	0.00	0.00	0.00
Cedar Rim Ute Tribal 2-2C8	24a	1	0.74	3287	0.91	1.51	0.10	0.59	0.05	0.00	0.02	0.25	0.13	0.27
Cedar Rim Ute Tribal 2-24C7	38a	1	0.95	0	1.03	1.01	0.00	0.00	0.00	0.00	0.00	0.00	0.00	0.00
Cedar Rim Ford 2-13C7	38a	1	0.97	0	1.02	1.00	0.00	0.00	0.00	0.00	0.00	0.00	0.00	0.00
Antelope Creek Ute Tribal 1-5 (05-07)	11a	2	0.58	0	1.01	0.96	0.00	0.00	0.00	0.00	0.00	0.00	0.00	0.00
Nutter Canyon Ute Tribal 10-21	21a	2	0.85	102	0.99	1.04	0.09	0.64	0.77	0.90	0.00	0.13	1.65	1.02
Bluebell Preston 2-8B1	4a	3	0.75	0	0.99	0.98	0.00	0.00	0.00	0.00	0.00	0.00	0.00	0.00
Bluebell Fay Mecham Fee Federal 1	27a	3	0.62	284	1.01	0.98	0.03	0.59	0.52	0.29	0.08	0.10	1.32	0.43
Bluebell 1-33A1 Lili Pack	33a	3	0.56	818	1.02	1.05	0.21	0.64	0.13	0.07	0.11	0.08	0.21	0.26
Chevron Blanchard 1-33-3	73a	3	0.53	62	1.01	1.02	0.05	0.57	0.39	0.12	0.03	0.12	0.38	0.38
Eight Mile Wash State 33-52D (33-32)	16a	4	0.92	78	0.97	1.07	0.06	0.58	0.70	0.65	0.03	0.08	1.13	0.96
Natural Buttes Old Squaws Crossing 4A	20a	4	0.43	497	0.99	1.06	0.02	0.64	0.49	0.23	0.03	0.09	0.46	0.51
Pleasant Valley Federal 24-15-H	22a	4	0.54	290	0.99	1.05	0.07	0.61	0.62	0.38	0.05	0.11	1.36	0.86
Monument Butte Federal 15-20	31a	4	0.67	110	1.01	1.04	0.09	0.61	0.54	1.00	0.00	0.00	1.78	1.23
Panette Bench Federal 14-5	51a	4	0.79	240	0.97	1.07	0.06	0.63	0.65	0.41	0.03	0.08	0.79	0.68
CNG 3-25B	78a	4	0.88	68	1.01	1.02	0.08	0.61	0.53	0.44	0.04	0.09	0.60	0.67
Wonsits Valley 133&71	8a	5	0.54	224	1.00	1.03	0.08	0.58	0.57	0.35	0.03	0.09	0.68	0.54
Wonsits Valley Whitton Valley 1-19-3C	24a	5	0.35	754	0.98	1.04	0.03	0.61	0.38	0.07	0.02	0.10	0.63	0.45
Gypsum Hills Federal 3	48a	5	0.44	292	1.01	1.02	0.08	0.59	0.58	0.31	0.03	0.09	0.61	0.57
Wonsits Valley Federal 105	55a	5	0.53	306	1.02	1.05	0.04	0.60	0.56	0.35	0.03	0.09	0.73	0.52
Wonsits Valley Unit 88-2	63a	5	0.80	403	0.98	0.97	0.07	0.60	0.65	0.53	0.04	0.10	0.58	0.63
White River Unit 47-10	84a	5	0.52	583	0.95	1.06	0.03	0.61	0.40	0.27	0.06	0.11	0.42	0.76
Wonsits Valley Federal 24	71a	5	0.58	530	0.98	1.05	0.07	0.57	0.55	0.40	0.04	0.11	0.62	0.61
Conoco Tribal 31-55A	74a	5	0.82	832	0.95	1.17	0.06	0.60	0.10	0.02	0.03	0.23	0.15	0.21
Conoco Tribal 35-51	75a	5	0.64	1067	0.98	1.20	0.07	0.50	0.11	0.02	0.04	0.24	0.16	0.24
Gypsum Hills Costas Federal 2-20-3b	70a	5	0.62	400	0.99	1.03	0.08	0.60	0.68	0.47	0.04	0.09	0.71	0.67
Coyote Basin E Red Wash 1-5	5a	6	0.59	0	0.96	1.03	0.16	0.53	0.63	0.90	0.12	0.17	0.47	0.23
Coyote Basin Federal 12-13	15a	6	0.66	0	1.01	0.99	0.19	0.55	0.70	0.56	0.11	0.09	0.49	0.25
Red Wash 20 1 32-28C	34a	6	0.81	173	1.02	0.99	0.15	0.59	0.63	0.49	0.10	0.12	0.52	0.24
Federal 1-27	67a	6	0.85	127	0.98	1.02	0.02	0.58	0.66	0.61	0.14	0.12	0.52	0.33
Coyote Basin E Red Wash Fed 4-6	69a	6	0.66	156	1.03	1.01	0.16	0.61	0.68	0.52	0.10	0.11	0.47	0.26
E Red Wash 1/91-26C (State 1-41-36C)	9a	6	0.44	323	0.86	1.11	0.20	0.48	0.28	0.04	0.10	0.12	0.24	0.42

Sample	No	Map-group	GC				Terpanes								
			C <sub>11</sub> /C <sub>12</sub>	β-sitostane µg/g LOC	R22	CPI	C <sub>19</sub> C <sub>21</sub> Tricyclic terpanes	22S/(22S+22R)	C <sub>19</sub> hopane	Ts/Ts+Tm	Dihopane index	Oleane index	Moritane/(moritane+hopane) C <sub>29</sub>	Tricyclics/pentacyclics	Gammacerane index
Walker Hollow															
Pearl Broadhurst 21	23a	7	0.35	329	1.09	1.03	0.11	0.59	0.44	0.00	0.05	0.12	0.61	0.45	
Walker Hollow	52a	7	0.45	506	0.99	1.06	0.02	0.59	0.40	0.16	0.05	0.12	0.61	0.46	
Pearl Broadhurst 1															
Walker Hollow	53a	7	0.49	301	1.02	1.02	0.02	0.64	0.49	0.20	0.04	0.11	0.60	0.31	
Pearl Broadhurst 15															
Walker Hollow	54a	7	0.42	550	0.95	1.08	0.01	0.58	0.38	0.18	0.04	0.14	0.58	0.43	
Pearl Broadhurst 18															
Walker Hollow	59a	7	0.31	966	0.98	1.09	0.05	0.60	0.46	0.17	0.05	0.12	0.54	0.44	
Pearl Broadhurst 12															
Walker Hollow Unit 1	60a	7	0.39	766	0.99	1.05	0.02	0.58	0.43	0.04	0.04	0.13	0.51	0.38	
Horseshoe Bend 2/22-34 Federal	8a	8	0.58	327	1.02	1.08	0.09	0.58	0.42	0.14	0.04	0.09	0.57	0.29	
Brennan Bottom Federal 2-20	13a	8	0.65	239	0.98	1.07	0.04	0.64	0.59	0.62	0.06	0.10	0.78	1.15	
Brennan Bottom Federal 15-8	42a	8	0.47	219	0.99	0.99	0.05	0.55	0.44	0.34	0.10	0.09	0.80	0.50	
Horseshoe Bend Federal 4-2-F	47a	8	0.52	229	1.01	1.08	0.07	0.59	0.65	0.44	0.06	0.05	1.04	0.52	
Horseshoe Bend Federal 5-SH	48a	8	0.52	144	1.06	1.04	0.06	0.63	0.58	0.34	0.06	0.11	0.91	0.58	
Brennan Bottom Federal 6	57a	8	0.55	156	0.97	1.03	0.06	0.58	0.47	0.51	0.12	0.10	0.80	0.58	
Brennan Bottom Federal 1	68a	8	0.74	625	0.96	1.00	0.07	0.58	0.40	0.53	0.17	0.12	0.58	0.82	
Twelve Mile Wash Fed 1 6958-6960ft	7a	9	0.60	1330	1.03	1.21	0.01	0.62	0.08	0.01	0.02	0.20	0.37	0.25	
Twelve Mile Wash Federal 1 7398-7420ft	10a	9	0.51	693	1.02	1.20	0.02	0.62	0.08	0.00	0.02	0.18	0.39	0.28	
Twelve Mile Wash Federal 1 DST 5960ft	26a	9	0.59	2175	0.95	1.21	0.06	0.56	0.07	0.01	0.02	0.21	0.35	0.30	
Gusher Gov 4-14	61a	9	0.59	234	1.04	1.01	0.05	0.58	0.62	0.29	0.07	0.10	0.93	0.50	
Gusher Gusher 3	30a	9	0.48	240	1.00	1.08	0.06	0.54	0.50	0.27	0.05	0.10	0.95	0.48	
Red Wash Whole Field	3a	-	0.53	427	1.05	1.05	0.08	0.55	0.41	0.18	0.05	0.11	0.51	0.46	



## APPENDIX 9

Sample	No.	Map-group	Terpanes						Sesqui-, diterpanes					
			Gammatocene µg/g oil	C <sub>29</sub> C <sub>30</sub>	17 $\alpha$ -hopanes	Methyl hopanes	C <sub>29</sub> Tetracyclic terpane	C <sub>29</sub> S/C <sub>31</sub> S/ab-hopane	Unknown terpane/C <sub>29</sub> ab-hopane	Sesqui-/sesqui + diterpanes	Sesqui-/sesqui + pentac terpanes	Sesqui-/sesqui steranes	Diterpanes/diterpanes + pentac terpanes	Diterpanes/steranes
Texaco D-1 Ute Trbal 4700ft	1e	1	304	0.52	+	+	0.08	0.00	0.61	0.05	0.21	0.03	0.15	0.37
Texaco D-1 Ute Trbal 9251ft	2e	1	0	0.00	-	-	0.00	0.00	0.64	1.00	1.00	1.00	1.00	0.00
Cedar Rim Ute Trbal 2-2C8	34e	1	230	0.63	+	++	0.05	0.00	0.51	0.04	0.14	0.04	0.14	0.40
Cedar Rim Ute Trbal 2-24C7	38e	1	0.00	0.00	-	-	0.00	0.00	0.92	1.00	1.00	1.00	1.00	1.00
Cedar Rim Ford 2-13C7	38e	1	0.00	0.00	-	-	0.00	0.00	0.90	1.00	1.00	1.00	1.00	0.53
Antelope Creek Ute Trbal 1-5 (05-07)	11e	2	0	0.00	-	-	0.00	0.00	0.45	1.00	1.00	1.00	1.00	0.32
Nutter Canyon Ute Trbal 10-21	21e	2	151	0.34	-	-	0.00	0.31	0.67	0.40	0.93	0.25	0.87	0.43
Bluebell Freston 2-8B1	4e	3	0	0.00	-	-	0.00	0.00	0.78	1.00	1.00	1.00	1.00	0.49
Bluebell Fay Mecham Fee Federal 1	27e	3	336	0.38	-	+	0.11	0.00	0.58	0.21	0.88	0.16	0.84	0.50
Bluebell 1-33A1 Lith Pack	33e	3	538	0.65	+	++	0.21	0.02	0.62	0.10	0.09	0.07	0.06	0.56
Chevron Blanchard 1-33-3	73e	3	2823	0.48	+	+	0.13	0.02	0.55	0.01	0.07	0.00	0.06	0.41
Eight Mile Wash State 33-52D (33-32)	18e	4	2841	0.35	+	-	0.22	0.13	0.68	0.15	0.78	0.08	0.63	0.34
Natural Buttes Old Squaws Crossing 4A	20e	4	170	0.34	+	-	0.27	0.03	0.66	0.15	0.79	0.08	0.66	0.37
Pleasant Valley Federal 24-15-H	22e	4	381	0.41	-	+	0.17	0.00	0.54	0.22	0.86	0.19	0.84	0.34
Monument Butte Federal 15-20	31e	4	221	0.48	-	+	0.62	0.00	0.68	0.44	0.93	0.27	0.87	0.40
Panette Bench Federal 14-5	51e	4	3258	0.37	+	-	0.23	0.08	0.39	0.03	0.40	0.05	0.51	0.19
CNG 3-25B	76e	4	1002	0.22	+	+	0.02	0.00	0.76	0.14	0.68	0.05	0.38	0.41
Wonsits Valley 133&71	6e	5	874	0.34	+	-	0.13	0.00	0.64	0.19	0.81	0.12	0.71	0.35
Wonsits Valley Whiton Valley 1-19-3C	24e	5	1658	0.47	+	+	0.12	0.02	0.60	0.11	0.61	0.08	0.51	0.45
Gypsum Hills Federal 3	48e	5	862	0.36	+	-	0.22	0.06	0.70	0.26	0.89	0.13	0.78	0.35
Wonsits Valley Federal 105	55e	5	0	0.34	+	+	0.13	0.05	0.55	0.16	0.81	0.14	0.77	0.28
Wonsits Valley Unit 88-2	83e	5	858	0.25	+	-	0.18	0.14	0.80	0.13	0.81	0.09	0.74	0.27
White River Unit 47-10	64e	5	1023	0.36	+	+	0.19	0.00	0.00	0.00	0.00	0.00	0.00	0.00
Wonsits Valley Federal 24	71e	5	713	0.38	+	-	0.18	0.06	0.81	0.15	0.80	0.11	0.72	0.37
Conoco Trbal 31-5SA	74e	5	3870	0.66	+	++	0.12	0.00	0.56	0.00	0.01	0.00	0.01	0.43
Conoco Trbal 35-51	75e	5	3476	0.68	+	++	0.14	0.01	0.57	0.00	0.01	0.00	0.01	0.52
Gypsum Hills Costas Federal 2 20-3b	70e	5	538	0.36	+	+	0.24	0.10	0.60	0.17	0.83	0.12	0.76	0.28
Coyote Basin E Red Wash 1-5	5e	6	142	0.38	-	+	0.18	0.19	0.83	0.45	0.87	0.14	0.58	0.40
Coyote Basin Federal 12-13	15e	6	87	0.42	-	+	0.27	0.00	0.78	0.42	0.86	0.17	0.63	0.34
Red Wash 20 1 32-28C	34e	6	188	0.40	-	+	0.19	0.00	0.77	0.38	0.81	0.16	0.58	0.41
Federal 1-27	67e	6	85	0.52	-	+	0.34	0.15	0.70	0.25	0.78	0.12	0.80	0.34
Coyote Basin E Red Wash Fed 4-6	69e	6	85	0.45	+	+	0.22	0.21	0.78	0.30	0.80	0.12	0.57	0.31
E Red Wash 1/91-26C (State 1-41-36C)	9e	6	748	0.44	-	+	0.13	0.00	0.28	0.03	0.06	0.08	0.13	0.34

Sample	No	Map-group	Terpanes						Sesqui-, diterpanes					
			Gammacerane (μg/g oil)	C <sub>29</sub> C <sub>30</sub> hopanes	Methyl hopanes	C <sub>n</sub> Tetracyclic terpane	C <sub>n</sub> SIC <sub>11</sub> S <sub>12</sub> hopane	Unknown terpane/C <sub>n+1,4</sub> hopane	Sesqu/ sesqu + diterpanes	Sesqu/ sesqu + pentac terpanes	Sesqu/ sesqu + steranes	Diterpanes/ diterpanes + pentac terpanes	Diterpanes/ diterpanes + steranes	B <sub>10</sub> (H)-dimane/B <sub>10</sub> (H) dimane/bornane
Walker Hollow Pearl Broadhurst 21	23a	7	1318	0.41	-	-	0.12	0.00	0.52	0.10	0.62	0.10	0.61	0.29
Walker Hollow Pearl Broadhurst 1	52a	7	1330	0.46	-	-	0.12	0.03	0.54	0.09	0.58	0.08	0.54	0.38
Walker Hollow Pearl Broadhurst 15	53a	7	576	0.36	-	-	0.19	0.06	0.50	0.10	0.64	0.10	0.64	0.29
Walker Hollow Pearl Broadhurst 18	54a	7	515	0.41	-	-	0.13	0.06	0.45	0.08	0.61	0.10	0.66	0.30
Walker Hollow Pearl Broadhurst 12	59a	7	n.a.	0.46	-	-	0.15	0.03	0.38	0.04	0.47	0.07	0.61	0.21
Walker Hollow Unit 1	60a	7	554	0.40	-	-	0.24	0.00	0.46	0.08	0.56	0.07	0.59	0.34
Horseshoe Bend 2/22-34 Federal	8a	8	600	0.30	-	-	0.16	0.00	0.61	0.19	0.84	0.13	0.77	0.41
Brennan Bottom Federal 2-20	13a	8	536	0.33	-	-	0.17	0.00	0.49	0.15	0.73	0.16	0.74	0.18
Brennan Bottom Federal 15-8	42a	8	502	0.40	-	-	0.14	0.00	0.65	0.23	0.71	0.14	0.57	0.34
Horseshoe Bend Federal 4-2-F	47a	8	391	0.39	-	-	0.16	0.00	0.63	0.26	0.86	0.17	0.78	0.38
Horseshoe Bend Federal 5-5H	48a	8	524	0.38	-	-	0.23	0.00	0.56	0.19	0.83	0.16	0.79	0.30
Brennan Bottom Federal 6	57a	8	1487	0.38	-	-	0.26	0.11	0.56	0.02	0.16	0.01	0.13	0.22
Brennan Bottom Federal 1	68a	8	247	0.39	-	-	0.28	0.00	0.57	0.11	0.49	0.09	0.42	0.25
Twelve Mile Wash Fed 1 6958-6980ft	7a	9	529	0.60	-	-	0.12	0.00	0.27	0.02	0.15	0.06	0.32	1.00
Twelve Mile Wash Federal 1 7396-7428ft	70a	9	984	0.59	-	-	0.09	0.00	0.51	0.07	0.32	0.06	0.31	0.55
Twelve Mile Wash Federal 1 DST 5960ft	71a	9	2412	0.73	-	-	0.13	0.00	0.56	0.08	0.37	0.06	0.32	0.64
Gusher Gov 4-14	61a	9	317	0.38	-	-	0.15	0.05	0.57	0.14	0.83	0.11	0.79	0.37
Gusher Gusher 3	30a	9	438	0.37	-	-	0.23	0.07	0.61	0.22	0.88	0.16	0.82	0.47
Red Wash Whole Field	3a	-	1062	0.36	-	-	0.28	0.03	0.50	0.10	0.53	0.10	0.53	0.34

waxy type

immature type

regular type

## APPENDIX 9

Sample	No	Map-group	Steranes, dinanes										% Terpanes		
			Isopimarane/ isoprismarane+phytocadinane	Homodimethoxy- dimane/isopimarane	Dimane/ dimane+phytocadinane	20S/(20S+20R) $\alpha$ C <sub>n</sub>	(S)/(D) $\alpha$ C <sub>n</sub>	Dinanes/sternanes	Sterane/terpanes	Methyl steranes	Disterane index	% Sesquiterpanes	% Diterpanes	% Tricyclic terpanes	
Texaco D-1 Ute Tribal 4700ft	10	1	0.50	0.92	0.88	0.33	0.27	0.00	0.21	-	0.00	4.6	3.0	7.6	
Texaco D-1 Ute Tribal 9251ft	20	1	0.00	0.00	0.00	0.00	0.00	0.00	0.00	-	0.00	63.9	36.1	0.0	
Cedar Rim Ute Tribal 2-2C8	140	1	0.54	0.87	0.84	0.32	0.19	0.00	0.24	--	0.00	3.1	3.0	8.5	
Cedar Rim Ute Tribal 2-24C7	380	1	0.00	0.00	1.00	0.00	0.00	0.00	0.00	-	0.00	92.3	7.7	0.0	
Cedar Rim Ford 2-13C7	390	1	0.00	1.00	1.00	0.00	0.00	0.00	0.00	-	0.00	89.5	10.5	0.0	
Antelope Creek Ute Tribal 1-5 (05-07)	110	2	0.71	0.59	0.62	0.00	0.00	0.00	0.00	-	0.00	45.0	55.0	0.0	
Nutter Canyon Ute Tribal 10-21	210	2	0.69	0.73	0.82	0.58	0.55	0.00	0.05	-	0.24	34.1	16.7	29.0	
Bluebell Freston 2-8B1	40	3	1.00	0.77	1.00	0.00	0.00	0.00	0.00	-	0.00	78.3	21.7	0.0	
Bluebell Fay Mecham Fee Federal 1	270	3	0.36	0.87	0.79	0.47	0.51	0.00	0.04	+	0.47	18.3	13.3	37.4	
Bluebell 1-33A1 Lih Pack	330	3	1.00	0.88	1.00	0.47	0.58	0.01	1.18	--	0.02	4.8	3.0	7.0	
Chevron Blanchard 1-33-3	730	3	0.35	0.85	0.87	0.47	0.47	0.02	0.07	+	0.07	0.5	0.4	25.3	
Eight Mile Wash State 33-52D (33-32)	160	4	0.67	0.80	0.80	0.48	0.67	0.00	0.05	-	0.00	14.7	69	39.3	
Natural Buttes Old Squaws Crossing 4A	200	4	0.34	0.83	0.79	0.43	0.46	0.00	0.05	-	0.22	14.8	7.8	23.2	
Pleasant Valley Federal 24-15-H	220	4	0.85	0.72	0.71	0.60	0.66	0.00	0.05	+	0.49	19.1	16.1	35.5	
Monument Butte Federal 15-20	310	4	0.76	0.71	0.84	0.39	0.67	0.00	0.06	+	0.00	37.5	17.3	27.3	
Panette Bench Federal 14-5	510	4	0.45	0.73	0.34	0.48	0.61	0.00	0.05	-	0.38	3.4	5.5	38.0	
CNG 3-25B	760	4	1.00	0.88	1.00	0.40	0.49	0.00	0.08	+	38.0	14.3	4.4	27.7	
Wansits Valley 133&71	60	5	0.44	0.87	0.74	0.47	0.51	0.00	0.06	-	0.27	18.1	10.3	27.3	
Wansits Valley Whiton Valley 1-19-3C	240	5	0.31	0.90	0.78	0.48	0.50	0.00	0.08	+	0.02	10.3	6.9	29.5	
Gypsum Hills Federal 3	460	5	0.52	0.87	0.80	0.48	0.49	0.00	0.04	-	0.32	24.1	10.3	23.9	
Wansits Valley Federal 105	550	5	0.40	0.85	0.59	0.44	0.53	0.00	0.05	+	0.23	15.2	12.3	29.2	
Wansits Valley Unit 88-2	630	5	0.50	0.86	0.69	0.46	0.62	0.00	0.04	-	0.46	13.3	8.9	27.4	
White River Unit 47-10	640	5	0.00	0.00	0.00	0.35	0.31	0.01	0.06	+	0.18	0.0	0.0	27.7	
Wansits Valley Federal 24	710	5	0.40	0.86	0.70	0.44	0.45	0.02	0.05	-	0.24	14.6	9.5	27.7	
Conoco Tribal 31-55A	740	5	0.38	0.88	0.78	0.30	0.28	0.01	0.24	--	0.00	0.2	0.1	10.2	
Conoco Tribal 35-51	750	5	0.42	0.86	0.83	0.31	0.27	0.01	0.26	--	0.00	0.2	0.2	10.7	
Gypsum Hills Costas Federal 2 20-3b	700	5	0.56	0.82	0.69	0.47	0.63	0.03	0.04	+	0.47	18.3	10.8	28.8	
Coyote Basin E Red Wash 1-5	50	6	0.68	0.87	0.91	0.47	0.44	0.00	0.12	-	0.76	39.6	7.9	14.9	
Coyote Basin Federal 12-13	150	6	0.77	0.85	0.91	0.46	0.48	0.00	0.12	+	0.33	36.2	10.2	15.7	
Red Wash 20 1 32-28C	340	6	0.71	0.88	0.92	0.44	0.43	0.15	0.15	+	0.53	32.2	9.6	16.9	
Federal 1-27	670	6	0.87	0.79	0.80	0.45	0.48	0.02	0.09	+	0.50	21.5	9.2	21.5	
Coyote Basin E Red Wash Fed 4-8	690	6	0.74	0.84	0.86	0.50	0.50	0.03	0.11	-	0.56	26.3	8.5	18.7	
E Red Wash 1/91-28C (State 1-41-38C)	90	6	0.20	0.79	0.34	0.20	0.16	0.00	0.58	+	0.13	2.2	5.6	10.6	

Sample	No	Map-group	Steranes, diginanes												% Diterpanes % Sesquiterpanes % Triterpanes	
			Isopimarane/ isopimarane+phylocladane	Homodimane/homo- dimane+isopimarane	Dimane/ dimane+phylocladane	20S/(20S+20R) $\mu\text{C}_{27}$	$\Delta^{30}(18+20)$ C <sub>27</sub>	Diginanes/steranes	Sterane/terpanes	Methyl steranes	Diasterane index	% Sesquiterpanes	% Diterpanes	% Triterpanes		
Walker Hollow Pearl Broadhurst 21	23o	7	0.30	0.89	0.59	0.36	0.40	0.00	0.07	-	0.00	9.5	8.9	28.9		
Walker Hollow Pearl Broadhurst 1	52o	7	0.19	0.92	0.62	0.33	0.34	0.00	0.07	-	0.06	8.5	7.3	29.7		
Walker Hollow Pearl Broadhurst 15	53o	7	0.25	0.91	0.57	0.36	0.41	0.00	0.06	-	0.06	9.0	9.1	29.0		
Walker Hollow Pearl Broadhurst 18	54o	7	0.26	0.88	0.53	0.30	0.42	0.00	0.06	-	0.12	7.7	9.5	28.7		
Walker Hollow Pearl Broadhurst 12	59o	7	0.30	0.85	0.39	0.40	0.40	0.01	0.05	-	0.09	4.0	7.0	29.8		
Walker Hollow Unit 1	60o	7	0.28	0.86	0.56	0.36	0.31	0.00	0.05	-	0.11	5.7	6.6	28.2		
Horseshoe Bend 2/22-34 Federal	8o	8	0.33	0.89	0.74	0.40	0.39	0.00	0.04	-	0.00	17.1	10.9	25.1		
Brennan Bottom Federal 2-20	13o	8	0.35	0.90	0.49	0.44	0.58	0.12	0.06	+	0.80	14.0	14.8	29.0		
Brennan Bottom Federal 15-8	42o	8	0.48	0.90	0.81	0.54	0.44	0.03	0.12	+	0.87	20.0	10.9	27.0		
Horseshoe Bend Federal 4-2-F	47o	8	0.47	0.86	0.76	0.41	0.50	0.00	0.06	+	0.38	22.7	13.1	30.9		
Horseshoe Bend Federal 5-5H	48o	8	0.44	0.85	0.65	0.38	0.54	0.02	0.05	+	0.27	17.3	13.4	31.4		
Brennan Bottom Federal 6	57o	8	0.44	0.90	0.66	0.51	0.48	0.01	0.09	-	0.68	1.6	1.3	33.1		
Brennan Bottom Federal 1	68o	8	0.48	0.89	0.72	0.50	0.48	0.02	0.13	-	0.86	9.9	7.6	26.6		
Twelve Mile Wash Fed 1 6956-6960ft	7o	9	0.32	0.00	0.72	0.45	0.35	0.00	0.14	+	0.00	2.1	5.8	21.7		
Twelve Mile Wash Federal 1 7396-7428ft	10o	9	0.29	0.92	0.84	0.38	0.29	0.00	0.16	+	0.00	8.0	5.6	21.3		
Twelve Mile Wash Federal 1 DST 5960ft	20o	9	0.31	0.89	0.87	0.40	0.23	0.01	0.14	+	0.00	6.7	5.3	19.9		
Gusher Gov 4-14	61o	9	0.51	0.81	0.73	0.48	0.58	0.02	0.03	-	0.30	13.3	9.9	35.7		
Gusher Gusher 3	30o	9	0.53	0.80	0.81	0.39	0.46	0.00	0.04	+	0.00	20.2	13.1	31.0		
Red Wash Whole Field	3o	-	0.37	0.86	0.66	0.31	0.33	0.00	0.10	-	0.05	8.9	8.9	25.1		

waxy type

immature type

regular type

## APPENDIX 9

Sample	No	Map-group	%Hopanes	%Steranes+stearanes	%Duganane+homoduganane	%	%C <sub>17</sub>	%C <sub>18</sub>	%C <sub>20</sub>	Maximum carbon number in GC	Maximum peak in GC	Modal
Texaco D-1 Ute Tnbal 4700ft	1a	1	67.3	17.5	0.0	13.0	49.8	37.2	41	B-carot	2	
Texaco D-1 Ute Tnbal 9251ft	2a	1	0.0	0.0	0.0	0.0	0.0	0.0	50	n-C <sub>24</sub>	1	
Cedar Rim Ute Tnbal 2-2C6	2ba	1	68.3	19.1	0.0	13.1	43.8	43.2	39	B-carot	2	
Cedar Rim Ute Tnbal 2-24C7	38a	1	0.0	0.0	0.0	0.0	0.0	0.0	50	n-C <sub>26</sub>	1	
Cedar Rim Ford 2-13C7	39a	1	0.0	0.0	0.0	0.0	0.0	0.0	50	n-C <sub>28</sub>	1	
Antelope Creek Ute Tnbal 1-5 (05-07)	11a	2	0.0	0.0	0.0	0.0	0.0	0.0	47	n-C <sub>26</sub>	1	
Nutter Canyon Ute Tnbal 10-21	21a	2	17.6	2.5	0.0	21.7	31.2	47.2	48	n-C <sub>27</sub>	1	
Bluebell Freston 2-8B1	4a	3	0.0	0.0	0.0	0.0	0.0	0.0	50	n-C <sub>24</sub>	1	
Bluebell Fay Mecham Fee Federal 1	27a	3	28.4	2.6	0.0	27.3	23.0	49.7	49	n-C <sub>24</sub>	2	
Bluebell 1-33A1 Lili Pack	33a	3	33.5	50.9	0.7	20.7	33.0	48.3	45	Ph	2	
Chevron Blanchard 1-33-3	73a	3	68.4	7.2	0.1	30.8	25.7	43.5	52	n-C <sub>27</sub>	1	
Eight Mile Wash State 33-52D (33-32)	18a	4	34.9	4.1	0.0	28.9	32.0	39.1	49	n-C <sub>23</sub>	1	
Natural Buttes Old Squaws Crossing 4A	20a	4	50.3	4.0	0.0	27.8	28.4	43.8	48	n-C <sub>27</sub>	1	
Pleasant Valley Federal 24-15-H	22a	4	26.1	3.1	0.0	27.0	46.5	26.5	49	n-C <sub>25</sub>	1	
Monument Butte Federal 15-20	31a	4	15.3	2.6	0.0	37.8	24.4	37.8	49	n-C <sub>23</sub>	1	
Panette Bench Federal 14-5	51a	4	47.9	5.2	0.0	31.5	30.5	38.0	48	n-C <sub>23</sub>	2	
CNG 3-25B	78a	4	48.3	7.3	0.0	36.6	18.0	45.4	53	n-C <sub>26</sub>	2	
Wonsits Valley 133&71	6a	5	40.1	4.2	0.0	44.8	17.5	37.9	49	n-C <sub>27</sub>	1	
Wonsits Valley Whiton Valley 1-19-3C	24a	5	46.6	6.7	0.0	29.1	29.5	41.4	50	n-C <sub>27</sub>	1	
Gypsum Hills Federal 3	46a	5	38.8	2.9	0.0	30.7	26.8	42.5	50	n-C <sub>27</sub>	2	
Wonsits Valley Federal 105	55a	5	39.7	3.6	0.0	30.7	24.2	45.1	49	n-C <sub>25</sub>	1	
Wonsits Valley Unit 88-2	63a	5	47.3	3.1	0.0	34.5	23.7	41.7	39	n-C <sub>24</sub>	2	
White River Unit 47-10	64a	5	65.9	6.3	0.0	39.3	21.9	38.8	50	n-C <sub>28</sub>	2	
Wonsits Valley Federal 24	71a	5	44.5	3.8	0.1	33.2	23.8	42.9	50	n-C <sub>25</sub>	1	
Conoco Tnbal 31-55A	74a	5	69.3	20.1	0.1	20.8	26.8	52.4	53	Pr	1	
Conoco Tnbal 35-51	75a	5	67.3	21.5	0.1	21.1	30.3	48.8	53	Pr	1	
Gypsum Hills Costas Federal 2-20-3b	70a	5	40.6	3.3	0.1	36.0	24.0	40.0	42	n-C <sub>25</sub>	1	
Coyote Basin E Red Wash 1-5	5a	6	31.7	5.8	0.0	42.7	15.8	41.5	50	n-C <sub>25</sub>	1	
Coyote Basin Federal 12-13	15a	6	31.9	8.0	0.0	43.2	14.1	42.7	47	n-C <sub>26</sub>	2	
Red Wash 20 1 32-28C	34a	6	32.7	7.5	1.2	48.4	17.1	34.5	48	n-C <sub>22</sub>	2	
Federal 1-27	67a	6	41.4	6.2	0.1	45.5	16.1	38.4	50	n-C <sub>13</sub>	2	
Coyote Basin E Red Wash Fed 4-6	69a	6	39.8	6.5	0.2	49.7	17.1	33.2	52	n-C <sub>27</sub>	1	
E Red Wash 1/91-28C (State 1-41-36C)	9a	6	45.2	36.3	0.0	85.3	13.5	21.2	47	n-C <sub>28</sub>	2	

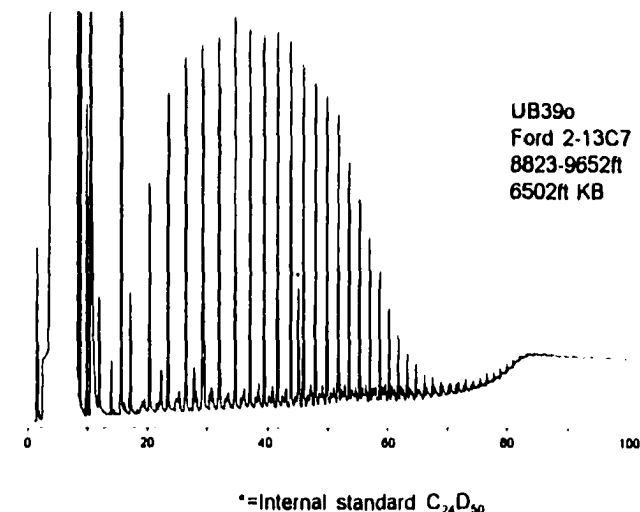
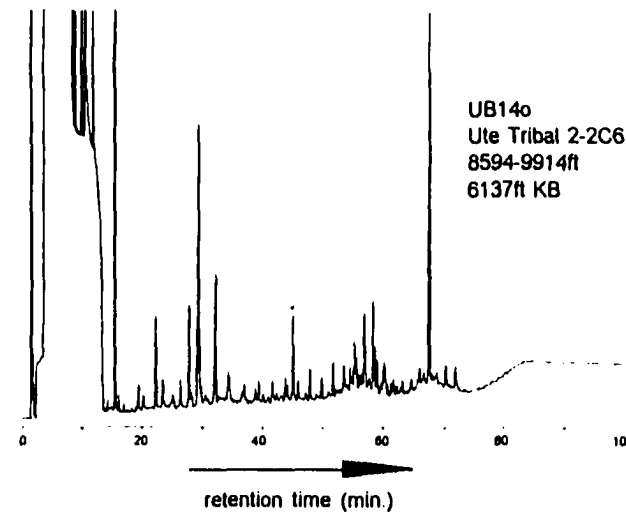
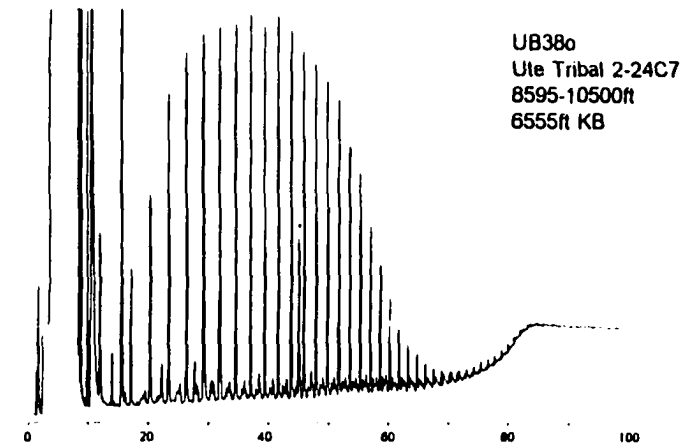
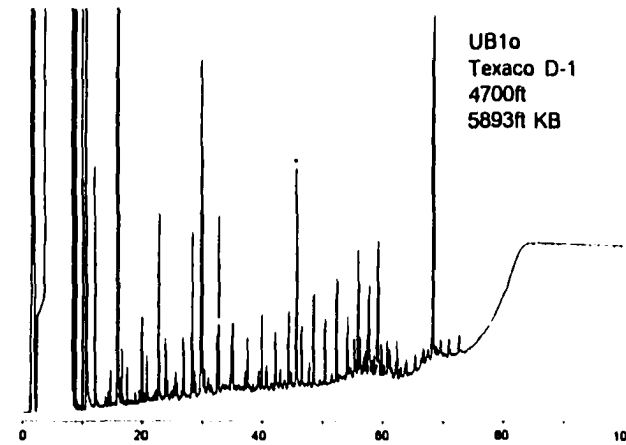
Sample	No.	Map-group	% Hopanes	% Steranes/stananes	% Dignanes+ homodignane	% C <sub>29</sub>	% C <sub>30</sub>	% C <sub>31</sub>	Maximum carbon number in GC	Maximum peak in GC	Modal
Walker Hollow Pearl Broadhurst 21	230	7	47.0	5.7	0.0	35.6	25.1	39.3	54	n-C <sub>29</sub>	1
Walker Hollow Pearl Broadhurst 1	520	7	48.3	6.3	0.0	33.1	28.1	40.8	47	n-C <sub>29</sub>	1
Walker Hollow Pearl Broadhurst 15	530	7	47.9	5.0	0.0	31.3	25.7	43.0	49	n-C <sub>29</sub>	1
Walker Hollow Pearl Broadhurst 18	540	7	49.2	4.9	0.0	40.5	20.7	38.8	40	Ph	1
Walker Hollow Pearl Broadhurst 12	590	7	54.7	4.5	0.0	37.4	27.5	35.1	45	Pr	
Walker Hollow Unit 1	600	7	55.0	4.5	0.0	32.1	25.9	42.0	44	n-C <sub>27</sub>	
Horseshoe Bend 2/22-34 Federal	80	8	43.7	3.2	0.0	35.0	28.5	36.8	48	Pr	2
Brennan Bottom Federal 2-20	130	8	36.6	5.1	0.6	37.6	28.2	34.3	47	n-C <sub>29</sub>	1
Brennan Bottom Federal 15-8	420	8	33.7	8.2	0.2	55.0	17.4	27.5	49	n-C <sub>27</sub>	2
Horseshoe Bend Federal 4-2-F	470	8	29.6	3.7	0.0	31.9	25.4	42.6	50	n-C <sub>27</sub>	1
Horseshoe Bend Federal 5-5H	480	8	34.3	3.5	0.1	37.4	22.8	39.8	49	n-C <sub>22</sub>	1
Brennan Bottom Federal 6	570	8	55.1	8.7	0.1	46.1	17.7	38.2	49	n-C <sub>27</sub>	1
Brennan Bottom Federal 1	680	8	45.5	10.3	0.2	50.1	13.0	37.0	53	Pr	2
Twelve Mile Wash Fed 1 6958-6960ft	700	9	58.2	12.1	0.0	20.2	38.9	40.9	39	Pr	1
Twelve Mile Wash Federal 1 7396-7426ft	700	9	54.5	12.7	0.0	16.8	34.2	49.0	39	Pr	2
Twelve Mile Wash Federal 1 DST 5960ft	700	9	56.7	11.3	0.1	19.7	31.8	48.5	39	Pr	1
Gusher Gov 4-14	610	9	38.3	2.7	0.0	36.1	25.9	38.0	51	n-C <sub>34</sub>	
Gusher Gusher 3	300	9	32.8	2.9	0.0	24.9	18.8	56.3	49	n-C <sub>27</sub>	1
Red Wash Whole Field	30	-	49.2	7.9	0.0	35.9	23.1	41.0	52	n-C <sub>25</sub>	1

waxy type   
 immature type   
 regular type

## APPENDIX 10

### High temperature gas chromatograms of Uinta Basin crude oils Map-group 1 - Cedar Rim

A10.1-1

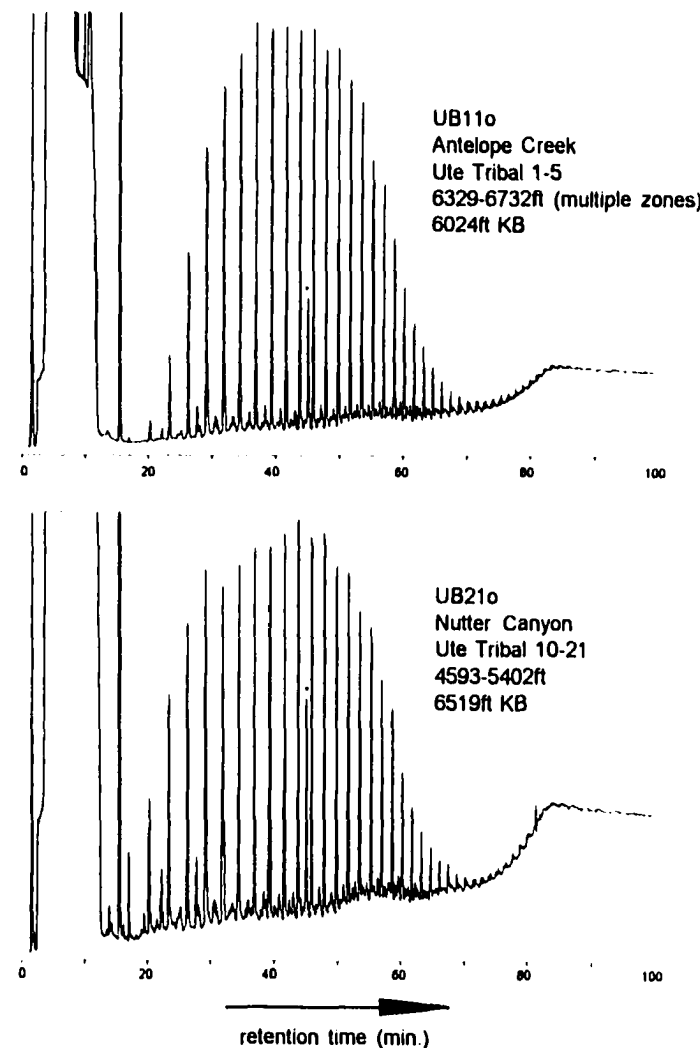


retention time (min.)

\*=Internal standard C<sub>24</sub>D<sub>50</sub>

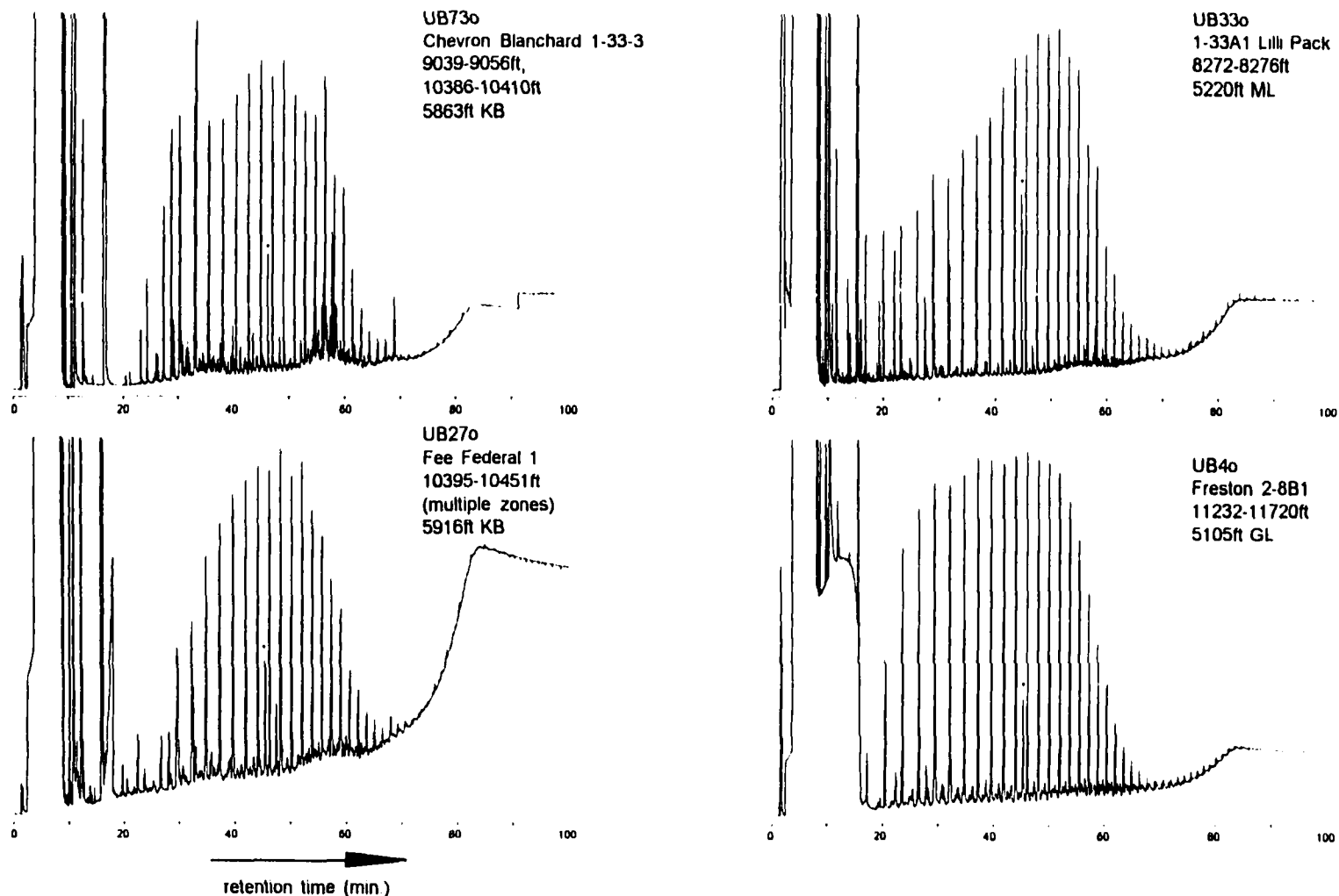
**APPENDIX 10**  
**High temperature gas chromatograms of Uinta Basin crude oils**  
**Map-group 2 - South-central fields 1**

10.2-1



**APPENDIX 10**  
**High temperature gas chromatograms of Uinta Basin crude oils**  
**Map-group 3 - Bluebell field**

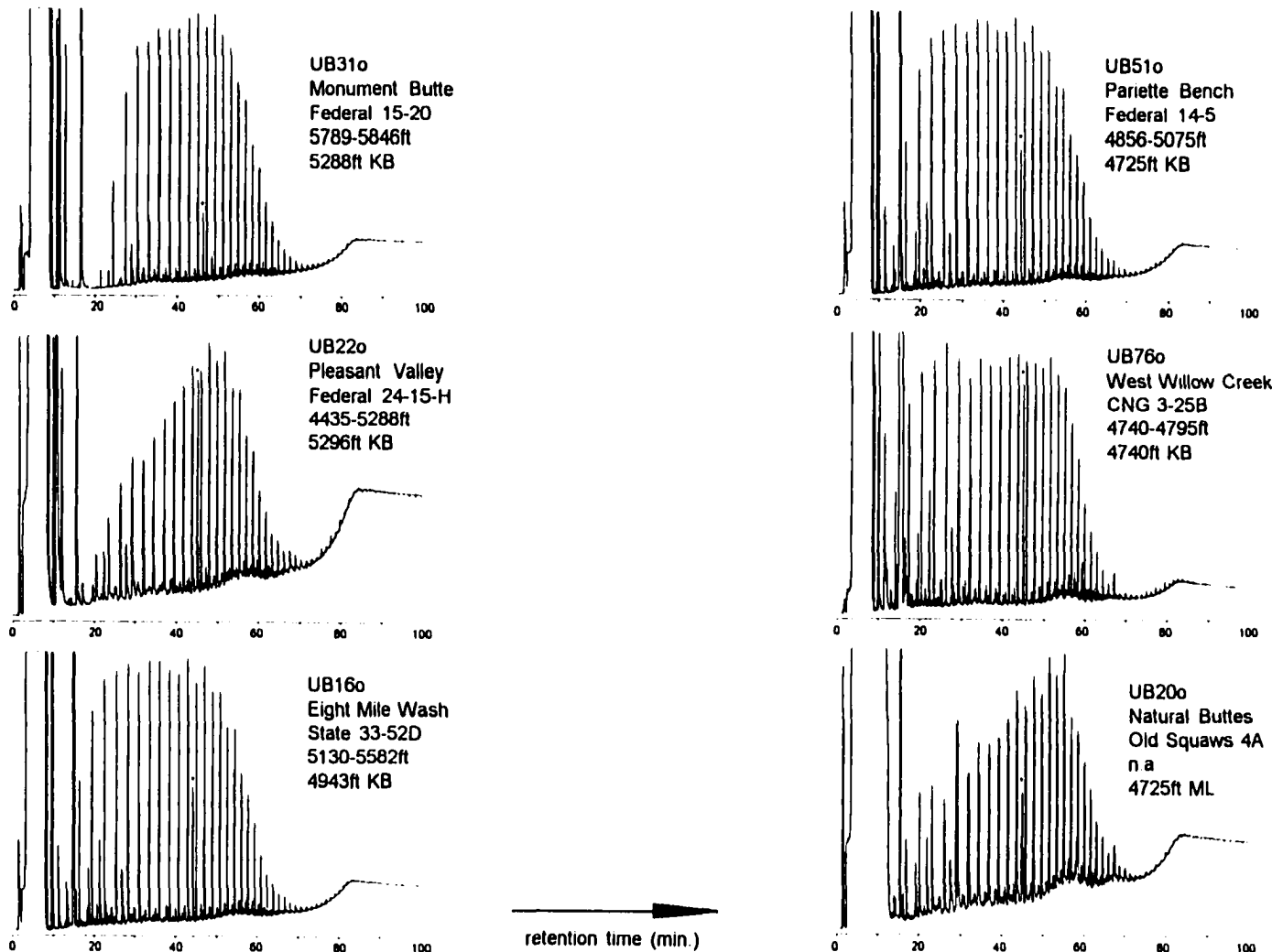
10.3-1



## APPENDIX 10

### High temperature gas chromatograms of Uinta Basin crude oils Map-group 4 - South-central fields 2

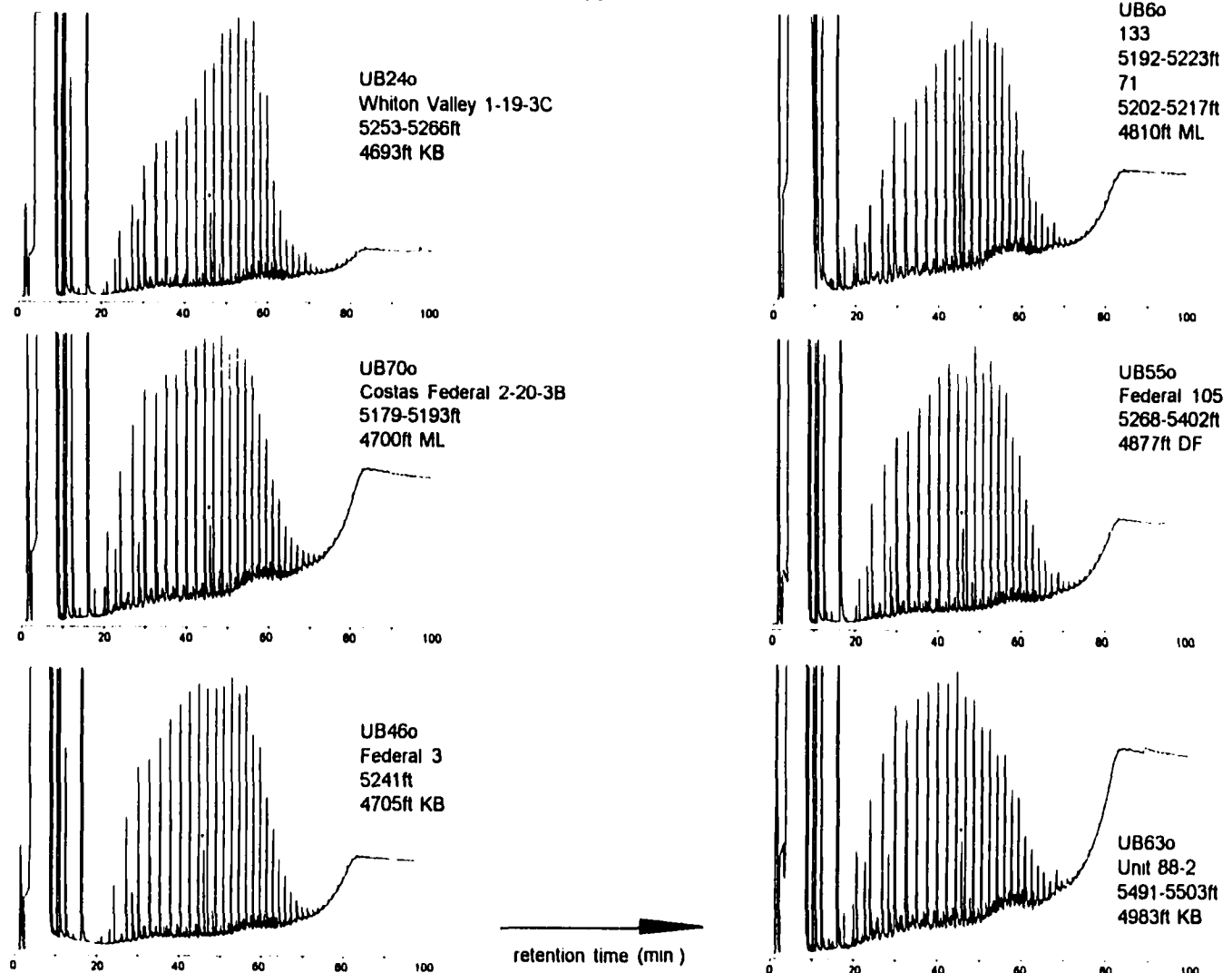
1041



## APPENDIX 10

### High temperature gas chromatograms of Uinta Basin crude oils Map-group 5 - Wonsits Valley/White River Unit - Gypsum Hills

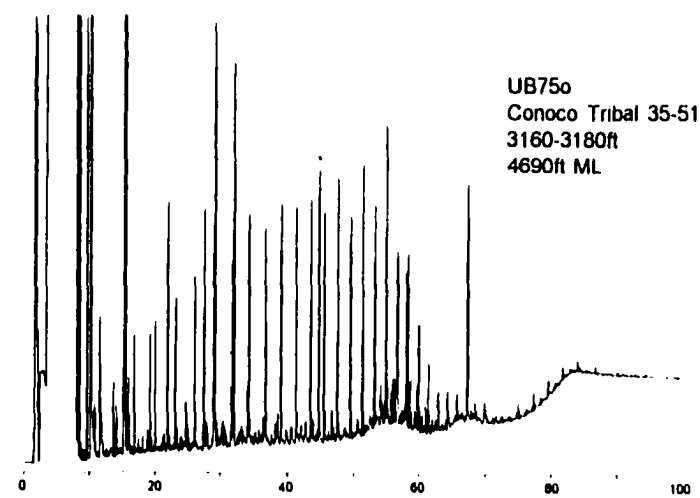
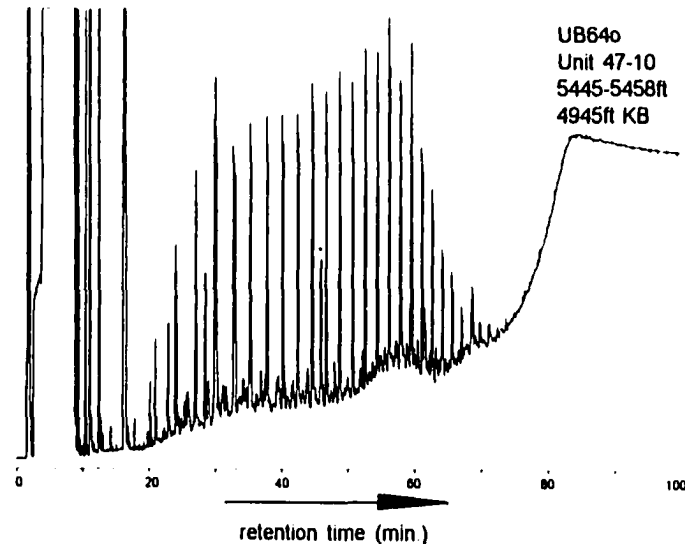
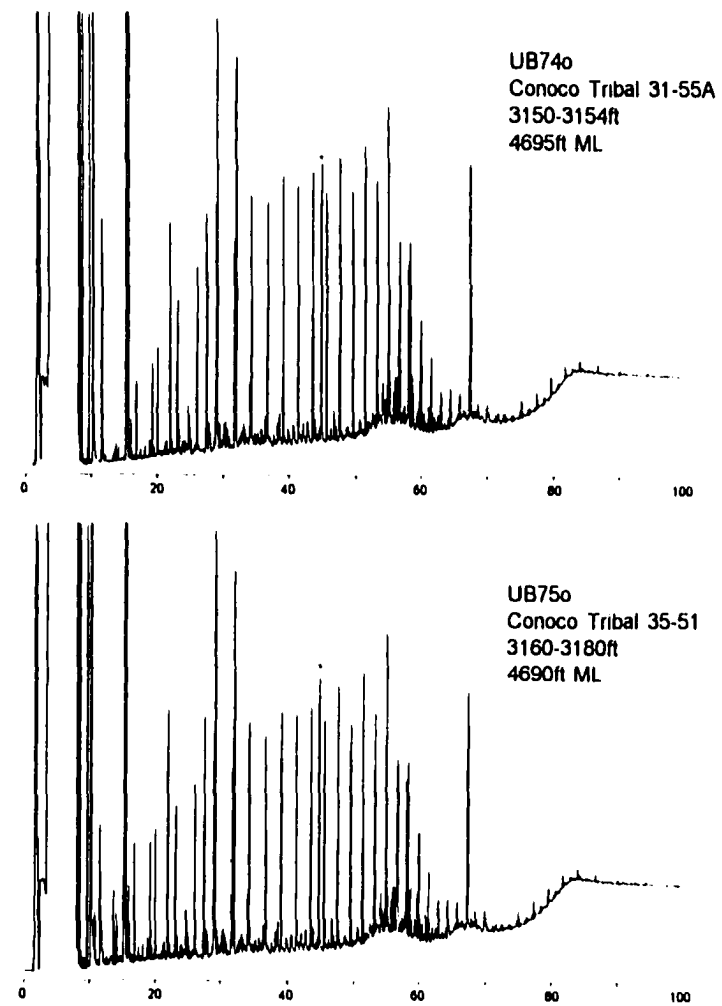
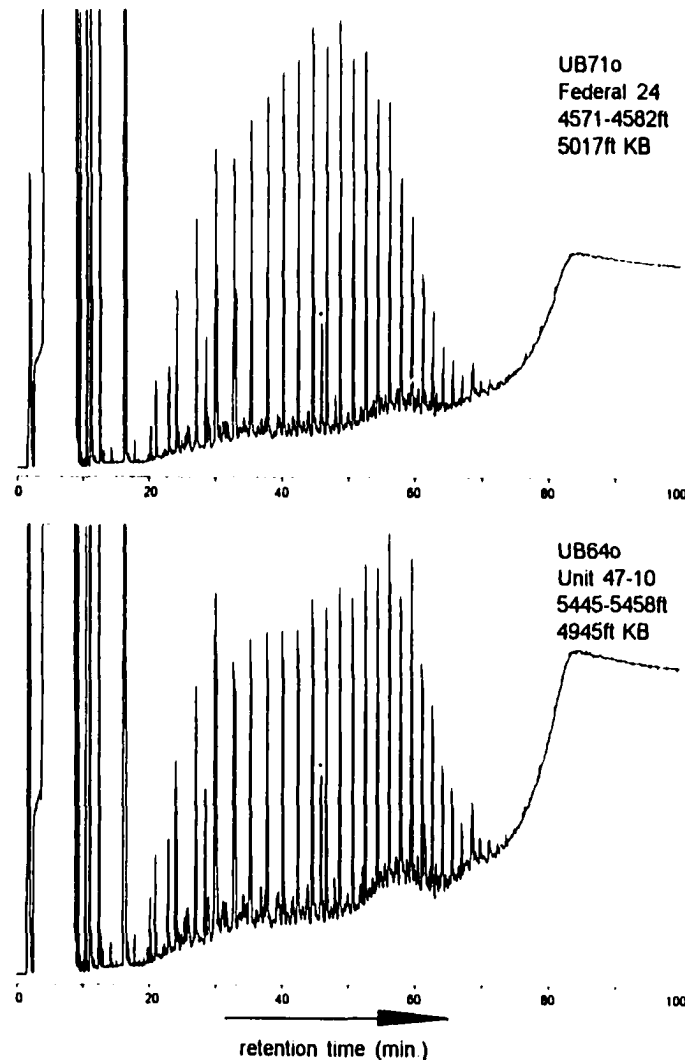
10-5-1



## APPENDIX 10

### High temperature gas chromatograms of Uinta Basin crude oils Map-group 5 - Wonsits Valley/White River Unit - Gypsum Hills

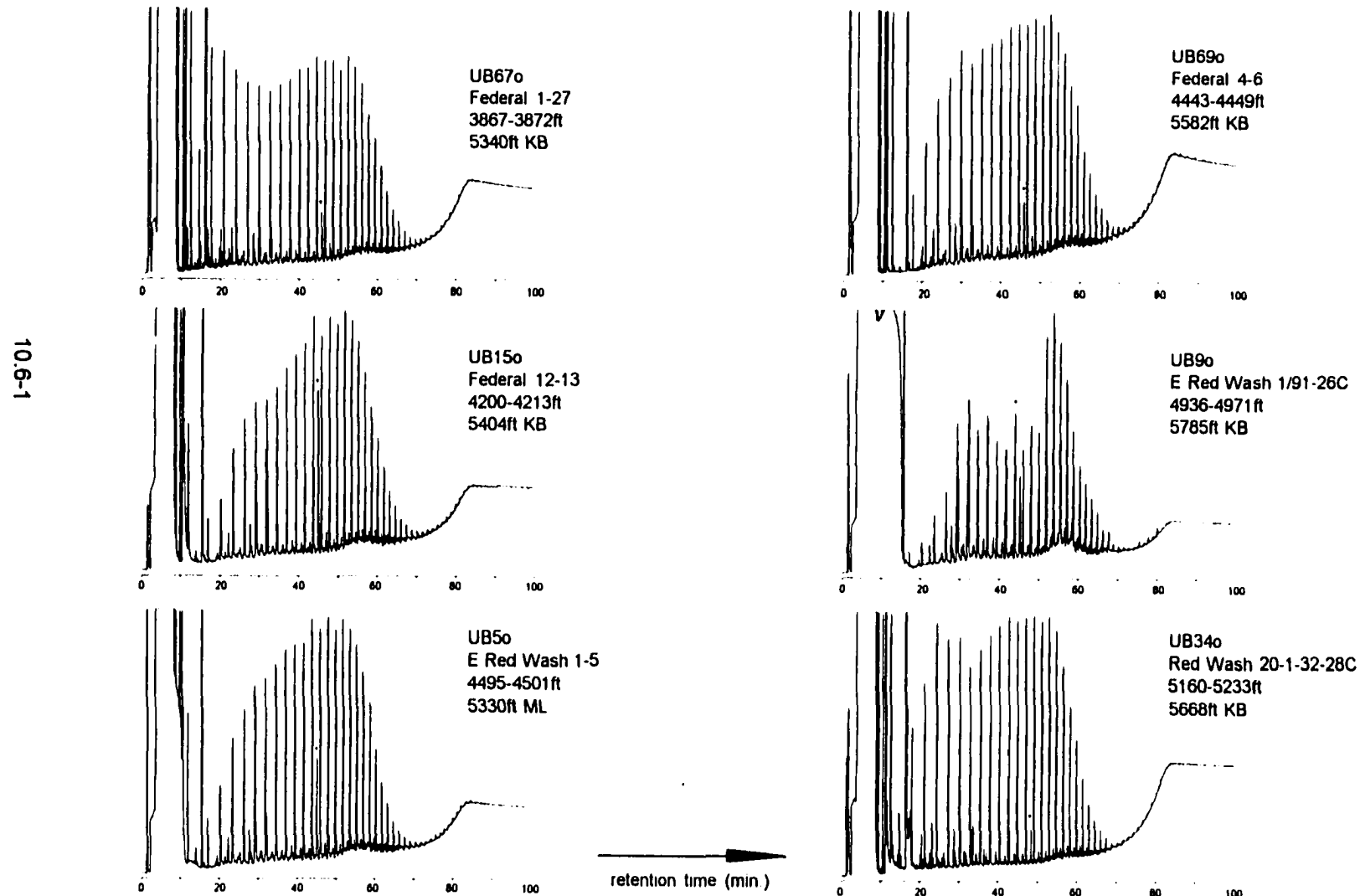
10.5-2



retention time (min.)

## APPENDIX 10

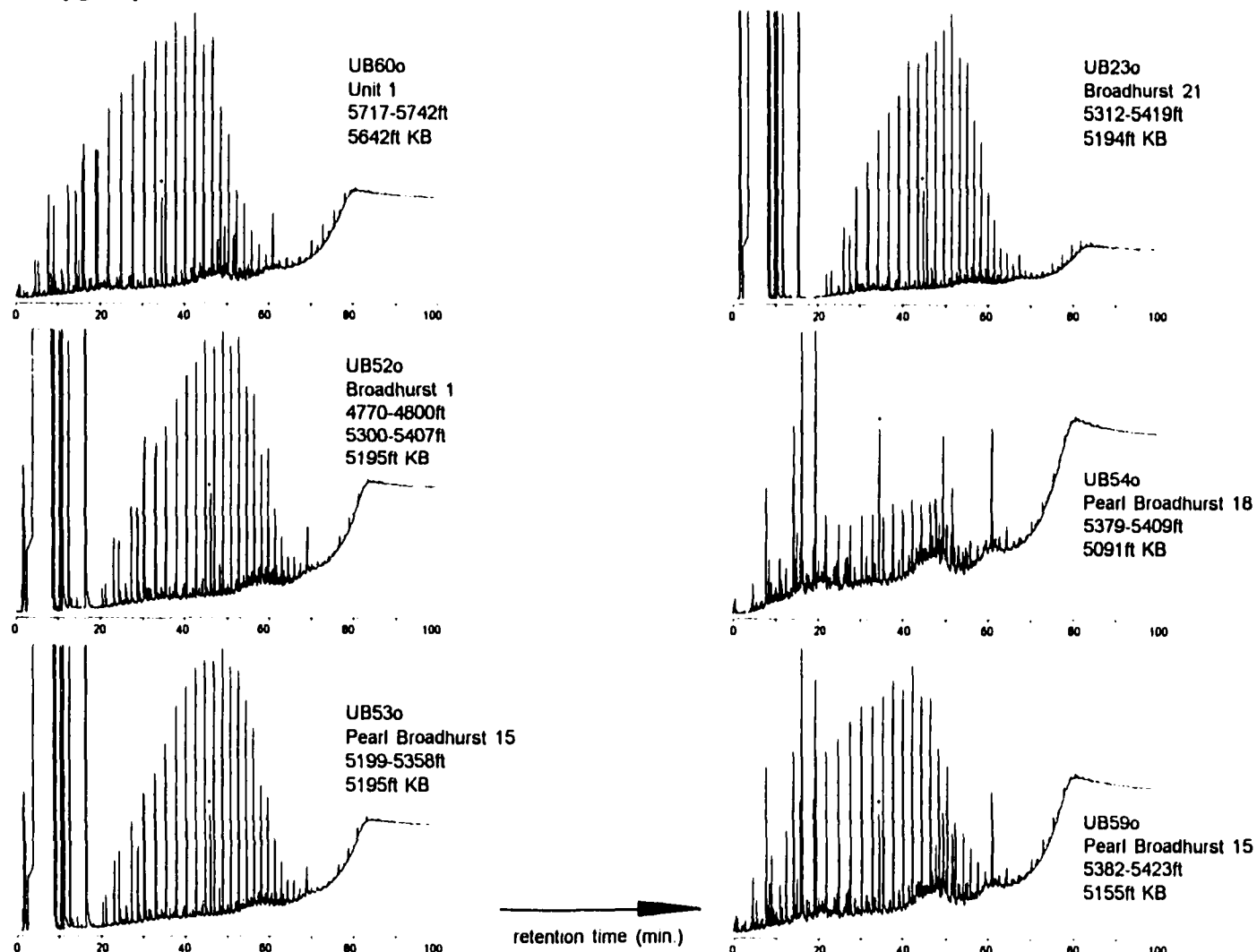
### High temperature gas chromatograms of Uinta Basin crude oils Map-group 6 - Coyote Basin / E Red Wash



## APPENDIX 10

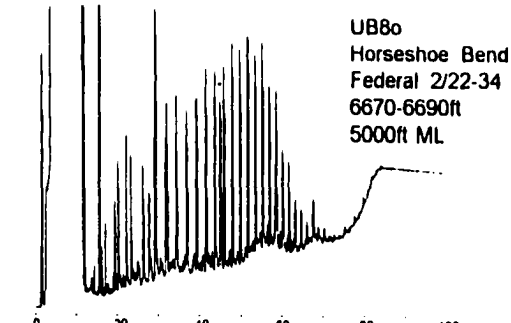
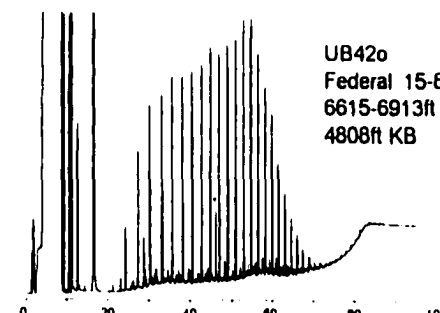
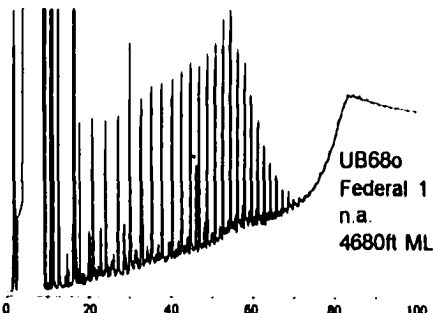
### High temperature gas chromatograms of Uinta Basin crude oils Mapgroup 7 - Walker Hollow Unit / Greater Red Wash area

10.7.1

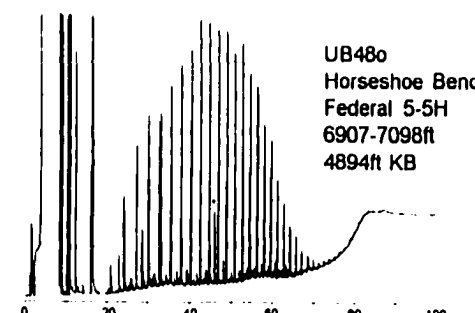
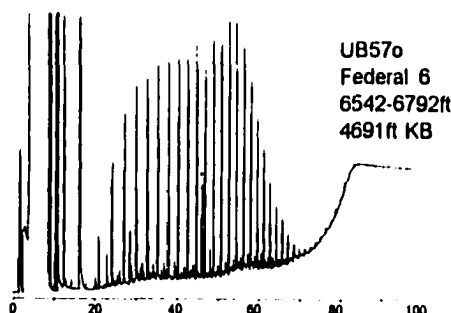


## APPENDIX 10

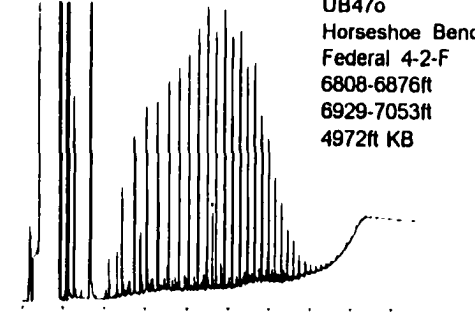
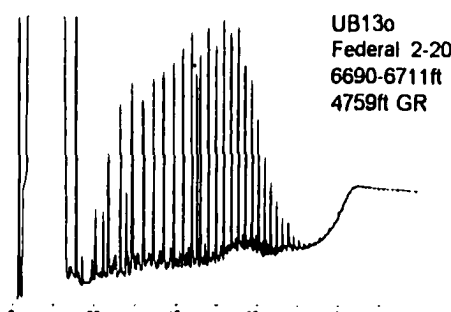
### High temperature gas chromatograms of Uinta Basin crude oils Map-group 8 - Brennan Bottom



10.8-1



retention time (min.)

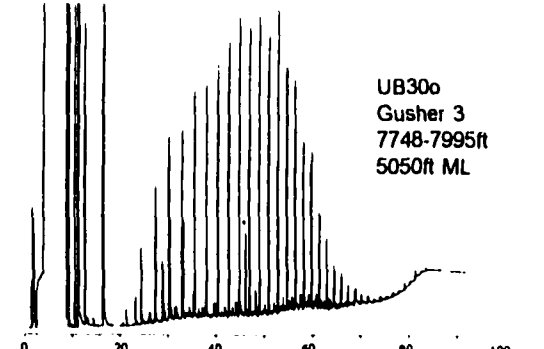
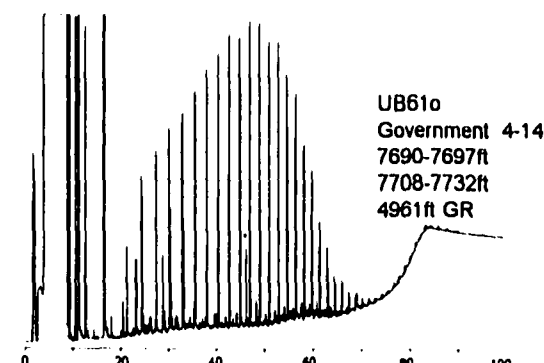
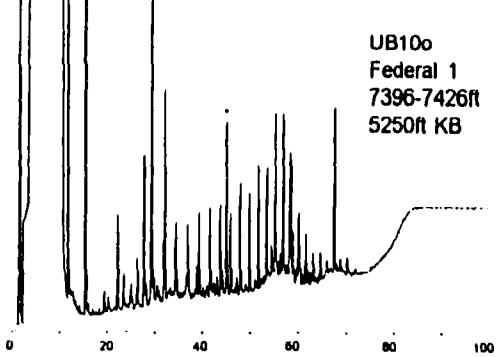
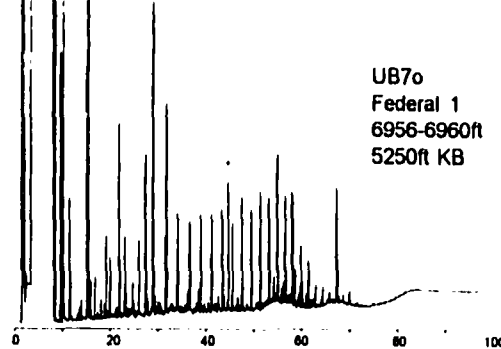
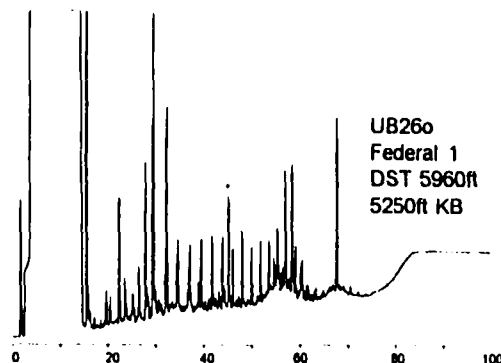


## APPENDIX 10

### High temperature gas chromatograms of Uinta Basin crude oils

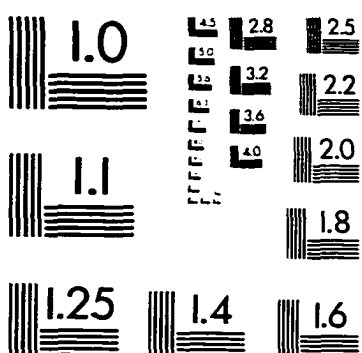
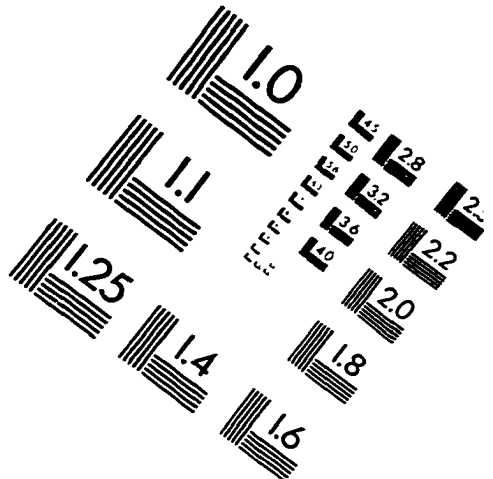
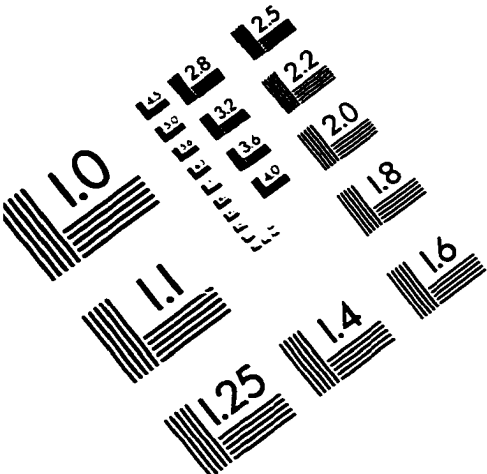
Map-group 9 - Twelve Mile Wash / Gusher

10.9-1



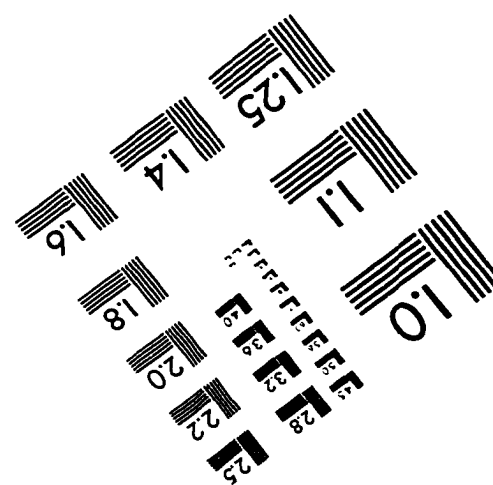
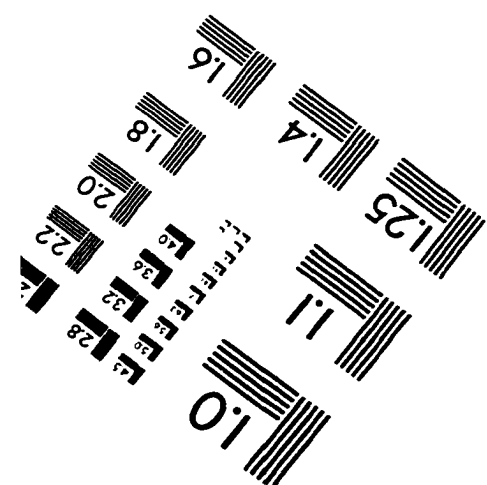
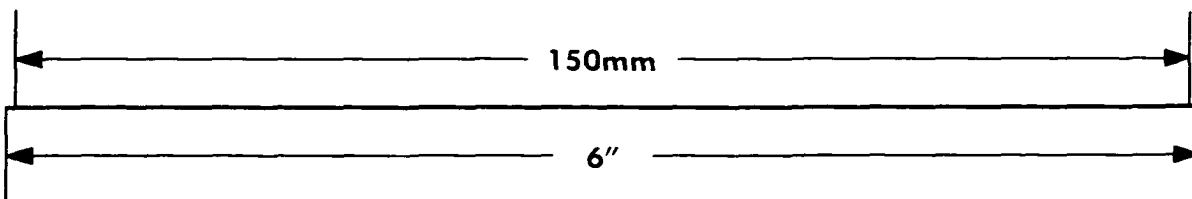
retention time (min)

**IMAGE EVALUATION  
TEST TARGET (QA-3)**



150mm

6"



**APPLIED IMAGE . Inc**  
1653 East Main Street  
Rochester, NY 14609 USA  
Phone: 716/482-0300  
Fax: 716/288-5989

© 1993. Applied Image, Inc., All Rights Reserved